Part III　Conclusion and Proposal

Chapter 1:　Conclusion

This project started in anticipation of whether we can find Noril'sk style copper-nickel-PGE sulfide ore deposits in the Paraná flood basalts. Studies on LIPs (Large Igneous Provinces), including the flood basalt that formed ore deposit of this type, have just made rapid development since 1995. Because discussions are still on the progress on the characteristics and origin of LIP, researchers have naturally different opinions.

Given this situation, this survey began, based on existing literature, by reviewing the characteristics and genesis of flood basalts around the world, chemical stratigraphy and geological structure of the Noril'sk ore deposits and Siberian trap, and considering the exploration criteria of the Noril'sk style ore deposits. According to the exploration criteria studied, the approaches from analyzing both the geological structure and the geochemistry of the basalts were conducted in order to extract an area with similar geological environment to the Noril'sk region in the Paraná Basin. That is, the geological structure analysis of the entire basin was carried out using the existing documents, satellite images, and gravity/geomagnetic data. At the same time, the analysis of the major chemical compositions and trace elements, such as Pt, Pd, Au, and REE, and isotope analysis for rock samples collected during the survey were also carried out. This resulted in defining the geochemical characteristics of the Paraná flood basalts. Based on comprehension of these results, we carried out study for the area that has a potential for existence of ore deposits.

1-1　Genesis of Flood Basalt and PGE Sulfide Ore Deposit

A number of theories exist concerning the genesis of flood basalt, including a theory that supports active involvement of the mantle plume and a theory that emphasizes ascensions of the asthenosphere in continent breaking up. However, there has been no established theory yet concerning the genesis of flood basalt. Since 1995, a new theoretical model has been attracting researchers. According to this model, vast amounts of oceanic crust (slab) that subducted from continental margins deposited at the deep of the mantle, and ascended as heterogeneous mantle plume. The flood basalt magma characteristically erupted huge amounts of lava in a short period generally within 1 Ma or less. The heterogeneous plume that consists of basalt constituent having low melting temperature and peridotite constituent. In addition to such variety of the theory, magma activities of flood basalt vary depending on the location, so

the theory of flood basalt formation does not necessarily lead to direct linkage to the existence of PGE ore deposits.

Most PGE concentrate in the earth's core and are rarely included in the continental crust that is markedly differentiated. Therefore, it is reasonable to think that the original magma of PGE deposit was brought from the deep part of the earth. The source materials of flood basalt that yielded the PGE mineralization may have been brought from mantle plume that ascended from the core and mantle boundary zone. The magma is also expected to be generated with large scale melting of plume and surrounding mantle. During the formation of flood basalt, large magma quantities are generated compared to periods of ordinary igneous activity. At this stage, PGE that ordinarily concentrates in solid phases is considered to have a high possibility to be caught in the melt with relatively large quantity. Since PGE concentration is affected by factors of the supplies of SiO_2 and sulfur by crustal contamination, and the local tectonic setting, such factors that influence to PGE concentration are important for forming PGE ore deposits from the magmas generated by the above process.

1-2 Exploration criteria of the Noril'sk style deposit

Assuming that the Noril'sk ore deposits in Russia belong to a type of orthomagmatic sulfide ore deposit, we considered the geological environment that satisfies the common requirements for the genesis of orthomagmatic sulfide has been formed connected to the flood basalt magmatism in the Noril'sk region. Based on such standpoint, a document survey regarding the world orthomagmatic sulfide deposits and the Noril'sk ore deposits was carried out.

The magmas related to the genesis of the Noril'sk ore deposits were initially sulfur undersaturated and rich in PGE, and were also picritic to basaltic compositions of high temperature. The Noril'sk ore deposits were formed in an area with large quantities of such magmas, that is the center of plume related magmatic activity. Considering the forming environment of the Noril'sk ore deposits from the view point of the condition of orthomagmatic sulfide ore deposit forming, the follows are presented as the exploration criteria for orthomagmatic ore deposit accompanied with flood basalt:

(1) The existence of sulfur undersaturated PGE rich magmas as lavas or intrusions.
(2) The existence of magmas showing the signatures of crustal contamination and sulfide segregation associated with above PGE rich magmas as lavas or intrusions.
(3) It is desirable that the magmas are high temperature picritic to basaltic composition that easily contaminates the crust materials.

(4) The center of the magmatic activity where the large volume of silicate magmas are supplied through crustal suture zone.

1-3 Geology and Geological Structure of the Paraná Basin

After Paleozoic in age, intracratonic basins such as Parana Basin, etc. were formed in the Gondwana continent. M. S. M. Mantovani et al. (2001) calculated the thickness of lithosphere of South-American plates using the tidal gravity anomalies. According to the results, the thickness of lithosphere of Parana Basin is 10 to 20 km or more thinner than that of surrounding basement rocks. At this kind of portion with thin lithosphere, intracratonic basins are formed by changes of regional stress field and mantle plume (Bott, 1971; Makenzie et al., 1978). The Noril'sk ore deposit was formed in Gydansk-Omsk rift (Zonnenshain et al., 1990) and Duluth ore deposit in Midcontinent Rift (MCR) of North America.

From Paleozoic to Mesozoic in age, the Parana Basin was repeatedly deposited and eroded due to dilation and constriction of mantle plume. The present total thickness of the sedimentary rocks attains a maximum of more than 4,000 meters. In Early Cretaceous in age, tholeiite basaltic magma was active in rift and subsequently Gondwana continent was ruptured (Rezende, 1972). The sedimentary rocks and volcanic rocks of Parana Basin can be divided into the following six Supersequences (SS) according to geologic ages (Milani et al., 1998; Fig. II-1-4-9). They are the Rio Ivai SS (Ordovician to Silurian), the Parana SS (Devonian), Gondwana I SS (Late Carboniferous to Early Triassic), the Gondwana II SS (Early to Middle Triassic), the Gondwana III SS (Early Cretaceous) which mostly comprises thoreiitic flood basalt (maximum thickness 1,723 m) and the Bauru SS (Late Cretaceous).

As the flood basalt lava is distributed thickly in the NE-SW direction along the Parana River, the area is estimated to have been a rift. Drillings for oil exploration revealed that a large amount of sills and dykes associated with flood basalt magmatism intruded into the rift. There are two zones which accumulated thickness of sills and dykes are larger. The one is an area where extends in the NW-SE direction from the east of Parana River to Ponta Grossa Arch and the other an area where are located in the boundaries between Matto Grosso do Sul Province and Sao Paulo province in the northern area of the Basin and extends in the N-S direction. In the TM false color image (RGB=234), they are expressed as geographyic features uplifted in the form of thin strings and sometimes continue over 100 kilometers.

Based on the residual gravity anomaly map (M. C. L. Quintas, 1995), A large and high anomaly is present along Parana River in the NE-SW direction of the central area of Basin. The high gravity anomaly of the rift may be due to the density difference between asthenosphere (3.33 g/cm^3) and lithosphere (2.80 g/cm^3). Other large high anomalies and large low anomalies are considered to indicate basement structures blocked by faults in the N-S

direction, NE-SE direction, and NW-SE direction.

With respect to the basement structure of the cetral region of the Basin based on aeromagnetic anomalies, large and high pseudogravity anomalies are recognized in the N-S direction in the eastern part and the western part, while a large and low pseudogravity anomaly is recognized in the N-S direction at the central part of the central region. The former are inferred to be regions with basement rocks in comparatively shallow depth and the latter a region where basement rocks collapsed due to flood basalt magmatism. The high pseudogravity anomaly in the western part may be possibly a part of Paraguay-Araguay belt and the high pseudogravity anomaly in the eastern part a part of Sao Francisco craton under the flood basalt lava pile. In the large low anomaly of the central part, high anomalies and low anomalies are recognized in the NE-SW direction, which run nearly in the same direction as Parana River. The low anomaly along the right side of Parana River coincides with high residual gravity anomaly and thick part of flood basalt lava.

Many magnetic lineaments which indicate faults are present on the pseudogravity anomaly map and so on. Principal directions of faults are NW-SE direction, NE-SW direction, and E-W direction. The magnetic lineaments in the NW-SE direction are continuous faults which have sharp boundaries. The magnetic lineaments in the E-W direction are poorly continuous. Most of faults in the E-W direction seem to be secondary shear faults derived from sinstral wrench faults in the NW-SE direction. The unclockwise rotations of them coincide with those mentioned by Turner et al. (1994) and W.M. de Rezende (1972). A large amount of sills and dykes are recognized in the areas where Rio Alonzo fault in the NW-SE direction and rift along Parana River in the NE-SW direction intersect.

1-4 Promising Areas of Emplacements of Ni-Cu-PGE Ore Deposits Estimated from Geological structure

We will present a comprehensive explanation of Precambrian basement rocks, sedimentary rocks and flood basalts in Post- Early Paleozoic, and faults in the Parana Basin and consider the relation among the rift zone and the regional stress field, and promising areas of emplacement of Noril'sk-type Cu-Ni-PGE ore deposit (Fig.II-1-5-25).

A large low anomaly zone in the central part of the pseudogravity anomaly map overlaps with a zone where sedimentary sequence and flood basalt lava are thicker, with a zone where a large quantity of sills and dykes intruded, with a high residual gravity anomaly zone, and with a high attenuation factor zone. Based on these facts, it is concluded that the large low anomaly zone was rift zone associated with flood basalt magmatism.

The direction of the rift zone extends in the N-S directions in the northern Basin; in the NE-SW directions the central Basin, and branches into the NE-SW and NW-SE directions in the

southern Rio Alfonzo fault. The inside of the rift zone has repetitions of high anomaly zones and low anomaly zones in the NE-SW direction. These anomaly zones in the NE-SW directions were formed by stair-step normal faults (vertical direction: maximum compressive principal stress axis σ_1) in the extensional stress in the NW-SE directions field (minimum compressive principal stress axis σ_3).

Many magnetic lineaments which represent faults in the NW-SE direction are recognized on the pseudogravity anomaly map. For example, Rio Alfonzo fault on the geological map are represented by several magnetic lineaments on the pseudogravity aomaly map. The faults in the NW-SE directions are estimated to be sinistral transcurrent faults because they have sharp boundaries and are accompanied with many secondary shear faults in E-W directions. In the Duluth ore deposit, many secondary shear fractures occurred in the form of Cymoid Loop-like tensional fractures in areas where the rift zone and transcurrent faults cross. The Duluth Complex intruded there and formed the ore deposit. The Noril'sk ore deposit was also formed in the volcano-center where magma extruded most instensely in the Gydansk-Omsk rift zone (Tamrazyan, 1962).

As the results mentioned above, we propose the following four promising areas, which rift zone and transcurrent faults cross, of emplacements of Ni-Cu-PGE ore deposits.

(1) The area where the Tiete structural line in the NW-SE direction crosses through Paran River
(2) The area where the Guapiara fault in the NW-SE direction crosses through Parana River.
(3) The area where Rio Alfonzo fault in the NW-SE direction crosses through Parana River.
(4) The western part of Torres‐Posadas fault in the southern region of Parana Basin

All of these areas are estimated to have been the volcano-center of flood basalt magmas. The largest volcano-center is found in the area (3) where the Rio Alfonzo fault crosses through Parana River. Among four areas, it is concluded that areas where the Guapiara fault and the Rio Alfonzo fault in the NW-SE directions cross through Parana River are the most promising area of emplacements of Ni-Cu-PGE ore deposits.

1-5 Geochemical Characteristics of Paraná Flood Basalts

(1) Classification of Magma Type

Six types of lava units of Paraná flood basalts are divided into Low-Ti type and High-Ti type by Peate et al. (1992). Since the Ti contents of Paranápanema and Ribeira are intermediate in this survey, the two above were geochemically judged not to be classified into Low-Ti type nor High-Ti type. Therefore, the two above were newly classified as the

Intermediate-Ti type, and the magma types of Paraná flood basalts were classified as follows. The difference of Ti contents among the three types is obvious, and each type shows different trends of fractionation in Mg#-TiO_2 diagram.

	Peate et al. (1992)	This survey
Low-Ti type	Gramado	Gramado
	Esmeralda	Esmeralda
	Ribeira	
Intermediate-Ti Type	—	Paranápanema-Ribeira
High-Ti Type	Paranápanema	Pitanga
	Pitanga	Urubicí
	Urubicí	

Ggeochemical examinations were carried out for both lava samples and intrusion samples in this survey. Both samples show entirely the same geochemical trend. Therefore, both lava and intrusion samples were classified into the above five magma types. As for distribution, Pitanga is distributed in the northern part of the Paraná Basin, Pitanga and Paranápanema-Ribeira are distributed in the central part, and Gramado, Esmeralda and Urubici are distributed in the southern part. Pitanga and Paranápanema-Ribeira are intermingled in the intrusions of the Ponta Grossa Arch in the central part. The results of the geochemical examinations are summarized in Table II-4-5-1.

(2) Partial Melting and Crustal Contamination

Pitanga, High-Ti type, is distributed from the northern to the central part of the Paraná Basin. This magma type shows the smallest degree of partial melting. It is thought to have been generated in relatively deeper portion in the upper mantle. Paranápanera-Ribeira, the Iintermediate type, is distributed in the central area of the Paraná Basin. The degree of partial melting of this type is shown larger than that of Pitanga. This means that it has been generated in a shallower portion than Pitanga was generated. The effect of the crustal contamination is considered limited in these two types of magma because of poor contents of U and Th that concentrate in the crust. Mantovani et al. (2000) described that the two types above were generated from a similar magma source with different degrees of partial melting. The large quantities of the two magma types above erupted and were piled with a thickness of approximately 1,800 meters along the Paraná River in the central part of the Paraná Basin, which is thought to be the center of the magmatic activity.

The Low-Ti type magmas (Gramado and Esmeralda) show relatively large degree of partial melting. They are thought to have been generated in relatively shallower portions compared to the other magma types. The increases of LIL elements such as Th, U and the likes that concentrate in crust, and Sr isotopic ratio are observed in both magma types. It is thought to be the effect of crustal contamination. The effect is particularly marked in Gramado. Esmeralda is considered to be the most primitive magma among all the magma types because of its low contents of light rare earth elements and a relatively high Nd isotopic ratio.

As regards the Low-Ti types of magma, the following three points are thought to have a close relationship. The first is that the magma was generated in a shallow portion. The second is that the magma was highly affected by crustal contamination, and the third is the existence of acidic rocks, which are considered to be the products of lower crust melting, in the southern part of the Paraná Basin. More specifically, the following process is thought to have occured. That is, the acidic magma was generated from the melt of the lower crust by the mantle plume heating. After generating the acidic magma, this magma and the magma generated by the melting of the mantle plume itself mixed and yielded Gramado type magma. Finally, just after the commencement of expanding the Atlantic, Esmeralda type magma is thought to have been generated that is less influenced by crustal contamination although the origin is the same as Gramado.

(3) PGE Contents of the Paraná Flood Basalts

The original magmas of the Paraná flood basalts are thougth to be PGE rich as a whole, particularly Pd rich (Refer to Table II-3-5-1) although there are some differences among the magma types. The most PGE enriched magma is Paranápanema-Ribeira. The average content of Pt and Pd summing is approximately the same as that of the Tuklonsky lava, the most PGE enriched lava in the Noril'sk region. Paranápanema-Ribeira is also rich in Cu. The magma of this type as lavas is distributed along the Paraná River in the central part of the Paraná Basin, and much native copper is observed in the cavities. The geochemical anomaly in PGE, Ni, Cu, and other elements that is observed in the western part of the state of Paraná (by the stream sediment geochemical survey carried out by MINEROPAR) possibly shows the distribution of Paranápanema-Ribeira that has high PGE contents. Paranápanema-Riberia as intrusions is distributed in the Ponta Grossa Arch intermingled with Pitanga of High-Ti type. The magma type of the higher PGE content next to Pitanga is Esmeralda that has the most primitive chemical composition. The PGE depletion by sulfur saturation is rarely observed in Paranápanema-Ribeira and Esmeralda.

Regarding Gramado and Pitanga, there are two populations of samples, PGE enriched and depleted. These two types are thought to have been initially PGE enriched. The depletion of PGE, however, is thought to have occurred due to sulfur saturation in a part of the magma. As

the cause of sulfur saturation, the crustal contamination in Gramado, and the crystallization differentiation in Pitanga are both thought to have occurred. Pd contents of 133.8 ppb were obtained by analyses of the intrusion sample (KN104) of Pitanga type that was collected in the Ponta Grossa Arch. This value exceeds the Pd content of ordinary basaltic magma, and suggests the existence of sulfide that includes Pd.

According to the facts above, all magma types of Paraná basalts are considered to be initially sulfur undersaturated and rich in PGE. They have the potential to form the ore deposits if satisfy other requirements demonstrated above.

1-6 Mineralization Potential of the Paraná Flood Basalts

In the Noril'sk region, the majority of the lava and intrusion is basaltic, however, the sills which embed ore deposits contain picritic parts and the assimilation of country rock on a large scale in the picritic sill is observed. Picritic magma, however, is rarely observed in the Paraná flood basalts, and the basalts are more differentiated than in the Noril'sk region. The magma temperature of the Paraná flood basalts is thought to be lower than that of the Noril'sk region. It is thought to be possible that this low temperature obstruct the assimilation of country rock and the large scale segregation of immiscible sulfides. As assumed in Pitanga, though, there is a possibility of segregating immiscible sulfides by the progress of the simple crystallization differentiation without the influence of contamination. The saturation mechanism on sulfur mentioned above is the same process considered in the Skaergaard intrusion in East Greenland (Anderson et. al., 1998) and the Sonju Lake intrusion in Minnesota, USA(Refer to Appendix 2).

All the samples of intrusion including the Ponta Grossa Arch sill that could be collected in this survey were distributed in the marginal area of the Basin, the edge area away from the center of magmaic activity. The sills are mostly poor in sulfide, and the maximum thickness is approximately 200 m, which is comparatively thin. The rock compositions show basaltic, and although show high PGE contents, the magma temperature is lower than that of the magma of Noril'sk. The contamination effect of country rock in such intrusions is weak. This is considered to be the reason why only a faint dissemination of sulfides is observed (pyrite/pyrrhotite/chalcopyrite/sphalerite). The segregation of sulfides in a large scale magma chamber like the Skaergaard intrusion under the high R factor is necessary to generate sulfide ore deposit from basaltic magma with high PGE contents.

The location with the highest possibility of generating sulfide ore deposit is thought to be the eruption center of Paranápanema-Ribeira and Pitanga types, which have the largest quantities of magmas among the Patana flood basalts. The eruption center is thought to be located in the central area of the Paraná Basin along the Paraná River where the lava piles are the thickest. Based on the existing data analysis, the strong shrinkage of lithosphere by the

ascension of the asthenosphere is observed in this area, and magma intrusion is estimated to be the most active in this area.

Chapter 2: Proposal

From analyses of existing geological papers, geological survey on the ground surface, geophysical anomaly maps, drilling data of coal exploration and so on resulted in identifying geotectonic characteristics of the Parana Basin and geochemical characteristics of flood basalt magmas and possibility of emplacements of Ni-Cu-PGE ore deposits such as the Noril'sk, Duluth and Skaergaard ore deposits.

According to the dykes and sills in the basement rocks, although the drilling cores of coal exploration and the outcrops were investigated, no Ni-Cu-PGE mineralization was almost identified.

Hereafter, diamond drillings are proposed for identifying mineralization of dykes and sills in the basement rocks in the promising area where have been located at vocano-centers of flood basalt magmas. But, as most of volcano-centers are located at more than 1,000 meters below the ground surface, it is difficult for ore deposits to be economic.

References

Ahern, J.L. and Mrkvicka, S.R. (1984) A mechanical and thermal model for the evolution of the Williston Basin. Tectonics, vol.3, no.1, pp.79-102.

Anderson, D.L. (1982) Hotspots, poler wander, Mesozoic convection and geoid. Nature, vol. 297, no.3, pp.391-393.

Anderson, D.L. (1994a) Superplumes or supercontinents? Geology, vol.22, pp.39-42.

Anderson, D.L. (1994b) The sublithospheric mantle as the source of continental flood basalts; the case against the continental lithosphere and plume head reservoirs. Earth and Planetary Science Letters, vol.123, pp.269-280.

Anderson, J.C.Ø., Rasmussen, H., Neilsen, T.F.D., and Rønsbo, J.G. (1998) The Triple Group and the Platinova gold and palladium reefs in the Skaergaard intrusion: Stratigraphic and petrographic relations. Economic Geology, vol.93, no.4, pp.488-509.

Arioli, E.E. (2000) The Mesozoic Igneous rocks of the Parana basin. Curitiba, MINEROPAR.

Arnason, J.G. and Bird, D.K. (2000) A gold- and platinum-mineralized layer in gabbros of the Kap Edvard Horm Complex: field, petrologic, and geochemical relations. Economic Geology, vol.95, no.5, pp.945-970.

Atalla, L.T., Civetta, L., Innocenti, F., Mantovani, M.S.M., Marques, L.S. and Sousa, M.A. (1982) Geochemistry of Paraná plateau basalts (Southern Brazil). Abstract: Generation of major basalt types, IAVCEI-IAGC Scientific Assembly, August 15-22, No.62, Reykjavik, Iceland.

Austin, J.A. and Uchupi, E. (1982) Continental-oceanic crustal transition off southwest Africa, Bull. Am. Ass. Petrol. Geol., vol.66, pp.1328-1347.

Bailes, A.H., Christiansen, E.H., Galley, A.G., Jenner, G.A., Keith, J.D., Kerrich, R., Lentz, D.R., Lesher, C.M., Lucas, S.B., Ludden, J.N., Pearce, J.A., Peloquin, S.A., Stern, R.A., Stone, W.E., Syme, E.C., Swinden, H.S., Wyman, D.A. (1996) Trace element geochemistry of volcanic rocks: Application for massive sulphude exploration. edt: Wyman, D.A., Geological Association of Canada, WINNPEG'96 Short course note 12.

Bailey, R.C. and Halls, H.C. (1984) Estimate of confidence in paleomagnetic directions derived from mixed remagnetization circle and direct observational data. Journal of Geophysics, vol.54, pp.174-182.

Barner, S.J. and Maier, W.D. (1999): The Fractionation of Ni, Cu and the Noble Metals in Silicate and Sulphide Liquids, in Keays, R.R., Lesher, C.M., Lightfoot, P.C. and Farrow, C.E.G. (editors), Dynamic Processes in Magmatic Ore Deposits and their Application in Mineral Exploration; Geological Association of Canada, Short Course Notes, no.13, pp.69-106.

Barnes, S.-J., Boyd, R., Korneliussen, A., Nilsson, L.-P., Often, M., Pedersen, R.B. and Robins, B. (1987) The use of mantle normalization and metal rations in discriminating between the effects of partial melting, crystal fractionation and sulphide segregation on platinum-group elements, gold, nickel and copper: examples from Norway. Geoplatinum symposium, pp.113-143.

Barnes, S.-J., Makovicky, E., Makovicky, M., Rose-Hansen, J. and Karup-Moller, S. (1997) Partition coefficients for Ni, Cu, Pd, Pt, Rh, and Ir between monosulfide solid solution and sulfide liquid and the formation of compositionally zoned Ni-Cu sulfide bodies by fractional crystallization of sulfide liquid. Canadian Journal of Earth Sciences, vol.34, pp.366-374.

Barnes, S.-J., Zientek, M.L. and Severson, M.J. (1997) Ni, Cu, Au, and platinum-group element contents of sulphides associated with intraplate magmatism: asynthesis. Canadian Journal of Earth Sciences, vol.34, pp.337-351.

Bellieni, G. Comin-Chiaramonti, P., Marques, L.S., Martinez, L.A., Melfi. A.J., Nardy, A.J.R., Piccirillo, E.M. And Stolfa, D. (1986) Petrogenetic aspects of acid and basic lavas from the Parana plateau (Brazil): geological, mineralogical and petrochemical relationship. Journal of Petrology, vol.27, pp.915-944.

Bellieni, G., Brotzu, P., Comin-Chiaramonti, P., Ernesto, M., Melfi, A.J., Pacca, I.G. and Piccirillo, E.M. (1984) Flood basalt to rhyolite suites in the southern Paraná plateau (Brazil): paleomagnetism, petrogenesis and geodynamic implications. Journal of Petrology, vol.25, pp.579-618.

Bellieni, G., Comin-Chiaramonti, P., Marques, L.S., Melfi, A.J., Piccirillo, E.M., Mardy, A.J.R. and Roisenberg, A. (1984a) High- and low-Ti flood basalts from the Paraná plateau (Brasil): petrology and geochemical aspects bearing on thir mantle origin. N.Jb. Miner. Abh., vol.150, pp.272-306.

Bellieni, G., Comin-Chiaramonti, P., Marques, L.S., Melfi, A.J., Piccirillo, E.M. and Stolfa, D. (1984b) Low-pressure evolution of basaltic sills from boreholes in the Paraná basin, Brazil. Tschermaks Min. Pet. Mitt., vol.33, pp.25-47.

Bennett, V.C., Norman, M.D. and Garcia, M.O. (2000) Rhenium and platinum group element abundances correlated with mantle source components in Hawaiian picrites: sulphides in the plume. Earth and Planetary Science Letters, vol.183, no.3-4, pp.513-526.

Bigarella, J.J. (1973) Geology of the Amazon and Parnaiba basins. The ocean basins and magmas, Chapter 2, pp.25-86.

Bonatti, E. (1996) Anomalous opening of the Equatorial Atlantic due to an equatorial mantle thermal minimum. Earth and Planetary Science Letters, vol.143, no.1-4 pp.147-160.

Bond, G.C., Kominz, M.A. (1984) Construction of tectonic subsidence curves for the early Paleozoic miogeocline, southern Canadian Rocky Mountains: Implications for subsidence mechanisms, age of breakup, and crustal thinning. Geological Society of America Bulletin, vol.95, pp.155-173.

Bott, M.H.P. (1976) Mechanisms of basin subsudence - an introductory review. Tectonophysics, vol.36, pp.1-4.

Brooks, C.K. (1973) Rifting and doming in Southern East Greenland. Nature Physical Science, vol.244, pp.23-25

Brooks, C.K., Keays, R.R., Lambert, D.D., Frick, L.R., Nielsen, T.F.D. (1999) Re-Os isotope geochemistry of Tertiary picritic and basaltic magmatism of East

Greenland: constrains on plume-lithosphere interactions and the genesis of the Platinova reef, Skaergaard intrusion. Lithos, vol.47, pp.107-126.

Brooks, C.K., Larsen, L.M., Nielsen, T.F.D. (1991) Importance of iron-rich tholeiitic magmas at divergent plate margins: a reappraisal. Geology, vol.19, pp.269-272.

Brügmann, G.E., Naldrett, A.J., Asif, M., Lightfoot, P.C., Gorbachev, N.S. and Fedorenko, V.A. (1993) Siderophile and chalcophile metals as tracers of the evolution of the Siberian Trap in the Noril'sk region, Russia. Geochimica et Cosmochimica Acta, vol.57, pp.2001-2018.

Buchanan, D.L. (1998) Platinum-Group Element Exploration, Chapter 7 Exploration Guidelines, Chapter 8 Evaluation Guidelines, Chapter 9 Summary and Conclusions. DEVELOPMENT IN ECONOMIC GELOGY, 26, ELSEVIER 1988.

Castillo, P.R., Natland, J.H., Niu, Y. and Lonsdale, P.F. (1998) Sr, Nd and Pb isotopic variation along the Pacific-Antarctic risecrest, 53-57° S: Implications for the composition and dynamics of the South Pacific upper mantle. Earth and Planetary Science Letters, vol.154no.1-4, pp.109-125.

CBC (1986) Mapa Geologico Resional. 1/50,000, Projet Lavras do Sul. Companhia Brasileira do Cobre.

Celso Pinto Ferraz (2000) Brazil. Mining Annual Review 2000.

Chai, G. and Naldrett, A.J. (1992a) The Jinchuan ultramafic intrusion: cumulate of a high-Mg basaltic magma. Journal of Petrology, vol.33, part 2, pp.277-303.

Chai, G. and Naldrett, A.J. (1992b) Characteristics of Ni-Cu-PGE Mineralization and Genesis of the Jinchuan Deposit, Northwest China. Economic Geology, vol.87, pp.1475-1495.

Chang, H.K., Kowamann, R.O., Figueiredo, A.M.F. and Bender, A.A. (1992) Tectonics and stratigraphy of the east Brazil rift system: an overview. Tectonophysics. Vol.213, pp.97-138.

Chase, C.G. and Gilmer, T.H. (1973) Precambrian plate tectonics: the midcontinent gravity high. Earth and Planetary Science Letters, vol.21, pp.70-78.

Chen, J.Y., Mingliang, J. (1987) Jin Chuan Nickel: difficult mining problems confront expansion at China's Jin Chuan mines. Engineering and Mining Journal, September, pp.44-57.

CIA. Nacional de Mineraçao (1995) Palnta de Detalhe (Index maps of mining licence).

Cloos, E. (1955) Experimental analysis of fracture patterns. Bulletin of the Geological Society of America, vol.66, pp.241-256.

Coffin, M.F., Eldholm, O. (1994) Large igneous provinces: crustal structure, dimensions, and external consequences. Reviews of Geophysics, vol.32, no.1, pp.1-36.

Comin-Chiaramonti, P., Gomes, C.B., Piccirillo, E.M. and Rivalenti, G. (1983) High TiO_2 dykes in the coastline of São Paulo and Rio de Janeiro States. N. Jahrb. Miner. Abh., vol.146, pp.133-150.

Coedani, U.G., Civetta, L., Mantvani, M.S.M., Petrini, R. Kawashita, K., Hawkesworth, C.J., Taylor, P.N., Longinelli, A., Cavazzini, G. and Piccirillo, M. (1988) Isotope geochemistry of flood volcanics from the Paraná basin (Brazil). In The Mesozoic Flood Volcanism of Paraná Basin: Petrogenetic and Geophysical Aspects, Piccirillo, E.M. and Melfi, A.J. (edts), IAG-USP, São Paulo, pp.157-178.

Courtillot, V., Jaupart, C., Manighetti, I., Tapponnier, P. and Besse, J. (1999) On causal links between flood basalts and continental breakup. Earth and Planetary Science Letters, vol.166, no.3-4, pp.177-195.

Cox, K.G. (1980) A model for flood basalt vulcanism. Journal of Petrology, vol.21, part 4, pp.629-650.

CPRM (1977) Volta Grande, Condicionamento Estrutural. 1/8,000. and others., Companhia Riograndense de Minerasao, Estado do Rio Grande do Sul.

CPRM (1994) Carta de Previsao pare Planejamento de Acoes Governamentais.

CPRM (1995a) Mapa de Indice de Prospectividade Demandata Area RS-01, Lavras do Sul/Casapava do Sul-RS. Programa Nacional de Prospecsao de Ouro-PNPO.

CPRM (1995b) Mapa de Jazimentos Auriferos, Area RS-01, Lavras do Sul/Cas[ava dp Sul-RS.

CPRM (1997) Programa levantamentos geológicos básicos do Brasil: Florianópolis (Folha SG-22-2-D-V), Lagoa (Folha SG-22-2-D-VI) , estado de Santa Catarina.

CPRM (1998) Mapeamento Geologica Integrado da Bacia Hidrografica do Guaiba (1/500,000).

CPRM (2000a) Cobre de Bom Jardim, Estado de Goias. Goiania 2000, Serie Oportunidades Minerais-Exame atualizado de Projeto, 03, Informe de Recursos Minerais.

CPRM (2000b) Ouro de Natividade, Estado de Tocantins. Goiania 2000, Serie Oportunidades Minerais-Exame atualizado de Projeto, 08, Informe de Recursos Minerais.

CPRM (2000c) Mapa Gemologico do Estado do Rio Grande do Sul/Percio de Moraes Blanco; Claudio Antonio Gil.-Porto Alegre.

CPRM GOIANIA (2000) Field Excursion Guide for MMAJ Mission.

Crocket J.E. (1981) Geochemistry of the platinum-group elements. In Platinum-Group Elements: Mineralogy, Geology, Recovery, Chapter 4 (ed: Cabri, L.J.), Canadian Institute of Mining and Metallurgy Spec., vol.23, pp.49-64.

Czamanske, G.K., Zen'ko, T.E., Fedorenko, V.A., Calk, L.C., Budahn, J.R., Bullock Jr., J.H., Fries, T.L., King, B.W. and Seims, D.F. (1995) Petrographic and Geochemical Characterization of Ore-bearing Intrusions of the Noril'sk Type, Siberia; With Dissccussion of Their Origin. Resource Geology Special Issue, no.18, pp.1-48.

Davies, G. (1988) Ocean bathymetry and mantle convection, 1, Large scale flow and hotspots, Journal of Geophisics Research, vol.93, no.10, pp.467-480.

Davino, A., Sinelli, O. and Souza, A. and Correa, C.T. (1982) Diabásios na região nordeste da Bacia do Paraná. An. XXXI Congr. Bras. Geol., Soc. Bras. Geol., vol.4, pp.1736-1744.

Deckart, K, Féraud, G, Marques, L.S. and Bertrand, H. (1998) New time constraints on dyke swarms related to the Paraná-Etendeka magmatic province, and subsequent South Atlantic opening, southeastern Brazil. Journal of Volcanology and Geothermal Research, vol.80, no.1-2, pp.67-83.

Deshmukh, S.S. and Sehgal, M.N. (?) Mafic dyke swarms in Decan volcanic province of Madhya Pradesh and Maharashtra. pp.323-340.

DNPM (1975) Availiação regional do setor Mineral- Rio Grande do Sul. Brasilia.

DNPM (1983) Carta Metalogenetica, Sao Gabriel Folha SH.21-S-B. Projeto Mapas Metalogenieticos e de

Previsao de Recursos Minerais.
DNPM (1984) Carta Metalogenetica, Cachoeira do Sul, Folho SH22-Y-A. Projet Mapas Metalogeneticos e de Previsao de Recusos Minerais.
DNPM (1986) Mapa Geológico do Estado de Santa Catarina (1:500,000). República federativa do Brazil, Ministerio das Minas e Energia, Departamento Nacional da Produção Mineral, Divisão de Geologia e Mineralogia-DGM, Distrito Regional do DNPM; Governo do Estado de Santa Catarina, Secretaria da Indústrial e Comércio, CODISC, Superintendéncia de Tecnologia Minas e Energia, Coordenação dos Recursos Minerais.
DNPM (1987) Cachoeira do Sul Folha SH.22-Y-A, Carta Metalogenetica, Carta de Previsao de Recursos Minerais, Carta de Previsao de Asoes Governamentais, Escala 1/250,000., Texto e Mapas.
DNPM (1989) Mapa Geológico do Estado de Paraná (1:650,000). República federativa do Brazil, Ministerio das Minas e Energia, Departamento Nacional da Produção Mineral, Divisão de Geologia e Mineralogia-DGM, Distrito Regional do DNPM; Governo do Estado de Paraná, Secretário Especial da Ciência, Tecnologai e Desenvolvimento Econômico, Minerais do Paraná S.A.-MINEROPAR.
DNPM (1989) Mapa Geológico do Estado de Rio Grande do Sul (1:600,000). República federativa do Brazil, Ministerio das Minas e Energia, Departamento Nacional da Produção Mineral, Divisão de Geologia e Mineralogia-DGM, Distrito Regional do DNPM.
DNPM (1989) Mapa Geologico do Estado do Rio Grande do Sul, escala 1/1,000,000 e Parte do Escudo Sul-Rio-Grandense, escala 1/600,000.
DNPM (1995) 2nd Edition, Geologic Map of Brazil and Adjoining Ocean Floor including Mineral Deposits (1981), 1/2,500,000. DNPM, MME. (4 Sheets).
DNPM (1995) Economia mineral do Brasil, mapas, DNPM, Estudis de Oikutuca e Economia Mineral, 8, 280p.
DNPM (2000) Mineral Summary 2000. DNPM, Brasilia.
DNPM (2000) Mining in Brazil - Basic Information for the Investor. Brasilia. p.88.
DNPM-CGMW-UNESCO (1978) Tectonic Map of Souith America 1:5,000,000; Explanatory Note. Brasilia.
DNPM-CPRM (1973a) Projeto Hidrogeologia da Fronteira Sudoeste do Rio Grande do Sul. Mapa Geológico (1:250,000) : Alegrete, SH.21-X-C, Anexo 18.
DNPM-CPRM (1973b) Projeto Hidrogeologia da Fronteira Sudoeste do Rio Grande do Sul. Mapa Geológico (1:250,000) : Cacequi, SH.21-X-D, Anexo 19.
DNPM-CPRM (1973c) Projeto Hidrogeologia da Fronteira Sudoeste do Rio Grande do Sul. Mapa Geológico (1:250,000) : Livramento, SH.21-Z-A, Anexo 21.
DNPM-CPRM (1973d) Projeto Hidrogeologia da Fronteira Sudoeste do Rio Grande do Sul. Mapa Geológico (1:250,000) : São Gabriel, SH.21-Z-B, Anexo 22.
DNPM-CPRM (1984a) Projeto a Borda Leste Da Bacia Do Paraná: Integração Geológica e Avaliação Econômica. Mapa Geológico (1:100,000) : Castro, SF.22-X-A-V, MI-2824, Anexo 36. Companhia de Pesquisa de Recursos Minerais Superintendência Regional de São Paulo Superintendência Regional de Porto Alegre.
DNPM-CPRM (1984a) Projeto a Borda Leste Da Bacia Do Paraná: Integração Geológica e Avaliação Econômica. Mapa Geológico (1:100,000) : Venceslau Brás, SF.22-Z-C-VI, MI-2787, Anexo 23. Companhia de Pesquisa de Recursos Minerais Superintendência Regional de São Paulo Superintendência Regional de Porto Alegre.
DNPM-CPRM (1984b) Projeto a Borda Leste Da Bacia Do Paraná: Integração Geológica e Avaliação Econômica. Mapa Geológico (1:100,000) : Jaguariaíva, SG.22-X-A-III, MI-2808, Anexo 31. Companhia de Pesquisa de Recursos Minerais Superintendência Regional de São Paulo Superintendência Regional de Porto Alegre.
DNPM-CPRM (1984c) Projeto a Borda Leste Da Bacia Do Paraná: Integração Geológica e Avaliação Econômica. Mapa Geológico (1:100,000) : Reserva, SG.22-X-A-IV, MI-2823, Anexo 35. Companhia de Pesquisa de Recursos Minerais Superintendência Regional de São Paulo Superintendência Regional de Porto Alegre.
DNPM-CPRM (1984d) Projeto a Borda Leste Da Bacia Do Paraná: Integração Geológica e Avaliação Econômica. Mapa Geológico (1:100,000) : Irati, SG.22-X-C-I, MI-2839, Anexo 38. Companhia de Pesquisa de Recursos Minerais Superintendência Regional de São Paulo Superintendência Regional de Porto Alegre.
DNPM-CPRM (1984e) Projeto a Borda Leste Da Bacia Do Paraná: Integração Geológica e Avaliação Econômica. Mapa Geológico (1:100,000) : Ponta Grossa, SG.22-X-C-II, MI-2840, Anexo 39. Companhia de Pesquisa de Recursos Minerais Superintendência Regional de São Paulo Superintendência Regional de Porto Alegre.
DNPM-CPRM (1986) Projeto a borda leste da bacia do Paraná: integração geológia e avaliação econômica. Figura 9c (Geological section). Companhia de Pesquisa de Recursos Minerais Superintendência Regional de São Paulo Superintendência Regional de Porto Alegre.
DNPM-CPRM (1986a) Projeto a Borda Leste Da Bacia Do Paraná: Integração Geológica e Avaliação Econômica. Relatório Final Volume I - Texto. Companhia de Pesquisa de Recursos Minerais Superintendência Regional de São Paulo Superintendência Regional de Porto Alegre, 210p.
DNPM-CPRM (1986b) Projeto a Borda Leste Da Bacia Do Paraná: Integração Geológica e Avaliação Econômica. Mapa Geológico (1:100,000) : Arroio Piraju, SH.21-X-C-III, Anexo 62. Companhia de Pesquisa de Recursos Minerais Superintendência Regional de São Paulo Superintendência Regional de Porto Alegre.
DNPM-CPRM (1986c) Projeto a Borda Leste Da Bacia Do Paraná: Integração Geológica e Avaliação Econômica. Mapa Geológico (1:100,000) : Vila Kramer, SH.21-X-D-I, Anexo 63. Companhia de Pesquisa de Recursos Minerais Superintendência Regional de São Paulo Superintendência Regional de Porto Alegre.
DNPM-CPRM (1986d) Projeto a Borda Leste Da Bacia Do Paraná: Integração Geológica e Avaliação Econômica. Mapa Geológico (1:100,000) : Alegrete, SH.21-X-C-VI, Anexo 65. Companhia de Pesquisa de Recursos Minerais Superintendência Regional de São Paulo Superintendência Regional de Porto Alegre.
DNPM-CPRM (1986e) Projeto a Borda Leste Da Bacia Do Paraná: Integração Geológica e Avaliação Econômica. Mapa Geológico (1:100,000) : S. Francisco de Assis, SH.21-X-D-IV, Anexo 66. Companhia de Pesquisa de Recursos Minerais Superintendência Regional de São Paulo Superintendência Regional de Porto Alegre.
DNPM-CPRM (1986f) Projeto a Borda Leste Da Bacia Do Paraná: Integração Geológica e Avaliação Econômica. Relatório Final Volume XIV - Anexos. Companhia de Pesquisa de Recursos Minerais Superintendência Regional

de São Paulo Superintendência Regional de Porto Alegre.
Doan, D.B. and Bond, A.R. (1994) Russia's Platinum-Group Metals: A Current Survey, International Geology Review. vol.36, pp. 92-100.
Druecker, M.D. and Gay, S.P. (1987) Mafic dyke swarms associated with Mesozoic rifting in eastern Paraguay. in Mafic Dyke Swarms, Spec. Pap. No.34, Halls, H.C. and Fahrig, W.F. (edts), Geological Association of Canada, Toronto, ON, pp.187-193.
Dunbar, J.A. and Sawyer, D.S. (1988) Continental rifting at pre-existing lithospheric weaknesses. Nature, vol.333, no.2, pp.450-452.
Duncan, A.R., Marsh, J.S., Milner, S.C. and Erlank, A.J. (1988) Distribution and petrogenesis of the basic rocks of the Etendeka Formation of northwestern Namibia. in Geochemical Evolution of the Continental Crust, Poços de Caldas, Brasil, pp.10-19.
Duncan, R.A. and Richards, M.A. (1991) Hotspots, mantle plumes, flood basalts, and true polar wander. Reviews of Geophysics, vol.29, no.1, pp.31-50.
E.I.U. (2000) Country Profile Brazil 1999-2000. The Economic Intelligence Unit. 15 Regent St., London SW1Y 4LR, United Kingdom.
Ebel, D.S. and Naldrett, A.J. (1996) Fractional Crystallization of Sulfide Ore Liquids at High Temperature. Economic Geology, vol.91, pp.607-621.
Eckstrand, O.R. (1996) Magmatic nickel-copper-platinum group elements; in Geology of Canadian Mineral Deposit Types. Eckstrand, O.R., Sinclair, W.D. and Thorpe, R.I. (Eds), Geological Survey of Canada, Geology of Canada, no.8, pp.583-614.
Eckstrand, O.R., Good, D.J. (2000) World distribution of nickel deposits. Geological Survey of Canada Open File 3791a, 19p.
Edu Lucas dos Santos (1999a) Geologia e Potencialidade das Mineralizasoes de Cobre (Au) e Ouro na Regiao de Lavras do Sul- RS. Porto Alegre.
Ellam, R.M. (1992) Lithospheric thickness as a control on basalt geochemistry. Geology, vol.20, pp.153-156.
Erlank, A.J., Duncan, A.R., Marsh, J.S., Sweeney, R.J., Hawkesworth, C.J., Milner, S.C., Miller, R.M. and Rogers, N.W. (1988) A laterally extensive geochemical discontinuity in the subcontinental Gondwana lithosphere. in Geochemical Evolution of the Continental Crust, Poços de Caldas, Brasil, pp.1-10.
Erlank, A.J., Marh, J.S., Duncan, A.R., Miller, R.McG., Hawkesworth, C.J., Betton, P.J. and Rex, D.C. (1984) Geochemistry and petrogenesis of the Etendeka volcanic rocks from SWA/Namibia. Geological Society of Africa, Special Publication vol.13, pp.195-245.
Ernesto, M. and Pacca, I.G. (1988) Palaeomagnetism of Paraná basin flood volcanics, southern Brazil. in Mesozoic Flood Volcanism from the Paraná Basin (Brazil): Petrogenetic and Geophysical Aspects, Piccirillo, E.M. and Melfi, A.J. (edts), IAG-USP. São Pauro, pp.229-255.
Farina, M. (1996a) Platinum-Group Metal Prospecting National Program -A Summary-. CPRM.
Farina, M. (1996b) Programma Nacional de Prospecson de Metais do Grupo da Platina-Uma Sintese (parte 1). A Terra em Revista, no.1, pp.50-56.
Farina, M., Matos, G.M.M. and Gallart, R. (1998) Programa Nacional de Porspecção de Oouro Natureza e Metodos. Serie Ouro- Informe Gerais, no.02, Informe de Recusos Minerais. CPRM, Txt and two maps (Lavras do Sul/Casapava do Sul).
Farrow, C.E.G. and Watkinson, D.H. (1999) An Evaluation of the Role of Fluids in Ni-Cu-PGE-Bearing, Mafic-Ultramafic Systems. in Keays, R.R., Lesher, C.M., Lightfoot, P.C. and Farrow, C.E.G. (eds), Dynamic Processes in Magmatic Ore Deposits and their Application in Mineral Exploration; Geological Association of Canada, Short Course Notes, vol.13, pp.31-67.
Fedorenko, V.A. (1994a) Evolution of magmatism as reflected in the volcanic sequence of the Noril'sk region. In Proceedings of the Sudbury-Noril'sk Symposium, Ontario Geological Survey, Special vol.5, pp171-183.
Fedorenko, V.A. (1994b) Model of genetic relationships between flood basalts, ore-bearing intrusions, and Cu-Ni-Pt ores in the Noril'sk region, NW Siberian platform, Russia. 7th International Platinum Symposium, Moscow, Abst., pp.26.
Fedorenko, V.A., Lightfoot, P.C., Naldrett, A.J., Czamanske, G.K., Hawkesworth, C.J., Wooden, J.L. and Ebel, D.S. (1996) Petrogenesis of the Flood-Basalt Sequence at Noril'sk, North Central Siberia. International Geology Review, vol.38, pp.99-135.
Ferreira, C.F. (1982) Alinhamentos estructurais magnéticos da região centro-oriental da bacia do Paraná. Instituto de Pesquisas Tecnológicas (São Paulo) Spec. Publ. Vol.12, pp.143-166.
Ferreira, C.F., Naldrett, A.J. and Asif, N. (1995) Distribution of platinum-group elements in the Niquelândia layered mafic - ultramafic intrusion, Brazil: implications with respect to exploration. Canadian Mineralogist, vol.33, pp.165-184.
Fodor, R.V. (1987) Low and high TiO_2 flood basalts of Southern Brazil: origin from picritic parentage and a commom mantle source. Earth and Planetary Science Letters, vol.84, pp.423-430.
Fodor, R.V. and Vetter, S.K. (1984) Rift-zone magmatism: petrology of basaltic rocks transitional from CFB to MORB, southeastern Brazil margin. Contribution of Mineralogy and Petrology, vol.88, pp.307-321.
Fodor, R.V., Corwin, C. and Roisenberg, A. (1985) Petrology of Serra Geral (Paraná) continental flood basalts, southern Brazil: crustal contamination, source material, and South Atlantic magmatism. Contributions of Mineralogy and Petrology, vol.91, pp.54-65.
Fontignie, D. and Schilling, J-G. (1996) Mantle heterogeneities beneath the South Atlantic: a Nd-Sr-Pb isotope study along the Mid-Atlantic Ridge (3° S-46° S). Earth and Planetary Science Letters, vol.142, no.1-2, pp.209-221.
Fram, M.S. and Lesher, C.E. (1993) Geochemical constraints on mantle melting during creation of the North Atlantic basin. Nature, vol.363, pp.712-715.
Friedinger, P.J.J. (1988) Basta - Subsidence and paleotemperature modeling of rift basins. Computers & Geosciences, vol.14, no.4, pp.505-526.
Fujii, T. (1998) Eruption of flood basaltic magma. Magma and Earth, The 12th The university and science disclosure symposium. (in Japanease)
Fukao, Y., Obayashi, M., Inoue, H. and Nenbai, M. (1992) Subducting slabs stagnant in the mantle tarnsition zone. Journal of Geophysics Research, vol.92, pp.14065-14090.
Fulfaro, V.J., Saad, A.R., Santos, M.V., and Vianna, R.B.

(1982) Vompartimentação e evolução tectonica da Bacia do Paraná. Rev. Bras. Geocienc, vol.12, pp.590-611.
Gallagher, K and Hawkesworth, C.J. (1992) Dehydration melting and the generation of continental flood basalts. Nature, vol.358, pp.57-59.
Gallagher, K and Hawkesworth, C.J. (1994) Mantle plumes, continental magmatism and asymmetry in the South Atlantic. Earth Planetary Science Letters, vol.123, pp.105-117.
Gallagher, K., Hawkesworth, C.J. and Mantovani, M.S.M. (1994) The denudation history of the onshore continental margin of SE Brazil inferred from apatite fission track data. Journal of Geophysics Research, vol.99, pp.18117-18145.
Garfunkel, Z. (1986) Review of oceanic transform activity and development. Journal of the Geological Society, London, vol.143, pp.775-784.
Garland, F.E., Hawkesworth, C.J., Mantovani, M.S.M. (1995) Description and Petrogenesis of the Paraná Rzhyolites, Southern Brazil. Journal of Petrology, vol.36, no.5, pp.1193-1227.
Garland, F.E., Turner, S. and Hawkesworth, C. (1996) Shifts in the source of the Paraná basalts through time. Lithos, vol.37, no.2-3, pp. 223-243.
Geul, J.J.C. (1970) Geology of Devon and Pardee Townships and the Stuart Location; district of Thunder Bay. Ontario department of mines (pbs), Geological Report 87, pp.31-36.
Gomes, M.E.B. (1996) Mecanismos de resfriamento, estruturação e processos pós-magmáticos em basaltos da bacia do Paraná - Região de Frederico Westphalen (RS) - Brasil. Doctor thesis of University of Rio Grande do Sul, 219p.
Governo do Estado do Rio Grande do Sul Secretaria da Coordenação e Planejamento Pró-Guaiba (1998) Cntrole e Administração Ambiental da Bacia Hidrográfica do Guaíba Módulo I - Subprojeto Monitoramento do Uso e Ocupação Territorial; Mapeamento Geológico Integrado da Bacia Hidrográfica do Guaíba, Escala 1:250,000.
Grant Cawthorn, R. (1999) Seventy-fifth Anniversary of the Discovery of the Platiniferous Merensky Reef. Platinum-Metals Review, vol.43, no.4, pp.146-148.
Green, D.H., et al. (1974) Contribution of Mineralogy and Petrology, vol.48, pp.33-43.
Green, J.C. (1983) Geologic and geochemical evidence for the nature and development of the Middle Proterozoic (Keweenawan) midcontinent rift of North America. Tectonophysics, vol.94, pp.413-437.
Griffiths, R.W. and Campbell, I.H. (1990) Stirring and structure in mantle starting plumes. Earth and Planetary Science Letters, vol.99, pp.66-78.
Griselin, M., Arndt, N.T. and Baragar, W.R.A. (1997) Plume-lithosphere interaction and crustal contamination during formation of Coppermine River basalts, Northwest Territories, Canada. Canadian Journal of Earth Sciences, vol.34, pp.958-975.
Hamlyn, P.R., Keays, R.R., Cameron, W.E., Crawford, A.J. and Waldron, H.M. (1985) Precious metals in magnesian low-Ti lavas: implications for metallogenesis and sulfur saturation in primary magmas. Geochimica et Cosmochimica Acta, vol.49, pp.1797-1811.
Handbook of exploration geochemystry, volume 6 Drainage geochemystry
Harris, C., Smith, H.S., Milner, S.C., Erlank, A.J., Duncan, A.R., Marsh, J.S. and Ikin, N.P. (1989) Oxygen isotope geochemistry of the Mesozoic volcanics of the Etendeka Formation, Namibia. Contribution of Mineralogy and Petrology, vol.102, pp.454-461.
Hart, S.R. (1984) A large-scale isotope anomaly in the southern hemisphere mantle. Nature, vol.309, pp.753-757.
Harris, C., Whittingham, A.M. and Armstrong, R.A. (1990) Oxygen isotope geochemistry of the silica volcanic rocks of the Etendeka-Paraná province: source constraints. Geology, vol.18, pp.1119-1121.
Hauri, E.H. (1996) Major-element variability in the Hawaiian mantle plume. Nature, vol.382, pp.415-419.
Hawkesworth, C.J., Gallagher, K., Kelley, S., Mantovani, M.S.M., Peate, D.W., Regelous, M., Rogers, N.W. (1992) Paraná magmatism and the opening of South Atlantic. in: Magmatism and the causes of continental break-up. eds.: Storey, B.C. , Alabaster, T. and Pankhurst, R.J., Geological Society, Special Publication, no.68, pp.221-240.
Hawkesworth, C.J., Gallagher, K., Kirstein, L., Mantovani, M.S.M., Peate, D.W., Turner, S.P. (2000) Tectonic controls on magmatism associated with continental break-up: an example from the Paraná-Etendeka Province. Earth and Planetary Science Letters, vol.179, no.2, pp.335-349.
Hawkesworth, C.J., Mantovani, M.S., Peate, D.W. (1988) Lithosphere remobilization during Paraná CFB magmatism. In Menzies & Coxx (eds.) Oceanic and continental lithosphere: similaritie and differences. Journal of Petrology, Special Volume, pp. 205-223.
Hawkesworth, C.J., Mantovani, M.S.M., Taylor, P.N. and Palacz, Z. (1986) Evidence from the Parana of South Brazil for a Continental Contribution to Dupal Basalts. Nature, vol.322, no.24, pp.356-359.
Hergt, J.M., Peate, D.W. and Hawkesworth, C.J. (1991) The petrogenesis of Masozoic Gondwana low-Ti flood basalts. Earth and Planetary Science Letters, vol.105, pp.134-148.
Hill, R.I., Campbell, I.H., Davies, G.F. and Griffiths, R.W. (1992) Mantle plumes and continental tectonics, Science, vol.256, pp.186-193.
Hirose, K. and Kushiro, I. (1993) Partial melting of dry peridotites at high pressures: determination of compositions of melts segregated from peridotite using aggregates of diamond. Earth and Planetary Science Letters, vol.114, pp.477-489.
Honda, S., Yuen, D.A., Balachander, S. and Reuteler, D. (1993) Three-dimensional mantle dynamics with multiple phase transitions. Science, vol.259, pp.1308-1311.
Housh, T.B., Luhr, J.F. (1991) Plagioclase-melt equilibria in hydrous systems. American Mineralogist, vol.76, pp.477-492.
Hulbert, l., Grégoire, D.C., Wildner, W., Albuquerque, L.F.F. and Chieregati, L.A. (1999) Geochemical examination of Paraná magmatism in Southern and South-central Brazil with respect to potential for Noril'sk-type Ni-Cu-PGE deposits. Canada-Brazil Cooperation Project for suitainable development in the mineral sector. CPRM special paper, 74p.
Humphris, S.E., Thompson, G., Schilling, J.G., Kingsley, R.H. (1985) Petrological and geochemical variations along the mid-Atlantic ridge between S and S: Influence of the Tristan da Cunha mantle plume. Geochimica et

Cosmochimica Acta. Vol.49, pp.1445-1464.
Iwamori, H., McKenzie, D., Takahashi, E. (1995) Melt generation by isentropic mantle upwelling. Earth and Planetary Science Letters, vol.134, pp.253-266.
Iwata, N. (1997) Geochronological study of the Deccan volcanism by the $^{40}Ar-^{39}Ar$ method. docter's thesis, University of Tokyo.
Jackson, S.E., Fryer, B.J., Gosse, W., Healey, D.C., Longerich, H.P. and Strong, D.F. (1990) Determination of the precious metals in geological materials by inductively coupled plasma-mass spectrometry (ICP-MS) with nickel sulphide fire-assay collection and tellurium coprecipitation. Chemical Geology, vol.83, pp.119-132.
Jefferson, C.W., Hulbert, L.J., Rainbird, R.H., Hall, G.E.M., Gregorie, L.I. and Grinenko, L.I. (1994) Mineral Resource Assessment of the Neoproterozoic Franklin Igneous Events of Arctic Canada: Comparison with the Permo-Triassic Noril'sk-Talnakh Ni-Cu-PGE Deposits of Russia. Geological Survey of Canada, open file 2789.
Kaneoka, I. (1983) Noble gas constraints on the layered structure of the mantle. Nature, vol.302, pp.698-700.
Keays, R.R. (1995) The role of komatiitic and picritic magmatism and S-saturation in the formation of ore deposits. Lithos, vol.34, pp.1-18.
Keays, R.R. (1997) Requirements for the formation of giant Ni-Cu-PGE sulfide deposits: the role of magma generation. Transactions of the American Geophysical Union, 1997 Fall Meeting, V32F MC:304 Web 1330h, Geodynamics of giant magmatic ore systems II, p.F799.
Kelley, S. (2002) Excess argon in K-Ar and Ar-Ar geochronology. Chemical Geology (Article in Press) 13993.
Kogiso, T., Tatsumi, Y., Shimoda, Y. and Barsczus, H.G. (1997) HIMU ocean island basalts in southern Polynesia: new evidence for whole mantle scale recycling of subducted oceanic crust. Journal of Geophysics Research.
Kurita, K. and Kobayashi, Y. (1991) Activity of the continental flood basalt as global event. Monthly The Earth.
Kushiro, I. (1996) Partial melting of a fertile mantle peridotite at high pressures: an experimental study using aggregates of diamond. American Geophysical Union, Earth Processes: Reading the Isotopic Code, Geophysical Monograph 95, pp.109-122.
Lambert, D.D., Foster, J.G., Frick, L.R., Ripley, E.M. and Zientek, M.L. (1998) Geodynamics of Magmatic Cu-Ni-PGE Sulfide Deposits: New Insights from the Re-Os Isotope System. Economic Geology, vol.93, no.2, pp.121-136.
Lanphere, M.A. and Dalrymple, G.B. (1978) The use of 40Ar/39Ar data in evaluation of disturbed K-Ar systems. U.S.G.S., Open-File Report, vol.78-701, pp.241-243.
Leinz, V., Bartorelli, A. and Isotta, C.A. (1968) Contribuição ao estudo do magmatismo basáltico Mesozóic da bacia do Paraná. An. Acad. bras. Ciênc., vol.40, pp.167-181.
Lesher, C.M. and Campbell, I.H. (1993) Geochemical and fluid dynamic modeling of compositional variations in Archean komatiite-hosted nickel sulfide ores in weatern Australia. Economic Geology, vol.88, pp.804-816.
Lesher, C.M., Burnham, O.M., Keays, R.R., Barnes, S.J. and Hulbert, L. (1999) Geochemical Discrimination of Barren and Mineralized Komatiites in Dynamic Ore-forming Magmatic Systems, in Keays, R.R., Lesher, C.M., Lightfoot, P.C. and Farrow, C.E.G. (eds), Dynamic Processes in Magmatic Ore Deposits and their Application in Mineral Exploration; Geological Association of Canada, Short Course Notes, vol.13, pp.451-477.
Licht, O.A.B. (2000) Conceptual model for Cu-Ni-sulfides and PGM mineralizations in the Parana Basin igneous rocks. Otavio Augusto Boni Licht. Mineropar, Curitiba, October 2000. Unbublished
Licht, O.A.B. (2000, unpublished) Mineral prospection in the State of Parana Third Plateau. For MMAJ Mission Guidance. Secretaria de Estado da Industria, Comercia e Desenvolviento Economico Minerais do Parana S.A.
Licht, O.A.B. (2001) A geoquímica multielementar na gestão ambiental - identificação e caracterização de províncias geoquímicas naturais, alterações antrópicas da paisagem, áreas favoráveis à prospecção mineral e regiões de risco para a saúde no estado do Paraná , Brasil. Universidade Federal do Paraná; Tese.
Lightfoot, P.C., Hawkesworth, C.J., Devey, C.W., Rogers, N.W. and Van Calsteren, P.W.C. (1990) Source and differentiation of Deccan Trap lavas: implications of geochemical and mineral chemical variations. Journal of Petrology, vol.31, part 5, pp.1165-1200.
Lightfoot, P.C., Hawkesworth, C.J., Hergt, J., Naldrett, A.J., Gorbachev, N.S., Fedorenko, V.A. and Doherty, W. (1993) Remobilisation of the continental lithosphere by a mantle plume: major-, trace-element, and Sr-, Nd-, and Pb-isotope evidence from picritic and tholeiitic lavas of the Noril'sk District, Siberian Trap, Russia. Contribution of Mineralogy and Petrology, vol.114, pp.171-188.
Lightfoot, P.C., Naldrett, A.J., Gorbachev, N.S., Doherty, W. and Fedorenko, V.A. (1990) Geochemistry of the Siberian Trap of the Noril'sk area, USSR, with implications for the relative contributions of crust and mantle to flood basalt magmatism. Contributions to Mineralogy and Petrology, vol.104, pp.631-644.
Long, P.E. and Wood, B.J. (1986) Structures, textures and cooling histries of Columbia River basalt flows. Bulletin of the Geological Society of America, vol.97, pp.1144-1155.
Lorand, J.-P., Pattou, L. and Gros, M. (1999) Fractionation of Platinum-group elements and gold in the upper mantle: a detailed study in Pyrenean orogenic lherzolites. Journal of Petrology, vol.40, issue6.
McKenzie, D. and Bickle, M.J. (1988) The volume and composition of melt generated by extension of the lithosphere. Journal of Petrology, vol.29, pp.625-679.
Mahoney, J.J., Coffin, M.F.(edts) (1997) Large igneous provinces: continental, oceanic, and planetary flood volcanism. Geophysical Monograph 100, American Geophysical Union (publisher), 438p.
Maksimov, Y.M. and Rudkevich, M.Y. (1971) Quantitative evaluation of the dynamics of Mesozoic and Cenozoic vertical movements over the West-Siberian plate. Geotectonics, no.1-6, pp.245-248.
Mantes-Lauer, C.L., Pacca, I.G., Melfi, A.J., Piccirillo, E.M., Bellieni, G., Petrini, R. and Rizzieri, R. (1995) The Anari and Tapirapuã Jurassic Formations, western Brazil: palaeo-magnetism, geochemistry and geochronology. Earth and Planetary Science Letters, vol.128, pp.357-371.
Mantovani, M.S.M. and Hawkesworth, C.J. (1990) An inversion approach to assimilation and fractional crystallisation processes. Contribution of Mineralogy and

Petrology, vol.105, pp.289-302.
Mantovani, M.S.M., Freitas, S.R.C., Shukowsky, W. (2001) Tidal gravity anomalies as a tool to measure rheological properties of the continental lithosphere: application to the South American Plate. Journal of South American Earth Sciences, vol.14, pp.1-14.
Mantovani, M.S.M., Marques, L.S., Sousa, M.A., Civetta, L., Atalla, L.T. and Innocenti, F. (1985) Trace element and strontium isotope constraints on the origin and evolution of Paraná continental flood basalts of Santa Catarina State (Southern Brazil). Journal of Petrology, vol.26, part 1, pp.187-209.
Mantovani, M.S.M., Wildner, W., Juchem, P.L. (2000) Paraná basin magmatism, stratigraphy and mineralization (southern Brazil). 31st International Geological Congress, Pre-congress Field Trip-Bft01.
Mapa das Trencheitras-DNPM-No.810526/93, Terra Santa.
Maruyama, S. (1994) Plume tectonics. The Journal of The Geological Society of Japan. Vol.100, pp.24-49.
Maruyama, S., Isozaki, Y., Kimura, G. and Terabayashi, M. (1997) Paleogeographic maps of the Japanese Islands: plate tectonic synthesis from 750Ma to the Present. The Island Arc, vol.6, pp.121-142.
Masuda, A., Nakamura, N., Tanaka, T. (1973) Fine structures of mutually normalized rare-earth patterns of chondrites. Geochimica et Cosmochimica Acta, vol.37, pp.239-248.
Matthey, J. (2000) Platinum 2000. Johnson Matthey Public Limited Company, 40-42 Hatton Garden, London EC1N 8EE, England. (Japanease version: Tanaka noble metal Co., Ltd.)
Mavrogenes, J.A. and O'Neill, H.S.C. (1999) The relative effects of pressure, temperature and oxygen fugacity on the solubility of sulfide in mafic magmas. Geochimica et Cosmochimica Acta, vol.63, no.7/8, pp.1173-1180.
McDonough, W.F., Sun, S.-s. (1995) The composition of the Earth. Chemical Geology, vol.120, pp.223-253.
McDougall, J.D. (edt.) (1988) Continental flood basalts. Kluwer Academic Publishers, 341p.
McKenzie, D. (1978) Some remarks on the development of sedimentary basin. Earth and Planetary Science Letters, vol.40, pp.25-32.
Mckenzie, D. and Bickle, M.J. (1988) The volume and composition of melt generated by extention of the lithosphere. Journal of Petrology, vol.29, part3, pp.625-679.
McKenzie, D. and O'Nions, R.K. (1991) Partial melt distributions from inversion of rare earth element concentrations. Journal of Petrology, vol.32, part 5, pp.1021-1091.
McKenzie, D. and O'Nions, R.K. (1995) The source regions of ocean island basalts. Journal of Petrology, vol.36, no.1, pp.133-159.
Melfi, A.J., Piccirillo, E.M. and Nardy, A.J.R. (1988) Geological and magmatic aspects of the Paraná basin -an introduction. in Piccirillo, E.M., Melfi, A.J.(eds.), The Mesozoic Flood Volcanism of the Paraná Basin, pp.1-14.
Metal Mining Agency of Japan (1977) Magmatic Segregation copper-nickel deposits of the Soviet Union, Data of Survey Analysis Committee, Mineral Resources Information Center, no.26.
Metal Mining Agency of Japan (2000) Rare Metals Data book (Revised Edition), Platinum Group Metals. (in Japanese)
Metal Mining Agency of Japan (2001) Rare Metals Stockpiling Data (31 rare metals). (in Japanese)
Milani E.J. (1997) Evoluçãao tectono-estratigráfica da bacia do Paraná e seu relacionamento com a geodinâmica fanerozóica do Gondwana sul-ocidental. volume I -Texto, Porto Alegre. UFRGS. CPGG. Tese de Doutorado. 2v.
Milani, E.J., Faccini, U.F., Scherer, C.M., Araújo, L.M. and Cupertino, J.A. (1998) Sequences and Stratigraphic Hierarchy of the Paraná Basin (Ordovician to Cretaceous), Southern Brazil. Bol. IG. USP, série científica, no.29.
Miller, J.D., Jr. and Severson, M.J. (2002) Geology of the Duluth Complex. University of Minnesota, Report of investigations 58, ISSN 0076-9177, pp.106-143.
Miller, J.D., Jr., Severson, M.J., and Hauch, S.A. (2002) History of the geologic mapping and mineral exploration in the Duluth Complex. University of Minnesota, Report of investigations 58, ISSN 0076-9177, pp.21-51.
Milner, S.C., Duncan, A.R., Whittingham, A.M. and Ewart, A. (1995a) Age of Mesozoic igneous rocks in northwestern Namibia, and their relationship to continental break-up. Journal of Geological Society of London, vol.152, pp.97-104.
Milner, S.C., Duncan, A.R., Whittingham, A.M. and Ewart, A. (1995b) Trans-Arlantic correlation of eruptive sequences and individual silicic units within the Paraná-Etendeka igneous province. Journal of Volcanology and Geothermal Research, vol.69, pp.137-157.
MINERAR (1997) Mina Volta Grande. Minerar, Consultoria e Projetos.
Minerar-CRM (1997) Mapa Geologico da Retiao de Lavras do Sul. Diagnostico do Potencial Mineral do Municipio de Lavras do Sul.
MINEROPAR (1986) Geologia do Estado do Paraná (1:1,400,000).
MINEROPAR (1986) Geologia do Estado do Paraná. 1/500,000 Mapa geologico(1984) da Mineropar. Secretaria de Estado da Industria e do Comercio, Governo do Estado do Paraná, 1998.
MINEROPAR (1994) Parana, Avaliasao Regional do Sector Mineral, Boletim no. 60, Governo do Estado do Parana.
MINEROPAR (2000) Field Trip Guidance for MMAJ Mission.
Mining Journal Ltd.(Publisher) (2000) Greenland. Mining Journal and Mining Magazine country and area review, pp.1-16.
Miyashiro, A. (1986) Hot regions and the origin of marginal basins in the western Pacific. Tectonophysics, vol.122, pp.195-216.
Mizusaki, A.M.P., Petrini, R., Bellieni, G., Comin-Chiramonti, P., Dias, J., De Min, A. and Piccirillo, E.M. (1992) Basalt magmatism along the passive continental margin of SE Brazil (Campos basin). Contribution of Mineralogy and Petrology, vol.111, pp.143-160.
Momme, P., Tegner, C., Brooks, C.K., Keays, R.R. (2002) The behaviour of platinum-group elements in basalts from the East Greenland rifted margin. Contribution of Mineralogy and Petrology, vol.143, pp.133-153.
Morgan, W.J. (1981) Hotspot tracks and opening of the Atlantic and Indian Ocean, in The Sea, vol.7: The Oceanic Lithosphere, Emiliani, C. (edt.), Wiley, New York, pp.443-487.
MSS (2000) Programa Levantamentos Geológicos Básicos do Brasil-PLGB; Subprograma de Integração geológica-Metalogenética Projeto Folhas Porto Alegre Sh.22E Lagoa Mirim SI.22,A0 Milionésimo, Carta Geológica Escala 1:250,000.

Nakagawa, M. and Ohta, E. (1995) Preponderance of Ir-Os-Ru Alloys in Depleted Ophiolite, Hokkaido, Japan: A Window to the Mantle. Resource Geology Special Issue, no.18, pp.49-56.

Naldrett, A.J. (1989a) Magmatic Sulfide Deposits. Oxford University Press, Oxford Monographs on Geology and Geophysics No.14, 181p.

Naldrett, A.J. (1989b) Selected Nickel-Sulfide Deposits, 4 Genetic Impications, Magmatic Sulfide Deposits. Clarendon Press, Oxford University Press 1989.

Naldrett, A.J. (1992) A model for the Ni-Cu-PGE Ores of the Noril'sk Region and Its Application to other Areas of Flood Basalt. Economic Geology, vol.87, no.8, pp.1945-1962.

Naldrett, A.J. (1999) World-class Ni-Cu-PGE deposits: key factors in their genesis. Mineralium Deposita, no.34, pp.227-240.

Naldrett, A.J., Brügmann, G.E. and Wilson, A.H. (1990) Models for the concentration of PGE in layered intrusions. Canadian Mineralogist, vol.28, pp.389-408.

Naldrett, A.J., Fedorenko, V., Shushen, L., Asif, M., Kunilov, V.E., Stekhin, A.I., Lightfoot, P.C. and Gorbachev, N.S. (1996) Controls on the Composition of Ni-Cu Sulfide Deposits as Illustrated by Those at Noril'sk, Siberia. Economic Geology, vol.91, pp.751-773.

Naldrett, A.J., Llightfoot, P.C., Fedorenko, V., Doherty, W. and Gorbachev, N.S. (1992) Geology and Geochemistry of Intrusions and Flood Basalts of the Noril'sk Region, USSR, with Implications for the Origin of the Ni-Cu Ores. Economic Geology, vol.87, no.4, pp.975-1004.

Naldrett, A.K. and Macdonald, A.J. (1980) Tectonic settings of Ni-Cu sulphide ores: their importance in genesis and exploration. The Continental Crust and Its Mineral Deposits(edt: Strangway, D.W.), Geological Association of Canada Special Paper 20, pp.633-657.

New Metals Association (2000) Nickel. New Metals Data Book 2000. (in Japanease)

Nürnburg, D. and Müller, R.D. (1991) The tectonic evolution of the South Atlantic from Late Jurassic to present. Tectoniphysics, vol.191, pp.27-53.

O'Connor, J.M. and Duncan, R.A. (1990) Evolution of the Walvis Ridge – Rio Grande Rise hotspot system: implications for African and South American plate motions over plumes. Journal of Geophysics Research, vol.95, no.17, pp.474-502.

Olson, P. and Singer, H. (1985) Creeping plumes. Journal of Fluid Mechanisums, vol.158, pp.511-531.

Oliveira, L.O.A. (1989) Aspectos da evolução termomecánica da Bacia do Paraná no Brasil. Rev. Bras. Geocienc. Vol.19, pp.330-342.

Oman, C.L., Finkelman, R.B. and Tewalt, S.J. (2001) Concentrations of platinum group elements in 122 U.S. coal samples. U,S, Geological Survey Open-File Report 97-53.

Onuma, N. and Montoya, M. (1984) Sr/Ca-Ba/Ca systematics of volcanic rocks from the central Andes, southern Peru, and its implication for Andean magmatism. Geochemical Journal, vol.18, pp.251-262.

Paulipetro (1982) Geology of the Paraná basin: reevaluation of hydrocarbon potential and prospects. Consorcio CESP/IPT, pp.198.

Pearce, J.A. (1996): A use's guide to basalt discrimination diagrams. in Wyman, D.A. (editor), Geological Association of Canada, WINNPEG'96 Short Course Note, vol.12, pp.79-113.

Peate, D.W. (1990) Stratigraphy and petrogenesis of the Paraná continental flood basalts, southern Brazil, Ph.D. thesis, The Open University, Milton Keynes.

Peate, D.W. (1997) The Paraná – Etendeka Province. Geophysical Monograph 100, "Large Igneous Provinces: Continental, Oceanic, and Planetary Flood Volcanism", The American Geophysical Union, pp.217-245.

Peate, D.W. and Hawkesworth, C.J. (1996) Lithospheric to asthenospheric transition in Low-Ti flood basalts from southern Paraná, Brazil. Chemical Geology, vol.127, no.1-3, pp.1-24.

Peate, D.W., Hawkesworth, C.J., Mantovani, M.S.M. (1992) Chemical stratigraphy of Paraná lavas (South America): classification of magma types and their spatial distribution. Bulletin of Volcanology, vol.55, pp.119-139.

Peate, D.W., Hawkesworth, C.J., Mantovani, M.S.M., Rogers, N.W., Turner, S.P. (1999) Petrogenesis and Stratigraphy of the High-Ti/Y Urubici Magma Type in the Paraná Flood Basalt Province and Implications for the Nature of Dupal-Type Mantle in the South Atlantic Region. Journal of Petrology, vol.40, no.3, pp.451-473.

Peate, D.W., Hawkesworth, C.J., Mantovani, M.S.M., Shukowsky, W. (1990) Mantle plumes and flood basalt stratigraphy in the Paraná, South America. Geology, vol.18, pp.1223-1226.

Peate, D.W., Mantovani, M.S.M., Hawkesworth, C.J. (1988) Geochemical stratigraphy of the Paraná continental flood basalts: bore-hole evidence. Rev Bras Geoc., vol.18, pp.212-221.

Peng, Z.X. and Mahoney, J. (1995) Drillhole lavas from the northwestern Deccan Traps, and the evolution of Réunion hotspot mantle. Earth Planetary Science Letters, vol.134, pp.169-185.

Peng, Z.X., Mahoney, J., Hooper, P., Harris, C. and Beane, J. (1994) A role for lower continental crust in flood basalt genesis? Isotopic and incompatible element study of the lower six formations of the western Deccan Traps. Geochimica et Cosmochimica Acta, vol.58, pp.267-288.

Petrini, R., Civetta, L., Piccirillo, E.M., Bellieni, G., Comin-Chiaramonti, P., Marques, L.S. and Melfi, A.J. (1987) Mantle heterogeneity and crustal contamination in the genesis of low-Ti continental flood basalts from the Paranà Plateau (Brazil): Sr-Nd isotope and geochemical evidence. Journal of Petrology, vol.28, part 4, pp.701-726.

Piccirillo, E. M. and Melfi, A. J. (eds.) (1988) The Mesozoic flood volcanism of the Paraná basin: petrogenetic and geophysical aspects. Sao Paulo, IAG-USP (Univ. Sao Paulo, Instituto Astronomico e Geofisico), 600p.

Piccirillo, E.M., Bellieni, G., Comin-Chiaramonti, P., Ernesto, M., Melfi, A.J., Pacca, I.G. and Ussami, N. (1988) Significance of the Paraná flood volcanism in the disruption of western Gondwanaland. in Piccirillo, E.M., Melfi, A.J.(eds.), The Mesozoic Flood Volcanism of the Paraná Basin, pp.285-296.

Piccirillo, E.M., Comin-Chiaramonti, P., Bellieni, G., Civetta, L., Marques, L.S., Melfi, A.J., Petrini, R., Raposo, M.I.B. and Stolfa, D. (1988) Petrogenetic aspects of continental flood basalt-rhyolite suites from the Paraná basin (Brazil). in Piccirillo, E.M., Melfi, A.J.(eds.), The Mesozoic Flood Volcanism of the Paraná Basin, pp.179-206.

Piccirillo, E.M.; Melfi, A.J.; Comin-Chiaramonti, P.; Bellieni, G.; Ernesto, M.; Pacca, I.G. (1988) Continental flood

vulcanism from the Parana Basin (Brazil). In: McDougall, J.D. ed. Continental Flood Basalts. Kluwer Academic Publishers, pp.195-238.

Pierce, K.L. and Morgan, L.A. (1993) The track of the Yellowstone hot spot: volcanism, faulting and uplift. Geological Society of America, vol.179, pp.1-53.

Prendergast, M.D. (2000): Layering and Precious Metals Mineralization in the Rincon del Tigre Complex, Eastern Bolivia. Economic Geology, vol.95, pp.113-130.

Quintas, M.C.L. (1995) O embasamento da bacia Paraná: reconstrução geofisica de seu arcabouço. Universidade de São Paulo (Dr. thesis), 213p.

Quintas, M.C.P., Mantovani, M.S.M. and Zalan, P.V. (1999) Contribuisao ao Estudo da Evolusao Mecanica da Bacia do Parana. Revista Brasileira de Geociencias, vol. 29, no. 2, pp.217-226.

Raposo, M.I.B., Ernest, M. (1995) Anisotropy of magnetic susceptibility in the Ponta Grossa dyke swarm (Brazil) and its relationship with magma flow direction. Physics of the Earth and Planetary Interiors, vol.87, pp.183-196.

Regelous, M. (1993) Geochemistry of dolerites from the Paraná flood basalt province, southern Brazil. Ph. D thesis, The Open University, Milton Keynes.

Rehkämper, M. Halliday, A.N., Fitton, J.G., Lee, D.-C., Wieneke, M. and Arndt, N.T. (1999) Ir, Ru, Pt, and Pd in basalts and komatiites: new constraints for the geochemical behavior of the platinum-group elements in the mantle. Geochimica et Cosmochimica Acta, vol.63, no.22, pp.3915-3934.

Renne, P.R., Deckart, K., Ernesto, M., Féraud, G. and Piccirillo, E.M. (1996) Age of the Ponta Grossa dike swarm (Brazil), and implications to Paraná flood volcanism. Earth and Planetary Science Letters, vol.144, no.1-2, pp. 199-211.

Renne, P.R., Ernesto, M., Pacca, I.G., Coe, R.S., Glen, J.M., Prévot, M., Perrin, M. (1992) The age of Paraná Flood Volcanism, rifting of Gondwanaland, and the Jurassic-Cretaceous Boundary. Science, vol.25, pp.975-978.

Renne, P.R., Glen, J.M., Milner, S.C., Duncan A.R. (1996) Age of Etendeka flood volcanism and associated intrusions in southwestern Africa. Geology, v.24, no.7, p.659-662.

Renne, P.R., Mertz, D.F., Ernesto, M., Marques, L., Teixeira, W., Ens, H.H. and Richards, M.A. (1993) Geochronologic constraints on magmatic and tectonic evolution of the Paraná province (abstract). Eos Trans. AGU, no.74, pp.553.

Renne, P.R., Zichao, Z., Richards, M.A., Black, M.T. and Basu, A.R. (1995) Synchrony and causal relations between Permian-Traiassic boundary crises and Siberian flood volcanism. Science, vol.269, pp.1413-1416.

Rezende, W.M.D (?) Post paleozoic geotectonics of South America related to plate tectonics and continental drift.

Ribeiro, M.J. (1978) Mapa Previsional do Cobre no Escudo Sul-Rio-Grandense, Brasilia. DNPM, Map and Explanation.

Richards, M.A., Duncan, R.A., Courtillot, V.E. (1989) Flood basalts and hotspot tracks: plume heads and tails. Science, vol.246, no.6, pp.103-107.

Rickwood, P.C. (1990) The anatomy of a dyke and the determination of propagation and magma flow directions. Mafic dykes and emplacement mechanisms, Rickwood and Tucker (eds.), pp.81-101.

Ringwood, A.E. (1994) Role of the transition zone and 660 km discontinuity in mantle dynamics. Physics of the Earth and Planetary Interiors, vol.86, pp.5-24.

Ringwood, A.E. and Irifune, T. (1988) Nature of the 650-km seismic discontinuity: implications for mantle dynamics and differentiation. Nature, vol.331, no.14, pp.131-136.

Ripley, E.M. (1999) Systematics of Sulphur and Oxygen Isotopes in Mafic Igneous Rocks and Related Cu-Ni-PGE Mineralization, in Keays, R.R., Lesher, C.M., Lightfoot, P.C. and Farrow, C.E.G. (editors), Dynamic Processes in Magmatic Ore Deposits and their Application in Mineral Exploration; Geological Association of Canada, Short Course Notes, no.13, pp.133-158.

Roach, T.A. and Roeder, P.L. (1998) Composition of chromite in the upper chromitite, Muskox Layered Intrusion, Northwest Territories. The Canadian Mineralogist, vol.36, pp.117-135.

Rocha-Campos, A.C., Cordani, U.G., Kawashita, K., Sonaki, H.M. and Sonaki, I.K. (1988) Age of the Paraná flood volcanism. in Mesozoic Flood Volcanism from the Paraná Basin (Brasil): Petrogenetic and Geophysical Aspects, Piccirillo, E.M. and Melfi, A.J. (edts), IAG-USP São Paulo, pp.25-45.

Romanini S.J., Albuwuerque L.F.F. (1996) Geological aspects of the basic intrusions characterized by CPRM's national program for prospection of the PGE in the Parana Basin. Port Alegre: CPRM. Internal Report.

Sano, T. (1996) Magma genesis of continental flood basalts: a case study of Deccan Trap basalts, India. docter's thesis, University of Tokyo.

Sano, T., Fujii, T., Deshmukh, S.S., Fukuoka, T. and Aramaki, S. (2001) Differentiation processes of Deccan Trap Basalts: contribution from geochemistry and experimental petrology. Juranal of Petrology.

Santos, E.L.D. (1999) Potencialidade das Mineralizasoes de Cobre (Au e Ag), Chunbo e Zinco (Ag, Au e Cu) da Janela Bom Jardim-RS. Porto Alegre.

Santos, E.L.D., Azevedo, G.C., Maciel, L.A.C., Mossmann, R. (1994) Mapa Geiologico da Regiao Leste-Sudeste de São Gabriel-RS. Escala 1/50,000. Porto Alegre, DNPM, 1998.

Santos, E.L.D., Maciel, L.A.C., Filho, J.A.Z. (1998) Distritos Mineriros do Estado do Rio Grande do Sul. Porto Alegre, DNPM.

Sato, H. (1977) Lithos, vol.10, pp.113-120.

Saunders, A.D., Storey, M., Kent, R.W. and Norry, M.J. (1992) Consequences of plume-lithosphere interations. in Magmatism and the Causes of Continental Break-up, Spec. Publ. No.68, The Geological Society, London, pp.41-60.

Scheibe, L.F. (1986) Geologia e petrologia do distrito alcalino de Lages, SC. Universidade de São Paulo instituto de geociências; Tese de doutoramento, 224p.

Schilling, J.-G. (1985) Geochemical and isotopic variation along the Mid-Atlantic Ridge axis 79 ° N to 0 ° N. in "The Geology of North America, vol. M., The Western North Atlantic Region", The Geological Society of America, pp.137-155.

Schouwstra, R.P., Kinloch, E.D. and Lee, C.A. (2000) Ashort Geological Review of the Bushveld Complex. Platinum-Metals Review, vol.44, no.1, pp.33-39.

Self, S., Thordarson, Th., Keszthelyi, L., Walker, G.P.L., Hon, K., Murphy, M.T., Long, P. and Finnemore, S. (1996) A new model for the emplacement of Columbia

River basalts as large, inflated pahoehoe lava flow fields. Geophysical Research Letters, vol.23, no.19, pp.2689-2692.

Severson, M.J., Miller, J.D., Jr., Peterson, D.M., Green, J.C., and Hauch, S.A. (2002) Mineral potential of the Duluth Complex and related intrusions. University of Minnesota, Report of investigations 58, ISSN 0076-9177, pp.164-200.

Shaw, D.M. (1970) Trace element fractionation during anatexis. Geochimica et Cosmochimica Acta, vol.34, pp.237-243.

Silver, P.G., Carlson, R.W. (1988) Deep slabs, geochemical heterogeneity, and the large-scale structure of mantle convection: investigation of an enduring paradox. Annual Revews of Earth Planetaly Science, vol.16, pp.477-541.

SMM (2001) Mineral exploration program in the Paraná basin, Brazil. Tecnical cooperation project between Brazil and Japan. in Oguino, K., Tadokoro, K. (Eds).

Stewart, K., Turner, S., Kelley, S., Hawkesworth, C.J., Kirstein, L., Mantovani, M.S.M. (1996) 3-D, ^{40}Ar-^{39}Ar geochronology in the Paraná continental flood basalt province, Earth and Planetary Science Letters, vol.143, no.1-4, pp. 95-109.

Sumiko Consultants CO., LTD. (2001a) Nickel of the world -Actual condition and the problem of the Ni resources-. (in Japanease)

Sumiko Consultants CO., LTD. (2001b) Nickel of the world II -Main articles on the nickel resources-. (in Japanease)

Sun, S.-s. and McDonough, W.F. (1989) Chemical and isotopic systematics of oceanic basalts: implications for mantle composition and processes. in Saunders, A.D. and Norry, M.J. (eds), Magmatism in the Ocean Basins, Geological Society Special Publication, no.42, pp.313-345.

Tackley, P.J., Stevenson, D.J., Glatzmaier, G.A. and Schubert, G. (1993) Effect of an endothermic phase transition at 670 km depth in a spherical model of convection in the Earth's mantle. Nature, vol.361, pp.699-704.

Tadokoro, K. (2000a) Report of Paraná area. (in Japanese)

Tadokoro, K. (2000b) RGS Report. (in Japanease)

Takahashi, E. (1986) Origin of basaltic magmas: implication from peridotite melting experiments and an olivine fractionation model. Volcanological Society of Japan, Volcano Spetial publication, vol.2, no.30, p.S17-S40.

Takahashi, E. (1996) Global mantle circulations and mantle plume. Earth Planetary Science Letters 1996 Fall Meeting, V72C-7 1525h, F769.

Takahashi, E, Shimazaki, T., Tsuzaki, Y. and Yoshida, H. (1993) Melting study of peridotite KLB-1 to 6.5 Gpa and the origin of basaltic magmas. Philos. Trans. R. Soc. London A342, pp.105-120.

Takahashi, E, Nakajima, K. and Wright, T.L. (1998) Origin of the Columbia River basalts: melting model of a heterogeneous plume head. Earth and Planetary Science Letters, vol.162, no.1-4, pp.63-80.

Takahashi, E., Nakajima, K. (1997) Origin of flood basalts: new model of mantle plumes. Science Journal Kagaku, vol.67, no.7, pp.519-529.

Tamrazyan, G.P. (1971) Siberian continental drift. Tectonophysics, vol.11, pp.433-460.

Tegner, C., Lesher, C.E., Larsen, L.M. and Watt, W.S. (1998) Evidence from the rare-earth-element record of mantle melting for cooling of the Tercialy Iceland plume. Nature, vol.395, pp.591-594.

The Geological Society of America Inc. (1989) Volcanism and tectonism in the Columbia River Flood Basalt Province. In Reidel, S.P., Hooper, P.R. (eds.), Geological Society of America, spetial paper, 386p.

The World Economic Information Service (WEIS) (1999) ARC Report 1999, The Activity and Expectation of Brazil.

Thériault, R.D., Barnes, S.-J. and Severson, M.J. (1997) The influence of country-rock assimilation and silicate to sulfide rations (R factor) on the genesis of the Dunka Road Cu-Ni-platinum-group element deposit, Duluth Complex, Minnesota. Canadian Journal of Earth Sciences, vol.34, pp.375-389.

Theriault, R.D., Barnes, S.J. and Severson, M.J. (2000) Origin of Cu-Ni-PGE sulfide mineralization in the Partridge River Intrusion, Duluth Complex, Minnesota. Economic Geology, vol.95, no.5, pp.929-943.

Thompson, R.N. and Gibson, S.A. (1991) Subcontinental mantle plumes, hotspots and pre-existing thinspots, The Journal of Geology, London, vol.147, pp.973-977.

Tokarski, A.K. (1990) Dyke swarms as stress indicators: tow constraints. Mafic Dykes and Emplacement Mechanisms, eds: Rickwood and Tucker, pp.101-104.

Tommasi, A., Vauchez, A. (2001) Continental rifting parallel to ancient collisional belts: an effect of the mechanical anisotropy of the lithospheric mantle. Earth and Planetary Science Letters, vol.185, no.1-2, pp.199-210.

Turner, S., Hawkesworth, C. (1995) The nature of the sub-continental mantle: constraints from the major-element composition of continental flood basalts. Chemical Geology, vol.120, no.3-4, pp.295-314.

Turner, S., Hawkesworth, C.J., Gallagher, K., Stewart, K., Peate, D.W. and Mantovani, M.S.M. (1996) Mantle Plumes, flood basalts, and thermal models for melt generation beneath continents: Assessment of a conductive heating model and application to the Paraná. Journal of Geophysics Research, 101(B5): 11.503-11.518.

Turner, S., Regelous, M., Kelley, S., Hawkesworth, C.J., Mantovani, M.S.M., (1994) Magmatism and continental break-up in the South Atlantic: high precision 40Ar-39Ar geochronology. Earth Planetary Science Letters, vol.1221, pp.333-348.

Turner, S.P., Kirstein, L. A, Hawkesworth, C.J., Peate, D.W., Hallinan, S., Mantovani, M.S.M. (1999) Petrogenesis of an 800 metre lava sequence in eastern Uruguay: insights into magma chamber processes beneath the Paraná flood basalt province. Journal of Geodynamics, vol.28, no.4-5, pp.471-487.

Turner, S.P., Peate, D.W., Hawkesworth, C.J., Mantovani, M.S.M. (1999) Chemical stratigraphy of the Paraná basalt succession in western Uruguay: further evidene for the diachronous nature of the Paraná magma types. Journal of Geodynamics, vol.28, no.4-5, pp.459-469.

UFRGS (1996) Mecanismos de resfriamento, estruturação e processos pós-magmáticos em basaltos da bacia do Paraná - Região de Frederico Westphalen (RS) - Brasil/ Márcia Elisa Boscato Gomes - Porto Alegre.

Uto, K. and Ishizuka, O. (1999) The current state and the future of K-Ar and $^{40}Ar/^{39}Ar$ dating of volcanic rocks. Journal of the Japanese Association for Petroleum Technology, vol.64, no.1, pp.63-71 (in Japanease).

Vacquier, V. (1962) A machine method for computing the magnitude and the direction of magnetization of a

uniformly magnetized body from its shape and a magnetic survey. Proceedings of the Benedum Earth Magnetism Symposium 1962, pp.124-137.

VanDecar, J.C., James, D.E. and Assumpção, M. (1995) Seismic evidence for a fossil mantle plume beneath South America and implications for plate driving forces, Nature, vol.378, pp.25-31.

Vidotti, R.M., Ebinger, C.J. and Fairhead, J.D. (1998) Gravity signature of the western Paraná basin, Brazil. Earth and Planetary Science Letters, vol.159, no.3-4, pp. 117-132.

Vogel, D.C. and Keays, R.D. (1997) The petrogenesis and platinum-group element geochemistry of the Newer Volcanic Province, Victoria, Australia. Chemical Geology, vol.136, pp.181-204.

Wallace, P.J., Carmichael, I.S.E. (1994) S speciation in submarine basaltic glasses as determined by measurements of SK αX-ray wavelength shifts. American Mineralogist, vol.79, pp.161-167.

Weiblen, P.W. (1982) Keweenawan intrusive igneous rocks. Geological Society of America Memoir 156, pp.57-82.

Weiblen, P.W. and Morey, G.B. (1980) A summary of the stratigraphy, petrology, and structure of the Duluth Complex. American Journal of Science, vol.280-A, pp.88-133.

White, R. and McKenzie, D. (1989) Magmatism at rift zones: the generation of volcanic continental margins and flood basalts. Journal of Geophysical Research, vol.94, no.B6, pp.7685-7729.

White, R.S. and McKenzie, D. (1995) Mantle plumes and flood basalts. Journal of Geophysical Research, vol.100, no.B9, pp.17543-17585.

Wildner, W. (1998) Mapeamento Integrado da Bacia Hidrográfica do Guaíba, 1:250.000 (faciologia do vulcanismo Serra Geral). CPRM – Serviço Geológico do Brasil, documento interno, 10 folhas 1:250.000. Convênio CPRM, FEPAM.

Wildner, W., Silva, L.A.C. (1999) Minerais de Os-Ir-Pd em concentrados de Batéia folhas jacupiranga e Rio Guaraú - São Paulo. Report of CPRM.

Wooden, J.L., Czamanske, G.K., Bouse, R.M., Likhachev, A.P., Kunilov, V.E. and Lyul'ko, V. (1992) Pb Isotope data Indicate a Complex, Mantle Oigin for the Noril'sk-Talnakh Ores, Siberia. Economic Geology, vol.87, pp.1153-1165.

Wooden, J.L., Czamanske, G.K., Fedorenko, V.A., Arndt, N.T., Chauvel, C., Bouse, R.M., King, B-S.W., Knight, R.J. and Siems, D.F. (1993) Isotopic and trace-element constraints on mantle and crustal contributions to Siberian continental flood basalts, Noril'sk area, Siberia. Geochimica et Cosmochimica Acta, vol.57, pp.3677-3704.

Wright, T.L., Mangan, M. and Swanson, D.A. (1988) Chemical data for flows and feeder dyke of the Yakima basalt group, Columbia River Basalt Group. Washington, Oregon and Idaho, and their bearing on a petrogenetic model. U.S.G.S. bulletin, vol.1821, 71p.

Yamashita, S., Tatsumi, Y. and Nohda, S. (1996) Temporal variation in primary magma compositions in the northeast Japan Arc. The Island Arc, vol.5, pp.276-288.

Yasuda, A and Fujii, T. (1994a) Melting phase relations of an anhydrous mid-ocean ridge basalt from 3 to 20 Gpa: implocations for the behavior of subducted oceanic crust in the mantle. Journal of Geophysical Research, vol.99, no.B5, pp.9401-9414.

Yasuda, A. and Fujita, T. (1994b) The flood basalt and plateau. Monthly The Earth Special Issue. (in Japanease)

Yuen, D.A. and Fleitout, L. (1985) Thinning of lithosphere by small scale convective destabilisation, Nature, vol.313, pp.125-128.

Zalán, P.V., Wolff, S., Conceição, J.C.J., Astolfi, M.A.M., Vieira, I.S., Appi, V.T. and Zanotto, O.A. (1987) Tectônia e Sedimentação da Bacia do Paraná. ATAS do III Simposio Sul-Brasileiro de Geologia, Curitiva. vol.1, pp.441-447.

Zindler, A. and Hart, S.R. (1986) Chemical geodynamics. Ann. Rev. Earth and Planetary Science Letters. Vol.14, pp.493-571.

Zolotukhin, V.V. and Al'Mukhamedov, A.I. (1988) Trap of the Siberian Platform. Continental Flood Basalts (Kluwer Academic Publishers), pp.273-310.

APPENDIX

CONTENTS OF APPENDIX

APPENDIX 1

Report of

the 9th

International Platinum Symposium

- Summary of the symposium -

9th International Platinum Symposium

Summary

The 9th International platinum symposium was held at Billings City, State of Montana, USA from July 21 to 25, 2002. Such a symposium has been held every four years to report results of platinum ore deposit studys around the world. This symposium had 70 presentations of lectures and 61 exhibitions of posters.

The participants totaled 204, including 83 from the United States, 49 from Canada, 13 from South Africa, 10 from Finland, 9 from the United Kingdom, 6 each from Brazil and Japan, 4 from China, 3 each from Germany, France, Albania, and Australia, 2 each from Russia and India, and 1 each from Denmark, Austria, Italia, and Egypt. The titles of abstracts and major presentations of platinum ore deposit studys are stated below.

Platinum-Group Elements in the Upper Zone of the Rustenburg Layered Suite of the Bushveld Complex: Preliminary Results from the Bellevue Borehole

Sarah-Jane Barnes[1] and Wolfgang D. Maier[2]
[1]Sciences de la Terre, Universite du Quebec, Chicoutimi, Canada, G7H 2B1
[2] Centre for Research on Magmatic Ore Deposits, Department of Earth Sciences,
University of Pretoria, Pretoria 0002, South Africa
email:sjbarnes@uqac.uquebec.ca, wdmaier@scientia.up.ac.za

The Rustenburg Layered Suite (RLS) is generally divided into five zones (Hall, 1932): the basal Marginal Zone (0-800 m of norites), overlain by the Lower Zone (800-1300 m of cyclic units of harzburgite and pyroxenites), the Critical Zone (1300 to 1800 m of cyclic units of chromitite, pyroxenites, and norites), the Main Zone (3000 to 3400 m of norites, gabbronorites and anorthosites), and the Upper Zone (2000 to 2800 m of cyclic units of magnetitites, gabbronorites anorthosites, and diorites). The Lower Zone and Critical Zone are enriched in Platinum-group elements (PGE) relative to the marginal rocks (Fig. 1). This enrichment culminates in the formation of the world famous Merensky and UG-2 reefs. In contrast the Main Zone contains little PGE. The PGE content of the Upper Zone is poorly documented. Page et al. (1982) published an initial survey, of Pt, Pd and Rh concentrations of the Upper Zone. For most of the rocks the PGE were present at less than the detection limits. However, Page et al. (1982) do report one location with high values in the lower portions of Upper Zone. Harney et al. (1990) investigated 17 samples from the 300 meters of stratigraphy around the Main Magnetite layer. They found that the samples above the Main Magnetite layer have low levels of PGE (Pt+Pd = 5-10 ppb). Samples below the Main Magnetite layer were somewhat richer (Pt+Pd=40-100 ppb). Subsequently, Harney and von Gruenewadlt (1995) quoted company reports that suggest the presence of up to 6 ppm Pt + Pd in the upper part of the Main Zone. They attribute this enrichment and the enrichment reported by Page et al. (1982) to local hydrothermal action.

As part of a larger project "The Bushveld Complex: its origin, crystallization and interaction with the Kaapvaal lithosphere" headed by Prof. Lew Ashwal we have determined PGE, Ni, Cu, S and full major and trace element analyses in 56 samples of Upper Zone from the Bellevue borehole. This borehole provides a complete section through the Upper Zone and the upper part of the Main Zone. The aims of our project are:

a) To characterize the distribution of the PGE in Upper Zone;

b) To investigate whether there is any enrichment of Pd and Au as is found in the upper parts of the Skaergaard intrusion (Andersen et al., 1998). It is intriguing to note that in the Bushveld the reefs have higher Pt/Pd ratios than the silicate liquids from which they formed (2.3 vs. 1.5) requiring that Pd be concentrated elsewhere (Barnes and Maier, 2002). In contrast the Platinova reef of Skaergaard contains little Pt implying that it has been extracted from the magma before the formation of the Platinova reef. Further the Bushveld reefs form from a relative unfractionated magma with chromite and orthopyroxene on the liquidus. The Skaergaard Platinova reef forms from a highly fractionated magma. Could there be a Platinova type reef in the Upper Zone of the Bushveld, or a Merensky type reef in the lower parts of Skaergaard?

c) To investigate whether there is any PGE enrichment of the type reported by Harney and von Gruenewaldt (1995) and Page et al. (1982).

d) To investigate whether magnetite will concentrate Os, Ir, and Ru . Capobianco et al. (1994) have shown in experiments run at high oxygen fugacity that magnetite can concentrate Ru by analogy one would expect Os and Ir to also be concentrated in the magnetite.

Our preliminary results show that for most of the Upper Zone the PGE concentrations are extremely low. In most rocks Pt and Pd do not exceed 1 ppb. Osmium and Ru are present at less than detection limits of 0.2 and 1 ppb respectively. Iridium concentrations range from 0.08 to 0.3 ppb, Au from 0.1 to 7 ppb, Rh from <0.1 to 0.5 ppb. There does not appear to be an enrichment of Pd over Pt so the Pd "missing" from the reef rocks remains to be found. There is an enrichment in all of the PGE, with Pt+Pd = 3 ppm in the cyclic unit of the lower most magnetite layer of the Upper Zone. While is difficult to make a direct stratigraphic correlation with the enrichments reported by Page et al. (1982) and Harney and von Gruenewadlt (1995), the enrichments are in approximately the same stratigraphic position, i.e. close to the change from the Main Zone to the Upper Zone. The magnetite layers do not appear to be enriched in Os, Ir, and Ru and hence magnetite

does not appear to have concentrated these elements. Iridium, Pd, Re, Au, Se and Cu all show a positive correlation with S suggesting that sulfides control these elements.

References

Andersen, J. C. O., Rassmussen, H., Nielsen, T. E. D., and Ronsbo, J. C., 1998, The Triple group and the Platinova gold and palladium reefs in the Skaergaard intrusion: Stratigraphic and petrographic relations. Econ. Geol., v. 93, p. 488-509.

Barnes, S-J. and Maier W.D., 2002, Platinum-group Elements and Microstructures of Normal Merensky Reef from Impala Platinum Mines, Bushveld Complex. Jour. Petrol., v. 43, 103-128.

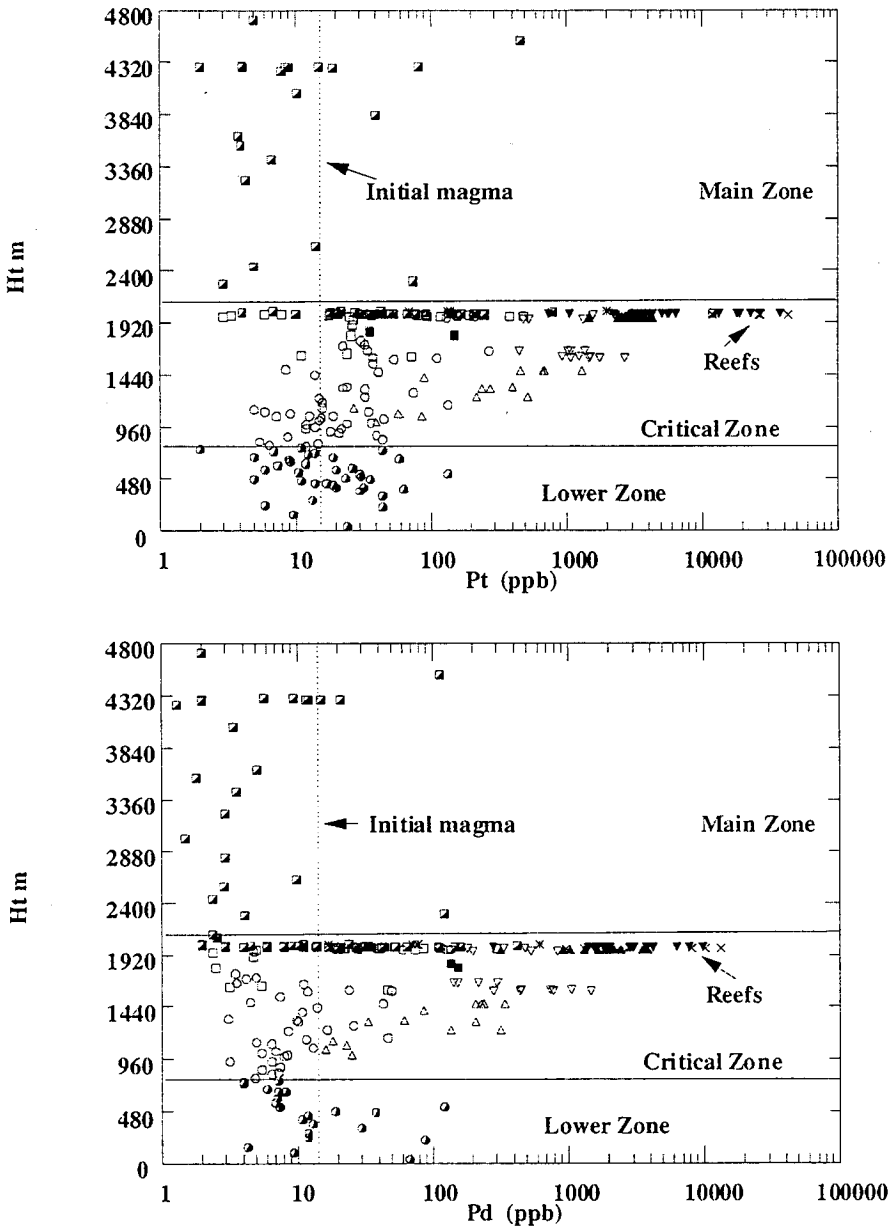

Figure 1. Variations in Pt and Pd content through the Bushveld Complex. Data from Barnes and Maier (in press) and references therein. Circles = peridotites and pyroxenites, triangles = chromitites, x = reefs; squares = mafic rocks.

Barnes, S-J. and Maier, W.D., (in press), Platinum-group Element Distributions in the Rustenburg Layered Suite of the Bushveld Complex, South Africa. *in* Cabri, L.J. ed. The Geology, Geochemistry and Mineral Benefication of Platinum-Group Elements, Canadian Institute Mining, Metallurgy and Petroleum Special vol. 54

Capobianco, C.J., Hervig, R.L. and Drake, M.J., 1994, Experiments on Ru, Rh and Pd compatibility for magnetite and hematite solid solutions crystallised from silicate melts. Chemical Geology, v. 113, p. 23-44.

Hall, A.L., 1932, The Bushveld Igneous Complex in the central Transvaal. Geological Society South Africa Memoir, 28, 544 p.

Harney, D.M.W., Merkle, R.K.W., and Von Gruenewaldt, G., 1990, Platinum-group element behavior in the Lower part of the Upper Zone, Eastern Bushveld Complex - Implications for the formation of the Main Magnetite Layer. Econ. Geol., v. 85, p. 1777-1789.

Harney, D.M.W., and Von Gruenewaldt, G., 1995, Ore-forming processes in the upper part of the Bushveld Complex, South Africa. Jour. Afri. Earth Sciences., v. 20, p. 77-89.

Page, N. J., Von Gruenewaldt, G., Haffty, J., AND Aruscavage, P.J., 1982, Comparison of platinum, palladium and rhodium distribution in some layered intrusions with special reference to the late differentiates (upper zone) of the Bushveld Complex, South Africa. Econ. Geol., v. 77, p. 1405-1418.

The Stillwater and Bushveld Magmas Were Wet!

Alan E. Boudreau
Division of Earth and Ocean Sciences, Nicholas School of the Environment and Earth Sciences, Duke University, Box 90227, Durham NC 27708\
e-mail: boudreau@duke.edu

Basic magmas that crystallized layered igneous intrusions such as the Stillwater complex have traditionally been considered to have been relatively "dry", largely because of the paucity of hydrous minerals. However, investigations of halogen variations suggest that the high-Cl, high-Mg parent liquids of the Stillwater and Bushveld complexes, like their modern-day boninitic counterparts, contained a much higher volatile content than previously recognized - possibly in excess of 1.0 wt. % H_2O (Boudreau *et al.*, 1997). Although volatile components can have a marked effect on crystallization behavior of these magmas, most existing models for the crystallization of these intrusions and the formation of their economically important platinum-group element deposits either ignore or downplay their potential importance.

Evidence for high volatile concentrations comes from several lines of evidence: 1) Presence of hydrous phases as common late (interstitial) minerals, 2) high Cl/F ratio of halogen-bearing minerals, 3) Cl and H isotopes consistent with a primary origin of the volatile components and 4) boninite-like nature of Stillwater and Bushveld magmas.

The range of apatite compositions in the Stillwater and Bushveld Complex and a few other intrusions are shown in figure 1, as well as chilled margin and associated contemporaneous sills dikes. In most intrusions, apatite is predominantly fluorian, with the mole fraction chlorapatite component typically less than 40 mole % and more commonly less than about 20 mole %. Furthermore, the apatite compositions generally become poorer in Cl (and richer if F) in the more evolved cumulates. These Cl-poor compositions are reflected in apatite in associated sills, dikes and chilled margins (Boudreau 1995). In contrast, those from the Stillwater and Bushveld complexes at and below the major PGE reefs are unusually Cl-Rich.

This is consistent with both Cl and H isotopic evidence as well (fig. 2). While Stillwater Cl isotope values are equivocal (but see below), most Bushveld samples overlap the range of values for pristine MORB and altered seafloor samples ($\delta^{37}Cl \sim +4$ ‰ relative to sea water). This contrasts with the sedimentary floor rocks ($\delta^{37}Cl \sim +0$ ‰), with little evidence of contamination away from the marginal rocks. The Cl isotope composition and high Cl/F ratio is therefore a fundamental characteristic of the first magmas and not derived from marginal samples.

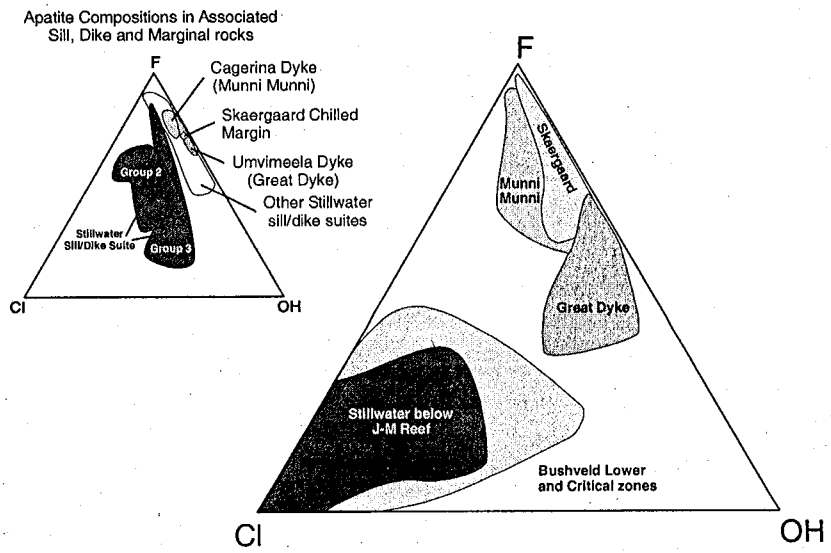

Figure 1. Composition apatite from some layered intrusions. Inset at left: Composition of apatite from coeval sills and dikes as well as those from chilled margins.

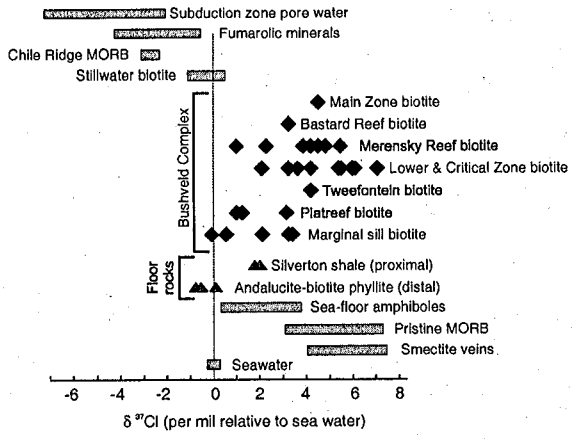

Figure 2. Comparison of Cl isotopic variations of the Stillwater and Bushveld complexes with those of other geologic environments. Data from Boudreau et al (1997), Willmore et al. (2002) and reference therein.

Similarly, a number of studies have shown that the O and H isotopes are largely constant with the volatile components being magmatic and not introduced. Of interest for this discussion is the overlap of Bushveld H isotopes with those of boninites (fig. 3).

The Boninite Analog

The Stillwater group 2 and 3 coeval sills and dikes, as well as the B1 sills of the Bushveld Complex, are high-Mg basalt with boninitic affinities, i.e. generally low TiO_2, but high K_2O and light REE (LREE) contents (fig.2). As has been proposed for boninites (e.g., Hickey and Frey, 1982), these compositional characteristics suggest that these magmas were generated from mantle that had undergone a previous basalt extraction event—but was subsequently enriched by a metasomatic (fluid) agent (Hatton and Sharpe, 1989; Wooden et al., 1991). An early melting event would have resulted in loss of halogen-bearing minerals, leaving a source depleted in F as well as Cl. Later infiltration by a Cl- rich metasomatic agent (fluid or volatile-rich silicate liquid) would have produced a metasomatized mantle with a high Cl/F ratio.

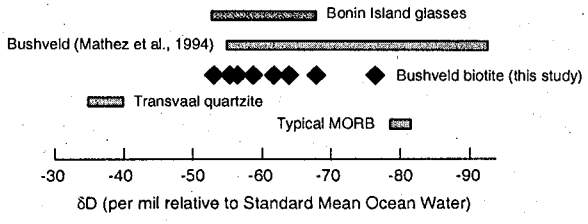

Figure 3. Comparison of H isotopes of the Bushveld complex with those of other geologic environments.

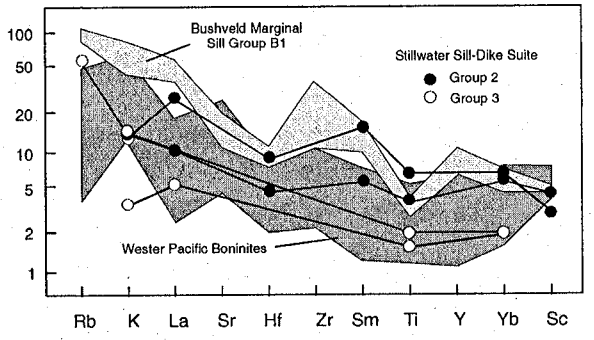

Figure 4. Spider diagram comparing Stillwater, Bushveld and boninite compositional characteristics. Data from Helz, 1985; Hatton and Sharpe, 1989.

In their discussion of potential isotopic sources for Stillwater magmas, Wooden et al. (1991) suggested that the metasomatic component was derived from subducted crustal rocks. As summarized by McCallum (1996), this model satisfies most of the known isotopic constraints for a Stillwater parent liquid, as it would elevate Pb and Sr but lower Nd isotopic ratios while having little effect on Os ratios as the high Os content of the mantle is unaffected by crustal contamination.

Incorporation of subducted material also provides a straightforward mechanism to recycle Cl back into the mantle (e.g., Anderson, 1974). In addition, as discussed by Keppler (1996) and You et al. (1996), a Cl-bearing hydrous fluid will preferentially incorporate alkalis, Pb, Sr and the light REE over Ti and the heavy REE as compared with a silicate liquid at mantle pressures. Thus a slab-derived fluid could give rise to observed elevated Cl/F, K and the LREE in the Stillwater source regions.

Subduction also appears able to fractionate the Cl isotopes, with light Cl characteristic of subduction zone pore water (Fig. 2). The light Cl of the Stillwater biotite and Chile Ridge MORB Cl zone as compared with more typical mantle values (Fig. 3) is consistent with the influenced of shallow subducted crustal fluids. This suggests more incorporation of light (shallow) crustal Cl (and water?) in the case of the Stillwater than occurred in the Bushveld.

A fluid involvement in the Stillwater and Bushveld source regions is also consistent with the high Cl/F weight ratio of Stillwater assemblages. Cl/F weight ratios in modern magmas are typically higher in arc-related magmas (melts generally considered to be the result of fluxing by volatiles derived from the subducted slab) as compared with MORB magmas (melts generated by decompression of upwelling mantle) (Table 1). MORB magmas

typically have Cl/F ratios less than about 1.0. Where unusually high Cl concentrations are reported in MORB, they are associated with higher water contents. In contrast are data from subduction-related magmas, particularly boninites, for which Cl/F ratios are typically an order of magnitude higher. As for arc-related magmas, the high Cl/F ratio of Stillwater assemblages suggest that melting in the Stillwater source region was initiated by an infiltrating fluid.

In addition, as noted by Schilling et al. (1980) for oceanic magmas and illustrated by the data of Table 1 for basic magmas in general, the Cl/F weight ratio is a useful indicator of overall volatile contents. In this regard, the high Cl/F ratio of the Stillwater and Bushveld mineral assemblages is indicative of an overall higher volatile content in the primitive magmas than is generally assumed. If the compositional comparison with modern boninites noted previously holds true for volatile elements as well, these parent liquids could have had in excess of 1 wt % H_2O.

Finally, the higher water content of Bushveld and Stillwater magmas needs to be incorporated in estimates of initial magma compositions as well as in crystallization models. The added water allows for the stabilization of olivine and has a strong effect on liquidus temperatures. In addition, the eventual separation of a volatile-rich fluid phase from interstitial liquids can transport the PGE and cause extensive recrystallization and even melting within the crystal pile.

References

Anderson, A. T., Jr, 1974. Chlorine, sulfur and water in magmas and oceans. Geological Society of America Bulletin 85:1485-1492.

Boudreau, A. E., 1999. Fluid fluxing of cumulates: The J-M Reef and associated rocks of the Stillwater Complex, Montana. Journal of Petrology, 40:755-772.

Boudreau, A.E., Stewart, M.A. and Spivack, A.J. 1997. Stable chlorine isotopes and the origin of high-Cl magmas of the Stillwater Complex, Montana. Geology, 25: 791-794.

Dobson, P.F, and O'Neil, J.R. 1987. Stable isotope compositions and water contents of boninite series volcanic rocks from Chichi-jima, Bonin Islands, Japan. Earth and Planetary Science Letters, 82: 75-86.

Hatton, C.J., and Sharpe, M.R., 1989. Significance and origin of boninite-like rocks associated with the Bushveld Complex, in Crawford, A.J., ed. Boninites, Unwin Hyman, Boston, 174-207.

Hickey, R., and Frey, F.A., 1982. Geochemical characteristics of boninite series volcanics: Implications for their sources. Geochemica et Cosmochimica Acta, 46: 2099-2115.

Keppler, H., 1996. Constraints from partitioning experiments on the composition of subduction zone fluids: Nature 380:101-117.

Table 1. Some representative Cl, F and H_2O contents of basic magmas from different geologic environments.

Environment	Cl (ppm)	F (ppm)	Cl/F	H_2O (wt. %)
Divergent margins (decompression melts)				
Mid-Atlantic Ridge(average)	100	200	0.5	0.21
Galapagos Spreading Center	400 - 3200	100-700	4 - 12	0.13 - 0.96
Flanking seamounts,				
East Pacific Rise	30 - 2260	40-240	1.9 - 15	0.1- 1.0
Convergent margins (flux melts)				
Continental arcs				
Columbia	830 ± 520	430 ± 200	1.1 - 9.1	<~2.0
Etna	1700	470	3.6	1.42
Crater Lake	1880 ± 70	400 ± 40	4.7	3.8-5.3
Island Arc Basalt				1.0 - 2.9
Boninites				1.2 - 2.5
Bonin Island		800 - 1740	67-116	8.6 - 15
Stillwater sill and dike group 2 and 3	Estimate from apatite composition		10-100	~1.0
Bushveld Lower and Critical zones	Estimate from apatite composition		10-100	~1.0

References: Boudreau et al (1997) and reference therein, Willmore et al. (2002)

Kyser, T.K., and O'Neil, J.R., 1984. Hydrogen isotope systematics of submarine basalts. Geochimica et Cosmochimica Acta, 48: 2123-2133.

Mathez, E.A, Agrinier, and Hutchens, R. 1994. Hydrogen isotope composition of the Merensky reef and related rocks, Atok section, Bushveld Complex. Economic Geology, 89: 791-802.

Schilling, J.-G., Bergeron, M.B., and Evans, R. 1980. Halogens in the mantle beneath the North Atlantic. Phil. Trans. Royal Society of London, A297: 147-178.

Sharpe,M. R. , Hulbert L. J., 1985. Utramafic sills beneath the eastern Bushveld Complex: Mobiized suspensions of early lower zone cumuates in a parent magma with boninitic affinities Econ. Geol. 80: 849 - 871.

Willmore C.C., Boudreau, A.E., and Kruger, F. J. 1999. The Halogen Geochemistry of the Bushveld Complex, Republic of South Africa: Implications for Chalcophile Element Distribution in the Lower and Critical zones. Journal of Petrology, 41: 1517-1539.

Wilmore, C.W., Boudreau A. E., Spivack, A. and Kruger, F.J. (2002). Halogens of the Bushveld complex, South Africa □^{37}Cl and Cl/F evidence for hydration melting of the source region in a back-are setting. Chemical Geology, v. 182, p. 503-511.

PGM and Complex Ni-Fe-Cu-Co Arsenide-Sulfide Paragenesis Associated with Fe-Ti-V Oxides of the Gulçari Magnetitite Pod, Rio Jacaré Sill, Bahia, Brazil

Reinaldo Santana Correia de Brito[1], Ariplinio Antonio Nilson[2] and Gilles Laflamme [3]
[1]CPRM, Geological Survey of Brazil, SUREG-RE, Recife, Pernambuco
[2] Instituto de Geociências, Universidade de Brasilia, Brasília, Brazil
[3]CANMET, Mining and Mineral Sciences Laboratories, Ottawa, Ontario, Canada
e-mail: rscdebrito@bol.com.br, aanilson@unb.br, glaflamme@nrcan.gc.ca

Introduction

Mafic and ultramafic layered intrusions are well known repositories of important magmatic metalic ore deposits. The best example of such intrusions is the Bushveld Complex in South Africa which exhibits mineralization of chromite, platinum-group metals, and Fe-Ti-V magnetic iron ores. Orthomagmatic processes driven by differentiation of large magma chambers are commonly used to explain such mineralization. Special regard has been historically given to Cu-Ni sulfide-related PGE mineralization and also to PGE-enriched sulfide-bearing chromitites. As the magnetitite ore bodies in layered intrusions have been mined solely for the Fe-Ti and V their role as potential PGE carrier have been seldomly studied. In this paper we intend to contribute to this particular issue by investigating one of these magnetite ore deposits as an alternative source of PGE. We present petrographic and mineral chemistry studies of the magnetic iron ores of the layered gabbroic Rio Jacaré Sill (RJS), Bahia (Brazil) and the associated PGE mineralization.

Magnetite pod-like bodies occur in the layered units of the Rio Jacaré Sill. The Gulçari pod is the main RJS magnetite deposit; it is located in the Lower Transition Zone of this intrusion. The pod consists a sequence of magnetitite, pyroxenite and gabbro layers. The known reserves are $2{,}0 \times 10^6$ tons of vanadiferous iron ore, bearing a mean grade of 2% V2O5. The magnetic iron ore also exhibits PGE values up to 4 ppm Pt, 1ppm Pd, and average grade of 400 ppb total PGE. Complex platinum-group minerals, PGM, were identified in the anomalous PGE intervals which were studied by Sá et al (1993). They form an oxide-PGM-arsenide/sulfide paragenesis which shows three distinct textural features. The first, considered as a primary feature, refers to exsolved Pt-Cu alloys within complex sulfide grains poikilitically enclosed in cumulus magnetite and ilmenite. The second one corresponds exsolution fringes of PGM on arsenides that occupy intercumulus space. The third textural type is represented by fracture-filling tiny PGE alloy particles in both silicate and Fe-Ti-V-oxide grains.

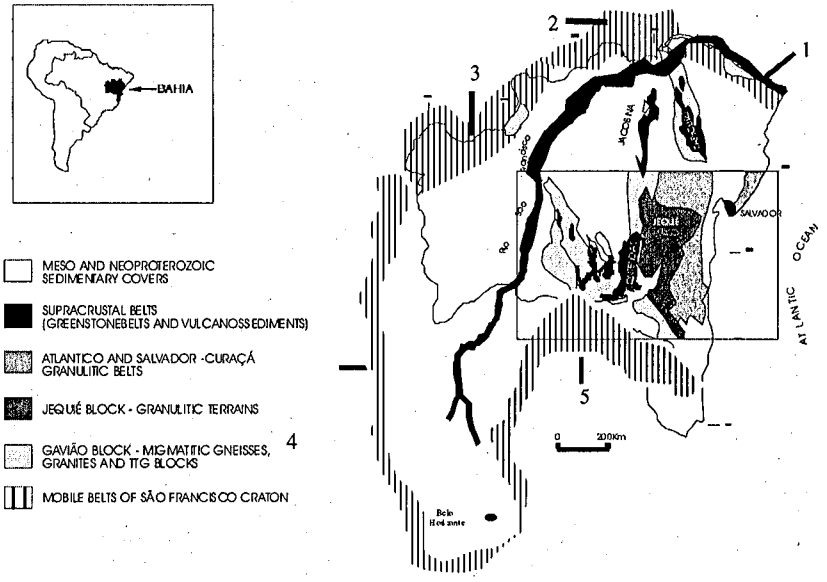

Figure 1. Geological outline of the S. Francisco Craton and the localization of the Rio Jacaré Sill. After Mascarenhas, (1976) and Almeida and Hasui, (1981).

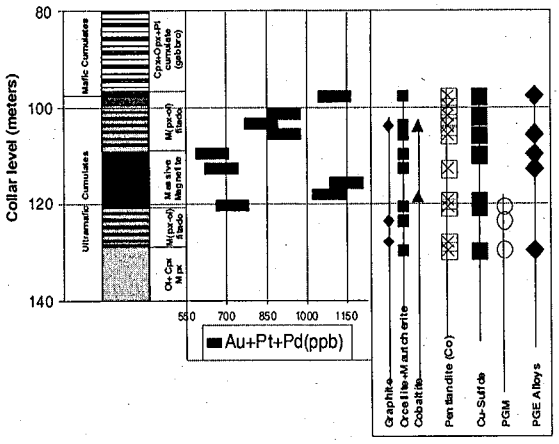

Figure 2. PGE, PGM and associated sulfide- arsenide paragenesis of the Fe-Ti-V oxide minerallization ofthe FGA40 drill core of. the Gulçari Farm prospect. (After Brito 2000).

Geology

The Rio Jacaré Sill is a 70km long, 1km wide synvolcanic Archean (2,841 ± 68 Ma Sm-Nd age, Brito et al. 1999) layered intrusion. It is intruded into folded and metamorphosed basaltic and andesitic rocks interbedded with continental sediments of the Archean Mirante Complex (Brito 2000). This Complex consists of the Mirante Formation (MFm.) and RJS; it is equivalent to the intermediate unit of the Contendas-Mirante Group of Marinho et al. (1994). The complex lies along the southern part of the Contendas-Jacobina Lineament, (fig1), which defines the limit between the Jequié and Gavião Blocks in the central-northern part of the São Francisco Craton.

The Rio Jacaré Sill

R.J.S. is divided up into three zones: a Lower Zone (LZ) which is 300m thick, a Transition Zone (TZ), 200-100 thick and an Upper Zone (UZ) which is 600 to 1000m thick. Lz consists of medium-grained gabbros that exhibit increase in clinopyroxene modal proportion and plagioclase grain size decrease towards TZ. TZ is made up of ultramafic cumulates consisting of cumulus olivine, clinopyroxene, magnetite and ilmenite that grade from magnetite peridotite, magnetitite with pyroxene and magnetite pyroxenite and mafic cumulates with cumulus plagioclase and clinopyroxene and minor hypersthene. Magnetite is usually a cumulus phase but sometimes it may be an intercumulus mineral. Monomineralic and bimodal cumulates define a microrythmically layered sequence of pyroxenite and gabbros with variable amounts of magnetite. Varied-textured fine to medium-grained gabbroic rocks occur in TZ as enclaves of decimetric to block size of fine-grained gabbro, sometimes pillow-shaped; they also may be present as thin sill-like sheets of diabasic rocks. These varied-textured rocks are interpreted as the result of mixing between different magmas. The Upper Zone consists of two subzones: UZ1 is gabbroic to pyroxenitic and UZ2 is gabbroic and leucogabbroic to anorthositic. UZ1 is a rhythmically banded sequence of micro-layered gabbro-pyroxenite-magnetitite, pyroxenite-ferro-gabbro and magnetite-bearing anorthosite. UZII consists of modally layered rocks divided in three units, a, b, and c. Unit a is made of medium to coarse-grained leucogabbro, unit b is composed of coarse-grained leucogabbro and unit c consists of medium to coarse-grained leucogabbro and anorthosite.

Mineralization

RJS hosts massive magnetitite pod-like bodies confined to a layered sequence of mafic and ultramafic cumulates. They are named lower and upper magnetite seams.

The lower magnetite seam is represented by the Gulçari pod which occurs within the lower Transition Zone. This pod is a 300m long, 150m thick sequence of magnetite, pyroxenite and gabbro layers carrying 2 million tons of vanadiferous iron ore with mean grade of 2% V2O5, that displays PGE values up to 4 ppm Pt, 1ppm Pd and average grade of 400ppb total PGE. Magnetite layers are interbeded with ultramafic and mafic cumulates (fig 2). The ultramafic cumulates are transgressive towards the contact with the Lower Zone gabbros and consist of olivine-magnetite cumulates, and clinopyroxene-magnetite heteradcumulates.

The massive magnetite layers are made up of ilmenite-magnetite heteradcumulates that form 2 cm to 3 meters thick layers that contain variable amounts of clinopyroxene (En 32-38). Associated mafic cumulates are rythmically microlayered gabbro, magnetite, and magnetite-piroxenite bands. The outer contacts of the magnetite pod exibit hornblende-rich rocks and dunite in places. These features are suggestive of a zoned pattern that Brito (1984) interpreted as similar to the magnetite pipe-like bodies of the Bushveld Complex (Willemse 1979). The upper Transition Zone pod-like magnetite bodies are groupings of magnetite seams and pyroxenites that form 150m long, 20m thick masses of 150,000 tons of vanadiferous iron ore with mean grade of 0.5% V2O5 and maximum total PGE contents of 1.3 ppm and mean grade of 380 ppb. The upper Transition

Zone also contains a low grade Cu sulfide mineralization which is confined to the lowermost layers of the upper magnetite seams.

Ore Mineralogy and Microtextural Features

Fe-Ti-V Oxides. The main ore minerals are the Fe-Ti-V oxides, magnetite and ilmenite, which occur together with olivine (Fo 46), clinopyroxene, and metamorphic minerals such as amphiboles (cummingtonite, and Fe-tschermackite), and serpentine. Clinopyroxene is altered to chlorite, especially at the borders of grains. Magnetite and ilmenite show cumulus texture; ilmenite is the early crystallizing phase.

Individual grains of magnetite and ilmenite show round shapes suggesting adcumulate growth. Magnetite and ilmenite also show poligonized shapes, curved borders, and policrystalline mosaics with 120 degrees dihedral angles at triple junctions. This suggests that annealing processes took place during subsolidus cooling. Magnetite shows rare broad ilmenite lamellar intergrowths of the so-called sandwich microtexture. It also show trellis microtextutres, which is a network of fine ilmenite lamellae exsolved at acute angles. Ilmenite also forms round to irregular shaped exsolved grains at the trellis intersections.

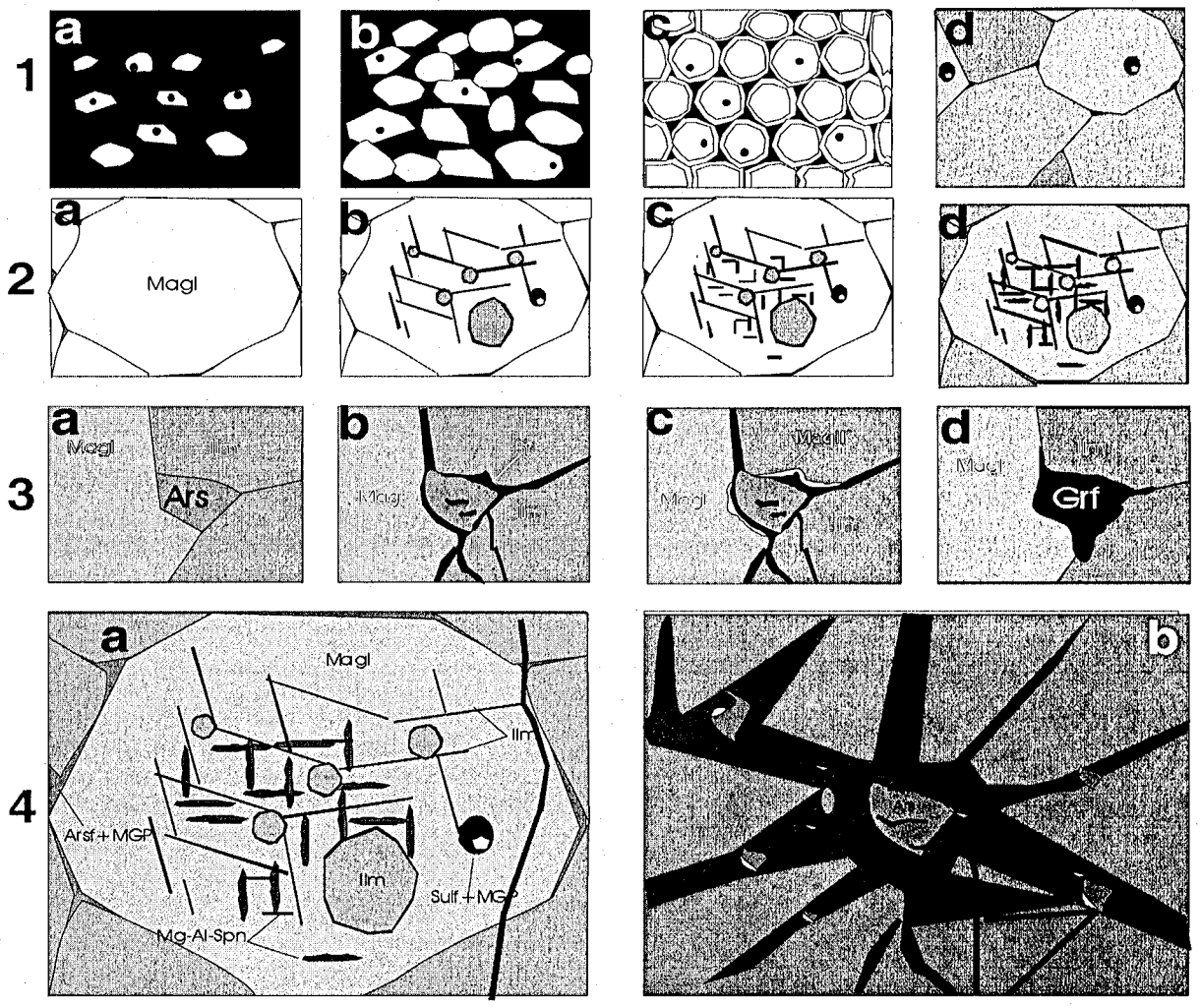

Figure 3. Microtextural evolution of the mineralization:1-Cumulus stage:1 a-nucleation of ilmenite and magnetite around EGP-rich sulfides. 1b and 1c, adcumulate overgrowth. 1d- Annealing and Al-rich spinel formation external to magnetite.2-Exsolutions: 2a.-Arsenic-bearing fluid injection at triple junctions. 2b- Formation of tellis-type oxiexsolution. 2c - Separation of ulvospinel via cloth texture exsolution. 2d- Exsolution of Mg-Al spinel from ulvospinel.3- Hydrothermal mineralization: 3a. Increasing fluid pressure promotes separation of grains by dilation of conctacts. 3b-Sulphur-enriched fluid arrival at arsenide and oxide interfaces. 3d. - Oxidation of sulfides.4- Current aspect of the mineralization: 4a.- Syngenetic Fe-Ti-V oxide-hosted PGE mineralization. 4b- Hydrothermal PGE mineralization associated with arsenides, sulfides and fracture-bound PGE alloys.Abreviations : Mag1=primary magnetite; Mag2= Secondary (hydrothermal) magnetite; Ilm = Ilmenite; Sf = Sulfide; Ars = Arsenide; Grf = Grafite; Spn = spinel.

Magnetite also shows the typical cloth microtexture which the exsolution of ulvospinel lamellae inthe 100 plane of the magnetite crystals. Aluminous magnesian spinel also occurs as fine exsolution lamellae within magnetite grains. Geothermo-barometric studies indicate that these ores underwent interoxide re-equlibration under reducing conditions defined by ilmenite. Ilmenite and olivine show equilibrium temperatures from 950 to 550oC. Ilmenite and magnetite coexisting grains yielded temperatures as low as 450-550 C at low fO2.

Platinum-Group Minerals and associated sulfides and Asenides

Eleven PGM-bearing phases have been identified. These minerals are associated with sulfides and arsenides within the iron-oxide grains and sometimes they are silicate-hosted. Sperrylite occurs as tiny (10μm) round grains whithin magnetite; sometimes it is silicate-hosted. It also shows external exsolution of gversite which is associated to cobaltite. Gversite also is associated with cobaltite in grains where it forms coronas around mautcherite. Cabriite occurs as very tiny grains (1μm) external to orcellite, in contact with silicate (cummingtonite). Cabriite also forms fracture-filling tiny grains (1μm) associated with oxidized chalcopyrite , orcellite and secondary magnetite (pure Fe3O4) . Cu-Pt alloys are usually enclosed in magnetite and form complex grains, that exhibit intergrowths with pyrrotite, chalcopyrite and bornite. These Pt-Cu alloys have been identified as isoferroplatinum. Platinum also occurs as platinian awaruite (5% Pt) forming 5μm round euhedral grains. Pt-free awaruite usually forms larger grains (10μm).

Discussion

The PGM, arsenides, sulfides, Fe-Ti-V oxides and silicate paragenesis exhibit textural features indicative of a sequence of magmatic and hydrothermal events. Aiming to explain the exotic relationship between Fe-Ti-V spinels and PGE mineralization we present a simple model of textural evolution via a three stage mineralizing process (figure 3). We suggest a first stage represented by the classic PGE collection by sulfides which were later captured within Fe-Ti-V oxides during cumulus processes. The second stage consisted of PGE-bearing arsenic post-cumumlus fluid injections which were deposited as PGE-bearing arsenides in intercumulus space. The third stage refers to the redistribution of these syngenetic PGE concentrations by late post-magmatic/metamorphic fluids.

The first stage represents orthomagmatic PGE mineralization which could to a certain extent be compared with PGM particles enclosed in chromite grains as shown in other layered intrusions. The second stage could be related to hydrothermal late arsenic-rich syn-magmatic fluids possibly related to crystallization compaction. The last phase may be ascribed to post-magmatic redistribution of PGE via a metamorphic fluid.

References

Brito, R.S.C.de. 1984, Geologia do Sill Estratificado do Rio Jacaré: In Actas Congresso Brasileiro de Geologia Rio de Janeiro., v. IX, p. 4316-4334

_____ 2000. Geologia e petrologia do sill máfico ultramamáfico do Rio Jacaré - Bahia e estudo das mineralizações de Fe-Ti-V e platinóides associados: Unpub. Ph.D. thesis, n. 39, I.G. Univ. of Brasília 325p.

Brito, R.S.C.de.; Pimentel, M.M.; Nilson, A.A.; Gioia, S.M. 1999. Samarium-Neodymium and Rubidium-strontium isotopic systematics of the Rio Jacare Sill – Bahia – Brazil: In Actas II South American Symposium on isotope geology. Cordoba. p. 44-47.

Marinho, M.M.; Galvão, C.F.; Nonato, I.F.; Silva, L.; D. da; Brito, R.S.C. de., 1994, Geologia e Potencialidade mineral de Borda Nordeste da faixa Contendas Mirante e do Sill do Rio Jacaré Bahia: CBPM, Série Arquivos Abertos, n. 6, 30 p.

Sá J.H.S.; Barnes, S.J.; Prichard, H.M.; Bowles, J.F.W.1993 Platinum-Paladium in iron-rich rocks of Rio Jacaré Complex: In I Brazilian PGE Meeting, extended abstracts p.77-78.

Willemse, J. 1969 The vanadiferous magnetic iron ore of the Bushveld Complex: ECON. GEOL., MON., v. 4, p. 187-208.

Review of Brazilian Chromite Deposits Associated with Layered Complexes: Constraints for the Postulated Genetic Models

Cesar F. Ferreira Filho[1], Juliana C. Marques[1], Carlos A. Spier[2], Sylvia M. Araújo[1] and Filipe S. M. Porto[1]
[1]Instituto de Geociências, Universidade de Brasília, Brasília, DF, 70910-900.
[2]Mineraçoes Brasileiras Reunidas, Av. de Ligação 3580, Nova Lima, MG, 34000-000
e-mail: cesarf@unb.br

Introduction

Chromitites represent a special case of cumulate rock where chromite is the only cumulus phase. Formation of chromitites thus requires that phase relations of the appropriate system be somehow changed to allow the system to fall into the chromite stability field. Several mechanisms for the formation of chromitite seams have been postulated. They include the contamination of the basic parental magma by sialic rocks, the change in total pressure, the influx of fresh magma into the magma chamber, and changes in oxygen fugacity. In order to test the postulated models, chromitites and hosting mafic and ultramafic rocks from three layered complexes in Brazil were investigated (Fig. 1). The main purpose of these studies was to provide an integrated understanding of the primary igneous evolution of chromitite seams and their host rocks, focusing on magma chamber processes leading to the formation of chomitites. In this paper we summarize the previous results and use them to review the genetic models.

The layered intrusions investigated: Bacuri Complex (Amapá), Niquelândia Complex (Goiás), and Ipueira-Medrado Sill (Bahia), have distinct geological settings and igneous stratigraphy, thus providing an opportunity to look at chromitites formed in different geological-petrological environments.

The Chromite Deposits of the Bacuri Complex

The tectonic setting, geology and chromite deposits of the Bacuri mafic-ultramafic layered complex (Fig. 1) were recently investigated (Spier and Ferreira Filho, 2001; Pimentel et al., 2002; Prichard et al., 2001). The chromite deposits of the Bacuri Mafic-Ultramafic Complex (BMUC) consist of 8.8 Mt. of ore grading 34% Cr_2O_3, representing the second largest reserves of chromite in Brazil. The BMUC is a major Paleoproterozoic (ca. 2.2 Ga) layered intrusion overprinted by ductile deformation and associated regional amphibolite facies metamorphism of the Transamazonian Cycle (ca. 2.0 Ga). The BMUC is intrusive into gneiss-migmatite terranes of the Guyana Shield.

The BMUC consists of a Lower Mafic Zone (> 500 meters-thick), an Ultramafic Zone (30-120 meters-thick) and an Upper Mafic Zone (> 300 meters-thick). The Ultramafic Zone consists of interlayered serpentinite (olivine cumulate) and chromitite (chromite cumulate). Most of the chromite is concentrated in a few meters-thick chromitite layer located at the base of the Ultramafic Zone in direct contact with the underlying Lower Mafic Zone (Fig. 2). Cryptic variation data (Fig. 2) are consistent with extensive fractionation within the UZ. The stratigraphic position of the main chromitite and cryptic variations in the UZ strongly supports a model for its origin associated with a major new influx of primitive magma, and mixing with more fractionated resident magma. The composition of chromite in massive chromitite of the BMUC is compared with other deposits in Table 1. The Mg ratio of chromite from the BMUC extends over a wide range (0.15-0.55), while the Cr ratios are very high (0.66 - 0.89) and vary through a smaller range.

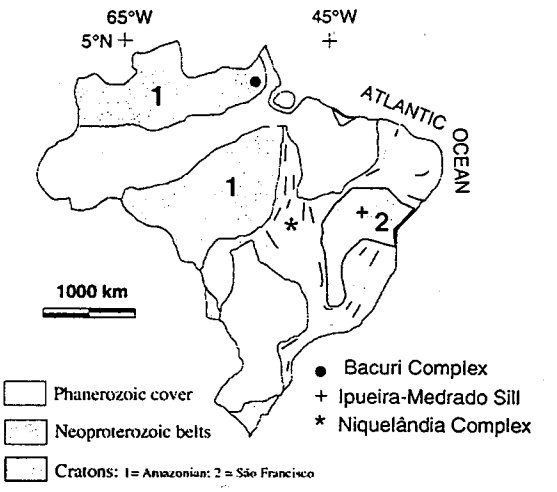

Figure 1. Schmatic location of the chromite mineralizatied layered complexes in Brazil.

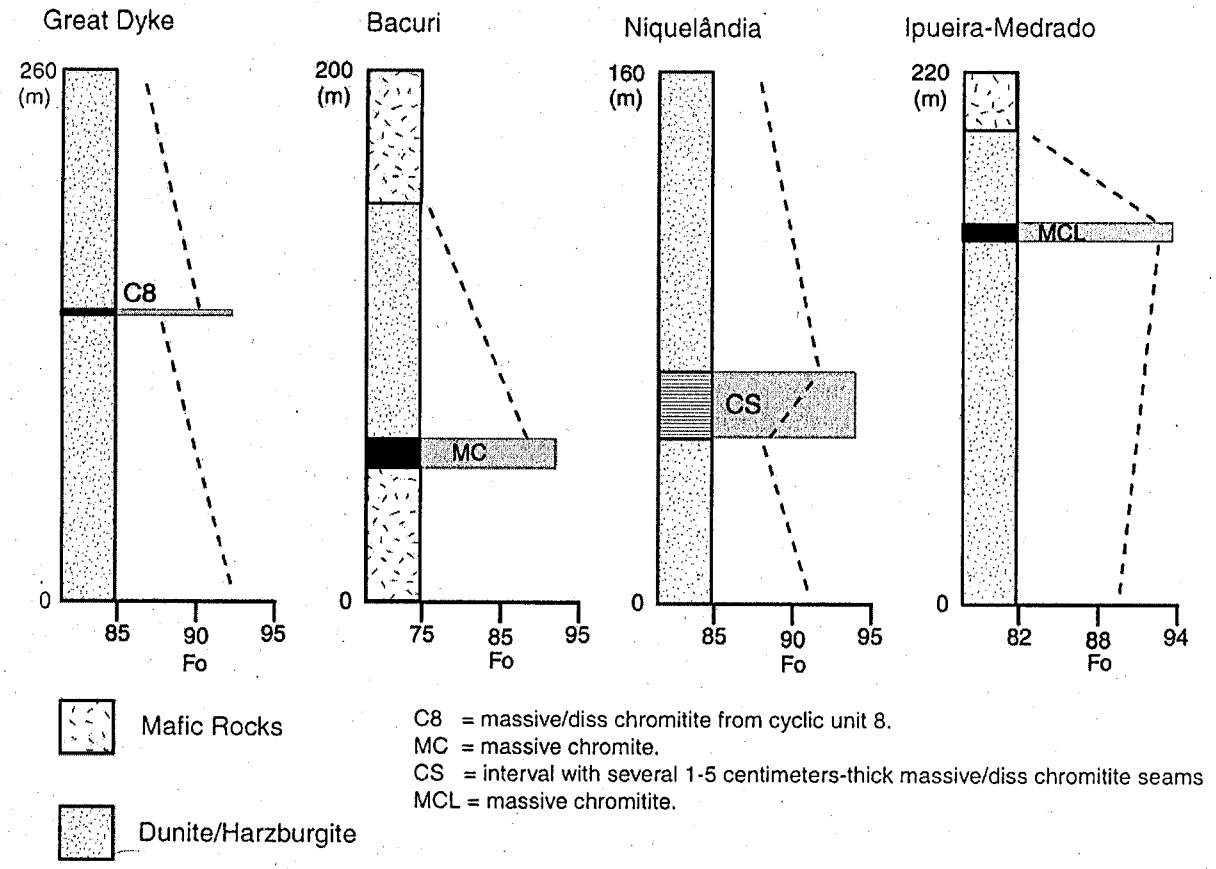

Figure 2. Schematic sections of chromitites from different layered complexes. Olivine cryptic variations indicate the general fractionation trend closely associated to chromitites. Data from the great Dyke are from Wilson et al. (1982).

The Chromitites of the Niquelândia Complex

The tectonic setting, geology and petrology of the Niquelândia Complex were considered in several papers and recently reviewed by Ferreira Filho et al. (1998; 2000). Previous investigations of the non-economic chromitite seams of the Niquelândia Complex were mainly focused on their anomalous PGE contents (Ferreira Filho et al., 1995). The Niquelândia Complex is a major layered intrusion that was affected by tectonic-metamorphic events during the Neoproterozoic. The estimated age for the Lower Layered Series (LS) of the Niquelândia Complex is Paleoproterozoic (ca. 2.0 Ga). The LS has an estimated thickness of several km, consisting of a Lower Mafic Zone (mainly gabbronorite), an Ultramafic Zone (interlayered dunite/pyroxenite) and an Upper Mafic Zone (mainly gabbronorite and pyroxenite).

The chromitite seams consist of several few centimeters-thick layers restricted to a 20 meters-thick interval of the estimated 3 km-thick Ultramafic Zone of the LS. Detailed study of the mineralized interval (Ferreira Filho et al., in prep) indicates that chromitites are interlayered with homogeneous dunite (olivine ± chromite adcumulate) of the Ultramafic Zone (Fig. 2). Cryptic variations indicate that the 20 meters-thick interval marks a slight reversal of the fractionation path (Fig. 2). The data support a model for its origin associated with new influx of primitive magma, and mixing with slightly more fractionated resident magma. The composition of chromite in massive chromitite of the Niquelândia Complex is compared with other deposits in Table 1. The Mg ratio of chromite from the Niquelândia Complex extends over a narrow range (0.48-0.57), while the Cr ratios extend over a wider range (0.58-0.71). The small range of Mg ratio is compatible with the very restricted variation of olivine (Fo 87-93) from interlayered dunites.

Table 1. Compositional features of chromite and olivine from different chromite-mineralized layered complexes.

Layered Complex	Crhomite in massive chromitite			Olivine		Age (Ga)
	Mg ratio	Cr ratio	Ti^{+4}	Fo	NiO	
Bushveld	0.24-0.58	0.60-0.75	0.13-1.06	77-88	na	2.05
Great Dyke	0.36-0.67	0.70-0.80	0.02-0.13	84-92	0.18-0.44	2.74
Stillwater	0.39-0.57	0.60-0.66	0.02-0.28	79-90	0.11-0.33	2.46
Bacuri	0.15-0.55	0.66-0.89	0.03-0.70	76-91	0.18-0.66	ca. 2.2
Ipueira-Medrado	0.45-0.72	0.58-0.68	0.09-0.44	84-93	0.18-0.47	ca. 2.0
Niquelândia	0.48-0.57	0.58-0.71	0.04-0.07	87-93	0.20-0.45	ca. 2.0

Adapted from Spier & Ferreira Filho (2001), Marques & Ferreira Filho (2002), and Stowe (1994)
na = systematic data not available.
Mg ratio = $Mg/(Mg+Fe^{+2})$; Cr ratio = $Cr/(Cr+Al)$.

The Chromite Deposit of the Ipueira-Medrado Sill

The geology, petrology and chromite deposits of the Ipueira-Medrado sill, a Paleoproterozoic (ca. 2.0 Ga) mafic-ultramafic intrusion, were recently investigated (Marques and Ferreira Filho, 2002; Marques et al., 2002). The chromite deposit of the Ipueira-Medrado sill consists of 4.5 Mt. of ore grading 30-40 wt. % Cr_2O_3, representing one of several chromite-mineralized intrusions of the Jacurici Complex, the largest reserve of chromite in Brazil with over 30 Mt of ore. The Jacurici Complex consists of a NS trending (70 km-long to 20 km-wide) swarm of mafic-ultramafic chromite mineralized bodies hosted by granulite-gneiss terranes of the São Francisco Craton (Fig. 1).

At the Ipueira-Medrado Sill, a 5-8 meters-thick massive chromitite layer (MCL) is hosted by a 200-300 meters-thick layered intrusion. The sill is subdivided in a Marginal Zone, consisting of sheared gabbro and harzburgite; an Ultramafic Zone consisting of dunite, harzburgite, chromitite and minor orthopyroxenite; and an upper Mafic Zone consisting of leuco- to melanorites. The MCL is located at the upper part of the Ultramafic Zone. Cryptic variations of olivine and orthopyroxene throughout the stratigraphy indicate that the sill consists of two intervals with distinct magmatic evolution. The interval located below the MCL is characterized by slow evolution of mineral compositions toward more primitive compositions. The interval located above the MCL is characterized by fast upward evolution toward more fractionated compositions (Fig. 2). The data suggest that the interval below the MCL crystallized in a dynamic magma chamber undergoing frequent replenishment with primitive magma. The magmatic evolution above the MCL suggests that crystallization occurred in a mainly closed magma chamber. The MCL is located at the transition from dynamic open system to mainly closed system magma chamber. The most primitive compositions are observed just below or at the MCL. Cryptic variations are the opposite to what is expected as the result of mixing new influxes of primitive liquid with residual fractionated liquid in the magma chamber. Re-Os and Sm-Nd data indicate strong contamination of the magma at or above the MCL, suggesting that chromite crystallization was triggered by changes of physical-chemical conditions associated to crustal contamination. The composition of chromite in massive chromitite of the Ipueira-Medrado sill is compared with other deposits in Table 1. The Mg ratio of chromite from the Ipueira-Medrado sill extends over a wide range (0.45-0.72), while the Cr ratios (0.58 - 0.68) vary through a smaller range.

Conclusions

Chromitites occur at the base of cyclic units in several layered complex suggesting that chromitites are formed by mixing new influxes of primitive liquid with residual fractionated liquid in the magma chamber (Irvine 1977). Evidence for such model is suggested by changes in the cryptic variation and/or the sequence of cumulus phases illustrated at the Great Dyke, Bacuri and Niquelândia complexes (Fig. 2). However, cryptic variations at the Ipueira-Medrado chromite deposit do not support such model for the origin of the main chromitite layer. Isotope data suggest that chromite crystallization was triggered by changes of physical-chemical conditions associated to crustal contamination at the Ipueira-Medrado sill. The data indicate that chromitite layers are always

associated with major changes in the magma chamber. This study also indicates that the specific mechanism responsible for appropriate phase changes leading to chromite crystallization may be different for each deposit. The compositions of chromite from massive chromitites investigated in our studies occupy a broader compositional field than previously stated for stratiform chromites (Stowe, 1994). Compositional fields currently considered to be typical of stratiform chromite should be reviewed.

References

Ferreira Filho, C.F., Naldrett, A.J., and Asif, M., 1995, The distribution of Platinum-Group elements in the Niquelândia layered mafic and ultramafic intrusion, Brazil: implications with regard to exploration: Canadian Mineralogist, v. 33, p. 165-184.

Ferreira Filho, C.F., and Pimentel, M. M., 2000, Sm-Nd isotope systematics and REE data of troctolites and their metamorphic equivalents of the Niquelândia Complex, central Brazil: further constraints for the timing of magmatism and metamorphism: Journal of South American Earth Sciences, v. 13, p. 647-659.

Ferreira Filho, C.F., Naldrett, A.J., and Gorton, M.P., 1998, REE and pyroxene compositional variation across the Niquelândia mafic and ultramafic layered intrusion, Brazil: Petrological and metallogenetic implications: Transactions of the Institution of Mining and Metallurgy (section B: Appl Earth Sci.), v. 107, p. B1-B22.

Irvine, T.N., 1977, Origin of chromitite layers in the Muskox intrusion and other layered intrusions: a new interpretation: Geology, v. 5, p. 573-577.

Marques, J.C., and Ferreira Filho, C.F., 2002, The chromite deposits of the Ipueira-Medrado Sill, Bahia, Brazil: Submitted to Economic Geology.

Marques, J.C., Ferreira Filho, C.F., Carlson, R.W., and Pimentel, M.M., 2002, Re-Os and Sm-Nd isotope systematics and trace elements geochemistry constraints for the origin of the chromite deposits of the Ipueira-Medrado sill, Bahia, Brazil: Submitted to Journal of Petrology.

Pimentel, M.M., Spier, C.A., and Ferreira Filho, C.F., 2002, Estudo Sm-Nd do Complexo Máfico-Ultramáfico Bacuri, Amapá: Idade da Intrusão, Metamorfismo e Natureza do Magma Original: Submitted to Revista Brasileira de Geociências.

Prichard, H.M., Sá, J.H.S., and Fischer, P.C., 2001, Platinum-group mineral assemblages and chromite composition in the altered and deformed Bacuri Complex, Amapá, Northeastern Brazil: Canadian Mineralogist, v. 39, p. 377-396.

Spier, C.A., and Ferreira Filho, C.F., 2001, The chromite deposits of the Bacuri mafic-ultramafic layered complex, Guyana Shield, Amapá State, Brazil: Economic Geology, v. 96, p. 817-835.

Stowe, C.W., 1994, Compositions and tectonic settings of chromite deposits through time: Economic Geology, v. 89, p. 528-546.

Wilson, A.H., 1992, The Geology of the Great "Dyke", Zimbabwe: The Ultramafic Rocks: Journal of Petrology, v. 23, p. 240-292.

Multimillion-Ounce PGE Deposits of the Portimo Layered Igneous Complex, Finland

M. Iljina and E. Hanski
Geological Survey of Finland, P.O. Box 77, FIN-96101 Rovaniemi, Finland
e-mail: markku.iljina@gsf.fi, eero.hanski@gsf.fi

Structure and Megacyclic Units

The ca. 2440 Ma Portimo Layered Igneous Complex (Portimo Complex) is located in the central part of an intrusion belt that crosses Finland almost along the Arctic Circle. Other intrusions in this belt include the Kemi and Penikat intrusions containing a chromitite deposit and PGE reefs, respectively. The Portimo Complex is composed of three principal structural units (Fig. 1): 1) the Portimo Dikes, 2) the Narkaus intrusion, and 3) the Suhanko-Konttijärvi intrusion with the last one having two separate igneous bodies, Suhanko and Konttijärvi.

The Narkaus and Suhanko-Konttijärvi intrusions contain a marginal series and an overlying layered series. The two marginal series differ in thickness and their prevailing rock types. The Narkaus Marginal Series generally varies from 10 to 20 m in thickness, while the Suhanko-Konttijärvi Marginal Series reaches several tens of meters. The Narkaus Marginal Series is mainly composed of pyroxenites, whereas olivine cumulates commonly constitute the upper half of the Suhanko-Konttijärvi Marginal Series.

A striking difference between the layered series of the two intrusions is the presence of marked reversals in the Narkaus intrusion, as shown by thick ultramafic olivine-rich cumulate layers, whereas crystallization in the Suhanko-Konttijärvi intrusion proceeded without any notable reversals (Fig. 1). The major reversals in the Narkaus Layered Series resemble those of the Penikat intrusion and enable its layered series to be divided into three megacyclic units (MCU). The Megacyclic unit II is, however, found only in the central part of the Narkaus intrusion and fades away eastwards.

Mafic and ultramafic dikes called the Portimo Dikes are encountered in the basement below the Suhanko-Konttijärvi intrusion in the Konttijärvi and Ahmavaara areas (Fig. 1). The dikes have not been dated, and their inclusion in the same magmatic event as the intrusions proper is based on geochemistry. The dikes are subparallel to the basal contact of the intrusion and merge with it locally, so that a dike can actually form the basement of the intrusion.

The MCUs of the intrusions and the dikes were generated from two kinds of parental magmas differing slightly in composition: Cr-richer and Cr-poorer, in this order. The former type resembles SHMB or the Bushveld B1 magma. The Portimo Dikes and MCU I-II have been interpreted to have crystallized from the Cr-richer magma, while the Cr-poorer magma was parental for the Suhanko-Konttijärvi intrusion and MCU III of the Narkaus intrusion.

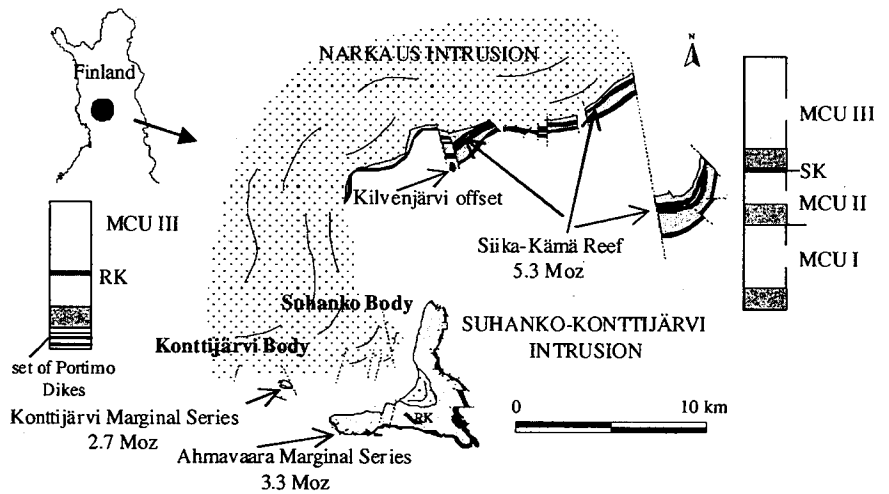

Figure 1. General geology, stratigraphic columns of the Suhanko-Konttijärvi (left) and Narkaus intrusions (ultramafic cumulates in gray). Archean rocks in white, layered intrusions in yellow (gabbros) and green (ultramafic) and younger supracrustal rocks stippled. SK = Siika-Kämä Reef and RK = Rytikangas Reef. Pt+Pd+Au resources, Outokumpu oyj press release.

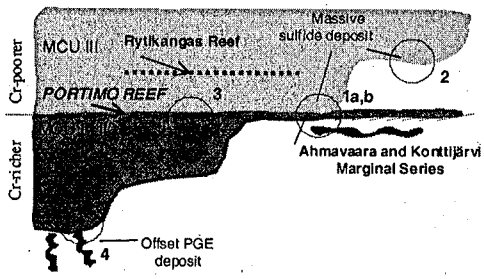

Figure 2. Structural interpretation of the Portimo Complex and the location of the PGE mineralization. Circles 1 - 4 refer to drill hole intersections depicted in Figures 3 - 6, respectively.

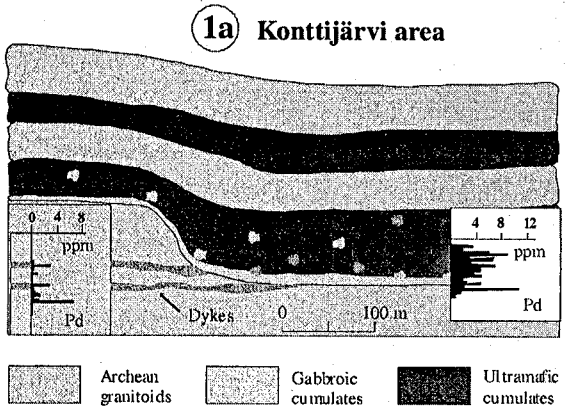

Figure 3. A: Incline cross-section through the Konttijärvi Marginal Series.

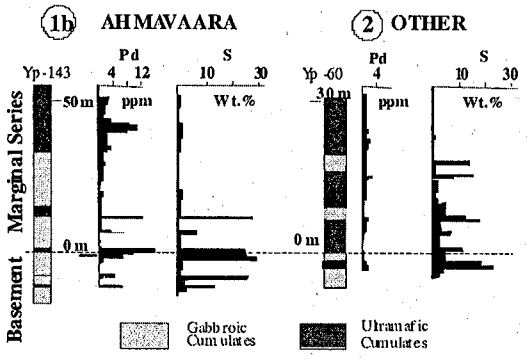

Figure 4. Comparison of Ahmavaara and another marginal series section of the Suhanko Body.

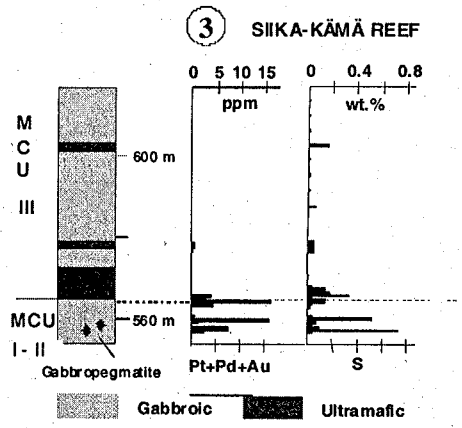

Figure 5. Drill hole section through the Siika-Kämä Reef.

PGE-Cu-Ni Mineralization

Among the layered intrusions in Fennoscandia, the Portimo Complex is exceptional in hosting a variety of PGE mineral deposits. Published resources are indicated in Fig. 1. The mineralization types include (Figs 2-6): a) PGE-bearing Cu-Ni sulfide disseminations in the marginal series of the Suhanko-Konttijärvi intrusion and Portimo Dikes; b) predominantly massive pyrrhotite deposits located close to the basal contact of the Suhanko-Konttijärvi intrusion; c) the Siika-Kämä PGE Reef in the Narkaus Layered Series; d) the Rytikangas PGE Reef in the layered series of the Suhanko Body; e) the offset Cu-PGE mineralization below the Narkaus intrusion

Disseminated PGE-bearing base metal sulfide concentrations (10–30 m thick) are encountered throughout the marginal series of the Suhanko-Konttijärvi intrusion (Alapieti et al., 1989; Iljina, 1994). Their distribution is erratic, and they generally extend from the lower peridotitic layer downwards for some 30 m into the basement. The PGE content varies from only weakly anomalous values to 2 ppm in most places in the marginal series of the Suhanko Body, but rises to over 10 ppm in several places in the Konttijärvi and Ahmavaara areas (Ni and Cu contents are generally less that 1 wt.% combined). In the same areas, the Portimo Dikes locally carry PGE up to several ppm (Circle 1a, Figs. 2 and 3). Co-precipitation of thorium and uranium minerals with Pd-Se minerals is also found within the Portimo Dikes.

Recent exploration has revealed that the small Konttijärvi Body has deep embayment structure in its center (Fig. 7). Highly PGE-enriched marginal series as encountered in the Konttijärvi-Ahmavaara areas are rare in layered intrusions, and the only other well-known occurrence is the Plat-

reef in the northern Bushveld Complex.

Massive sulfide concentrations are characteristic of the marginal series of the Suhanko Body. The massive sulfide deposits are slab-like concentrations generally varying in thickness from 20 cm to 20 m, and the individual slabs within deposit are separated from each other by more silicate-rich cumulate layers or granitoids. The slabs vary in location from 30 m below the basal contact of the intrusion to a position 20 m above it, within the marginal series. The massive sulfide concentrations vary in size from less than one million tonnes to more than ten million tonnes. The sulfide paragenesis is composed almost exclusively of pyrrhotite, except in the Ahmavaara deposit, which also contains chalcopyrite and pentlandite. Accordingly, the sulfide fraction of Ahmavaara contains 2.7 wt. % Ni and 2.4 wt. % Cu, while the other massive deposits hardly reach a half of these values.

The massive pyrrhotite deposits show low PGE values, with the maximum Pt+Pd normally reaching a few ppm (exemplified by Circle 2, Figs 2 and 4). Similarly to the sulfide disseminated marginal series, the PGE concentrations are much higher in the Ahmavaara deposit, attaining a level of 20 ppm (Circle 1b, Figs 2 and 4).

The Siika-Kämä PGE Reef of the Narkaus intrusion is located most typically at the base of MCU III (Figs 1, 2 and 5), but it can lie even tens of meters below that or in the middle of the olivine cumulate layer of MCU III (Huhtelin et al., 1989; Iljina, 1994). The reef is continuous over the whole strike length of ca. 15 km. The thickness varies from less than one meter to several meters, and many drill cores contain a number of mineralized layers separated by PGE-poor layers, which can be some meters thick. The PGE concentration varies from anomalous values of several hundred ppb to some tens of ppm. The Siika-Kämä mineralization is one of the sulfide-deficient PGE mineralizations in the Portimo Complex, sometimes containing no visible sulfides at all and hardly ever having a whole-rock sulfur content in excess of 1 wt.%.

The main PGE occurrence in the layered series of the Suhanko-Konttijärvi intrusion is the Rytikangas PGE Reef (Figs 1-2). Its position is known over a distance of 1.5 km. The Rytikangas Reef is hosted by poikilitic plagioclase, plagioclase-bronzite, and plagioclase-bronzite-augite orthocumulates, all containing augite oikocrysts. The orthocumulate layer varies in thickness from 30 cm to 10 m. The thickness of the Reef itself is 30–50 cm, and it is usually encountered on top of the poikilitic orthocumulate layer. PGE + Au concentration are up to 20 ppm.

The offset mineralization is sporadically distributed in the basement gneisses and granites below the Narkaus intrusion (Figs. 1, 2 and 6). The largest deposit, and also the best-known one, is that situated below the Kilvenjärvi block. The offset mineralization represents the richest PGE deposit type within the Portimo area with its Pt + Pd content reaching occasionally 100 ppm. The offset is a Pd-dominated deposit with much higher Pd/Pt than in the other Portimo deposits and extremely low concentrations of Os, Ir, Ru, and Rh. Furthermore, it is irregular in form, being composed of disseminated sulfide-PGM 'clouds', massive sulfide veins or bodies, and breccias, in which sulfide veins brecciate granitoids.

The proportions of base metal sulfides and PGM are variable, but the massive sulfide bodies are always rich in PGE, while some samples containing hardly any visible sulfides can have several tens of ppm of Pd as well. In general terms, the more sulfide-rich occurrences are situated closer to the basal contact of the intrusion and those poorer in sulfides are encountered in a wider zone below the intrusion (Fig. 6).

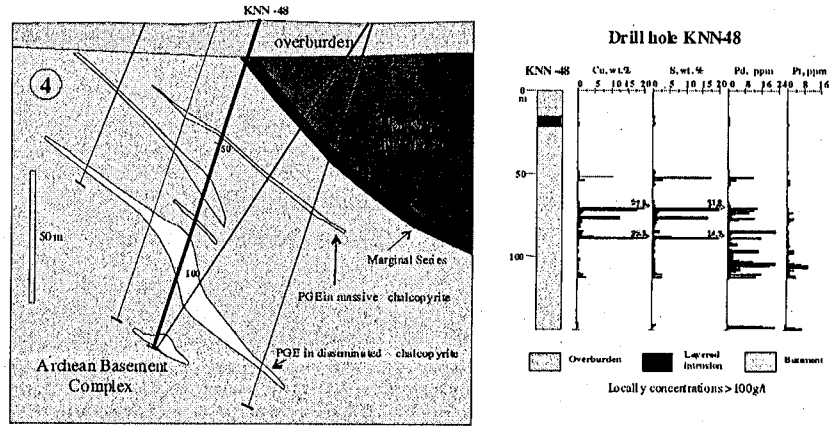

Figure 6. An example of an offset deposit, Kilvenjärvi.

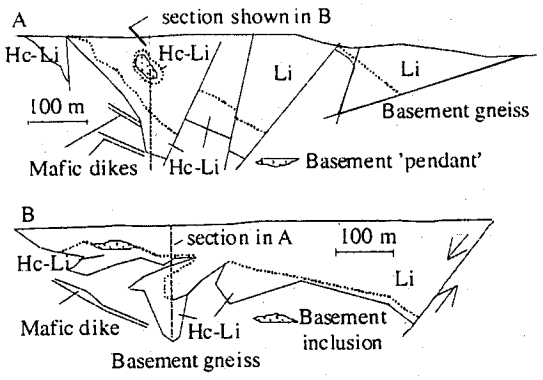

Figure 7. Cross-section (A) and longitudinal section (B) of the Konttijärvi Body. Li, layered intrusion, Hc-Li, heavily contaminated layered intrusion. Redrawn from Arctic Platinum Partnership Oy material.

Figure 2 shows a structural model for the Portimo Complex and the position of the above described mineralization sites and deposits. Taking the boundary region of the two parental magmas as a reference level, it can be seen that the Siika-Kämä Reef, the highly mineralized Ahmavaara and Konttijärvi Marginal Series, and the mineralized Portimo Dikes are located in the same positions in terms of the magma stratigraphy. Accordingly, they were referred to as a group name the 'Portimo Reef' by Iljina (1994). In the Konttijärvi and Ahmavaara areas, the pulses of the earlier parental magma are represented by the Portimo Dikes lying immediately below the marginal series. It is crucial that a marked decrease in PGE values and Ni and Cu contents of the sulfide fraction in the Suhanko-Konttijärvi Marginal Series takes place as soon as the Portimo Dikes disappear below it. In addition, regardless of the quantity of base metal sulfides present, the PGE ratios and chondrite-normalized PGE patterns are practically constant throughout the Portimo Reef. This is the case in the Ahmavaara Marginal Series, for instance, where the variation from disseminated to massive sulfides has only a marginal effect on the PGE patterns.

Discussion

The 'Portimo Reef' seems to lie in an ideal position in the light of the magma mixing model for PGE ore genesis. The two parental magmas inevitably mixed, at least in the Narkaus chamber, while the Portimo Dikes may have had thickenings in the Konttijärvi and Ahmavaara areas, which were not totally solidified at the time of subsequent magma injection, allowing the magmas to mix. The magma mixing model entails, however, certain problems. One is that the Reef can sometimes be located in cumulates or gabbropegmatites far below the first signs of a new magma. Another problem is found in the Konttijärvi and Ahmavaara areas, where higher tenor of PGE is sporadically found in the footwall granitoids and Portimo Dikes. These PGE enrichments are disseminated in character and therefore not indicative of a stream of immiscible sulfide liquid. Local co-precipitation of U- and Pd-Se minerals refers to co-trasportation and mineralization through a fluid phase. The above-mentioned features rule out magma mixing as the sole cause of ore formation.

The location of the 'Portimo Reef' excludes the possibility that its genesis could be exclusively related to the processes that took place in the present intrusions, but suggests that the ore-forming processes started much earlier in some intermediate magma chamber in the crust below the Narkaus and Suhanko-Konttijärvi intrusions and the last batch of the Cr-richer magma was already highly enriched in PGE at the time of emplacement. The PGE was possibly carried by a fluid phase and/or small amounts of immiscible sulfides. The multi-million ounce PGE deposit in the Konttijärvi Body demonstrates that the small size of a mafic body does not make it non-prospective when it is related to large volumes of magma of the whole intrusion belt.

References

Alapieti, T.T., Lahtinen, J.J., Huhma, H., Hänninen, E., Piirainen, T., Sivonen, S.J., 1989. Platinum-group element-bearing Cu-Ni sulphide mineralization in the marginal series of the early Proterozoic Suhanko-Konttijärvi layered intrusion, northern Finland. In: Prendergast, M.D., Jones, M.J. (Eds.), Magmatic sulphides – the Zimbabwe volume. Inst. Mining Metall., London, pp. 177–187.

Huhtelin, T.A., Lahtinen, J.J., Alapieti, T.T., Korvuo, E., Sotka, P., 1989. The Narkaus intrusion and related PGE and sulphide mineralizations. In: Alapieti, T. (Ed.), 5th International Platinum Symposium. Guide to the post-symposium field trip, August 4–11, 1989. Geol. Surv. Finland, Guide 29, 145–161.

Iljina, M., 1994. The Portimo Layered Igneous Complex with emphasis on diverge sulphide and platinum-group element deposits. Acta Univ. Ouluensis. Ser. A, Sci. Rer. Natur. 258. (Thesis).

Exploration for Platinum-Group Element (PGE) Deposits in Mafic and Ultramafic Rocks

Reid R. Keays[1] and Peter C. Lightfoot[2]
[1]Mineral Exploration Research Center, Laurentian University, Sudbury, Ontario, Canada, P3E 2C6
[2]Inco Technical Services Limited, Highway 17 West, Copper Cliff, Ontario, Canada, P0M 1N0
e-mail: rkeays@nickel.laurentian.ca, lightfootpc@inco.com

Most economic PGE deposits belong to a continuum of Ni-Cu-PGE sulfide mineralization styles from those that tend to be sulfide-poor and mined mainly for their PGE contents, through to those that are sulfide-rich and are mined mainly for their Ni and Cu contents. These sulfide deposits occur in association with mafic and ultramafic rocks in a variety of settings:

- Narrow "reefs" with low sulfide content within layered mafic/ultramafic intrusions (e.g., the Merensky Reef, South Africa; the J-M Reef of the Stillwater Complex, USA; and the Great Dyke, Zimbabwe).
- Wider zones of PGE sulfide enrichment within mafic/ultramafic intrusions (e.g., Munni Munni, Australia; River Valley and East Bull Lake Intrusions, Canada).
- Stratiform lenses of massive to disseminated Ni-Cu (PGE) sulfides at the base of komatiitic flow units (e.g., Kambalda, Australia; Cape Smith Fold Belt, Canada).
- In association with the outer contact phase of the Sudbury Igneous Complex, Canada, and concentrated in early-formed Offset dykes and the proximal country rocks.
- Stratabound zones of disseminated Ni-(Cu-PGE) sulfides within komatiitic rocks (e.g., Mount Keith, Australia).
- Within feeder zones of magmatic systems (e.g., Voisey's Bay, Canada).
- Within subvolcanic sills which acted as feeders to continental mafic volcanic sequences (e.g., Noril'sk, Russia; and possibly the Thompson Nickel Belt, Canada).

Many Ni-Cu sulfide deposits contain appreciable amounts of the PGEs, although the PGE tenor (calculated in 100% sulfide) varies enormously. Most of the mineralization was formed from magmas that were initially S-under-saturated but became S-saturated either by assimilation of S-bearing crustal rocks (e.g., komatiite-associated Ni sulfide deposits) or by magma mixing (e.g., Bushveld). During the fractionation of S-under-saturated mafic magmas, incompatible elements such as Cu, S, Se, Pd, and Pt accumulate in the residual silicate melt, whereas compatible elements such as Ni, Ir, Ru and Os are removed with the early silicate and/or oxide phases (Keays, 1995). Once a magma achieves S-saturation and fractionates even small quantities of immiscible magmatic sulfides, it will become strongly depleted in the PGE because of their very high Nernst partition coefficients (i.e. concentration element in sulfide melt/concentration element in silicate melt). The depletion in the PGE will be much more pronounced than the depletion in the other chalcophile elements such as Cu, S, and Se because the PGE have partition coefficients 1-3 orders of magnitude higher than these siderophile and chalcophile elements. A good example of this is provided by the Ni-Cu-PGE sulfide ores of the Sudbury camp; the noritic rocks of the Main Mass of the Sudbury Igneous Complex overlying the Sudbury ores are depleted in Cu and Ni, and, they are extremely depleted in PGE (Keays and Lightfoot, 1999).

In the case of layered intrusions, the ratios of the PGE to elements such as S, Cu and Se are much more useful exploration tools than absolute PGE concentrations. We show that data sets from the Munni Munni Complex, Great Dyke, Stillwater Complex, and the Bushveld Complex exhibit cross-overs in PGE/chalcophile metal ratios proximal to mineralized horizons. This is illustrated for the Merensky Reef of the Bushveld Complex (Fig. 1). The Pd/Cu and Pt/Cu ratios of rocks occurring above the mineralized horizons are all significantly lower than for rocks occurring below the mineralized horizons in these intrusions. The reason for this is that prior to ore formation, the magmas below the mineralized horizons were S-under-saturated whereas those from above it were S-saturated. The advantage of this approach to exploration for PGE deposits is that stratigraphically controlled analyses of ordinary, non-mineralized rocks will provide valuable clues as to the probable presence and location of PGE mineralization within an intrusion.

A feature of all of these mineralized layered intrusions is that the S-under-saturated magmas, which formed the rocks underlying the mineralized horizons, were high Pd- and high Pt-

bearing Siliceous High Magnesian Basaltic Magmas (SHMB). In all but the Munni Munni Complex, the ultramafic rocks are dominated by orthopyroxene, and so they crystallized from Si-rich melts. It is unclear whether these SHMB magmas were boninites or crustally contaminated komatiites. However, it appears that these magmas were initially S-under-saturated, a feature that we suggest is critical to the formation of important magmatic PGE deposits.

The Bushveld magmas appear to have contained more than an order of magnitude higher concentrations of the PGE than "normal" S-under-saturated magmas, such as komatiites that contain about 10 ppb Pd. The UG-2 and the Merensky Reef lie at the bases of cyclic units of rocks, termed the UG-2 Cycle and the Merensky Cycle that are both located in the Upper Critical Zone (Figure 1). They formed from discrete units of magma and possibly within double diffusion convection cells. All of the PGE decline in abundance from the base to the top of each cycle (Figures 1 and 2). In the UG-2 cycle, Pd drops off from 3100 ppb Pd at the base to 0.7 ppb Pd at the top. These variations indicate that the magma that formed the UG-2 was initially S-under-saturated but became S-saturated as it cooled; the first sulfides to segregate from the magma were Pd-rich reflecting the high partition coefficient. Sulfides that formed at the top of the UG-2 cycle have very low Pd contents; by the time they formed, the bulk of the Pd had been removed from the magma. Mass balance considerations suggest that the magma that formed the UG-2 contained 57 ppb Pd and 73 ppb Pt, while the Merensky Reef magma contained 106 Pd and 266 Pt.

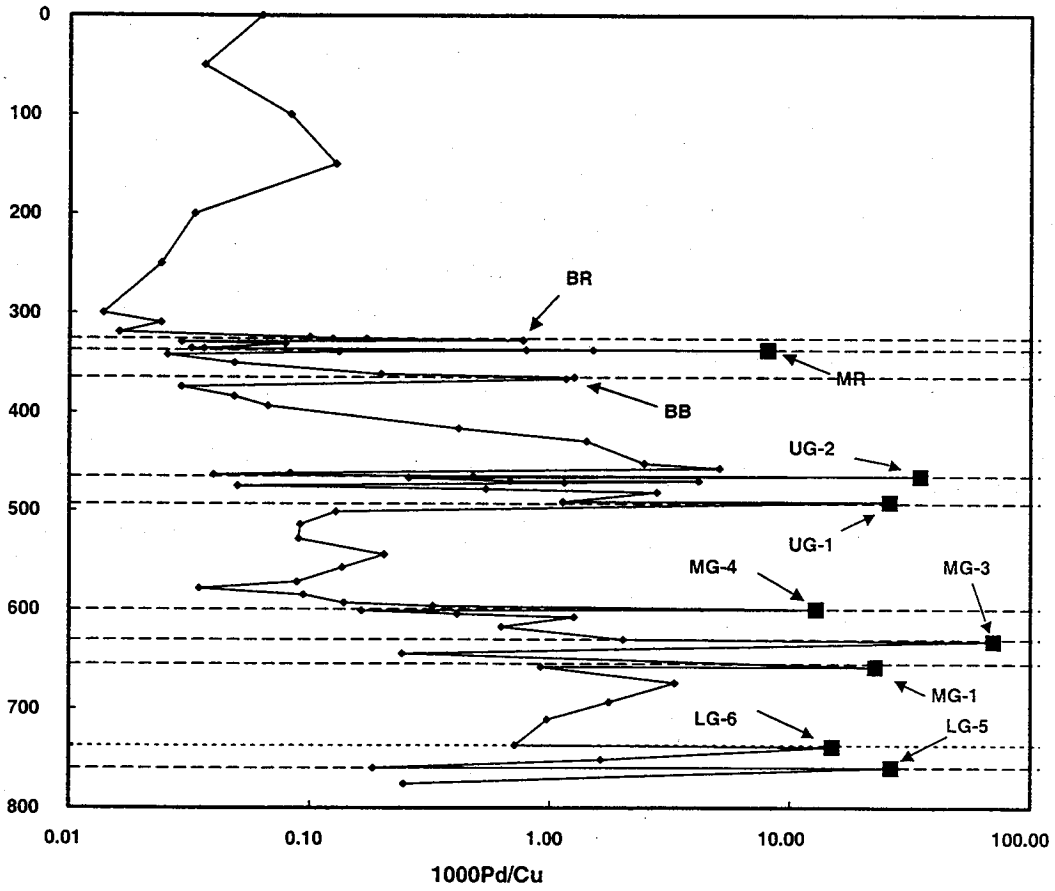

Figure 1. Variation in Pd/Cu ratios of rocks from a drill hole traverse across the Rustenberg Mine (Bushveld Complex). Note that the Pd/Cu ratios decrease upwards from the chromitite seams (solid black squares) located at the base of each package of rocks. Except for the low Pd/Cu values at the top of these packages, Pd/Cu ratios in rocks below the Merensky Reef are higher than those of rocks above. Copper and Pd data for the chromite samples are from Hiemstra (1986) and Lee & Parry (1988)). Symbols: BR-Bastard Reef, MR-Merensky Reef, BB-Boulder Bed, UG-1 & UG-2 are Upper Group chromitite seams, MG-1, -3 and –4 are Middle Group chromitite seams and LG-5 and –6 are Lower Group Chromitites.

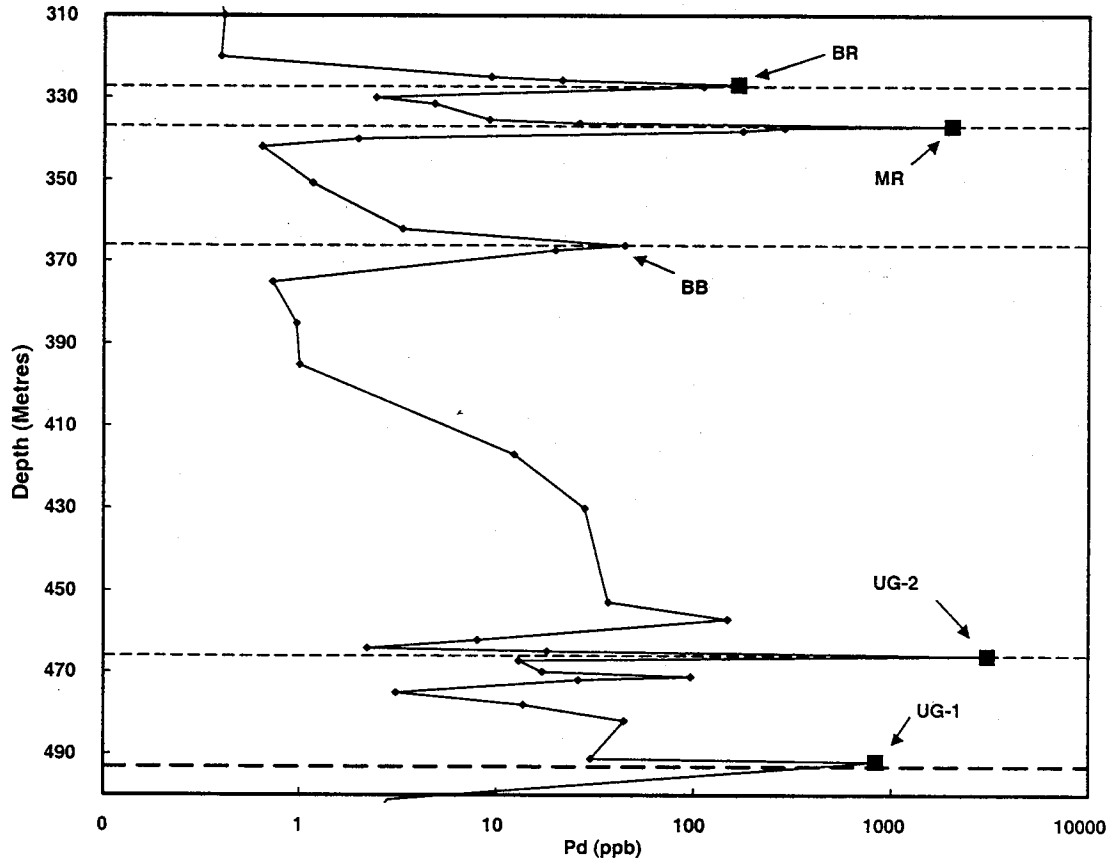

Figure 2. Variation in Pd contents of samples from the base of the UG-1 to the top of the Bastard Reef in samples from a traverse across the Upper Critical Zone of the Bushveld Complex in the Rustenberg Mine. Note that Pd contents in the UG-2 cycle decrease from 3100 ppb Pd at the base of the cycle (in the UG-2) to 0.7 ppb Pd at the top of the cycle (immediately below the Boulder Bed). See Figure 1 for symbols.

A mechanism is required to explain the very high PGE content of the Bushveld magmas. It is suggested that PGE-rich sulfides were initially deposited in a magma chamber at a deeper level than that of the present Bushveld Complex, as a result of interaction between a mantle-derived magma and the crust. Evidence for such interaction is provided by the strongly radiogenic Os-isotope signature of samples from the UG-2 and the Merensky Reef (Schoenberg et al., 1999). At some later stage, these PGE-rich sulfides were dissolved by a second, strongly S-under-saturated magma, such as a SHMB, and introduced into the Bushveld magma chamber where they eventually became S-saturated due to cooling and consequently precipitated the PGE-rich sulfides in the UG-2 and the Merensky Reef.

Many other Ni-Cu-(PGE) sulfide deposits (e.g. Noril'sk, Voisey's Bay) are probably products of two-stage processes initially involving deposition of Ni-Cu-PGE sulfides at depth due to interaction of mantle-derived magmas with crustal materials and subsequent transport of these sulfides to higher levels in the crust. However, unlike the Bushveld, instead of dissolving the PGE-rich sulfides, the second "carrier" magma simply transported these as immiscible sulfide droplets into the higher-level magma chambers.

References

Hiemstra, S. A., 1986. The distribution of chalcophile and platinum-group elements in the UG-2 chromitite layer of the Bushveld Complex, Econ. Geol., v. 81, p. 1080-86

Hoatson, D. M. and Keays, R. R. 1989, Formation of Platiniferous sulfide horizons by crystal fractionation and magmatic mixing in the Munni Munni layered intrusion, West Pilbara Block, Western Australia: Econ.

Geol., v. 84, p. 1775-1804.

Keays, R. R., 1995. The role of komatiitic and picritic magmatism and S-saturation in the formation of ore deposits: Lithos v. 34, p. 1-18.

Keays, R.R., and Lightfoot, P.C. 1999 The role of meteorite impact, source rocks, protores and mafic magmas in the genesis of the Sudbury Ni-Cu-PGE sulfide ore deposits in R.R. Keays, C.M. Lesher, P.C. Lightfoot, and C.E.G. Farrow (Editors), Dynamic Processes in Magmatic Ore Deposits and their Application in Mineral Exploration, Geological Association of Canada Short Course, v. 13, p. 329-366.

Lee, C. A. and Parry, S. J. 1988, Platinum-group element geochemistry of the Lower and Middle Group Chromitites of the Eastern Bushveld Complex, Econ. Geol., v. 83, p. 1127-39.

Schoenberg, R., Kruger, F. J., Nagler, T. F., and Kramers, J. D., 1999, PGE enrichment in chromitite layers and the Merensky Reef of the Western Bushveld Complex; a Re-Os isotope study. Earth Planet.Sci. Lett., v. 172, p. 49-64

Chromite is the Key to PGE

F. Johan Kruger[1], Judith A. Kinnaird[1], Paul A. M. Nex[2] and R. Grant Cawthorn[2]
[1]Economic Geology Research Institute – Hugh Allsopp Laboratory
[2]School of Geosciense, University of the Witwatersrand, WITS 2050, South Africa.
Email: 106fjk@cosmos.wits.ac.za

Introduction

Chromitite layers in the Bushveld Complex have long been known to host anomalous concentrations of PGE. Indeed, the first recorded occurrence of PGE is from a chromitite in the area around Mineral Range in 1908. Initially these discoveries did not flourish due to metallurgical constraints, and the discovery in 1924 of the pipe-like (Onverwacht, Mooihoek and Driekop) bodies with payable Pt-Fe alloys, and then the chromite bearing (but S-enriched) Merensky Reef (both metallurgically amenable) suppressed interest in chromitite as a source of PGE (see Cawthorn, 1999 for a historical overview of the discovery of the Merensky Reef), until in the late 1970's and 1980's when metallurgical breakthroughs and increased demand led to mining of the UG2.

In the 1980's the model of Naldrett and co-workers. (see e.g. Naldrett, 1989), in which a very high ratio of magma to an immiscible sulfide liquid (R-factor) associated with magma influx and mixing is invoked, gained favour due to the presence of sulfide in the Merensky Reef. However, this model has recently been discredited for PGE in the Bushveld Complex (Cawthorn, in press).

Mineralogy, Geochemistry and Sr-Isotope Data

The chromitite layers of the Bushveld Complex host platinum group elements as platinum group minerals (PGM) which principally include PGE-sulfide minerals, (laurite, braggite and cooperite), but antimonides (geversite, stibio-paladinite), arsenides (sperrylite), bismuthides (insizwaite), tellurides (merenskyite, moncheite) and alloys (isoferro-platinum) are major contributors (see e.g. Lee, 1996). Base metal (Ni-Cu-Fe) sulfides also occur, but are not sufficiently abundant to be the residue of a PGE enriched immiscible sulfide liquid. Furthermore, many of these minerals occur as euhedral crystals enclosed in chromite grains. The R-factor modelling depends on large sulfide liquid/silicate liquid partition coefficients which obey Henry's Law. The presence of liquidus PGM negates this assumption – which can only be sustained by special pleading (e.g. assumed post-crystallization sulfur loss).

Chromitite is highly enriched in PGM, and chromite compared to most silicate host rocks and potential primary magmas (see e.g. Scoon & Teigler (1994)). The enrichment of chromium in chromitite (Cr ±20% in UG2) compared to a tholeiitic liquid (±250 ppm) is about 800, and the enrichment in PGE in chromitite (8 ppm for the UG2) relative to a potential tholeiitic liquid (±40 ppb (Davies & Tredoux, 1985)) is about 200. These ball-park figures are within a factor of 4 and suggest that the *process* that led to the crystallization of chromite simultaneously led to the crystallization *and* co-concentration of PGM. This requires the processing of a large volume of liquid (some 200-800 times the mass of the precipitated chromitite).

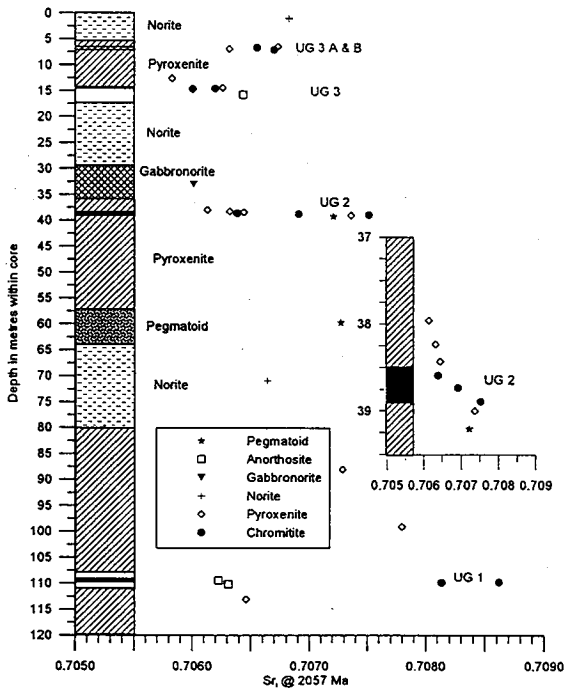

Figure 1. Strontium isotope profile in upper Critical Zone silicates and chromitite-hosted plagioclase from 10m below UG1 to 5m above UG3 in KF17 core, north of the Steelpoort lineament. The expanded inset for isotopic ratios through the UG2 chromitite illustrates the upward decrease in initial ratios from base to top of the chromitite. Source of data, Richardson (2002).

Seminal papers by Irvine (1975 & 1977) showed that chromite crystallization can be induced by felsic (silica) contamination (1975) or by mixing of "parental" magma and more evolved residua (1977); the process of mixing dissimilar magmas forcing the mixture into the chromite phase field.

Recently, Schoenberg *et al.* (1999) showed that chromitite layers have exotic enriched Sr-isotope systematics which are completely different from those of the host silicate rocks, and which imply sudden and major contamination by a 'granitic' crustal component. Furthermore, this contamination was only active while the chromitite was forming and ceased once the chromitite stopped forming. These observations have been confirmed and extended by Kinnaird *et al.* (in press) an example of which is shown in Figure 1.

These mineralogical, geochemical and isotopic data suggest a mechanism for chromitite formation that revives Irvine's (1975) model in combination with his 1977 parental magma mixing model, but negates the later (1981) double diffusive convection model and the Irvine & Sharpe (1986) U- and A-type magma mixing models for these rocks.

A Model for Accumulation of Chromite and PGM

In this model we envisage that influxes of new magma into the Bushveld magma chamber rose up as fountains that interacted with and entrained granophyric roof-rock melt. This process contaminated both the new magma and the resident entrained melt with a SiO_2 rich component that induced crystallization of copious chromite and the concomitant crystallization of PGM. The small PGM crystals are collected and incorporated by the more abundant chromite grains as suggested by Hiemstra (1979). The chromite with adherent PGM and magma was carried to the floor of the chamber by the collapsing fountain to form chromitite layers enriched in PGE. Chromite (and PGM) only crystallize while there is roof-melt interaction or there is sufficient compositional contrast to force the mixture into the chromite phase field. The contamination process ceases when the head of the fountain ceases to impinge on the floating roof-rock melt. Continued magma influx may occur which is uncontaminated by the roof-rock melt. This process is illustrated in Figure 2

This process involves mixing three component magmas to produce chromitite. These are the resident (residual) magma, the new influx of magma and the roof-rock (granophyric) melt. The resident magma need not be a derivative of the second new magma as required by some models for PGE mineralisation and chromitite formation such as those of Campbell & Naldrett (1983) or Irvine (1977).

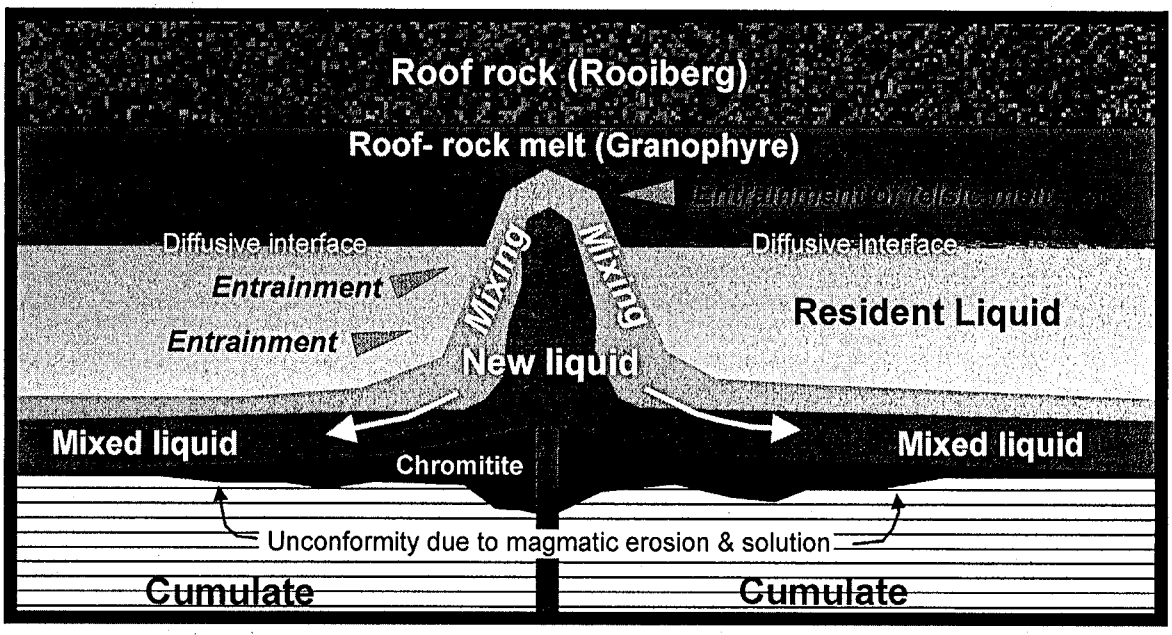

Figure 2. Introduction of a new magma (Ro = 0.705 - 0.706) as an active fountain results in entrainment of the resident mafic liquid and if there is sufficient upward momentum roof-rock melt (Ro > 0.72) is also entrained. This results in contamination by a silica-rich component with the resulting forced crystallisation of chromite. The mixed liquids are out of equilibrium with the floor cumulates and react and erode to form an unconformity onto which the chromite/PGM ore is deposited.

In the Bushveld Complex, the influxing magmas are not a single primitive "parental" magma, but a diverse series of different magmas as shown by Harmer & Sharpe (1985).

Conclusion

The model outlined here provides an explanation for the following features of chromitites and their PGM mineralization:

1. The apparent random stratigraphic positions of chromitites with respect to the evolving layered silicates, which cannot be predicted in the sequence as they they are induced by magma addition events and not fractional crystallization.
2. The apparent unconformable relationships to underlying sequences.
3. The co-enrichment of Cr and PGE.
4. The unusual isotopic, mineralogical and chemical properties.

References

Campbell, I., Naldrett, A.J. & Barnes S.J. (1983). A model for the origin of the platinum-rich sulfide horizons in the Bushveld and Stillwater Complexes. Journal of Petrology 24, 133-165

Cawthorn, R.G. (in press). Magma mixing models for Merensky-style mineralisation: the fallacy of binary diagrams. Econ. Geol.

Cawthorn, R.G. (1999). The discovery of the platiniferous Merensky Reef in 1924 S. Afr. J. Geol. 103, 178-183

Harmer, R.E. & Sharpe M.R. (1985). Field relations and strontium isotope systematics of the Marginal rocks of the Eastern Bushveld Complex. Economic Geology 80, 813-837

Hiemstra, S.A. (1979). The role of collectors in the formation of the platinum deposits in the Bushveld Complex. Canad. Mineral. 17, 469-482.

Irvine, T.N. (1975). Crystallization sequences in the Muskox intrusion and other layered intrusions-II. Origin of chromitite layers and similar deposits of other magmatic ores. Geochim. Cosmochim. Acta 39 991-1020.

Irvine, T.N. (1977). Origin of chromitite layers in the Muskox intrusion and other stratiform intrusions: a new interpretation. Geology 5, 273-277.

Irvine T.N. (1981). A liquid-density controlled model for chromitite formation in the Muskox intrusion. Ann. Rep. Geophysical Laboratory 80: 317-324

Irvine, T.N. & Sharpe, M.R.(1986). Magma mixing and the origin of stratiform oxide ore zones in the Bushveld and Stillwater Complexes. In: Metallogency of Basic and Ultrabasic Rocks_Inst. Mining and Metall. 183-198

Kinnaird, J.A., Kruger, F.J., Nex P.A.M. & Cawthorn, R.G. (in press). Understanding chromitite formation – a key to understanding processes of platinum enrichment. Trans. Inst. Mining and Metall.

Naldrett, A.J. (1989). Stratiform PGE deposits in layered intrusions. Rev. Econ. Geol., 4, 135-166

Lee, C.A. (1996). A review of mineralisation in the Bushveld Complex and some other layered intrusions, In: Layered intrusions" Ed. R.G. Cawthorn, Elsevier, pp103-145

Richardson, T.R. (2002). Stratigraphy of the upper Critical Zone in the eastern Bushveld. MSc thesis, Univ. Witwatersrand, Johannesburg, South Africa.

Schoenberg, R., Kruger, F.J., Nagler, T.F., Meisel, T. and Kramers, J.D. (1999). PGE enrichment in chromitite layers and the Merensky Reef of the western Bushveld Complex; a Re-Os and Rb-Sr isotope study. Earth Planet. Sci. Lett. 172, 49-64.

Scoon, R.G. and Teigler, B. (1994). Platinum Group element mineralisation in the Critical Zone of the western Bushveld Complex: 1. Sulphide-poor chromitites below the UG2. Econ. Geol., 89, 1094-1121.

Discrimination between Magmatic and Hydrothermal Ni-Cu-PGE and PGE Mineralization

C. M. Lesher and **R. R. Keays**
Mineral Exploration Research Centre, Department of Earth Sciences, Laurentian University, Sudbury, ON P3E 6B5, Canada
e-mail: lesher@sympatico.ca

Introduction

Mafic-ultramafic-hosted Ni-Cu-(PGE) and PGE deposits are believed to have formed by segregation of immiscible sulfide melts and/or alloys from mafic-ultramafic magmas in dynamic magmatic systems such as lava channels, feeder dikes, and magma chambers. However, some of the mineralization in some deposits (e.g., hydrothermal veins at Kambalda: Lesher & Keays, 1984; Stillwater J-M reef: Boudreau et al., 1986; Sudbury footwall ores: Farrow & Watkinson, 1996) is associated with hydrous and/or halogen-bearing phases and is interpreted to have formed from or been modified by hydrothermal fluids.

Different base, precious, and semi-metals have different solubilities and partition differently between silicate magmas, sulfide melts, and supercritical fluids/volatiles (e.g., Keays & Crocket, 1970; Keays et al., 1982; Barnes & Maier, 1999; Mathez, 1999; Wood, in press). For example, the solubilities of Fe, Co, Ni, Cu, PGEs, and Au are different in sulfide melts and hydrothermal fluids; Au, Cu, and platinum-group PGEs (PPGE: Pt, Pd, Rh) behave differently than Ni, Co, and iridium-group PGEs (IPGE: Ru, Ir, Os); and Ru and Ir behave differently than other IPGEs. Therefore, it should be possible to distinguish between those ores deposited by magmatic processes and only modified by hydrothermal fluids and those ores deposited directly from hydrothermal fluids. Unfortunately, very few deposits have been systematically analyzed for complete suites of base, precious, and semi-metals, but it is possible to make some preliminary interpretations.

Discrimination

Although the behavior of the different metals varies with magma/fluid composition, temperature, pressure, fO_2, and fS_2, the general order of partitioning into sulfide melts appears to be PGE ~ Au > Cu > Ni > Co > Fe, whereas the general order of solubility in hydrothermal fluids appears to be Fe > Cu ~ Au > Pt ~ Pd > Ni > Co >> Ru ~ Ir. Differential crystallization/ precipitation processes can further fractionate different elements, but it is possible, at least in most cases, to distinguish between magmatic and hydrothermal mineralization on the basis of Au/Cu/Pt/Pd, Ir/Ni, and Cr/Fe ratios. These differences are best illustrated on primitive mantle-normalized variation diagrams (Figs. 1-5)

For example, the majority of the ores at Kambalda (Fig. 1), Langmuir (not shown), Donaldson West (Fig. 2), and Sudbury (Fig. 3) exhibit relatively systematic variations in metal ratios with fractionations consistent with magmatic segregation from komatiitic, basaltic komatiitic, and noritic magmas (see Barnes & Naldrett, 1985), respectively, and local mobilization of Au, Pd, Pt, and/or Cu. However, hydrothermal veins and Ni-enriched metasediments in these localities are strongly depleted in Ir, sometimes depleted in other IPGE (e.g., Rh at Sudbury, Rh-Ru-Os at Donaldson), and also depleted (where data are available) in Cr. In contrast, ores at Lac des Iles, New Rambler, and Rathbun Lake (Fig. 4) are strongly enriched in PPGE relative to IPGE and strongly depleted in Ir relative to Ni and/or other PGE. Their compositions are consistent with hydrothermal modification of magmatic sulfides (Lac des Iles and some Rathbun Lake samples) or with hydrothermal transport and deposition (New Rambler and some Rathbun Lake samples).

The ores in the Bushveld and Stillwater complexes (Fig. 5) are depleted in Ni and Cu relative to other metals, but are not significantly depleted in Ir or other IPGE. Their Ir contents are more consistent with magmatic segregation (e.g., Campbell et al., 1983) and hydrothermal modification than with hydrothermal generation (e.g., Boudreau et al., 1986). However, Stillwater ores appear to have lower Cu and much higher Pd and Pt contents, consistent with stronger hydrothermal modification.

Clearly, more experimental data are required to establish the relative mobilities of PGEs in hydrothermal fluids, but if the observed fractionations in known hydrothermal ores are characteristic, then they suggest that the PGE mineralization in the Bushveld and Stillwater Complexes segregated via magmatic processes and was subsequently modified by hydrothermal processes.

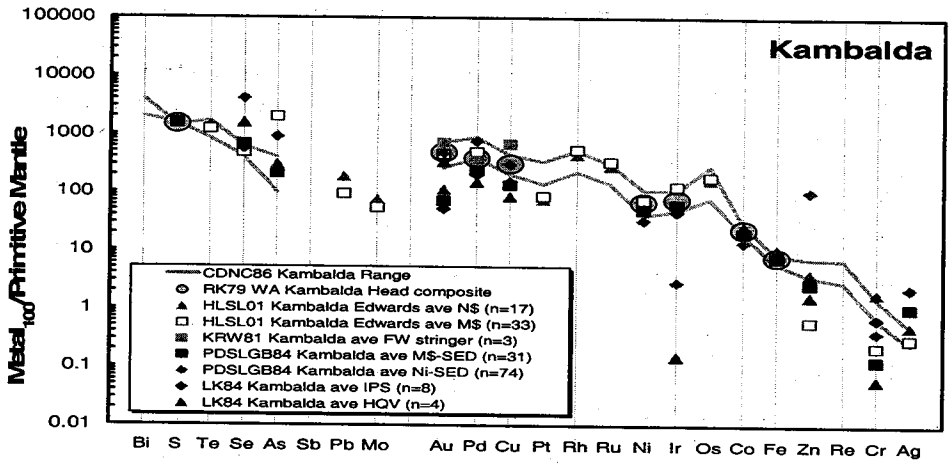

Figure 1. Kambalda ores. For this and subsequent figures, data sources shown as initials of authors and year; ore types: D$ = disseminated, N$ = net-textured, RN$ = reverse net-textured, M$ = massive, IPS = Interpillow, Ni-SED = Ni-enriched metasedimentary, V$ = hydrothermal vein.

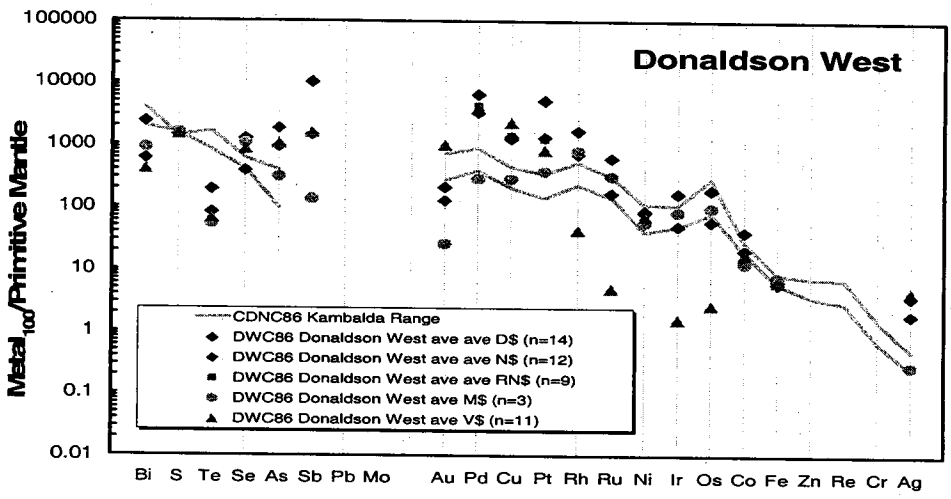

Figure 2. Donaldson West ores.

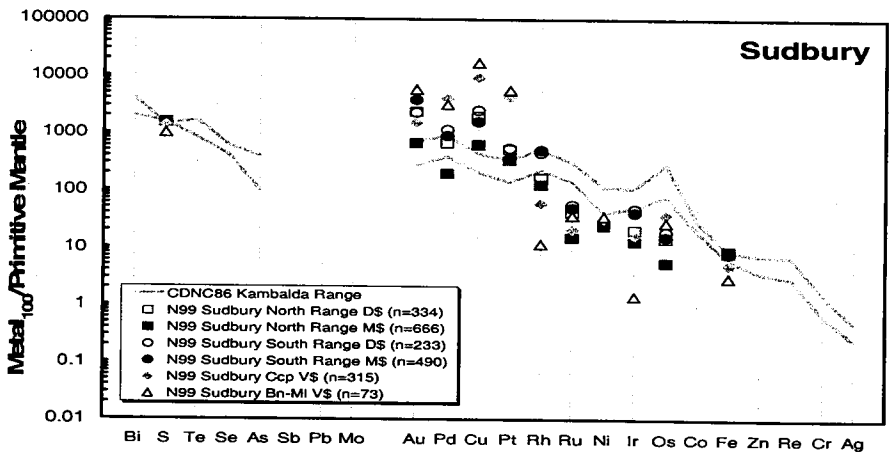

Figure 3. Sudbury ores.

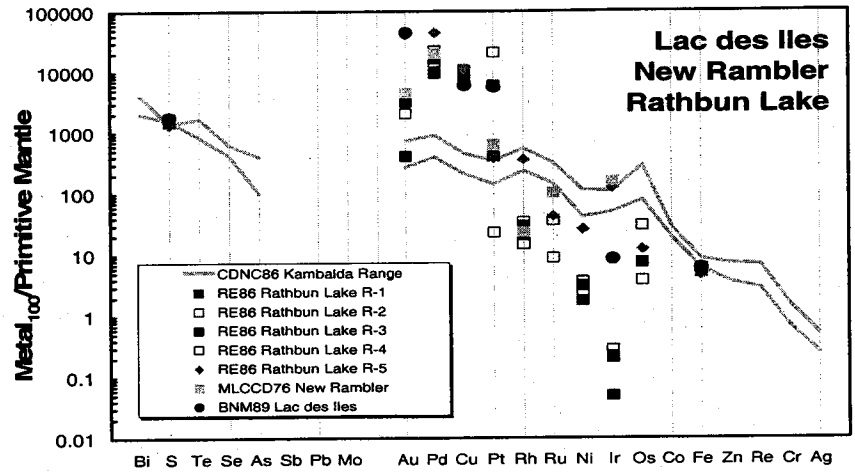

Figure 4. Lac des Iles, New Ramber and Rathbun Lake ores.

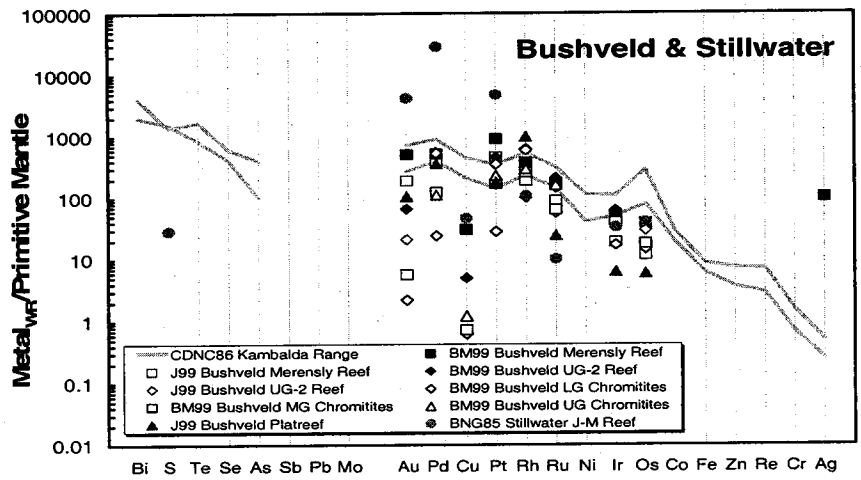

Figure 5. Bushveld and Stillwater ores.

References

Barnes, S.-J., and Maier, W.D., 1999, The fractionation of Ni, Cu, and the noble metals in silicate and sulphide liquids *in* Dynamic Processes in Magmatic Ore Deposits and their Application to Mineral Exploration, GAC Short Course Notes, v. 13, p. 69-106.

Barnes, S.-J., Naldrett, A.J., and Gorton, M.P., 1985, The origin of the fractionation of the platinum-group elements in terrestrial magmas, Chem. Geol., v. 53, p. 303-323.

Boudreau, A.E., Mathez, E.A., and McCallum, I.S., 1986, Halogen geochemistry of the Stillwater and Bushveld Complexes: Evidence for transport of the platinum-group elements by Cl-rich fluids, J. Pet., v. 27, p. 967-986.

Brügmann, G.E., Naldrett, A.J., and Macdonald, A.J., 1989, Magma mixing and constitution zone refining in the Lac des Iles Complex, Ontario; genesis of platinum-group element mineralization, Econ. Geol., v. 84, p.1557-1573.

Campbell, I.H., Naldrett, A.J., and Barnes, S.J., 1983, A model for the origin of platinum-rich sulphide horizons in the Bushveld and Stillwater Complexes, J. Pet., v.24, p. 133-165.

Cowden, A., Donaldson, M.J., Naldrett, A.J., and Campbell, I.H., 1986, Platinum-group elements and gold in the komatiite-hosted Fe-Ni-Cu sulfide deposits at Kambalda, Western Australia, Econ. Geol., v. 81, p. 1226-1235.

Dillon-Leitch, H.C.H., Watkinson, D.H., and Coats,

C.J.A., 1986, Distribution of platinum-group elements in the Donaldson West deposit, Cape Smith Belt, Québec, Econ. Geol., v. , 81, p. 1147-1158.

Farrow, C.E.G., and Watkinson, D.H., 1996, Geochemical evolution of the Epidote Zone, Fraser Mine, Sudbury: Ni-Cu-PGE remobilization by saline fluids, Expl. Min. Geol., v. 5, p. 17-31.

Green, A.H., and Naldrett, A.J., 1981, The Langmuir volcanic peridotite-associated nickel sulphide deposits, Econ. Geol., v. 76, p. 1503-1523.

Heath, C., Lahaye, Y., Stone, W.E., and Lambert, D.D., 2001, Origin of variations in nickel tenor along the strike of the Edwards Lode nickel sulfide orebody, Kambalda, Western Australia, Can. Min., v. 39, p. 655-672.

Jones, R.T., 1999, Platinum Smelting in South Africa (http://www.mintek.ac.za/Pyromet/Platinum/Platinum.htm)

Keays, R. R. and Crocket, J. H., 1970, A study of the precious metals in the Sudbury nickel irruptive ores: Econ. Geol., v. 65, 438-450.

Keays, R.R., Nickel, E.H., Groves, D.I. and McGoldrick, P.J., 1982, Iridium and palladium as discriminants of volcanic exhalative, hydrothermal, and magmatic nickel sulfide mineralization, Econ. Geol., v. 77, p. 1535-1547.

Keays, R.R., Ross, J.R., and Woolrich P., 1981, Precious metals in volcanic peridotite-associated nickel sulfide deposits in Western Australia, II: Distribution within ores and host rocks at Kambalda, Econ. Geol., v. 76, p. 1645-1674.

Lesher, C.M., and Keays, R.R., 1984, Metamorphically and hydrothermally mobilized Fe-Ni-Cu sulphides at Kambalda, Western Australia, *in* Buchanan, D.L., and Jones, M.J. (Eds.), Sulphide Deposits in Mafic and Ultramafic Rocks, Inst. Min. Metall., London, p. 62-69.

Mathez, E.A., 1999, Factors controlling the concentrations of platinum-group elements in layered intrusions and chromitites, *in* Dynamic Processes in Magmatic Ore Deposits and their Application to Mineral Exploration, GAC Short Course Notes, v. 13, p. 251-286.

McCallum, M.E., Loucks, R.R., Carlson, R.R., Cooley, E.F., and Doerge, T.A., 1976, Platinum metals associated with hydrothermal copper ores of the New Rambler mine, Medicine Bow Mountains, Wyoming, Econ. Geol. v.71, p.1429-1450.

Naldrett, A.J., Asif, M., Schandl, E., Searcy, T., Morrison, G.G., Binney, W.P., and Moore, C, 1999, Platinum-group elements in the Sudbury ores; significance with respect to the origin of different ore zones and to the exploration for footwall orebodies, Econ. Geol, v. 94, p.185-210.

Paterson, H.L., Donaldson, M.J., Smith, R.N., Lenard, M.F., Gresham, J.J., Boyack D.J., and Keays, R.R., 1984, Nickeliferous sediments and sediment-associated nickel ores at Kambalda, Western Australia, *in* Buchanan, D.L., and Jones, M.J. (Eds.), Sulphide Deposits in Mafic and Ultramafic Rocks, Inst. Min. Metall.,, London, p. 81-94.

Ross, J.R., and Keays, R.R., 1979, Precious metals in volcanic-type nickel sulfide deposits in Western Australia: I. Relationships with the composition of the ores and host rocks, Can. Min., v. 17, p. 417-436.

Rowell, W.F, and Edgar, A.D., 1986, Platinum-group element mineralization in a hydrothermal Cu-Ni sulfide occurrence, Rathbun Lake, northeastern Ontario, Econ. Geol, v. 81, p.1272-1277.

Wood, S.A, in press, The aqueous geochemistry of the platinum-group elements with applications to ore deposits, *in* Cabri, A. (Ed.), The Geology, Geochemistry, Mineralogy, and Mineral Beneficiation of the Platinum-Group Elements, Canadian Institute of Mining, Metallurgy and Petroleum, Special Volume 54.

Olivine and S Isotope Systematics of Ore-Bearing Intrusions at Noril'sk, Siberia

C. Li[1], E. M. Ripley[1] and A. J. Naldrett[2]
[1]Department of Geological Sciences, Indiana University, Bloomington, IN 47401, USA
[2]Department of Geology, University of Toronto, Toronto, Ontario, M5S 3B1 Canada
E-mail: cli@indiana.edu

Introduction

The Ni-Cu-PGE ore-bearing intrusions of the Noril'sk area such as the Noril'sk I and the Main and NW Talnakh intrusions have been recognized to be comagmatic with the voluminous Permo-Triasic Siberian Traps flood basalts (Lightfoot et al., 1992; Naldrett et al., 1992; Czamanske et al., 1994; Fedorenko, 1994). These intrusions contain at least 50 times more sulfides than the magmas represented by their rocks could have dissolved (Naldrett et al., 1992). Although there is a common consensus that much of the sulfides and their metals were possibly derived from the associated lavas as well as the intrusive rocks, opinions as to where the sulfide segregation took place are still divided. Naldrett et al. (1995, 1996), Lightfoot and Hawkesworth (1997) and Naldrett and Lightfoot (1999) have proposed that the ore-bearing intrusions were volcanic feeders in which immiscible sulfide liquids segregated and reacted with continuous surges of magmas *en route* to the surface. Others have suggested that the ore-bearing intrusions are blind sills formed by sulfide-laden magmas derived from a dynamic staging magma chamber (Naldrett et al., 1992; Brügmann et al., 1993; Naldrett and Lightfoot, 1993; Lightfoot et al., 1994) or a series of staging magma chambers (Fedorenko, 1994). This study is concerned with the systematic variations of olivine and S isotopic compositions that can be used to discriminate these two competing genetic models.

Types of Olivine and Their Compositional Variations

Olivines from the ore-bearing intrusions occur as (1) inclusions in augite and plagioclase oikocrysts (Fig. 1); (2) discrete grains with granular or subpoikilitic pyroxenes and plagioclase, and interstitial sulfides; and (3) poikilitic crystals enclosing pyroxenes and plagioclase. There is a special type of olivine that occurs as olivine-rich schlieren and masses referred to as "olivinites" by many Russian geologists.

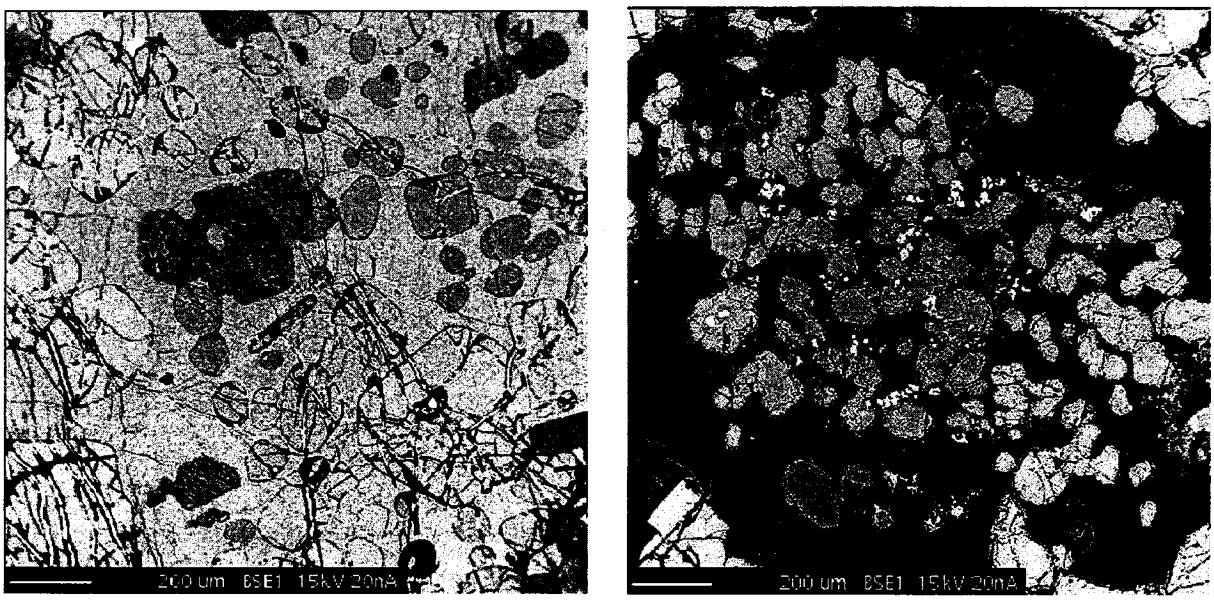

Figure 1. BSE images showing olivine inclusions in augite (left) and plagioclase (right)

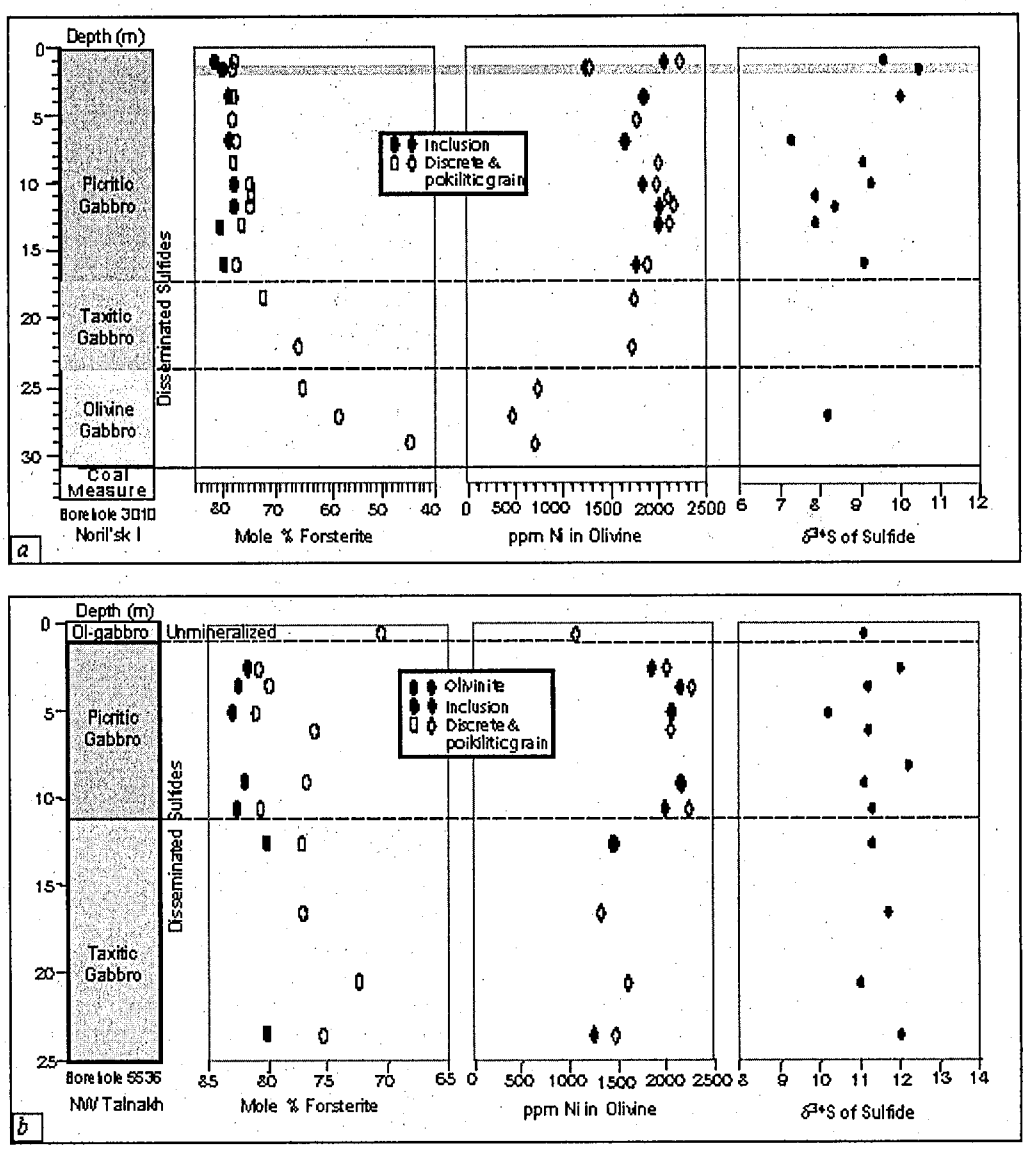

Figure 2. Stratigraphic variations of olivine and S isotopic compositions at Noril'sk (a) and Talnakh (b).

The compositional relationships between olivine inclusions and coexisting discrete olivines are different in sulfide-poor (<0.3 wt.% S) and sulfide-bearing samples. In sulfide-poor samples, olivine inclusions contain higher Fo and Ni than coexisting discrete olivines, consistent with the results of fractional crystallization. In sulfide-bearing samples, discrete olivines also have lower Fo contents than coexisting olivine inclusions. However, the Ni contents of the discrete olivines are higher instead of lower. In addition, the discrete olivines together define an inverse Ni-Fo relationship that apparently has resulted from subsolidus re-equilibration of olivine with trapped sulfide liquid. The difference in olivine composition between an olivinite and its sulfide-bearing gabbroic host is similar to the difference between olivine inclusions and coexisting discrete olivines in the sulfide-bearing samples.

The main points inferred from the compositional variations of different types of olivine are summarized below: (1) olivine inclusions were early cumulus crystals that have been largely protected by their host oikocrysts from re-equilibration with trapped silicate and/or sulfide liquids; (2) olivinites were either cognate inclusions of early olivine cumulates or they represent *in situ* segregation of cumulus olivine aggregates; and (3) discrete and poikilitic olivines crystallized later and their compositions were variably modified by trapped silicate and/or sulfide liquids.

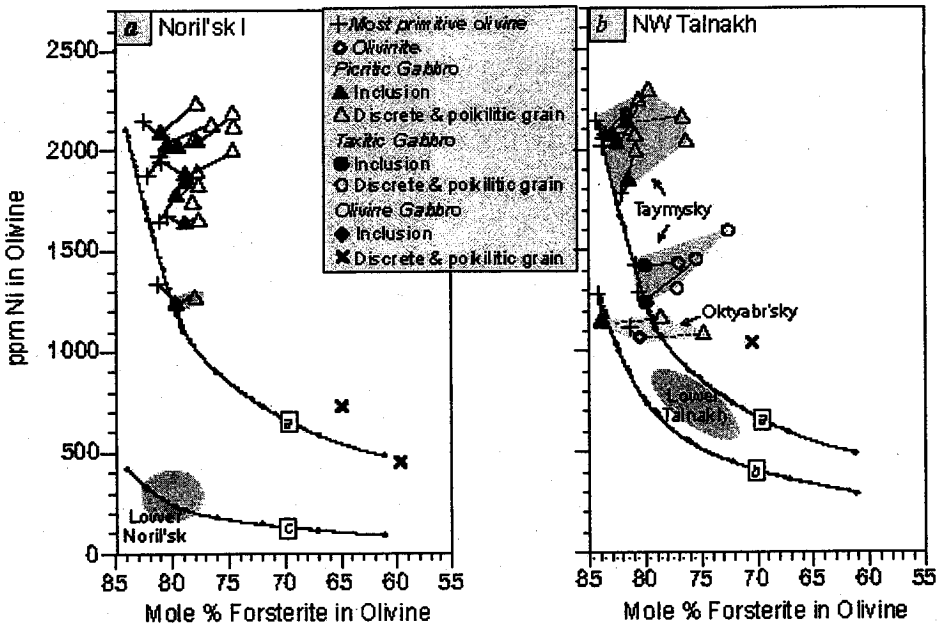

Figure 3. Modeling of olivine fractionation. a. Noril'sk I and Lower Noril'sk intrusions. b. NW Talnakh and Lower Talnakh intrusions. See text for discussions.

Stratigraphic Variations of S Isotopic and Olivine Compositions

Fig. 2a illustrates the stratigraphic variations of olivine and S isotopic compositions in borehole 3010 in the northern part of the Noril'sk I intrusion. The Fo contents of olivines from the olivine gabbro unit decrease downward from 67 mole % to less than 45 mole %. In the overlying taxitic gabbro unit, the Fo contents of olivines are slightly higher and appear to extend the trend of the gabbro unit. But the Ni contents of olivine in the taxitic gabbro unit are much higher, varying between 1700-1900 ppm. In the picritic gabbro, olivine inclusions contain Fo up to 81 mole %. The Fo variations of olivine inclusions from this unit are rather small, mostly less than 3 mole %. The Fo contents of discrete olivines are several mole % less than coexisting olivine inclusions. The contents of Ni in both olivine inclusions and coexisting discrete olivines display an inverse correlation with their Fo contents. Olivines from a sample close to the top of the unit have much lower Ni contents than others from this unit, which may be related to lower Ni content in the sulfide. The content of Ni in the bulk sulfide of this sample is 7 wt%. The contents of Ni in other samples of this unit vary mostly between 9 and 12 wt%. The $\delta^{34}S$ values of the samples from this borehole vary between 7.9 and 10.5 ‰. Within the picritic gabbro unit, the sample with low Ni content in olivine has a higher $\delta^{34}S$ value than other samples.

The stratigraphic variations of olivine and S isotopic compositions in borehole 5536 located at the Taymysky Mine in the northern part of the NW Talnakh intrusion is shown in Fig. 2b. The $\delta^{34}S$ values of sulfides from different rock units in this borehole are similar, varying between 10.2 and 12.2 ‰. In contrast, olivines from different units have distinctly different compositions. Olivines from the picritic gabbro unit are the most primitive and have the highest Ni contents. Olivines from the underlying taxitic gabbro unit have slightly lower Fo contents and significantly lower Ni contents. Olivines from the top olivine gabbro unit are the most evolved and have the lowest Ni contents.

In summary, there are significant discontinuities of olivine compositions, particularly Ni contents, at the contacts of different rock units in the Noril'sk I and Talnakh intrusions. In contrast, the stratigraphic variations in S isotopic compositions are only subtle or minor. This is only explicable if multiple magmas with distinctly different Ni contents and similar S isotopic compositions were involved in the development of the intrusions.

Comparison of Different Intrusions

The compositions of olivine from different intrusions are compared in Fig. 3. The model curves represent the compositional variations of the olivines expected to crystallize from magmas with variable initial Ni contents and the same major

element compositions during fractional crystallization. The model lines labeled *a*, *b* and *c* represent initial Ni contents of 300, 180 and 60 ppm, respectively. The major element compositions are from the average values of the Noril'sk-type sills given by Zen'ko and Czamanske (1994). The simulation of crystallization was performed for 1 kb at the QFM buffer using the silicate liquid model MELTS of Ghiorso and Sack (1995). Olivine is predicted to crystallize at 1230 °C. Plagioclase starts to join olivine at 1198 °C, and clinopyroxene starts to join both olivine and plagioclase at 1175 °C. This crystallization sequence is in good agreement with petrographic observation. Nickel fractionation was calculated assuming that D^{Ni} for olivine, clinopyroxene and plagioclase are 7, 1 and 0, respectively.

Olivine inclusions from the Noril'sk I intrusion have Fo contents similar to the same type of olivine from the Lower Noril'sk intrusion, but have much higher Ni contents and thus require a much higher initial Ni content in magma (300 ppm, line *a* versus 60 ppm, line *c*). It is seen that 5% crystallization in accordance with the model of 300 ppm initial Ni in magma accounts well for the most primitive olivines from the Noril'sk I intrusion, except for one sample which has a much lower Ni content and falls closer to the model line at >20% of crystallization. The displacement of the coexisting discrete olivines to the right can be attributed to reaction with trapped silicate liquid and/or sulfide liquid. Olivines from the olivine gabbro unit of the Noril'sk I intrusion are broadly consistent with the modeled compositions after >50% crystallization.

Compared to the Noril'sk I intrusion, the contents of Fo in olivine inclusions from the picritic gabbro unit of the NW Talnakh intrusion at Taymysky are slightly higher (Fig. 5b). Most of the olivine inclusions from this unit fall closer to the model of 300 ppm initial Ni in magma at <5% crystallization. The olivine inclusions from the taxitic gabbro unit of the NW Talnakh intrusion at Taymysky are more fractionated and fall near the model line at 10-12 % crystallization. Olivine inclusions from the picritic gabbro unit of the NW Talnakh intrusion at Oktyabr'sky have significantly lower Ni contents than the same type of olivine from the same type of rock unit at Taymysky, and require a much lower initial Ni content in magma (180ppm, line *b*). Olivines from the olivinites have compositions similar to the olivine inclusions from the same rock units. Similar to the Noril'sk I intrusion, there are notable displacements to the right for the discrete olivines from the NW Talnakh intrusion, possibly due to re-equilibration with trapped silicate liquid and/or sulfide liquid. Olivines from the Lower Talnakh intrusion plott slightly to the right of the model *b* fractionation trend (180 ppm initial Ni content in magma).

Lower Ni contents in olivine from the Oktyabr'sky mine than from the Taymysky mine are coupled with lower Ni, Cu and PGE contents in their associated sulfide ores. At Oktyabr'sky, the bulk sulfide ores of the picritic gabbro unit contain 2.0-3.6 wt% Ni, 5.2-9.4 wt% Cu and 8-19 ppm Pd (Naldrett et al., 1996). At Taymysky, the bulk sulfide ores of the same rock unit intercepted by borehole 5536 contain 3.6-9.3 wt% Ni, 7.1-11.5 wt% Cu and 15-28 ppm Pd. It seams that a higher R-factor would explain the higher chalcophile element contents in the sulfide ores at Taymysky. But this is not supported by the similar sulfur isotopic compositions at both locations. Similarly, the disseminated sulfides in the different rock units at Taymysky are also not related to each other by different R-factors. The content of Pd in the bulk sulfide of a sample from the olivine gabbro unit is <4ppm, which is >3 times less than the contents of Pd in the bulk sulfides of the underlying picritic gabbro unit. The $\delta^{34}S$ values of the sulfides from these two units however, are similar and all close to ~11 ‰.

The main conclusions from the proceeding discussions are summarized below: (1) with respect to major element compositions, the parental magmas of the picritic gabbro units of the Noril'sk and Talnakh intrusions were similar; (2) with respect to Ni contents, however, the parental magma of the picritic gabbro unit at Oktyabr'sky was significantly depleted in Ni as compared to that of the same type of rock unit at Taymysky and Noril'sk (180 versus 300 ppm); and (3) the disseminated sulfides in the same type of rock units in different intrusions, as well as in different rock units of a single borehole, were often not related to each other by different *R*-factors. Rather, compositional differences appear to be related to emplacement of multiple magmas that contained sulfide liquids with similar S isotopic compositions but significantly different chalcophile element concentrations.

Summary

Our S isotopic and olivine data are more consistent with the interpretation that sulfide segregation occurred in staging chambers. The sulfide liquids were then episodically upgraded in their chalcophile element concentrations by new surges of magmas into the chambers. Some of these sulfide magmas were simultaneously transported by the episodic surges of magmas to higher levels to form the composite sills of the ore-bearing intrusions.

Attributes of Skaergaard-Type PGE Reefs

James D. Miller, Jr.[1] and Jens C. Ø. Andersen[2]
[1]Minnesota Geological Survey, c/o NRRI, University of Minnesota-Duluth, 5013 Miller Trunk Hwy., Duluth, MN, 55811 , USA
[2]Camborne School of Mines, University of Exeter, Redruth, Cornwall, TR15 3SE UK
e-mail: mille066@tc.umn.edu, andersen@csm.ex.ac.uk

Stratiform, platinum group element (PGE) deposits have long been known to occur in ultramafic-mafic intrusive complexes such as Bushveld and Stillwater (Naldrett, 1989b). Commonly known as PGE reefs, such deposits are typically found near the transition from ultramafic to mafic cumulates where they occur as 1-3 meter thick intervals enriched in PGEs (1-20 ppm) and trace to moderate amounts of sulfide (0.5-5 wt %). However, relatively recent discoveries have demonstrated that potentially economic stratiform PGE mineralization may also occur in tholeiitic mafic layered intrusions. Au- and PGE-bearing layers have been found most notably in the Middle Zone of the Skaergaard Intrusion (Bird et al., 1991; Andersen et al., 1998), but also in related Palaeogene intrusions of East Greenland (Arnason et al., 1997; Arnason and Bird, 2000); in the Jurassic Freetown Layered Complex of Sierra Leone (Bowles, 2000); in thick Mesozoic tholeiitic diabase sheets of the eastern United States; in the 990 Ma Rincón del Tigre complex (Prendergast, 2000); in several intrusions associated with the 1.1Ga Midcontinent Rift of North America (Miller, 1999, this volume; Miller et al., 2002); in the Paleoproterozoic Lake Owen intrusion of Wyoming (Loucks and Glasscock, 1989); and in the 1.27 Ga Muskox Intrusion (Barnes and Francis, 1995). These and other discoveries reinforce previous suggestions that reef-type PGE deposits hosted by tholeiitic intrusions make up a new class of mineral deposits, which is best represented by the Platinova reefs of the Skaergaard Intrusion (Nielsen and Brooks, 1995; Prendergast, 2000). In this presentation, we summarize the distinctive attributes of this type of deposit, which we refer to as Skaergaard-type PGE reefs and discuss how their metallogenesis may differ from classic PGE reefs.

Tholeiitic mafic layered intrusions refer to a class of intrusions formed from aluminous, olivine tholeiitic parent magmas that are commonly associated with active rift settings, especially in plume-affected areas. Troctolite, anorthosite, olivine gabbro and oxide-rich olivine gabbro are common rock types in such intrusions whereas peridotite, pyroxenite, and dunite are usually quantitatively minor. When well-differentiated, such intrusions display a simplified cumulus stratigraphy following the scheme: Ol or Pl only-> Ol + Pl -> Pl + Cpx + FeOx ± Ol -> Pl + Cpx + FeOx + Ol + Ap. They have a strong cryptic layering towards iron-enrichment indicative of Fenner-type differentiation. They differ from classic PGE reef-bearing intrusions by lacking a significant ultramafic component (early olivine-only crystallization is minor to absent in most tholeiitic intrusions) and by being poor in orthopyroxene (inverted pigeonite is rarely a cumulus phase).

Skaergaard-type PGE reefs in well-differentiated tholeiitic intrusions are similar to classic reefs hosted by ultramafic-mafic complexes such as Bushveld and Stillwater complexes, in that they occur as sulfide-poor, PGE-rich intervals that are meters in thickness and are conformable with igneous layering. However, Skaergaard-type PGE reefs differ from classic reefs in many significant ways as summarized in Table 1. Also like many classic reef deposits, Skaergaard-type PGE reefs appear to have formed by predominantly orthomagmatic processes related the saturation, exsolution, and settling of magmatic sulfide melt from silicate magma and the accumulation of sulfide in stratiform cumulate layers. And like classic reefs, some believe that postcumulus hydromagmatic processes may be predominately responsible for the formation of Skaergaard-type reefs as well (Boudreau and Meuer, 1999).

One very significant difference in their metallogenesis, however, appears to be the manner by which sulfide becomes saturated in the magma system. Although magma mixing appears to be an important triggering mechanism for sulfide saturation (or oversaturation) in classic PGE reef systems (Naldrett, 1989b), the nearly constant solubility of sulfur during differentiation of tholeiitic magmas implies that magma recharge may not be capable of producing sulfide saturation in these systems.

To demonstrate this characteristic of sulfide solubility in a differentiating tholeiitic, the sulfide solubility curve and the liquid line of descent for FeO, S and temperature were modelled for the Sonju Lake intrusion (SLI) of northeastern Minnesota (Figure 1A). The SLI is a 1-km-thick, unidirectionally differentiated, sheet-like intrusion

that formed as a closed magmatic system during Midcontinent Rift magmatism (Miller and Ripley, 1996). The variation in FeO and temperature during crystallization differentiation of the SLI have been calculated by applying the fractional crystallization model of Nielsen (1990) to an estimated parent magma composition with 14.7% FeO (Miller and Ripley, 1996). The FeO model curve is similar to a FeO liquid line of descent curve (Fig. 1A) that has been calculated from mass balance of whole rock compositions through the SLI. Based on the experimental studies of Haughton et al. (1974), a 14-20% range of FeO contents at a temperature of 1200°C corresponds to sulfide solubility increasing from 0.11 to 0.19%. Over this range of increased FeO, temperature decrease has an opposite effect on sulfide solubility. The effect of temperature is not completely known in detail, but a number of experimental studies conducted between 1400 and 1000 °C reported by Naldrett (1989a) suggest a decrease in sulfide solubility by a factor of 3 to 8.5 per 100°C drop in temperature (or a 0.04 –0.09 wt. % decrease in sulfide solubility per 100°C), with a greater effect at lower overall temperatures. The estimated variations in sulfide solubility due to the changes in model FeO and temperature during fractional crystallization of the SLI are shown in Figure 1B. The resultant flat solubility curve (Fig. 1B) demonstrates the offsetting effects of increasing FeO and decreasing temperature throughout most of the SLI's crystallization history.

TABLE 1: Comparision of Attributes of Skaergaard-type and Classic PGE Reefs.

	Skaergaard-type PGE Reefs	Classic PGE Reefs
Tectonic Setting	Plume-influenced continental rifts, occur as subvolcanic intrusions	Unclear, occur as large, isolated intrusions within Precambrian cratons
Age	Mesoproterozoic and younger	Neoarchean to Paleoproterozoic
Parent Magma	Aluminous, olivine tholeiite (E-MORB)	High-Cr/Mg/Si boninite/komatiite (U-type) with aluminous tholeiite (A-type)
Host Rock	Gabbroic to ferrogabbroic cumulates (Pl+Cpx±Ox±Ol); some associated with layering.	Pyroxenitic to noritic cumulates; locally associated with chromitite layers, early anorthositic cumulates, and pegmatite.
Sulfide Composition **of Mineralized Intervals**[1]	Cu/Ni >100 (closed systems) Cu/Ni >1 (open systems)	Cu/Ni = 0.3-5.0 (open systems)
Precious Metal Ratios of Mineralized Intervals[1]	Pt/Pd = 7 – 0.1 Pt+Pd/Au = 1 - 10	Pt/Pd = 2.5 - 0.2 Pt+Pd/Au > 10
Stratigraphic Distribution of Peak Concentrations[1] (⇒ below, ⇔ coincident with, / or)	Pt ⇒/⇔ Pd ⇒⇒ Au Pt + Pd ⇒ Cu (±Ni)⇔ Au	Pd ⇒/⇔ Pt ⇒/⇔ Au Pt + Pd ⇒/⇔ Ni ⇔ Cu ⇔ Au
Examples[2]	Closed systems - Skaergaard, Sonju Lake Intrusion, New Haven diabase Open systems- Layered Series at Duluth, Kap Edvard Holm Complex, Lake Owen Intrusion, Freetown Complex, Muskox Intrusion, Rincón del Tigre Complex	Bushveld Complex, Stillwater Complex, Great Dyke, Munni Munni Complex, Jimberlana Intrusion, Penikat, Portimo and other Fenno-scandian intrusions, Rum Intrusion, Muskox Intrusion, Rincón del Tigre Complex

[1] *Based on data from this study; Arnason and Bird, 2000; Prendergast, 2000; Andersen et al., 1998; Lee, 1996; Barnes and Francis, 1995; Naldrett, 1989b.*

[2] *PGE reefs in the Muskox and Rincón del Tigre intrusions have attributes in common with both reef types.*

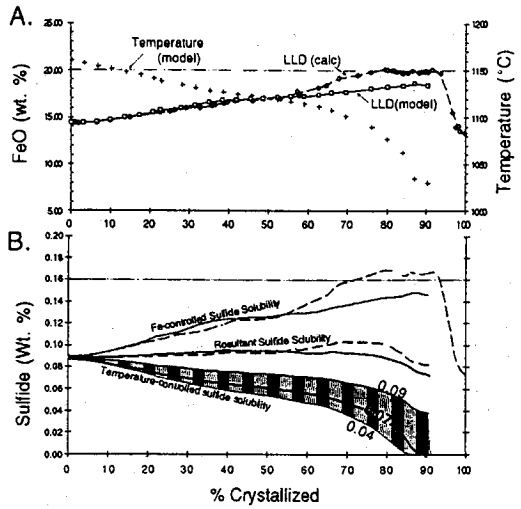

Figure 1. Model curves for FeO, temperature, and sulfide solubility variation during crystallization differentiation of the Sonju Lake intrusion. A) Variation in FeO and temperature based on fractional crystallization model of Nielsen (1990) and variation in FeO based on mass balance calculation (Miller and Ripley, 1996). B) Variation in sulfide solubility due to effects of temperature (factor range of 0.04–0.09 wt% sulfide/100 °C after Naldrett, 1989a) and FeO concentration (based on experimental data from Haughton et al., 1964). Resultant solubility curves are based on a median temperature factor of 0.07 wt% sulfide/100 °C.

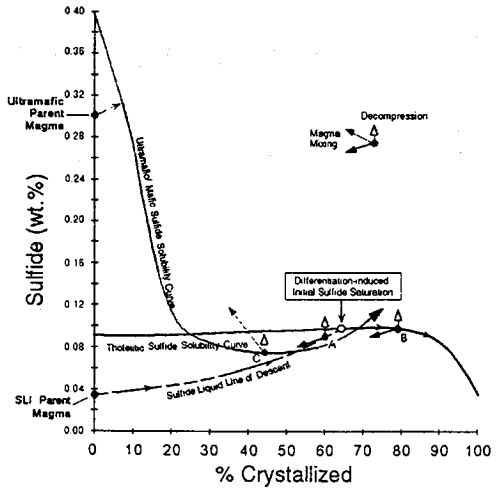

Figure 2. Resultant sulfide solubility curve for Sonju Lake intrusion compared to solubility curve estimated for ultramafic/mafic magma systems (Naldrett, 1989b). Liquid line of descent for sulfide in the SLI magma calculated by Rayleigh distillation and based on sulfide saturation at 65% crystallized. Vector arrows show effects of magma mixing and decompression for three different situations. Point A shows effects on tholeiitic SLI magma just prior to sulfide saturation. Point B shows effects on sulfide-saturated SLI magma. Point C shows effects on evolved ultramafic magma system.

Chemostratigraphic studies show that the Sonju Lake intrusion reached sulfide saturation at 65% crystallized (Miller, 1999; this volume). Treating sulfide as an incompatible component up to the point of saturation, the liquid line of descent of sulfide during fractional crystallization can be calculated by simple Rayleigh distillation. Assuming a sulfide concentration of 1.1 wt.% at saturation, the calculated liquid line of descent curve implies an initial sulfide concentration of the parent magma of 0.35 wt.% (Fig. 2). It is clear that magmatic recharge of this parental composition will not result in saturation or oversaturation of sufide. Also plotted in Figure 2 is the sulfide solubility curve estimated for ultramafic/mafic magma systems by Naldrett (1989b), which shows how magma mixing can result in sulfide oversaturation is such systems. Although stratiform PGE mineralization in the Kap Edvard Holm intrusion appears to be related to magma mixing (Arnason and Bird, 2000), it is not clear how this has occurred from an uncontaminated tholeiitic parent magma.

Rather than magma recharge, magmatic processes of crystallization differentiation, decompression due to magma venting, and changes in phase equilibrium appear to be important in the formation of most Skaergaard-type reef occurrences. The Sonju Lake intrusion looks to be the most clear cut example of sulfide saturation triggered by straightforward crystallization differentiation, though a detail examination of the reef is underway to confirm this interpretation. Andersen et al. (1998) have similarly interpreted the Pd and Au mineralization of the Skaergaard to have formed by fractional crystallization driving the magma to sulfide saturation. However, the cyclical nature of PGE mineralization and modal layering in the host gabbro may suggest a more dynamic triggering mechanism. Miller (this volume) has interpreted the PGE mineralization and the related macrocyclic layering in the Layered Series at Duluth as resulting from periodic decompression due to magma venting from a shallow (<5km) depth. Perhaps the Platinova reefs of the Skaergaard formed in a similar manner. Sulfide saturation triggered by changes in phase equilibrium, especially the onset of Fe-oxide crystallization, is evident in the Rincón del Tigre complex (Prendergast, 2000).

In conclusion, the suggestion by Nielsen and Brooks (1995) that the stratiform PGE and Au mineralization discovered over a decade ago in the Skaergaard intrusion may constitute an important new type of mineral deposit now seems prophetic in light of similar discoveries in other igneous provinces. Although an economically viable deposit has yet to be found, the search for

Skaergaard-type PGE reefs has only just begun. Like their classic reef cousins, exploration for this subtle style of mineralization requires systematic sampling and a thorough understanding of the crystallization history of the host intrusion.

References

Andersen, J.C.Ø., Rasmussen, H., Nielsen, T.F.D., Rønsbo, J.G., 1998, The Triple Group and the Platinova gold and palladium reefs in the Skaergaard Intusion: stratigraphic and petrographic relations: ECONOMIC GEOLOGY, v.93, p. 488-509.

Arnason, J.G., and Bird, D.K., 2000, A gold- and platinum-mineralized layer in gabbros of the Kap Edvard Holm complex: field, petrologic, and geochemical relations: ECONOMIC GEOLOGY, v. 95, p. 945-970.

Arnason, J.G., Bird, D.K., Bernstein, S. and Kelemen, P.B., 1997, Gold and platinum-group element mineralization in the Kruuse Fjord Gabbro complex, East Greenland: ECONOMIC GEOLOGY, v.92, p. 490-501.

Barnes, S-J., and Francis, D., 1995, The distribution of platinum-group elements, nickel, copper, and gold in the Muskox layered intrusion, Northwest Territories, Canada: ECONOMIC GEOLOGY, v. 90, p. 135-154.

Bird, D.K., Brooks, C.K., Gannicott, R.A., Turner, P.A., 1991, A gold-bearing horizon in the Skaergaard Intrusion, East Greenland: ECONOMIC GEOLOGY, v. 86, p. 1083-1092.

Boudreau, A.E. and Meuer, W.P., 1999, Chromatographic separation of platinum-group elements, gold, base metals, and sulfur during degassing of a compacting and solidifying igneous crystal pile: Contributions to Mineralogy and Petrology, v. 134, p. 174-185.

Bowles, J.F.W., 2000, A primary platinum occurrence in the Freetown Layered Intrusion, Sierra Leone: Mineralium Deposita, v. 35, p. 583-586.

Haughton, D.R., Roeder, P.L., Skinner, B.J., 1974, Solubility of sulfur in mafic magmas: Economic Geology, v. 69, p. 451-467.

Lee, C.A., 1996, A review of mineralization in the Bushveld Complex and some other layered intrusions, *in* Cawthorne, R.G., ed., Layered Intrusions: Amsterdam, Elsevier Sci., p. 103-145.

Loucks, R.R.,and Glasscock, J.W., 1989, Petrology and PGE mineralization of the early Proterozoic Lake Owen layered mafic intrusion, southern Wyoming, USA: Bulletin of the Geological Society of Finland, v. 61, p.11-12.

Miller, J.D., Jr., 1999, Geochemical evaluation of platinum group element (PGE) mineralization in the Sonju Lake Intrusion, Finland, Minnesota: Minnesota Geological Survey Information Circular 44, 32 p.

Miller, J.D., Jr., and Ripley, E.M., 1996, Layered intrusions of the Duluth Complex, Minnesota, USA, *in* Cawthorne, R.G., ed., Layered Intrusions: Amsterdam, Elsevier Sci., p. 257-301.

Miller, J.D., Jr., Green, J.C., Severson, M.J., Chandler, V.W., Hauck, S.A., Peterson, D.E., and Wahl, T.E., 2002, Geology and mineral potential of the Duluth Complex and related intrusions, northeastern Minnesota. Minnesota Geological Survey Report of Investigations 58, 208 p. w/CD-ROM.

Naldrett, A.J., 1989a, Sulfide melts: crystallization temperatures, solubilities in silicate melts, and Fe, Ni, and Cu partitioning between basaltic magmas and olivine, *in* Whitney, J.A., and Naldrett, A.J., eds., Ore deposition associated with magmas: Reviews in Economic Geology, v. 4, p. 5-20.

Naldrett, A.J., 1989b, Stratiform PGE deposits in layered intrusions, *in* Whitney, J.A., and Naldrett, A.J., eds., Ore deposition associated with magmas. Reviews in Economic Geology v. 4, p. 135-165.

Nielsen, R.L., 1990, Theory and application of a model of open system processes, *in* Nicholls, J. and Russell, J.K., eds., Modern Methods of Igneous Petrology: Mineralogical Society of America, Reviews in Mineralogy, v. 24, p. 56-106.

Nielsen, T.F.D., and Brooks, C.K., 1995, Precious metals in magmas of East Greenland: Factors important to the mineralization in the Skaergaard Intrusion: Economic Geology, v. 90, p. 1911-1917.

Prendergast, M.D., 2000, Layering and precious metal mineralization in the Rincón del Tigre complex, eastern Bolivia: Economic Geology, v. 95, p. 113-130.

On the Formation of Platinum Group Element–Rich Continental Flood Basalt and the Platinova Reefs of the Skaergaard Intrusion

Peter Momme[1,2], Christian Tegner[1,2] and C. Kent Brooks[2,3]
[1]Geologisk Institut, University of Aarhus, DK-8000 Århus C, Denmark
[2]Danish Lithosphere Centre, Øster Voldgade 10, DK-1350 København K, Denmark
[3]Geologisk Institut, Københavns Universitet, Øster Voldgade 10, DK-1350 København K, Denmark
e-mail: christian.tegner@geo.au.dk

Platinum Group Element reefs associated with layered mafic intrusions require a parental magma that contains at least several parts per billion (p.p.b.) Pd or Pt. The extemely high distribution coefficient for PGE between sulphide and magma predicts that PGE–rich magmas can only form if all sulphides are melted out of the mantle. For standard peridotite mantle with 250±50 p.p.m. S (McDonough and Sun, 1995), the mantle sulphides are exhausted only if the mean degree of mantle melting (F) exceeds 20%. Komatiite is of course the type example of a Pd–rich magma (8–21 p.p.b., Fig. 1) formed by high F: well above 20% (Keays, 1995). Mid-ocean ridge basalt (MORB) mostly form by moderately high F (8-20%; Klein and Langmuir, 1987), but rarely contains more than 1 p.p.b. Pd (Fig. 1); this is ascribed either to retention in mantle sulphides or to subsequent sulphide saturation during basalt differentiation (Barnes et al., 1987).

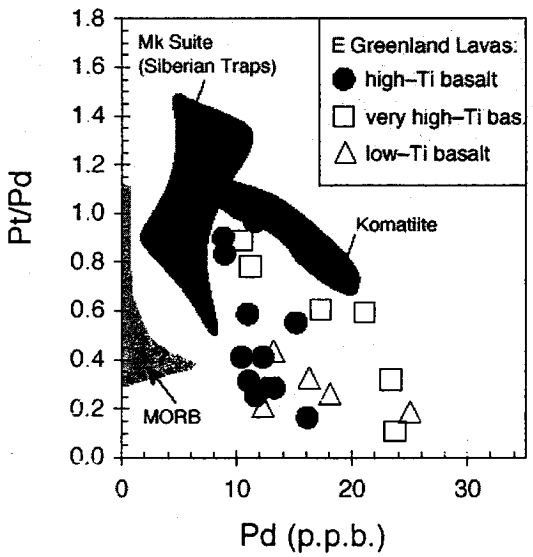

Figure 1. Pd and Pt composition of the Paleogene East Greenland flood basalt province (Momme et al., 2002), recent MORB and old komatiite (Rehkämper et al., 1999), and PGE–rich flood basalts of the Permo–Triassic Siberian traps (Mokulaevsky Suite; Brügmann et al., 1993).

For continental flood basalts, the constraints on mantle melting conditions are conflicting. On the one hand, the presence of prominent PGE reefs of continental mafic intrusions such as Noril'sk, Bushveld, Stillwater, and Skaergaard associated with flood basalts implies PGE–rich parental magmas. This would suggest high F. On the other hand, the lithophile trace element composition, in particular the rare–earth elements (REE), indicate that most continental flood basalts formed by moderate F in the range from 5 to 15% (Fram and Lesher, 1993). Although most continental flood basalts are inferred to originate from hot mantle plumes, the reason F remains moderate is that the top portion of the melting regime is truncated by thick non–melting lithosphere – this is referred to as the 'lid'–effect (Ellam, 1992). In this contribution we explore the effects of the lithospheric lid on the PGE and REE composition of continental flood basalt with particular emphasis on the Paleogene East Greenland Igneous Province, following Momme et al. (in press, in review), and the Platinova Pd–Au reef of the Skaergaard intrusion (Andersen et al., 1998).

PGE of the East Greenland Continental Flood Basalt Province

This Paleogene flood basalt province formed during continental rifting immediately before the opening of the Northeast Atlantic. The major element and REE composition show the 6 km thick lava pile of the Blosseville Kyst is composed mainly of high–Ti basalt [mg#, = molar Mg/(Mg+Fe) range from 60 to 43] and with subordinate and intercalated low–Ti and very–high–Ti basalt, all largely unaffected by crustal contamination (Tegner et al., 1998). All three magma suites are PGE–rich with Pd ranging from 3 to 25 p.p.b., but we will focus only on the dominant high–Ti suite that contains 6 to 16 p.p.b. Pd (Fig. 1). The concentration of Pd increase with decreasing mg# (Fig. 2), demonstrating that Pd was excluded during igneous differentiation. This can only be obtained if the magma was undersaturated with respect to S and thus did not reach the point

where sulphide droplets are exsolved (Momme et al., 2002). In summary the East Greenland flood basalts contain moderate amounts of PGE between that of komatiite and MORB (Fig. 1) and did not exsolve sulphide.

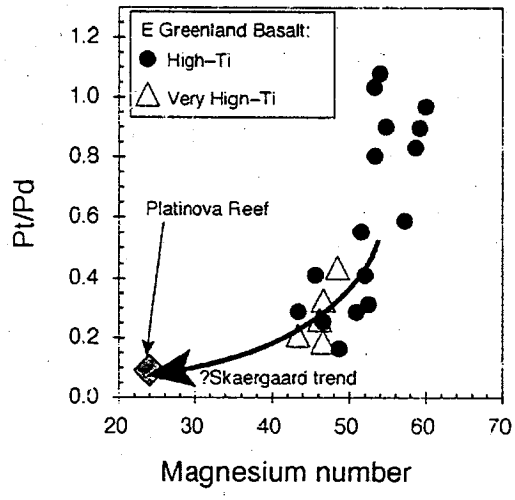

Figure 2. Variation in Pd and Pt with mg# [molar Mg/(Mg+Fe)] for high–Ti and very high–Ti basalt lavas of the East Greenland flood basalt province. Also shown is the typical Pd/Pt of the Platinova Pd–Au reef of the coeval Skaergaard intrusion.

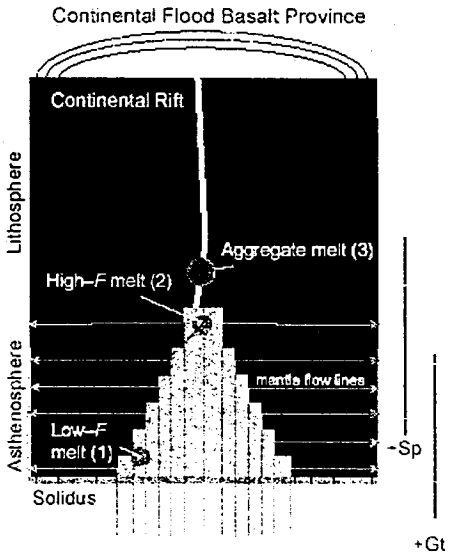

Figure 3. Schematic cross-section showing the melting regime of a corner–flow model (Langmuir et al., 1992) for upwelling mantle plume beneath a continental rift. The mantle solidus is intersected at ~120 km depth and the top of the melting column is at ~60 km depth (Tegner et al., 1998). Predicted melts labelled 1, 2 and 3 are: 1) low–F, high La/Sm$_N$, low PGE content, and S–saturated; 2) high–F, low La/Sm$_N$, high PGE content, and S–undersaturated; 3) aggregate melt, intermediate F, PGE content, and La/Sm$_N$.

Mantle Melting Model

Forward modelling of the REE composition suggests the high–Ti basalts from Greenland formed by mean degrees of melting (F) ranging from 5 to 9%, of mantle depleted slightly (0.5%) relative to Primitive Mantle (Tegner et al., 1998). In this model it was assumed that the melting regime is triangular and governed by upwelling and corner flow as suggested for melting beneath mid–ocean ridges (Langmuir et al., 1992). As depicted in Fig. 3, the mantle starts melting when its solidus is crossed and mantle parcels undergo progressive melting as they ascend. In a forward model, this is approximated by melting mantle parcels at the pressure of the solidus intersection by one percent, extract the magma, recalculate the residual mantle composition and mineralogy, and so forth with pressure of steps decreasing by 1 kbar for each computation. If this is the way the mantle melts, the mantle parcels that reach the top of the melting regime undergo a large degree of melting whereas mantle parcels at the side of the triangle only melts by a few percent before they flow to the side and out of the melting zone (Fig. 3). If melt at any given time is pooled from the entire melt zone it will be a mixture of low and high degree melts. Clearly, the low–degree melts stem from mantle in which sulphides retain the PGE inventory and they will be S–saturated and contain little or no PGE, and will have high concentrations of incompatible lithophile trace elements such as REE. On the other hand, the higher degree melts from the top of the melting column eventually will reach the point at which the sulphides are dissolved and the magmas become PGE–rich. The geometric relations predict that F is half of the maximum degree of melting reached for the topmost mantle parcel of the triangle Rehkämper et al. (1999) was the first to propose that such a melting model may explain the formation of ocean–island basalts with moderate PGE as the result moderate F.

The results of our forward modelling of the PGE composition of basalt formed during continental breakup is summarised in Fig. 4 and indicate that if the mantle contains 200 S and the magma can dissolve 1000 p.p.m. S, then magmas with 10 p.p.b. Pd may be produced for F larger than 10%. In summary, forward modelling of REE suggests that the high-Ti East Greenland flood basalts may form for F ranging from 5 to 9% and forward modelling of PGE suggests the same basalts may form only for F above 10% for reasonable mantle compositions. The F estimated from REE modelling obviously depends more on assumptions about source composition than that of PGE modelling. Hence, the major element, the REE, and the PGE composition of the high–Ti

flood basalts may all be explained by approximately 10% mantle melting.

The 'Lid'-Effect Drives Magma to S–Undersatuation

The pooled melts of the above model is a mixture of S–undersaturated (high–degree melts) and S–saturated basalts (low–degree melts) and it is not clear whether this mixed product is over– or undersaturated at the depth of the source. In any case, it appears unlikely that the S–undersaturated nature of the East Greenland flood basalts may be so strong without additional effects that drive the magma to S–undersaturation. In fact, there are two mechanisms that may increase the amount of S that may be dissolved in basalt, that is FeO content and pressure. Poulson and Ohmoto (1990) showed that the S–capacity of a magma increases with its FeO content. Because the high–Ti basalts diffentiate towards iron enrichment (Brooks et al., 1991) it appears that the S–capacity of the magma may increase solely as a consequence of differentiation. Further, the REE's indicate garnet is present in the source. Hence the lid–effect predicts that the mean pressure of melting, *P*, is elevated. The FeO content of magma increase with *P* during melting and thus suggest that continental flood basalts have high S–capacity relative to MORB. Finally, but perhaps most important, Mavrogenes and O'Neill (1999) showed that magmas at high pressure can dissolve less S than the same magma at low pressure. For the reasons outlined above, we believe the high *P* of melting followed by adiabatic ascent of the magma may be very important in driving continental flood basalts to S–undersaturation.

Formation of the Platinova Reef, Skaergaard intrusion

The Platinova Reef consists of several orthomagmatic palladium– and gold–rich magnetite–gabbro layers at the top of the Middle Zone (Andersen et al., 1998). In terms of igneous differentiation, the host pyroxene and plagioclase composition indicates the reef formed from an evolved magma with mg# close to 23. Compared to PGE reefs of the Bushveld and Stillwater complexes, the Platinova Reef is not only unusual in that the magma was evolved, but also in that it is a Pd reef with Pt/Pd below 0.1 A surprising feature of the Greenland high–Ti basalts is that the Pt content, which ranges from 2 to 11 p.p.b., decreases slightly with fractionation, indicating Pt is incorporated into the fractionating gabbro assemblage (D^{bulk} is 2–3), perhaps as tiny Platinum–Group Minerals hosted by olivine (Momme et al., 2002). Hence Pd is fractionated from Pt and Pt/Pd decreases with differentiation (Fig. 2). In the same way as the Pt/Pd of the high–Ti basalts decrease with mg# ranging from 60 to 43, we speculate that the low Pt/Pd of Platinova Reef (mg# ~25) may result from prolonged fractionation where Pt is included into and Pd excluded from the cumulates. This is illustrated as the Skaergaard trend in Fig. 2.

Implications for the Siberian Trap Magmatism

The Noril'sk mafic intrusions are associated with the Siberian Traps flood basalts and the parental magmas must have contained considerable amounts of PGE. Almost all the flood basalts of the region are depleted in PGE, saturated in S, and show isotopic evidence for the assimilation of S–rich sediments (Brügmann et al., 1993). However, in the top section of the volcanic pile there are lavas that contain significant amounts of PGE (Brügmann et al., 1993) and may not be S-saturated.

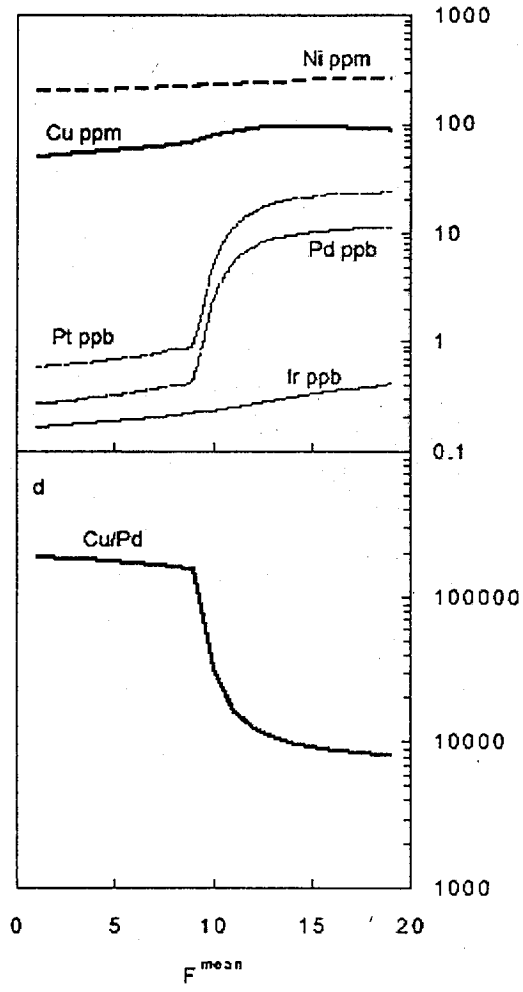

Figure 4. Modelled Ni, Cu, Pt, Pd and Ir composition with mean degree of mantle melting (F). Model calculations assume corner–flow melting regime as shown in Fig. 3, the mantle contains 200 S, and the magma can dissolve 1000 p.p.m. S (Momme et al., in review).

In the Mokulaevsky Suite, the concentration of PGE is similar to the high–Ti basalts of East Greenland (Fig. 1) whereas the REE patterns are steeper. The differences in REE may reflect a more enriched source for the Siberian flood basalts. We speculate that the primary mantle–derived versions of the Siberian Traps flood basalts was very similar to those of the East Greenland high–Ti basalts and that they could have formed at comparable mantle melting conditions. If so, the main difference between the two provinces lie in the crustal processes indicating abundant assimilation in the Siberian case and very little crustal contamination in the East Greenland basalts. However, we speculate whether mantle plume melting beneath a thick lithospheric 'lid' could also account for the composition of these occurrences.

References

Andersen, J.C.Ø., Rasmussen, H., Nielsen, T.F.D., and Rønsbo, J.G. (1998). The Triple Group and the Platinova gold and palladium reefs in the Skaergaard intrusion: stratigraphic and petrographic relations. Economic Geology, v. 93 p. 488–509.

Barnes S-J, Boyd R, Korneliussen A, Nilsson L-P., Often M, Pedersen RB, and Robins B (1987). The Use of Mantle Normalization and Metal Ratios in Discrimination between the Effects of Partial Melting, Crystal Fractionation and Sulphide Segregation on Platinum-Group Elements, Gold, Nickel and Copper: Examples from Norway. In: H.M. Prichard, P.J. Potts, J.F.W. Bowles and S.J. Cribb (eds) Geo-platinum symposium volume. Elsevier, London, p. 113-143.

Brooks, C.K., Larsen, L.M., Nielsen, T.F.D (1991). Importance of iron–rich tholeiitic magmas at divergent plate margins: a reppraisal. Geology, v. 19, p. 269–272.

Brügmann, G.E., Naldrett, A.J., Asif, M., Lightfoot, P.C., Gorbachev, N.S., and Fedorenko, V.A. (1993) Siderophile and chalcophile metals as tracers of the evolution of the Siberian Trap in the Noril'sk region, Russia, Geochimica et Cosmochimica Acta, v. 57, p. 2001-2018.

Ellam R.M. (1992) Lithospheric thickness as a control on basalt geochemistry. Geology v. 20, p. 153-156.

Fram MS, Lesher CE (1993). Geochemical constraints on mantle melting during creation of the North Atlantic basin. Nature, v. 363, p. 7112-715.

Keays, R.R. (1995). The role of komatiitic magmatism and S-saturation in the formation of ore deposits. Lithos, v. 34, p. 1-18.

Klein E.M., Langmuir, C.H. (1987). Global correlations of ocean ridge basalt chemistry with axial depth and crustal thickness. Journal of Geophysical Research 92(B8):8089-8115

Langmuir C.H., Klein, E.M., Plank, T. (1992). Petrological systematics of mid-ocean ridge basalts: Constraints on melt generation beneath ocean ridges. In: J.P. Morgan, D.K. Blackman and J.M. Sinton (eds): Mantle flow and melt generation at mid-ocean ridges. Geophysical Monographs, v. 71, p. 183-275.

Mavrogenes, J.A. and O'Neill, H.S.C. (1999). The relative effects of pressure, temperature and oxygen fugacity on the solubility of sulfide in mafic magmas, Geochimica et Cosmochimica Acta, v. 63, p. 1173-1180.

Momme, P., Tegner, C., Brooks, C.K., and Keays, R.R. (in press). The behaviour of platinum-group elements in basalts from the East Greenland Rifted Margin Contributions to Mineralogy and Petrology.

Momme, P., Brooks, C.K., Tegner, C., and Keays, R.R. (in review).Modeling platinum-group elements during mantle melting and comparison beetween East Greenland and Siberian continental flood basalts. Earth and Planetary Science Letters.

Poulson, S.R. and Ohmoto, H. (1990). An evaluation of the solubility of sulfide sulfur in silicate melts from experimental data and natural samples. Chemical Geology, v. 85, p. 57-75.

Rehkämper, M., Halliday, A.N., Fitton, J.G., Lee, D.-C., Wieneke M., and Arndt, N.T. (1999). Ir, Ru, Pt and Pd in basalts and komatiites: new constraints for the geochemical behaviour of the platinum-group elements in the mantle, Geochimica et Cosmochimica Acta, v. 63(22), p. 3915-3934.

McDonough WF, Sun S-s (1995). The composition of the Earth, Chemical Geology, v. 120, p. 223-253.

Tegner, C., Lesher, C.E., Larsen, L.M., and Watt, W.S. (1998). Evidence from the rare-earth-element record of mantle melting for cooling of the Tertiary Iceland Plume, Nature, v. 395, p. 591-594.

Local Variations and Regional Trends in PGE Geochemistry and Mineralogy in the Main Sulfide Zone of the Great Dyke, Zimbabwe

Thomas Oberthür[1], Thorolf W. Weiser[1] and Kari Kojonen[2]
[1]Federal Institute for Geosciences and Natural Resources (BGR), Stilleweg 2, D-30655 Hannover, Germany.
[2]Geological Survey of Finland, Betonimiehenkuja 4, FIN-02150 Espoo, Finland
e-mail: thomas.oberthuer@bgr.de

Introduction

The Great Dyke of Zimbabwe constitutes the world's second largest reserve of PGE after the Bushveld Complex in neighbouring South Africa. In the Great Dyke, economic concentrations of PGE are restricted to sulfide disseminations of the Main Sulfide Zone (MSZ). The present work is based on the study of samples from new exposures of economic grade primary ores of the MSZ created in the course of exploration and mining at Hartley, Mhondoro, Ngezi, Unki and Mimosa (Fig. 1). New findings are reported on the geochemical distribution and the mineralogical siting of the PGE, the mineralogy of the PGM, and the regional variations of these parameters. The findings are discussed in view of the contrasting "magmatic sulfide" and "hydrothermal fluid" genetic models.

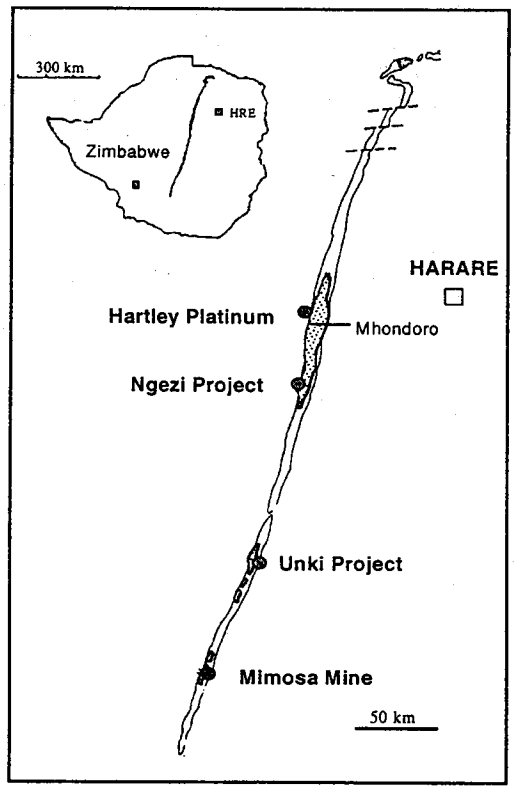

Figure 1. Sketch of the Great Dyke showing the localities of mines and prospects mentioned in the text.

Geologic Setting

The 2575.4 ± 0.7 Ma Great Dyke layered intrusion has a linear shape and strikes over 550 km NNE at a maximum width of about 11 km, cutting Archean granites and greenstone belts of the Zimbabwe craton. Stratigraphically, it is divided into a lower Ultramafic Sequence of dunites, harzburgites, olivine bronzitites and pyroxenites, together with narrow layers of chromitite, and an upper Mafic Sequence mainly consisting of plagioclase-rich rocks (norites, gabbro-norites, olivine gabbros). Economic concentrations of PGE, Ni and Cu in the form of disseminated sulfides occur some meters below the transition from the Ultramafic to the Mafic Sequence, in the several meters thick "Main Sulfide Zone", in pyroxenitic host rocks.

Samples and Methods

Twenty-one vertical profiles across the MSZ, between 1.5 and 5 m long, were taken from drill cores (Hartley, Mhondoro, Ngezi, Unki) or were cut underground (Hartley, Mimosa). The whole rock samples were analysed by XRF and ICP-MS. PGE contents were determined by INAA after Ni-sulfide extraction. Polished sections were investigated by reflected light microscopy, XRD, SEM/EDX, and electron microprobe.

Geochemical Distribution of PGE in the MSZ

Our study of 21 MSZ sections corroborated that, apart from minor variations, the MSZ is characterized by a typical vertical pattern of base metal sulfide and PGE distribution as known from the work of e.g. Prendergast (1988), Prendergast and Wilson (1989), and Wilson (2001). This pattern is characterized by "offsets", i.e. a certain degree of decoupling, and separation of the respective element distribution patterns and peak concentrations, namely of Pd from Pt, and also of all PGE from the base metals. Our data also confirm the subdivision of the MSZ into a lower PGE subzone and an upper BMS subzone, and the further subdivision of the PGE subzone into a lower (Pd>Pt) and an upper part (Pd<Pt).

The vertical distributions of the base metals and sulfur (BMS; Cu, Ni, S), Pt and Pd are shown in Fig. 2, which is an idealized profile across the MSZ, about 3 metres wide, mainly based on data from Hartley mine. Notable are three variably pronounced peaks in the PGE subzone. (i) PGE-1 close to the base is a broader area characterized by slightly increasing PGE contents at low levels of base metals and sulfur, Pd > Pt, and low contents of ΣPPGE relative to ΣIPGE (ΣPPGE/ΣIPGE ratios are ca. 9 at PGE-1 compared to ca. 20 at positions PGE-2 and PGE-3 at Hartley mine). Further upward, ΣIPGE remain at nearly constant levels, Pd values exceed those of Pt, and the base metal and sulfur contents continue to increase slightly. (ii) At position PGE-2, the peak of Pd is reached, which coincides with a subsidary peak of Pt and slightly elevated BMS contents. (iii) PGE-3 is the peak of Pt, distintcly offset from the peak of Pd. At this position, shortly before or overlapping with the strongest BMS peak, Pd shows a subsidary peak and Rh, Ru, Ir and Os reach maxima. The elevated contents of ΣIPGE relative to ΣPPGE (low ΣPPGE/ΣIPGE ratios) in the PGE-1 area indicate a certain offset of the IPGE group from Pt and Pd. This justifies a further refinement of the structure of the PGE subzone (basal, centre and top part; indicated by the peaks PGE-1, PGE-2 and PGE-3).

Chondrite-normalized patterns of the averages of the PGE subzone of the MSZ show steep upward trending curves from Os to Pd (Fig. 3). This type of pattern is regarded typical for PGE mineralization produced by magmatic scavenging of PGE through segregating sulfides. The tight array displayed by the various MSZ localities indicates consistent contents and proportions of PGE within the MSZ over wide areas.

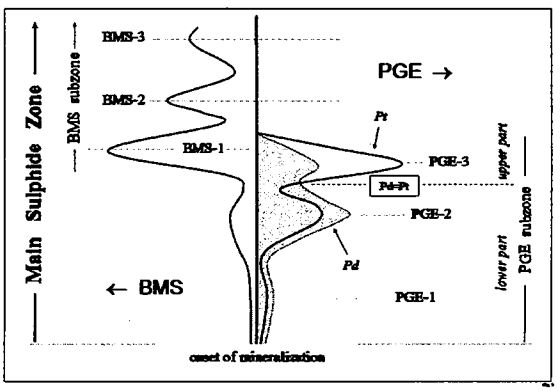

Figure 2. Sketch of key features of element distributions and subdivision of the MSZ. BMS = base metal sulfides.

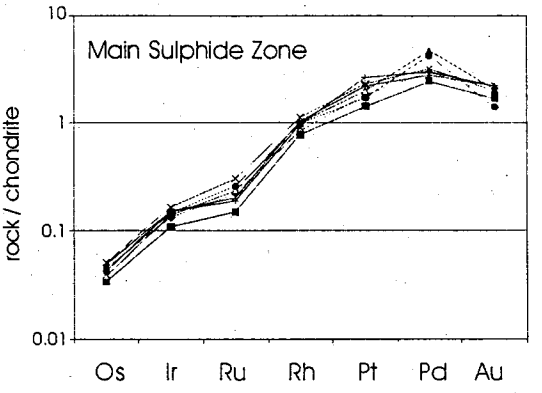

Figure 3. C-1 normalized average PGE contents of the MSZ (PGE subzone) from various Great Dyke localities.

Platinum-Group Minerals (PGM)

The pyroxenites of the MSZ contain between 0.5 and 10 vol% of sulfides – pyrrhotite, pentlandite, chalcopyrite and subordinate pyrite – which mainly occur interstitially to cumulus orthopyroxene. The PGM are usually included in pyrrhotite or chalcopyrite, rarely in pentlandite, or they occur at sulfide/sulfide or sulfide/silicate contacts or within silicates. PGM intergrown with pyrite are extremely rare. PGM grain sizes (apparent maximum diameters) range from < 5 to 50 μm in general, but may reach up to 373 μm in the longest dimension.

Altogether, 801 grains of PGM were analyzed by electron microprobe. The suite of PGM (proportions by number) comprises (Pt,Pd)-bismuthotellurides, mainly moncheite, maslovite, merenskyite, and michenerite (50.1%), followed by sperrylite (19%), the PGE-sulfarsenides hollingworthite, platarsite, irarsite and ruarsite (11.9%), the (Pt,Pd)-sulfides cooperite and braggite (8.5%), laurite (5.0%), and some rarer phases.

The various PGM are heterogeneously distributed within the MSZ sequence. At Hartley for example, sperrylite occurs throughout the PGE subzone of the MSZ, whereas cooperite/braggite only occur in samples from and below the Pt peak. The (Pt,Pd)-bismuthotellurides concentrate in the upper portion of the PGE subzone of the MSZ only, mainly in the regions around PGE-3 and BMS-1.

Trace PGE Contents in Sulfides

Micro-PIXE studies had shown that pentlandite from the lower PGE subzone of the MSZ at Hartley, Unki and Mimosa had elevated contents of Pd (maximum value 2,236 ppm Pd), and Rh (max. 259 ppm Rh), and SIMS analysis revealed that pyrite was a carrier of Pt (0.4-244, mean 35.5 ppm; n=37). Electron microprobe analysis using the CSIRO-Trace program was performed on pentlandite from Hartley, Unki and

Mimosa. Maximum Pd and Rh contents measured are 2,506 ppm Pd and 562 ppm Rh. In the example below (Fig. 4; core CD-02, Hartley mine), Pd contents in pentlandite appear to attain and stay at a plateau level of ca. 1,200 ppm Pd through most of the PGE subzone of the MSZ (maximum average value = 1,379 ppm Pd), interrupted by a return to lower values (≈ 300 ppm Pd) between PGE-1 and PGE-2. Further up-sequence, Pd contents in pentlandite drop to values below the detection limit of the method (about 40 ppm Pd) just before reaching the Pt peak (PGE-3). The data therefore underline that most of the Pd is generally hosted by pentlandite in the lower and central parts of the PGE subzone.

Figure 5 summarizes the major geochemical and mineralogical variations and trends in the MSZ. Note the elevated contents of Pd in pentlandite in the lower part of the PGE subzone, overlapping distributions of the various PGM groups in the profile, and the preferred concentration of laurite in the basal part of the PGE subzone. Gold and the tellurides of Bi, Ag, Ni and Pb mainly occur in the transition from the PGE to the BMS subzone of the MSZ. Changes in pyrrhotite compositions, and the presence of pyrite in the upper part of the PGE subzone and the BMS subzone indicate increasing fS_2 up sequence.

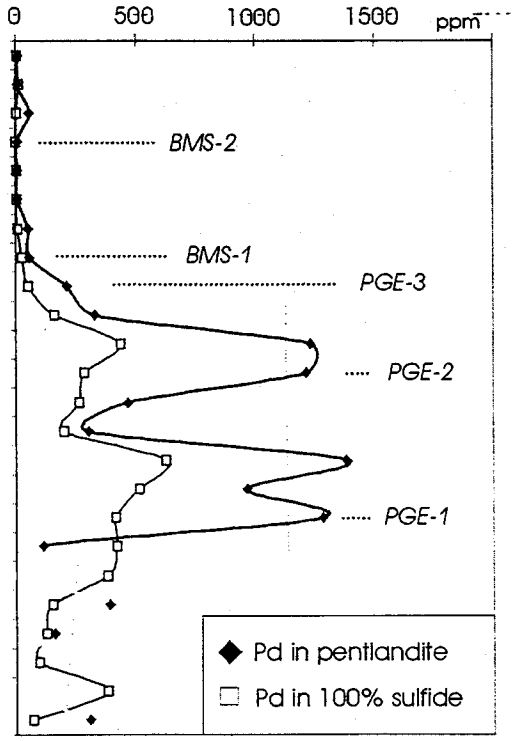

Figure 4. Vertical distribution of Pd in pentlandite (ppm) analyzed by electron microprobe, and Pd in 100% sulfide (ppm) calculated from whole rock data.

Regional Variations in PGM Proportions

Major regional differences were observed in PGM proportions (Table 1) and grain sizes. The MSZ samples of the North Chamber (Hartley + Mhondoro + Ngezi) have higher proportions of (Pt,Pd)-bismuthotellurides (63.8%) and cooperite plus braggite (12.7%), and lower proportions of sperrylite (11.0%), PGE-sulfarsenides (2.4%), and laurite (1.7%) compared to those of the South Chamber. The respective South Chamber (Unki + Mimosa) values are: (Pt,Pd)-bismuthotellurides (35.2%), cooperite/braggite (3.9%), sperrylite (27.6%), PGE-sulfarsenides (22.1%) and laurite (8.6%). The different PGM proportions and accompanying different apparent average PGM grain sizes (39 μm in the North Chamber versus 18.5 μm in the South Chamber) must be considered in the metallurgical treatment of the ores.

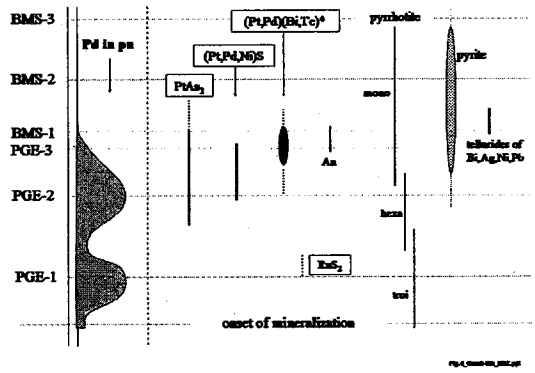

Figure 5. Summary of key geochemical and mineralogical features of MSZ profiles as exemplified at Hartley mine. Pd in pn = Pd contents in pentlandite. (Pt,Pd)(Bi,Te) = (Pt,Pd)-bismuthotellurides. Pyrrhotite: mono = monoclinic; hexa = hexagonal; troi = troilite.*

*Table 1. Comparison of PGM proportions by number of various MSZ localities. (Pt,Pd)(Bi,Te) * = (Pt,Pd)-bismuthotellurides. PGE-AsS + = PGE-sulfarsenides.*

locality →	Hartley	Mhondoro	Ngezi	Unki	Mimosa
PGM (n) → type [%] ↓	*181*	*43*	*199*	*250*	*134*
(Pt,Pd)(Bi,Te) *	71	58	60	39	28
$PtAs_2$	11	9	11	28	26
(Pt,Pd)S	11	5	16	4	3
PGE-AsS +	2	4	2	16	33
Pt-Fe alloys	1	11	6	—	—
others	4	11	5	12	13

Discussion and Conclusions

The combination of geochemical and mineralogical data suggests the following model for the formation of the PGM in relation to PGE distributions. It is postulated that all PGE were primarily scavenged by sulfide in the magmatic stage due to their high partition coefficients in favour of sulfide. The metal profiles indicate sulfide accumulation in a number of distinct successive layers, each with its own geochemical characteristics. The general trend within the MSZ is one of upward increases in ΣPPGE / ΣIPGE, Pt/Pd and Cu/Ni ratios, as well as fS_2. Apparently, the various elements were extracted from the magma in consecutive batches which show successive enrichments of the chalcophile elements according to their apparent D values (in case of the MSZ, $D_{Pd} > D_{Pt}$, for example). Upon cooling, in the subliquidus stage, the PGE-bearing sulfide droplets recrystallized to form aggregates of pyrrhotite, pentlandite, chalcopyrite and some pyrite. The development down-temperature was accompanied by continuous subsolidus annealing of the sulfides and their internal crystal ordering. Ballhaus and Ryan (1995) demonstrated that Pd and Rh are accommodated within the crystal lattice of pentlandite down to low temperatures, a finding corroborated by our direct measurements of these elements in pentlandite. In contrast, Pt is incompatible with any of the sulfides forming (except for low levels in pyrite) and was thus expelled from their crystal lattices. Pt released from sulfides during the annealing process readily reacted with As, Bi and Te due to the high affinity of these metalloids for Pt, to form sperrylite and bismuthotellurides. Although occasional intergrowths of cooperite/braggite and (Pt,Pd)-bismuthotellurides indicate that these mineral groups do not exclude each other, their distribution patterns within the MSZ are antipathetic.

Furthermore, the high concentrations of Bi and Te combined with the availability of Bi and Te at the position of the main BMS peak (BMS-1) led to a pronounced competition also for Pd. It is postulated that a chemical gradient existed between sulfide-bound Pd in pentlandite and Te and Bi which favoured the formation of Pd-rich bismuthotellurides. It is assumed that these reactions largely took place under isochemical conditions on a sample scale, and interstitial magmatic-hydrothermal fluids probably aided the mass transfer. It can also be speculated that a general upward gradient within the MSZ (peak concentrations of reactive Te and Bi at BMS-1) led to a certain chromatographic control, which may have supported the small-scale redistribution, the separation of certain metals, and the reactions that formed the PGM in a vapor-refining zone as fluids evolved during solidification of the cumulus pile (Boudreau and Meurer 1999). Furthermore, the elevated ΣIPGE / ΣPPGE ratios at the base of the MSZ, closely following the onset of mineralization, are conspicious. They may be explained by the preferential extraction of IPGE first, probably due to the formation of laurite, as indicated by elevated proportions of laurite in the basal part of the MSZ.

PGE distribution patterns and average contents in the MSZ are near-identical at the various localities studied. In contrast, PGM proportions differ widely between the ores of the North and South Chambers. This finding underlines that the formation of the PGM is mainly controlled by the local availibility of reaction partners for the PGE. The elevated proportions of PGE-arsenides and -sulfarsenides in the South Chamber (together 49.7%) probably indicate higher fugacities of arsenic in the South Chamber magmas at the stage of MSZ formation, possibly due to contamination of the magmas by assimilation of country rocks (e.g. Oberthür et al. 2002).

The findings provide new indications towards the mechanisms that led to the distinct vertical element and mineral distribution patterns of the MSZ. Sulfide segregation appears to be the most important factor in the primary magmatic concentration of the PGE. It is concluded here that the orthomagmatic model elegantly explains the observed metal zonation patterns in principle. The degree to which internal fluids and certain metalloids (As, Te, Bi) have influenced the redistribution of the PGE and the formation of PGM still has to be ascertained.

References

Ballhaus, C.G. and Ryan, C.G. (1995). Contributions to Mineralogy and Petrology 122, 241-251.

Boudreau, A.E. and Meurer, W.P. (1999). Contributions to Mineralogy and Petrology 134, 174-185.

Oberthür, T., Davis, D.W., Blenkinsop, T.G. and Höhndorf, A. (2002). Precambrian Research 113, 293-305.

Prendergast, M.D. (1988). *In* Geoplatinum 87. *Edited by* H.M. Prichard et al. Elsevier, 281-302.

Prendergast, M.D. and Wilson, A.H. (1989). *In* Magmatic sulphides - the Zimbabwe volume. *Edited by* M.D. Prendergast and M.J. Jones. The Institution of Mining and Metallurgy, London, 21-42.

Wilson, A.H. (2001). Journal of Petrology 42, 1845-1867.

Evaluation of PGE Potentiality of Layered Gabbros in the Samail Ophiolite, Oman: Results of Geochemical Exploration and Petrological Examination

M. Ogasawara[1], H. Al-Azri[2], H. H. Al-Hashmi[2], H. A. Qidwai[2], M. Al-Araimi[2] and K. Al-Toobi[2]
[1]Geological Survey of Japan/AIST, Tsukuba, Japan, 305-8567
[2]Directorate General of Minerals, MCI, Oman
e-mail: masa.ogasawara@aist.go.jp

Introduction

Major PGE deposits are found in the mafic-ultramafic layered intrusions in the continental environment, and most of them are located in the stable cratons. Discoveries of PGE and gold mineralizations have been reported from the Skaergaard intrusion and several other Tertiary mafic-ultramafic layered intrusions of North Atlantic Igneous Province in Greenland and northwest Scotland (Bird et al., 1991; Bird et al., 1995; Butcher et al., 1999). Magmatism formed those intrusions in the North Atlantic Igneous Province was resulted from mantle plume activity at the opening of the north Atlantic Ocean (Saunders et al., 1997). Therefore, the discoveries of the PGE mineralizations in the gabbros related to the opening of the north Atlantic Ocean encourage to search the PGE mineralization in the oceanic environment. Large gabbro bodies are present in the oceanic crust, though exposures of the gabbro bodies are limited. The layer 3 of oceanic crust is composed of gabbro with typical thickness of 4km. The oceanic crust is exposed in ophiolite bodies representing upper part of oceanic lithosphere. The ophiolite consists of thin sediments, pillow basalts, sheeted dyke complexes, gabbros, and ultramafic mantle unit. Lower part of the gabbros is typically layered with ultramafic cumulate, thus, the oceanic gabbros have lithology similar to the typical layered mafic-ultramafic intrusions which host the major PGE deposits. However, limited evaluations of oceanic gabbros for PGE resources have been conducted. The Samail ophiolite in Oman is one of the best exposed ophiolite complexes in the world, therefore it is best place to evaluate the potentiality of PGE mineralization in the oceanic gabbros. Furthermore, at one locality in the Samail ophiolite, magmatic sulphide ores were found in the gabbro (Lachize, et al., 1991; Lorand and Juteau, 2000). Although, Prichard et al. (1996) considered that the Samail ophiolite is a member of low PGE type ophiolite. Present study evaluates PGE and gold potentiality in the gabbros of the Samail ophiolite, and examines the exploration methodology in the ophiolite area.

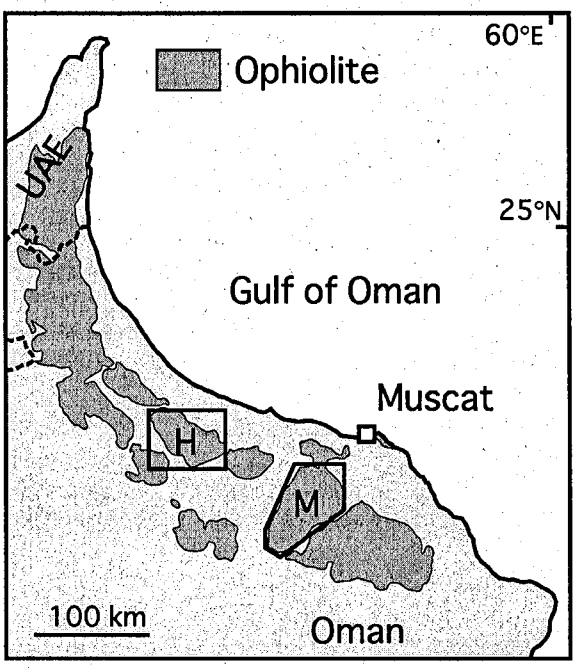

Figure 1. The Samail ophiolite and studied areas. H: Haylayn block. M: Maqsad block.

General Geology

The Samail ophiolite comprises of rocks derived from the Cretaceous oceanic crust and mantle which were obducted on to the Arabian continent during the late Cretaceous, and occurs in northern Oman (Fig. 1). The ophiolite is divided into 13 blocks. Magmatic sulphide ores were found from the Wadi Haymiliyah in the Haylayn block (Lachize, et al., 1991; Lorand and Juteau, 2000). The Haymiliyah outcrop is only known location of gabbro-hosted magmatic sulphide ores in the Samail ophiolite. The Haylayn and Maqsad blocks (Fig. 1) are selected for present study. In the Haylayn block, the ophiolite unit has northwest general trend. Gabbros occur in the central part of the block, and lower mantle unit is present southwest of the gabbros. In the Maqsad block, gabbros are present subhorizontally on the mantle ultramafic rocks, and occur mainly in the north and southeastern parts of the block. Layered gabbros are found in the lower portion of the gabbro unit,

and laminate and massive gabbros are present in the upper portion of the unit.

Geochemical Survey

As the exploration in East Greenland resulted in discovery of PGE and gold mineralization of the Skaergaard intrusion had used the stream sediment geochemical survey at the initial stage (Brooks, 1989), the geochemical survey was conducted in present study. Streams or rivers in the Oman Mountain are generally dry, and are described as wadi. However, occasional rainfalls are sufficient to form thick stream sediments in the dry river. We have collected stream sediments of under 60-mesh grain size by dry sieving at the sampling locations. Samples were collected mainly in the area where gabbros are exposed. Major and trace element data were obtained by XRF. Standard fire assay using PbO as collector with ICP-MS finish was used to obtain concentrations of Pt, Pd, and Au. Selected samples were analyzed with NiS fire assay with ICP-MS finish. Most of samples were also analyzed by ICP-AES with sample dissolution by acid reaching method, and the results were compared with whole rock XRF data. Our survey also checked host lithology and structure of gabbros and possible occurrences of sulfide minerals in the gabbros.

Results

SiO_2 contents of the stream sediments from the study areas range from 42 % to 49 %, indicating that those have similar chemical composition to the ophiolite unit. N-MORB normalized plot (Fig. 2) of average chemical compositions of the stream sediments for two blocks shows that the stream sediments are depleted in incompatible elements and enriched in MgO, Cr, and Ni. Although the stream sediments are collected in the area with exposure of gabbros, the difference of the chemistry from N-MORB may be resulted by selective depletion or enrichment of some elements during erosion, transportation, and deposition to form the stream sediments. High Cr concentrations must be resulted by incorporation of chromite grains in the sediments. Furthermore, as the area contains sub-recent alluvial terraces typically consist of calcrete, high concentrations of CaO and Sr must be derived from those. The average MgO, Ni, and Cr values of the stream sediments from the Haylayn block are higher than those of the Maqsad block, suggesting the stream sediments of the Haylayn block contain more materials from ultramafic part of the ophiolite.

Concentrations of Pd, Pt, and Au in the stream sediments are generally low. As detection limit of Pt is high (10ppb), most of the stream sediments have Pt concentration less than the detection limit. Pd content ranges from less than 2ppb to 16ppb. Although the range of the Pd concentration is small, Pd values show systematic geochemical relationships with other elements. Pd vs. Cr_2O_3 diagram (Fig. 3) indicates two trends. The first trend indicates small Pd enrichment with increase of Cr_2O_3, suggesting enrichment of Pd associated with chromites. The other trend is Pd enrichment without or with only small increase of Cr_2O_3 value. This trend might suggest the presence of PGE mineralization related with primary magmatic sulfide.

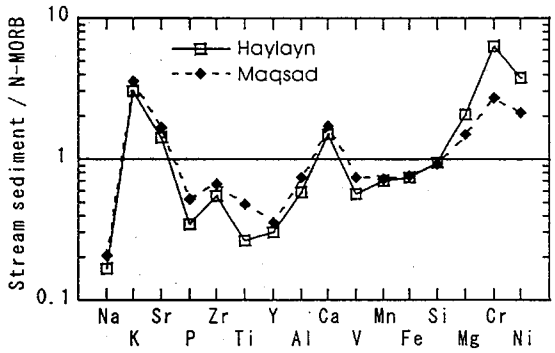

Figure 2. N-MORB normalized diagram for average compositions of stream sediments from the Haylayn and Maqsad blocks in the Samail ophiolite. N-MORB values are calculated from data of Sun et al. (1979). Elements are positioned according to their relative incompatibility for partial melting of mantle rocks.

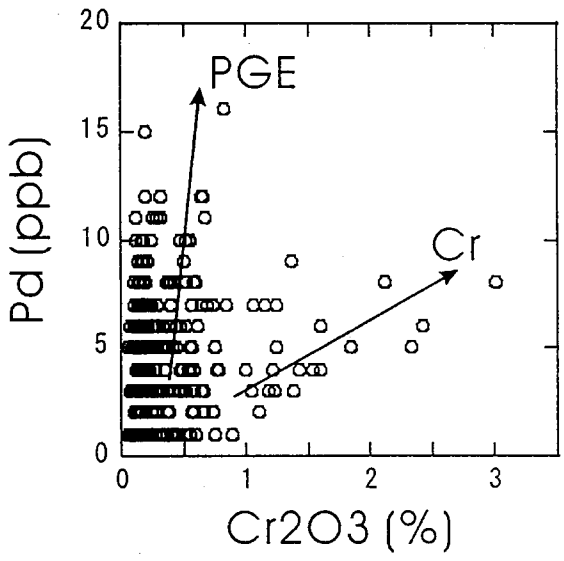

Figure 3. Pd vs. Cr_2O_3 variation diagram for stream sediments from the Haylayn block in the Samail ophiolite. The small Pd enrichment trend associated with chromites is indicted by the arrow (Cr). Another trend (PGE) may be associated with sulphide minerals.

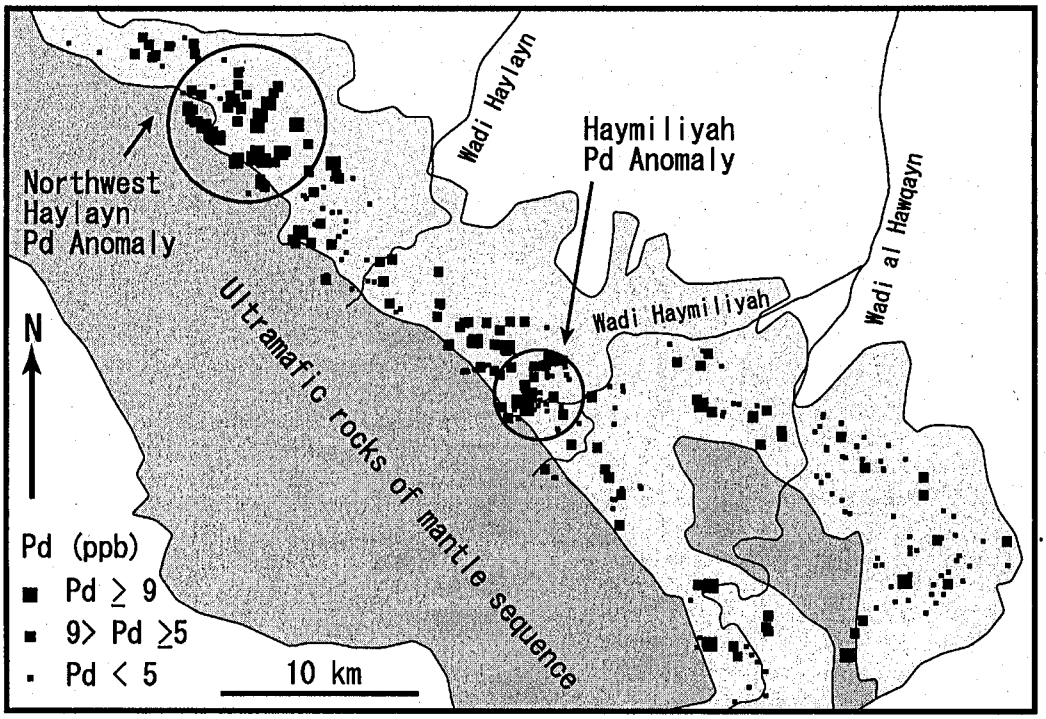

Figure 4. Stream sediment geochemical anomaly map of Pd for the Haylayn block. Light gray area is crustal sequence of the ophiolite unit.

Various geochemical maps have been constructed. Most of the maps reflect main lithology, and are conformable to geologic maps. For example, MgO, Cr, and Ni values increase in the area closed to the mantle sequence. Stream sediments with high Pd values are found in the two areas from the Haylayn block (Fig. 4). Small anomaly in the central part of the block is situated around Wadi Haymiliyah. Occurrence of sulphide ores (Lachize, et al., 1991; Lorand and Juteau, 2000) is located in the center of the anomaly, indicating the stream sediment geochemical survey is an effective method to show presence of such sulfide ores. Another area is located in the northwestern part of the block. The area is considered to be potential area for the PGE mineralization, and further detailed stream sediment sampling and geological survey have been conducted.

During the stream sediment sampling, observation of the gabbros has been made to find any sulphide bearing zone. Copper stains are fond at many outcrops, indicating presence of chalcopyrites in the gabbro. Primary sulphide bearing zones have been found at two new locations. However, PGE concentrations of samples from the sulphide rich zones are low, and are similar level to those from the Wadi Haymiliyah (Lorand and Juteau, 2000). Characteristically yellow alteration zones that were resulted by weathering of primary sulphide minerals, have been found at various location in the gabbro. In the centre of the northwest Pd anomaly of Haylayn block, extensive yellow alteration zones are found. Full PGE analysis of an altered sample indicates slightly high Pd concentration.

Summary

Present study intends to evaluate PGE and gold potentiality in the gabbros of the Samail ophiolite, and to examine the exploration methodology in the ophiolite area. The stream sediment geochemical survey was conducted in the two blocks of the Samail ophiolite. The geochemical characteristics of stream sediments are resulted by two components, ophiolitic rocks and alluvial sediments. Pd in the stream sediments shows two enrichment trends, one with small enrichment with chromites and other may be related with sulphide ores. Two Pd geochemical anomaly areas were found in the Haylayn block. Although absolute level of Pd anomaly is not too high, it is

significantly higher than the back ground level. The one of Pd anomaly area indicates the location of sulphide ores, suggesting the stream sediment geochemical survey is an effective method to find such sulfide ores. Yellow alteration zones that were resulted by weathering of primary sulfide minerals, have been found at various locations in the gabbro. In addition to the alteration zones, primary sulphide mineral bearing zones in the gabbro have been found at two new locations. The findings of additional primary sulphide zones in the gabbro suggest that unusual condition to form primary sulphide zones in the oceanic gabbro may not be necessary.

References

Bird, D.K., Brooks, C.K., Gannicott, R.A., and Turner, P.A., 1991, A gold-bearing horizon in the Skaegaard intrusion, East Greenland: Economic Geology, 86, 1083-1092.

Bird, D.K., Arnason, J.G., Brandriss, M.E., Nevle, R., Radford, G., Bernstein, S., Ganicott, R.A., and Keleman, P.B., 1995, A gold-bearing horizon in the Kap Holm complex, East Greenland: Economic Geology, 90, 1288-1300.

Brooks, K., 1989, Major gold find in Greenland: Tera Nova, 1, 591-593.

Butcher, A.R., Pirrie, D., Prichard, H.M., and Fisher, P., 1999, Platinum-group mineralization in the Rum layered intrusion, Scottish Hebrides, UK: Jour. Geol. Soc., London, 156, 213-216.

Lorand, J.P. and Juteau, T., 2000, The Haymiliyah sulphide ores (Haylayn massif, Oman ophiolite): in-situ segregation of PGE-poor magmatic sulphides in a fossil oceanic magma chamber: Marine Geophys. Res., 21, 327-349.

Lachize, M., Lorand, J.P. and Juteau, T., 1991, Cu-Ni-PGE magmatic sulfide ores and their host layered gabbros in the Haymiliyah magma chamber (Haylayn block, Semail ophiolite nappe, Oman): in Tj. Peters et al. (eds), Ophiolite Genesis and Evolution of the Oceanic Lithosphere: 209-229.

Prichard, H.M., Load, R.A., and Neary, C.R., 1996, A model to explain the occurrence of platinum- and palladium- rich ophiolite complexes: Journal of the Geological Society, London, v. 153, p. 323-328.

Saunders, A.D., Fitton, J.G., Kerr, A.C., Norry, M.J., and Kent, R.W., 1997, The North Atlantic Igneous Province, Geophysical Mon., 100, 45-93.

Sun, S.S., Nesbitt, R.W., and Sharaskin, A.Y., 1979, Geochemical characteristics of mid-ocean ridge basalts: Earth Planet. Sci. Lett., 44, 119-138.

APPENDIX 2

Report of

the 9th

International Platinum Symposium

- Geology, mineral occurrences and PGE exploration in the Duluth Complex -

The survey team attended the pre-symposium excursion of the 9th International Platinum Symposium," PGE Occurrences in Mafic Intrusions around Western Lake Superior, USA and Canada", which are held from July 13 to July 20, 2002. We summarize as follows the geology and mineral deposits of the Duluth Complex based on the pre-symposium excursion guide, Miller and Severson (2002), Severson et al. (2002), and Miller et al. (2002), and so on. The purpose of attending the symposium and the excursion was securing new insight and exploration criteria on Cu-Ni-PGE deposits, which is a mineralization being targeted in the present project of the Parana Basin Area, Brazil.

１－１． Geology of the Duluth Complex

１－１－１． Tectonic Setting

The Duluth Complex and associated Keweenawan intrusions in northeastern Minnesota constitute one of the largest mafic intrusive complexes in the world, second only to the Bushveld Complex of South Africa. These rocks cover an arcuate area of over 5,000 square Kilometers (Fig.1, Fig.2, and Fig.3). The intrusive rocks and comagmatic flood basalts underlying most of northeastern Minnesota were emplaced during the development of the Mesoproterozoic Midcontinent rift about 1.1 billion years ago.

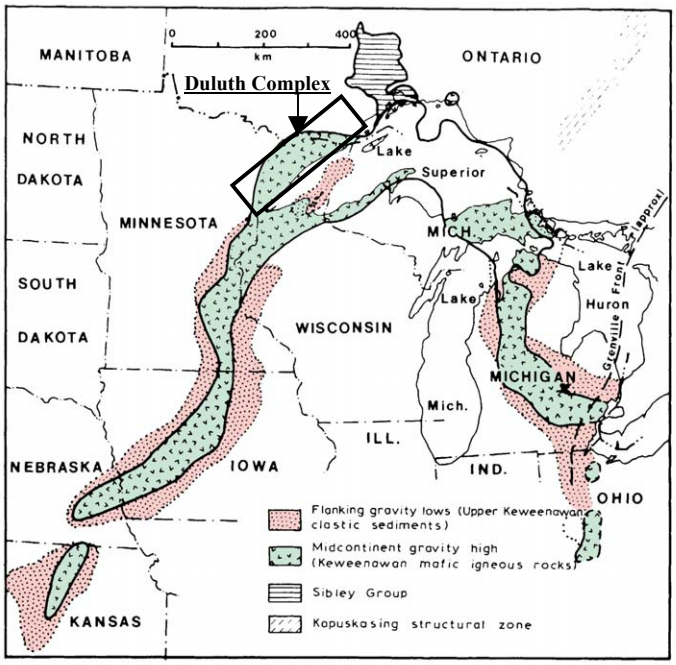

Fig.1 Generalized geological map of the Midcontinent Rift of North America(Weiblen, 1980).

The Midcontinent rift can be traced by its geophysical signature from its exposure in the Lake Superior region along a 2,000- kilometer-long, segmented, arcuate path from Kansas to lower Michigan. The rift is infilled with a lower sequence of volcanic rocks, locally as much as 20-kilometersthick, and an upper sequence of fluvial sedimentary rocks. Conceptually, the evolution of the Duluth Complex and related igneous rocks is interpreted in terms of the interactions between a deep mantle plume and mature continental lithosphere. Geochronologic studies indicate that the magmatic activity occurred in four distinct stages within the span of about 23 million years.

The early magmatic stage (1109 to 1107 Ma) occurred during a time of reversed magnetic polarity and was characterized by the rapid and voluminous eruption of initially primitive magmas derived directly from the plume. This quickly gave way to more evolved and crustally contaminated mafic magmas as well as felsic melts. This stage is thought to represent the impact of the mantle plume head with the initially cool and brittle lithosphere, the rapid heating of the lithosphere by mantle-derived melts, and the eventual contamination of those melts by their staging in the lower crust. This mafic underplating likely resulted in felsic melts being formed by partial melting of the lower crust.

The latent magmatic stage (1107 to 1102 Ma) was a period during which volcanic activity was largely dormant, except for possibly rhyolitic volcanism. This stage is thought to represent a period of continued mantle plume upwelling and melting, extensive crustal underplating, and lower crustal melting. Crustal anatexis created a rheological and density barrier to the passage of mafic magmas to the upper crust.

The main magmatic stage (1102 to 1094 Ma) was a period of normal magnetic polarity conditions during which volcanic activity was renewed. This stage was characterized by moderate rates of eruption of uncontaminated (except for rhyolite) but diverse magma compositions. It is thought to represent the onset of upper crustal separation, the evacuation of lower crustal magma chambers, and continued mantle plume melting.

The late magmatic stage (1094 to 1086 Ma) was a period of waning volcanic activity but continued subsidence of the rift basin. This led to the development of evolved composite volcanoes and the interbedding of lava flows and basin sediments. This period probably represents the loss of the plume heat source by plate drift and the thermal collapse of the rift basin.

U-Pb ages indicate that various intrusions of the Duluth Complex were emplaced during the early and main magmatic stages of the Midcontinent rift. Early stage intrusions include the large granophyre bodies occurring in the roof zone of the Duluth Complex (the Cucumber Lake, Misquah Hills, and Whitefish Lake granophyres) and the gabbroic intrusions occurring at the northeastern end of the Duluth Complex (the Crocodile Lake and Poplar Lake intrusions). Gradational

relationships between the roof zones of these gabbros and the overlying granophyre bodies imply that the felsic rocks preceded emplacement of the gabbros. The overall evolved nature of these mafic and felsic intrusions implies that they were emplaced late in the early magmatic stage, probably contemporaneous with the eruption of the evolved and contaminated Hovland lavas. A precise age of 1106.9 ± 0.8 Ma for the basal gabbro of the Poplar Lake intrusion is consistent with this interpretation. The large volume of anorthositic rocks and the eleven discrete mafic layered intrusions that make up the remainder of the Duluth Complex were emplaced during the main magmatic stage.

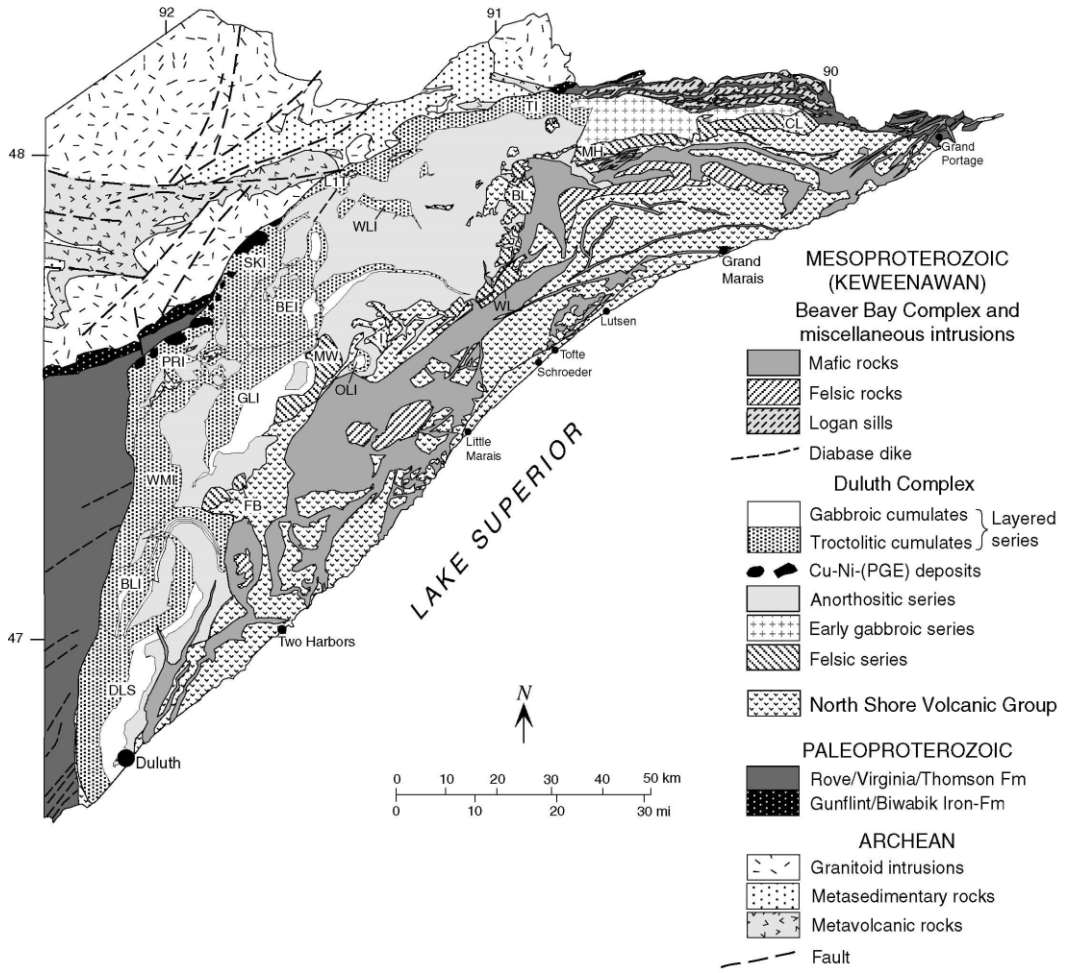

Generalized geology of northeastern Minnesota highlighting individual intrusions of the Duluth Complex. Layered series intrusions are:

BEIÑ Bald Eagle intrusion
BLIÑ Boulder Lake intrusion
DLSÑ Layered series at Duluth
GLIÑ Greenwood Lake intrusion
L1TÑ Lake One troctolite
OLIÑ Osier Lake intrusion
PRIÑ Partridge River intrusion
SKIÑ South Kawishiwi intrusion
TIÑ Tuscarora intrusion
WMIÑ Western Margin intrusion
WLIÑ Wilder Lake intrusion

Felsic Series intrusions:

BLÑ Beth Lake granophyre (and Wine Lake monzodiorite)
CLÑ Cucumber Lake granophyre
FBÑ Fairbanks/Brimson granophyres
IÑ Isabella granophyre
MHÑ Misquah Hills granophyre
MWÑ Mt. Weber granophyre
WLÑ Whitefish Lake granophyre

Fig.2 Generalized geology of the Duluth Complex and surrounding area (Miller and Severson, 2002).

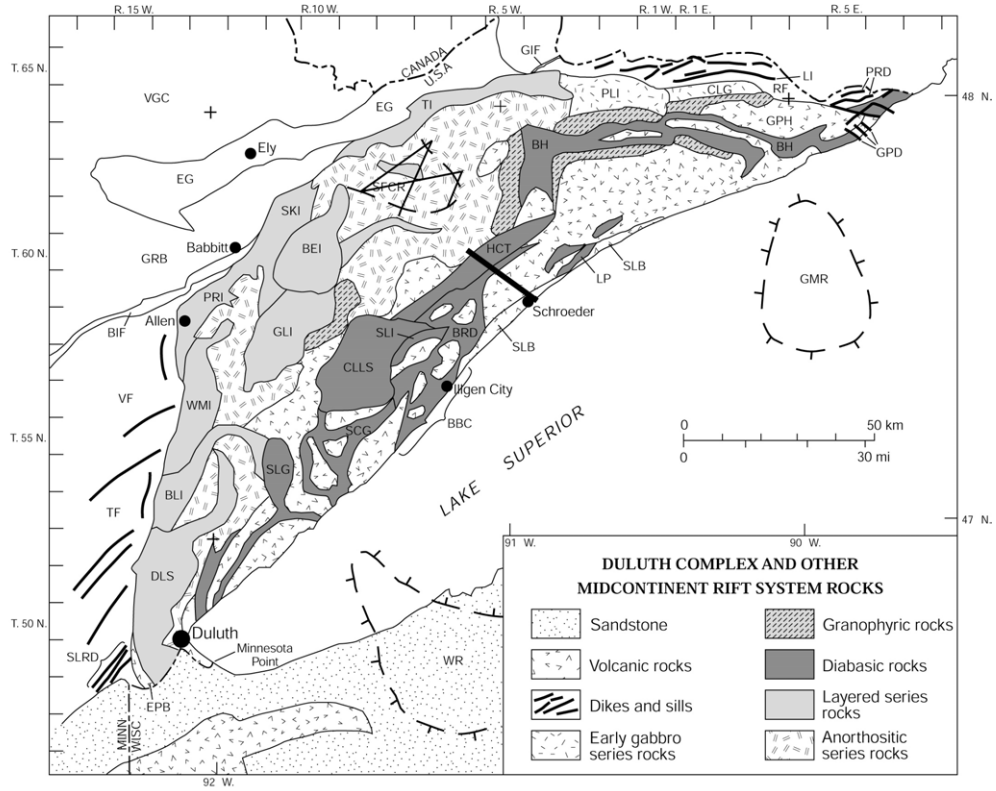

Abbreviation of geological units:BEI—Bald Eagle intrusion, BIF—Biwabik Iron Formation (Paleoproterozoic), BLI—Boulder Lake intrusion, BBC—Beaver Bay Complex, BH—Brule Lake and Hovland gabbros, BRD—Beaver River diabase, CLG—Crocodile Lake gabbro, CLLS—Cloquet Lake layered series, DLS—Layered series at Duluth, EG—Ely Greenstone (Archean), EPB—Ely's Peak basalts, GIF—Gunflint Iron Formation, GLI—Greenwood Lake intrusion GPH—Grand Portage basalts & Hovland lavas GRB—Giants Range batholith (Archean), GPD—Grand Portage dikes HCT—Houghtaling Creek troctolite LI—Logan intrusions, LP—Leveaux porphyritic diorite PLI—Poplar Lake intrusion PRD—Pigeon River diabase, PRI—Partridge River intrusion RF—Rove Formation (Paleoproterozoic) SCG—Silver Creek gabbro, SLRD—St. Louis River dikes SLB—Schroeder–Lutsen basalts SKI—South Kawishiwi intrusion, SLG—Sawmill Lake gabbro SLI—Sonju Lake intrusion TF—Thomson Formation (Paleoproterozoic), TI—Tuscarora intrusion VGC—Vermilion Granitic Complex (Archean) VF—Virginia Formation (Paleoproterozoic), WMI—Western Margin intrusion

Areas with heavy hatchures designate basement highs as follows:GMR—Grand Marais ridge SFCR—Schroeder–Forest Center ridge WR—White's ridge

Fig.3 Generalized geology of the Duluth Complex and associated rocks with emphasis on each intrusions(Chandler, 2002).

１－１－２． General Definition of the Duluth Complex

The Duluth Complex is defined as a more or less continuous mass of mafic to felsic plutonic rocks that extends in an arcuate fashion from Duluth nearly to Grand Portage. It is bounded by a footwall of predominantly Paleoproterozoic and Archean rocks, a hanging wall of largely mafic volcanic rocks and hypabyssal intrusions.

Defining the Duluth Complex more genetically, it is composed of multiple discrete intrusions of mafic to felsic tholeiitic magmas that were episodically emplaced into the base of a comagmatic volcanic edifice between 1108 and 1098 Ma. Within the nearly continuous mass of intrusive igneous rock forming the Duluth Complex, four general rock series are distinguished on the basis of age, dominant lithology, internal structure, and structural position within the complex.

Felsic series - Massive granophyric granite and smaller amounts of intermediate rock that occur as a semicontinuous mass of intrusions strung along the eastern and central roof zone of the complex emplaced during early stage magmatism (~1108 Ma).

Early gabbro series - Layered sequences of dominantly gabbroic cumulates that occur along the northeastern contact of the Duluth Complex that were also emplaced during early stage magmatism (~1108 Ma).

Anorthositic series - A structurally complex suite of foliated, but rarely layered, plagioclase-rich gabbroic cumulates that was emplaced throughout the complex during main stage magmatism (~1099 Ma). The upper contact of the anorthositic series against volcanic or granophyric rocks is typically sharp and somewhat chilled.

Layered series - A suite of stratiform troctolitic to ferrogabbroic cumulates that comprises at least 11 variably differentiated mafic layered intrusions and occurs mostly along the base of the Duluth Complex. These intrusions were emplaced during main stage magmatism, but generally after the anorthositic series (~1099 Ma).

１－１－３ The main intrusions of the Duluth Complex

The layered series at Duluth is a well differentiated, 3- to 4.5-kilometer-thick, eastdipping, sheetlike mafic layered intrusion(Fig.4). Aeromagnetic data show that the layered series at Duluth has a north-south strike length of about 60 kilometers and eventually pinches out into the Boulder Lake intrusion. The hanging wall of the layered series at Duluth consists of olivine gabbroic and troctolitic anorthosite of the anorthositic series. The footwall of the layered series at Duluth at its southern end is composed of reversed polarity lavas of the Ely's Peak basalts.

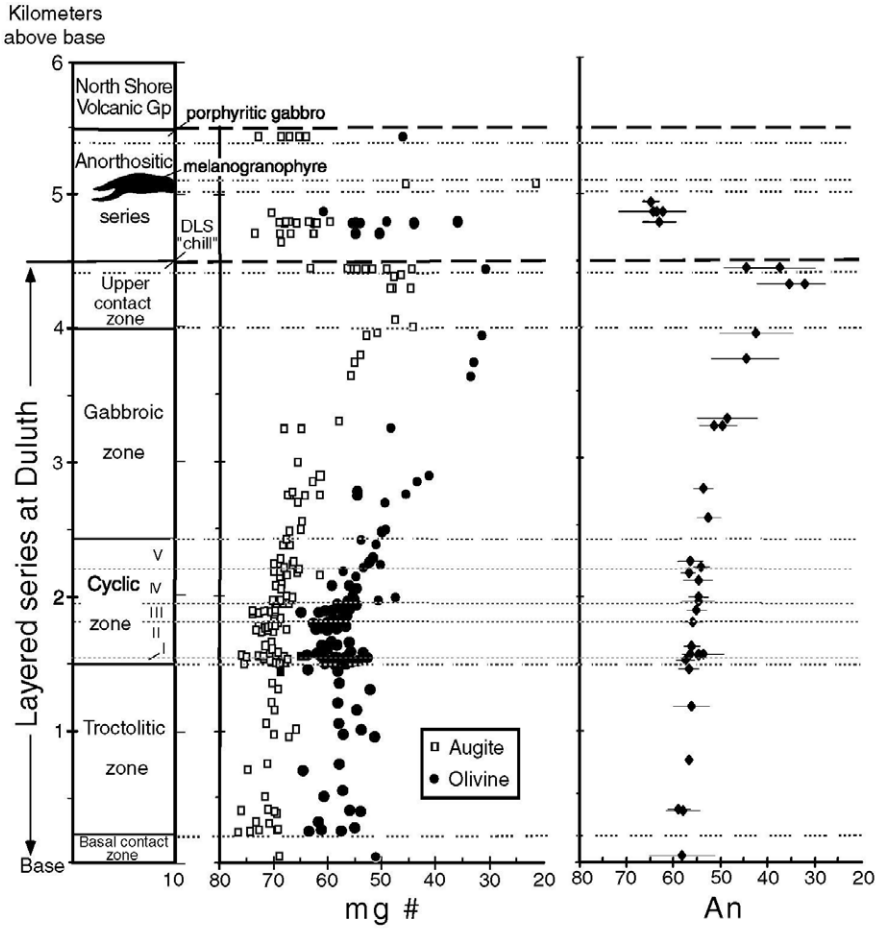

Igneous stratigraphy and cryptic variation of olivine, pyroxene, and plagioclase composition through the layered series at Duluth. Mg values of olivine and pyroxene and An content of plagioclase are based on multiple microprobe analyses (error bars indicate one standard deviation).

Fig.4 Igneous stratigraphy and cryptic variation through the Layered Series at Duluth (Miller and Severson, 2002).

The layered series at Duluth is divided into five major zones based on dominant rock type. The basal contact zone is composed of coarse-grained, taxitic olivine gabbro and augite troctolite. The

lowermost cumulate sequence is the troctolite zone. It is 1- to 2-kilometers-thick, consists mostly of homogeneous foliated troctolitic cumulates(Fig.5A). The cyclic zone forms the medial section of the layered series at Duluth and is characterized by cyclical variations in cumulus mineralogy between troctolitic and gabbroic cumulates(Fig.5B). The persistent occurrence of gabbroic cumulates defines the gabbro zone. Gabbroic cumulates, in turn, grade upward into unlaminated (noncumulate) apatitic quartz ferromonzodiorite, which composes most of the upper contact zone. This quartz ferromonzodiorite complexly mixes with a fine-grained biotitic ilmenite ferrodiorite, which ultimately forms a "chilled" contact with anorthositic series rocks. A body of melanogranophyre that irregularly cuts through the anorthositic series probably represents the uppermost differentiate of the layered series at Duluth.

Although the layered series at Duluth is overall a well-differentiated intrusion, the repeated progression from troctolitic to gabbroic cumulates in the cyclic zone indicates that it did not fractionally crystallize as a closed system. The cyclic zone consists of at least five macrocycles within which troctolitic cumulates grade upward to gabbroic cumulates. Macrocycle boundaries are marked by the abrupt regression in the cumulus mineralogy from gabbroic back to troctolitic cumulates(Fig.5B). The gabbroic parts of the macrocycles commonly contain inclusions of anorthositic series rocks and the very uppermost parts of the macrocycles locally have discontinuous layers of fine-grained gabbroic adcumulate. Miller and Ripley (1996) suggested that the macrocyclic phase layering is predominantly related to devolatilization and decompression that attended magma venting events from a shallow chamber (less than 5-kilometers-deep), with magma recharge possibly having a secondary effect.

Fig.5 Photographs of
A)Troctolite zone(layered augite troctolite) and
B)Cyclic zone

The Partridge River intrusion has been studied in detail because it hosts at least four sub-economic copper-nickel deposits and at least seven potential Fe-Ti deposits. The Partridge River intrusion consists mainly of troctolitic cumulates that are exposed in an arc shaped area that extends from the Water Hen Fe-Ti deposit area to the Babbitt copper-nickel deposit. Miller and Ripley(1996) estimated that the Partridge River intrusion is 2.5-kilometers-thick. Its footwall includes the Paleoproterozoic Virginia Formation (slate and graywacke), and to a lesser extent, the Biwabik Iron Formation. The top of the Partridge River intrusion is in complex contact with anorthositic rocks, gabbroic rocks, and mafic volcanic. This assemblage of anorthositic, gabbroic, and hornfelsic rocks are also present as large inclusions within the interior of the Partridge River intrusion.

The basal 900 meters of the Partridge River intrusion are known in great detail from the abundance of exploration drill core. This marginal zone, consisting of varied troctolitic and gabbroic rock types, is subdivided into seven stratigraphic units that can be correlated over a strike length of 24 kilometers. All of these igneous units generally exhibit shallow dips (10o to 20°) to the southeast. The stratigraphy shown in Fig.6 is based on the re-logging of almost 700 drill holes, or 205 kilometers of drill core.

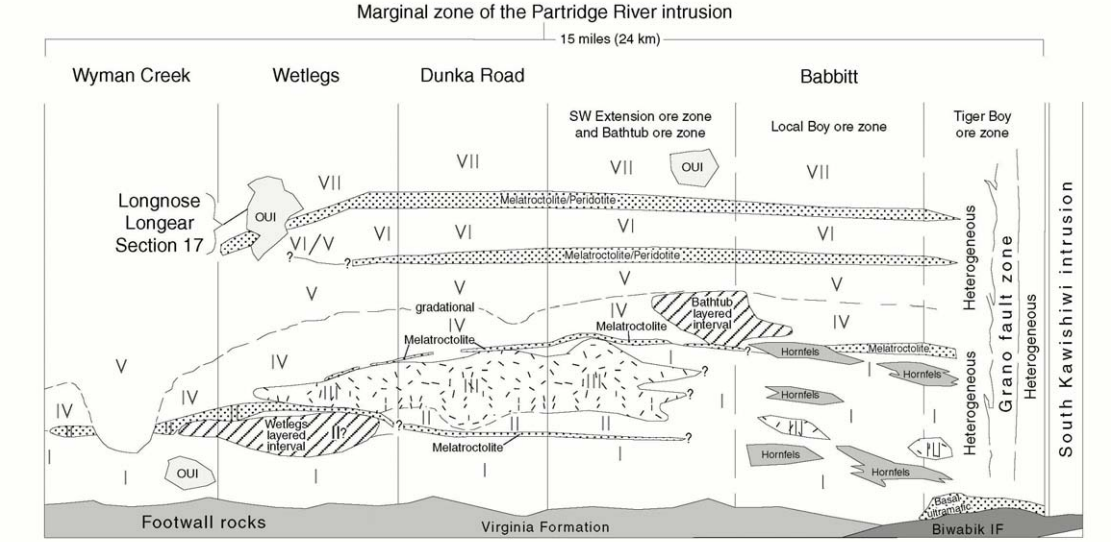

Generalized stratigraphy of the marginal zone of the Partridge River intrusion (modified from Severson, 1994). Stratigraphic relationships for the area between the Wyman Creek deposit and the Water Hen deposit are poorly understood and are not portrayed on this figure.

Fig.6 Generalized stratigraphy of the marginal zone of the Partridge River Intrusion (Miller and Severson, 2002).

Unit I:

Unit I is the dominant sulfide-bearing member of the Partridge River intrusion. It consists of a heterogeneous mixture of ophitic troctolitic to gabbroic rocks that contain abundant inclusions of hornfelsic sedimentary footwall rocks and minor thin, discontinuous layers of melatroctolite and peridotite. Noritic rocks are common at the basal contact and peripheral to sedimentary hornfels inclusions, probably due to contamination of the magma. An ultramafic interval, consisting of an oxide-bearing peridotite overlying an oxide-bearing pyroxenite, is present at the base of Unit I in areas where the Partridge River intrusion is in direct contact with the Biwabik Iron Formation .

Unit II **:**

This unit exhibits considerable variation from one copper-nickel deposit to the next. At the Dunka Road and Babbitt deposits, Unit II consists of homogeneous troctolitic rocks, with minor sulfide mineralization, and a fairly persistent basal ultramafic layer that separates Unit II from Unit I. The upper contact with Unit III is gradational at the Dunka Road deposit. At the Wetlegs deposit, Unit II is either a single ultramafic layer immediately beneath Unit III, and/or the Wetlegs layered interval, which consists of repeated, thin cyclic units that internally grade upward from ultramafic rock to troctolite. Still farther to the west at the Wyman Creek deposit, Unit II consists of a single ultramafic horizon that separates sulfide-bearing and heterogeneous troctolitic rocks of Unit I from homogeneous troctolitic rocks of Unit IV.

Unit III:

This unit consists of poikilitic leucotroctolite that commonly grades into poikilitic/ophitic augite troctolite. Because of its fine-grained texture and distinctive olivine oikocrysts that impart a mottled appearance, Unit III is a useful marker horizon, although it is absent from the Wyman Creek deposit and portions of the Babbitt deposit. Hornfelsed basalt inclusions, or roof rocks, are commonly associated with Unit III at the Dunka Road deposit. This relationship, and the highly gradational contact of Unit III with Unit II, suggest that Unit III may have formed as a roof cumulate during crystallization of Unit II.

Unit IV:

Homogeneous ophitic augite troctolite that contains a local basal unit of ultramafic rock. Unit IV typically exhibits a highly gradational upper contact with Unit V. A cyclic sequence of alternating troctolitic and ultramafic layers, termed the Bathtub layered interval, is present in the Bathtub ore zone of the Babbitt deposit.

Unit V:

Unit V consists of homogeneous, coarse-grained leucotroctolite. At the Wyman Creek deposit, drill hole relationships suggest that Unit V cuts downward into the lower units.

Units VI and VII:

Each of these units consist of homogeneous leucotroctolite that locally grades into ophitic augite troctolite; both also contain a fairly persistent ultramafic base. Several other similar units

(Unit VIII and up) are present above these two units, but they are not defined by drilling.

***Oxide ultramafic intrusions (OUI)*:**

Several late-stage pegmatitic plugs and vertical lenses of oxide-bearing ultramafic intrusions intrude the troctolitic rocks of the Partridge River intrusion. Severson and Hauck (1990) first used the acronym OUI to designate crosscutting pegmatitic bodies of peridotite, melatroctolite, melagabbro, and clinopyroxenite that contain a high percentage of coarse-grained oxides (15 to 100 percent). The OUI are spatially arranged along linear trends, suggesting that structural control was important to their genesis. In addition, the Longnose.Longear.Section 17 group of OUIs is positioned over a window in the basal contact where the Biwabik Iron Formation is the footwall rock. This relationship suggests a genetic link between assimilation of iron formation at the basal contact and formation of OUI along a coincident fault zone.

Wetlegs deposit, Unit I (D.H. W-8B): heterogeneous sulfide-bearing augite troctolite (Cu:0.25-0.34%, Ni:0.07-0.10%).

Wetlegs deposit, Unit II : abundant ultramafic layers in the Wetlegs area.

Fig.7 Photographs of A) Unit I, and B) Unit II of the Partridge River Intrusion.

Attributes of the more heterogeneous units (I and II) near the base of the Partridge River intrusion are interpreted to indicate rapid magma replenishment in a progressively developing magma chamber, and magmatic contamination from assimilated footwall rocks. The more homogeneous upper units (IV through VII), each floored by a persistent ultramafic layer, were probably emplaced later in a well-developed magma chamber. The ultramafic layers in the upper units, and abundant ultramafic layers of the Wetlegs and Bathtub layered intervals, probably represent the inception of episodic magma injection that crystallized more primitive ultramafic layers before mixing with the resident magma.

The South Kawishiwi intrusion hosts at least five subeconomic copper-nickel deposits and a potential platinum group element-copper-nickel deposit. The South Kawishiwi intrusion is dominantly composed of troctolitic cumulates that are exposed in an 8- by 32-kilometer arcuate band. Footwall rocks include the Virginia Formation in the Serpentine and Dunka Pit deposits, the Biwabik Iron Formation in the Dunka Pit and Birch Lake deposits, and the Archean Giants Range batholith in the Dunka Pit deposit north to the Spruce Road deposit. The presence of Biwabik Iron Formation as inclusions as far north as the Spruce Road deposit indicates that the majority of Paleoproterozoic units were assimilated and removed from the footwall during emplacement of the South Kawishiwi intrusion, leaving the Giants Range batholith as the dominant footwall rock type. Also present as inclusions in the Dunka Pit and Serpentine deposits are mafic volcanic hornfels (probably North Shore Volcanic Group) and quartz sandstone hornfels (probably equivalents to the Puckwunge and Nopeming Sandstones).

The South Kawishiwi intrusion consists of five major map units. These are, from the base upward:

1. A basal contact zone that is a heterogeneous mix of sulfide-bearing troctolitic, gabbroic, and noritic rocks with abundant hornfels inclusions;
2. A thick unit of subophitic to ophitic augite troctolite that contains an internal ophitic olivine gabbro unit;
3. A discontinuous and localized layer of poikilitic leucotroctolite;
4. A thick, homogeneous sequence of ophitic troctolite;
5. An uppermost, thick sequence of homogeneous troctolite that contains numerous lensoidal layers and inclusions of anorthositic rocks.

Severson (1994) and Zanko and others (1994) further subdivided the marginal zone of the South Kawishiwi intrusion into 17 different lithostratigraphic units (Fig.8) that are present in over 180 drill holes over a strike length of 31 kilometers. Sulfide mineralization is confined to the BH, BAN, UW, and U3 units, and to a lesser extent the U1 and U2 units. Major marker horizons that are

correlated in drill holes include three horizons with abundant cyclic ultramafic layers (U1, U2, and U3 units) and a pegmatite-bearing unit (PEG unit). A large, anorthositic inclusion (less than 1-kilometer-thick) is intersected in six deep drill holes in the State Highway One corridor area.

The lowest units of the marginal zone are the most varied with respect to textures, rock type, and sulfide content. They are unevenly distributed along the strike length of the South Kawishiwi intrusion in a "compartmentalized" fashion, suggesting a complicated intrusive history(Fig.8). The lowest units were emplaced early into several restricted magma chambers via repeated and close-spaced magmatic pulses. The U1, U2, and U3 units represent periods of rapid and continuous magma injection that crystallized more primitive ultramafic layers before mixing with the resident magma. The U3 unit is unique among the lower units in that it contains several massive oxide pods (titanomagnetite-rich) along its entire length. A spatial correspondence between the U3 unit and footwall iron-formation suggests that most of the massive oxide pods are iron-rich "restite" produced by the magmatic digestion of iron-formation. The U3 unit also contains the majority of the high platinum group element values that have been sampled within the South Kawishiwi intrusion.

The upper units of the South Kawishiwi intrusion are continuous throughout the intrusion. Their continuity and monotonous troctolitic composition suggest that they crystallized in a more quiescent and open magmatic system characterized by widely spaced magmatic pulses.

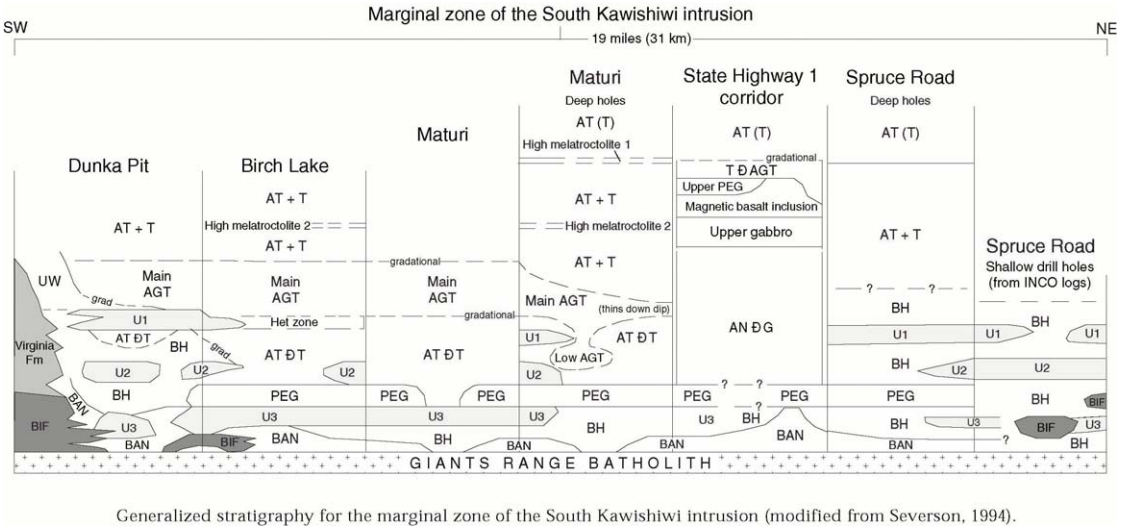

Generalized stratigraphy for the marginal zone of the South Kawishiwi intrusion (modified from Severson, 1994).

Fig.8 Generalized stratigraphy of the marginal zone of the South Kawishiwi Intrusion (Miller and Severson, 2002).

１－２． Mineral Deposits of the Duluth Complex

Increased demand and commodity prices for platinum group elements (PGEs) have recently reinvigorated exploration activity in the Duluth Complex and related Keweenawan intrusions in northeastern Minnesota. Known copper-nickel deposits along the base of the complex are being reassessed for their PGE concentrations, and intrusions stratigraphically higher in the Duluth and Beaver Bay Complexes are being evaluated using new models for stratiform PGE mineralization within well-differentiated tholeiitic systems.

１－２－１． Copper-Nickel-(PGE) Sulfide Mineralization

The fundamental characteristics of this style of mineralization involve sulfur contamination of mafic magmas by pre-Keweenawan footwall rocks, and mineralization occurring in the vicinity of the basal contact of mafic intrusions. The variants of this style of mineralization that may potentially exist in the Duluth Complex include:

a) Disseminated copper-nickel-(PGE) sulfide mineralization in basal contact zones of mafic intrusions
b) Massive sulfide mineralization at the basal intrusive contact and in footwall rocks
c) Sulfide mineralization in major feeder zones (Noril'sk/Voisey's Bay-type; Naldrett, 1997)

Only disseminated copper-nickel sulfide mineralization and basal massive sulfide mineralization are presently known to occur in the Duluth Complex.

a) Disseminated Sulfide Mineralization

Large resources of low-grade copper-nickel sulfide ore that locally contain anomalous PGE concentrations are well documented by drilling in the basal zones of the South Kawishiwi and Partridge River intrusions(Fig.9, Table.1). At least nine subeconomic deposits have been delineated in the basal 100 to 300 meters of both intrusions. The mineralization consists predominantly of disseminated sulfides that collectively constitute over 4.4 billion tons of material averaging 0.66 percent copper and 0.2 percent nickel (Listerud and Meineke, 1977). Overall, the copper to nickel ratio averages 3.3:1, ranging from 2.4:1 to 4.11:1. PGE concentrations average about 10 parts per million platinum + palladium (recalculated to 100 percent sulfide), but may range as high as 50 parts per million platinum + palladium (recalculated to 100 percent sulfide) in associated stratabound zones, such as the Birch Lake and Dunka Road deposits. Sulfur isotope analyses consistently indicate that the source of sulfur was from the pelitic country-rocks of the Virginia Formation, which form much of the footwall to the Partridge River intrusion and locally to the South Kawishiwi intrusion.

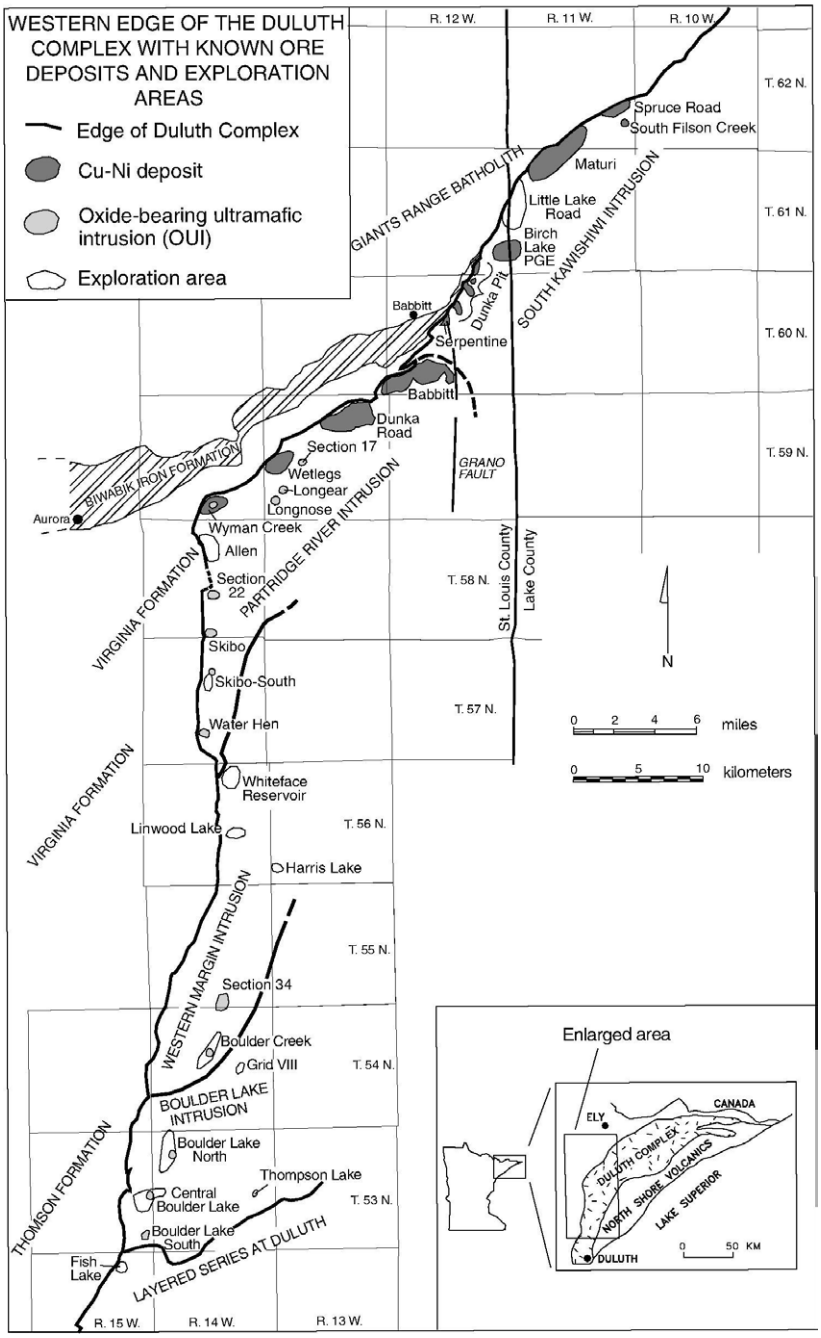

Fig.9 Location of the mineral deposits and exploration areas along the western base of the Duluth Complex(Miller at al., 2002).

Table 1 Calculated copper-nickel resources for various deposits along the western margin of the Duluth Complex(Miller et al., 2002).

(-) not available

Deposit (company)	Resources (in Mt)	Average Cu%	Average Ni%	Cu% cutoff	Cu/Ni ratio (x/1)
South Filson Creek (Hanna)	-	-	-	-	3.00
Spruce Road (INCO)	248	0.46	0.17	-	2.63
Maturi (INCO)	247 underground	0.50	0.19	-	2.40
Maturi Deep (Duval)	411	0.74	0.22	-	-
Dunka Pit (many)	272	0.25	-	-	-
Serpentine (Bear Cr., AMAX)	7	0.88	0.30	0.60	2.85
Babbitt/Minnamax (Bear Cr., AMAX)	364	0.84	0.19	0.60	4.11
Babbitt/Mesaba (Arimetco)	3300	0.46	0.12	0.38	-
Dunka Road (USS)	100 underground	0.77	0.24	-	3.43
Dunka Rd/NorthMet (PolyMet)	808	0.43	0.11	-	-
Wetlegs (Bear Creek, Exxon)	38	0.29	0.10	0.15	-
Wyman Creek (USS)	-	-	-	-	-
All deposits (Listerud and Meineke, 1977)	4400	0.66	0.20	0.50	3.30

The sulfide deposits are hosted by taxitic troctolitic to gabbroic rocks that contain abundant inclusions of the various footwall rock types. Within the Partridge River intrusion, the basal unit(Unit-I) hosts the vast majority of the disseminated sulfides. Similarly, mineralization within the South Kawishiwi intrusion is confined to the basal heterogeneous (BH), ultramafic 3 (U3), basal augite troctolite/norite (BAN), and updip wedge (UW) units.

The disseminated sulfide minerals occur as interstitial grains that make up between trace amounts and 10 percent of the rock by volume (visual estimation). The average sulfide mineral content is between 1 and 5 percent. Major sulfide minerals are pyrrhotite, chalcopyrite, cubanite, and pentlandite. Pyrrhotite is generally the dominant sulfide, especially closer to the basal contact. Chalcopyrite is generally the dominant copper-sulfide with variable amounts of cubanite. Also

present are minor amounts of bornite, talnakhite, chalcocite, digenite, mackinawite, valleriite, violarite, native copper, and platinum group minerals.

Although this mineralization type is described as being present within the basal units of the South Kawishiwi and Partridge River intrusions, the basal zones do not contain sulfides in all areas. Mineralized zones are extremely erratic in their spatial extent and ore grades. Zones that are barren of sulfides commonly interfinger with mineralized zones in a random pattern. This erratic pattern of mineralization, in part, mirrors the lithologic heterogeneity of the basal units. The only exception to this random mineralization pattern is the Maturi deposit (and its downdip eastward extension), where the upper portion of the basal heterogeneous (BH) unit consistently exhibits copper values in excess of 1.0 percent that gradually decrease with depth toward the basal contact. The change to more consistent mineralization at Maturi may be related to a thinning of the basal heterogeneous unit in the area and thus the sulfides are more restricted to a specific horizon.

Although the style of mineralization in all of the deposits is dominated by disseminated copper-nickel sulfides, differences occur between the deposits in copper-nickel and PGE grade, thickness, and tonnage. Mineralization profiles from single drill holes within each of the deposits of the South Kawishiwi intrusion are presented in Fig.10. Peterson (2001) attributed the higher-grade, sheetlike mineralization of the Maturi and Maturi Extension deposits to confined magma flow of the lower South Kawishiwi intrusion beneath a large pillar of older anorthositic series rocks.

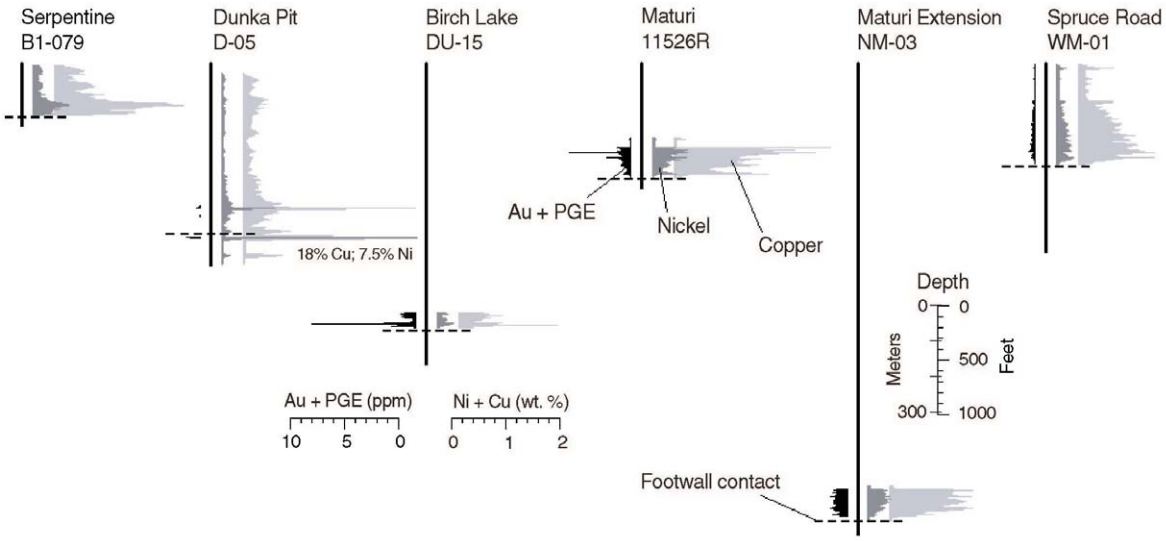

Fig.10 Assay from drill holes in each of the copper-nickel deposits of the South Kawishiwi Intrusion(Peterson, 2002).

Contrasting with this heterogeneity of rock types and mineralization, some internal PGE bearing sulfide zones within the lower units exhibit a stratabound relationship to the igneous stratigraphic section. For example, at the Dunka Road and Babbitt deposits, the top of Unit I immediately beneath an ultramafic layer commonly exhibits increased copper-PGE grades (Fig.11). These PGE-bearing zones are often copper enriched.

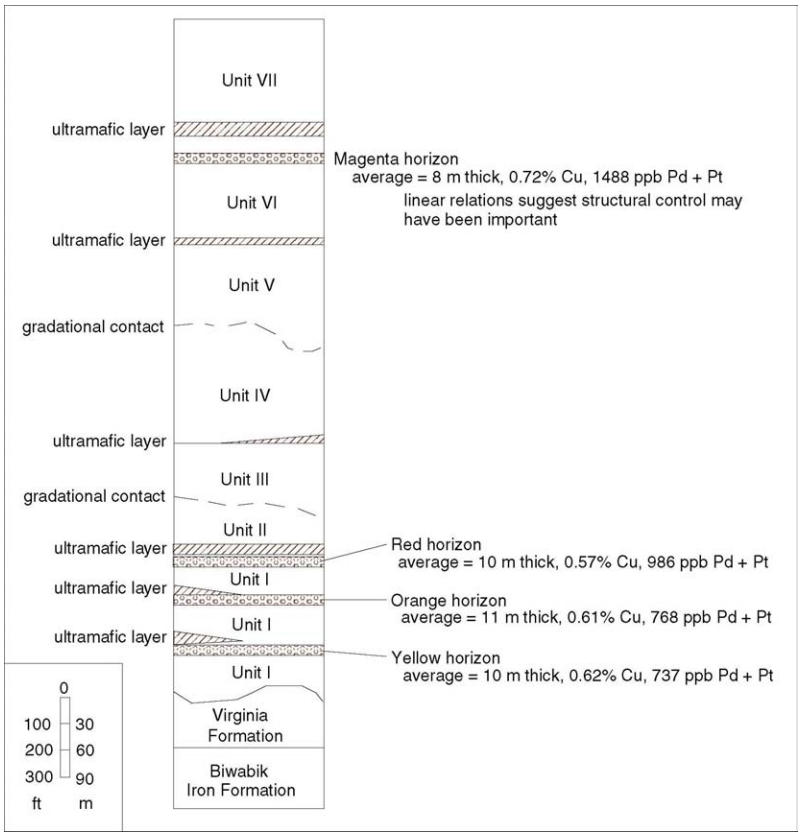

Fig.11 Distribution of PGE-bearing stratabound horizons relative to the igneous stratigraphy at the Dunka Road deposits(modified from Geerts, 1991). (Severson et al., 2002)

Two other stratabound copper-rich (±PGE) zones are present beneath discontinuous ultramafic horizons within the interior of Unit I at Dunka Road. At the Maturi deposit, a copper-enriched (and possibly PGE-enriched) zone also occurs immediately beneath an ultramafic unit (U3) at the top of the basal heterogeneous unit.

Copper-enrichment often occurs locally near fault zones as in the Wyman Creek, Wetlegs, and Dunka Road deposits close to the basal contact, and at the South Filson Creek deposit, 670 meters above the basal contact. The causes of copper-PGE enrichment along faults are not entirely clear,

but probably involve the remobilization and redeposition of copper and PGEs by circulating chlorine-rich hydrothermal fluids, possibly during the latest stages of magmatic crystallization. Evidence for such fluids is given by the presence of chlorine-rich brown liquid drops that commonly coat the surfaces of drill core after exposure to air. These drops form by a deliquescent process and are found on core from the Fish Lake area north to the Spruce Road deposit and the Gunflint Trail area. Analyses of the drops indicate high chlorine content values up to 3,000 parts per million. The drops are most common on core from the ultramafic layers (variably serpentinized) and the oxide ultramafic intrusions (OUI). They are also locally associated with disseminated sulfide zones, massive sulfides at the Local Boy ore zone of the Babbitt deposit, massive oxides and ultramafic layers from the U3 unit of the South Kawishiwi intrusion, pre-Duluth Complex sills (Logan-type sill and Cr-sill), and olivine-bearing portions of the metamorphosed footwall Biwabik Iron Formation. In addition to the liquid drops, chlorine-rich coatings on the core occur in a variety of colors and precipitate forms.

In summary, the disseminated sulfide mineralization at each of the copper-nickel deposits, with the exception of the Maturi deposit, can be classified as chaotic with diverse ore grades that are unevenly distributed throughout the basal mineralized units. This diverse nature makes it difficult to predict the overall spatial distribution of ore zones based on widely scattered drill holes and little to no outcrop. More in-fill drilling is needed in order to address ore controls. The cause of the erratic mineralization is probably related to a variety of factors that include:

- The nature of magma emplacement (turbulent versus quiescent)
- The mode of emplacement (along bedding planes in the footwall rocks versus overplating previous magma pulses)
- The volume of magmatic inputs (small incremental batches versus wide-spaced and large-volume batches)
- The total sulfide content of the magma prior to final emplacement
- The sulfide content of the footwall rocks (in-situ source)
- The secondary enrichment/depletion of copper and PGEs along faults

Magma pulses in the basal heterogeneous units appear to have formed dispersed sulfides that were unable to coalesce and form massive sulfides. Exceptions include pyrrhotite-rich massive sulfides at the Serpentine and Dunka Pit deposits; however, in these two cases a local sulfur source is also present in the footwall Virginia Formation. Most of the disseminated mineralization appears to have formed from a sulfide melt that interacted with low volumes of silicate magma, as indicated by low to moderate R-factors ranging from 50 to 3,000. The low R-factors are probably the result of close-spaced magma inputs of limited volume in progressively developing magma chambers accompanied by contamination from the footwall rocks. Conversely, the copper-PGE-enriched

zones beneath ultramafic horizons formed from a sulfide melt that apparently interacted with large volumes of silicate magma as indicated by high R-factors in the range of 5,000 to 17,000. The high R-factors of these zones are indicative of more turbulent magma conditions following a new magma input that crystallized the ultramafic layers. Overall, copper and PGE-enriched zones within the disseminated sulfide mineralization are associated with a dynamic changeover in the style of emplacement from close-spaced, low-volume, and contaminated pulses to wide-spaced, large-volume, and uncontaminated pulses. Some late hydrothermal secondary enrichment of copper and PGEs also took place adjacent to faults during later stages of emplacement.

b) Basal massive sulfide mineralization

In a few localized areas along the basal zones of the South Kawishiwi and Partridge River intrusions, semi-massive to massive sulfide mineralization is present at the basal contact. In most cases, the massive to semi-massive sulfide is proximal to either sulfide-rich footwall rocks or structures such as faults and pre-complex folds. Massive sulfide zones that are spatially related to sulfide-rich footwall rocks are intersected in scattered drill holes in the Dunka Pit, Babbitt, and Serpentine deposits. All of these massive sulfides are pyrrhotite-rich (with generally less than 2 percent copper) and are present at, or slightly above, the basal contact. In all cases, a pyrrhotite-rich member of the footwall Virginia Formation (bedded pyrrhotite unit) is located at the basal contact and is situated updip of the massive sulfide occurrences. This relationship suggests that the bedded pyrrhotite unit acted as a local sulfur source that generated a copper-poor, sulfide-rich melt that was concentrated downdip along the basal contact, via gravity settling.

The massive sulfide occurrence in the Local Boy ore zone of the Babbitt deposit is clearly structurally controlled. At this locality, the massive sulfide zones are copper-rich (generally 5 to 25 percent copper) and are situated along the axis of an anticline defined by the footwall rock units. The highest PGE values (11 parts per million palladium and 8 parts per million platinum) found to date within the Duluth Complex are associated with these structurally controlled, copper-rich, massive sulfides. The massive sulfides are almost exclusively hosted by the Virginia Formation, present as both inclusions above the basal contact and in the footwall rocks below the basal contact, while interfingering intrusive rocks are relatively barren of massive sulfide. These relationships, plus sulfide textures that are indicative of structural preparation, suggest that the massive sulfides were "injected" into the footwall rocks. Ripley (1986) and Severson and Barnes (1991) proposed that an immiscible sulfide melt, formed in an auxiliary magma chamber at depth, was injected into structurally prepared zones in the footwall rocks along the anticline to form the Local Boy ores. Late movement of chlorine-rich fluids along the axis of the anticline further redistributed and concentrated the PGEs. Recent studies indicated that there is an overall increase in the copper-PGE content of the massive sulfide in an east-to-west direction; this is possibly the result of fractional crystallization of immiscible sulfide melt as it migrated into the footwall rocks. In this scenario, the

north-south-trending Grano fault is inferred to be a potential feeder zone.

Structurally controlled veins and irregular pods of massive sulfide are locally present within granitic footwall rocks immediately beneath the South Kawishiwi intrusion. These occurrences are intersected in scattered holes that outline two northeast-trending belts(Fig.12). The linearity of the belts suggests they are fault controlled. One of these belts crudely aligns with the Birch Lake fault zone that trends through the Birch Lake PGE prospect. The massive sulfide veins were probably formed by the downward expulsion of a basal immiscible sulfide melt into fractured and faulted footwall rocks. The veins are moderately copper enriched due to fractional crystallization of the sulfide melt as it moved down through the footwall rocks.

The occurrence of local massive sulfide veins near and below the basal contact of the Duluth Complex is an indication that larger, potentially economic footwall massive sulfide deposits may yet be found.

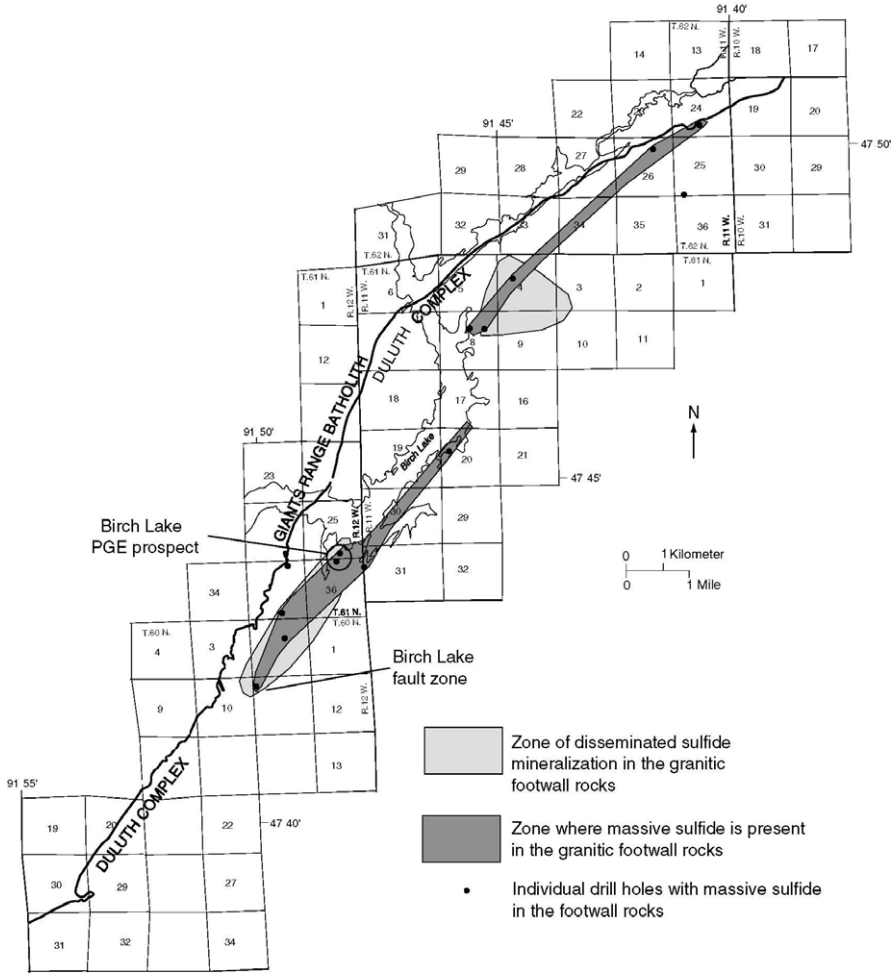

Fig.12 Linear distribution of massive sulfide, disseminated sulfide, and copper rich veins in the footwall rocks beneath the South Kawishiwi Intrusion(Severson et al., 2002).

c) Feeder Zone Sulfide Mineralization

Some of the attributes of the Duluth Complex copper-nickel-PGE sulfide deposits resemble those of deposits at Noril'sk, Russia and Voisey's Bay, Canada that are associated with sulfide mineralization in intrusive feeder zones. The common attributes include occurrence in shallow tholeiitic intrusions associated with plateau basalt volcanism, an external sedimentary source of sulfur, and openness to repeated magma influx and expulsion. A critical attribute of the high-grade Noril'sk.Talnakh and Voisey's Bay deposits, not yet positively identified in the Duluth Complex deposits, is the location of a magma conduit. A conduit that experienced repeated influxes of magma appears to be key to the formation of high grade copper-nickel-PGE deposits. Although this type of mineralization has not been recognized in the Duluth Complex, the conceptional model of magma flow has been established in the South Kiwishiwi and the Partridge River Intrusions and promissing areas of the mineralization have been delineating.

One of the difficulties in evaluating the potential for feeder zone mineralization in the Duluth Complex is determining whether intrusions were fed one-by-one by local magma conduits or by master conduits that sequentially fed several intrusions.

１－２－２． Stratabound and Stratiform PGE Mineralization

PGE-enriched zones in the Duluth Complex and related intrusions can be classified into two categories, stratabound and stratiform. The term *stratabound* refers to PGE-enriched horizons that are restricted to a general stratigraphic unit; however, the PGE-enriched zones are often transgressive relative to the enclosing stratigraphy because they are associated with a wide variety of internal rock types that characterize the stratigraphic unit. The term *stratiform* denotes specific PGE-enriched horizons that are sheetlike in form, concordant, and strictly coextensive with laterally persistent igneous layers. The stratiform PGE horizons differ from the stratabound ones because they are consistently sulfide-poor and tend to occur at mid levels of well differentiated intrusions.

a) Stratabound PGE mineralization

Stratabound PGE-enriched horizons, with low to moderate sulfide concentrations (0.05 to 1.0 weight percent sulfur), are commonly associated with ultramafic layers in the Dunka Road, Babbitt, Wetlegs, and Birch Lake deposits, and occur at the extreme top of Unit I immediately beneath a laterally persistent ultramafic layer(Fig.11). At Dunka Road, this stratabound horizon averages about 10-meters-thick and contains an average of 1.0 part per million palladium + platinum. Recent work suggested that the sulfur was largely derived from the mafic magma and that this stratabound horizon was formed as a result of magma mixing. Two similar stratabound PGE enriched horizons, related to laterally discontinuous ultramafic layers, occur toward the middle of Unit I at Dunka Road. To the west of Dunka Road, the stratabound PGE horizon at the top of Unit I is also present at the Wetlegs and Wyman Creek deposits. At the Dunka Road and the Wetlegs deposits, PGE-

enriched stratabound horizons also span across the ultramafic layer that separates Units VI and VII.

Another example of a PGE stratabound horizon is at the Birch Lake PGE prospect within the South Kawishiwi intrusion. There, PGE contents as high as 9 parts per million palladium + platinum, and Cr_2O_3 contents locally as high as 10 weight percent are associated with a wide variety of rock types within the U3 unit. The U3 unit consists of alternating troctolitic and ultramafic layers in which variably sulfide mineralized zones and discontinuous pods of Cr-bearing massive oxide both occur. As stated above, the massive oxide pods are interpreted based on empirical relationships to have been produced by assimilation and partial melting of the Biwabik Iron Formation. This oxide-rich partial melt may have initially acted as a trap that concentrated chromium and titanium, and through further assimilation and contamination of the magma, may have led to precipitation of PGEs. However, because the ultramafic layers of the U3 unit are interpreted to record new influxes of more primitive magma, magma mixing may have had a more significant effect on PGE mineralization. Furthermore, the presence of chlorine-rich drops on the surface of drill core from the Birch Lake area suggests that a hydrothermal model of concentrating the PGE could also be invoked. As depicked in Fig.13, ascending chlorine-rich hydrothermal fluids may have remobilized and further concentrated the PGE along the northeast trending Birch Lake fault.

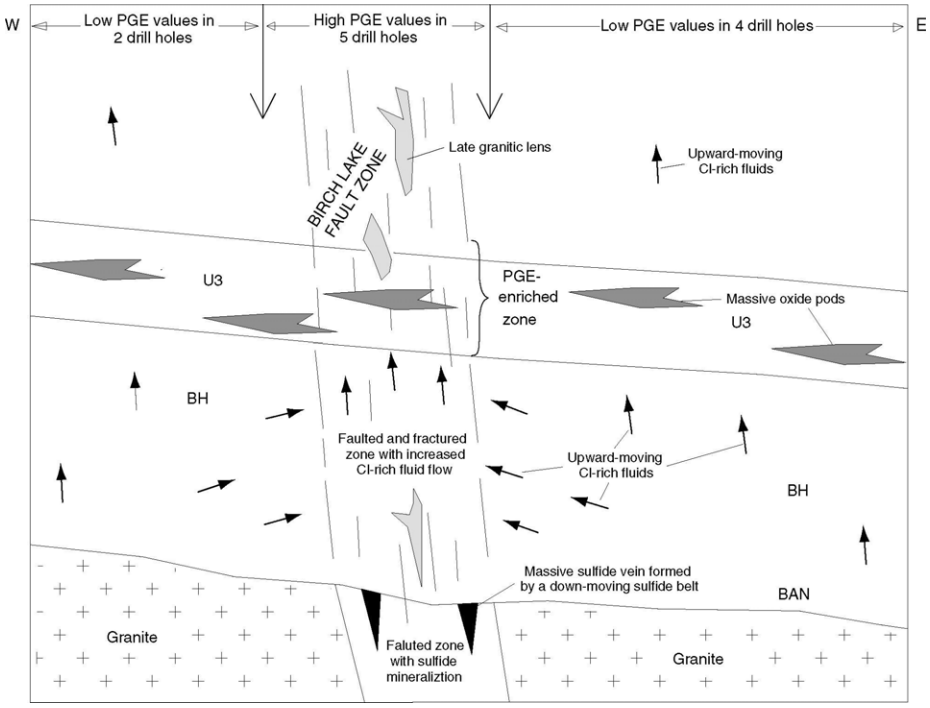

Fig.13 Schematic diagram showing the possible role of the Birch Lake fault for concentration PGE in U3 unit(Severson et al., 2002).

Fig.14A Photograph of Ni-Cu-PGE ore (disseminated ore).

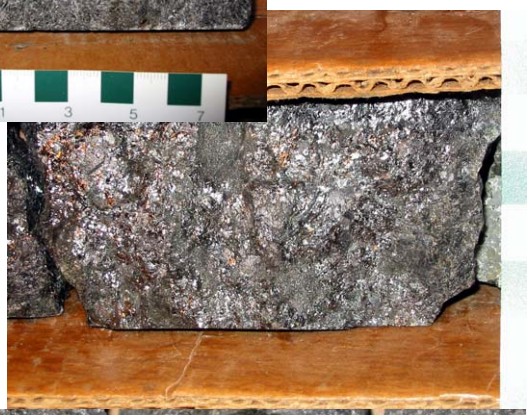

Birch Lake area (D.H. BL-89-2): troctolite in the vicinity of 2595.5ft (2593-2597ft, Cu:0.71%, Ni:0.18%, Pd:1100ppb, Pt:520ppb)

Fig.14B Photograph of Ni-Cu-PGE ore (stratabound mineralization?).

Babbitt deposit (D.H. BI-120): mela-troctolite in the vicinity of 1307ft (the top of Unit I), with native copper (1305-1315ft, Cu:0.72%, Ni:0.16%, Pd:1728ppb, Pt:837ppb).

Fig.14C Photograph of Ni-Cu-PGE ore(massive ore).

Babbitt deposit (D.H.10198): mixed norite and hornfels with massive sulfide in the vicinity of 21ft (20-25ft, Cu:14%, Ni:0.28%, Pd:1700ppb, Pt:260ppb, Au:250ppb**).**

b) Stratiform PGE mineralization

Recent discoveries of gold- and PGE-enriched horizons (or PGE reefs) in the upper part of the Skaergaard intrusion and related Tertiary intrusions of east Greenland have stimulated exploration for such deposits in other tholeiitic layered intrusions such as those comprising the Duluth Complex. Stratiform PGE mineralization in well-differentiated tholeiitic intrusions are similar to classic PGE reef deposits hosted by ultramafic-mafic complexes, such as the Bushveld and Stillwater Complexes, in that they occur as sulfide-poor (less than 1 weight percent), PGE-rich intervals that are several meters thick and are conformable with igneous layering. However, stratiform PGE mineralization in tholeiitic intrusions, termed Skaergaard-type PGE mineralization, differs from the classic PGE reefs because it is:

- Exclusively associated with mantle plume influenced, continental rift environments
- Of Middle Proterozoic age or younger
- Associated with aluminous, olivine tholeiitic parent magma compositions that experience Fenner-type crystallization differentiation
- Hosted by ferrogabbroic cumulate rocks
- Associated with copper-rich, nickel-poor sulfide
- Associated with significant gold that is stratigraphically offset above peak PGE concentrations

Although there is considerable disagreement about how classic PGE reefs formed, most believe that Skaergaard-type reefs are orthomagmatic (formation by the saturation, exsolution, and settling of sulfide melt from silicate magma).

The key requirements for the orthomagmatic formation of an economic PGE reef in a tholeiitic intrusion are:

- The parent magma must be initially sulfide undersaturated
- The parent magma must have a high initial PGE concentration and/or experience a considerable amount of fractional crystallization to build up noble metal concentrations prior to sulfide saturation
- The initial segregation of sulfide melt must be associated with a large R-factor (silicate/sulfide melt ratio)

These required conditions imply that the best chance for significant stratiform PGE mineralization in a tholeiitic intrusion should be at a mid- to upper-level horizon that marks the first "cumulus arrival" of immiscible sulfide melt. Given a well-differentiated, initially sulfide undersaturated tholeiitic intrusion, its ability to form an economic PGE reef depends on the manner by which sulfide becomes saturated in the magma. Mechanisms that may trigger sulfide saturation include:

Fractional crystallization - Because sulfur is an incompatible element in silicate minerals, sulfide will become enriched in differentiating magmas ultimately to the point of saturation and exsolution.

Magma recharge and mixing - Unlike variable sulfide solubility in ultramafic-mafic magmas that produce classic PGE reefs, sulfide solubility in differentiating tholeiitic magmas remains fairly constant over the course of fractional crystallization due to the offsetting effects of temperature and Fe enrichment. Therefore, mixing of magmas with comparable sulfide solubilities is unlikely to produce sulfide saturation or oversaturation.

Decompression due to magma venting - At shallow crustal depths, sulfide solubility appears to positively correlate with pressure. Consequently, in a magma that is close to sulfide saturation, decompression due to magma venting can potentially trigger system wide exsolution of sulfide melt.

Phase changes - The cumulus arrival of a mineral phase that abruptly lowers the iron content of the magma can potentially trigger sulfide saturation. Magnetite crystallization would be the most effective phase change. This was the apparent trigger for sulfide saturation in the Rincon del Tigre magma system of Bolivia(Prendergast, 2000).

Most intrusions of the Duluth and Beaver Bay Complexes formed from initially sulfide undersaturated magmas and show evidence of having undergone one or more of the above mentioned processes during crystallization. Two of these intrusions, the Sonju Lake intrusion and the layered series at Duluth, have been studied for their potential to host stratiform PGE mineralization, and subeconomic mineralization has been found in both areas. The Sonju Lake intrusion was a closed magmatic system and the layered series at Duluth was a more open magmatic system.

Stratiform PGE mineralization in the Sonju Lake intrusion

The Sonju Lake intrusion is a 1,200-meter-thick, shallow-dipping, sheetlike intrusion that forms part of the Beaver Bay Complex(Fig.3). Although its exposed strike-length is only about 3 kilometers, the Sonju Lake intrusion has a distinctive aeromagnetic signature that can be traced for at least 20 kilometers. The Sonju Lake intrusion is predominantly composed of well-laminated, mafic mesocumulates that define a unidirectionally differentiated sequence. Between a lower contact zone of fine grained melatroctolite cumulates (unit slmt - OP cumulate) and an upper zone of unlaminated olivine ferromonzodiorite (unit slmd), five units are distinguished on the basis of cumulus mineral assemblages. In ascending order these units are: sld - dunite (O), slt - troctolite (PO), slg - gabbro (POC), slfg - ferrogabbro (PCF $\pm$ O), and slad - apatite olivine ferrodiorite (PCFOA). This cumulus stratigraphy is complemented by a smooth cryptic variation in mineral compositions. The parent magma composition of the Sonju Lake intrusion is estimated to be an uncontaminated, moderately evolved olivine tholeiite. Cumulus stratigraphy and cryptic variation

suggests that the Sonju Lake intrusion formed by unidirectional fractional crystallization under nearly closed conditions.

To determine the possible location of a stratiform PGE reef in the Sonju Lake intrusion, a total of 67 outcrop and drill core samples that profile the intrusion were analyzed for platinum, palladium, gold, sulfur, copper, and other major and trace elements(Fig.15). These data indicate that a narrow PGE-enriched interval exists within the ferrogabbro unit and lies immediately below the stratigraphic level marking the initial saturation of sulfide melt in the Sonju Lake intrusion magma. Initial saturation and segregation of sulfide melt is inferred to occur at the +322-meter level, where an increase in copper abundance is recognized. Copper content increases from consistently less than 100 parts per million below the +322-meter level to greater than 500 parts per million above, and then gradually decreases to below 100 parts per million in the upper part of the intrusion. This pattern is consistent with:

- Sulfide undersaturated conditions below the +322-meter level
- The saturation and cumulus segregation of sulfide melt at the +322-meter level
- The gradual depletion of copper abundance due to continued exsolution of sulfide melt above the +322-meter level

Nickel was strongly depleted in the magma at the time of inferred sulfide saturation, presumably by prolonged olivine crystallization.

Interestingly, the onset of sulfide saturation at the +322-meter level implied by the abrupt increase in copper abundance is not reflected in the sulfur data. Theoretically, a gabbro cumulate saturated in sulfide melt should contain a minimum of 400 parts per million sulfur based on sulfide solubility of 0.1 weight percent for a moderately evolved mafic magma. The sulfur abundance in cumulates below the +322 meter level are consistently less than the theoretical saturation benchmark. However, sulfur concentrations above the +322 meter level vary unsystematically between less than 100 and 500 parts per million, and only sustain greater than 400 parts per million sulfur concentrations above about +460 meters. Petrographic observations confirm that this zone of presumed sulfide saturation is locally poor in modal sulfide and where present, the sulfide is dominated by copper rich varieties (chalcopyrite, bornite, and digenite). A possible explanation for the high copper, low sulfur samples in the zone between +322 meters and +460 meters is that oxidizing deuteric fluids caused dissolution of sulfur without mobilizing copper. A similar oxidation/desulfurization process has been noted in the low-sulfide PGE reefs in eastern Greenland intrusions. The Sonju Lake intrusion displays several features that are consistent with such a process of oxidation and desulfurization:

- Moderate degrees of chloritic and uralitic alteration of pyroxene are common in ferrogabbroic cumulates of the ferrogabbro unit
- Copper-rich sulfides (chalcopyrite, bornite, and digenite) predominate in samples near the +322 meter level

・Secondary veins of pyrite with hematite occur locally above the +322-meter level

If deuteric desulfurization is a widespread phenomenon in mafic layered intrusions, variations in copper abundance rather than total sulfur may be better indicators of magmatic sulfide saturation.

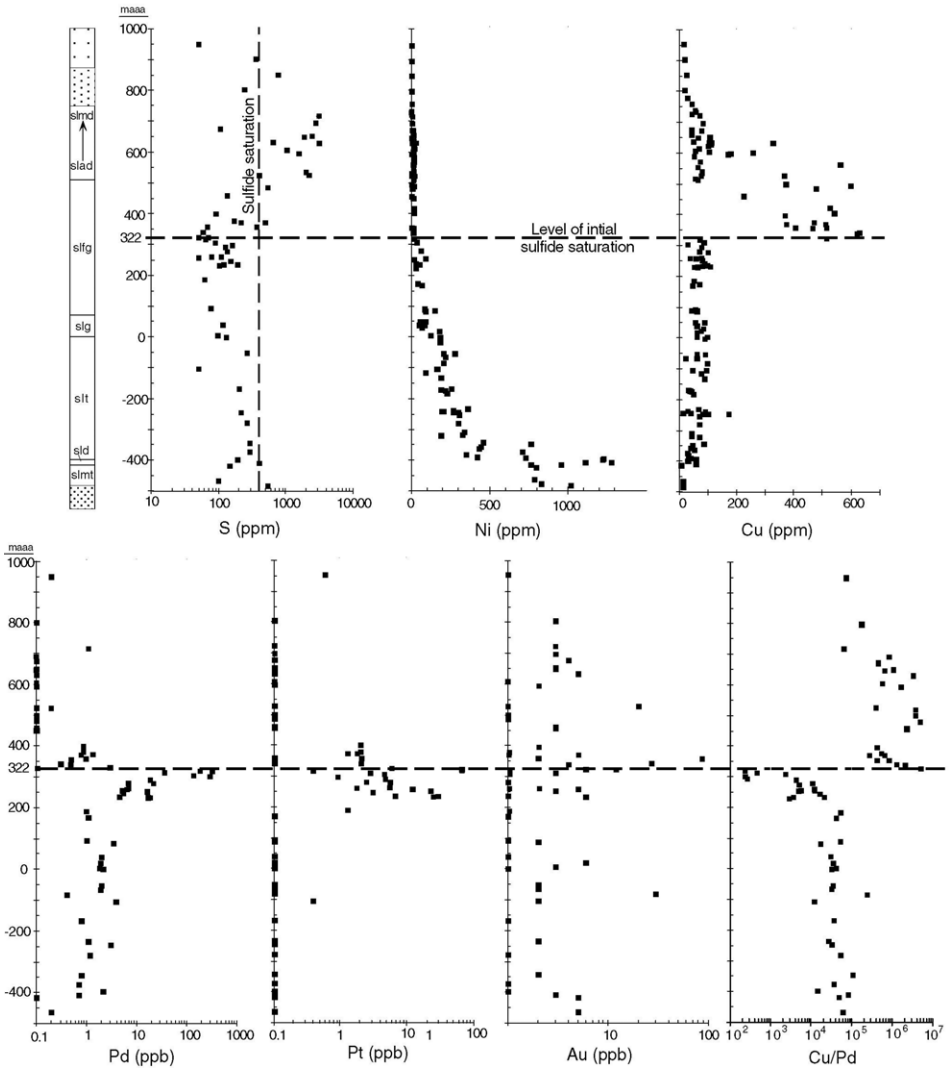

Fig.15 Chemostratigraphic variation in whole rock concentrations of S, Ni, Cu, Pd, Pt, Au, and Cu/Pd through the Sonju Lake intrusion(Severson et al., 2002).

There are no overt changes in lithology evident from field observations across the horizon of increased copper abundance (and PGE enrichment) that would suggest sulfide saturation was triggered by a significant perturbation to the magma system (such as magma recharge, assimilation, or venting). The only notable change observed across the horizon of initial sulfide saturation is the gradual changeover from titanomagnetite-dominated to ilmenite-dominated cumulus oxide phases. However, this also seems an unlikely triggering mechanism because such a change should have minimal effect on the FeO content of the magma and thus sulfide solubility. Rather, given the well-differentiated and closed nature of the Sonju Lake intrusion system, it is concluded that simple crystallization differentiation was the process primarily responsible for not only driving the magma to sulfide saturation, but also for triggering the initial sulfide exsolution event.

Upward from about the +230-meter level, palladium abundance increases regularly to a peak concentration of 320 parts per billion in the sample just below the first known sample to display an abrupt jump in copper to greater than 500 parts per million. This high palladium sample also yields the greatest platinum concentration (66 parts per billion), although a secondary platinum peak (less than 30 parts per billion) seems to exist about 90 meters below the sulfide saturation level. The highest gold concentration (85 parts per billion) occurs 35 meters above the level of initial sulfur saturation, although its variation is less systematic than palladium and platinum. In the first high concentration copper sample (greater than 500 parts per billion) and in most overlying samples, palladium and platinum abundances drop to below detection limits (less than 0.1 part per billion).

The efficiency with which PGEs were scavenged from the Sonju Lake intrusion magma with the "cumulus arrival" of sulfide melt is indicated by the 10^4 increase in copper/palladium observed across the +322-meter horizon. Changes in the copper/palladium ratio reflect the fact that the sulfide melt/silicate magma partition coefficient for palladium is several orders-of magnitude greater than that for copper.

When directly comparing the Sonju Lake and Skaergaard intrusions, not only are their petrologic similarities evident, but also when comparably scaled, their patterns of precious metal and sulfide mineralization are remarkably similar (Fig.16). Their similar paragenetic sequences of cumulus minerals imply comparable closed-system crystallization differentiation of aluminous, olivine tholeiitic parent magmas. Both parent magmas were initially sulfide-undersaturated and became saturated at proportionally similar levels in their crystallization histories. Both intrusions were crystallizing a cumulus mineral assemblage of plagioclase + augite + iron oxide at the time of sulfide saturation. Both show peak PGE concentrations at or just below the level of initial sulfide saturation. Both show low and variable levels of palladium in the lower sulfide undersaturated part of the intrusions and almost complete and persistent palladium depletion above the sulfide saturation horizon. Finally, both show an upward displacement of peak gold concentration from the PGE peak.

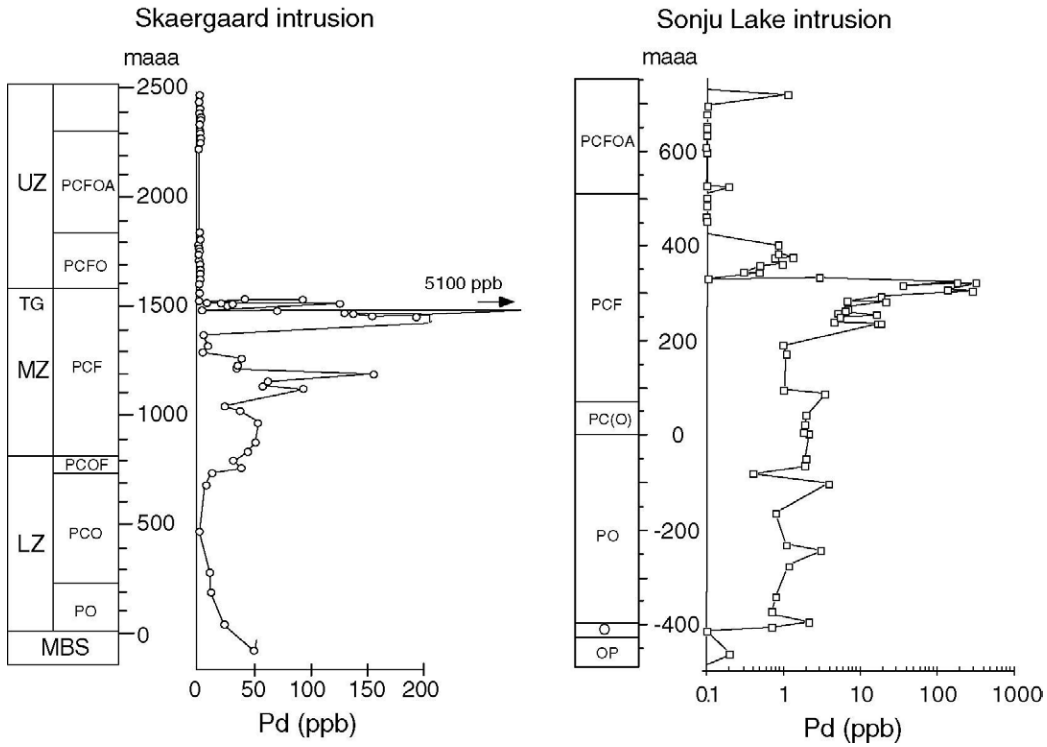

Fig.16 Comparison of generalized igneous stratigraphy and stratigraphic variation of Pd concentrations in the Skaergaard and Sonju Lake intrusions(Severson et al., 2002).

Stratiform PGE mineralization in the layered series at Duluth

The layered series at Duluth is a 3.5 to 5kilometer-thick, sheetlike, mafic layered intrusion, and the igneous stratigraphy of the layered series at Duluth is divided into five major zones. The repeated progression from troctolitic to gabbroic cumulates in the cyclic zone indicates that the layered series at Duluth, unlike the Sonju Lake intrusion, did not crystallize as a closed system. Based on these characteristics, Miller and Ripley (1996) suggested that the macrocyclic phase layering is predominantly related to devolatilization and decompression that attended magma venting events from a shallow (less than 5 kilometers) chamber, with magma recharge possibly having a secondary affect.

Geochemical data were acquired from 83 hand samples that profile the general stratigraphy of the layered series at Duluth. Most of the samples have platinum + palladium concentrations below 15 parts per billion, 14 samples have concentrations between 15 and 150 parts per billion, and five samples have concentrations greater than 150 parts per billion(Fig.17). Whole rock sulfur and copper concentrations imply that the layered series at Duluth magma was consistently sulfide

undersaturated during troctolite-zone crystallization, achieved intermittent saturation during crystallization of the cyclic zone, and was fairly consistently saturated as the gabbro zone accumulated. In contrast to the singular large increase in copper abundance and copper/palladium ratio observed in the Sonju Lake intrusion system (Fig.15), the layered series at Duluth shows erratic variability in these parameters (Fig.17). Such variability probably reflects the openness of the layered series at Duluth system to magmatic recharge.

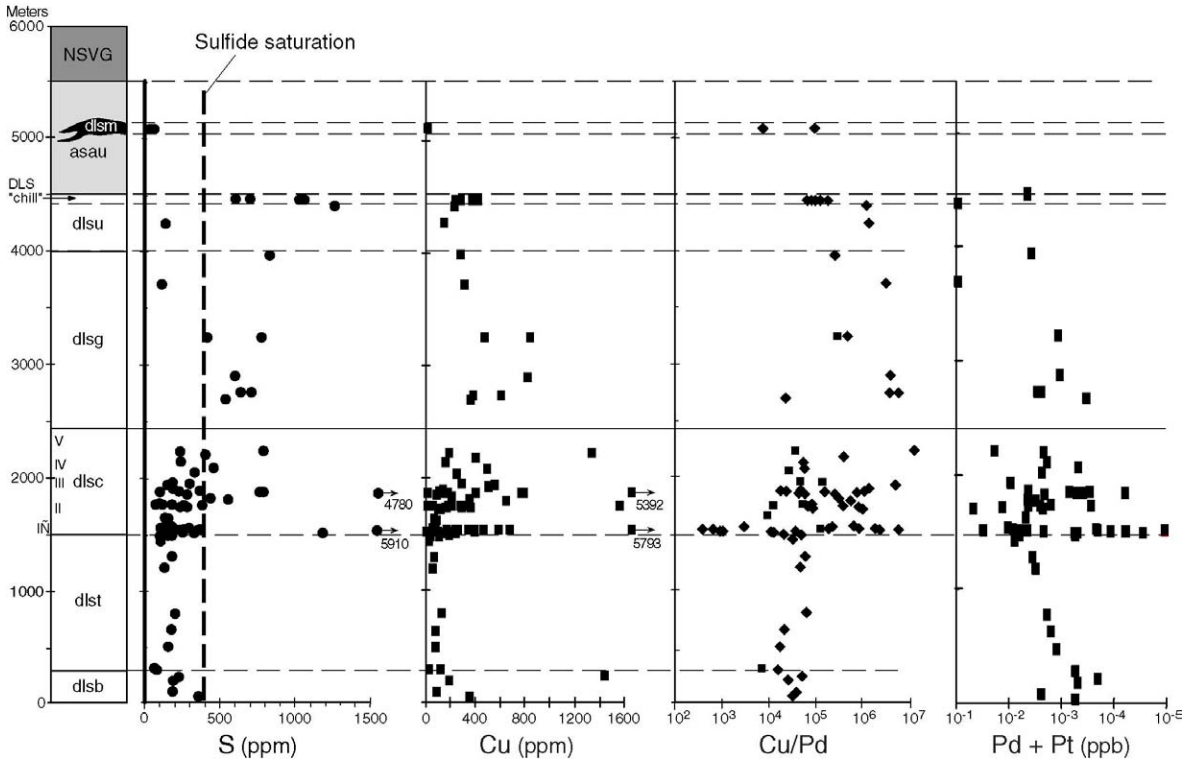

Fig.17 Stratigraphic variation in S, Cu, Cu/Pd, and Cu+Pd abundances through the Layered Series of Duluth(Severson et al., 2002).

１－３． Mineral Exploration in the Duluth Complex

１－３－１． Copper-Nickel Exploration activity at the Base of the Duluth Complex

Exploration for copper-nickel sulfide deposits along the base of the Duluth Complex began in 1948 and has continued intermittently. Between 1951 and 2000, at least 22 companies conducted drilling campaigns in 28 areas. During this period, over 1,700 holes totaling over 1.4 million feet (427 kilometers) of core have been drilled in the basal zone of the complex. At least ten copper nickel deposits, portrayed on Fig.9

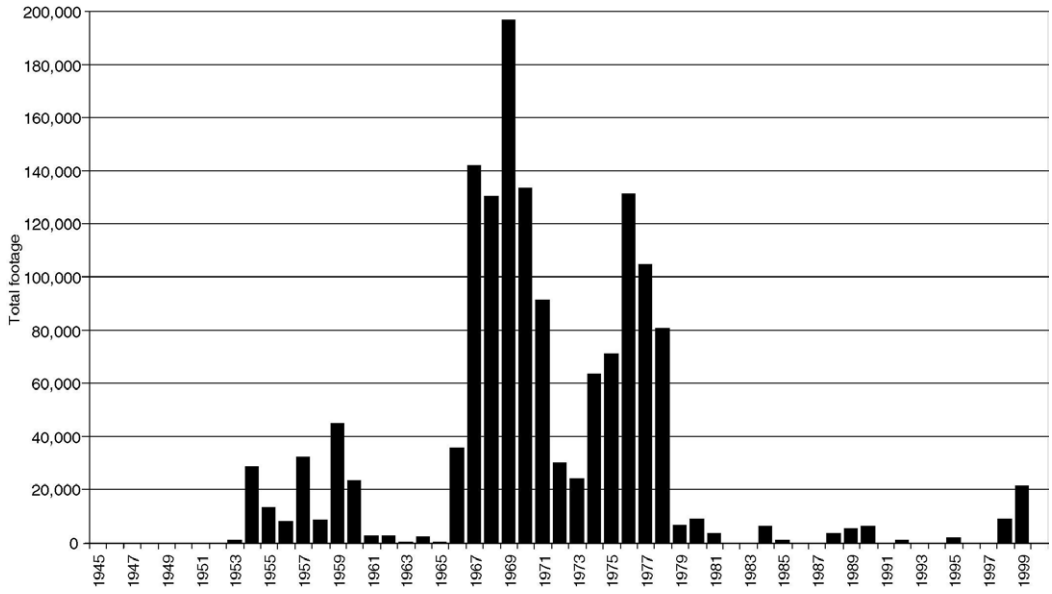

Fig.18 Histgram of annual exploration drilling footage along the basal contact of the Duluth Complex(Miller et al., 2002).

Outcrops that contain disseminated sulfide minerals were first noted at the base of the Duluth Complex by Grant(1899). However these occurrences were too sporadic and weakly mineralized to spark any exploration interest. More strongly mineralized rocks with copper stains were discovered in 1948 by prospector F.S. Childers at the area of present Spruce Road deposit. In 1951, a 188-foot (57-meter) exploration drill by Childers and partner R.V. Whiteside, situated within what is now referred to as the Maturi deposit, intersected disseminated sulfides in gabbroic rock that averaged 0.36 percent copper and 0.13 percent nickel.

This discovery sparked the exploration activity. In 1952, INCO and Bear Creek Mining(a

subsidiary of Kennecott Mining Company) conducted reconnaissance geological and geophysical surveys, which were beginning of the exploration activities by major mining companies. The drilling campaign commenced in 1954 is divided into two phases, the first phase(1954-1960), and the second phase(1966-1981).

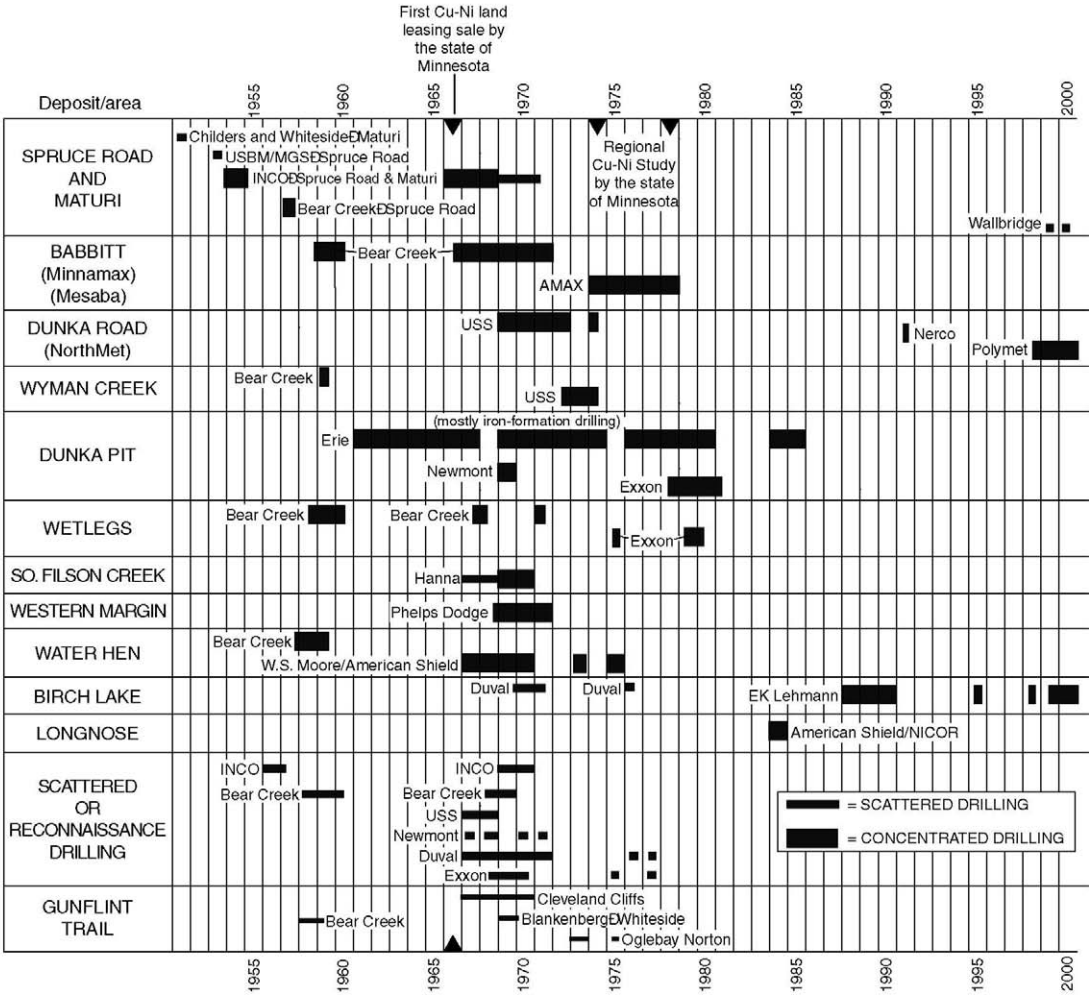

Fig.19 Chronology of drilling activities between 1950 and 2000 along the basal contact of the Duluth complex(Miller et al., 2002).

The first phase

INCO conducted drillings during 1954 and 1955 at the Spruce Road and Maturi deposits. A potentially large tonnage of low grade copper-nickel ore was indicated by this work. During 1956 and 1957, on the basis of geophysical surveys, INCO drilled reconnaissance holes into other areas.

However the results from these areas were disappointing.

Between 1957 and 1960, Bear Creek Mining conducted an extensive drilling program that targeted scattered geophysical anomalies, and the most interesting holes were located at the Babbitt Lake deposit.

After 1960, all drilling activities were suspended due to the low grade nature of the ore, coupled with low metal price, and unavailability of state-owned mineral lands.

The second phase

In 1966, regulations covering mining leases for copper and nickel on state lands were established. Leases were awarded to many companies and the second phase drilling activities began. Between 1967 and 1978, extensive drilling programs were conducted along the base of the Duluth Complex.

INCO completed a major drilling effort at its Spruce Road and Maturi deposits, and sunk a shaft at the Maturi deposit in 1966 and 1967. They decided that the mineralization at the Maturi deposit was too low grade to support an underground mine and concentrated their efforts at the Spruce Road deposit. In 1974, INCO announced their plan to establish an open-pit mine at the site.

Bear Creek Mining concentrated most of their effort at the Babbitt and Serpentine deposits between 1967 and 1971. After the activity of Bear Creek Mining, Amax renamed the deposit, "the Minnamax deposit", and conducted an extensive exploration program at the deposit that consisted of 228 surface drill holes(from 1974 to 1978), sinking a shaft with four drifts into massive sulfide mineralization near the basal contact at the Local Boy ore zone, and drilling 219 underground holes at Local Boy.

Between 1974 and 1978, in response to environment concerns regarding the impact of sulfide mining, "The Regional Copper and Nickel Study" was conducted by the state. Coincident with the study, the leasing of state lands was suspended between 1974 and 1981. The impact of the study on exploration activity in the Duluth Complex was significant. Development of both the Spruce Road and Babbitt deposits was delayed pending results of the study. By the end of the study in 1978, copper and nickel markets had weakened. As a result AMAX relinquished their land position at the Babbitt deposit and the Minnamax shaft was closed in 1981. INCO continues to maintain their leases, but has not pursued any further developments.

１－３－２． PGEs exploration activity

During the early phases of drilling (prior to about 1980), all of the exploration companies recognized that the copper-nickel deposits had some potential for hosting precious metals, especially platinum group elements (PGEs). However, PGEs were rarely analyzed for in the early exploration period because PGE assays were too, and the assays were often inaccurate and not replicable. Based on limited PGE sampling, the companies assumed that the typical copper-nickel ore contained no more than a few hundred parts per billion combined platinum and palladium. In

1985, the Minnesota Department of Natural Resources and University of Minnesota (Minerals Resource Research Center [MRRC]) discovered significant values of about 9 parts per million combined platinum + palladium in the chromium bearing drill core from the Birch Lake area. A short time later, Morton and Hauck (1987) compiled all of the unpublished company PGE data for the Duluth Complex and reported the presence of significant PGE values, often associated with high copper contents. These discoveries sparked renewed interest in the copper-nickel deposits of the Duluth Complex as potential polymetallic deposits.

At least four companies are currently evaluating the polymetallic potential of five areas along the basal contact. PolyMet Mining Corporation has acquired the Dunka Road deposit and renamed it the NorthMet deposit. PolyMet has recently drilled over 90 holes (from 1998 to 2001) and is conducting pre-feasibility studies. They plan on using a hydrometallurgical process to treat the copper-nickel-cobalt-PGE-gold sulfide ore. Cominco American Incorporated has acquired the Babbitt deposit and has renamed it the Mesaba deposit. They also plan on using a hydrometallurgical process. Between 1988 and 2000, Lehmann drilled 20 surface holes to evaluate the PGE potential of the Birch Lake area at depths of 2,000 to 2,600 feet (610 to 792 meters) below the surface. In 1997, INCO began to renew their interest in the Maturi and Spruce Road deposits following the discovery of high-grade copper-PGE massive sulfide veins in the footwall rocks beneath the Sudbury Igneous Complex. In 1999, INCO's U.S. subsidiary, American Copper and Nickel Company, joint-ventured their properties with Wallbridge Mining Company Limited. Wallbridge has recently drilled two holes at Spruce Road to evaluate the high-grade vein potential, and one hole at Maturi to evaluate the PGE potential associated with the disseminated copper-nickel mineralization.

In addition to the recent activity along the basal contact of the Duluth Complex stated above, companies are showing interest in the possibilities of discovering PGE reef deposits at higher stratigraphic levels. Miller (1999) proposed that several intrusions within the Duluth and Beaver Bay Complexes appear to have petrologic attributes favorable for reef formation. Exploration companies that held mineral leases in the interior of the Duluth Complex and in the Beaver Bay Complex in 2001 include Falconbridge Limited, McVicar Minerals Limited, Polymet Mining Incorporated, and E.K. Lehmann and Associates.

APPENDIX 3

Report of

the 9th

International Platinum Symposium

- Geology and PGE mineralization of the Lac de Iles mine and others in Ontario, CANADA -

Lac des Iles

The mafic to ultramafic Archean Lac des Iles Intrusive Complex (2692Ma) (LDI-IC) is located approximately 85 kilometres north of the City of Thunder Bay in northwestern Ontario,CANADA. The LDI-IC is host to numerous zone of platinum group element(PGM) mineralization,including the Roby Zone(open-pit). The Roby Zone has been in commercial production since 1993 and as of December 31,2001 has produced 629,272 ounces of palladium,44,086 ounces of platinum,42,073 ounces of gold,11,139,923 pounds of copper and 7,765,647 pounds of nickel. As of December 31,2001 measured and indicated resources for the 950 metres long by 815 metres wide Roby Zone deposit total 159 million tones grading 1.55g/t Pd,0.17g/t Pt,0.12g/t Au,0.05 % Cu and 0.05 % Ni at a palladium cut-off grade of 0.7g/t.

Lac des Iles Intrusive Complex (LDI-IC) (Fig.1)

The LDI-IC is the largest of a series of mafic to ultramafic intrusions defining a circular pattern in the Lac des Iles area that is approximately 30 kilometres in diameters. The LDI-IC consists of three chambers,each a distinct lithological domain. Ultramafic intrusions(North Lac des Iles Intrusion) are centerd on Lac des Iles, chaotic gabbroic intrusions(Mine Block Intrusion) occur immediately south of Lac des Iles, and a relatively homogeneous hornblende gabbro(Camp Lake Intrusion) is located southwest of Camp Lake.

North Lac des Iles Intrusion(NLDI-I)

The NLDI-I can be sub-divided into four domains based on lithological variations and structure.

(1) massive to broadly layered,east-trending clinopyroxenite,with lesser websterite and minor olivine bearing units underlying the extreme north-northwest portion of The NLDI-I
(2) massive to locally well layered north trending clinopyroxenite,websterite,thin olivine rich units and underlying gabbro in the northeastern portion of of The NLDI-I
(3) east-trending massive gabbro,gabbronorite,varitextured gabbro/gabbronorite,and heterolithic gabbro/gabbronorite breccia interfingered with massive clinopyroxenite and minor websterite and olivine-bearing units in the south central portion of of The NLDI-I
(4) clinopyroxenite with less abundant olivine-bearing units,websterite and gabbro underlying the southern portion of of The NLDI-I

Laterally,the most continuous unit is a 50m thick gabbro that can be traced over 2 kilometres on a northerly strike in the northeastern part of The NLDI-I. The most

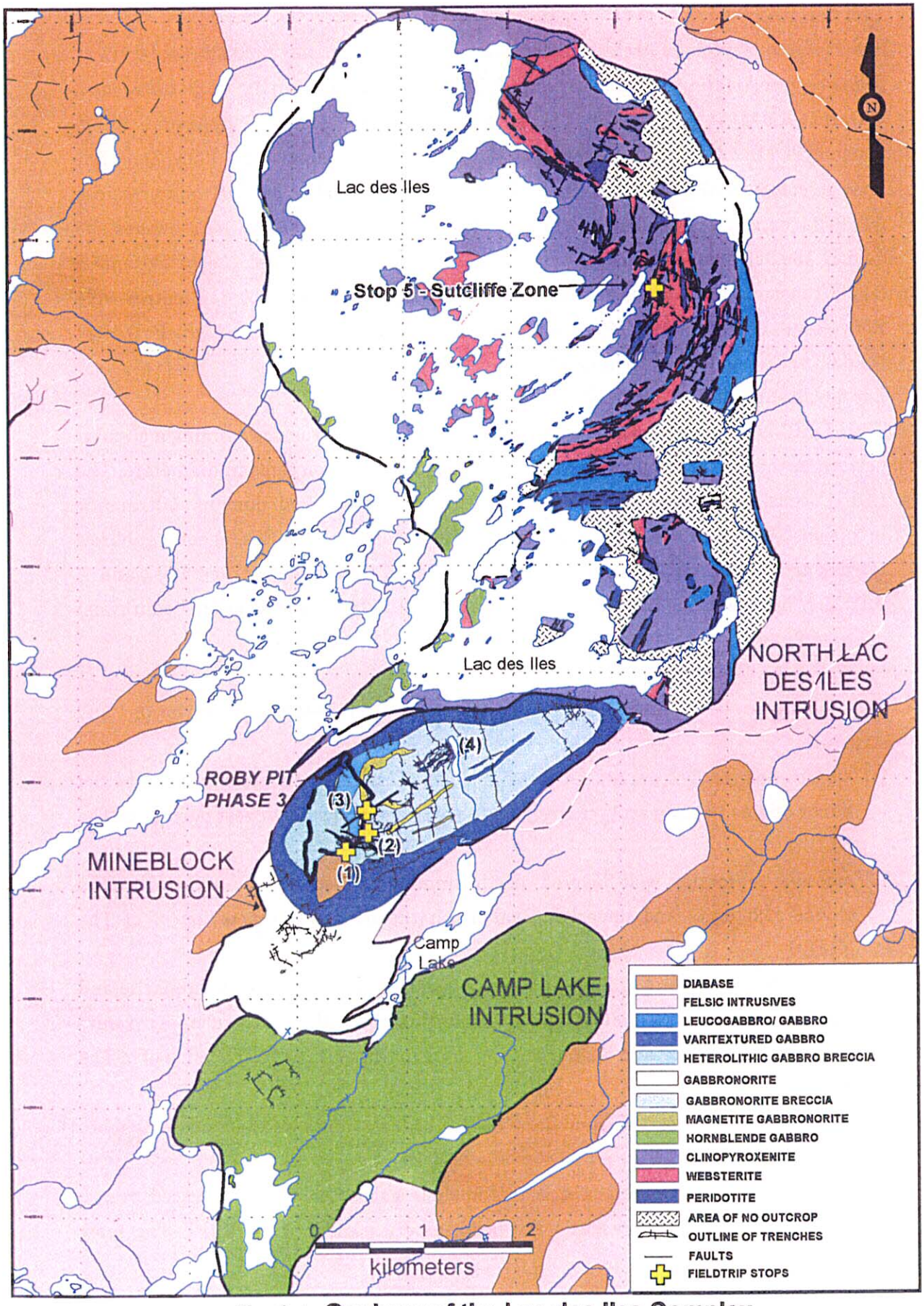

Fig. 1 Geology of the Lac des Iles Complex

common style of mineralization in the NLDI-I consists of disseminated chalcopyrite containing up to 1.0g/t Pd+Pt.

Mine Block Intrusion(MBI) (Fig.2)

MBI is texturally and compositionally complex. Its composition ranges from anorthosite to clinopyroxenite,leuco-gabbronorite to melanonorite and includes magnetite-rich gabbro. Textures include equigranular, fine-to coarse-grained, porphyritic, and pegmatitic, varitextured units and heterolithic gabbro breccia. These last three textural types are the most common host to PGE mineralization, including the Roby Zone. The most laterally continuous unit is a massive medium-grained gabbro, referred to as East Gabbro. It is adjacent to a varitextured gabbro "rim" to the west and more equigranular gabbronorite to the east. The varitextured rim is host to the Roby Zone palladium deposit where heterolithic gabbro breccia is common, occurring as pipes and pods, and large blocks(～60m) of varying composition.

Camp Lake Intrusion

Camp Lake Intrusion is dominantly a medium-grained hornblende gabbro, with lesser leucocratic, melanocratic, porphyritic, varitextured, and monolithic breccia. Minor PGE mineralization occurs along the northern edge of this intrusion.

Roby Zone (Fig.3,4,5,6)

The Roby Zone is a bulk mineable deposit with a minimum north to south length of 950 metres, a width of 815 metres and has been intersected at a depth of 1,000 metres by core drilling. The Roby Zone is comprised of three distinct ore types.

High Grade Ore(7.6% of volume), North Roby Ore(5.3%) and Breccia Ore(87.1%)

High Grade Ore

The High Grade Ore is mostly hosted by a portion of a 15 to 25 metres thick unit of pyroxenite/melanogabbro. It is located in the east-central portion of the Roby Zone, bounded by the PGE-barren East Gabbro hanging wall and Breccia Ore to the west. The High Grade Ore is confined to a 400-metres long segment of the pyroxenite, while the on strike extensions are barren to low grade.

Sulfide mineralization within the pyroxenite consists of 0.25% to 3.0% fine-grained disseminated sulfides with local net textured patches with up to 10% sulfide. The dominant sulfides are pyrite, pyrrhotite, chalcopyrite and pentlandite. Palladium and platinum mineralization within the High Grade Ore consists of predominantly fine-grained PGE sulfide, braggite and telluride minerals,merenskyite and kotulskite, which are present interstitially to cumulus grains and as inclusions within secondary silicates. The mean grade of the High Grade Ore is 7.89g/t Pd,with a maximum of

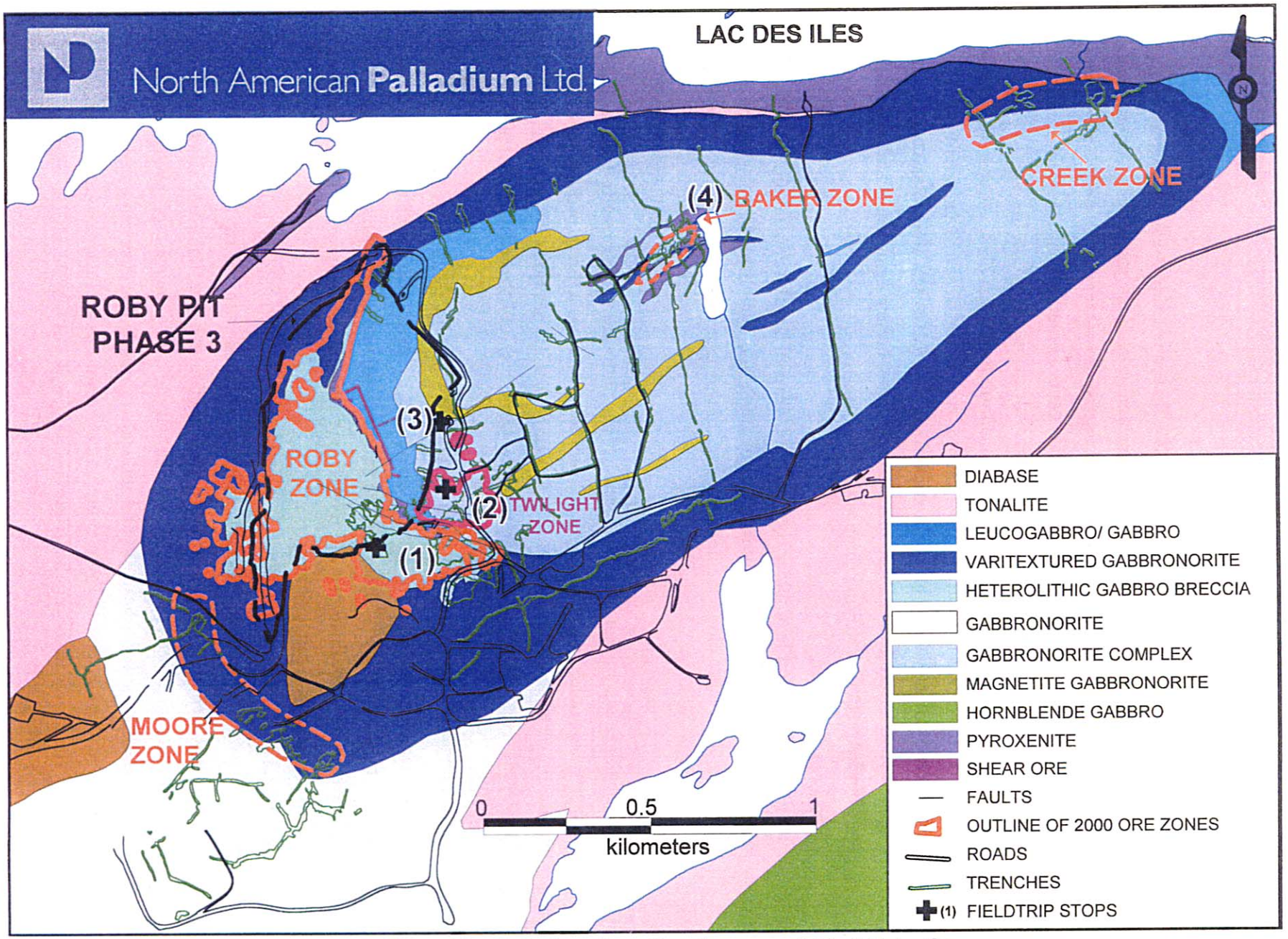

Fig. 2 Mineblock Intrusion Geology and Fieldtrip Stops

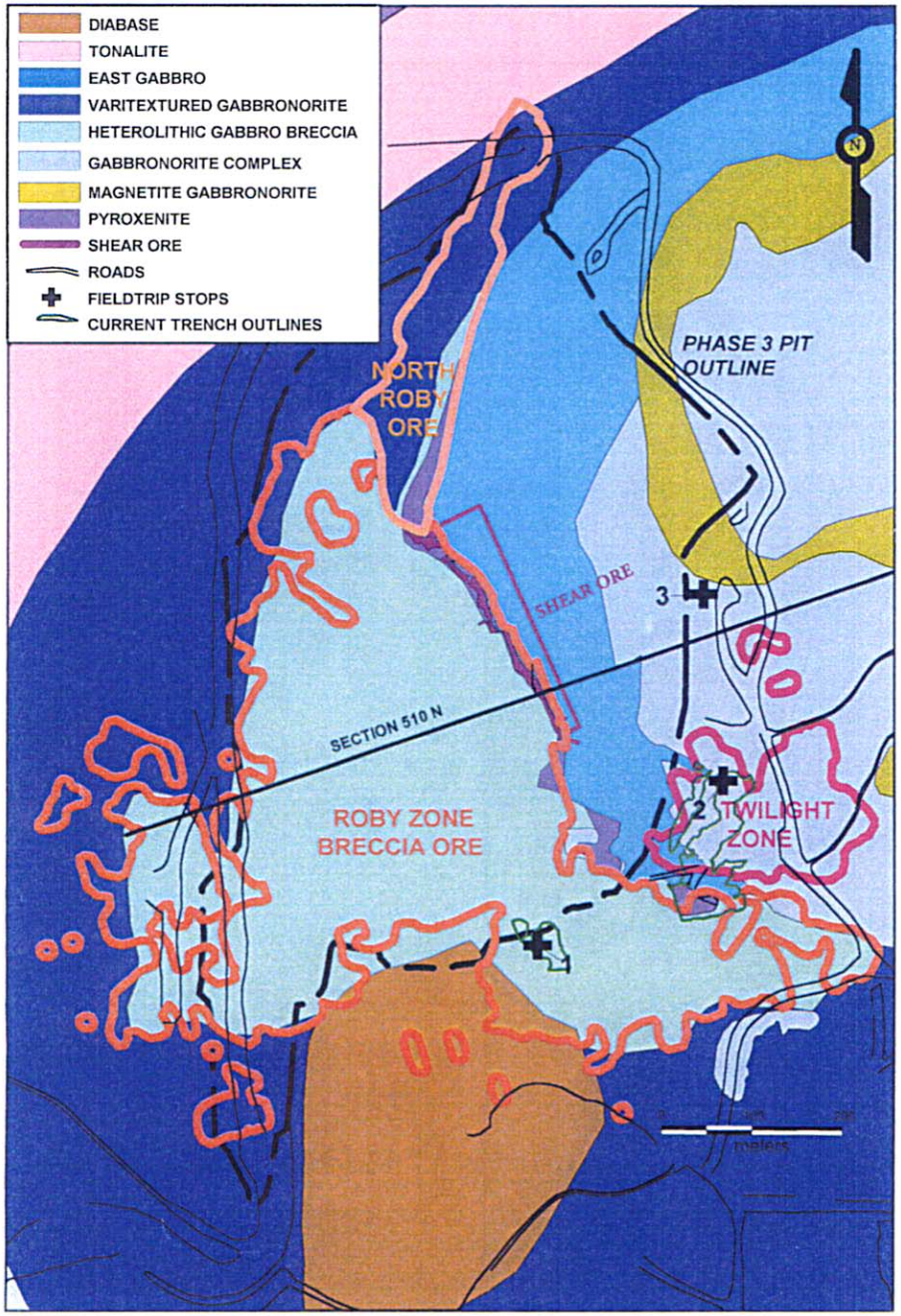

Fig. 3 ROBY ZONE GEOLOGY

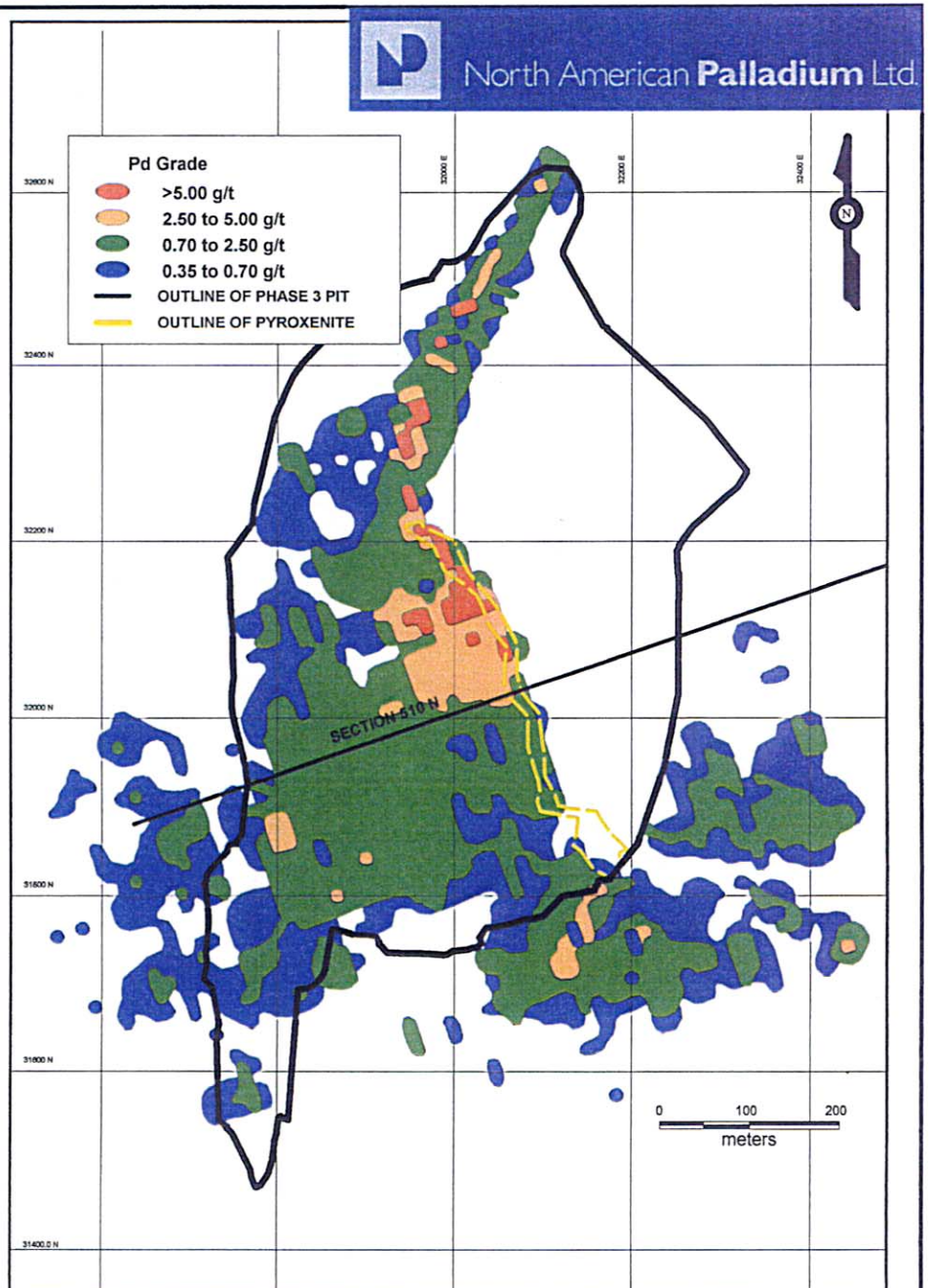

Fig. 4 ROBY ZONE Pd GRADE CONTOURS

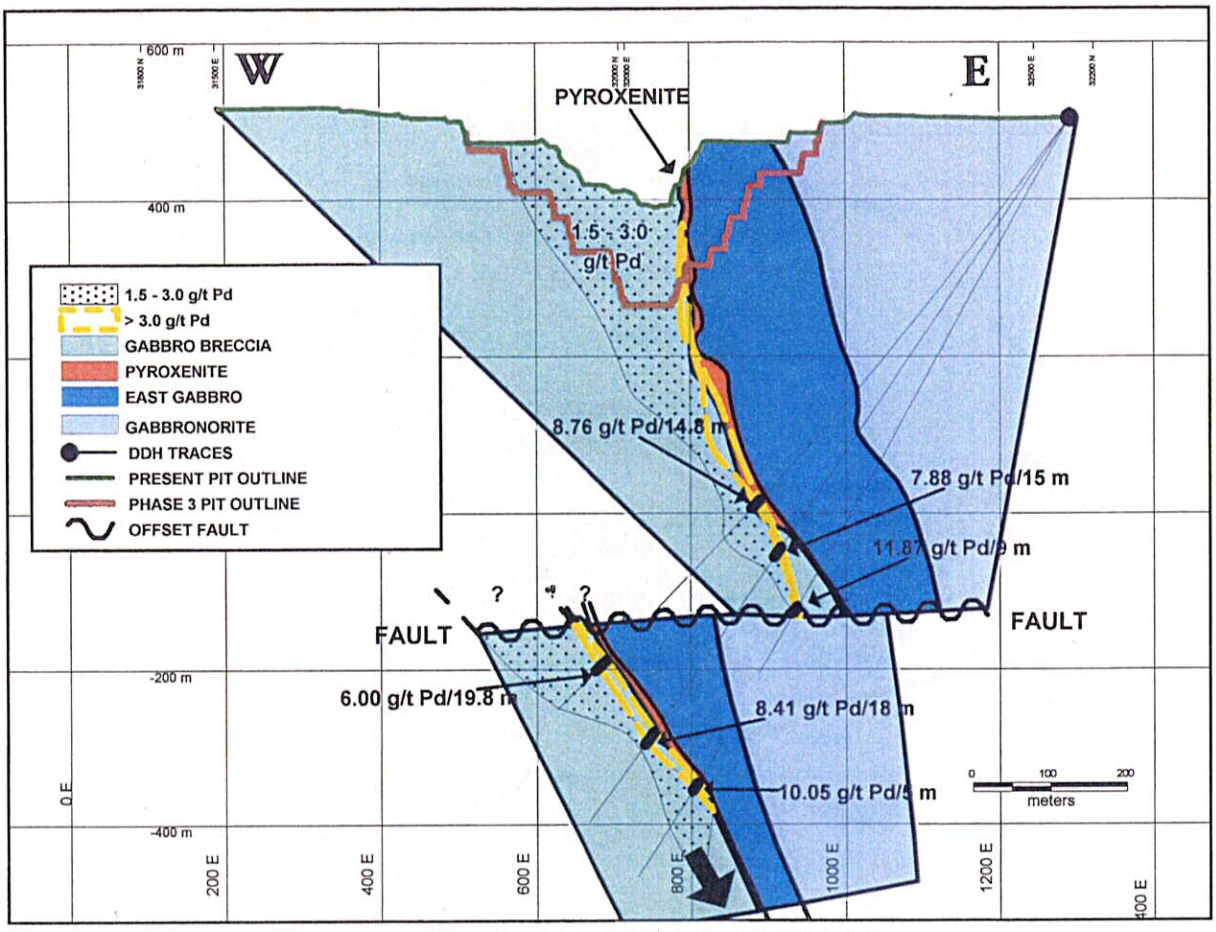

Fig. 5 SECTION 510 - GENERAL GEOLOGY

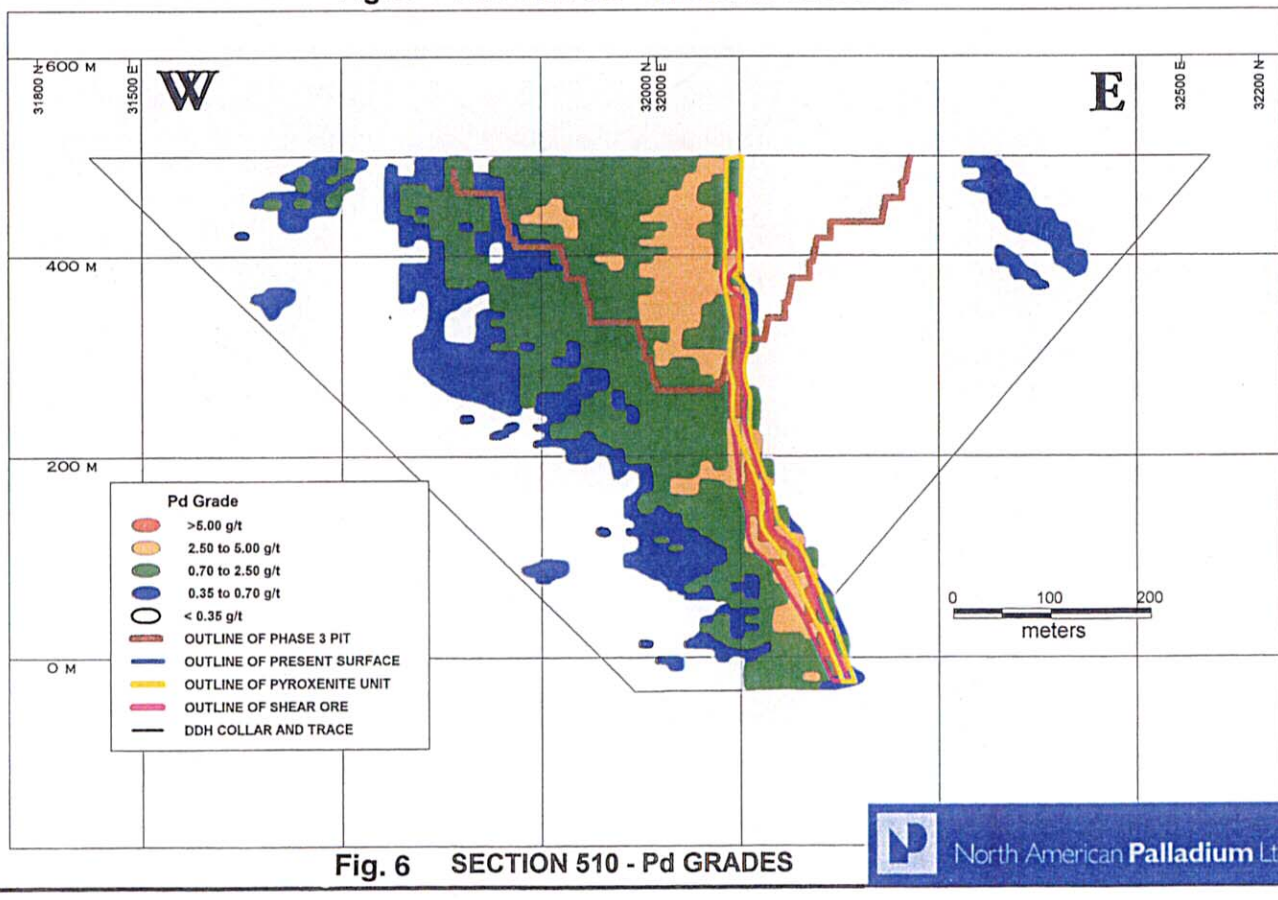

Fig. 6 SECTION 510 - Pd GRADES

North American Palladium Ltd

55.95g/t Pd.

North Roby Ore

The North Roby Ore is a tabular zone that is 20 to 40 metres thick, and 200 metres long. Surfide mineralization occurs primarily within gabbronorite and clinopyroxenite, ranging from trace amounts to 4%, and typically is less than 0.25%. The dominant sulfides are pyrrhotite, pentlandite, chalcopyrite and pyrite. Net-textured sulfides are common in gabbronorite and clinopyroxenite and occur locally within the gabbroic matrix of the heterolithic gabbro. PGE mineralization of the North Roby Ore, occurs primarily within gabbronorite and clinopyroxenite layers. The mean grade of the North Roby Ore is 1.7g/t Pd, and a maximum assay value of 39.7g/t Pd.

Breccia Ore

Southwest of the High Grade Ore, the central mass of the Breccia Ore is contained within a mineralized complex that measures 550 metres north-south by 350 metres wide. An arm of this mineralization has been traced for an additional 250 metres to the southeast. This complex contains lithologies that range in composition from clinopyroxenite to anorthosite to norite. Textures include equigranular fine to coarse grain, porphyrytic, pegmatiteic, varitextured and heterolithic gabbroic breccia, of which the latter three textures are host to the PGE mineralization. Sulfide mineralization within the Breccia Ore often comprises up to 5% of the rock and consists of intergrown chalcopyrite, pentlandite, pyrrhotite and pyrite. PGE mineralization within the Breccia Ore is associated with heterolithic gabbro breccia and accompanying varitextured gabbro. The mean grade of the Breccia Ore is 1.2g/t Pd,with a maximum of 36g/t Pd.

Twilight Zone

The Twilight Zone is a small pod of gabbronoritic breccia found on the eastern side of the Roby Pit. It is separated from the Roby Zone on its western boundary by the 50-70m thick East Gabbro and separated from the southeastern extension of the Roby Zone by a 100m thick barren, post-mineralization gabbro dike. The breccia is characterized by large, sub-round noritic clasts set within a matrix of melanogabbro.

Baker Zone

The Baker Zone is a lower grade deposit situated approximately 1km ENE of the Roby Zone Pit. The zone is situated in the northern/central portion of the Lac des Iles Complex and consists mostly of equigranular norite/gabbronorite that has been intruded by heterolithic melanogabbro breccia, melanogabbro, and a small amount of varitextured gabbro.

Keweenawan Supergroup

Mesoproterozoic intrusive, volcanic and minor sedimentary rocks associated with the Midcontinent Rift(MCR) comprise the Keweenawan Supergroup. On the northern margin of the MCR, Keweenawan rocks include a variety of intrusive rocks.

Copper-Nickel-Platinum Group Element Deposits Associated with the MCR

Rift-related intrusive rocks, such as the Duluth Complex in Minnesota, the Mellen Complex in Wisconsin, the Logan sills and Nipigon plate near Thunder Bay, as well as the alkalic-carbonatite complexes near Marathon, are most commonly exposed along the margins of the MCR. The presence of widespread disseminated Ni-Cu-sulphide mineralization in basal units of the the Duluth Complex , the Mellen Complex, the Coldwell alkalic complex, and in a number of gabbroic to peridotitic dykes and sills, shows that processes necessary for the formation of sulphide deposits were active in some intrusions locally in the MCR.

Intrusion / Lithology	Mineralization Style	Local Examples *(Associated PGE-Mineralized Areas)*
Reversed Magnetic Polarity??? < (1005-1102 Ma):		
Layered gabbro-anorthositic intrusions: Crystal Lake Gabbro	Disseminated and blebby sulphides in medium- to coarse-grained, varied-textured (*a.k.a.* 'taxitic') gabbro	Crystal Lake Gabbro *(Great Lakes Nickel deposit)*
	Disseminated sulphides in Cr-spinel-bearing cumulate layers	*(Cr-spinel-bearing, anorthositic gabbro above Cu-Ni deposit)*
Pine Point - Mount Mollie Gabbro	Disseminated, intergranular sulphides, fracture fillings	*(Mount Mollie; Pine River)*
Normal Magnetic Polarity < (1005-1102 Ma):		
Pigeon River and Arrow River diabase dykes	Disseminated sulphides in medium- to coarse-grained gabbro and diabase	*(Wallenius; Naomi Island; Jarvis Point)*
Reversed Magnetic Polarity (ca. 1108 Ma):		
Logan diabase sills, cone sheets	Sparse, disseminated sulphides	(Numerous)
Nipigon gabbros		
Tholeiitic to alkaline complexes: Coldwell alkaline complex Killala Lake alkaline complex	Disseminated sulphides in medium- to coarse-grained, vari-textured (*a.k.a.* taxitic) gabbro	**Coldwell**: Two Duck Lake gabbro *(Marathon deposit)*; Geordie Lake gabbro — **Killala Lake**: Border gabbro *(Sandspit - Killala)*
	Disseminated sulphides in massive Fe-Ti-oxide cumulate layers	**Coldwell**: Eastern Border gabbro *(Skipper Lake zone)* — **Killala Lake**: *(Unknown)*
Layered(?) picritic ultramafic intrusions	Disseminated sulphides and native metals in lherzolite, dunite, peridotite, etc.	Leckie Lake *(Wolf Mountain)*; Hele Township; Eva-Kitto townships

Exploring for PGM near the Lake Nipigion area (Fig.7,8,9)

The Lake Nipigion area near Thunder Bay where ultramafic rocks of the Nipigion embayment are being testing for their potential to host prolific Noril'sk-type nickel deposits.Many active companies are mentioned by this district.

Campany's names are as follows.

North American Palladium Ltd.

New Millennium Metals Corp.

Platinum Group Metals Inc.

Jonpol Explorations Ltd and Wolfden Resources Inc.

East West Resources Corp.

Canadian Golden Dragon Resources Ltd.

McVicar Mineral Ltd.

Geomaque Explorations Ltd.

LEH Ventures Ltd.

Aurora Platinum Corp.

PGM Ventures Corp.

Spider Resources Inc.

Landore Resources Inc.

Canplats Resources Corp.

Hunter Dickinson Inc.

East West Resources Corp. and joint-venture partner Canadian Golden Dragon Resources Ltd. on exploring the Seagull and Disraeli intrusions for PGM.The project is 90km northeast of Thunder Bay, and forms part of the Wolf Mountain project.Diamond drilling has been conducted on magnetic anomary in Seagull pluton, it`s conical phase measures 3km long 2km wide and is composed of an upper phase of pink granophyric gabbro and a pyroxenite-gabbro unit that contains a magnetite-rich layer with elevated PGE values(1to 3g/t Pd+Pt).The sulphide zone with elevated PGE values ranges up to 16m in thickness and sometimes forms two layers containing more elevated values.

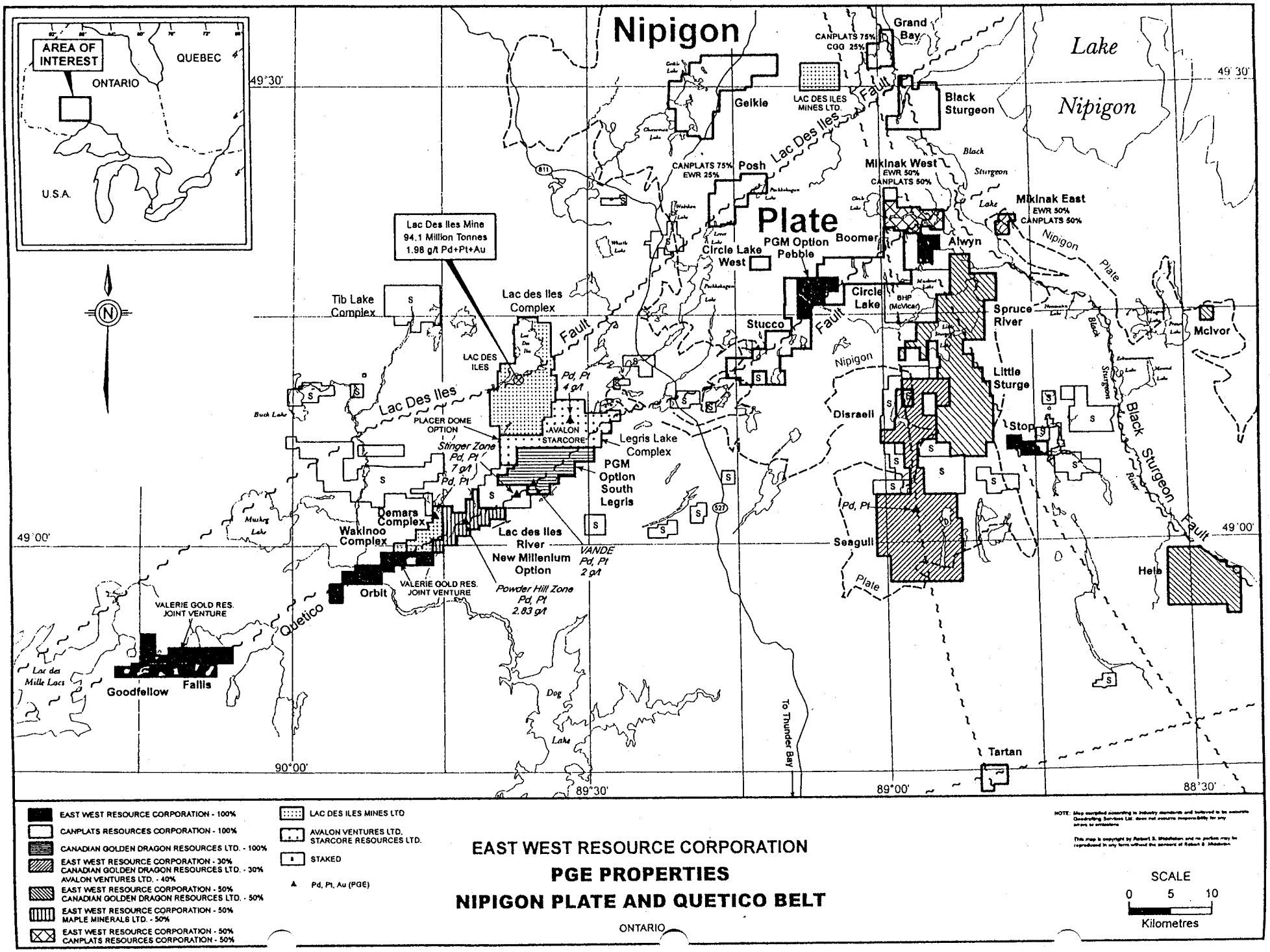
AREA OF INTEREST
QUEBEC
ONTARIO
U.S.A.
Nipigon
Plate
Lake Nipigon
Grand Bay
CANPLATS 75%
CGG 25%
Gelkie
LAC DES ILES MINES LTD.
Black Sturgeon
Lac Des Iles Fault
CANPLATS 75%
EWR 25%
Posh
Mikinak West
EWR 50%
CANPLATS 50%
Mikinak East
EWR 50%
CANPLATS 50%
Lac Des Iles Mine
94.1 Million Tonnes
1.98 g/t Pd+Pt+Au
Circle Lake West
PGM Option
Pebble
Boomer
Alwyn
Circle Lake
BHP (McVicar)
Spruce River
McIvor
Tib Lake Complex
Lac des Iles Complex
Stucco
Fault
LAC DES ILES
Pd, Pt
4 g/t
Lac Des Iles
PLACER DOME OPTION
AVALON STARCORE
Stinger Zone
Pd, Pt
7 g/t
Pd, Pt
Legris Lake Complex
PGM Option South Legris
Little Sturge
Disraeli
Stop
Black Sturgeon River
Fault
Demars Complex
Wakinoo Complex
Lac des Iles River
New Millenium Option
VANDE
Pd, Pt
2 g/t
Powder Hill Zone
Pd, Pt
2.83 g/t
Orbit
VALERIE GOLD RES. JOINT VENTURE
Seagull
Pd, Pt
Hele
Plate
Quetico
Goodfellow
Fallis
Lac des Mille Lacs
Dog Lake
To Thunder Bay
Tartan
49°30'
49°00'
90°00'
89°30'
89°00'
88°30'
EAST WEST RESOURCE CORPORATION - 100%
CANPLATS RESOURCES CORPORATION - 100%
CANADIAN GOLDEN DRAGON RESOURCES LTD. - 100%
EAST WEST RESOURCE CORPORATION - 30%
CANADIAN GOLDEN DRAGON RESOURCES LTD. - 30%
AVALON VENTURES LTD. - 40%
EAST WEST RESOURCE CORPORATION - 50%
CANADIAN GOLDEN DRAGON RESOURCES LTD. - 50%
EAST WEST RESOURCE CORPORATION - 50%
MAPLE MINERALS LTD. - 50%
EAST WEST RESOURCE CORPORATION - 50%
CANPLATS RESOURCES CORPORATION - 50%
LAC DES ILES MINES LTD
AVALON VENTURES LTD.
STARCORE RESOURCES LTD.
STAKED
Pd, Pt, Au (PGE)
EAST WEST RESOURCE CORPORATION
PGE PROPERTIES
NIPIGON PLATE AND QUETICO BELT
ONTARIO
SCALE
0 5 10
Kilometres

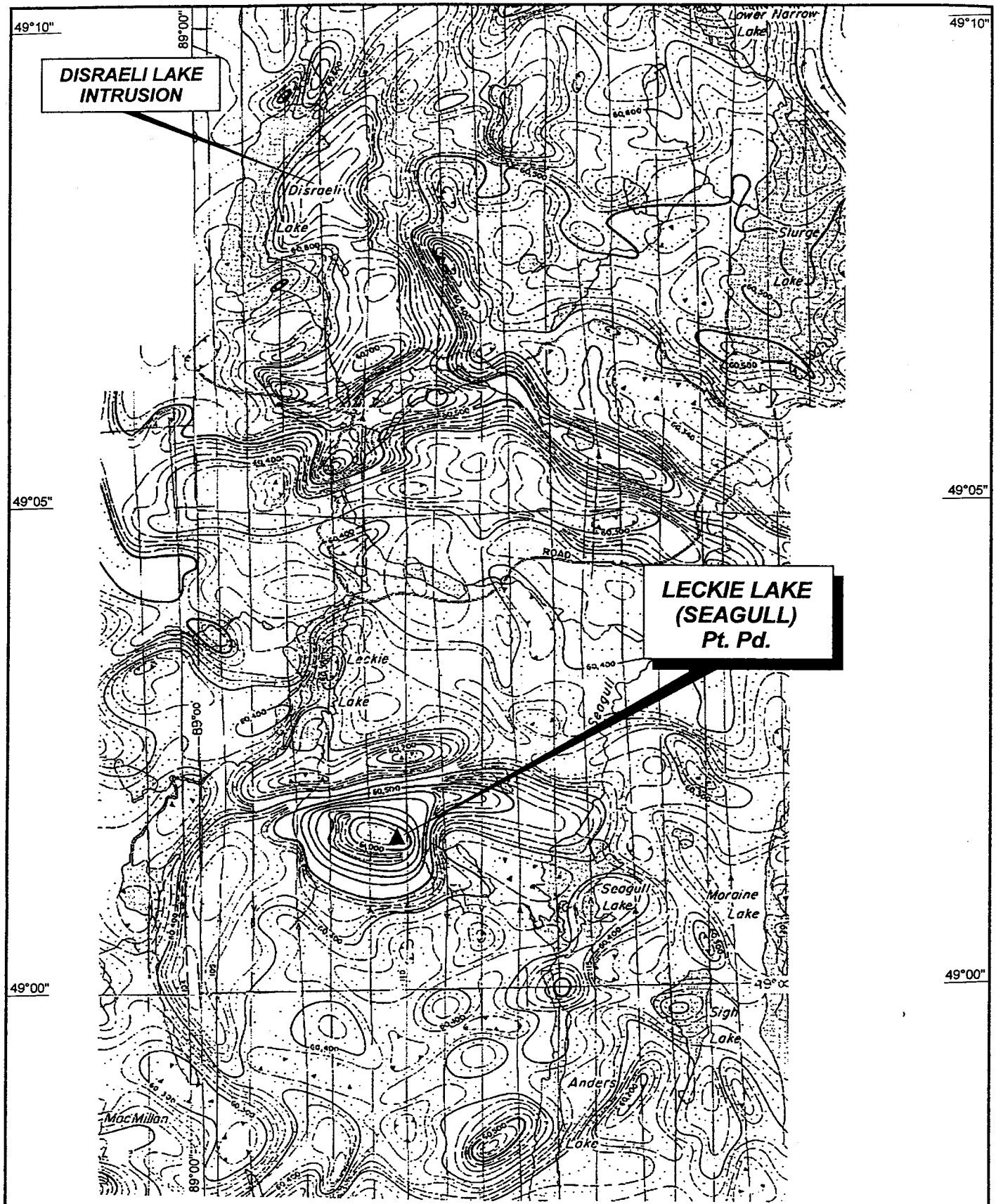

Fig. 8 EAST WEST RESOURCE CORPORATION

DISRAELI LAKE INTRUSION AND SEAGULL PLUTON (Wolf Mountain)

KILOMETRES 0 1 2 3

0 1 2 MILES

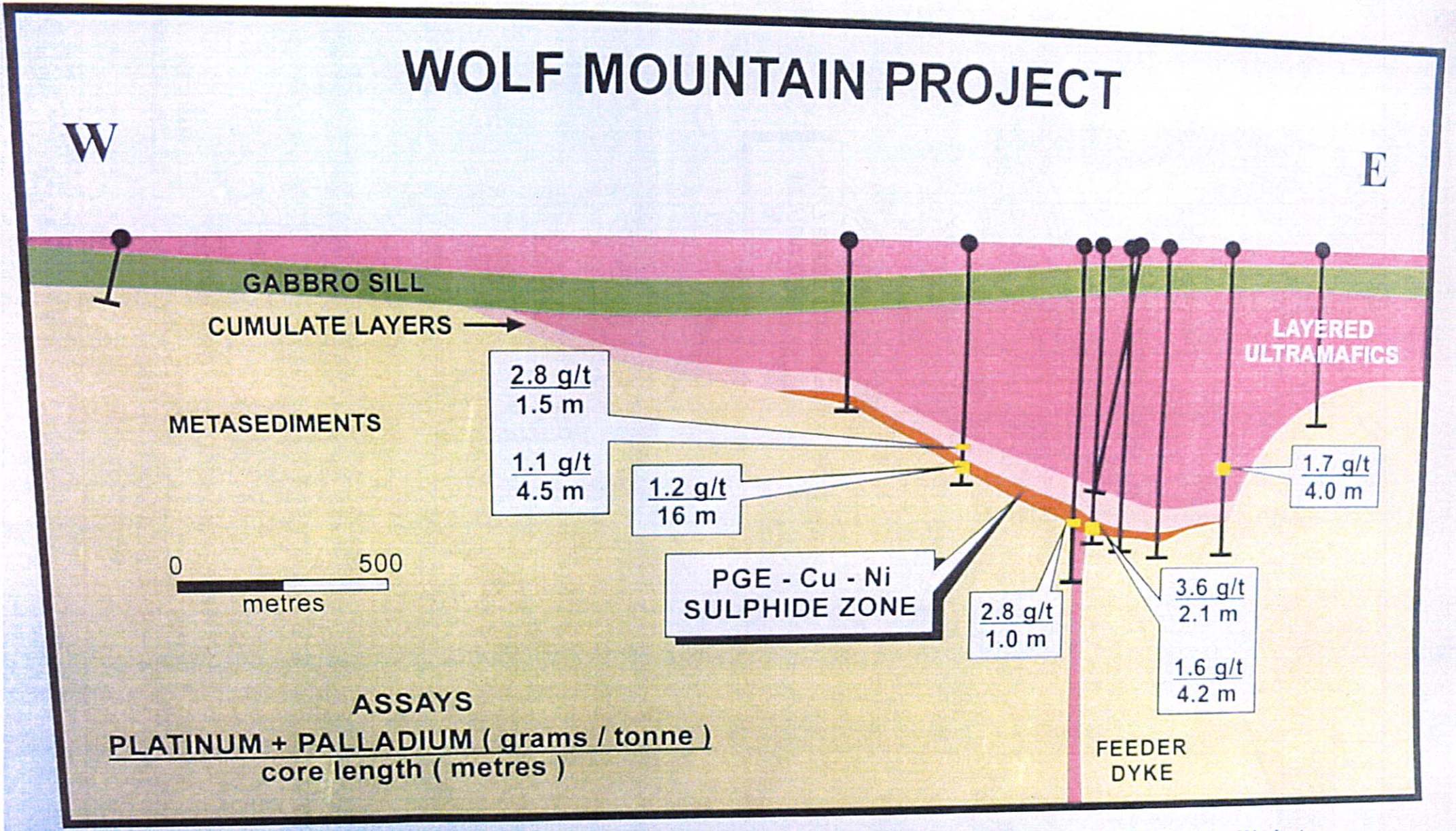

Fig. 9 Geological Cross section of the Seagull Intrusion (Wolf Mountain Project). The Noril'sk-type Cu-Ni-PGE target is indicated in red. Sulphides from this area display composite blebby textures and a high base metal-PGE to sulphur ratio similar to Noril'sk-type mineralization.

Crystal Lake gabbro (Fig.10,11)

Crystal Lake gabbro, which is Y-shaped in plan view, with a west-northwest-striking limb 5km long and an east-northeast-striking, southern limb 2.75km long.This intrusion was subdivided into four major, roughly equivalent, lithologic zone.

(1) an upper zone(60 to 80m) of sulfide-barren troctolite, olivine gabbro and anorthositic gabbro

(2)a middle zone(30 to 42m) of cyclic, layered anorthositic and olivine gabbro, Cr-spinel-bearing anorthosite, and olivine gabbro

(3)a lower, unlayered zone(50m) of vari-textured gabbro and leucotroctolite, which hosts the bulk of the Cu-Ni-sulfide deposit

(4)a basal zone(1 to 7m) of fine-grained, chilled melagabbro and hornfelsed country-rock xenoliths

The sulphides which comprise the Great Lakes Nickel deposit are disseminated, interstitial and included grains and droplets.Pyrrhotite, chalcopyrite, cubanite and pentlandite are the main sulphides.A grab sample of the lower adit area returned 116ppb/t Au, 688ppb/t Pd, 14ppb/t Pt, 13494ppm/t Cu, 4756ppm/t Ni and 255ppm/t Zn.This deposit reserves 45.6 million tons at a grade of 0.334% Cu and 0.183% Ni.

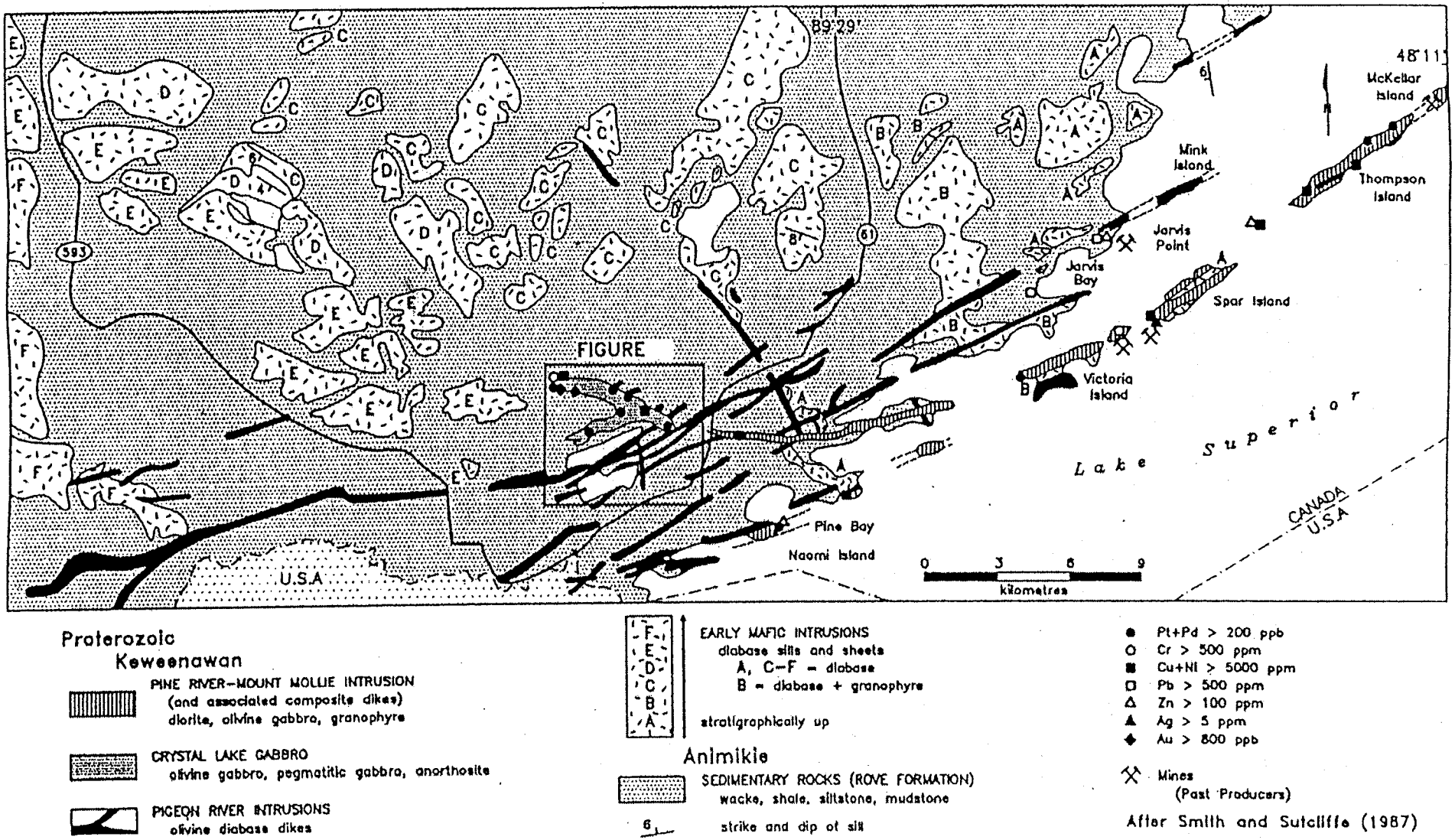

Figure Geology and distribution of intrusive Keweenawan rocks of the Crystal Lake–Pigeon River Region (*after* Smith and Sutcliffe 1987).

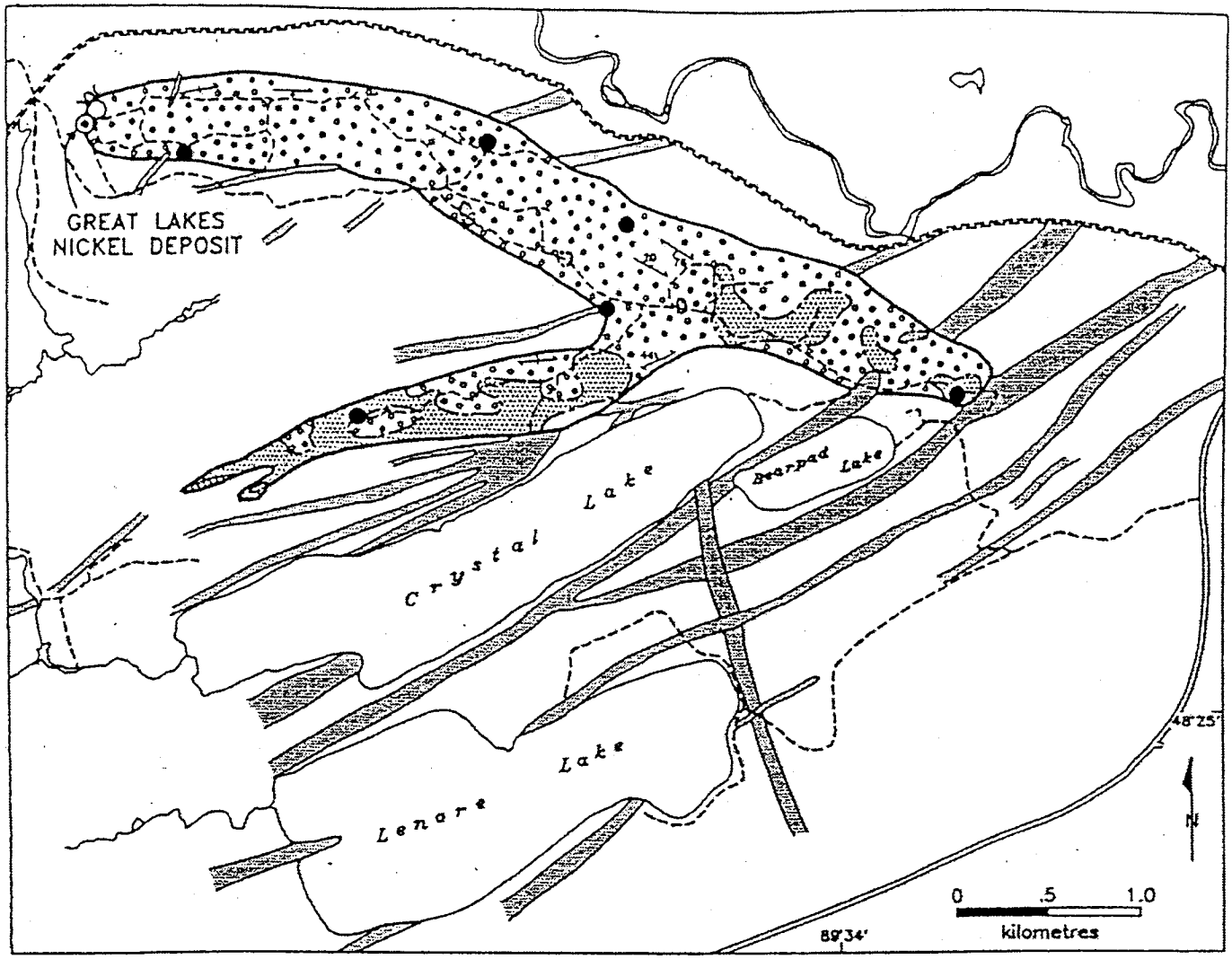

Figure . Distribution of rock types in the Crystal Lake Intrusion (*after* Smith and Sutcliffe 1987).

Coldwell alkaline complex (Fig.12,13,14(1),(2),Tab.1)

A variety of Mesoproterozoic, Midcontinent Rift-related alkaline and carbonatitic rocks comprise several intrusive complexes on the north shore of Lake Superior.They include the Coldwell and Killala Lake alkaline complexes, the Prairie Lake carbonatite and numerous diatremes and related dykes in the vicinity of Dead Horse Creek.the Coldwell complex covers an area of approximately 580km2.The complex comprises three, superimposed ring subcomplexes or magmatic centers that young progressively(Centers 1⇒3) to the southwest.

Center 1 : saturated alkaline rocks with oversaturated residue ; chiefly gabbro and Fe-rich augite syenite

Center 2 : miaskitic alkaline rocks with oversaturated residue ; chiefly alkaline biotite gabbro and nephline syenite

Center 3 : alkaline rocks with oversaturated residue ; chiefly syenite and quartz syenite

A variety lamprophyric and other dyke rocks occur within the complex.

Mafic(+ultramafic) intrusive rocks occur within Centers 1 and 2 and are tabulated, with their associated mineralized zones.Mineralized zones occur in the border gabbro at the eastern(Marathon deposit; Skipper Lake Zone) and western(Middleton occurrences) margins of the complex, and in its interior at Geordie Lake.

Marathon deposit

The mineralization has a north-south strike length of about 1.9 kilometers and dips 30° to 40° to the west, and has a true thickness ranging from 15 to 100m.The Southern Extension Zone incorporates two targets(BR Target and the RD Target) situated to the south of the known resource area(Main Zone) in the under-explored southern 2.3km of the Marathon Property.Grades of up to 4.70g/t Pt+Pd over 15.5m have been intersected in past drilling in the BR Target.The BR Target has a strike length of 225m.The RD Target is located 500m south of the BR Target.Several grab samples grading in the 2.0g/t Pt+Pd range have been found.The significant sulphide occurrences are restricted to the layered olivine gabbro(Eastern Border gabbro), with major concentrations as pods, lenses and interstitiall, disseminated grains in the coarse basal phase at or near the contact with the Archean supracrustal rocks.Pyrrhotite and chalcopyrite are the pricipal sulphide minerals.

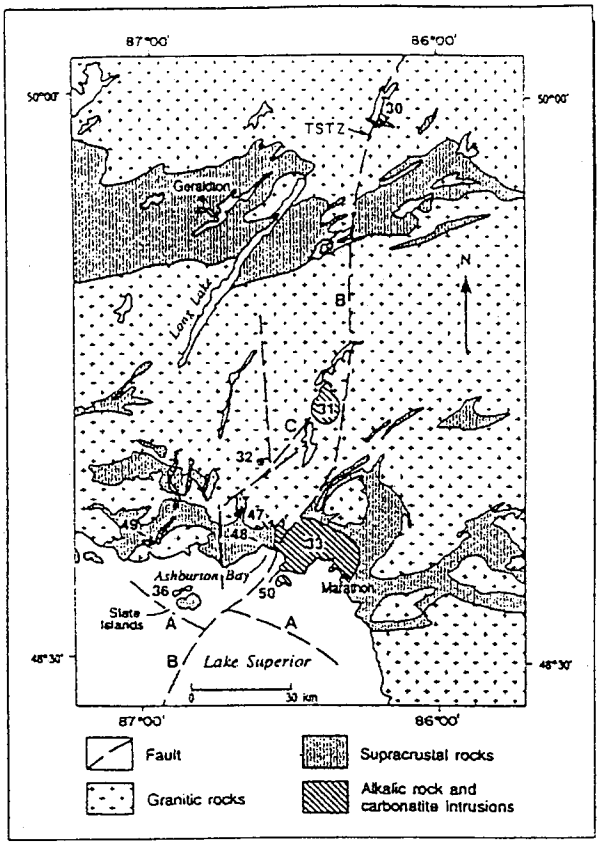

Regional geology (Sage 1991) in the vicinity of the Trans-Superior Tectonic Zone (TSTZ), extension of the Thiel Fault (B)

Key to numbering:
30 - Chipman Lake fenites / carbonatite dykes
31 - Killala Lake alkaline complex
32 - Prairie Lake Carbonatite
33 - Coldwell alkaline complex
47 - Dead Horse Creek diatremes
48 - McKellar Creek diatreme

Generalized geology of the Coldwell alkaline complex after Mitchell and Platt (1994)

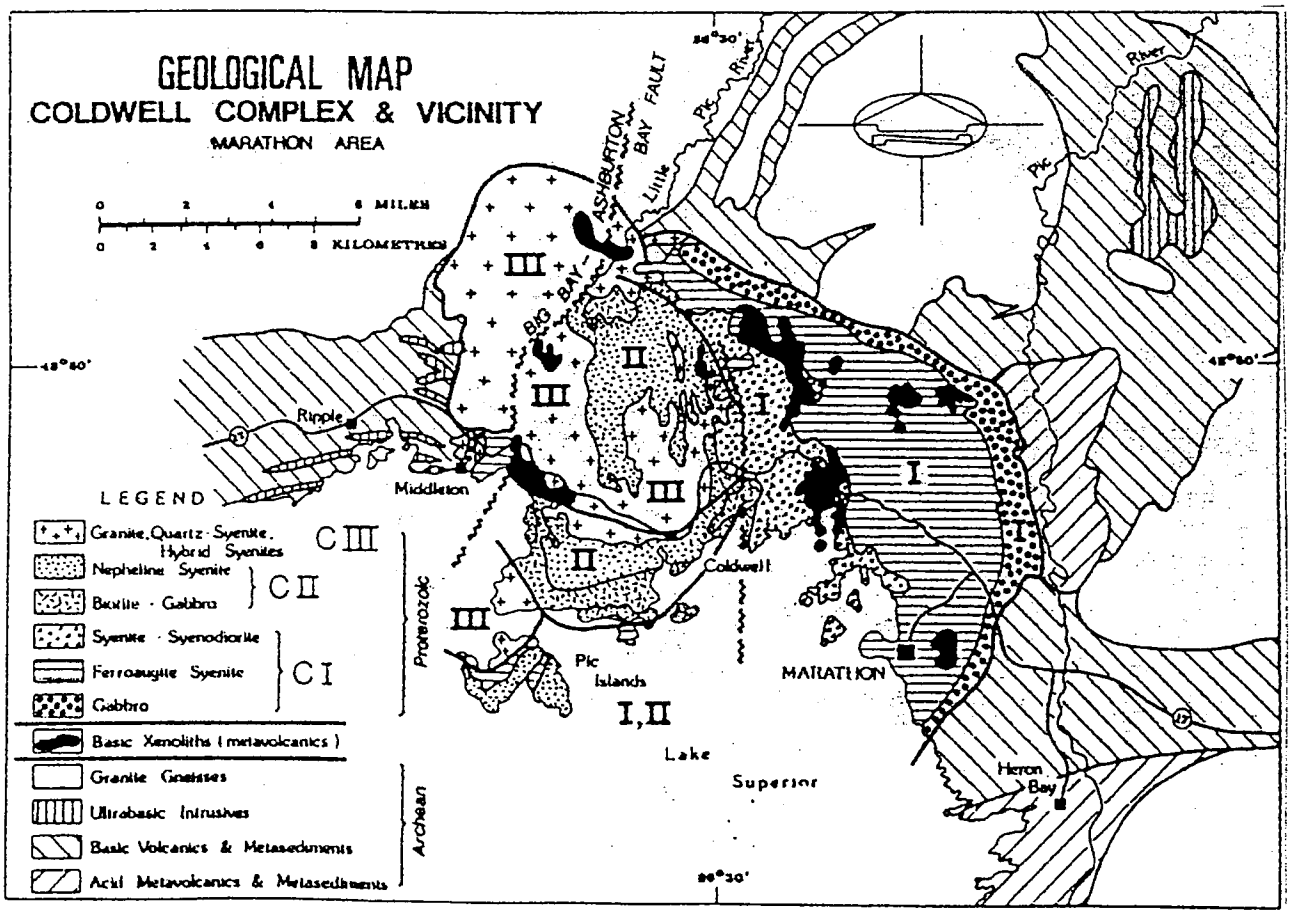

Intrusion (Center)	Lithologic Units	Reference(s)
Eastern Gabbro (1)	layered gabbro cumulates (olivine gabbro, gabbro, troctolite, anorthositic gabbro)	Shaw (1994, 1997); Lum (1973)
Western Gabbro (1)	Massive and layered series gabbro; olivine-bearing	Penczak (1992); Wilkinson (1983)
Two Duck Lake (1)	Gabbronorite, olivine gabbronorite, olivine-bearing gabbro, leucogabbro	Shaw (1994, 1997)
	Hornblende gabbro to monzodiorite; olivine ferrogabbro to ferrodiorite; olivine gabbro to diorite	Dahl *et al.*(1987)
Malpas Lake (1)	Amphibole-bearing olivine gabbro	Shaw (1994, 1997)
Geordie Lake (?)	Troctolite, olivine gabbro	Mulja (1989); MacTavish *et al.* (1987)
Alkaline gabbro (2)	Biotite gabbro	Mitchell and Platt. (1982)
	Biotite- and olivine-gabbro	Walker *et al.* (1993a)

Deposit / Mineralized Zone	Grade / Significant Assays	Ore Mineralogy	Reference(s)
Marathon	37 million tonnes averaging 1.1 g/t Pd, 0.27 g/t Pt, 0.21 g/t Au 1.85 g/t Ag, 0.38% Cu and 0.032% Ni	Chalcopyrite ≥ pyrrhotite >> pentlandite > cubanite ≥ pyrite; sphalerite, hollingworthite, atokite-zvyaginstevite, sperrylite, Bi-kotulskite, michenerite, merenskyite, monceite, stibiopalladinite, paolovite, merteite II, palladoarsenide, unnamed (Pd_5As_2), nickeline, majakite, aregentian gold	Ohnenstetter *et al.* (1991); Watkinson and Ohnenstetter (1992); Good and Crocket (1994a,b)
Geordie Lake	5.2 g/t Pd, 1.71% Cu, 244 ppb Pt, 373 ppb Au, 28.8 g/t Ag; drilling in 2000 yielded 1.164 g/t Pd, 0.054 g/t Pt and 0.070 g/t Au over 5.95 metres	Chalcopyrite, bornite, pyrite, millerite, siegenite, pentlandite, galena, chalcocite, melonite, hessite, unnamed (Ag_3Te_2), altaite, kotulskite, merenskyite, michenerite, sopcheite, Pd-bismuthotelluride, paolovite, Pd-arsenide, guanglinite, Pd-antimonide, sperrylite, electrum, $Pd_{1.6}As_{1.5}Ni$, $AgSb_4$	Mulja (1989); Mulja and Mitchell (1990, 1991)
Middleton		Chalcopyrite, pyrrhotite, pentlandite, sphalerite, pyrite	Penczak (1992)
Skipper Lake	average grade of 1.05 g/t Pd+Pt+Au over 12 m	Chalcopyrite, bornite, pentlandite, cobaltite, galena, chalcocite; telargpalite, polarite, kotulskite, taimyrite, merteite, zvyaginstevite, plumbopalladinite, majakite, tetraferroplatinum	MacTavish (2000)

	MEASURED				INDICATED				INFERRED			
CUT-OFF (g/t Pd)	TONNES	Pd (g/t)	Pt (g/t)	Cu (%)	TONNES	Pd (g/t)	Pt (g/t)	Cu (%)	TONNES	Pd (g/t)	Pt (g/t)	Cu (%)
0.001	24 602 220	0.698	0.182	0.264	46 450 710	0.621	0.168	0.243	51 637 320	0.460	0.130	0.218
0.04	16 963 200	0.912	0.229	0.317	29 387 070	0.658	0.221	0.306	24 245 100	0.749	0.194	0.302
0.8	8 649 000	1.215	0.296	0.357	13 613 805	1.163	0.287	0.347	7 940 340	1.135	0.279	0.386
1.2	3 357 765	1.588	0.391	0.389	4 614 560	1.523	0.378	0.377	2 374 290	1.633	0.378	0.424

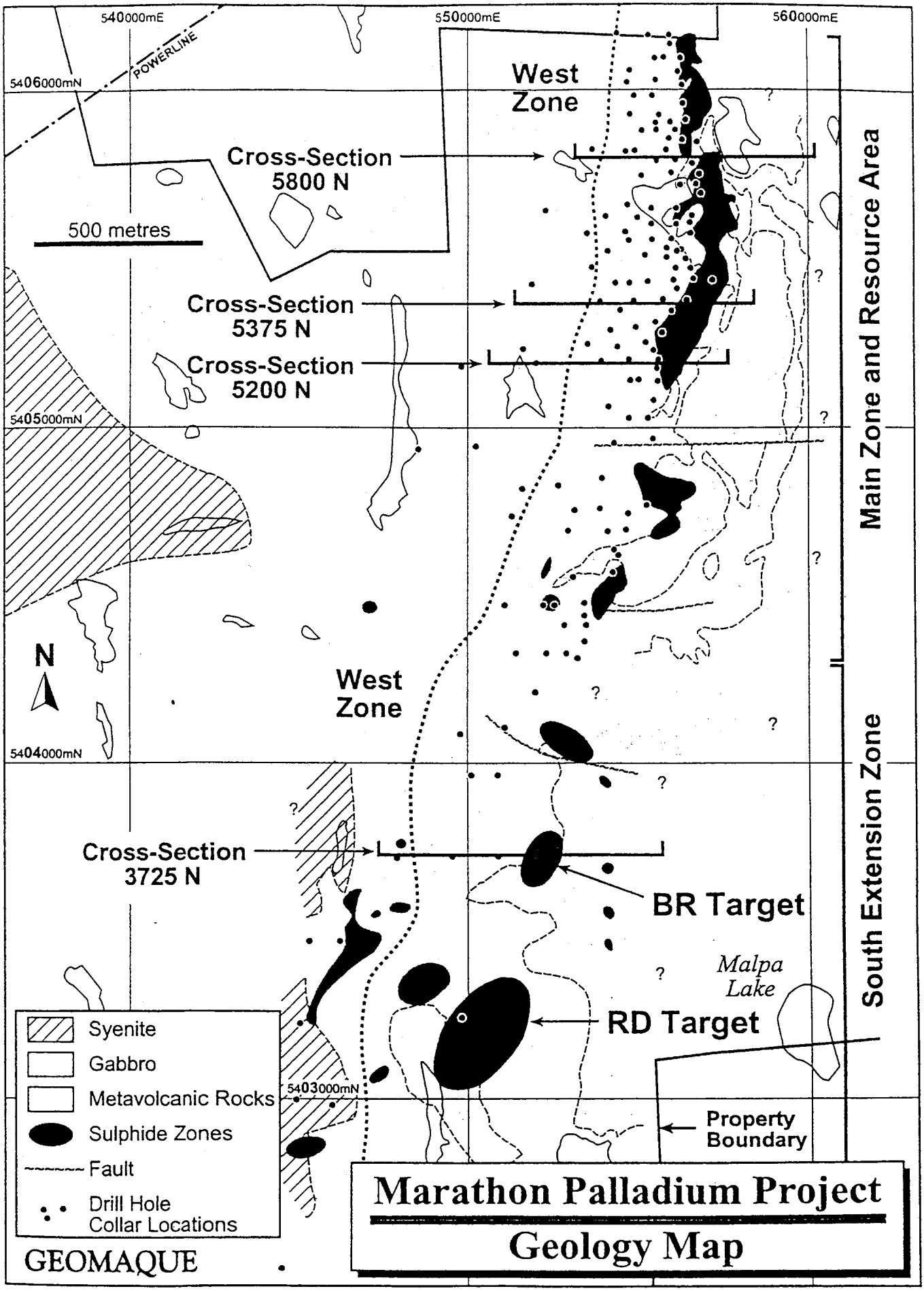
540000mE
550000mE
560000mE
5406000mN
5405000mN
5404000mN
5403000mN
POWERLINE
West Zone
Cross-Section 5800 N
500 metres
Cross-Section 5375 N
Cross-Section 5200 N
Main Zone and Resource Area
N
West Zone
Cross-Section 3725 N
BR Target
Malpa Lake
RD Target
South Extension Zone
Property Boundary
Syenite
Gabbro
Metavolcanic Rocks
Sulphide Zones
Fault
Drill Hole Collar Locations
GEOMAQUE
Marathon Palladium Project
Geology Map

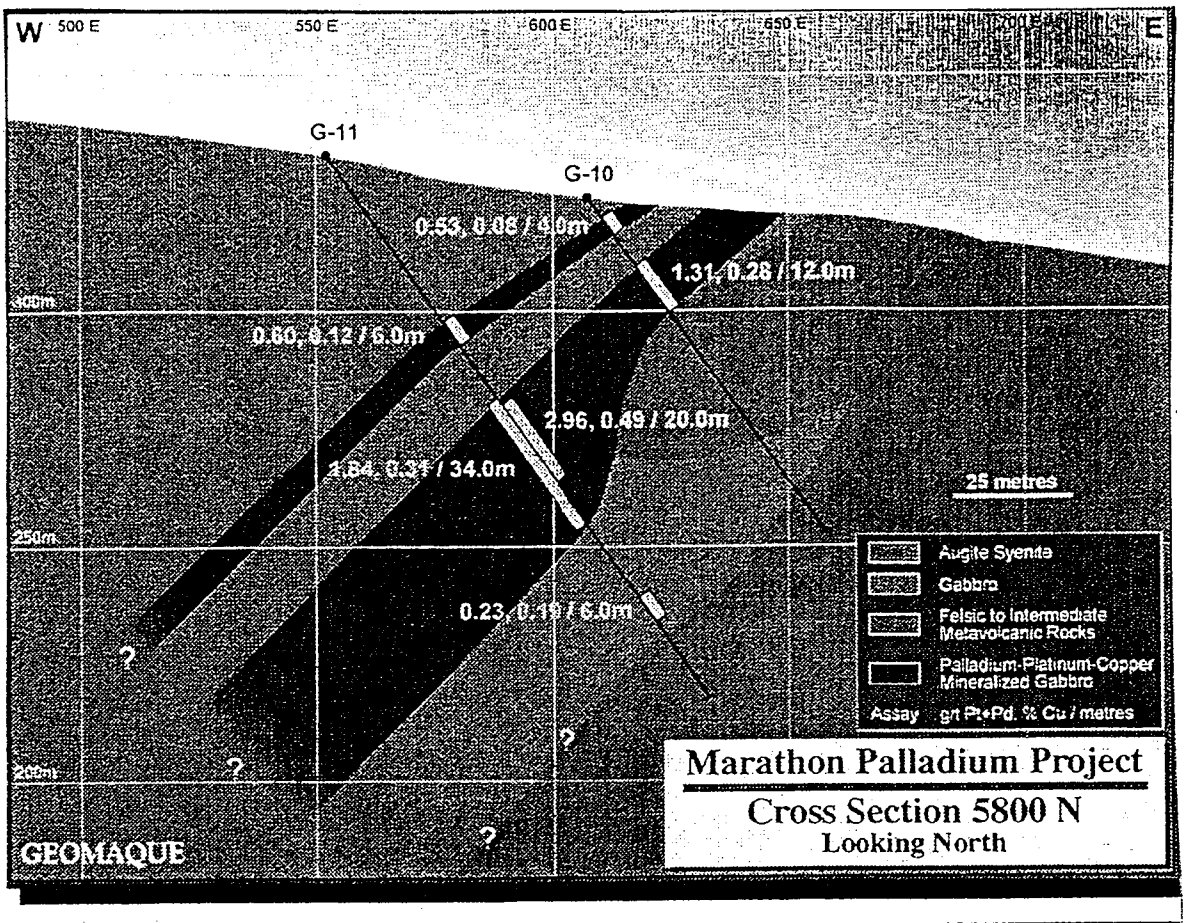
W
500 E
550 E
600 E
650 E
E
G-11
G-10
0.53, 0.08 / 4.0m
1.31, 0.28 / 12.0m
300m
0.60, 0.12 / 6.0m
2.96, 0.49 / 20.0m
1.84, 0.31 / 34.0m
25 metres
250m
0.23, 0.19 / 6.0m
?
?
?
200m
?
Augite Syenite
Gabbro
Felsic to Intermediate Metavolcanic Rocks
Palladium-Platinum-Copper Mineralized Gabbro
Assay g/t Pt+Pd, % Cu / metres
GEOMAQUE
Marathon Palladium Project
Cross Section 5800 N
Looking North

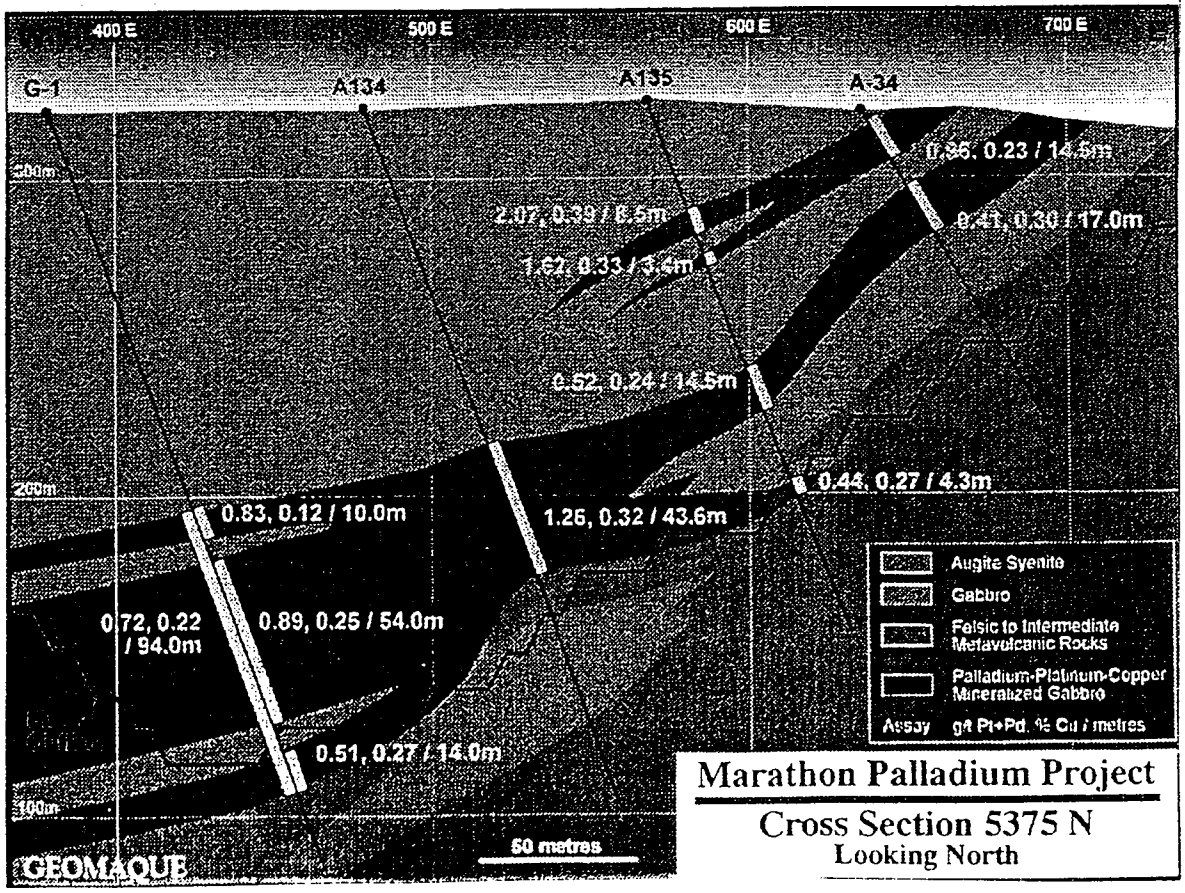
400 E
500 E
600 E
700 E
G-1
A134
A135
A-34
200m
0.36, 0.23 / 14.5m
2.07, 0.39 / 6.5m
0.41, 0.30 / 17.0m
1.62, 0.33 / 3.4m
0.52, 0.24 / 14.5m
0.44, 0.27 / 4.3m
0.83, 0.12 / 10.0m
1.26, 0.32 / 43.6m
0.72, 0.22 / 94.0m
0.89, 0.25 / 54.0m
0.51, 0.27 / 14.0m
100m
50 metres
Augite Syenite
Gabbro
Felsic to Intermediate Metavolcanic Rocks
Palladium-Platinum-Copper Mineralized Gabbro
Assay g/t Pt+Pd, % Cu / metres
GEOMAQUE
Marathon Palladium Project
Cross Section 5375 N
Looking North

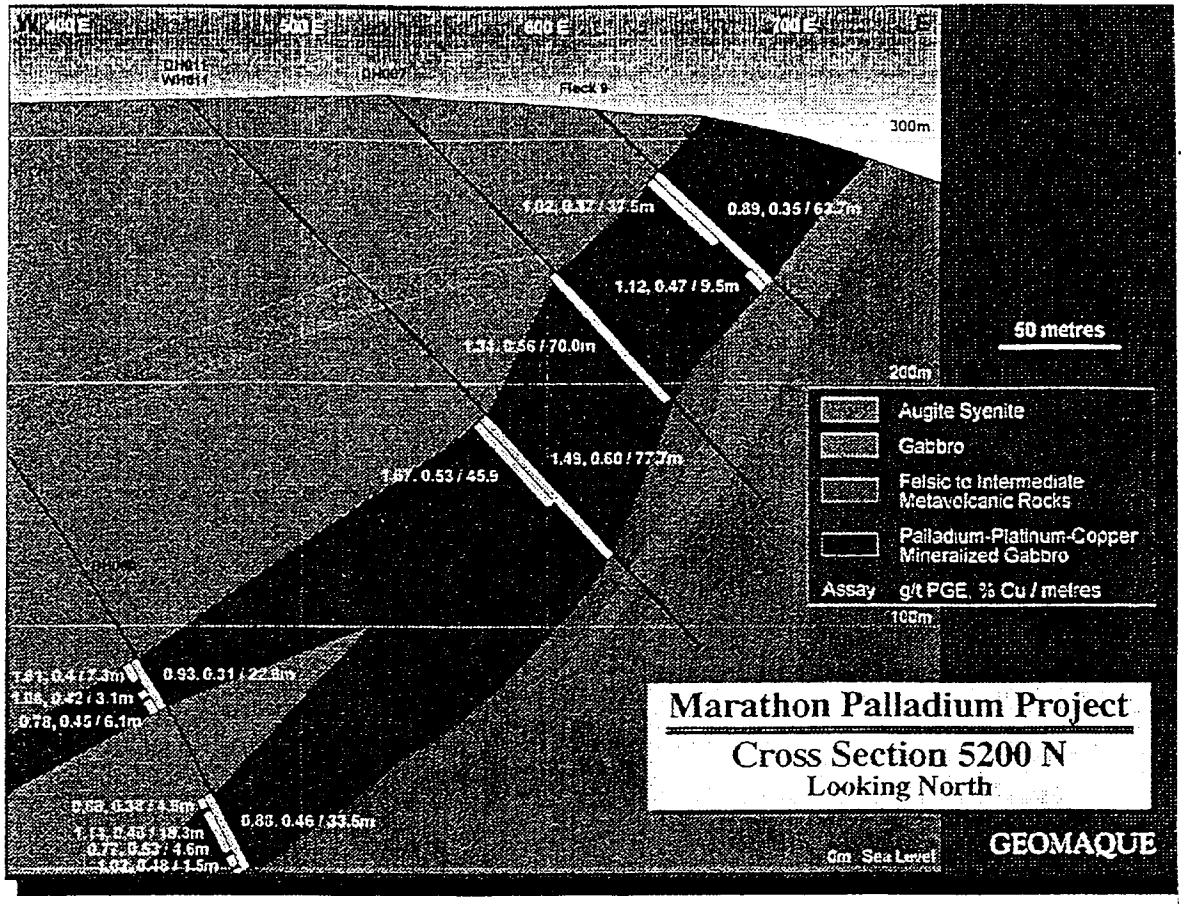
DH01
Wn01
DH07
Fleck 9
300m
1.02, 0.37 / 37.5m
0.89, 0.35 / 62.7m
1.12, 0.47 / 9.5m
1.34, 0.56 / 70.0m
1.49, 0.60 / 77.7m
1.67, 0.53 / 45.9
50 metres
200m
Augite Syenite
Gabbro
Felsic to Intermediate Metavolcanic Rocks
Palladium-Platinum-Copper Mineralized Gabbro
Assay g/t PGE, % Cu / metres
100m
1.91, 0.4 / 7.3m
0.93, 0.31 / 22.8m
1.08, 0.42 / 3.1m
0.78, 0.45 / 6.1m
0.83, 0.46 / 33.5m
1.13, 0.49 / 19.3m
0.72, 0.53 / 4.6m
0m Sea Level
Marathon Palladium Project
Cross Section 5200 N
Looking North
GEOMAQUE

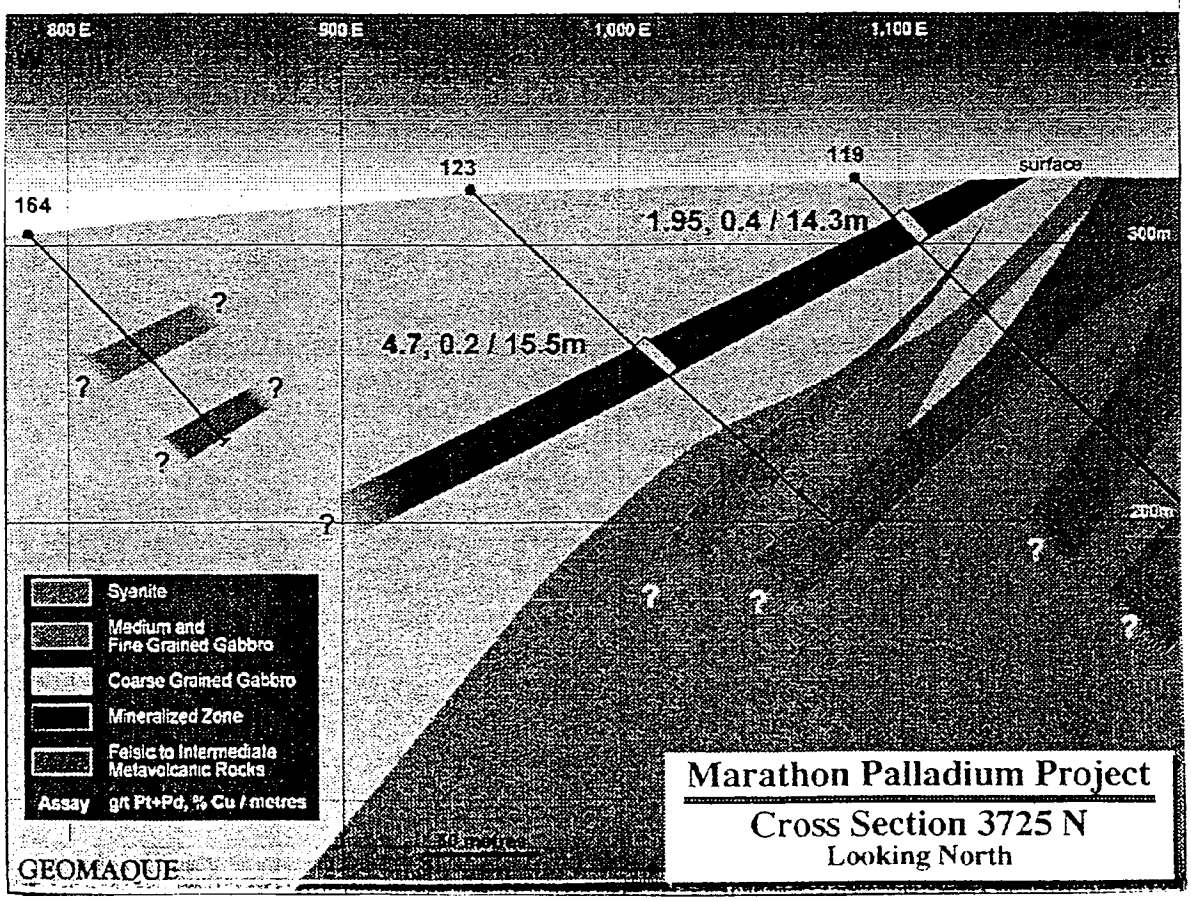
800 E
900 E
1,000 E
1,100 E
164
123
119
surface
1.95, 0.4 / 14.3m
300m
4.7, 0.2 / 15.5m
200m
Syenite
Medium and Fine Grained Gabbro
Coarse Grained Gabbro
Mineralized Zone
Felsic to Intermediate Metavolcanic Rocks
Assay g/t Pt+Pd, % Cu / metres
50 metres
Marathon Palladium Project
Cross Section 3725 N
Looking North
GEOMAQUE

APPENDIX 4

Description of rock and drill core samples

Sample No.	Depeth	Longitude			Latitude			Altitude	Sample Type		Rock Name	Description	Mineral-ization	Weathering	Analysis method								
	m	D	M	S	D	M	S	m							Bulk	PGE	Ar-Ar	Thin	P-Thin	X-ray	EPMA	Nd-Sr Isotope	S-Isotope	NRM
AS001	---	51	8	49.2	28	52	38.7		basic lava	outcrop	basalt	lava, dark gray, fine, massive, native copper included	native copper	---	1		1	1				1		
AS002	---	53	8	51.3	25	12	25.2	703	basic lava	outcrop	basalt	lava, greenish dark gray, fine, massive, rarely quartz in amygdaloidal texture	---	---	1			1						
AS003	---	53	11	10.8	25	22	14.9	590	basic lava	outcrop	basalt	lava, gray, fine, massive	---	---	1		1	1				1		
AS004A	---	53	3	29.2	25	23	59.8	508	basic lava	outcrop	basalt	lava, weak greenish gray, fine, massive	---	---	1			1			1			
AS004B	---	53	3	29.2	25	23	59.8	508	basic lava	outcrop	basalt	lava, greenish gray, coarse grained part of outcrop, malachite/celadonite included, many vesicle	malachite	---	1									
AS005	---	52	48	13.2	25	24	50.8	665	basic lava	outcrop	basalt	lava, greenish gray, fine, partly reddish weathered, malachite/celadonite included	malachite	weathering	1			1						
AS006	---	52	39	49.1	25	21	5.1	605	basic lava	outcrop	basalt	lava, dark gray, fine, massive, rarely greenish celadonite included	---	weak weathering	1		1	1				1		
AS007	---	52	25	0.8	25	23	22.5	902	basic lava	outcrop	basalt	lava, dark gray, fine, massive	---	---	1			1						
AS008	---	52	31	51.2	25	29	24.9	685	basic lava	outcrop	basalt	lava, dark gray, fine, massive	---	---	1			1						
AS009	---	53	20	50.0	25	4	33.9	720	basic lava	outcrop	basalt	lava, brownish-greenish, fine, massive, weekly weathered	---	weak weathering	1			1						
AS010	---	50	29	40.0	24	47	54.9	955	basic intrusion	outcrop	dolerite	dyke, black-dark gray, massive, pyrite included	pyrite	---	1			1				1	1	
AS011	---	50	30	30.6	24	47	9.2	914	basic intrusion	outcrop	dolerite	dyke, black-dark gray, massive, pyrite included	pyrite	---	1			1				1		
AS012	---	50	33	23.4	24	42	31.5	808	sediment	outcrop	shale	black shale of Irati Fm.	---	---										
AS013	---	50	46	25.6	24	39	28.0	829	basic intrusion	outcrop	dolerite	dyke, weak greenish, massive, sulfide invisible	sulfide	---	1			1						
AS014	---	50	51	49.5	24	38	3.6		basic intrusion	outcrop	gabbro	sill, gray, pyrite included mainly in crack, large phenocryst:cpx, pl(2-3cm)	pyrite	---	1			1				1		1
AS015A	---	50	50	0.0	24	30	15.0	987	acidic intrusion	outcrop	dolerite **(Acidic Rock)**	dyke, gray **(Acidic Rock)**	---	---	1			1						
AS015B	---	50	50	0.0	24	30	15.0	987	basic intrusion	outcrop	chilled margin of dyke	dyke, fine, pyrite veinlet included	pyrite	---	1			1						
AS016A	---	50	46	18.1	24	27	9.2	942	basic intrusion	outcrop	dolerite	dyke, gray, fine, sulfide invisible	sulfide	---	1			1						
AS016B	---	50	46	18.1	24	27	9.2	942	basic intrusion	outcrop	dolerite	dyke, gray, coarse, sulfide invisible	sulfide	---	1			1						
AS017	---	50	42	21.5	24	25	4.9	911	basic intrusion	outcrop	dolerite	dyke, dark gray, coarse, rarely pyrite included	pyrite	---	1			1						
AS018	---	49	46	39.5	23	34	7.7	572	basic intrusion	outcrop	dolerite	sill, dark gray, middle grained(phenocryst:2-3cm), pyrite included in matrix	pyrite	---	1			1						
AS019	---	49	45	15.3	23	34	6.2	551	basic intrusion	outcrop	gabbro	sill, black-dark gray, coarse,pyrite rich in matrix	pyrite	---										
AS020	---								others	outcrop	coal ore	Pyrite rich coal ore of Rio Bonito Fm.	pyrite	---								1	1	
AS021	---	50	10	18.5	27	50	50.7	1034	basic lava	outcrop	basalt	dark gray fine-grained basalt, native copper observed (1grain, film-like)	native copper	---	1			1			1			
AS022A	---	50	8	51.0	27	50	56.8	1074	sediment?	outcrop	altered rock	greenish altered rock (mudstone or altered volvanic rock), rarely pyrite included	pyrite	weathering	1					1				
AS022B	---	50	8	51.0	27	50	56.8	1074	others	outcrop	altered rock	white argillized rock, strong py-diss	pyrite	---	1					1				
AS022C	---	50	8	51.0	27	50	56.8	1074	sediment	outcrop	altered rock	weak silicified sand stone, py-diss.	pyrite	---	1									
AS022D	---	50	8	51.0	27	50	56.8	1074	others	outcrop	altered rock	white argillized rock, strong py-diss	pyrite	---	1									
AS023	---	50	12	21.6	27	51	36.3	958	basic intrusion	outcrop	possible basalt?	dark gray fine-grained basalt or intrusion, fine-grainrd py/cp(?) included	pyrite, chalcopyrite?	---	1		1	1				1		
AS024A	---	50	5	38.2	27	56	33.3	1219	basic intrusion	outcrop	possible basalt?	black aphanitic rock, conpact and very homogenious, columner joint(10-30cm) well developed	---	---	1		1	1				1		
AS024B	---	50	5	38.2	27	56	33.3	1219	basic intrusion	outcrop	basalt	dyke, width=50cm, black, glass rich, N40W	---	---	1			1						
AS025	---	50	5	42.0	27	56	30.4	1199	basic lava	outcrop	basalt				1			1						
AS026	---	50	6	26.5	27	46	53.5	993	others	outcrop	kimberlite				1			1						
AS027	---	50	6	21.3	27	46	49.6	975	others	outcrop	kimberlite				1			1						
AS028A	---	50	13	44.9	27	46	41.5	1005	others	outcrop	phonolite				1			1						

Description of rock and drill core samples

Sample No.	Depeth	Longitude			Latitude			Altitude	Sample Type		Rock Name	Description	Mineral-ization	Weathering	Analysis method									
	m	D	M	S	D	M	S	m							Bulk	PGE	Ar-Ar	Thin	P-Thin	X-ray	EPMA	Nd-Sr Isotope	S-Isotope	NRM
AS028B	---	50	13	44.9	27	46	41.5	1005	others	outcrop	phonolite				1									
AS028C	---	50	13	44.9	27	46	41.5	1005	others	outcrop	phonolite									1				
AS029	---	50	16	20.0	27	38	59.6	966	others	outcrop	carbonatite?													
AS030	---	50	13	50.4	27	32	45.4	866	others	outcrop	phonolite													
AS031	---	50	12	23.7	27	39	41.4	894	others	outcrop	kimberlite													
KM101	---	50	24	42.5	25	22	12.6	820	sediment	outcrop	shale	Irati Fm.(?), black shale, pyrite invisible	pyrite	---										
KM102	---	50	37	23.3	25	22	15.8	829	sediment	outcrop	shale	Irati Fm., black shale, pyrite invisible	pyrite	---										
KM103	---	50	48	28.9	25	11	9.7		basic intrusion	outcrop	dolerite	dyke, dark gray, fine massive	---	---	1									
KM104	---	51	12	57.3	25	19	15.1		basic lava	outcrop	basalt	weak greenish gray (celadonite?), very fine, weakly weathered, possible Pitanga type	---	weak weathering	1	1		1						
KM105	---	51	20	58.6	25	21	50.0	1,107	basic lava	outcrop	basalt	weakly greenish gray f.~m.grained basalt, weakly weathered, celadonite/black glass(rare) included	---	weak weathering	1									
KM106	---	51	39	59.6	25	25	13.8	1,107	basic lava	outcrop	basalt	brown-black, fine and very compact, fine radical columnar joint(30cm) develop, secondary pyrite along joint plain.	pyrite	---	1							1		1
KM107	---	52	9	41.8	25	41	35.6	814	basic lava	outcrop	basalt	greenish dark gray-black, amygdaloidal, fine, opal and greenish glass (celadonite?) included	---	---	1									
KM108	---	52	18	33.0	25	17	43.7	852	basic lava	outcrop	basalt	dark gray, compact, fresh	---	---	1									
KM109	---	52	17	19.8	25	8	2.9	677	basic lava	outcrop	basalt	black, very fine and compact, partly green dot included	---	---	1									
KM110	---	52	4	7.7	24	52	19.4	984	basic lava	outcrop	basalt	reddish brown, weathered, amygdaloidal, cal-network	---	weathering										
KM111	---	51	45	53.5	24	48	11.0	977	basic lava	outcrop	basalt	black, massive and compact, fresh	---	---	1			1						
KM112	---	51	49	7.6	24	40	13.5	955	basic lava	outcrop	basalt	similar to KM111, dark gray, fine and fresh, partly black glass included	---	---	1									
KM113	---	51	57	45.9	24	29	23.0	709	basic lava	outcrop	basalt	dark gray, massive/amygdaloidal, zeolite(?) in amygdal, wk weathered	---	weak weathering										
KM114	---	52	13	30.8	24	29	46.2	855	basic lava	outcrop	basalt	pale gray, fine-m. grained, wk weathered, green mineral included	---	weak weathering	1									
KM115	---	52	28	58.5	24	38	35.7		basic lava	outcrop	basalt	black, fine and very compact, partly black glass included	---	---	1									
KM116	---	52	45	35.5	24	36	44.5	531	basic lava	outcrop	basalt	greenish brown-brown, m.weathered, fine	---	weathering	1	1								
KM117	---	52	19	42.5	24	6	10.7	584	basic lava	outcrop	basalt	gray, massive, fine-m.grained, compact, fresh	---	---	1									1
KM118	---	52	6	15.3	24	18	36.8	435	basic lava	outcrop	basalt	dark gray, massive, fine-m.grained, wk weathered(partly greenish)	---	weak weathering	1									
KM119	---	52	10	9.0	24	7	34.6	700	basic lava	outcrop	basalt-andesite	pale gray, fine-m. grained, wk weathered,	---	weak weathering										
KM120	---	52	9	14.8	24	7	6.4	682	basic lava	outcrop	basalt	dark gray (wk greenish) fine-medium grained, wk weathered	---	weak weathering	1	1						1		
KM121	---	51	59	46.8	24	1	8.4	385	basic lava	outcrop	basalt	pale gray(greenish) wk weathered, green dott included	---	weak weathering	1									
KM122	---	51	51	9.3	23	51	41.3	419	basic lava	outcrop	basalt	dark gray, massive and compact, partly black glass included	---	---	1									
KM123	---	51	49	13.9	23	42	59.6	499	basic lava	outcrop	basalt	greenish pale gray, wk weathered	---	weak weathering										
KM124	---	52	1	54.0	23	31	33.7	411	basic lava	outcrop	basalt	brown, wk amygdaloydal, moderate weathered, white clay in amygdal(a little)	---	weathering	1									
KM125	---	51	39	57.7	23	35	58.1	734	basic lava	outcrop	basalt	greenish gray, fine-m. grained	---	---	1									
KM126	---	51	38	34.8	23	46	48.2	590	basic lava	outcrop	basalt	dark gray(wk greenish), compact, fine	---	---	1									1
KM127	---	51	30	13.8	23	59	15.9	622	basic lava	outcrop	basalt	dark gray(part reddish stained) , fine, compact, partly greenish dot included	---	---										
KM128	---	51	19	43.7	23	59	31.1	807	basic lava	outcrop	basalt	similar to KM127	---	---	1									
KM129	---	51	7	18.0	23	41	46.2	792	basic lava	outcrop	basalt-picrite?	black, wk amygdaloidal, wk greenish weathered	---	weak weathering	1			1						
KM130A	---	51	6	30.1	23	39	15.1	686	basic lava	outcrop	basalt	grey (brown net stained), compact, wk weathered	---	weak weathering	1									

Description of rock and drill core samples

Sample No.	Depeth	Longitude			Latitude			Altitude	Sample Type		Rock Name	Description	Mineral-ization	Weathering	Analysis method								
	m	D	M	S	D	M	S	m							Bulk	PGE	Ar-Ar	Thin	P-Thin	X-ray	EPMA	Nd-Sr Isotope	S-Isotope	NRM
KM130B	---	51	6	30.1	23	39	15.1	686	basic intrusion	outcrop	dolerite (dyke/sill)	dark gray-black, coarse grained, fresh	---	---	1			1						
KM131	---	51	7	52.1	23	29	42.4	612	basic lava	outcrop	basalt?	pale gray (wk greenish), compact, medium grain	---	weathering	1									1
KM132	---	51	18	27.2	22	55	58.5	356	basic lava	outcrop	basalt	dark gray (brownish stained), fine, wk weathered, compact	---	weak weathering										
KM133	---	51	15	1.7	22	51	28.0	480	basic lava	outcrop	basalt	pale gray-gray (partly grrenish dot), fine, wk weathered	---	weak weathering	1									
KM134	---	51	11	34.1	22	51	3.7	387	basic lava	outcrop	basalt	greenish dark gray, wk weathered	---	weak weathering	1									
KM135	---	50	56	59.5	22	57	49.1	354	basic lava	outcrop	basalt	greenish dark gray, compact, partly black glass included	---	---	1									
KM136	---	50	48	38.7	22	54	30.8	395	basic lava	outcrop	basalt	greenish dark gray, compact, fine, wk weathered	---	weak weathering	1									
KM137	---	50	44	1.1	23	5	7.1	487	basic lava	outcrop	basalt	black, compact and fresh, partly fine black glass included	---	---	1			1						
KM138	---	50	40	43.2	23	13	51.8	469	basic lava	outcrop	basalt	black, compact and fresh, fine	---	---	1									
KM139	---	51	0	39.9	23	15	38.5	419	basic lava	outcrop	basalt	brownish gray, wk amygdaloydal, wk weathered, white clay(zeolite?) in amygdal.	---	weak weathering	1									
KM140	---	50	42	17.3	23	29	2.8	753	basic lava	outcrop	basalt	dark gray(wk greenish), small green dot included, wk weathered, compact, m. grained	---	weak weathering	1									
KM141	---	50	27	23.8	23	24	45.0	482	basic lava	outcrop	basalt	darlk gray, m.grained, partly green dot included	---	---	1									
KM142	---	50	50	23.2	23	20	19.5	508	basic lava	outcrop	basalt	black-dark gray, fresh and compact, small black glass included	---	---	1							1		
KM143	---	50	2	20.0	23	14	21.0	542	basic lava	outcrop	basalt	dark gray, compact, pyroxene(1mm) →partly clay	---	---	1									
KM144	---	50	15	22.8	23	4	3.9	490	basic lava	outcrop	basalt	black-dark grey, compact and fresh, m.grained	---	---	1			1						
KM145	---	51	20	45.2	23	19	34.0	634	basic lava	outcrop	basalt	reddish-greenish gray, m.weathered, greenish dot included	---	weathering	1									
KM146	---	51	22	5.0	23	39	41.2	799	basic lava	outcrop	basalt	brownish gray(wk greenish), wk weathered, m.grained	---	weak weathering	1									
KM147	---	51	38	11.6	24	3	31.8	455	basic lava	outcrop	basalt	dark gray, fine granined, fresh and compact	---	---	1									
KM148	---	51	40	9.2	24	22	13.7	1,100	basic lava	outcrop	basalt	black, compact, very fine grained	---	---	1									1
KM149	---	51	43	48.6	24	51	45.1	974	basic lava	outcrop	basalt	dark gray-black, fine grained, fresh and compact, partly black glass included	---	---										
KM150	---	51	32	15.9	25	5	19.6	1,141	basic lava	outcrop	basalt	dark gray(wk greenish), compact, fine, mafic mineral→partly clay	---	weak weathering	1									
KM151	---	48	25	55.4	22	47	28.4	639	basic lava	outcrop	basalt	dark gray, medium grained, very weak weathered.	---	weak weathering	1									
KM152	---	48	50	20.1	22	34	29.3	556	basic lava	outcrop	basalt	dark gary, massive, few amygdal, very weak weathered	---	weak weathering	1									
KM153	---	48	53	36.2	22	18	16.2	557	basic lava	outcrop	basalt	dark gray, aphyric, massive, fine-m.grained	---	---	1							1		1
KM154	---	48	59	16.0	21	46	1.0	435	basic lava	outcrop	basalt	ditto	---	---	1									
KM155	---	49	4	43.9	21	36	16.9	386	basic lava	outcrop	basalt	ditto	---	---	1									
KM156	---	49	47	51.0	21	17	26.3	354	basic lava	outcrop	basalt	greenish gray, part amygdaloidal, greenish chalcedony included	---	weathering	1									
KM157	---	50	9	33.9	21	16	37.9	351	basic lava	outcrop	basalt	greenish gray, m.grained, massive, greenish celadonite and opal included	native copper?	weathering	1									
KM158	---	51	19	30.5	20	45	18.5	317	basic lava	outcrop	basalt	greenish gray, weak-m,weathered, greenish dott included	---	weathering	1									
KM159	---	51	22	22.8	20	30	10.1	325	basic lava	outcrop	basalt	reddish gray, m.weathered, partly greenish dott included	---	weathering	1									
KM160	---	51	21	12.9	20	23	51.2	347	basic lava	outcrop	basalt	greenish gray, m.weathered	---	weathering	1									
KM161	---	50	54	13.7	20	18	2.9	328	basic lava	outcrop	basalt	dark gray, massive and compact, fresh, a few amygdal included	---	---	1			1						
KM162	---	50	10	45.9	20	27	48.9	409	basic lava	outcrop	basalt	dark gray, fine grained, glassy, fresh	---	---	1									
KM163	---	50	9	2.6	20	51	13.9	393	basic lava	outcrop	basalt	ditto	---	---	1			1						
KN001	---	51	2	27.0	29	49	16.0	130	basic intrusion	outcrop	dolerite	sill, dark greenish grey, fine grain(glassy), phenocryst: pyroxene+plagioclase, olivine?.	---	---	1	1		1						

Description of rock and drill core samples

Sample No.	Depeth	Longitude			Latitude			Altitude	Sample Type		Rock Name	Description	Mineral-ization	Weathering	Analysis method								
	m	D	M	S	D	M	S	m							Bulk	PGE	Ar-Ar	Thin	P-Thin	X-ray	EPMA	Nd-Sr Isotope	S-Isotope	NRM
KN002	---	51	2	27.0	29	49	16.0	130	basic intrusion	outcrop	gabbro	sill, dark greenish grey and redish dots, coarse grain, picritic, pyroxene+plagioclase+olivine.	---	---	1	1	1	1				1		
KN003	---	51	8	55.7	29	37	53.2	102	basic intrusion	outcrop	basalt	feeder dyke, dark greenish grey, fine grain(glassy), phenocryst: pyroxene+plagioclase.	---	---	1		1	1			1	1		
KN004	---	50	22	2.5	29	14	18.9	100	acidic lava	outcrop	acidic rock (dacite?)	lava, dark grey, grassy, phenocryst: plagioclase+pyroxene, amygdaloidal texture(agate).	---	---										
KN005	---	50	57	17.5	28	32	4.5	932	basic lava	outcrop	basalt	lava, dark greenish grey, fine grain, phenocryst: plagioclase(+pyroxene).	---	---	1		1	1				1		
KN006	---	51	6	23.7	28	21	28.4	923	basic lava	outcrop	basalt	lava, dark greenish grey, fine grain, phenocryst: plagioclase+pyroxene, magnetite rich, native copper.	native copper	---	1			1				1		
KN007	---	51	28	55.0	27	37	6.3	677	acidic lava	outcrop	dacite	lava, pale grey, coarse grain, phenocryst: plagioclase+pyroxene.	---	---										
KN008	---	51	29	12.1	27	37	8.3	677	acidic lava	outcrop	rhyorite	lava, dark grey, grassy, flow band, amygdaloidal texture(agate).	---	---										
KN009	---	51	28	8.0	27	36	22.2	563	basic lava	outcrop	basalt	lava, dark greenish grey, fine grain, phenocryst: plagioclase+pyroxene, magnetite rich.	---	---	1			1				1		
KN010	---	51	20	31.7	27	20	7.3	863	basic lava	outcrop	basalt	lava, dark greenish grey, fine grain, phenocryst: plagioclase+pyroxene, magnetite rich.	---	---	1									
KN011	---	51	24	3.0	27	17	47.1	840	basic lava	outcrop	basalt	lava, greenish grey, fine grain, massive, phenocryst: plagioclase+pyroxene.	---	---	1			1						
KN012	---	51	40	52.2	27	3	29.4	874	basic lava	outcrop	basalt	lava, greenish grey, medium grain, phenocryst: plagioclase+pyroxene, native copper.	native copper	---	1		1	1				1		
KN013	---	51	47	35.2	26	58	56.1	1,135	acidic lava	outcrop	dacite	lava, grey, coarse grain(porphyritic), phenocryst: plagioclase(max 1cm)+pyroxene.	---	---										
KN014	---	51	59	36.8	26	53	18.5	1,054	basic lava	outcrop	basalt	lava, greenish grey, fine grain, massive, phenocryst: plagioclase+pyroxene, magnetite.	---	---	1			1				1		
KN015	---	53	15	29.2	26	45	56.6	593	basic lava	outcrop	basalt	lava, dark greenish grey, fine grain, phenocryst: pyroxene+plagioclase, amygdaloidal texture(zeolite).	---	---										
KN016	---	53	30	38.6	26	34	18.9	753	basic lava	outcrop	basalt	lava, greenish grey, fine grain, massive, phenocryst: plagioclase+pyroxene, magnetite, native copper.	native copper	---	1		1	1				1		
KN017	---	52	49	6.6	26	18	7.6	831	basic lava	outcrop	basalt	lava, grey, medium grain, massive, phenocryst: plagioclase+pyroxene, magnetite.	---	---	1			1						
KN018	---	52	41	25.3	26	14	34.7	818	basic lava	outcrop	basalt	lava, grey, medium grain, heterogeneity, phenocryst: plagioclase, magnetite, interstitial glass-spheriform black glass.	---	---	1			1						
KN019	---	53	1	20.2	26	4	23.2	640	basic lava	outcrop	basalt	lava, grey, fine-medium grain, massive, phenocryst: plagioclase(+pyroxene), magnetite, (weak weathered).	---	weak weathering	1			1				1		
KN020	---	53	17	25.8	25	52	17.1	567	basic lava	outcrop	basalt	lava, dark greenish grey, fine grain, massive, glassy, phenocryst: plagioclase(+pyroxene).	---	---	1		1	1				1		
KN021	---	53	10	59.1	25	55	31.8	606	basic lava	outcrop	basalt	lava, dark greenish grey, fine grain, massive, glassy, phenocryst: plagioclase, spheriform black glass.	---	---	1			1						
KN022A	---	53	19	40.6	25	45	1.9	545	basic lava	outcrop	basalt	lava, greenish grey, fine-medium grain, phenocryst: plagioclase, magnetite rich.	---	---	1			1				1		
KN022B	---	53	19	40.6	25	45	1.9	545	basic lava	outcrop	basalt	glass rich part, coase grain, phenocryst: plagioclase, native copper	native copper	---	1			1						
KN022C	---	53	19	40.6	25	45	1.9	545	basic lava	outcrop	gabbro	gabbroic part.	---	---							1			
KN023A	---	53	32	54.9	25	46	48.2	463	basic lava	outcrop	basalt	lava, grey, fine grain, glassy, phenocryst: plagioclase, magnetite, native copper.	native copper	---	1			1						
KN023B	---	53	32	54.9	25	46	48.2	463	basic lava	outcrop	gabbroic dolerite	glass rich and coarse grain part, phenocryst: plagioclase+pyroxene, black spheriform glass, native copper.	native copper	---	1			1						
KN023C	---	53	32	54.9	25	46	48.2	463	basic lava	outcrop	gabbroic dolerite	glass rich and coarse grain part.	---	---				1						
KN024A	---	53	48	40.2	25	40	54.2	374	basic lava	outcrop	basalt	lava, grey, fine grain, glassy, phenocryst: plagioclase, magnetite.	---	---	1		1	1				1		
KN024B	---	53	48	40.2	25	40	54.2	374	basic lava	outcrop	gabbroic dolerite	glass rich and coarse grain part, phenocryst: plagioclase+pyroxene, black spheriform glass.	---	---	1			1						
KN025A	---	53	48	18.6	25	38	19.2	314	basic lava	outcrop	basalt	lava, reddish grey, fine-medium grain, massive, glassy, phenocryst: plagioclase, amygdaloidal texture, weak weathered(celadonite).	---	weak weathering	1			1						
KN025B	---	53	48	18.6	25	38	19.2	314	basic lava	outcrop	basalt	lava, greenish grey, coarse grain, glass rich, amygdaloidal texture (zeolite, quartz, calcite).	---	---	1			1						
KN026	---	53	34	0.4	25	36	19.3	407	basic lava	outcrop	basalt	lava, greenish grey, fine grain, massive, phenocryst: plagioclase+pyroxene.	---	---	1			1						
KN027	---	54	12	6.5	25	20	16.6	385	basic lava	outcrop	basalt	lava, greenish grey, fine grain, massive, glassy, phenocryst: plagioclase, magnetite.	---	---	1		1	1				1		
KN028	---	53	51	51.6	25	0	58.1	544	basic lava	outcrop	basalt	lava, reddish grey, fine grain, phenocryst: plagioclase, weathered.	---	weathering	1			1						
KN029	---	53	42	4.5	24	43	44.9	516	basic lava	outcrop	basalt	lava, reddish grey, fine grain, massive, amygdaloidal texture(ϕ : Max 1cm), weathered.	---	weathering	1			1						
KN030	---	53	46	26.2	24	45	5.6	468	basic lava	outcrop	basalt	lava, reddish-greenish grey, fine-medium grain, massive, phenocryst: plagioclase, weak weatherd(hematite, celadonite).	---	weak weathering	1			1						

Description of rock and drill core samples

Sample No.	Depeth	Longitude			Latitude			Altitude	Sample Type		Rock Name	Description	Mineral-ization	Weathering	Analysis method								
	m	D	M	S	D	M	S	m							Bulk	PGE	Ar-Ar	Thin	P-Thin	X-ray	EPMA	Nd-Sr Isotope	S-Isotope	NRM
KN031	---	54	5	32.2	24	33	31.6	418	basic lava	outcrop	basalt	lava, grey, fine grain, massive, native copper along joint.	native copper	---	1		1	1				1		
KN032	---	54	14	29.9	24	27	21.9	278	basic lava	outcrop	basalt	lava, greenish grey, fine grain, phenocryst: plagioclase, weak weathered.	---	weak weathering	1			1				1		
KN033	---	54	1	40.1	24	47	16.6	348	basic lava	outcrop	basalt	lava, greenish grey, fine grain, massive, phenocryst: plagioclase, magnetite, native copper, weak weathered(hematite, celadonite).	native copper	weak weathering	1			1			1			
KN034A	---	50	51	52.3	25	12	21.6	922	basic intrusion	outcrop	basalt	sill, grey, fine grain, massive, phenocryst: plagioclase+pyroxene.	---	---	1			1						
KN034B	---	50	51	52.3	25	12	21.6	922	basic intrusion	outcrop	gabbro	sill, dark grey, coarse grain, phenocryst: pyroxene+plagioclase.	---	---	1			1						
KN035A	---	50	40	32.4	25	26	23.1	995	basic intrusion	outcrop	gabbro	sill, grey, coarse grain, phenocryst: pyroxene+plagioclase, magnetite, pyrite dissemination.	pyrite	weathering	1									1
KN035B	---	50	40	32.4	25	26	23.1	995	basic intrusion	outcrop	gabbro	sill, grey, coarse grain, phenocryst: pyroxene+plagioclase, magnetite, pyrite dissemination(abundant part of pyrite).	pyrite	---					1		1			
KN035C	---	50	40	32.4	25	26	23.1	995	others	outcrop	black clay	black clay and zeolite along joint.	---	---						1				
KN036A	---	50	37	28.8	24	19	23.7	739	basic intrusion	outcrop	dolerite	dyke, grey, coarse grain, phenocryst: plagioclase+pyroxene, pyrite dissemination.	pyrite	---	1									
KN036B	---	50	37	28.8	24	19	23.7	739	basic intrusion	outcrop	dolerite	dyke, grey, coarse grain, phenocryst: plagioclase+pyroxene, pyrite dissemination(abundant part of pyrite).	pyrite	---	1				1					
KN037	---	50	26	29.5	24	1	12.5	905	basic intrusion	outcrop	dolerite	dyke, grey-greenish grey, phenocryst: pyroxene+plagioclase.	---	---	1			1						
KN038	---	50	12	30.7	23	54	31.2	877	basic intrusion	outcrop	dolerite	sill, greenish grey, medium-coarse grain, massive, phenocryst: pyroxene+plagioclase, pyrite dissemination.	pyrite	---	1				1					
KN039A	---	49	51	18.3	23	39	27.4	812	basic intrusion	outcrop	dolerite	sill, grey-greenish grey, medium grain, massive, phenocryst: pyroxene+plagioclase, pyrite.	pyrite	---	1			1						
KN039B	---	49	51	18.3	23	39	27.4	812	basic intrusion	outcrop	gabbroic dolerite	sill, grey-greenish grey, coarse grain, phenocryst: pyroxene+plagioclase, pyrite.	pyrite	---	1			1						
KN040A	---	49	44	26.8	24	14	22.9	991	basic intrusion	outcrop	dolerite	sill, grey-greenish grey, medium grain, massive, phenocryst: pyroxene+plagioclase, pyrite dissemination.	pyrite	---	1			1				1		
KN040B	---	49	44	26.8	24	14	22.9	991	basic intrusion	outcrop	dolerite	sill, grey-greenish grey, medium grain, massive, phenocryst: pyroxene+plagioclase, pyrite dissemination(abundant part of pyrite).	pyrite	---	1				1			1	1	
KN040C	---	49	44	26.8	24	14	22.9	991	basic intrusion	outcrop	gabbro	sill, grey-greenish grey, coarse grain, phenocryst: pyroxene+plagioclase.	---	---	1			1						
KN041	---	54	45	24.8	29	19	34.1	338		outcrop	dacite	lava, ligh grey, massive, fine grain, phenocryst: plagioclase, weathered.	---	weathering										
KN042	---	54	49	27.1	29	15	1.5	450		outcrop	dacite	lava, ligh grey, massive, fine grain, phenocryst: plagioclase.	---	---	1			1						
KN043	---	55	6	31.0	29	35	28.6	170		outcrop	dacite **(Acidic Rock)**	lava, ligh grey, massive, fine grain, phenocryst: plagioclase, weak weathered.	---	weak weathering	1			1						
KN044	---	55	54	20.9	29	50	25.7	136		outcrop	dacite?	lava, grey, massive, fine grain, phenocryst: plagioclase, weathered.	---	weathering	1			1						
KN045	---	55	15	51.4	29	0	45.0	318		outcrop	basalt?	lava, dark greenish grey, fine-medium grain, phenocryst: plagioclase(+pyroxene?), weakly weathered.	---	weak weathering	1			1						
KN046A	---	56	3	4.8	29	54	46.2	130		outcrop	dacite?	lava, grey, medium grain, massive, phenocryst: plagioclase(+pyroxene?), weathered.	---	weathering	1			1						
KN046B	---	56	3	4.8	29	54	46.2	130		outcrop	dacite?	lava, grey, coarse grain, porphyritic, phenocryst: plagioclase(+pyroxene?), muscovite and zeolite, weathered.	---	weathering										
KN047	---	55	43	50.6	28	48	41.0	124		outcrop	basalt	lava, dark grey, medium grain, massive, phenocryst: plagioclase+pyroxene, native copper in.	native copper	---	1				1		1			
KN048A	---	55	8	24.4	28	28	51.7	173		outcrop	basalt	lava, greenish grey, medium grain, massive, phenocryst: plagioclase+pyroxene, weathered.	---	weathering	1			1						
KN048B	---	55	8	24.4	28	28	51.7	173		outcrop	gabbro	lava, greenish grey, coarse grain, porphyritic, phenocryst: plagioclase+pyroxene, weathered.	---	weathering	1			1						
KN049	---	55	22	34.0	28	27	19.0	135		outcrop	basalt	lava, grey, fine grain, massive, phenocryst: plagioclase+pyroxene, native copper in.	native copper	---	1				1					
KN050	---	54	26	37.4	28	23	47.9	268		outcrop	basalt	lava or Sill?, dark grey, medium-coarse grain, massive, phenocryst: plagioclase+pyroxene, sulfide dissemination.	sulfide	---	1		1		1			1		
KN051	---	54	16	11.5	28	20	15.7	264		outcrop	basalt	lava or sill?, dark grey, medium-coarse grain, massive, phenocryst: plagioclase+pyroxene, sulfide dissemination, weakly weathered.	sulfide	weak weathering	1				1					
KN052	---	54	21	52.8	27	46	39.4	235		outcrop	basalt	lava, grey, fine-medium grain, massive, phenocryst: plagioclase+pyroxene, native copper in.	native copper	---	1		1		1			1		
KN053	---	55	12	57.3	29	2	23.3	335		outcrop	dacite?	lava, grey-reddish grey, fine grain, massive, weathered.	---	weathering				1						
KN101	---	50	3	48.4	24	46	25.2	1,020	sediment	outcrop	tuff breccia	Castro Group, pale brown tuff breccia	---	---										
KN102	---	50	9	7.2	24	46	1.3		sediment	outcrop	sandstone	Furnas Fm., white, flat bedding	---	weathering										
KN103	---	50	26	43.2	24	30	2.9		sediment	outcrop	siltstone	Ponta Grossa Fm., pale grey, loose, flat bedding, lamina	---	weathering										

Description of rock and drill core samples

Sample No.	Depeth	Longitude			Latitude			Altitude	Sample Type		Rock Name	Description	Mineral-ization	Weathering	Analysis method								
	m	D	M	S	D	M	S	m							Bulk	PGE	Ar-Ar	Thin	P-Thin	X-ray	EPMA	Nd-Sr Isotope	S-Isotope	NRM
KN104	---	50	32	18.2	24	28	1.9	838	basic intrusion	outcrop	dolerite	dyke, dark greenish grey, medium grain	---	---	1	1			5					
KN105A	---	50	35	10.5	24	25	26.0	726	basic intrusion	outcrop	dolerite	dyke, dark greenish grey, coarse grain	---	weathering	1			1						1
KN106	---	50	46	17.8	24	27	10.6	934	basic intrusion	outcrop	dolerite	dyke. dark greenish grey. coarse grain.	---	weathering										1
KN107	---	50	59	48.0	24	24	50.2		sediment	outcrop	siltstone	Palermo Fm., pale grey, flat bedding.	---	weathering										
KN108	---	51	25	42.3	24	1	52.0	721	basic intrusion	outcrop	dolerite	dyke. dark greenish grey. fine grain.	---	weathering	1									
KN109	---	51	10	1.8	23	56	11.2		sediment	outcrop	sandstone	Rio do Rasto Fm., pale grey. medium grain.	---	weathering										
KN110A	---	51	5	6.8	23	59	5.2		basic intrusion	outcrop	gabbro	dyke/sill. dark greenish grey. medium grain	---	weathering	1	1								1
KN110B	---	51	5	6.8	23	59	5.2		sediment	outcrop	sandstone / siltstone	white. hornfelsed around dyke/sill weakly.	---	weathering										
KN111	---	50	47	38.8	24	17	57.5		sediment	outcrop	sandstone / shale	Itarare Fm.. pale grey - grey.	---	weathering										
KN112	---	50	43	0.9	24	30	21.2	869	basic intrusion	outcrop	dolerite	dyke. dark greenish grey. fine grain.	---	weathering	1	1								1
KN113	---	50	42	21.0	24	25	6.4		basic intrusion	outcrop	dolerite	dyke. dark greenish grey. medium grain.	---	weathering										
KN114	---	50	37	30.7	24	19	25.9		basic intrusion	outcrop	dolerite	dyke. dark greenish grey. medium grain.	---	weathering										
KN115	---	50	33	20.6	23	56	31.5		basic intrusion	outcrop	dolerite	dyke. dark greenish grey. medium grain.	---	weathering	1									
KN116	---	50	37	25.0	23	50	25.2	1,118	sediment	outcrop	sandstone	Rio do Rasto Fm.. white.	---	weathering										
KN117	---	50	36	51.3	23	52	5.7	907	basic intrusion	outcrop	gabbro	sill. dark greenish grey. coarse grain. olivine(?)	---	weathering	1			1						1
KN118	---	50	0	32.9	23	46	49.2	595	basic intrusion	outcrop	dolerite	dyke. dark greenish grey. medium grain.	---	weathering	1									
KN119	---	49	38	54.4	24	4	27.0		basic intrusion	outcrop	gabbro	sill, dark greenish grey, coarse grain, sulfide disteminated (chalcopyrite/pyrite).	chalcopyrite/ pyrite	weathering	1				1					1
KN120	---	49	39	14.7	24	8	11.8	758	sediment	outcrop	sandstone	Furnas Fm., white, flat bedding	---	weathering										
KN121	---	49	41	9.8	24	12	51.3		basic intrusion	outcrop	dolerite	(small quarry). dyke. dark greenish grey. medium grain.	---	---	1			1						1
KN122	---	49	49	31.9	24	22	12.1		sediment	outcrop	sandstone	Furnas Fm., white, flat bedding	---	weathering										
KN123	---	50	52	4.7	24	18	29.9	886	basic intrusion	outcrop	dolerite	dyke. dark greenish grey. coarse grain.	---	weathering	1			1						
KN124	---	50	55	39.8	24	13	35.5	835	basic intrusion	outcrop	dolerite	dyke, dark greenish grey, medium grain	---	weathering	1									
KN125	---	50	58	28.7	24	9	20.1	845	basic intrusion	outcrop	dolerite	dyke, dark greenish grey, fine grain	---	weathering	1									
KN126A	---	51	3	27.8	24	4	22.8	1,021	basic intrusion	outcrop	dolerite	dyke, dark greenish grey, medium grain	---	weathering	1									1
KN126B	---	51	3	27.8	24	4	22.8	1,021	sediment	outcrop	siltstone	Rio do Rasto Fm.,	---	weathering										
KN127	---	50	20	50.4	24	5	57.1		sediment	outcrop	sandstone	Itarare Fm.. pale brownish grey.	---	weathering										
KN128	---	50	0	14.1	24	29	55.6	1,125	basic intrusion	outcrop	dolerite	dyke, dark greenish grey, coarse grain, chalcopyrite/pyrite disseminated	chalcopyrite/ pyrite	weathering	1				1					
KN129A	---	49	57	48.1	24	32	26.2	1,018	sediment	outcrop	tuff	Castro Group, reddish brown	---	weathering										
KN129B	---	49	57	48.1	24	32	26.2	1,018	others	outcrop	granodiorite	Cunhaporanga pluton (upper Proterozoic), Qtz. Hor. Pyx. Fl	---	weathering										
KN130	---	49	51	28.9	24	53	30.4		others	outcrop	granophyre	Cunhaporanga pluton (Arkostic sandstone?)	---	weathering										
KN131	---	49	49	40.3	24	56	1.1	999	others	outcrop	schist	pelitic	---	weathering										
KN132	---	49	49	19.7	24	56	51.1		others	outcrop	schist	limestone quarry, alternation between pelitic schist and limestone	---	weathering										
KN133	---	49	56	46.2	25	7	55.0	946	others	outcrop	metabasite	Acungui group (upper Proterozoic),	---	---										
KN134	---	49	48	31.8	25	2	11.8	802	basic intrusion	outcrop	dolerite	dyke, dark greenish grey, medium grain	---	weathering	1									
KN135	---	49	46	31.7	24	59	56.0	806	others	outcrop	schist	pelitic	---	weathering										

Description of rock and drill core samples

Sample No.	Depeth	Longitude			Latitude			Altitude	Sample Type		Rock Name	Description	Mineral-ization	Weathering	Analysis method									
	m	D	M	S	D	M	S	m							Bulk	PGE	Ar-Ar	Thin	P-Thin	X-ray	EPMA	Nd-Sr Isotope	S-Isotope	NRM
KN136	---	49	45	38.9	25	0	36.5		others	outcrop	diorite	phenocryst: Hb. Pyx. K-Fl. Qtz., alteration min.:Epi	---	weathering										
KN137	---	49	42	49.5	25	2	24.2	596	others	outcrop	schist	mica	---	weathering										
KN138	---	49	37	34.7	25	11	21.8	719	others	outcrop	granite	megacrystal of feldspar (several mm to several cm), Hb, Pyx.	---	---										
KN139	---	49	35	59.3	25	14	6.5	614	others	outcrop	schist	pale green mica schist/white quartz schist	---	---										
KN140	---	49	33	41.0	25	16	29.4	740	others	outcrop	schist	mica	---	---										
KN141	---	48	24	26.7	23	31	41.7	787	basic intrusion	outcrop	gabbro	sill, dark greenish grey, medium grain	---	---	1									
KN142	---	48	23	15.2	23	28	35.6	706	basic intrusion	outcrop	gabbro	sill, dark greenish grey, medium grain, pyrite disseminated	pyrite	weathering	1				1					
KN143	---	48	17	22.8	23	29	30.9	755	basic intrusion	outcrop	dolerite	dyke, dark greenish grey, coarse grain	---	weak weathering	1									
KN144	---	48	56	25.1	23	7	57.1	624	basic lava	outcrop	basalt	lava, dark greenish grey, fine grain	---	weathering	1									
KN145	---	49	3	47.1	23	19	14.4	659	basic lava	outcrop	basalt	lava, dark greenish grey, fine grain	---	weathering	1									
KN146	---	49	14	18.3	23	31	18.0	619	basic intrusion	outcrop	gabbro	sill, dark greenish grey, coarse grain, pyrite disseminated	pyrite	weathering	1				1					1
KN147	---	49	19	53.9	23	28	25.3		sediment	outcrop	siltstone	Rio do Rasto Fm. White-pale green- greyish pink, ripple mark, bedding flat.	---	weathering										
KN148	---	49	20	49.0	23	28	3.5	679	basic intrusion	outcrop	dolerite	dyke, dark greenish grey, fine grain dyke in coarse grain dyke	---	weathering	1									1
KN149	---	49	21	13.1	23	27	42.5	673	basic intrusion	outcrop	dolerite	dyke, dark greenish grey,	---	weathering										
KN150	---	49	31	27.7	23	23	29.3	562	basic intrusion	outcrop	gabbro	sill, dark greenish grey, medium grain, pyrite disseminated	pyrite	weathering	1	1			1					1
KN151	---	49	29	9.6	23	22	15.1	558	basic intrusion	outcrop	dolerite	dyke, light greenish grey, porphyritic	---	weathering	1			1						
KN152	---	49	14	15.8	23	12	42.0	570	basic lava	outcrop	basalt **(Acidic Rock)**	lava, pale brownish grey, fine grain. **(Acidic Rock)**	---	weathering	1									
KN153	---	49	20	16.7	23	14	3.7	585	basic lava	outcrop	basalt	lava, greenish grey, medium grain,	---	weathering	1									
KN154	---	49	27	5.2	23	16	7.6	703	basic lava	outcrop	basalt	lava, dark greenish grey, fine grain	---	weathering	1									
KN155	---	49	28	9.7	23	18	42.0	828	sediment	outcrop	sandstone	Botucau Fm., red, fine grain,	---	weathering										
KN156	---	49	58	38.0	22	51	58.3	469	basic lava	outcrop	basalt	lava, greenish grey, fine grain, celadonite in cavities and cracks,	---	weathering	1									
KN157	---	50	29	28.2	22	36	17.7	473	basic lava	outcrop	basalt	lava, pale greenish grey, fine grain	---	weathering	1									1
KN158	---	50	34	4.8	22	30	9.7	441	basic lava	outcrop	basalt	lava, grey, fine grain,	---	weathering	1									
KN159	---	51	3	28.2	23	3	33.7	433	basic lava	outcrop	basalt	lava, greenish grey, medium grain, celadonite in cavities and cracks,	---	weathering	1									1
KN160	---	51	26	47.4	23	50	5.4	689	basic intrusion	outcrop	dolerite	dyke in basalt lava, dark greenish grey, medium grain	---	weathering	1									1
KN161	---	50	51	55.1	24	10	23.6	723	basic intrusion	outcrop	dolerite	dyke, dark greenish grey, medium grain	---	weathering	1									
KN162	---	50	48	9.5	24	11	2.2	891	basic intrusion	outcrop	gabbro	sill, dark greenish grey, medium grain, pyrite disseminated	sulfide	weathering	1				1					
KN163	---	50	46	34.1	24	6	33.8	674	basic intrusion	outcrop	dolerite	dyke, dark greenish grey	---	weathering	1									1
KN164	---	50	43	51.1	24	3	35.1	793	basic intrusion	outcrop	gabbro	dyke, dark greenish grey, pyrite disseminated	sulfide	weathering	1				1					
KN165	---	50	42	4.3	23	58	4.3	778	basic intrusion	outcrop	dolerite	dyke, dark greenish grey, coarse grain	---	weathering	1									
KN166	---	50	40	20.3	23	56	2.1	742	basic intrusion	outcrop	dolerite	dyke, dark greenish grey, coarse grain	---	weathering	1									
KN167B	---	50	36	54.0	23	55	12.0	696	basic intrusion	outcrop	gabbro	dyke/sill, dark greenish grey, coarse grain (pegmatic), sulfide disseminated	sulfide	weathering	1				1					1
KN168	---	50	38	12.2	23	47	38.7	1,174	acidic lava	outcrop	dacite	relic of lava in the Paleozoic sequence, phenocryst of Qtz	---	weathering	1				1					
KN169	---	50	49	17.5	24	27	47.2	1,016	basic intrusion	outcrop	gabbro	sill, dark greenish grey, sulfide disseminated	sulfide	weathering	1				1					
KN170	---	50	51	35.3	24	25	11.4	832	basic intrusion	outcrop	gabbro	sill, dark greenish grey, medium grain	---	weathering	1									1

Description of rock and drill core samples

Sample No.	Depeth	Longitude			Latitude			Altitude	Sample Type		Rock Name	Description	Mineral-ization	Weathering	Analysis method								
	m	D	M	S	D	M	S	m							Bulk	PGE	Ar-Ar	Thin	P-Thin	X-ray	EPMA	Nd-Sr Isotope	S-Isotope	NRM
KN171	---	50	55	11.8	24	24	29.7	894	basic intrusion	outcrop	gabbro	dark greenish grey, sulfide disseminated (?)	sulfide	weathering	1				1					
KN172	---	50	49	58.9	24	32	3.2	992	basic intrusion	outcrop	gabbro	sill, dark greenish grey, fine grain	---	weathering	1									
KN173	---	50	52	3.9	25	0	55.3	791	basic intrusion	outcrop	dolerite	dyke, dark greenish grey, fine grain	---	weathering	1	1								
KN174A	---	50	56	29.1	25	2	4.1	738	basic intrusion	outcrop	gabbro	sill, dark greenish grey, fine grain	---	weathering	1									1
KN174B	---	50	56	29.1	25	2	4.1	738	sediment	outcrop	mudstone	laminated, weak hornfelsed	---	---										
KN175	---	50	42	26.3	25	22	34.3	882	basic intrusion	outcrop	gabbro	sill, dark greenish grey, fine grain	---	weathering	1									
KN176	---	50	30	28.7	25	37	33.3	957	basic intrusion	outcrop	gabbro	sill, dark greenish grey, fine grain	---	weathering	1									
TM101	---	50	43	14.6	16	57	56.6	666	basic intrusion	outcrop	gabbro?	dyke, grey, coarse grain(glassy), phenocryst: pyroxene(max 1cm)+plagioclase,olivine?	---	---	1			1						
TM102	---	51	30	29.5	16	43	57.5	683	basic intrusion	outcrop	gabbro?	sill, dark greenish grey, coarse grain(glassy), phenocryst: pyroxene+plagioclase(max 5mm)	---	---	1									
TM103	---	51	37	46.9	16	49	47.6	713	basic intrusion	outcrop	gabbro?	sill, dark greenish grey, coarse grain(glassy), phenocryst: pyroxene+plagioclase	---	---	1									
TM104	---	51	43	16.2	16	54	18.2	753	basic intrusion	outcrop	dolerite	sill, dark greenish grey, medium grain(glassy), phenocryst: pyroxene+plagioclase	---	---	1									
TM105	---	51	52	54.3	16	52	18.4	720	basic intrusion	outcrop	gabbro?	sill, dark greenish grey, coarse grain(glassy), phenocryst: pyroxene+plagioclase, olivine?.	---	---	1			1						
TM106	---	51	54	33.5	16	50	28.7	731	basic intrusion	outcrop	dolerite	sill, dark grey, medium grain(glassy), phenocryst: pyroxene+plagioclase	---	---	1									
TM107	---	52	0	22.4	17	36	27.8	672	basic intrusion	outcrop	dolerite	sill, dark grey, medium grain(glassy), phenocryst: pyroxene+plagioclase	---	---	1									
TM108	---	52	3	38.9	17	29	1.2	775	sediment	outcrop	calcalious rock	pale grey, calcalious rock, pyrite dissemination.	pyrite	---									1	
TM109	---	52	3	38.9	17	29	1.2	775	basic intrusion	outcrop	dolerite	dyke-sill, dark grey, medium-coarse grain(glassy), phenocryst: pyroxene+plagioclase	---	---	1									
TM110	---	52	3	38.9	17	29	1.2	775	basic intrusion	outcrop	basalt	dyke-sill, grey, fine grain(glassy), phenocryst: plagioclase, pyrite film	pyrite	---	1								1	
TM111	---	52	3	21.2	17	28	27.5	768	basic intrusion	outcrop	dolerite?	dyke-sill, grey, medium grain(glassy), phenocryst: pyroxene+plagioclase, ((py diss?))	pyrite	---	1				1					
TM112	---	52	3	21.2	17	28	27.5	768	basic intrusion	outcrop	dolerite?	sill, grey,medium-fine grain(glassy), phenocryst: pyroxene+plagioclase, olivine?	---	---	1									
TM113	---	51	44	58.9	17	55	8.4	651	basic lava	outcrop	basalt?	pale purpple- grey, fine grain(glassy), phenocryst: plagioclase	---	---	1			1						
TM114	---	51	47	40.7	17	59	12.4	660	basic lava	outcrop	basalt	p-brownish grey, fine grain(glassy), phenocryst: pyroxene+plagioclase	---	---	1									
TM115	---	51	39	25.6	17	56	6.2	729	basic lava	outcrop	basalt	p-greenish grey, compact,fine-medium grain(glassy), phenocryst: pyroxene+plagioclase	---	---	1									
TM116	---	50	48	20.0	17	42	42.9	669	basic lava	outcrop	basalt	p-greenish grey, compact,medium-fine grain(glassy), phenocryst: pyroxene+plagioclase	---	---	1									
TM117	---	50	41	30.5	17	33	32.1	660	basic intrusion	outcrop	gabbro?	sill-like?, pale grey, partly redish,coarse grain (glassy), phenocryst: pyroxene (0.5cm)+plagioclase	---	---	1			1						
TM118	---	50	33	30.9	17	32	31.1	533	basic lava	outcrop	basalt	dark grey, compact,fine grain(glassy), phenocryst: pyroxene+plagioclase	---	---	1									
TM119	---	50	32	29.4	17	36	52.3	530	basic lava	outcrop	basalt	dark grey, compact,fine grain(glassy), phenocryst: pyroxene+plagioclase	---	---	1									
TM120	---	50	33	14.8	17	52	46.3	496	basic lava	outcrop	basalt	p-grey, compact,fine-medium grain(glassy), phenocryst: pyroxene+plagioclase	---	---	1									
TM121	---	50	42	30.4	17	52	37.1	573	basic lava	outcrop	basalt	dark grey, compact,fine grain(glassy), phenocryst: pyroxene+plagioclase,py film	sulfide	---	1							1		
TM122	---	49	31	46.5	18	0	28.4	526	basic lava	outcrop	basalt	dark greenish grey, medium-fine grain(glassy), phenocryst: pyroxene+plagioclase	---	---	1									
TM123	---	49	32	25.4	17	47	10.5	722	basic lava	outcrop	basalt	dark grey, compact,fine grain(glassy), phenocryst: pyroxene+plagioclase	---	---	1									
TM124	---	49	23	24.5	17	57	37.4	668	basic lava	outcrop	basalt	dark grey, compact,fine grain(glassy), phenocryst: pyroxene+plagioclase	---	---	1									
TM125	---	49	16	5.3	18	4	7.0	827	basic lava	outcrop	basalt	dark greenish grey,fine-medium grain(glassy), phenocryst: pyroxene+plagioclase	---	---	1									
TM126	---	49	18	38.8	18	24	2.5	678	basic lava	outcrop	basalt	dark grey, compact,fine grain(glassy), phenocryst: pyroxene+plagioclase	---	---	1	1						1		
TM127	---	49	1	23.9	18	30	34.3	650	basic lava	outcrop	basalt?	dark grey, fine-medium grain(glassy), phenocryst: pyroxene+plagioclase	---	---	1									
TM128	---	48	19	24.5	18	53	26.5	801	basic lava	outcrop	basalt	dark grey, compact,fine grain(glassy), phenocryst: pyroxene+plagioclase	---	---	1									

Description of rock and drill core samples

Sample No.	Depeth	Longitude			Latitude			Altitude	Sample Type		Rock Name	Description	Mineral-ization	Weathering	Analysis method									
	m	D	M	S	D	M	S	m							Bulk	PGE	Ar-Ar	Thin	P-Thin	X-ray	EPMA	Nd-Sr Isotope	S-Isotope	NRM
TM129	---	47	55	12.1	19	41	58.8	747	basic lava	outcrop	basalt	dark grey, compact,fine grain(glassy), phenocryst: pyroxene+plagioclase	---	---	1	1								
TM130	---	47	52	49.5	19	50	21.5	724	basic lava	outcrop	basalt	dark grey, compact,fine grain(glassy), phenocryst: pyroxene+plagioclase	---	---	1	1						1		
TM131	---	47	47	57.5	19	57	30.3	589	basic lava	outcrop	basalt	dark greenish grey, compact fine-medium grain(glassy), phenocryst: pyroxene+plagioclase	---	---	1									
TM132	---	47	47	19.5	20	3	37.7	602	basic lava	outcrop	basalt	dark grey, compact,fine grain(glassy), phenocryst: pyroxene+plagioclase, pyrite film?	pyrite	---	1				1					
TM133	---	47	28	20.0	20	9	11.2	939	basic lava	outcrop	basalt	dark grey, compact,fine grain(glassy), phenocryst: pyroxene+plagioclase	---	---	1									
TM134	---	47	16	53.0	20	37	12.0	714	basic intrusion	outcrop	dolerite?	sill,dark greenish grey, fine-medium grain(glassy), phenocryst: pyroxene+plagioclase	---	---	1									
TM135	---	47	18	49.3	20	41	36.3	695	basic lava	outcrop	dolerite	p-grey, medium grain(glassy), phenocryst: pyroxene+plagioclase	---	---	1									
TM136	---	47	19	14.2	20	34	47.1	923	basic lava	outcrop	basalt	dark grey, compact,fine grain(glassy), phenocryst: pyroxene+plagioclase	---	---	1									
TM137	---	47	18	49.4	21	6	1.3	667	basic intrusion	outcrop	dolerite	sill,dark greenish grey, medium grain(glassy), phenocryst: pyroxene+plagioclase	---	---	1									
TM138	---	47	17	39.8	21	10	12.2	762	basic intrusion	outcrop	dolerite	sill,dark greenish grey, medium grain(glassy), phenocryst: pyroxene+plagioclase	---	---	1									
TM139	---	47	19	42.3	21	20	34.5	720	basic intrusion	outcrop	dolerite	sill,dark grey, medium grain(glassy), phenocryst: pyroxene+plagioclase	---	---	1									
TM140	---	47	16	34.9	21	44	26.4	814	basic intrusion	outcrop	dolerite	sill,dark grey, medium-coarse grain(glassy), phenocryst: pyroxene+plagioclase	---	---	1									
TM141	---	47	18	28.2	21	50	50.2	644	basic intrusion	outcrop	dolerite?	sill,dark greenish grey,medium- coarse grain(glassy), phenocryst: pyroxene+plagioclase	---	---	1									
TM142	---	47	22	7.0	21	55	31.7	554	basic intrusion	outcrop	gabbro?	sill, dark greenish grey, coarse grain(glassy), phenocryst: pyroxene+plagioclase	---	---	1									
TM143	---	47	19	1.1	22	12	29.4	733	basic intrusion	outcrop	gabbro?	sill, dark grey, medium-coarse grain (glassy), phenocryst: pyroxene+plagioclase	---	---	1									
TM144	---	47	28	29.5	22	34	20.0	621	basic intrusion	outcrop	dolerite	sill, dark greenish grey, medium-coarse grain(glassy), phenocryst: pyroxene+plagioclase	---	---	1									
TM145	---	47	15	10.4	22	29	21.1	683	basic intrusion	outcrop	gabbro?	sill, dark greenish grey, medium-coarse grain(glassy), phenocryst: pyroxene+plagioclase	---	---	1									
TM146	---	47	10	28.3	22	25	14.6	614	basic intrusion	outcrop	dolerite	sill,dark grey, medium grain(glassy), phenocryst: pyroxene+plagioclase	---	---	1									
TM147	---	47	11	34.0	22	36	28.3	607	basic intrusion	outcrop	gabbro?	sill, dark greenish grey, medium-coarse grain(glassy), phenocryst: pyroxene+plagioclase	---	---	1									
TM148	---	47	21	24.6	22	36	51.8	534	basic intrusion	outcrop	gabbro?	sill, dark greenish grey, coarse grain(glassy), phenocryst: pyroxene+plagioclase	---	---	1			1						
TM149	---	47	35	36.1	21	42	18.8	700	basic lava	outcrop	basalt	dark grey, compact,medium-fine grain(glassy), phenocryst: pyroxene+plagioclase	---	---	1									
TM150	---	47	42	3.0	21	23	3.5	728	basic intrusion	outcrop	dolerite	sill,dark greenish grey, medium grain(glassy), phenocryst: pyroxene+plagioclase	---	---	1									
TM151	---	47	45	11.0	21	16	8.3	713	basic lava	outcrop	basalt	dark grey, compact,fine grain(glassy), phenocryst: pyroxene+plagioclase	---	---	1									
TM152	---	54	44	57.2	20	27	14.3	514	basic lava	outcrop	basalt	purple grey,compact,fine grain,weathering	---	weathering	1									
TM153	---	55	6	38.5	20	38	16.1	226	basic lava	outcrop	basalt	grey,compact,medium grain,weathering	---	weathering	1	1						1		
TM154	---	54	21	50.9	19	46	57.2	614	basic lava	outcrop	basalt	brown,medium grain,weathering	---	weathering	1									
TM155	---	54	22	36.9	19	17	45.7	577	basic lava	outcrop	basalt	brownish grey,medium grain,weathering	---	weathering	1									
TM156	---	53	23	19.2	19	49	38.1	392	basic lava	outcrop	basalt	dark greenish grey, fine grain(glassy), phenocryst: pyroxene+plagioclase	---	---	1									
TM157	---	54	31	52.1	20	59	53.5	428	basic lava	outcrop	basalt	brownish grey,medium grain,weathering	---	weathering	1									
TM158	---	55	26	10.8	21	11	1.9	551	basic lava	outcrop	basalt	brown,medium grain,weathering	---	weathering	1									
TM159	---	55	37	33.1	21	10	36.1	417	basic lava	outcrop	basalt	grey,medium grain,weathering,phenocryst:pyroxene+plagioclase	---	weak weathering	1									
TM160	---	55	49	17.2	21	29	3.1	448	basic lava	outcrop	basalt	purple-grey,medium grain,weathering	---	weathering	1									
TM161	---	54	59	13.6	21	37	26.6	318	basic lava	outcrop	basalt	pale purple grey,medium grain,weathering	---	weathering	1									
TM162	---	54	32	1.3	21	54	37.4	291	basic lava	outcrop	basalt	pale greenish grey, fine grain(glassy), phenocryst: pyroxene+plagioclase	---	---	1									1
TM163	---	56	7	46.7	22	9	12.2	360	basic lava	outcrop	basalt	dark greenish grey, medium grain(glassy), phenocryst: pyroxene+plagioclase	---	weak weathering	1									

Description of rock and drill core samples

Sample No.	Depeth	Longitude			Latitude			Altitude	Sample Type		Rock Name	Description	Mineral-ization	Weathering	Analysis method								
	m	D	M	S	D	M	S	m							Bulk	PGE	Ar-Ar	Thin	P-Thin	X-ray	EPMA	Nd-Sr Isotope	S-Isotope	NRM
TM164	---	55	23	38.4	22	54	29.0	394	basic lava	outcrop	basalt	dark grey,medium grain,weathering	---	weathering	1	1						1		
TM165	---	55	13	1.3	23	7	52.6	427	basic lava	outcrop	basalt	dark grey,partly red-brown,compact,medium grain,(weathering)	---	weathering	1									1
TM166	---	55	2	42.7	22	55	12.5	380	basic lava	outcrop	basalt	dark greenish grey, medium grain(glassy), phenocryst: pyroxene+plagioclase	---	weak weathering	1									
TM167	---	54	55	45.0	22	43	16.9	370	basic lava	outcrop	basalt	pale purple grey,green spot,medium grain,weathering	---	weak weathering	1									
TM168	---	54	52	31.5	22	15	33.1	389	basic lava	outcrop	basalt	dark grey,partly brown,compact,fine grain,(weathering)	---	weathering	1									
TM169	---	54	6	44.1	22	56	44.7	298	basic lava	outcrop	basalt	pale grey, medium grain(glassy), green spotted,onion structure	---	weak weathering	1									
TM170	---	54	5	27.4	22	58	5.5	292	basic lava	outcrop	basalt	pale greenish grey, medium grain(glassy), green spotted, phenocryst:px+pl	---	---	1									
TM171	---	54	15	50.4	24	7	13.5	255	basic lava	outcrop	basalt	brownish grey,medium grain,phenocryst:px+pl	---	weak weathering	1									
TM172	---	53	50	20.8	24	20	56.7	350	basic lava	outcrop	basalt	dark grey,partly green spot,medium grain,phenocryst:px+pl	---	---	1									
TM173	---	53	51	20.8	24	11	0.6	267	basic lava	outcrop	basalt	dark brownish grey, medium grain,phenocryst:px+pl	---	---	1									
TM174	---	53	45	58.1	24	34	47.1	462	basic lava	outcrop	basalt	brownish grey, medium grain,(weathering)	---	weathering	1									
TM175	---	54	12	45.3	24	36	4.5	332	basic lava	outcrop	basalt	brownish grey, medium grain, phenocryst:px+pl	---	---	1									1
TM176	---	54	15	32.4	24	46	56.1	344	basic lava	outcrop	basalt	brownish grey, medium grain, phenocryst:px+pl	native copper	---	1									
TM177	---	54	3	56.3	24	57	20.9	525	basic lava	outcrop	basalt	brownish grey, green spot, medium grain, phenocryst:px+pl	---	---	1									
TM178	---	54	9	37.2	25	12	7.9	369	basic lava	outcrop	basalt	brownish grey, green spot, fine grain, phenocryst:px+pl	---	---	1									1
TM179	---	54	15	32.7	25	10	31.4	324	basic lava	outcrop	basalt	dark greenish grey, fine grain(glassy), phenocryst: pyroxene+plagioclase	native copper	---	1									
WW013	---	50	44	21.1	28	36	3.0		basic lava	outcrop	andesitic basalt	lava, brown, fine-grain, amygdaloidal texture.	---	---										
WW017	---	50	17	16.1	28	39	7.2		acidic lava	outcrop	andesitic basalt **(Acidic Rock)**	lava, brown, fine-grain, weak amygdaloidal texture. **(Acidic Rock)**	---	---	1			1						
WW024	---	50	33	23.3	28	1	31.2		basic lava	outcrop	andesitic basalt	lava, brow-reddish grey, fine-grain, weak amygdaloidal texture.	---	---	1			1				1		
WW026	---	50	51	21.8	28	23	41.1		acidic lava	outcrop	andesitic basalt **(Acidic Rock)**	lava, brow-grey, fine-grain, amygdaloidal texture. **(Acidic Rock)**	---	---	1			1						
WW031	---	51	28	1.9	28	19	3.9		basic lava	outcrop	basalt	lava, greenish grey, fine grain.	---	---	1			1						
WW056	---	52	52	4.0	27	25	15.7		basic lava	outcrop	basalt	lava, greenish grey, fine grain.	---	---	1			1						
WW068	---	53	5	8.5	29	19	4.5		acidic lava	outcrop	andesite? **(Acidic Rock)**	lava, grey, coarse grain, phenocryst: pyroxene-plagioclase. **(Acidic Rock)**	---	---	1			1						
WW069	---	53	0	48.9	29	24	23.3		basic lava	outcrop	basalt **(Acidic Rock)**	lava, greenish grey, fine grain, rare amygdaloidal texture. **(Acidic Rock)**	---	---	1			1						
WW073	---	52	44	18.5	29	9	17.7		basic lava	outcrop	basalt	lava, dark grey, fine grain.	---	---	1			1						
WW076	---	51	55	40.4	29	22	57.2		basic lava	outcrop	andesitic basalt	lava, grey, coarse grain, phenocryst: pyroxene-plagioclase.	---	---	1			1						
WW077	---	51	52	57.0	29	11	37.9		basic lava	outcrop	andesitic basalt	lava, grey, coarse grain, phenocryst: pyroxene-plagioclase.	---	---	1			1						
WW083	---	51	6	33.3	29	28	46.6		basic lava	outcrop	basalt	lava, dark grey, fine grain.	---	---	1			1						
WW092	---	51	38	9.6	28	13	59.4		basic lava	outcrop	basalt	lava, dark grey, fine grain, rare amygdaloidal texture.	---	---	1			1						
WW095	---	52	15	50.6	28	4	4.8		basic lava	outcrop	basalt	lava, grey-dark brown, fine grain.	---	---	1			1						
WW097	---	50	52	26.0	29	45	21.6		basic lava	outcrop	basalt	lava, amygdaloidal texture	---	---										
WW099	---	50	43	41.8	29	33	2.5		basic lava	outcrop	basalt	lava, grey, fine grain, phenocryst: pyroxene+(plagioclase).	---	---	1			1				1		
WW117a	---	50	18	28.7	28	26	41.5		basic lava	outcrop	basalt	lava, reddish grey, fine grain.	---	---	1			1						
WW122	---	49	43	23.8	28	18	7.2		basic lava	outcrop	basalt	lava, reddish grey, fine grain, rare amygdaloidal texture.	---	---	1			1				1		
WW129	---	50	9	55.0	28	14	52.4		basic lava	outcrop	basalt	lava, grey, medium grain, rare amygdaloidal texture, (brown layer).	---	---	1			1						

Description of rock and drill core samples

Sample No.	Depeth	Longitude			Latitude			Altitude	Sample Type		Rock Name	Description	Mineral-ization	Weathering	Analysis method								
	m	D	M	S	D	M	S	m							Bulk	PGE	Ar-Ar	Thin	P-Thin	X-ray	EPMA	Nd-Sr Isotope	S-Isotope	NRM
WW130	---	50	2	58.0	28	7	40.7		basic lava	outcrop	basalt	lava, grey, medium grain.	---	---	1			1						
WW134	---	50	11	33.3	27	51	57.5		basic lava	outcrop	basalt	lava, grey, medium grain.	---	---	1	1		1						
WW-161	---	55	5	45.8	30	10	36.3		basic intrusion	outcrop	gabbro	sill, gabbro, host: Rosário Fm.	---	weak weathering	1									
WW-162	---	55	17	3.1	30	5	15.5		basic intrusion	outcrop	gabbro	sill, gabbro with native copper	native copper	weathering	1									
WW-163	---	55	34	11.0	29	53	56.3		basic lava	outcrop	andesitic basalt	andesitic basalt?	---	weathering	1									
WW-164	---	55	47	1.3	29	48	19.5		acidic lava	outcrop	acidic rock	acidic flow	---	weathering	1									
WW-165	---	55	38	25.8	29	45	54.0		acidic lava	outcrop	acidic rock	acidic flow	---	weathering	1									
WW-166	---	55	33	28.3	29	44	29.6		acidic lava	outcrop	acidic rock	acidic flow	---	weathering	1									
WW-167	---	55	58	9.6	29	35	53.1		basic lava	outcrop	basalt	basalt or andesitic basalt	---	weathering	1									
WW-174	---	55	38	9.7	29	58	10.9		acidic lava	outcrop	acidic rock	acidic flow	---	weak weathering	1									
WW-175	---	55	34	37.2	30	9	34.4		acidic lava	outcrop	acidic rock	acidic flow	---	weathering	1	1								
WW-177	---	55	52	11.9	29	55	47.8		acidic lava	outcrop	acidic rock	acidic flow	---	weathering	1									
WW-181	---	56	36	8.9	29	41	37.4		acidic lava	outcrop	acidic rock	lava, acidic or intermediate?	---	weathering	1									
WW-183A	---	56	35	20.0	29	57	24.0		basic lava	outcrop	basalt	autobrecciated lava, near bottom of one flow	---	weak weathering	1									
WW-184	---	56	27	51.7	30	0	20.6		acidic lava	outcrop	acidic rock	lava, acidic rock	---	weathering	1	1								
WW-191	---	55	33	47.6	30	50	28.1		acidic lava	outcrop	acidic rock	lava, near contact between lava and sandstone	---	weak weathering	1									
WW-196	---	56	12	58.9	30	29	12.4		basic lava	outcrop	basalt	lava, near contact between lava and sandstone (Botucatu Fm.)	---	weak weathering	1									
WW-197	---	56	23	59.5	30	24	27.5		basic lava	outcrop	basalt	lava.	---	weathering	1									
WW-203	---	55	51	24.0	30	52	43.3		acidic lava	outcrop	acidic rock	lava, acidic rock.	---	weathering	1									
WW-204	---	56	29	9.9	30	18	9.2		acidic lava	outcrop	acidic rock	lava, acidic rock.	---	weathering	1									
WW-205	---	56	33	2.6	30	8	25.7		acidic lava	outcrop	acidic rock	lava, acidic rock, flow texture.	---	weathering	1									
WW-209	---	57	6	56.0	29	53	1.3		acidic lava	outcrop	acidic rock	lava, acidic rock.	---	weathering	1									
WW-210	---	56	59	22.9	29	44	53.3		acidic lava	outcrop	acidic rock	lava, acidic rock.	---	weak weathering	1									
WW-219	---	55	5	42.4	29	2	37.1		acidic lava	outcrop	acidic rock	lava, acidic rock.	---	weak weathering	1									
WW-221	---	54	49	24.3	29	15	0.3		acidic lava	outcrop	acidic rock	lava, acidic rock.	---	weak weathering	1									
WW-222	---	53	20	35.0	29	43	17.6		basic intrusion	outcrop	gabbro	sill, gabbro, in sediment (Rosário Fm.).	---	weak weathering	1									
WW-223	---	53	0	0.1	29	44	44.7		basic intrusion	outcrop	gabbro	sill, gabbro.	---	weak weathering	1									
AC-028	---	53	13	20.6	26	45	26.4		basic lava	outcrop	basalt	lava, greenish grey, fine grain.	---	---	1			1						
AC-034B	---	53	30	5.0	26	52	28.3		basic lava	outcrop	dolerite	lava, greenish grey, coarse grain, phenocryst: pyroxene+plagioclase.	---	---	1			1						
AC-035	---	53	29	59.1	27	1	40.6		basic lava	outcrop	basalt	lava, reddish grey, fine grain.	---	---	1			1						
ACR-119	---	51	36	27.2	27	31	5.8		acidic lava	outcrop	basalt (Acidic Rock)	lava, reddish grey, fine grain. (Acidic Rock)	---	---	1			1						
ACR-125	---	52	35	54.1	27	4	5.3		basic lava	outcrop	basalt	lava, grey, fine grain, phenocryst: pyroene+plagioclase.	---	---	1			1						
ADR-033	---	52	5	9.8	26	44	36.7		basic lava	outcrop	basalt	lava, greenish grey, fine grain, weak weathered(hematite), rare amygdaloidal texture.	---	weak weathering	1			1						
YM105	---	54	57	28.8	28	33	51.4	181	basic lava	outcrop	basalt	lava, massive, greenish grey, medium grain, phenocryst: plagioclase+pyroxene, amygdaloidal texture, weathering.	---	weak weathering	1									
YM108	---	55	15	46.4	28	11	44.0	130	basic lava	outcrop	basalt	lava, massive, grey, fine grain, aphyric, reddish dots (hematite).	---	weathering	1	1		1						

Description of rock and drill core samples

Sample No.	Depeth	Longitude			Latitude			Altitude	Sample Type		Rock Name	Description	Mineral-ization	Weathering	Analysis method									
	m	D	M	S	D	M	S	m							Bulk	PGE	Ar-Ar	Thin	P-Thin	X-ray	EPMA	Nd-Sr Isotope	S-Isotope	NRM
YM109	---	55	19	47.9	28	6	47.1	93	basic lava	outcrop	basalt	lava, massive, grey, fine grain, aphyric, fine grained sulfide.	sulfide	---	1									
YM114	---	54	58	12.7	28	15	6.4	194	basic lava	outcrop	basalt	lava, massive, reddish grey, medium grain, phenocryst: olivine+plagioclase+cpx, weak weathering, reddish dots (hematite).	---	weak weathering	1	1								
YM115	---	55	1	37.6	28	6	48.2	148	basic lava	outcrop	basalt	lava, massive, greenish grey, fine grain, phenocryst: plagioclase+(cpx).	---	---	1	1								
YM117	---	55	8	12.9	27	57	16.1	259	basic lava	outcrop	basalt	lava, massive, grey, medium grain, phenocryst: plagioclase+(cpx), weak weathering (hematite).	---	weak weathering	1			1						
YM118	---	54	56	12.8	28	2	45.7	227	basic lava	outcrop	basalt	lava, massive, grey, fine grain, phenocryst: plagioclase+(cpx).	---	---	1									
YM119	---	54	45	42.8	28	7	42.5	308	basic lava	outcrop	basalt	lava, massive, grey, fine-medium grain, phenocryst: plagioclase+(cpx).	---	---	1	1		1						
YM120	---	54	33	35.0	28	9	34.1	317	basic lava	outcrop	basalt	lava, massive, grey, medium grain, phenocryst: plagioclase+(cpx), weak weathering (celadonite+hematite).	---	weak weathering	1									
YM121	---	54	5	52.6	28	35	6.4	272	basic lava	outcrop	basalt	lava, massive, greenish grey, medium grain, phenocryst: plagioclase+(cpx), weak weathering (celadonite).	---	weak weathering	1									
YM122	---	54	4	54.6	28	21	21.9	263	basic lava	outcrop	basalt	lava, massive, greenish grey,fine-medium grain, phenocryst: plagioclase+(cpx).	---	---	1				1					
YM124	---	53	32	29.1	28	14	4.5	411	basic lava	outcrop	basalt	lava, massive, grey, medium grain, phenocryst: plagioclase+(cpx), weak weathering.	---	weak weathering	1									
YM125	---	53	10	58.1	28	22	2.3	458	basic lava	outcrop	basalt	lava, massive, reddish grey, medium grain, phenocryst: plagioclase+(cpx), native copper along crack, weak weathering.	native copper	weak weathering	1	1								
YM126	---	53	32	36.9	28	39	50.9	396	basic lava	outcrop	basalt	lava, massive, greenish grey, fine-medium grain, phenocryst: plagioclase+(cpx), weak weathering (celadonite+hematite).	---	weak weathering	1									
YM127	---	54	3	14.0	28	8	24.5	379	basic lava	outcrop	basalt	lava, massive, greenish grey, fine grain, weak weathering (celadonite+hematite).	---	weak weathering	1									
YM128	---	54	9	4.2	27	58	41.0	364	basic lava	outcrop	basalt	lava, massive, greenish grey, fine grain, weak weathering (celadonite+hematite).	---	weak weathering	1									
YM129	---	54	47	5.6	27	48	21.9	322	basic lava	outcrop	basalt	lava, massive, greenish grey, medium-coarse grain, phenocryst: plagioclase(+cpx), weak weathering.	---	weak weathering	1									
YM130	---	55	1	44.6	27	52	14.1	128	basic lava	outcrop	basalt	lava, massive, grey, fine grain, native copper along cruck.	native copper	---	1	1								
YM131	---	54	46	42.4	27	39	23.7	250	basic lava	outcrop	basalt	lava, massive, reddish grey, medium grain, phenocryst: plagioclase, malachite along cruck, weak weathering.	native copper	weak weathering	1									
YM132	---	54	27	16.7	27	39	1.5	198	basic lava	outcrop	basalt	lava, massive, grey, fine grain, fine grain native copper in.	native copper	---	1									
YM133	---	54	30	27.4	27	52	48.1	259	basic lava	outcrop	basalt	lava, massive, grey, fine-medium grain, dissemination of fine grain native copper.	native copper	---	1									
YM134	---	54	7	59.2	27	31	46.7	211	basic lava	outcrop	basalt	lava, massive, grey, fine grain, fine grain native copper along cruck.	native copper	---	1									
YM135	---	53	48	17.5	27	39	3.8	417	basic lava	outcrop	basalt	lava, massive, grey, fine grain.	---	---	1									
YM136	---	53	54	17.3	28	13	32.1	379	basic lava	outcrop	basalt	lava, massive, greenish grey, fine grain, weak weathering.	---	weak weathering	1									
YM137	---	53	6	49.0	27	53	58.1	373	basic lava	outcrop	basalt	lava, massive, greenish grey, fine grain, native copper along cruck.	native copper	---	1									
YM138	---	52	56	29.2	27	50	20.7	407	basic lava	outcrop	basalt	lava, massive, grey, fine-medium grain, dots of native copper.	native copper	---	1									
YM139	---	53	2	7.4	27	48	44.5	396	basic lava	outcrop	basalt	lava, massive, greenish grey, coarse grain, weak weathering.	---	weak weathering	1			1						
YM140	---	53	31	23.0	27	40	37.8	513	basic lava	outcrop	basalt	lava, massive, grey, fine grain.	---	---	1									
YM141	---	53	10	11.4	27	26	23.3	287	basic lava	outcrop	basalt	lava, massive, grey, fine-medium grain, dots of native copper.	native copper	---	1									
YM142	---	53	22	36.1	27	20	48.2	520	basic lava	outcrop	basalt	lava, massive, grey, aphyric, a few vesicle, native copper in vesicles and along cruck, weak weathering.	native copper	weak weathering	1									
YM143	---	53	43	4.5	27	20	47.6	423	basic lava	outcrop	basalt	lava, massive, greenish grey, fine grain, a few vesicle, weathering.	---	weathering	1									
YM144	---	53	13	3.5	27	4	42.8	291	basic lava	outcrop	basalt	lava, massive, grey, fine grain, native copper along cruck.	native copper	---	1									
YM145	---	52	53	41.3	27	3	54.3	507	basic lava	outcrop	basalt	lava, massive, grey, aphyric, black glass in.	---	---	1									
YM146	---	52	34	54.3	27	10	13.3	647	basic lava	outcrop	basalt	lava, massive, fine grain.	---	---	1	1								
YM147	---	52	43	33.7	27	23	32.9	429	basic lava	outcrop	basalt	lava, massive, grey, aphyric, black glass in, dissemination of native copper.	native copper	---	1									
YM148	---	52	50	11.4	27	39	44.5	619	basic lava	outcrop	basalt	lava, massive, greenish grey, coarse grain, weak weathering.	---	weak weathering	1									
YM150	---	50	10	47.1	29	46	39.6	15	basic intrusion	outcrop	basalt	dyke?, width: 30cm, fine grain (glassy), dissemination of sulfide (pyrite), weak weathering.	sulfide	weak weathering	1				1					

Description of rock and drill core samples

Sample No.	Depeth	Longitude			Latitude			Altitude	Sample Type		Rock Name	Description	Mineral-ization	Weathering	Analysis method									
	m	D	M	S	D	M	S	m							Bulk	PGE	Ar-Ar	Thin	P-Thin	X-ray	EPMA	Nd-Sr Isotope	S-Isotope	NRM
YM151	---	50	10	47.1	29	46	39.6	15	basic lava	outcrop	basalt (Acidic Rock)	lava, massive, greenish grey, medium grain, vesicle (common), weak weathering. (Acidic Rock)	---	weak weathering	1									
YM152	---	50	10	47.1	29	46	39.6	45	basic intrusion	outcrop	basalt (Acidic Rock)	feeder dyke?, black, glassy. (Acidic Rock)	---	---	1									
YM153	---	50	9	38.3	29	25	29.5	100	basic lava	outcrop	basalt	lava, massive, greenish grey, medium grain, phenocryst: plagioclase+olivine, a few vesicle, weak weathering.	---	weak weathering	1									
YM154	---	50	11	31.1	29	22	56.7	185	basic lava	outcrop	basalt	lava, massive, greenish grey, aphyric, a lot of vesicles, weak weathering.	---	weak weathering	1									
YM155	---	50	11	3.0	29	22	25.4	415	basic lava	outcrop	basalt	lava, massive, grey, fine grain, phenocryst: plagioclase+olivine, a few vesicles.	---	---	1									
YM156	---	50	10	52.0	29	22	31.2	500	basic intrusion	outcrop	basalt	sill?, massive,greenish grey, porphyritic?, phenocryst: plagioclase+olivine, including of fine grained sulfide.	sulfide	---	1				1					
YM157	---	50	10	48.9	29	22	11.6	610	basic lava	outcrop	basalt (Acidic Rock)	lava, massive, black, glassy. (Acidic Rock)	---	---	1									
YM158	---	50	10	18.4	29	21	18.1	770	basic lava	outcrop	basalt	lava, massive, reddish grey, a few vesicles, weak weathering.	---	weak weathering	1									
YM159	---	50	11	6.1	29	20	8.7	850	basic lava	outcrop	dacite	lava, flow banding, grey, a few vesicles, weak weathering.	---	weak weathering	1									
YM160	---	50	11	6.1	29	20	8.7	850	basic lava	outcrop	basalt (Acidic Rock)	lava, massive, black, glassy, a few vesicles. (Acidic Rock)	---	---	1									
YM161	---	49	57	6.6	28	47	59.0	1,170	basic intrusion	outcrop	basalt	feeder dyke, fine pich columner joint, greenish grey, medium grain, phenocryst: plagioclase, weak weathering.	---	weak weathering	1									
YM162	---	49	56	57.1	28	48	1.9	1,090	basic lava	outcrop	basalt (Acidic Rock)	lava, massive, black, glassy, a few vesicles. (Acidic Rock)	---	---	1									
YM163	---	49	56	46.4	28	48	19.8	940	basic lava	outcrop	basalt	lava, massive, greenish grey, fine grain, including of fine grained native copper (rare), weak weathering.	native copper	weak weathering	1									
YM164	---	49	56	29.1	28	48	23.3	855	basic lava	outcrop	basalt	lava, massive, greenish grey, fine grain, weathering.	---	weathering	1									
YM165	---	49	56	4.2	28	48	17.0	750	basic lava	outcrop	basalt	lava, massive, reddish grey, fine grain, a few vesicles, fine grained native copper, weathering.	native copper	weathering	1									
YM166	---	49	55	46.1	28	48	26.0	630	basic lava	outcrop	basalt	lava, massive, grey, fine grain, weak weathering.	---	weak weathering	1									
YM167	---	49	55	27.9	28	48	12.8	440	basic lava	outcrop	basalt	lava, massive, grey, fine grain, a few vesicles, native copper (rare), weak weathering.	native copper	weak weathering	1									
YM168	---	49	55	13.8	28	48	27.4	370	basic lava	outcrop	basalt	lava, massive, grey, fine grain (aphyric), a few vesicles, weak weathering.	---	weak weathering	1	1								
YM169	---	49	22	18.4	28	45	1.3	130	basic intrusion	outcrop	basalt	sill, fine pich columner jpint, fine grain, dots of sulfide along cruck.	sulfide	---	1									
YM170	---	49	26	46.6	28	51	24.2	50	basic intrusion	outcrop	dolerite	sill, fine pich columner jpint, grey, phenocryst: plagioclase+cpx+olivine, dots of sulfide (along cruck).	sulfide	---	1									
YM171	---	49	26	46.6	28	51	24.2	60	basic intrusion	outcrop	dolerite	sill, fine pich columner jpint, grey, phenocryst: plagioclase+cpx+olivine, dots of sulfide (along cruck).	sulfide	---	1									
YM172	---	49	26	46.6	28	51	24.2	70	basic intrusion	outcrop	dolerite	sill, fine pich columner jpint, grey, phenocryst: plagioclase+cpx+olivine, dissemination of sulfide.	sulfide	---	1									
YM173	---	49	26	46.6	28	51	24.2	100	basic intrusion	outcrop	gabbro	sill, gabbroic part, coarse grain, plagiclase+cpx, dissemination of sulfide.	sulfide	---	1				1					
YM174	---	49	26	46.6	28	51	24.2	80	basic intrusion	outcrop	dolerite	sill, fine pich columner jpint, grey, phenocryst: plagioclase+cpx+olivine, dissemination of sulfide.	sulfide	---	1									
YM175	---	49	26	46.6	28	51	24.2	100	basic intrusion	outcrop	dolerite	sill, fine pich columner jpint, grey, phenocryst: plagioclase+cpx+olivine, dissemination of sulfide.	sulfide	---	1									
YM176	---	49	24	6.8	28	30	32.0	515	basic intrusion	outcrop	gabbro	sill (gabbroic part), massive, grey, coarse grain, plagioclase+cpx, dissemination of sulfide	sulfide	---	1				1					
YM177	---	49	12	55.1	28	30	16.7	168	basic intrusion	outcrop	basalt	dyke?, massive, grey, medium grain, phenocryst: plagioclase.	---	---	1									
YM178	---	49	31	38.0	28	23	38.5	760	basic lava	outcrop	basalt	lava, massive, medium grain, phenocryst: plagioclase+(olivine?), a few vesicles, weathering.	---	weathering	1									
YM179	---	49	32	13.7	28	23	34.9	905	basic lava	outcrop	basalt	lava, massive, fine grain, phenocryst: plagioclase+(olivine?), a few vesicles, weak weathering.	---	weak weathering	1			1						
YM180	---	49	32	26.4	28	23	42.0	1,000	basic lava	outcrop	basalt	lava, massive, grey, fine-medium grain, including of vesicles, weak weathering.	---	weak weathering	1									
YM181	---	49	32	42.6	28	23	47.0	1,075	basic lava	outcrop	basalt	lava, massive, fine grain, including of vesicles, weak weathering.	---	weak weathering	1									
YM182	---	49	39	0.4	28	6	40.8	1,374	basic lava	outcrop	basalt	lava, massive, greenish grey, fine grain, phenocryst: cpx, including of vesicles, weak weathering.	---	weak weathering	1	1								
YM183	---	49	38	18.6	28	5	16.7	1,495	basic intrusion	outcrop	dolerite	dyke, fine pich columner joint, phenocryst: cpx+plagioclase, sulfide along cruck.	sulfide	---	1									
YM184	---	49	36	29.4	28	1	51.8	1,275	basic lava	outcrop	basalt	lava, massive, grey, fine-medium grain, phenocryst: cpx+plagioclase, a few vesicles, weak weathering.	---	weak weathering	1	1								
YM185	---	49	34	16.0	27	54	42.4	1,195	basic intrusion	outcrop	dolerite	sill, massive, greenish grey, dissemination of sulfide, weak weathering.	sulfide	weak weathering	1									

Description of rock and drill core samples

Sample No.	Depeth	Longitude			Latitude			Altitude	Sample Type		Rock Name	Description	Mineral-ization	Weathering	Analysis method									
	m	D	M	S	D	M	S	m							Bulk	PGE	Ar-Ar	Thin	P-Thin	X-ray	EPMA	Nd-Sr Isotope	S-Isotope	NRM
YM186	---	49	3	26.0	27	41	35.8	980	basic intrusion	outcrop	basalt	sill, massive, greenish grey, medium grain, phenocryst: plagioclase+cpx+olivine?, weak weathering.	---	weak weathering	1									
YM187	---	48	34	9.1	27	45	29.9	20	basic intrusion	outcrop	gabbro (Acidic Rock)	dyke, wideth: >10m, leucocratic, plagioclase+cpx+olivine, fine grained sulfide. (Acidic Rock)	sulfide	---	1									
YM188	---	48	33	38.1	27	47	38.5	25	basic intrusion	outcrop	gabbro	dyke, massive, width: 20m, meranocratic, plagioclase+cpx+olivine, with fine grained sulfide.	sulfide	---	1				1					
YM189	---	48	30	18.9	27	43	24.4	22	basic intrusion	outcrop	gabbro	dyke, massive, wideth: 10m, N40E, meranocratic, plagioclase+cpx+olivine, with sulfide.	sulfide	---	1									
YM190	---	48	26	5.0	27	35	49.4	85	basic intrusion	outcrop	gabbro	dyke, massive, width>5m, meranocratic, plagioclase+cpx+olivine, with sulfide.	sulfide	---	1									
YM191	---	48	25	6.1	27	26	28.8	81	basic intrusion	outcrop	gabbro	dyke, massive, meranocratic, width: >50m, plagioclase+cpx+olivine, with sulfide, weak weathering.	sulfide	weak weathering	1									
YM192	---	49	31	41.4	28	23	32.3	810	basic intrusion	outcrop	dolerite	dyke, massive, reddish grey, coarse grain, phenocryst: plagioclase+cpx, a few vesicles, weathering.	---	weathering	1									
YM193	---	49	32	48.8	28	23	45.8	1,120	basic lava	outcrop	basalt	lava, massive, greenish grey, fine grain, with vesicles (rare), weak weathering.	---	weak weathering	1									
YM194	---	49	32	54.4	28	23	48.9	1,165	basic lava	outcrop	basalt	lava, massive, greenish grey, fine grain, a few vesicles, weathering.	---	weathering	1									
YM195	---	49	32	54.1	28	23	56.4	1,255	basic intrusion	outcrop	basalt	dyke, width: >100m, black, glassy, weak weathering.	---	weak weathering	1									
YM197	---	49	33	3.1	28	23	57.1	1,330	basic lava	outcrop	basalt	lava, massive, greenish grey, fine grain, aphyric, magnetite (common), a lot of vesicles, weathering.	---	weathering	1									
YM198	---	49	43	20.5	28	18	21.0	1,300	basic intrusion	outcrop	dolerite	dyke, fine pich columner joint, grey, phenocryst: plagioclase+cpx+olivine.	---	---	1			1						
YM199	---	49	48	42.9	28	14	25.4	1,480	basic lava	outcrop	basalt	lava, grey, fine grain, phenocryst: plagioclase+cpx+olivine?, a lot of vesicles, weak weathering.	---	weak weathering	1									
YM200	---	50	31	7.5	27	44	3.4	785	basic lava	outcrop	basalt	lava, massive, grey, fine-medium grain, fine grained native copper (rare), weak weathering.	native copper	weak weathering	1									
YM201	---	50	23	38.2	27	26	34.9	872	basic intrusion	outcrop	basalt	sill or dyke, grey, medium-coarse grain, phenocryst: plagioclase+cpx+olivine?, weak weathering.	---	weak weathering	1									
YM205	---	50	4	36.5	27	16	55.8	605	basic intrusion	outcrop	basalt	sill, fine piched columner jpint, fine grain, a lot of sulfide along cruck.	sulfide	---	1									
YM206	---	50	4	36.5	27	16	55.8	605	basic intrusion	outcrop	gabbro	sill, gabbroic part of YM205, plagioclase+cpx+olivine, weak weathering.	---	weak weathering	1									
YM207	---	50	8	35.7	26	58	1.0	570	basic intrusion	outcrop	basalt	sill, thickness: 10-15m, fine piched columner joint, grey, medium grain, phenocryst: plagioclase+cpx+olivine, sulfide along cruck.	sulfide	---	1									
YM208	---	50	25	59.7	26	56	10.0	1,070	basic lava	outcrop	basalt	lava, massive, grey, fine grain, a few vesicles, weak weathering.	---	weak weathering	1	1								
YM210	---	50	20	24.1	26	48	12.9	1,275	basic lava	outcrop	basalt	lava, massive, greenish grey, fine grain, weak weathering.	---	weak weathering	1	1								
YM211	---	50	32	15.6	26	4	22.2	755	basic intrusion	outcrop	dolerite	sill, thickness: 10-15m, massive, grey, porphyritic, phenocryst: cpx.	---	---	1				1					
YM212	---	50	32	15.6	26	4	22.2	755	basic intrusion	outcrop	basalt	sill (child margin), blackish green, fine grain, dissemination of sulfide.	sulfide	---	1				1					
YM215	---	51	34	37.0	26	35	20.1	1,325	basic intrusion	outcrop	basalt (Acidic Rock)	dyke, massive, greenish grey, fine grain, a few vesicles, weak weathering. (Acidic Rock)	---	weak weathering	1									
YM218	---	52	24	30.1	26	46	58.1	710	basic intrusion	outcrop	dolerite	sill (lava?), massive, coase grain, phenocryst: plagioclase+cpx.	---	---	1									
YM219	---	52	20	48.0	27	4	42.5	585	basic lava	outcrop	basalt	lava, massive, greenish grey, fine grain, weak weathering.	---	weak weathering	1									
YM222	---	50	42	23.0	26	55	26.2	1,010	basic lava	outcrop	basalt	lava, massive, greenish grey, fine grain, weathering.	---	weathering	1									
YM223	---	51	13	11.9	27	2	49.7	1,025	basic lava	outcrop	basalt	lava, massive, greenish grey, fine grain, weak weathering.	---	weak weathering	1	1								
YM225	---	51	34	26.5	27	15	32.5	600	basic lava	outcrop	dolerite	lava, massive, grey, coarse grain, phenocryst: plagioclase+cpx, dots of native copper, weak weathering.	native copper	weak weathering	1									
YM227	---	52	2	3.2	27	25	53.0	625	basic lava	outcrop	basalt	lava, massive, greenish grey, fine grain, a few vesicles, weak weathering.	---	weak weathering	1									
YM228	---	52	18	24.8	27	42	31.4	785	basic lava	outcrop	basalt?	lava, massive, greenish grey, green band (flow band?), fine grain.	---	---	1			1						
YM229	---	52	15	42.5	27	52	56.8	651	basic intrusion	outcrop	basalt	dyke, fine piched columner joint, greenish grey, medium grain, weathering.	---	weathering	1									
YM230	---	51	48	8.3	27	55	58.2	800	basic lava	outcrop	basalt	lava, massive, greenish grey, fine grain, weak weathering.	---	weak weathering	1									
YM231	---	51	39	19.5	27	47	14.7	780	basic lava	outcrop	basalt	lava, massive, greenish grey, medium grain, phenocryst: olivine?, weak weathering.	---	weak weathering	1			1						
AT03-486.0	486.0	49	45	19.6	29	11	34.1	---	basic intrusion	drill core		native copper in cavity, chalcedonic quartz druse	native copper	---					1		1			
AT03-486.3	486.3							---	sediment	drill core	black shale	black brecciated shale with pyrite	pyrite	---	1			1				1	1	

Description of rock and drill core samples

Sample No.	Depeth	Longitude			Latitude			Altitude	Sample Type		Rock Name	Description	Mineral-ization	Weathering	Analysis method								
	m	D	M	S	D	M	S	m							Bulk	PGE	Ar-Ar	Thin	P-Thin	X-ray	EPMA	Nd-Sr Isotope	S-Isotope	NRM
AT03-487.0	487.0							---	basic intrusion	drill core	dolerite	sill, gray aphanitic tholeiitic dolerite, strongly py-diss(dotted)	pyrite	---	1			1						
AT03-498.5	498.5							---	basic intrusion	drill core	dolerite	sill, gray coarse grained tholeiitic dolerite(gabbroic), weakly py-diss	pyrite	---	1			1						
AT03-509.4	509.4							---	basic intrusion	drill core	dolerite	sill, gray medium grained tholeiitic dolerite	---	---	1			1						
AT03-519.2	519.2							---	basic intrusion	drill core	dolerite	sill, gray medium grained tholeiitic dolerite, strong pyritization	pyrite	---	1			1				1		
AT03-528.9	528.9							---	basic intrusion	drill core	dolerite	sill, gray medium grained tholeiitic(or picritic) dolerite	---	---	1			1						
AT03-537.3	537.3							---	basic intrusion	drill core	dolerite	sill, gray medium grained tholeiitic dolerite, weak pyritization(film like)	pyrite	---	1			1						
AT03-547.4	547.4							---	basic intrusion	drill core	dolerite	sill, gray aphanitic tholeiitic dolerite, chilled margin(4m in width)	---	---	1			1						
AT03-590.1	590.1							---	basic intrusion	drill core	dolerite	sill, gray medium grained tholeiitic dolerite, weak pyritization(dotted dissemonation, film-like)	pyrite	---	1			1						
AT03-600.0	600.0							---	basic intrusion	drill core	dolerite	sill, gray medium grained tholeiitic dolerite, weak pyritization(dotted dissemonation, film-like)	pyrite	---	1			1						
AT03-607.9	607.9							---	basic intrusion	drill core	dolerite	sill, gray medium grained tholeiitic dolerite, weak pyritization(dotted dissemonation, film-like)	pyrite	---	1			1						
AT03-616.9	616.9							---	basic intrusion	drill core	dolerite	sill, gray aphanitic tholeiitic dolerite, chilled margin(4m in width), weak pyritization	pyrite	---	1			1						
AT08-792.4	792.4	49	43	12.4	29	18	15.8	---	basic intrusion	drill core	dolerite	sill, gray medium grained tholeiitic dolerite	---	---	1			1						
AT08-802.85	802.9							---	basic intrusion	drill core	dolerite	sill, gray coarse grained tholeiitic dolerite (gabbroic)	---	---	1			1						
AT08-815.1	815.1							---	basic intrusion	drill core	dolerite	sill, gray medium grained tholeiitic dolerite	---	---	1			1						
AT08-825.0	825.0							---	basic intrusion	drill core	dolerite	sill, gray medium grained tholeiitic dolerite	---	---	1			1						
AT08-834.4	834.4							---	basic intrusion	drill core	dolerite	sill, gray medium grained tholeiitic dolerite	---	---	1			1						
AT08-845.1	845.1							---	basic intrusion	drill core	dolerite	sill, gray medium grained tholeiitic dolerite	---	---	1			1				1		
AT08-853.05	853.1							---	basic intrusion	drill core	dolerite	sill, gray aphanitic tholeiitic dolerite, chilled margin(4m in width)	---	---	1			1						
AT08-925.3	925.3							---	basic intrusion	drill core	dolerite	sill, gray fine grained tholeiitic dolerite, weak pyritization	pyrite	---	1			1						
AT08-936.5	936.5							---	basic intrusion	drill core	dolerite	sill, gray medium grained tholeiitic dolerite	---	---	1			1						
AT08-947.75	947.8							---	basic intrusion	drill core	dolerite	sill, gray very fine grained tholeiitic dolerite	---	---	1			1						
TG07-235.0	235.0	50	26	55.9	29	57	57.4	---	basic intrusion	drill core	basalt	sill, black, fine	---	---	1			1						
TG07-250.0	250.0							---	basic intrusion	drill core	basalt	sill, black, fine, pyrite in fracture	pyrite	---	1			1						
TG07-270.0	270.0							---	basic intrusion	drill core	basalt	sill, black, fine	---	---	1			1						
TG114-272.0	272.0	50	39	51.9	30	1	52.9	---	basic intrusion	drill core					1			1						
TG114-275.0	275.0							---	basic intrusion	drill core					1			1						
TG114-278.9	278.9							---	basic intrusion	drill core					1			1						
TG114-283.8	283.8							---	basic intrusion	drill core					1			1						
TG114-286.4	286.4							---	basic intrusion	drill core					1			1						
TG114-289.9	289.9							---	basic intrusion	drill core					1			1			1	1		
TG114-293.7	293.7							---	basic intrusion	drill core					1			1						
TG114-295.0	295.0							---	basic intrusion	drill core					1			1						
TG228-725	725.0	50	5	37.4	29	50	26.4	---	basic intrusion	drill core	dolerite	sill, black, fine	---	---	1			1						
TG228-740	740.0							---	basic intrusion	drill core	dolerite	sill, black, fine	---	---	1			1						
TG228-755.0	755.0							---	basic intrusion	drill core	gabbro	sill, coarse grain, gabbroic	---	---	1			1						

Description of rock and drill core samples

Sample No.	Depeth	Longitude			Latitude			Altitude	Sample Type		Rock Name	Description	Mineral-ization	Weathering	Analysis method								
	m	D	M	S	D	M	S	m							Bulk	PGE	Ar-Ar	Thin	P-Thin	X-ray	EPMA	Nd-Sr Isotope	S-Isotope	NRM
TG228-758.5	758.5							---	basic intrusion	drill core		boundary of fine/coarse part	---	---				1						
TG228-770	770.0							---	basic intrusion	drill core	basalt	sill, black, fine	---	---	1			1						
TG228-785	785.0							---	basic intrusion	drill core	basalt	sill, black, fine	---	---	1			1						
TG228-800	800.0							---	basic intrusion	drill core	basalt	sill, black, fine	---	---	1			1						
TG228-817	817.0							---	basic intrusion	drill core	basalt	sill, black, fine	---	---	1			1				1		
TG228-830	830.0							---	basic intrusion	drill core	basalt	sill, black, fine	---	---	1			1						
TG27-112.0	112.0							---	basic intrusion	drill core	dolerite	sill, reddish black, porphyritic	---	---	1			1						
TG27-119.0	119.0							---	basic intrusion	drill core	basalt	sill, black, fine	---	---	1			1						
TG27-138.5	138.5							---	basic intrusion	drill core	basalt	sill, very fine, chilled margin	---	---	1			1						
TG27-91.5	91.5	50	30	48.2	29	51	31.7	---	basic intrusion	drill core	dolerite	sill, black, middle grained, possible high magnesian	---	---	1			1						
TG27-93.2	93.2							---	basic intrusion	drill core	basalt	sill, black, very fine, chilled margin, possible high magnesian	---	---	1			1						
TG62-176.5	176.5	50	41	8.2	30	2	21.7	---	basic intrusion	drill core					1			1						
TG62-183.5	183.5							---	basic intrusion	drill core					1			1						
TG62-188.0	188.0							---	basic intrusion	drill core					1			1						
TG62-196.7	196.7							---	basic intrusion	drill core					1			1						
TG62-200.5	200.5							---	basic intrusion	drill core					1			1						
TG62-204.0	204.0							---	basic intrusion	drill core					1			1						
TG62-207.7	207.7							---	basic intrusion	drill core					1			1						
TG62-211.4	211.4							---	basic intrusion	drill core					1			1						
TG62-215.4	215.4							---	basic intrusion	drill core					1			1						
TG62-220.0	220.0							---	basic intrusion	drill core					1			1						
TG62-220.4	220.4							---	basic intrusion	drill core					1			1						
TG62-223.4	223.4							---	basic intrusion	drill core					1			1						
TG62-225.0	225.0							---	basic intrusion	drill core					1			1						
TG62-226.3	226.3							---	basic intrusion	drill core					1			1			1			
TG62-226.8	226.8							---	basic intrusion	drill core					1			1						
TG62-227.8	227.8							---	basic intrusion	drill core					1			1						
TG62-234.8	234.8							---	basic intrusion	drill core					1			1						
TG62-237.6	237.6							---	basic intrusion	drill core					1			1				1		
TG62-238.5	238.5							---	basic intrusion	drill core					1			1						
TG95-639.3	639.3	50	10	56.9	29	48	37.0	---	basic intrusion	drill core	basalt	sill, black, chilled margin, pyrite in fracture	pyrite	---	1			1						
TG95-650.3	650.3							---	basic intrusion	drill core	basalt	sill, black, fine	---	---	1			1						
TG95-664.7	664.7							---	basic intrusion	drill core	basalt	sill, black, fine	---	---	1			1						
TG95-682.0	682.0							---	basic intrusion	drill core	dolerite	sill, black, coarse grain, gabbroic	---	---	1			1						
TG95-695.0	695.0							---	basic intrusion	drill core	basalt	sill, black, fine	---	---	1			1						

Description of rock and drill core samples

Sample No.	Depeth	Longitude			Latitude			Altitude	Sample Type		Rock Name	Description	Mineral-ization	Weathering	Analysis method								
	m	D	M	S	D	M	S	m							Bulk	PGE	Ar-Ar	Thin	P-Thin	X-ray	EPMA	Nd-Sr Isotope	S-Isotope	NRM
TG95-709.4	709.4							---	basic intrusion	drill core	basalt	sill, black, fine	---	---	1			1						
TG95-725.0	725.0							---	basic intrusion	drill core	basalt	sill, black, fine	---	---	1			1						
TG95-743.0	743.0							---	basic intrusion	drill core	basalt	sill, black, fine	---	---	1			1						
TG95-756.3	756.3							---	basic intrusion	drill core	basalt	sill, black, fine	---	---	1			1				1		
TG95-772.8	772.8							---	basic intrusion	drill core	basalt	sill, very fine, chilled margin	---	---	1			1						
TG95-825.7	825.7							---	sediment	drill core	shale	black shale of Irati Fm.	---	---										
TG97-563.2	563.2	50	7	46.6	29	51	19.2	---	sediment	drill core	siltstone	pyrite rich silt stone, pyrite conc. In fracture	pyrite	---										
TG97-569.2	569.2							---	basic intrusion	drill core	dolerite	sill, black, very fine, chilled margin	---	---	1			1						
TG97-590.0	590.0							---	basic intrusion	drill core	dolerite	sill, black, fine, pyroxene(1mm) included	---	---	1			1						
TG97-602.0	602.0							---	basic intrusion	drill core	dolerite	sill, black, fine, pyroxene(1mm) included	---	---	1			1						
TG97-615.0	615.0							---	basic intrusion	drill core	dolerite	sill, black, fine, pyroxene(1mm) included	---	---	1			1						
TG97-625.0	625.0							---	basic intrusion	drill core	dolerite	sill, black, fine, pyroxene(1mm) included	---	---	1			1						
TG97-630.0	630.0							---	basic intrusion	drill core	dolerite	sill, black, fine, pyroxene(1mm) included	---	---	1			1						
TG97-650.0	650.0							---	basic intrusion	drill core	dolerite	sill, black, fine, pyroxene(1mm) included	---	---	1			1						
TG97-664.0	664.0							---	basic intrusion	drill core	dolerite	sill, black, very fine, possible chilled margin	---	---	1			1						
FP-02	125.20-125.40	50	35	43.6	23	50	15.2	---	basic intrusion	drill core	dolerite	dark gray, dolerite	---	---	1									
FP-02	580.15-580.40							---	basic intrusion	drill core	dolerite	dark gray, fine, dolerite, py-network	pyrite	---	1				1					
FP-02	582.80-582.95							---	basic intrusion	drill core	dolerite	dark gray, fine, dolerite	---	---	1									
FP-02	586.15-586.35							---	basic intrusion	drill core	dolerite	dark gray, dolerite, chilled margin, py-diss(dot)	pyrite	---	1				1					
FP-02	596.60-596.75							---	basic intrusion	drill core	dolerite	dark gray, dolerite	---	---	1									
FP-02	604.60-604.80							---	basic intrusion	drill core	dolerite	dark gray, coarse grained dolerite(gabbroic), py-diss	pyrite	---	1									
FP-02	605.55-605.70							---	basic intrusion	drill core	dolerite	dark gray, coarse grained dolerite(gabbroic), py-diss	pyrite	---	1				1					
FP-09	24.75-24.95	50	57	20.0	24	32	43.0	---	basic intrusion	drill core	dolerite	greenish gray, amygdaloidal, chilled margin(fine)	---	---	1									
FP-09	173.20-173.40							---	basic intrusion	drill core	dolerite	dark gray, chilled margin (fine)	---	---	1									
FP-09	174.10-174.30							---	sediment	drill core	hornfels	white foot wall hornfels, py-net, native copper?	pyrite, native copper	---	1				2					
SP-21	129.80-130.00	50	30	26.1	23	46	58.7	---	basic intrusion	drill core	dolerite	dark gray fine dolerite(chilled margin), py-diss	py rite	---	1				1					
SP-33	74.50-74.70	50	27	54.4	23	46	29.4	---	basic intrusion	drill core	dolerite	dark gray, fine, dolerite, wk py-diss	pyrite	---	1									
SP-51	171.40-172.05	50	30	18.7	23	46	37.2	---	others	drill core	shale	Irati Py-conc	pyrite	---									1	
SP-64	76.65-76.75	50	28	39.3	23	44	37.7	---	basic intrusion	drill core	dolerite	black fine dolerite, py-diss (film)	pyrite	---	1									
SP-64	133.25-133.45							---	basic intrusion	drill core	dolerite	black fine dolerite, py-diss (film), py-diss along crack	pyrite	---	1									
SP-64	138.15-138.30							---	others	drill core	shale	Irati Py-conc	pyrite	---									1	
SP-65	138.40-138.60	50	28	39.2	23	45	10.2	---	basic intrusion	drill core	dolerite	black, fine and compact dolerite, chilled margin, py-diss along crack	pyrite	---	1									
SP-66	603.35-603.50	50	36	46.0	23	47	10.0	---	basic intrusion	drill core	dolerite	black, dolerite	---	---	1									
SP-66	776.50-776.70							---	basic intrusion	drill core	dolerite	dark gray, dolerite, py-diss(dot)	pyrite	---	1				1					
SP-66	777.50-777.65							---	basic intrusion	drill core	dolerite	dark gray, fine, dolerite, py-diss along crack, chilled margin	pyrite	---	1									

Description of rock and drill core samples

Sample No.	Depeth	Longitude			Latitude			Altitude	Sample Type		Rock Name	Description	Mineral-ization	Weathering	Analysis method									
	m	D	M	S	D	M	S	m							Bulk	PGE	Ar-Ar	Thin	P-Thin	X-ray	EPMA	Nd-Sr Isotope	S-Isotope	NRM
FP-08	216.40-216.60	50	57	28.5	24	52	59.0	---	basic intrusion	drill core	dolerite	gray, dolerite, py-diss(dot)	pyrite	---	1									
FP-08	218.50-218.70							---	basic intrusion	drill core	dolerite	gray, dolerite, py-diss(dot)	pyrite	---	1									
FP-08	249.90-250.10							---	basic intrusion	drill core	dolerite	gray, dolerite, py-diss?	pyrite	---	1									
SP-30	55.20-55.40	50	28	23.2	23	47	33.7	---	basic intrusion	drill core	dolerite	gray, dolerite, py-diss(dot)	pyrite	---	1									
NF-09	25.85-26.00	50	38	3.9	23	56	27.8	---	basic intrusion	drill core	dolerite	dark gray, dolerite	---	---	1									
NF-09	46.65-46.85							---	basic intrusion	drill core	gabbro	greenish gray, gabbro, m.weathered	---	weathering	1									
NF-09	58.70-58.90							---	basic intrusion	drill core	gabbro	greenish gray, gabbro, m.weathered, qtz-network included(a few %)	---	weathering	1									
NF-09	70.70-70.90							---	others	drill core	gabbro	greenish gray, gabbro, m.weathered, qtz-network included(30%), py-diss along qtz	pyrite	weathering	1				1					
NF-09	80.80-81.00							---	basic intrusion	drill core	dolerite	dark gray, dolerite, brown dot of stain (py-diss?)	pyrite	---	1									
NF-09	100.75-100.90							---	basic intrusion	drill core	dolerite	dark gray, dolerite	---	---	1									
NF-09	126.10-126.30							---	basic intrusion	drill core	gabbro	greenish gray, gabbro	---	---	1									
NF-09	141.80-142.00							---	basic intrusion	drill core	dolerite	greenish gray, dolerite, m.weathered	---	weathering	1									
NF-09	152.45-152.65							---	sediment	drill core	tuff	footwall Irati tuff? Py-conc.	pyrite	---	1									
SP-17	529.45-529.65	50	33	46.9	23	46	27.0	---	basic intrusion	drill core	dolerite	dark gray, dolerite(fine, basaltic), wk py-diss	pyrite	---	1									
SP-17	731.00-731.20							---	basic intrusion	drill core	dolerite	dark gray, dolerite(fine, basaltic), wk py-diss along crack	pyrite	---	1				1					
SP-17	734.40-734.55							---	sediment	drill core	mudstone	footwall wk sil mud、py-diss (pach)	pyrite	---	1				1		1		1	
SP-17	735.30-735.45							---	sediment	drill core	mudstone	footwall wk sil mud、py-diss(dot)	pyrite	---	1				1		1			
SP-23	625.60-625.70	50	33	16.9	23	44	11.8	---	basic intrusion	drill core	dolerite	dark gray, dolerite(fine, basaltic), chilled margin	---	---	1									
SP-23	701.80-701.90							---	basic intrusion	drill core	dolerite	dark gray, dolerite(fine, basaltic), wk py-diss, chilled margin	pyrite	---	1									
NF-05	168.20-168.30	50	34	50.2	23	51	59.1	---	basic intrusion	drill core	dolerite	dark gray-black dolerite	---	---	1									
SP-10	234.95-235.05	50	32	18.1	23	45	23.8	---	basic intrusion	drill core	dolerite	black, dolerite(fine), py-diss along crack	pyrite	---	1									
SW-01	285.30-285.40	49	42	23.0	28	56	43.7	---	basic intrusion	drill core					1									
SW-01	461.20-461.40							---	basic intrusion	drill core	basalt	dark grey, chilled margin, fine grain	---	---	1									
SW-01	533.05-533.25							---	basic intrusion	drill core	basalt	dark grey, chilled margin, fine grain	---	---	1									
SW-01	547.10-547.30							---	sediment	drill core	hornfels	sediment (hornfels), pyrite veinlet.	pyrite	---	1								1	
SW-01	553.15-553.35							---	basic intrusion	drill core	dolerite	dolerite, quartz vein with pyrite and chalcopyrite?	pyrite, chalcopyrite?	---	1					1				
SW-01	556.55-556.70							---	basic intrusion	drill core	basalt	dark grey, child margin, fine grain, dissemination of fine grained pyrite.	pyrite	---	1									
SW-03	234.00-234.20	49	40	6.5	28	41	39.9	---	basic intrusion	drill core	dolerite	dolerite, dissemination of pyrite (in matrix and along cruck).	pyrite	---	1					1			1	
SW-03	235.00-235.30							---	basic intrusion	drill core	basalt	basalt	---	---	1									
AT-09	365.30-365.50	49	51	39.3	29	25	8.1	---	basic intrusion	drill core	dolerite	dolerite, dark grey, a few pyrite.	pyrite	---	1					1				
AT-09	576.50-576.70							---	basic intrusion	drill core	dolerite	dark gray, dolerite, py-diss	pyrite	---	1									
AT-09	601.10-601.20							---	basic intrusion	drill core	dolerite	coase grained dolerite (gabbro), a few pyrrhotite.	pyrrhotite	---	1					1			1	
AT-09	657.70-657.90							---	basic intrusion	drill core	dolerite	dolerite, dark grey, CPX>>olivine+plagioclase, magnetite rich.	---	---	1									
AT-09	680.25-680.65							---	basic intrusion	drill core	dolerite	chilled margin, dark gray, very fine	pyrite?	---	1									
AT-06	715.40-715.50	49	45	16.4	29	15	54.4	---	basic intrusion	drill core	basalt	chilled margin, dark grey, pyrite along cruck.	pyrite	---	1					1				

Description of rock and drill core samples

Sample No.	Depeth	Longitude			Latitude			Altitude	Sample Type		Rock Name	Description	Mineral-ization	Weathering	Analysis method									
	m	D	M	S	D	M	S	m							Bulk	PGE	Ar-Ar	Thin	P-Thin	X-ray	EPMA	Nd-Sr Isotope	S-Isotope	NRM
AR-01-RS	30-40	52	19	39.0	27	24	16.0	---	basic lava	drill cuttings	---	---	---	---	1									
AR-01-RS	70-80							---	basic lava	drill cuttings	---	---	---	---	1									
AR-01-RS	110-120							---	basic lava	drill cuttings	---	---	---	---	1									
AR-01-RS	150-160							---	basic lava	drill cuttings	---	---	---	---	1									
AR-01-RS	190-200							---	basic lava	drill cuttings	---	---	---	---	1									
AR-01-RS	230-240							---	basic lava	drill cuttings	---	---	---	---	1									
AR-01-RS	270-280							---	basic lava	drill cuttings	---	---	---	---	1									
AR-01-RS	310-320							---	basic lava	drill cuttings	---	---	---	---	1									
AR-01-RS	350-360							---	basic lava	drill cuttings	---	---	---	---	1									
AR-01-RS	390-396							---	basic lava	drill cuttings	---	---	---	---	1									
PP-02-SP	240-250	51	24	50.5	22	7	19.6	---	basic lava	drill cuttings	---	---	---	---	1									
PP-02-SP	280-290							---	basic lava	drill cuttings	---	---	---	---	1							1		
PP-02-SP	320-330							---	basic lava	drill cuttings	---	---	---	---	1									
PP-02-SP	360-370							---	basic lava	drill cuttings	---	---	---	---	1									
PP-02-SP	400-410							---	basic lava	drill cuttings	---	---	---	---	1									
PP-02-SP	440-450							---	basic lava	drill cuttings	---	---	---	---	1							1		
PP-02-SP	480-490							---	basic lava	drill cuttings	---	---	---	---	1									
PP-02-SP	520-530							---	basic lava	drill cuttings	---	---	---	---	1									
PP-02-SP	560-570							---	basic lava	drill cuttings	---	---	---	---	1									
PP-02-SP	600-610							---	basic lava	drill cuttings	---	---	---	---	1							1		
PP-02-SP	640-650							---	basic lava	drill cuttings	---	---	---	---	1									
PP-02-SP	680-690							---	basic lava	drill cuttings	---	---	---	---	1									
PP-02-SP	720-730							---	basic lava	drill cuttings	---	---	---	---	1									
PP-02-SP	760-770							---	basic lava	drill cuttings	---	---	---	---	1							1		
PP-02-SP	800-810							---	basic lava	drill cuttings	---	---	---	---	1							1		
PP-02-SP	840-850							---	basic lava	drill cuttings	---	---	---	---	1									
PP-02-SP	880-890							---	basic lava	drill cuttings	---	---	---	---	1									
PP-02-SP	920-930							---	basic lava	drill cuttings	---	---	---	---	1									
PP-02-SP	960-970							---	basic lava	drill cuttings	---	---	---	---	1							1		
PP-02-SP	1000-1010							---	basic lava	drill cuttings	---	---	---	---	1									
PP-02-SP	1042-1052							---	basic lava	drill cuttings	---	---	---	---	1									
PP-02-SP	1070-1080							---	basic lava	drill cuttings	---	---	---	---	1									
PP-02-SP	1120-1130							---	basic lava	drill cuttings	---	---	---	---	1							1		
PP-02-SP	1160-1170							---	basic lava	drill cuttings	---	---	---	---	1									
PP-02-SP	1200-1210							---	basic lava	drill cuttings	---	---	---	---	1									

Description of rock and drill core samples

Sample No.	Depeth	Longitude			Latitude			Altitude	Sample Type		Rock Name	Description	Mineral-ization	Weathering	Analysis method									
	m	D	M	S	D	M	S	m							Bulk	PGE	Ar-Ar	Thin	P-Thin	X-ray	EPMA	Nd-Sr Isotope	S-Isotope	NRM
PP-02-SP	1240-1250							---	basic lava	drill cuttings	---	---	---	---	1									
PP-02-SP	1280-1290							---	basic lava	drill cuttings	---	---	---	---	1							1		
PP-02-SP	1320-1330							---	basic lava	drill cuttings	---	---	---	---	1									
PP-02-SP	1380-1390							---	basic lava	drill cuttings	---	---	---	---	1	1						1		
PP-02-SP	1420-1430							---	basic lava	drill cuttings	---	---	---	---	1									
PP-02-SP	1460-1470							---	basic lava	drill cuttings	---	---	---	---	1							1		
PP-02-SP	1500-1510							---	basic lava	drill cuttings	---	---	---	---	1									
PP-02-SP	1540-1550							---	basic lava	drill cuttings	---	---	---	---	1	1						1		
PP-02-SP	1590-1600							---	basic lava	drill cuttings	---	---	---	---	1	1						1		
RP-03-SP	220-230	49	22	23.7	20	48	27.1	---	basic lava	drill cuttings	---	---	---	---	1									
RP-03-SP	260-270							---	basic lava	drill cuttings	---	---	---	---	1									
RP-03-SP	400-410							---	basic lava	drill cuttings	---	---	---	---	1									
RP-03-SP	440-450							---	basic lava	drill cuttings	---	---	---	---	1									
RP-03-SP	480-490							---	basic lava	drill cuttings	---	---	---	---	1									
RP-03-SP	600-610							---	basic lava	drill cuttings	---	---	---	---	1									
RP-03-SP	640-650							---	basic lava	drill cuttings	---	---	---	---	1									
RP-03-SP	680-690							---	basic lava	drill cuttings	---	---	---	---	1									
RP-03-SP	800-810							---	basic lava	drill cuttings	---	---	---	---	1									
CA-85	432.20-432.70	50	40	46	29	43	50.9	---	basic intrusion	drill core					1									
CA-85	473.00-473.50							---	basic intrusion	drill core					1									
CA-85	522.50-522.95							---	basic intrusion	drill core					1									
CA-85	637.40-637.90							---	basic intrusion	drill core					1									
CA-85	666.15-666.65							---	basic intrusion	drill core					1									
CA-86	496.25-496.75	50	33	39.7	29	45	36.9	---	basic intrusion	drill core					1									
CA-86	516.50-517.00							---	basic intrusion	drill core					1									
CA-86	548.75-549.25							---	basic intrusion	drill core					1									

Analysis type

Bulk: Whole rock analysis (including of Au, Pt and Pd assay)
PGE: Measurement of Ir, Rh and Re contents (ICP)
Ar-Ar: $^{40}Ar-^{39}Ar$ dating
Thin: Microscopic observation of thin section
P-thin: Microscopic observation of polished-thin section
X-ray: Powdary X-ray diffraction
EPMA: Erectron microprobe analysis
Nd-Sr isotope: Measurement of $^{143}Nd/^{144}Nd$ and $^{87}Sr/^{86}Sr$ isotopic ratio
S-isotope: Measurement of $\sigma\ ^{34}S$ isotopic ratio
NRM: Measurement of natural remanent magnetism

APPENDIX 5

Microscopic observation of thin and polished-thin section for rock samples

Sampe No.	Sample Type	Rock Name	Magma Type	Mg#	Minerals																Note
					pl	am	opx	cpx	ol	qz	chl	ca	serp	opaque							
														mt	chr	sul	pyrr	py	cp	
AS001	lava	cpx basalt	Gramado	72.3	◎		・	○			・			△		・?				
AS002	lava	ol bearing cpx basalt	Paranapanema	60.6	◎		・	○			・		・	△		・?				coarse basalt(or dolerite)
AS003	lava	ol bearing cpx basalt	Ribeira	70.5	◎		・	○	・		・		・	△		・?				
AS004A	lava	ol bearing cpx basalt	Paranapanema	61.4	◎		・	○	・		・		・	△		・?				contact with cpx dolerite
AS005	lava	ol bearing cpx basalt	Paranapanema	64.3	◎		・	○	・		△		△	△		・?				
AS006	lava	ol bearing cpx basalt	Paranapanema	64.1	◎		・	○			・		・	△		・?				
AS007	lava	ol bearing cpx basalt	Paranapanema	63.6	◎		・	○			・		・	△		・?				
AS008	lava	ol cpx dolerite	Pitanga	66.7	◎		・	○	・		△		△	△		・?				
AS009	lava	ol bearing cpx basalt	Paranapanema	59.5	◎		・	○			・		・	△		・?				ferric hydroxide
AS010	dyke	cpx dolerite	Paranapanema	61.0	◎			○			・			△		・?				
AS011	dyke	cpx dolerite	Paranapanema	59.8	◎			○			・			△		・?				ol(idingsite) bearing?
AS013	dyke	cpx gabbro	Paranapanema?	52.1	◎		・	○		・	・			△		・?				
AS014	sill	ol bearing cpx gabbro	unclassify	43.1	◎		・	○	・	・	・		・	△		・?				needle shape cpx(1cm×0.2mm)
AS015A	dyke	ol bearing cpx dolerite	Acidic rock	23.1	◎		・	○	・		・		・	△		・?				
AS015B	dyke	cpx basalt	Pitanga	55.2	◎		・	○	・?		・			△		・?				partly brown glass matrix
AS016A	dyke	cpx dolerite	Paranapanema-Ribeira	63.5	◎		・	○			・			△		・?				
AS016B	dyke	cpx dolerite	Paranapanema-Ribeira	55.6	◎		・	○		・	・			△		・?				
AS017	dyke	cpx dolerite	unclassify	47.8	◎		・	○		・	・	・		△		・?				
AS018	sill	cpx dolerite	Paranapanema	60.4	◎		・	○			・			△		・?				
AS021	lava	ol bearing cpx basalt	Gramado	66.0	◎		・	○	・		・		・	△		・?				coarse basalt
AS023	lava	cpx basalt	Gramado?	53.5	◎		・	○			・			△		・?				partly brown glass matrix
AS024A	lava	cpx basalt	Esmeralda	70.1	◎		・	○			・			△		・?				
AS024B-1	dyke	cpx basalt (fragment)	unclassify	79.4	◎		・	○			・	・		△		・?				intergranular texture
AS024B-2	dyke	cpx ol basalt (matrix)	unclassify	79.4	◎		△	・	△		・	・		△		・?				glass matrix with phenocrysts
AS025	lava	weathered cpx basalt	unclassify	61.5	◎		・	○			△			△		・?				partly glass matrix
AS026	(Lajes district)	weathered basalt	kimberlite	80.5	◎		・	△			△	△	・	△		・?				hyaloclastite
AS027	(Lajes district)	cpx basalt	kimberlite	66.8	◎		・	○			△		・	△		・?				ferric hydroxide
AS028A	(Lajes district)	trachy andesite	phonolite	13.7	◎	○					△	・								alkaline feldspar and alkaline amphibole
KM104	lava	cpx basalt	Esmeralda	67.5	◎			△		・	・			△						cryptocrystalline
KM111	lava	ol-bearing cpx basalt	Paranapanema-Ribeira	67.0	◎		△	○	・		・			△			・			intergranular texture, iddingsite

Microscopic observation of thin and polished-thin section for rock samples

Sampe No.	Sample Type	Rock Name	Magma Type	Mg#	Minerals																Note
					pl	am	opx	cpx	ol	qz	chl	ca	serp	opaque							
														mt	chr	sul	pyrr	py	cp	
KM129	lava	cpx basalt	Paranapanema	57.4	◎		△	○			・			△						intersartal texture, iddingsite
KM130B	sill or dyke	cpx dolerite	Paranapanema-Ribeira	66.4	◎		・	○			△			△			・			
KM137	lava	cpx basalt	Paranapanema-Ribeira	66.7	◎		・	○		・	・			△						intergranular texture, gas cavity
KM144	lava	cpx basalt	Paranapanema	58.1	◎		・	○			・			△					・	glass matrix(partly)
KM161	lava	cpx basalt	Paranapanema-Ribeira	63.9	◎		・	○			・			△			・			intergranular texture, iddingsite
KM163	lava	cpx basalt	Paranapanema-Ribeira	65.4	◎		・	○			△			△						intersertal texture, iddingsite
KN001	sill	cpx basalt	Gramado?	78.0	◎			・						・						autobrecciated texture
KN002	sill	olivine gabbro	Gramado?	88.5	◎		△	△	◎					・	・					
KN003	dyke	olivine basalt	Gramado?	81.5	◎			○	○		・			・	・?					ferric hydroxide (reddish)
KN005	lava	cpx basalt	Gramado	59.8	◎			○		・	・			△						
KN006	lava	cpx basalt	Esmeralda	66.8	◎			○			・			△						
KN009	lava	cpx basalt	Esmeralda	68.9	◎			○		・	・			△						green clay mineral(malachite?)
KN011	lava	cpx basalt	Esmeralda	66.8	◎			○			・			△						
KN012	lava	ol-cpx basalt	Esmeralda?	67.8	◎			○			△		△	・		・?				coarse basalt
KN014	lava	ol-cpx basalt	Pitanga?	60.6	◎			○			△		△	・		・?				coarse basalt
KN016	lava	cpx basalt	Paranapanema	59.1	◎			○			・			△						
KN017	lava	cpx basalt	Ribeira	67.6	◎			○			・			△						
KN018	lava	ol-cpx basalt	Pitanga	56.7	◎			○			△		△	△		・?				
KN019	lava	cpx basalt	Ribeira	68.4	◎			○			・			△		・?				
KN020	lava	ol bearing cpx basalt	Paranapanema	65.0	◎			○			・		・	△		・?				
KN021	lava	ol-cpx basalt	Paranapanema	65.7	◎			○			△		△	△		・?				
KN022A	lava	ol-cpx basalt	Paranapanema	65.4	◎			○			△		△	△		・?				
KN022B	lava	weathered dolerite	---	47.3	◎			△			○			△		・?				ferric hydroxide, malachite?
KN023A	lava	ol bearing cpx basalt	Paranapanema	65.2	◎			○			・		・	△		・?				
KN023B	lava	cpx dolerite	---	49.9	◎			○			△			△		・?				chlorite-epidote
KN023C	lava	ol-bearing cpx basalt	---	---	◎			○			△		・	△		・?				
KN024A	lava	ol-bearing cpx basalt	Paranapanema	66.0	◎			○			△		・	△		・?				
KN024B	lava	weathered dolerite	---	49.7	○			△		・	○			△		・?				malachite? , needle shape weatherd mineral
KN025A	lava	ol cpx basalt	Ribeira	66.6	◎		・	○			△		・	△		・?				
KN025B	lava	cpx dolerite	---	52.2	◎		・	○		・	△			△		・?				malachite?(○)

Microscopic observation of thin and polished-thin section for rock samples

Sampe No.	Sample Type	Rock Name	Magma Type	Mg#	Minerals																Note
					pl	am	opx	cpx	ol	qz	chl	ca	serp	opaque							
														mt	chr	sul	pyrr	py	cp	
KN026	lava	ol cpx basalt	Paranapanema	65.7	◎		・	○			△		・	△		・?				
KN027	lava	ol bearing cpx basalt	Paranapanema	59.9	◎			○		・	・		・	△		・?				malachite?(・)
KN028	lava	cpx-basalt	Paranapanema	59.7	◎			○			・			△		・?				ferric hydroxide
KN029	lava	cpx-basalt	Paranapanema	54.1	◎			○			・			△		・?				ferric hydroxide
KN030	lava	cpx-basalt	Paranapanema	59.7	◎			○			・			△	・?	・?				
KN031	lava	cpx-basalt	Paranapanema	57.3	◎		・	○			・			△		・?				
KN032	lava	cpx-basalt	Ribeira	69.0	◎			○			・			△		・?				
KN033	lava	cpx-basalt	Paranapanema	57.3	◎			○			・			△		・?				
KN034A	sill	cpx-basalt	Pitanga	65.2	◎		・	○			・			△		・?				
KN034B	sill	cpx dolerite	---	48.4	◎		・	○			・			△		・?				
KN035B	sill	cpx gabbro	---	---	◎		・	○			・			△		・?				
KN037	dyke	cpx gabbro	Paranapanema	53.6	◎		・	○			・			△		・?				
KN039A	sill	cpx gabbro	Paranapanema-Ribeira	67.4	◎		・	○			・			△		・?				
KN039B	sill	cpx gabbro	---	52.8	◎		・	○		・	・			△		・?				
KN040A	sill	ol bearing cpx dolerite	Paranapanema	64.3	◎		・	○	・		・		・	△		・?				
KN040C	sill	ol bearing cpx dolerite	---	55.9	◎		・	○	・		・		・	△		・?				
KN042	lava	weathered pyroxene basalt	Gramado	67.6	◎			・		・	・	・		△		・?				or weathered basaltic andesite
KN043	lava	cpx basalt	Acidic rock	36.0	◎		・	○		・	・			△		・?				
KN044	lava	cpx basalt	Gramado	70.5	◎		・	○			・			△		・?				
KN045	lava	cpx basalt	Gramado?	63.4	◎		・	○			・			△		・?				
KN046A	lava	ol bearing cpx dolerite	Gramado	69.6	◎		・	○	・		・		・	△		・?				ferric hydroxide
KN047	lava	ol bearing cpx dolerite	Pitanga	56.1	◎		・	○	・		・		△	△		・?				ferric hydroxide
KN048A	lava	ol bearing cpx dolerite	Gramado	57.7	◎		・	○	・		・		・	△		・?				
KN048B	lava	weathered dolerite	---	43.0	◎			・			△		・	△		・?				
KN049	lava	ol cpx basalt	Ribeira	66.0	◎		・	○			・		・	△	・?	・?				
KN050	lava	ol cpx basalt	Paranapanema	65.4	◎		・	○			・		・	△	・?	・?				
KN051	lava	ol cpx basalt	Paranapanema	59.1	◎		・?	○			・		・	△		・?				
KN052	lava	ol cpx basalt	Ribeira	67.6	◎		・?	○			・		・	△		・?				coarse basalt(or dolerite)
KN053	lava	weathered cpx basalt	---	---	◎			・			△			△		・?				or weathered basaltic andesite
KN105A	dyke	cpx dolerite(-gabbro)	Paranapanema-Ribeira	57.4	◎		・	◎			・			△			△	・	・	

Microscopic observation of thin and polished-thin section for rock samples

Sampe No.	Sample Type	Rock Name	Magma Type	Mg#	Minerals																Note
					pl	am	opx	cpx	ol	qz	chl	ca	serp	opaque							
														mt	chr	sul	pyrr	py	cp		
KN117	sill	cpx gabbro	Paranapanema?	52.6	◎		・	○			△			△			△	・	・		
KN119	sill	cpx gabbro	Paranapanema	53.7	◎	・		○		・	・			△			・	・	・		
KN121	dyke	ol-bearing cpx basalt	Pitanga?	57.8	◎		・	○	・		・			△			△	・	・		intergranular texture, iddingsite
KN123	dyke	cpx gabbro	Paranapanema-Ribeira	57.1	◎	・	・	○			・			△			・	・			
KN128	dyke	cpx gabbro	Pitanga	56.4	◎	・	・	○		・	・	・		△			・	・			
KN142	sill	cpx dolerite	Paranapanema-Ribeira	48.8	◎			○			・			△			・				
KN146	sill	cpx basalt	Pitanga	58.2	◎		・	○		・	・	・		△			・				intergranular texture
KN150	sill	cpx gabbro	Pitanga	54.1	◎		・	○		・	・	・		△			・	・			
KN151	dyke	ol-bearing cpx basalt	Pitanga?	55.2	◎		・	○	・		・			△			・	・			intergranular texture, pyroxinite xenolith
KN162	sill	ol-bearing cpx dolerite	Pitanga?	35.7	◎	・	・	○	・	・	・			・			・				iddingsite
KN164	dyke	cpx gabbro	Ribeira	68.6	◎		・	○			・	・		△			・	・			
KN167B	dyke	cpx gabbro	Pitanga	45.7	◎		・	○			△			△			・	・			
KN168	lava	cpx basalt	Acidic rock	39.5	◎		・	△			・			△			△	・			intergranular texture
KN169	sill	cpx gabbro	Esmeralda	58.6	◎		・	○			・			△			・	・			
KN171	sill	cpx gabbro	Paranapanema-Ribeira	58.6	◎		・	○		・	・			△			・	・			
TM101	dyke	ol-bearing cpx basalt	Urubici?	78.7	◎		・	○	・		・			△							cryptocrystalline
TM105	sill	cpx gabbro	Pitanga	52.2	◎		・	○			・			△			・	・			
TM111	dyke	ol-bearing cpx basalt	Pitanga	57.7	◎			○	・		・	・		△			・	・			gas cavity, idingsite, cryptocrystalline
TM113	lava	cpx basalt	Pitanga	53.2	◎		・	○			・			△			・				intergranular texture
TM117	sill	ol-bearing cpx basalt	Pitanga?	74.6	○		・	○	・		△	・		△							glass-cryptocrystalline matrix
TM132	lava	ol-bearing cpx basalt	Pitanga	56.3	◎		・	△	・	・	△			・							gas cavity, idingsite, cryptocrystalline
TM148	sill	ol-bearing cpx gabbro	Pitanga	51.6	◎		・	○	・		△			△			・	・	・		
YM108	lava	cpx basalt	Gramado	64.1	◎		・	○			・			△			・				intergranular texture, iddingsite
YM117	lava	cpx basalt	Paranapanema	58.9	◎		・	○			・			△			・				intergranular texture, iddingsite
YM119	lava	ol-bearing cpx basalt	Paranapanema-Ribeira	68.7	◎		△	○	・		・			△			・				intergranular texture, iddingsite
YM122	lava	cpx basalt	Paranapanema	59.8	◎		・	○			△			△			△				idingsite, cryptocrystalline, native copper (2 grains)
YM139	lava	ol-bearing cpx dolerite	Pitanga?	47.4	◎		△	○	・	・	・			△			・				iddingsite
YM150	dyke	cpx basalt	Gramado	63.9	◎		・	△		・	・			・							cryptocrystalline
YM156	sill	ol-bearing cpx basalt	Gramado?	67.8	◎			○	・		・			△			・				intergranular texture
YM173	sill	cpx gabbro	Gramado	37.2	◎		・	○		・	・			△			・	・			iddingsite

Microscopic observation of thin and polished-thin section for rock samples

Sampe No.	Sample Type	Rock Name	Magma Type	Mg#	Minerals																Note
					pl	am	opx	cpx	ol	qz	chl	ca	serp	opaque							
														mt	chr	sul	pyrr	py	cp		
YM176	sill	cpx gabbro	Gramado?	40.9	◎		・	○		・	・			△			・	・			
YM179	lava	cpx basalt	Urubici	63.0	◎		・	△			・			△			・				glass-cryptocrystalline matrix, native cupper (3 grains)
YM188	dyke	cpx dolerite	Urubici?	61.3	◎	・	・	○		・	・			△			・	・			
YM198	dyke	cpx basalt(-dolerite)	Esmeralda	66.9	◎		・	○			・			△			・	・	・		intergranular texture, iddingsite
YM211	sill	cpx basalt	Urubici	62.2	◎		・	○		・	・			△			・				intergranular texture, iddingsite
YM212	sill	cpx basalt	Urubici	63.2	◎		・	○			・			・							intersertal texture, iddingsite
YM228	lava	cpx basalt	Esmeralda	55.6	◎		・	○		・	・			△							intergranular texture
YM231	lava	cpx basalt	Esmeralda?	58.6	◎		・	○			・			△			・				intergranular texture
WW017	lava	aphilic andesite	Acidic rock	45.9	◎					・				・							idingsite
WW024	lava	cpx basalt	Gramado	63.5	◎		・	○	・		・			△		・?					
WW026	lava	andesite	Acidic rock	42.9	◎			△		・	・			△		・?					
WW031	lava	cpx basalt	Esmeralda	57.7	◎			○			・			△		・?					
WW056	lava	cpx basalt	Paranapanema	64.4	◎			○			・		・	△		・?					ferric hydroxide (reddish)
WW068	lava	sandstone	Acidic rock	59.3	◎						・	・		△							medium grain size, rock fragment is absent
WW069	lava	cpx basalt	Acidic rock	49.5	◎			○			・		・	△		・?					ferric hydroxide (reddish)
WW073	lava	cpx basalt	Gramado	48.3	◎			△			・			・							fine
WW076	lava	ol-cpx dolerite	Gramado	70.9	◎			○	・		・		△	△							
WW077	lava	ol-cpx dolerite	Gramado	73.1	◎			○	・		・		△	△							
WW083	lava	cpx basalt	Gramado	58.6	◎			○			・			△		・?					
WW092	lava	ol bearing cpx basalt	Esmeralda	69.1	◎			○			・		△	△		・?					ferric hydroxide (reddish)
WW095	lava	ol bearing cpx basalt	Esmeralda	65.5	◎			○			・		△	△		・?					ferric hydroxide (reddish)
WW099	lava	ol bearing cpx basalt	Gramado	75.1	◎			○		・	・		・	△							
WW117a	lava	cpx basalt	Gramado	65.6	◎			○			・			△							ferric hydroxide (reddish)
WW122	lava	ol bearing cpx basalt	Urubici	59.0	◎			○		・	・		・	△							
WW129	lava	cpx basalt	Gramado	63.7	◎			○			・			△							ferric hydroxide (reddish)
WW130	lava	cpx basalt	Esmeralda	71.0	◎			○			・			△							
WW134	lava	cpx basalt	Gramado	66.3	◎			○			・			△							
AC-028	lava	cpx basalt	Ribeira	70.0	◎			○			・			△		・?					green clay mineral(malachite?)
AC-034B	lava	cpx dolerite	Paranapanema	63.4	◎			○			・			△							green clay mineral(malachite?)
AC-035	lava	cpx basalt	Paranapanema	59.4	◎			○			・			△							ferric hydroxide (reddish)

Microscopic observation of thin and polished-thin section for rock samples

Sampe No.	Sample Type	Rock Name	Magma Type	Mg#	Minerals																Note
					pl	am	opx	cpx	ol	qz	chl	ca	serp	opaque							
														mt	chr	sul	pyrr	py	cp	
ACR-119	lava	cpx basalt	Acidic rock	43.6	◎			○			・			△						partly spinifex-like texture,
ACR-125	lava	cpx olivine dolerite	Pitanga	55.7	◎			△			△		○	△		・?				
ADR-033	lava	cpx basalt	Gramado	61.0	◎			○			・			△		・?				green clay mineral(malachite?)
5AT03-SC-486.3	sill (drill core)	basalt with shear plane	Gramado?	66.3	○			・		・	・	・		・		・?				
5AT03-SC-487.0	sill (drill core)	cpx basalt	Gramado	62.7	○			・		・	・	・		△		・?				needle shape opaque,
5AT03-SC-498.5	sill (drill core)	cpx gabbro	Gramado	50.6	◎			○			・			△		・?				
5AT03-SC-509.4	sill (drill core)	cpx gabbro	Gramado	48.9	◎			○			・	・		△		・?				
5AT03-SC-519.2	sill (drill core)	cpx gabbro	Gramado	52.7	◎			○			・			△		・?				
5AT03-SC-528.9	sill (drill core)	cpx gabbro	Gramado	51.1	◎			○			・			△		・?				
5AT03-SC-537.3	sill (drill core)	cpx gabbro	Gramado	50.5	◎			○	・		・			△		・?				
5AT03-SC-547.4	sill (drill core)	cpx basalt	Gramado	50.5	◎			○		・	・			△		・?				fine, quartz vain,
5AT03-SC-590.1	sill (drill core)	cpx basalt	Gramado	52.1	◎			○		・	・			△		・?				
5AT03-SC-600.0	sill (drill core)	cpx dolerite	Esmeralda	51.8	◎			○		・	・			△		・?				
5AT03-SC-607.9	sill (drill core)	cpx dolerite	Esmeralda	51.9	◎			○		・	・			△		・?				
5AT03-SC-616.9	sill (drill core)	cpx basalt	Esmeralda	51.9	◎			○		・	・			△		・?				
5AT08-SC-792.4	sill (drill core)	cpx basalt	Gramado	47.8	◎			○		・	・			△		・?				
5AT08-SC-802.85	sill (drill core)	cpx gabbro	Gramado	37.4	◎			○			・			△		・?				
5AT08-SC-815.1	sill (drill core)	cpx dolerite	Gramado	50.6	◎			○			・			△		・?				
5AT08-SC-825.0	sill (drill core)	cpx dolerite	Gramado	51.4	◎			○			・			△		・?				
5AT08-SC-834.4	sill (drill core)	cpx dolerite	Gramado	51.5	◎			○			・			△		・?				coase
5AT08-SC-845.1	sill (drill core)	cpx dolerite	Gramado	50.9	◎			○			・			△		・?				
5AT08-SC-853.05	sill (drill core)	cpx basalt	Gramado	51.3	◎			○			△			△		・?				epidote-chlorite vein
5AT08-SC-925.3	sill (drill core)	cpx basalt	Gramado?	46.6	◎			○			・		・	△		・?				
5AT08-SC-936.5	sill (drill core)	cpx basalt	Gramado	45.6	◎			○			・			△		・?				
5AT08-SC-947.75	sill (drill core)	cpx basalt	Gramado	49.8	◎			○			・			△		・?				fine grained
TG07-235.0	sill (drill core)	basaltic andesite	Gramado?	39.6	◎			△	・	・	・			・						
TG07-250	sill (drill core)	basaltic andesite	Gramado?	39.1	◎			△	・	・	・			・						
TG07-270.0	sill (drill core)	basaltic andesite	Gramado?	37.2	◎			△	・	・	・			・						
TG114-272.0	sill (drill core)	cpx basalt	Gramado	71.0	◎		・	○			・			・						
TG114-275.0	sill (drill core)	cpx basalt	Gramado	71.0	◎		・	○			・			・						

Microscopic observation of thin and polished-thin section for rock samples

Sampe No.	Sample Type	Rock Name	Magma Type	Mg#	Minerals															Note
					pl	am	opx	cpx	ol	qz	chl	ca	serp	opaque						
														mt	chr	sul	pyrr	py	cp	
TG114-278.9	sill (drill core)	basalt with gabbro	Gramado?	78.7	◎		・	○			・		・	・	・	・?				mixed texture, contact part
TG114-283.8	sill (drill core)	olivine gabbro	Gramado?	88.8	◎		・	○	・		△		◎	・	・	・?				
TG114-286.4	sill (drill core)	olivine gabbro	Gramado?	90.5	◎		・	○	◎		・		・	・	・					
TG114-289.9	sill (drill core)	olivine gabbro	Gramado?	88.6	◎		・	○	◎		・		・	・	・					
TG114-293.7	sill (drill core)	olivine gabbro	Gramado?	84.8	◎		・	○	○		・		△	・	・					
TG114-295.0	sill (drill core)	olivine gabbro	Gramado?	82.8	◎		・	○	・		△		◎	・	・	・?				
TG228-725	sill (drill core)	cpx basalt	Gramado	61.1	◎		・	○			・			△		・?				
TG228-740	sill (drill core)	cpx dolerite	Gramado	60.7	◎		・	○			・			△		・?				
TG228-755	sill (drill core)	cpx gabbro	Paranapanema	51.5	◎		・	○			・			△						
TG228-758.5	sill (drill core)	cpx gabbro	Gramado	63.1	◎		・	○			・			△						
TG228-770	sill (drill core)	cpx gabbro	Gramado	64.7	◎		・	○			△			△						
TG228-785	sill (drill core)	cpx dolerite	Gramado	61.8	◎		・	○			・			△						
TG228-800	sill (drill core)	cpx dolerite	Gramado	61.8	◎		・	○			・			△						
TG228-817	sill (drill core)	cpx dolerite	Gramado	61.6	◎		・	○			・			△						
TG228-830	sill (drill core)	cpx dolerite	Gramado	61.6	◎		・	○			・			△						
TG27-112.0	sill (drill core)	basaltic andesite	Acidic rock	41.8	◎			△	・	・	・			・						ol bearing cpx basalt
TG27-119.0	sill (drill core)	basaltic andesite	Gramado	48.0	◎			△		・	・			・						
TG27-138.5	sill (drill core)	basaltic andesite	Gramado	42.2	◎			△		・	△			・						fine, strongly altered
TG27-91.5	sill (drill core)	olivine gabbro	unclassify	79.7	◎		・	△	・		△		△	△	・?	・?				
TG27-93.2	sill (drill core)	cpx basalt	unclassify	46.0	◎			△		・				・						fine, quartz-calcite veins
TG62-176.5	sill (drill core)	cpx basalt	Gramado	45.3	◎		・	○			・			・		?				
TG62-183.5	sill (drill core)	cpx basalt	Gramado	42.5	◎		・	○			・			・		?				
TG62-188.0	sill (drill core)	cpx basalt	Gramado	46.9	◎		・	○			・			・		?				
TG62-196.7	sill (drill core)	cpx basalt	Gramado	42.4	◎		・	○			・	△		・		・(pt?)				calcite vein with opaque
TG62-200.5	sill (drill core)	cpx basalt	Gramado	45.1	◎		・	○			・			・		?				
TG62-204.0	sill (drill core)	cpx basalt	Gramado	42.2	◎		・	○			・			・		?				
TG62-207.7	sill (drill core)	cpx basalt	Gramado	43.6	◎		・	○			・	・		・		?				two calcite veins with sulfide
TG62-211.4	sill (drill core)	cpx basalt	Gramado	42.5	◎		・	○			・			・		?				
TG62-215.4	sill (drill core)	Komatiite	Gramado	41.6	・					・	△		◎							spinifex texture
TG62-220.0	sill (drill core)	cpx basalt	Gramado	42.6	◎		・	○			・			・		?				

Microscopic observation of thin and polished-thin section for rock samples

Sampe No.	Sample Type	Rock Name	Magma Type	Mg#	Minerals																Note
					pl	am	opx	cpx	ol	qz	chl	ca	serp	opaque							
														mt	chr	sul	pyrr	py	cp	
TG62-220.4	sill (drill core)	olivine gabbro	unclassify	79.7	◎		・	○	○		・		△	・	・						
TG62-223.4	sill (drill core)	olivine gabbro	unclassify	77.3	◎		・	○	○		・		△	・	・						
TG62-225.0	sill (drill core)	olivine gabbro	Gramado?	74.1	◎		・	○	○		・		△	・	・						
TG62-226.3	sill (drill core)	olivine gabbro	unclassify	90.2	◎		・	○	◎		・		・	・	・						
TG62-226.8	sill (drill core)	olivine gabbro	unclassify	90.4	◎		・	○	○		△		△	・	・						
TG62-227.8	sill (drill core)	olivine gabbro	unclassify	90.7	◎		・	○	○		△		△	・	・	・?					chlorite vein
TG62-234.8	sill (drill core)	olivine gabbro	unclassify	89.9	◎		・	○	○		・		・	・	・						
TG62-237.6	sill (drill core)	olivine gabbro	unclassify	88.7	◎		・	○	○		△		△	・	・	・?					
TG62-238.5	sill (drill core)	olivine gabbro	unclassify	87.7	◎		・	○	○		・		・	・	・						
TG95-639.3	sill (drill core)	basaltic andesite	Gramado	57.9	◎			・				・		・		・?					cpx bearing aphilic basaltic andesite
TG95-650.3	sill (drill core)	cpx basalt	Gramado?	57.9	◎			△				・									calcite veins
TG95-664.7	sill (drill core)	cpx dolerite	Gramado	61.9	◎		・	○			・			△							
TG95-682.0	sill (drill core)	ol bearing cpx gabbro	Gramado?	49.9	◎		・	○	・		△			△		・?					coase,
TG95-695.0	sill (drill core)	cpx gabbro	Gramado	59.6	◎		・	○			・			△		・?					
TG95-709.4	sill (drill core)	cpx gabbro	Gramado	67.9	◎		・	○			・			△							
TG95-725.0	sill (drill core)	cpx gabbro	Gramado	65.6	◎		・	○			・			△							
TG95-743.0	sill (drill core)	cpx gabbro	Gramado	64.0	◎		・	○			・			△							
TG95-756.3	sill (drill core)	cpx gabbro	Gramado	62.8	◎		・	○			・			△							
TG95-772.8	sill (drill core)	cpx dolerite	Gramado	61.0	◎		・	○			・			△		・?					
TG97-569.2	sill (drill core)	cpx basalt	Gramado	61.7	◎		・	○			・	・		・							chlorite vein
TG97-590.0	sill (drill core)	cpx dolerite	Gramado	61.1	◎		・	○			・			△		・?					
TG97-602.0	sill (drill core)	cpx dolerite	Gramado	61.5	◎		・	○			・			△		・?					
TG97-615.0	sill (drill core)	cpx dolerite	Gramado	61.4	◎		・	○			・			△		・?					
TG97-625.0	sill (drill core)	cpx dolerite	Gramado	62.1	◎		・	○			・			△		・?					
TG97-630.0	sill (drill core)	cpx dolerite	Gramado	61.6	◎		・	○			・			△		・?					
TG97-650.0	sill (drill core)	cpx dolerite	Gramado	62.1	◎		・	○			・			△		・?					
TG97-664.0	sill (drill core)	cpx basalt	Gramado	61.3	◎		・	○			・			△		・?					
AT-06 (715.40-715.50)	sill (drill core)	weathered pyroxene basalt	Gramado	41.5	◎			・		・	△			・			・	△			intergranular texture, iddingsite
AT-09 (365.30-365.50)	sill (drill core)	cpx gabbro	Gramado?	80.0	◎		△	◎			・			△			・	・			iddingsite
AT-09 (601.10-601.20)	sill (drill core)	cpx gabbro	Gramado?	78.7	◎			◎			・			△			・	・			iddingsite

Microscopic observation of thin and polished-thin section for rock samples

Sampe No.	Sample Type	Rock Name	Magma Type	Mg#	Minerals																Note
					pl	am	opx	cpx	ol	qz	chl	ca	serp	opaque							
														mt	chr	sul	pyrr	py	cp	
FP-02 (580.15-580.40)	sill (drill core)	cpx basalt	Paranapanema?	57.9	◎		・	◎			・			・				△		intergranular texture
FP-02 (586.15-586.35)	sill (drill core)	cpx basalt	Paranapanema	58.0	◎		・	○			・			・				△		cryptocrystalline-intersertal texture
FP-02 (605.55-605.70)	sill (drill core)	cpx dolerite	Pitanga?	50.7	◎		・	◎		・	△	・		△			△			
FP-09 (174.10-174.30)	sediment (drill core)	altered clastic rock (silt)	---	---	△					○		△					・	△		
NF-09 (70.70-70.90)	sediment (drill core)	calcarious altered rock	---	---	△					△	△	△		・			・	△		
SP-17 (731.00-731.20)	sill (drill core)	cpx basalt	Pitanga	56.6	◎		・	○			△	△						△		calcite vein cutted the pyrite vein; cryptocrystalline
SP-17 (734.40-734.55)	sediment (drill core)	silt stone	---	---						◎		・						△		pyrite vein; muscovite
SP-17 (735.30-735.45)	sediment (drill core)	calcalious rock	---	---						○		◎						△		clay minerals (△)
SP-21 (129.80-130.00)	sill (drill core)	weathered pyroxene basalt	Pitanga	57.9	○			△			△	・						○		clay minerals (△), pyrite nodular (ϕ 5mm), pyrite vein
SP-66 (776.50-776.70)	sill (drill core)	cpx dolerite	Paranapanema	61.3	◎			○			△			△			△	△		
SW-01 (553.15-553.35)	sill (drill core)	weathered basalt	Esmeralda?	52.5	◎						○	△		△				○	・	clay minerals (△)
SW-03 (234.00-234.20)	sill (drill core)	cpx basalt	Esmeralda	62.6	◎		・	○		・	△			・			・	△	・	

Legend

◎: abundant; ○: common; △: minor; ・: rare

pl: plagioclase, am: amphibole, opx: ortho pyroxene, cpx: clino pyroxene, ol: olivine

qtz: quartz, chl: chlorite, ca: carbonate mineral (mainly calcite), serp: serpentine

mt: magnetite, chr: chromite, sul: sulfide, pyrr: pyrrhotite, py: pyrite, cp: chalcopyrite, chr: chromite

APPENDIX 6

Geochemical grade assay for rocks, drill cores and drill cuttings samples

Sample No.	SiO_2	Al_2O_3	Fe_2O_3	MnO	MgO	CaO	Na_2O	K_2O	TiO_2	P_2O_5	LOI	Total	Be	V	Cr	Co	Ga	Ge	As	Rb	Sr	Y	Zr	Nb	Mo	In	Sn	Sb	Cs	Ba	Sc
	%	%	%	%	%	%	%	%	%	%	%	%	ppm	ppm	ppm	ppm	ppm	ppm	ppm	ppm	ppm	ppm	ppm	ppm	ppm	ppm	ppm	ppm	ppm	ppm	ppm	ppm
Detection Limit	0.01	0.01	0.01	0.001	0.01	0.01	0.01	0.01	0.001	0.01	0.01		1	5	20	1	1	0.5	5	1	2	0.5	1	0.2	2	0.1	1	0.2	0.1	3	1
AC-028	49.81	13.81	12.75	0.192	6.37	10.57	2.36	1.16	1.900	0.21	1.21	100.34	<1	407	156	41	20	1.6	<5	34	363	24.3	138	12.6	<2	<0.1	<1	<0.2	0.3	323	38
AC-034B	49.65	12.77	14.65	0.231	5.44	9.30	2.39	1.22	2.263	0.25	2.04	100.22	<1	470	100	40	21	1.5	<5	30	263	35.6	163	14.2	<2	<0.1	<1	<0.2	0.3	311	43
AC-035	51.37	12.82	15.50	0.240	4.87	8.96	2.52	1.32	2.264	0.27	0.32	100.46	<1	443	66	40	21	1.6	<5	36	246	37.2	182	15.0	<2	<0.1	1	<0.2	0.5	333	41
ACR-119	67.53	12.68	6.27	0.099	1.04	3.08	3.37	3.75	1.021	0.32	1.02	100.16	3	80	<20	10	20	1.9	<5	203	146	52.8	277	22.3	<2	<0.1	5	0.3	7.9	641	17
ACR-125	50.40	12.61	15.18	0.205	4.09	8.13	2.68	1.61	3.645	0.57	1.30	100.43	1	429	21	38	23	1.7	<5	40	396	39.4	254	26.3	<2	<0.1	2	<0.2	0.4	564	33
ADR-033	56.95	12.95	11.58	0.160	3.88	6.67	2.58	2.81	1.089	0.15	1.63	100.44	1	261	21	33	20	1.9	<5	161	126	39.5	170	11.7	<2	<0.1	3	0.4	6.0	328	36
AS001	53.74	14.33	11.03	0.181	6.18	9.51	2.32	1.29	0.983	0.13	0.61	100.30	<1	259	71	42	19	1.6	<5	41	204	22.2	121	8.2	<2	<0.1	<1	0.5	0.6	287	39
AS002	51.28	12.92	14.91	0.236	4.91	8.59	2.58	1.23	2.210	0.25	0.89	100.01	<1	437	39	45	21	1.9	<5	27	267	34.1	177	15.0	<2	<0.1	1	<0.2	0.3	324	43
AS003	50.51	13.87	12.53	0.177	6.43	10.69	2.37	0.87	1.699	0.18	1.06	100.37	<1	382	167	41	19	1.6	<5	22	305	23.6	120	10.4	<2	<0.1	<1	<0.2	0.2	248	42
AS004A	51.26	12.97	14.75	0.210	5.04	9.23	2.55	1.10	2.103	0.26	0.81	100.28	<1	440	88	39	20	1.6	<5	27	277	32.9	155	12.2	<2	<0.1	<1	<0.2	0.3	320	40
AS004B	51.55	11.93	14.85	0.180	4.93	7.89	2.90	1.80	2.090	0.25	1.86	100.22	<1	492	57	38	20	1.8	<5	62	264	32.8	155	11.9	<2	<0.1	<1	<0.2	0.8	312	39
AS005	48.82	13.10	14.70	0.190	5.67	9.72	2.42	1.13	2.289	0.28	2.07	100.39	<1	422	106	28	18	0.7	<5	17	330	30.5	152	13.1	<2	<0.1	<1	<0.2	0.2	334	39
AS006	49.85	13.15	14.60	0.206	5.59	9.90	2.44	1.04	2.323	0.31	0.95	100.35	<1	436	121	43	22	1.7	<5	29	357	31.6	171	15.1	<2	<0.1	1	<0.2	0.3	324	37
AS007	49.72	13.12	14.98	0.211	5.61	9.98	2.46	1.12	2.110	0.25	0.92	100.47	<1	421	95	41	21	1.8	<5	30	348	28.5	158	13.6	<2	<0.1	<1	<0.2	0.4	321	39
AS008	48.82	11.69	15.68	0.219	6.75	9.30	2.31	1.19	2.664	0.32	1.17	100.12	1	478	116	49	22	1.9	<5	28	380	28.8	202	19.0	<2	<0.1	1	<0.2	0.2	380	37
AS009	50.72	12.69	15.73	0.228	4.95	8.95	2.57	1.06	2.376	0.28	0.96	100.52	<1	440	57	44	22	1.9	<5	30	240	42.1	200	15.7	<2	<0.1	1	0.2	0.5	322	42
AS010	50.10	12.93	15.24	0.213	5.12	9.22	2.59	1.09	2.385	0.30	0.97	100.15	<1	481	48	42	23	1.8	<5	32	335	33.2	183	16.3	<2	<0.1	1	0.3	1.2	360	38
AS011	50.45	12.89	15.33	0.210	4.89	9.22	2.73	1.17	2.490	0.33	0.57	100.29	<1	474	66	42	23	1.5	<5	32	355	33.5	193	17.2	<2	<0.1	2	0.5	0.8	371	36
AS013	50.54	12.27	17.03	0.231	3.97	8.17	2.56	1.38	3.003	0.41	0.61	100.17	1	542	<20	42	25	1.7	<5	40	327	40.4	234	20.2	<2	<0.1	2	<0.2	1.0	439	38
AS014	53.52	12.27	14.64	0.225	2.38	6.66	3.11	2.18	2.372	0.95	2.06	100.37	2	144	<20	23	27	1.9	<5	53	459	55.0	358	31.5	<2	<0.1	4	0.5	1.6	802	23
AS015A	61.10	12.39	11.63	0.175	0.75	4.26	3.43	3.26	1.364	0.39	1.67	100.42	3	<5	<20	11	30	1.9	<5	85	348	70.5	603	45.5	2	0.1	4	0.2	0.9	976	17
AS015B	50.26	12.66	14.54	0.212	3.85	7.71	2.99	1.48	3.595	0.71	2.09	100.08	1	329	<20	33	26	1.7	<5	46	465	45.5	297	27.4	<2	<0.1	2	0.7	12.0	506	30
AS016A	51.52	13.20	14.55	0.213	5.43	9.35	2.67	1.01	2.075	0.24	0.19	100.44	<1	432	73	42	21	1.9	<5	26	293	33.5	167	13.5	<2	<0.1	1	<0.2	0.6	302	42
AS016B	51.39	10.94	17.66	0.241	4.74	7.65	2.38	1.20	2.937	0.37	0.88	100.39	1	549	<20	48	23	1.8	<5	33	244	49.5	259	21.3	<2	<0.1	2	<0.2	1.2	379	42
AS017	53.87	13.39	13.90	0.193	2.73	7.41	2.81	1.59	2.413	0.46	1.64	100.39	1	251	<20	29	25	1.6	<5	45	303	49.7	289	23.8	<2	<0.1	2	0.3	0.9	489	30
AS018	49.07	12.71	16.32	0.201	5.34	9.42	2.44	1.07	2.958	0.30	0.67	100.50	<1	603	92	48	22	1.6	<5	31	331	34.0	169	15.2	<2	<0.1	1	<0.2	0.8	354	42
AS021	54.09	13.73	12.27	0.176	5.11	7.71	3.30	1.46	1.202	0.17	1.15	100.37	<1	297	25	40	20	1.7	<5	55	195	28.5	134	12.7	<2	0.2	43	5.7	2.9	332	37
AS022A	44.17	17.35	17.96	0.742	2.15	0.82	0.39	0.05	1.956	0.17	14.06	99.81	4	452	121	32	27	1.6	<5	10	22	118.0	152	10.5	<2	0.2	25	0.8	1.3	121	44
AS022B	54.28	24.25	4.68	0.063	1.48	0.43	0.42	0.20	2.878	0.05	11.17	99.90	1	643	310	37	41	1.5	<5	4	35	32.8	221	13.9	<2	0.2	18	0.7	0.3	88	56
AS022C	83.20	3.75	6.56	0.008	0.08	0.03	0.43	0.56	0.061	0.08	4.69	99.45	<1	160	<20	18	9	0.8	<5	21	38	5.5	63	3.1	<2	<0.1	20	0.6	1.2	164	3
AS022D	60.32	17.42	6.49	0.036	0.22	0.06	0.45	-0.01	1.505	0.02	12.39	98.91	<1	407	50	44	24	1.6	<5	2	28	10.2	164	12.3	<2	<0.1	13	0.2	0.3	53	45
AS023	52.34	12.43	15.70	0.217	3.87	8.13	2.95	0.88	1.952	0.25	1.61	100.31	<1	491	<20	40	22	1.9	<5	46	216	41.5	170	12.5	<2	<0.1	8	<0.2	3.7	355	40
AS024A	50.84	13.60	12.56	0.213	6.33	10.47	2.47	0.48	1.326	0.13	0.13	98.54	<1	362	70	39	19	1.4	<5	17	160	28.8	85	5.6	<2	<0.1	6	<0.2	0.4	114	43
AS024B	43.82	11.94	12.75	0.204	10.56	12.27	2.78	0.84	1.538	0.59	2.85	100.15	<1	273	261	47	18	1.4	<5	18	607	24.9	132	44.4	<2	<0.1	15	0.3	2.5	638	32
AS025	50.06	13.08	13.06	0.161	4.48	6.72	3.65	2.63	3.916	0.51	1.87	100.15	2	320	55	36	22	1.8	<5	62	347	36.6	300	27.8	<2	<0.1	10	<0.2	0.4	1050	25
AS026	45.33	10.84	9.95	0.194	8.81	9.05	2.65	2.26	1.746	0.69	7.86	99.38	2	227	150	35	16	1.3	<5	59	1200	33.6	207	83.4	<2	0.1	21	0.4	3.3	2830	24
AS027	47.09	13.42	13.65	0.186	5.90	7.04	2.36	2.69	4.433	0.61	2.77	100.13	2	361	42	37	26	1.4	<5	49	722	37.8	337	35.1	<2	<0.1	8	<0.2	<0.1	4350	26
AS028A	57.38	22.50	2.34	0.156	0.08	0.84	9.52	5.87	0.120	0.02	1.19	100.01	6	8	<20	<1	39	1.2	<5	222	90	12.6	710	106.3	<2	<0.1	33	0.3	7.5	152	<1
AS028B	55.46	21.82	1.76	0.101	1.38	2.54	3.66	5.21	0.133	0.02	8.09	100.17	5	7	<20	<1	34	1.3	<5	164	188	13.8	494	94.4	<2	<0.1	29	0.3	5.5	290	1
KM103	50.86	13.50	13.53	0.190	5.67	10.04	2.35	0.84	1.990	0.22	0.88	100.08	<1	414	111	41	19	1.5	<5	17	356	26.9	127	12.9	<2	<0.1	1	<0.2	0.3	339	38
KM104	53.53	13.75	11.94	0.260	5.31	8.72	2.57	1.20	1.294	0.18	1.01	99.77	1	339	34	39	18	1.5	<5	38	203	27.5	109	10.0	<2	<0.1	1	<0.2	1.3	295	37
KM105	55.59	12.23	13.88	0.206	3.02	6.94	2.68	2.31	1.678	0.27	0.77	99.59	2	378	<20	36	18	1.6	<5	87	140	39.0	146	12.1	<2	<0.1	2	<0.2	2.2	346	37
KM106	49.86	12.14	14.89	0.198	3.98	7.96	2.54	1.18	3.786	0.54	2.48	99.54	2	433	<20	38	22	1.4	<5	25	462	39.2	259	23.9	<2	<0.1	2	<0.2	0.8	629	29
KM107	50.28	12.24	14.93	0.211	4.16	8.10	2.72	1.14	3.877	0.53	1.79	99.99	2	391	<20	35	23	1.6	<5	21	474	37.5	257	24.6	<2	<0.1	2	<0.2	0.5	520	30
KM108	50.75	13.11	14.06	0.211	5.45	9.41	2.37	1.01	2.172	0.28	1.37	100.19	1	388	93	44	20	1.6	<5	22	326	33.6	149	15.3	<2	<0.1	1	<0.2	0.3	346	39
KM109	51.01	12.39	14.94	0.213	3.85	8.04	2.96	1.04	3.226	0.48	1.73	99.87	2	378	32	33	22	1.5	<5	33	417	39.4	248	24.7	<2	<0.1	2	<0.2	1.1	662	30
KM111	49.93	13.47	13.27	0.194	5.78	10.13	2.27	0.75	1.976	0.23	1.88	99.88	<1	370	98	42	19	1.4	<5	8	353	26.3	131	14.2	<2	<0.1	1	<0.2	<0.1	323	38
KM112	50.39	13.50	12.96	0.187	6.19	10.33	2.26	0.83	1.845	0.22	1.48	100.20	1	376	164	43	20	1.7	<5	15	367	27.0	134	13.6	<2	<0.1	1	<0.2	0.1	323	39
KM114	51.56	12.37	15.28	0.216	4.62	8.60	2.43	1.23	2.320	0.27	1.22	100.12	1	387	47	38	20	1.7	<5	31	219	49.4	174	14.9	<2	<0.1	2	<0.2	0.3	320	41
KM115	50.79	13.32	13.80	0.205	6.01	9.86	2.24	0.73	1.944	0.23	0.83	99.96	<1	376	145	44	19	1.5	<5	10	259	30.8	132	12.7	<2	<0.1	1	<0.2	0.3	273	41
KM116	49.58	12.51	15.47	0.183	4.80	7.82	2.53	1.91	2.375	0.30	2.43	99.92	1	424	30	41	21	1.6	<5	54	247	39.5	183	15.9	<2	<0.1	2	<0.2	0.3	417	41
KM117	52.12	12.41	15.45	0.213	4.63	8.54	2.45	1.10	2.393	0.29	0.83	100.42	1	400	42	38	20	1.6	<5	23	220	39.5	178	15.5	<2	<0.1	1	<0.2	0.2	327	41
KM118	49.40	13.06	13.38	0.185	6.04	9.84	2.19	1.00	1.831	0.22	2.15	99.29	<1	357	142	40	18	1.6	<5	22	246	28.2	123	11.7	<2	<0.1	1	<0.2	0.8	259	40
KM120	51.67	12.49	15.36	0.218	4.51	8.63	2.59	1.09	2.422	0.28	0.86	100.12	1	395	47	39	20	1.6	<5	23	218	39.6	177	14.9	<2	<0.1	2	<0.2	0.2	313	41
KM121	50.51	12.21	15.82	0.155	3.57	7.75	2.53	1.68	3.419	0.46	1.97	100.07	1	454	<20	35	22	1.4	<5	36	344	42.5	220	21.4	<2	<0.1	2	0.2	0.3	497	35

Geochemical grade assay for rocks, drill cores and drill cuttings samples

Sample No.	La	Ce	Pr	Nd	Sm	Eu	Gd	Tb	Dy	Ho	Er	Tm	Yb	Lu	Hf	Ta	W	Tl	Bi	Th	U	Ag	Cd	Cu	Ni	Pb	Zn	S
	ppm	ppm	ppm	ppm	ppm	ppm	ppm	ppm	ppm	ppm	ppm	ppm	ppm	ppm	ppm	ppm	ppm	ppm	ppm	ppm	ppm	ppm	ppm	ppm	ppm	ppm	ppm	%
Detection Limit	0.05	0.05	0.01	0.05	0.01	0.005	0.01	0.01	0.01	0.01	0.01	0.005	0.01	0.002	0.1	0.01	0.5	0.05	0.1	0.05	0.01	0.3	0.3	1	1	3	30	0.001
AC-028	18.97	42.62	4.87	21.49	4.64	1.599	4.85	0.77	4.56	0.92	2.71	0.373	2.27	0.315	3.7	0.83	<0.5	0.12	<0.1	2.05	0.36	<0.3	0.6	214	70	<3	91	<0.001
AC-034B	21.32	48.64	5.57	25.11	5.87	1.904	6.39	1.13	6.62	1.36	4.05	0.592	3.35	0.485	4.7	0.94	<0.5	0.12	<0.1	2.40	0.41	<0.3	<0.3	308	50	<3	117	<0.001
AC-035	22.84	51.74	5.89	25.98	6.02	1.980	6.42	1.14	6.87	1.41	4.11	0.615	3.47	0.509	5.0	1.01	<0.5	0.14	<0.1	2.51	0.48	<0.3	<0.3	228	41	16	111	<0.001
ACR-119	52.06	110.73	12.19	50.35	10.33	2.153	10.10	1.70	9.64	1.94	5.63	0.844	4.74	0.654	7.6	1.88	1.1	1.74	0.4	12.57	4.19	<0.3	<0.3	115	<1	12	86	<0.001
ACR-125	37.32	85.89	9.69	42.27	9.05	2.888	8.68	1.40	7.75	1.51	4.25	0.602	3.38	0.474	6.9	1.86	<0.5	0.24	<0.1	3.94	0.79	<0.3	<0.3	199	22	8	126	0.004
ADR-033	24.63	51.34	6.07	25.58	6.05	1.621	6.41	1.15	7.29	1.44	4.25	0.644	3.68	0.537	4.9	0.98	0.8	1.18	0.3	6.92	2.07	<0.3	0.5	126	26	<3	96	<0.001
AS001	16.32	35.23	4.03	17.05	3.75	1.145	4.02	0.70	4.16	0.85	2.55	0.371	2.37	0.349	3.1	0.50	<0.5	0.21	0.1	3.67	0.66	<0.3	<0.3	58	49	29	75	0.001
AS002	21.49	47.44	5.56	23.97	5.54	1.847	6.15	1.05	6.25	1.28	3.77	0.555	3.47	0.504	4.8	0.97	<0.5	0.09	0.1	2.48	0.47	<0.3	<0.3	203	38	40	103	<0.001
AS003	15.61	34.10	4.04	17.64	3.92	1.413	4.40	0.74	4.39	0.86	2.55	0.369	2.37	0.347	3.2	0.70	<0.5	0.05	<0.1	1.74	0.31	<0.3	<0.3	185	71	4	82	<0.001
AS004A	20.53	45.22	5.17	22.77	5.39	1.739	5.77	0.98	6.07	1.20	3.55	0.547	3.42	0.496	4.3	0.85	<0.5	0.11	0.1	2.72	0.51	<0.3	0.4	211	51	24	100	<0.001
AS004B	20.55	45.34	5.25	22.86	5.31	1.743	5.75	1.00	6.07	1.24	3.60	0.537	3.26	0.500	4.3	0.85	<0.5	0.19	<0.1	2.76	0.54	<0.3	<0.3	264	42	7	103	0.005
AS005	20.96	46.20	5.45	23.27	5.17	1.782	5.52	0.91	5.57	1.08	3.22	0.478	2.97	0.444	3.9	0.88	<0.5	0.05	<0.1	2.39	0.55	<0.3	<0.3	219	57	29	97	<0.001
AS006	24.07	53.78	6.33	26.90	6.23	2.120	6.28	1.02	6.16	1.17	3.50	0.528	3.07	0.470	4.5	1.04	<0.5	0.09	0.2	2.55	0.53	<0.3	<0.3	226	56	13	96	0.005
AS007	22.30	49.69	5.81	24.76	5.38	1.858	5.55	0.90	5.54	1.06	3.03	0.438	2.67	0.411	4.1	0.95	<0.5	0.09	<0.1	2.23	0.42	<0.3	<0.3	197	54	15	87	<0.001
AS008	28.25	63.02	7.43	31.45	6.75	2.236	6.85	1.06	5.99	1.14	3.26	0.440	2.65	0.411	5.3	1.30	<0.5	0.07	0.1	2.63	0.53	<0.3	0.6	209	73	<3	116	<0.001
AS009	24.19	53.11	6.34	27.86	6.35	2.099	7.34	1.20	7.45	1.50	4.42	0.655	4.06	0.608	5.2	1.04	<0.5	0.13	0.1	2.47	0.46	<0.3	<0.3	264	44	<3	121	<0.001
AS010	26.25	56.96	6.62	28.94	6.50	2.093	6.55	1.10	6.71	1.25	3.72	0.565	3.37	0.513	4.8	1.13	<0.5	0.30	0.3	2.83	0.57	<0.3	<0.3	260	44	4	117	0.356
AS011	26.76	58.28	6.85	29.38	6.54	2.103	6.79	1.11	6.58	1.25	3.78	0.552	3.27	0.505	5.0	1.14	<0.5	0.09	0.1	2.98	0.59	<0.3	<0.3	268	43	<3	117	0.363
AS013	31.29	69.47	8.13	34.55	7.73	2.508	8.14	1.33	7.89	1.54	4.60	0.675	4.13	0.586	5.9	1.38	<0.5	0.16	0.1	3.44	0.74	<0.3	0.6	299	26	<3	133	0.037
AS014	52.80	119.41	14.20	62.31	13.20	4.294	12.78	1.99	11.17	2.03	5.78	0.807	4.78	0.673	9.2	2.18	0.5	0.14	<0.1	4.68	0.96	<0.3	<0.3	79	1	11	155	0.133
AS015A	75.99	166.51	19.06	79.14	16.29	4.620	15.38	2.41	13.98	2.63	7.63	1.067	6.52	0.960	15.3	3.11	0.7	0.27	0.1	8.00	1.62	<0.3	<0.3	91	<1	4	179	0.109
AS015B	41.89	93.59	11.16	49.01	10.49	3.442	10.47	1.58	8.81	1.63	4.81	0.612	3.78	0.585	7.4	1.93	1.3	0.18	<0.1	3.65	0.71	<0.3	<0.3	45	7	<3	120	0.315
AS016A	22.07	49.19	5.73	24.92	5.72	1.903	5.99	1.03	6.42	1.23	3.65	0.566	3.46	0.533	4.5	0.94	<0.5	0.09	<0.1	2.38	0.44	<0.3	<0.3	246	47	12	107	0.011
AS016B	34.00	75.06	8.75	37.25	8.48	2.300	8.92	1.51	9.09	1.77	5.30	0.800	4.76	0.715	6.7	1.47	<0.5	0.10	<0.1	3.80	0.73	<0.3	<0.3	292	44	<3	137	0.011
AS017	37.92	83.24	9.61	40.97	8.93	2.624	9.18	1.53	9.12	1.79	5.33	0.777	4.62	0.702	7.3	1.58	<0.5	0.15	0.2	4.51	0.88	<0.3	<0.3	387	21	<3	123	0.063
AS018	23.86	52.89	6.21	27.00	6.10	2.060	6.29	1.07	6.27	1.24	3.73	0.548	3.34	0.520	4.6	1.06	<0.5	0.09	<0.1	2.64	0.54	<0.3	0.3	255	49	7	116	0.082
AS021	20.74	44.79	5.05	21.36	4.94	1.438	5.37	0.90	5.40	1.12	3.15	0.473	2.96	0.428	4.3	8.40	3.9	0.45	0.5	5.43	1.32	<0.3	0.7	112	41	8	93	0.013
AS022A	39.72	91.39	11.40	55.13	14.69	4.882	19.55	3.37	19.48	3.80	10.76	1.459	8.33	1.212	5.0	2.98	1.0	0.21	0.2	4.41	0.93	<0.3	1.1	144	67	<3	134	0.018
AS022B	17.16	33.91	3.61	15.65	3.78	1.377	4.79	0.89	5.59	1.23	3.82	0.648	4.04	0.632	7.0	2.41	0.8	0.15	0.1	6.26	2.41	0.7	0.9	276	78	24	138	0.246
AS022C	11.75	23.82	2.30	8.89	1.60	0.572	1.47	0.23	1.16	0.21	0.59	0.084	0.54	0.083	1.8	1.26	<0.5	0.37	<0.1	1.77	0.94	<0.3	0.6	14	63	4	<30	4.295
AS022D	11.87	21.39	2.21	8.50	1.75	0.517	1.87	0.32	1.95	0.39	1.14	0.173	1.11	0.162	5.0	2.01	0.9	0.45	<0.1	6.57	5.84	0.3	0.6	136	63	15	<30	7.055
AS023	23.52	51.34	5.86	26.23	6.26	1.962	7.31	1.30	7.74	1.59	4.56	0.687	4.20	0.608	5.2	1.70	<0.5	0.39	0.1	5.75	1.23	<0.3	0.8	208	24	5	130	0.048
AS024A	8.68	20.87	2.62	12.54	3.66	1.343	4.85	0.89	5.43	1.10	3.13	0.475	2.85	0.413	2.8	0.91	<0.5	0.08	<0.1	1.85	0.51	<0.3	0.7	160	65	4	74	0.020
AS024B	47.56	94.56	9.74	39.12	6.94	2.342	6.20	0.94	5.21	0.97	2.56	0.341	2.17	0.302	3.7	3.54	<0.5	0.29	<0.1	5.62	1.70	<0.3	0.7	102	202	7	345	0.099
AS025	43.93	98.58	11.44	50.46	10.68	3.655	10.66	1.50	8.12	1.45	3.75	0.464	2.99	0.393	8.7	2.46	<0.5	0.31	<0.1	4.67	1.00	0.4	0.7	143	54	7	135	0.012
AS026	102.39	179.37	17.18	64.65	10.91	3.199	9.01	1.32	7.05	1.27	3.38	0.437	2.85	0.388	5.6	3.56	0.8	0.52	0.1	23.65	3.57	<0.3	0.5	81	150	24	110	0.028
AS027	61.89	128.18	14.41	61.74	12.63	4.114	11.05	1.60	8.49	1.47	3.76	0.457	2.94	0.397	9.6	4.56	<0.5	0.11	<0.1	5.55	1.27	0.6	0.7	164	56	11	131	0.025
AS028A	129.71	165.14	10.59	24.91	2.32	0.495	1.39	0.24	1.50	0.34	1.24	0.234	1.66	0.281	13.1	3.03	<0.5	1.55	0.3	40.85	10.61	1.2	<0.3	3	<1	46	127	0.006
AS028B	132.27	163.95	10.45	24.49	2.37	0.552	1.32	0.25	1.68	0.38	1.39	0.260	1.88	0.298	10.1	2.87	<0.5	0.63	0.2	38.58	6.47	0.9	<0.3	2	<1	47	126	0.029
KM103	18.34	38.34	4.78	21.06	4.78	1.672	5.04	0.85	4.89	0.93	2.81	0.394	2.44	0.352	3.6	0.80	<0.5	0.09	<0.1	1.86	0.40	0.6	1.5	221	57	19	93	0.053
KM104	16.45	34.44	4.27	18.17	4.33	1.370	4.84	0.85	4.99	1.00	2.99	0.438	2.73	0.390	3.2	0.64	<0.5	0.21	0.2	3.59	0.99	0.4	0.4	141	28	<3	84	0.009
KM105	20.87	42.99	5.36	23.00	5.52	1.573	6.11	1.09	6.53	1.32	4.02	0.610	3.71	0.549	4.3	0.84	1.0	0.51	0.3	5.33	1.59	0.7	0.5	169	<1	15	109	0.008
KM106	35.80	77.31	9.89	43.10	9.47	3.097	9.09	1.42	7.80	1.41	4.05	0.547	3.31	0.462	7.1	1.74	<0.5	0.12	0.2	3.24	0.72	1.0	0.8	204	1	24	119	0.048
KM107	38.15	81.82	10.12	44.59	9.73	3.145	9.44	1.42	7.64	1.36	3.97	0.534	3.26	0.445	7.1	1.69	<0.5	0.11	<0.1	3.62	0.75	0.8	0.8	194	<1	10	113	0.037
KM108	23.75	47.76	6.06	26.48	6.03	2.002	6.32	1.03	5.97	1.14	3.56	0.528	3.12	0.458	4.1	0.86	<0.5	0.09	<0.1	2.67	0.56	0.3	1.0	242	31	9	103	0.010
KM109	37.94	79.32	9.68	42.18	9.01	2.898	8.98	1.39	7.69	1.37	4.10	0.580	3.56	0.498	6.9	1.65	<0.5	0.21	<0.1	3.87	0.77	0.9	0.8	241	<1	20	124	0.030
KM111	20.56	42.95	5.21	22.60	5.16	1.751	5.28	0.87	5.04	0.96	2.97	0.420	2.62	0.368	3.8	0.80	<0.5	<0.05	<0.1	2.26	0.41	0.7	1.1	228	57	13	100	0.015
KM112	20.30	41.61	5.04	22.32	4.97	1.658	5.12	0.83	4.79	0.90	2.75	0.410	2.46	0.356	3.6	0.77	<0.5	<0.05	<0.1	2.12	0.39	0.6	<0.3	221	73	<3	96	0.010
KM114	24.42	49.09	6.04	26.94	6.38	2.033	7.42	1.23	7.26	1.41	4.35	0.641	3.92	0.572	5.0	0.94	<0.5	0.13	<0.1	2.66	0.50	0.8	0.7	260	14	10	120	0.009
KM115	19.10	39.39	4.88	21.38	5.11	1.716	5.78	0.99	5.61	1.10	3.41	0.507	3.11	0.446	3.8	0.75	<0.5	0.07	<0.1	2.10	0.65	0.5	<0.3	264	80	8	102	0.009
KM116	26.22	55.22	6.70	29.21	6.73	2.154	7.38	1.22	7.24	1.37	4.31	0.631	3.81	0.561	5.0	1.00	<0.5	0.12	<0.1	2.88	0.56	0.7	0.9	151	21	10	126	0.007
KM117	23.30	49.19	6.10	26.43	6.51	2.027	7.16	1.24	7.26	1.40	4.33	0.645	3.94	0.574	5.0	0.94	<0.5	0.07	<0.1	2.67	0.51	0.7	<0.3	252	20	<3	124	0.011
KM118	17.75	37.38	4.57	20.33	4.71	1.636	5.42	0.91	5.36	1.00	3.18	0.461	2.83	0.417	3.6	0.69	<0.5	0.09	<0.1	1.91	0.35	0.6	0.4	219	71	21	97	0.012
KM120	23.52	49.51	6.07	26.67	6.44	2.023	7.24	1.22	7.19	1.40	4.38	0.651	3.81	0.564	5.0	0.95	<0.5	0.07	<0.1	2.65	0.50	0.6	1.1	279	23	21	122	0.010
KM121	36.39	72.90	8.93	38.55	8.49	2.731	8.61	1.36	7.68	1.44	4.49	0.644	3.91	0.570	6.0	1.45	<0.5	0.14	<0.1	3.92	0.81	0.8	1.4	175	22	13	137	0.012

Geochemical grade assay for rocks, drill cores and drill cuttings samples

Sample No.	Pd	Pt	Ir	Rh	Re	Au
	ppb	ppb	ppb	ppb	ppb	ppb
Detection Limit	0.2	0.2	0.1	0.2	0.1	2
AC-028	16.5	11.9				4
AC-034B	19.1	5.9				6
AC-035	15.2	7.6				5
ACR-119	2.0	1.4				1
ACR-125	1.3	0.6				3
ADR-033	7.4	3.3				3
AS001	0.6	0.3				17
AS002	17.0	4.8				8
AS003	16.4	10.2				3
AS004A	22.3	9.3				6
AS004B	20.4	5.2				4
AS005	15.1	11.7				4
AS006	13.3	11.3				4
AS007	17.9	11.0				4
AS008	0.2	0.6				<2
AS009	16.6	4.3				9
AS010	16.0	13.1				5
AS011	14.7	11.5				4
AS013	20.9	9.8				5
AS014	<0.2	<0.2				<2
AS015A	<0.2	<0.2				<2
AS015B	<0.2	<0.2				<2
AS016A	15.6	5.2				4
AS016B	14.9	1.2				5
AS017	15.1	2.9				5
AS018	17.6	6.4				3
AS021	4.7	6.0				69
AS022A	8.3	8.5				4
AS022B	13.6	11.1				5
AS022C	1.9	2.4				3
AS022D	3.8	5.1				3
AS023	14.1	15.2				6
AS024A	11.6	6.0				3
AS024B	6.2	3.9				2
AS025	7.8	4.4				4
AS026	5.4	2.8				<2
AS027	7.1	6.4				4
AS028A	<0.2	<0.2				<2
AS028B	<0.2	<0.2				<2
KM103	16.6	12.8				4
KM104	15.4	11.1	0.2	1.0	0.7	17
KM105	5.8	5.1				2
KM106	<0.2	<0.2				<2
KM107	<0.2	<0.2				<2
KM108	11.7	11.1				4
KM109	4.2	1.3				<2
KM111	14.8	12.9				4
KM112	14.3	11.2				4
KM114	9.4	5.1				4
KM115	16.3	9.0				4
KM116	37.0	3.3	0.5	0.7	0.8	22
KM117	11.7	6.2				3
KM118	16.4	9.8				3
KM120	15.3	5.1	0.1	1.0	1.2	8
KM121	0.2	<0.2				3

Geochemical grade assay for rocks, drill cores and drill cuttings samples

Sample No.	SiO_2	Al_2O_3	Fe_2O_3	MnO	MgO	CaO	Na_2O	K_2O	TiO_2	P_2O_5	LOI	Total	Be	V	Cr	Co	Ga	Ge	As	Rb	Sr	Y	Zr	Nb	Mo	In	Sn	Sb	Cs	Ba	Sc
	%	%	%	%	%	%	%	%	%	%	%	%	ppm	ppm	ppm	ppm	ppm	ppm	ppm	ppm	ppm	ppm	ppm	ppm	ppm	ppm	ppm	ppm	ppm	ppm	ppm	ppm
Detection Limit	0.01	0.01	0.01	0.001	0.01	0.01	0.01	0.01	0.001	0.01	0.01		1	5	20	1	1	0.5	5	1	2	0.5	1	0.2	2	0.1	1	0.2	0.1	3	1
KM122	50.05	13.49	13.18	0.186	6.11	10.31	2.30	0.56	1.826	0.19	1.62	99.82	<1	367	97	42	19	1.5	<5	7	335	24.2	113	12.0	<2	<0.1	1	<0.2	0.1	268	39
KM124	47.87	12.39	14.40	0.188	5.09	9.19	2.08	0.58	1.976	0.28	5.35	99.39	1	370	47	38	18	1.6	<5	13	392	31.3	133	12.5	<2	<0.1	2	<0.2	0.1	254	40
KM125	51.22	12.99	14.16	0.202	5.16	9.04	2.34	1.64	2.046	0.23	0.99	100.00	<1	378	87	38	19	1.6	<5	53	231	32.8	150	13.0	<2	<0.1	1	<0.2	0.3	290	42
KM126	51.04	13.33	13.97	0.201	5.87	9.71	2.37	0.88	2.051	0.23	0.43	100.06	<1	374	129	40	19	1.6	<5	17	248	30.1	131	12.3	<2	<0.1	1	<0.2	0.2	271	41
KM128	50.81	12.51	14.52	0.228	4.56	7.98	2.72	1.37	3.419	0.46	1.69	100.26	2	391	42	36	23	1.6	<5	28	438	34.9	227	20.7	<2	<0.1	2	<0.2	0.5	468	31
KM129	49.74	12.47	15.01	0.210	4.34	8.42	2.64	0.91	3.047	0.34	2.06	99.19	1	506	39	37	23	1.3	<5	27	394	38.8	211	15.9	<2	<0.1	2	0.4	0.6	558	33
KM130A	50.06	12.39	10.41	0.200	4.38	8.00	2.64	1.45	3.064	0.22	0.82	93.64	1	465	31	37	24	1.6	<5	31	362	39.4	198	19.9	<2	<0.1	1	<0.2	0.3	421	32
KM130B	51.04	15.18	11.36	0.171	4.81	9.95	2.57	0.98	1.902	0.22	0.90	99.10	1	335	86	32	20	1.1	<5	18	380	25.3	135	12.6	<2	<0.1	2	<0.2	0.2	346	32
KM131	49.16	13.52	13.23	0.183	6.28	10.00	2.24	0.95	1.725	0.20	1.84	99.33	<1	385	146	40	19	1.5	<5	14	296	26.1	120	10.7	<2	<0.1	<1	<0.2	<0.1	288	40
KM133	50.47	12.88	14.40	0.205	5.28	9.25	2.52	1.11	2.224	0.25	1.31	99.89	<1	411	94	38	20	1.4	<5	21	238	37.2	156	12.1	<2	<0.1	1	<0.2	0.3	279	42
KM134	50.53	12.60	14.85	0.211	5.03	8.71	2.30	1.46	2.165	0.25	1.26	99.37	1	431	70	38	20	1.0	<5	34	228	38.3	153	12.7	<2	<0.1	1	<0.2	0.4	315	42
KM135	50.62	12.92	15.14	0.216	5.16	9.22	2.41	1.02	2.147	0.26	0.83	99.92	1	462	100	43	21	1.5	<5	20	260	36.7	156	13.3	<2	<0.1	1	<0.2	0.1	331	42
KM136	51.08	12.88	15.42	0.210	5.12	9.14	2.43	1.14	2.211	0.28	0.50	100.39	1	465	92	41	21	1.6	<5	26	261	37.3	159	13.7	<2	<0.1	1	<0.2	0.3	340	41
KM137	50.19	13.15	13.24	0.215	5.68	9.93	2.41	0.46	1.804	0.20	1.84	99.12	<1	406	97	37	20	1.4	<5	15	290	31.4	132	11.6	<2	<0.1	1	<0.2	0.2	275	42
KM138	49.84	12.89	15.84	0.216	4.87	8.96	2.54	1.05	3.093	0.41	0.51	100.21	1	513	72	42	22	1.3	<5	21	379	37.8	193	18.3	<2	<0.1	2	1.0	0.4	466	36
KM139	49.06	13.52	13.31	0.179	6.40	10.29	2.26	0.67	1.786	0.20	2.25	99.94	1	393	160	41	20	1.6	<5	6	306	32.7	121	11.5	<2	<0.1	1	<0.2	<0.1	320	40
KM140	49.85	12.90	14.56	0.185	4.59	8.67	2.48	1.43	2.606	0.56	1.05	98.86	2	344	77	36	22	1.6	<5	30	346	39.4	187	17.6	<2	<0.1	2	<0.2	0.3	455	33
KM141	49.33	13.64	13.33	0.189	6.26	10.12	2.42	0.87	2.241	0.25	1.00	99.65	1	372	111	43	21	1.5	<5	18	430	27.2	139	12.4	<2	<0.1	1	<0.2	0.1	292	34
KM142	49.95	12.86	14.32	0.208	4.28	8.19	2.77	1.61	3.815	0.59	0.89	99.48	2	411	22	33	25	1.4	<5	30	565	38.2	257	23.4	<2	<0.1	2	<0.2	0.4	1020	27
KM143	49.03	12.93	14.39	0.199	5.40	9.22	2.55	1.16	3.291	0.34	1.57	100.07	1	470	87	42	24	1.6	<5	21	471	33.7	191	17.7	<2	<0.1	2	<0.2	0.2	386	33
KM144	51.04	12.51	15.98	0.229	4.76	9.19	2.45	0.94	2.254	0.25	0.70	100.31	1	446	40	45	21	1.6	<5	19	248	38.4	167	14.1	<2	<0.1	1	<0.2	0.2	292	42
KM145	50.24	13.21	13.93	0.208	5.83	9.70	2.28	1.04	1.919	0.22	1.14	99.71	1	411	103	44	20	1.6	<5	22	252	35.6	145	12.7	<2	<0.1	1	<0.2	0.3	283	42
KM146	51.40	12.91	14.58	0.215	5.10	9.19	2.53	1.20	1.971	0.24	0.65	99.98	1	417	55	43	20	1.5	<5	30	272	33.3	146	13.0	<2	<0.1	1	<0.2	0.4	321	41
KM147	50.59	12.51	14.79	0.213	3.99	7.85	2.86	1.49	3.495	0.61	0.80	99.21	2	381	<20	36	22	1.4	<5	29	416	43.4	235	21.6	<2	<0.1	2	<0.2	0.2	490	31
KM148	49.86	12.34	15.19	0.217	3.96	8.15	2.87	1.15	3.630	0.69	1.55	99.60	2	388	20	35	22	1.3	<5	34	422	42.0	249	25.6	<2	<0.1	2	<0.2	0.6	637	31
KM150	50.24	12.44	14.92	0.215	4.21	8.07	2.68	1.66	3.670	0.68	1.13	99.91	2	402	<20	46	23	1.6	<5	35	406	45.4	252	26.1	<2	<0.1	2	<0.2	0.4	566	31
KM151	49.70	12.24	15.56	0.205	3.75	7.86	2.70	1.38	3.804	0.64	2.08	99.92	2	391	<20	36	24	1.6	<5	30	482	42.9	300	29.5	<2	<0.1	2	<0.2	0.3	586	29
KM152	49.68	12.41	14.98	0.218	4.49	8.09	2.67	1.48	3.703	0.45	0.87	99.03	2	481	<20	40	25	1.7	<5	31	508	37.4	251	24.7	<2	<0.1	2	<0.2	0.3	505	30
KM153	49.85	12.59	15.13	0.201	4.58	8.43	2.73	1.41	3.693	0.48	0.43	99.52	2	473	33	38	23	1.6	<5	27	512	36.5	222	22.2	<2	<0.1	2	<0.2	0.2	450	32
KM154	49.32	12.30	15.75	0.200	4.34	8.49	2.61	1.54	3.729	0.48	1.01	99.76	1	478	68	38	23	1.6	<5	30	420	37.8	234	23.6	<2	<0.1	2	<0.2	0.2	485	32
KM155	49.55	12.39	15.74	0.220	4.52	8.56	2.66	1.50	3.749	0.49	0.62	99.98	2	477	67	40	23	1.6	<5	30	476	38.0	235	24.0	<2	<0.1	2	<0.2	0.2	493	33
KM156	47.30	12.65	12.73	0.186	6.45	9.69	2.82	1.19	1.554	0.20	3.88	98.66	1	384	97	43	18	1.7	<5	10	376	22.7	87	12.0	<2	<0.1	<1	<0.2	0.2	320	40
KM157	50.86	13.02	13.79	0.176	5.50	9.58	2.41	1.60	1.829	0.21	1.13	100.10	<1	429	93	43	19	1.7	<5	53	420	28.3	131	12.6	<2	<0.1	1	<0.2	0.5	397	40
KM158	50.90	12.69	15.23	0.224	4.93	9.13	2.65	1.28	2.091	0.24	0.93	100.30	<1	442	52	42	20	1.6	<5	23	245	34.3	144	12.9	<2	<0.1	1	<0.2	0.3	309	42
KM159	48.04	13.42	14.28	0.189	5.97	9.32	2.45	0.98	1.888	0.22	2.67	99.43	1	409	108	42	19	1.6	<5	17	270	57.6	123	11.8	<2	<0.1	1	<0.2	1.0	531	42
KM160	49.85	13.31	13.37	0.189	6.03	10.03	2.35	1.05	1.730	0.20	1.98	100.09	<1	391	98	41	18	1.6	<5	18	322	27.2	119	10.9	<2	<0.1	<1	<0.2	0.4	260	40
KM161	49.69	13.19	14.31	0.216	5.44	9.83	2.45	0.72	2.037	0.23	2.18	100.27	1	417	82	41	19	1.4	<5	7	441	29.1	136	12.3	<2	<0.1	1	<0.2	<0.1	337	41
KM162	50.55	12.77	15.27	0.228	4.86	9.16	2.51	0.80	2.445	0.30	1.34	100.22	1	435	90	41	21	1.7	<5	23	296	39.8	188	13.8	<2	<0.1	1	<0.2	0.3	682	40
KM163	48.76	12.95	13.93	0.210	5.65	9.98	2.45	0.54	1.943	0.23	1.90	98.54	1	398	101	42	20	1.7	<5	14	460	30.5	148	11.6	<2	<0.1	1	<0.2	0.2	434	40
KN001	46.93	14.73	11.88	0.163	9.02	10.80	2.08	0.78	1.530	0.15	2.15	100.22	<1	305	640	54	20	1.4	<5	22	259	22.9	123	9.5	<2	<0.1	13	5.1	0.4	198	39
KN002	46.01	11.67	11.42	0.173	18.92	10.01	1.25	0.30	0.518	0.07	0.02	100.36	<1	192	898	80	11	1.7	<5	6	178	10.2	42	2.5	<2	<0.1	<1	<0.2	<0.1	122	35
KN003	46.99	14.29	11.09	0.170	10.47	10.79	2.16	0.50	1.330	0.22	0.74	98.74	<1	250	602	51	17	1.4	<5	9	325	20.2	93	4.8	<2	<0.1	<1	<0.2	0.5	293	38
KN005	52.78	13.00	14.51	0.216	4.64	8.53	2.70	1.36	1.654	0.21	0.73	100.33	<1	436	30	40	21	1.6	<5	49	189	35.5	156	10.8	<2	<0.1	1	<0.2	0.9	327	39
KN006	50.64	13.39	14.20	0.219	6.13	10.41	2.51	0.66	1.361	0.15	0.72	100.39	<1	412	60	46	19	1.7	<5	15	168	29.7	106	6.8	<2	<0.1	<1	<0.2	0.2	196	46
KN009	51.69	13.69	12.58	0.186	5.97	10.47	2.65	1.26	1.341	0.18	0.21	100.21	<1	359	73	38	19	1.7	<5	58	206	24.8	119	7.8	<2	<0.1	<1	<0.2	1.8	189	39
KN010	51.78	13.78	13.56	0.210	5.58	9.49	2.45	1.17	1.369	0.17	0.63	100.18	<1	316	61	28	15	0.7	<5	35	167	28.5	118	7.0	<2	<0.1	<1	<0.2	0.6	248	40
KN011	52.30	13.76	13.13	0.204	5.66	9.92	2.58	1.09	1.349	0.20	0.22	100.41	<1	352	72	39	19	1.6	<5	41	179	29.0	125	7.9	<2	<0.1	<1	<0.2	1.3	247	40
KN012	51.28	14.79	11.91	0.214	5.38	10.90	2.55	0.76	1.233	0.14	0.95	100.11	<1	368	41	46	20	1.6	<5	17	184	29.3	103	6.9	<2	<0.1	<1	<0.2	0.2	193	42
KN014	49.11	12.77	15.39	0.213	5.08	8.91	2.66	1.39	3.569	0.47	0.34	99.90	1	512	<20	46	24	1.6	<5	33	422	34.9	205	22.4	<2	<0.1	1	<0.2	0.3	428	34
KN016	51.29	12.49	15.45	0.198	4.78	8.90	2.62	1.16	2.306	0.28	0.52	100.01	<1	409	54	42	22	1.9	<5	28	235	38.4	188	15.6	<2	<0.1	1	0.2	0.2	301	42
KN017	49.41	13.41	13.95	0.190	6.24	10.25	2.39	0.99	1.978	0.24	1.24	100.29	<1	409	143	44	21	1.6	<5	25	342	27.8	138	12.6	<2	<0.1	<1	<0.2	0.2	289	39
KN018	49.36	12.29	15.26	0.238	4.29	8.39	2.64	1.61	3.703	0.55	1.87	100.19	1	420	<20	38	24	1.8	<5	39	405	37.8	247	26.1	<2	<0.1	1	<0.2	0.3	477	32
KN019	49.05	13.31	13.40	0.190	6.21	10.50	2.37	0.73	1.920	0.20	0.99	98.88	<1	408	122	43	21	1.5	8	10	374	25.3	132	12.6	<2	<0.1	<1	<0.2	0.2	279	39
KN020	50.03	13.25	14.27	0.199	5.68	10.04	2.49	1.05	2.178	0.25	1.03	100.46	<1	425	93	43	22	1.6	<5	23	364	28.1	154	14.5	<2	<0.1	<1	<0.2	0.1	330	39

Geochemical grade assay for rocks, drill cores and drill cuttings samples

Sample No.	La	Ce	Pr	Nd	Sm	Eu	Gd	Tb	Dy	Ho	Er	Tm	Yb	Lu	Hf	Ta	W	Tl	Bi	Th	U	Ag	Cd	Cu	Ni	Pb	Zn	S
	ppm	ppm	ppm	ppm	ppm	ppm	ppm	ppm	ppm	ppm	ppm	ppm	ppm	ppm	ppm	ppm	ppm	ppm	ppm	ppm	ppm	ppm	ppm	ppm	ppm	ppm	ppm	%
Detection Limit	0.05	0.05	0.01	0.05	0.01	0.005	0.01	0.01	0.01	0.01	0.01	0.005	0.01	0.002	0.1	0.01	0.5	0.05	0.1	0.05	0.01	0.3	0.3	1	1	3	30	0.001
KM122	16.97	35.26	4.32	19.14	4.46	1.565	4.77	0.76	4.43	0.83	2.61	0.387	2.24	0.340	3.2	0.66	<0.5	0.07	<0.1	1.89	0.37	0.5	<0.3	214	70	11	92	0.015
KM124	19.21	40.36	4.95	21.78	5.27	1.721	5.68	0.97	5.72	1.09	3.47	0.507	3.07	0.446	3.8	0.75	<0.5	0.06	<0.1	2.17	0.34	0.5	<0.3	112	17	6	109	0.013
KM125	20.26	42.19	5.19	22.60	5.35	1.773	6.00	1.02	6.02	1.15	3.56	0.538	3.27	0.483	4.2	0.79	<0.5	0.07	<0.1	2.30	0.45	0.7	0.4	205	44	3	111	0.012
KM126	19.00	39.52	4.87	21.54	5.14	1.668	5.66	0.96	5.59	1.09	3.42	0.502	3.04	0.436	3.8	0.75	<0.5	0.05	<0.1	2.13	0.40	0.6	<0.3	239	65	12	105	0.016
KM128	33.40	71.09	8.96	39.71	8.72	2.887	8.51	1.31	7.10	1.23	3.64	0.487	2.96	0.420	6.2	1.41	<0.5	0.09	<0.1	3.19	0.66	0.7	0.6	127	23	6	116	0.009
KM129	26.11	56.46	7.30	32.36	7.34	2.471	7.59	1.26	7.08	1.31	4.00	0.575	3.46	0.502	6.0	1.26	<0.5	0.10	<0.1	3.22	0.67	0.7	0.4	220	15	7	124	0.028
KM130A	28.43	62.91	7.51	33.54	7.61	2.702	7.96	1.30	7.37	1.47	4.06	0.595	3.54	0.503	6.0	1.27	<0.5	0.09	0.1	2.99	0.61	0.8	0.5	218	25	12	123	0.009
KM130B	18.89	39.27	4.92	21.61	4.93	1.689	5.16	0.84	4.78	0.89	2.67	0.396	2.33	0.343	3.9	0.80	<0.5	<0.05	<0.1	2.43	0.49	0.5	0.8	226	35	11	92	0.013
KM131	15.83	33.79	4.19	18.33	4.32	1.496	4.63	0.80	4.64	0.90	2.78	0.406	2.52	0.375	3.5	0.67	<0.5	<0.05	<0.1	2.03	0.40	0.5	0.7	207	71	16	95	0.016
KM133	17.16	37.36	4.83	21.79	5.79	1.868	6.27	1.12	6.57	1.26	3.86	0.569	3.40	0.496	4.5	0.81	<0.5	0.12	<0.1	2.04	0.76	0.8	0.8	233	37	9	111	0.010
KM134	19.63	40.51	5.28	23.26	5.68	1.885	6.46	1.12	6.73	1.31	4.07	0.617	3.69	0.560	4.5	0.84	<0.5	<0.05	<0.1	2.51	0.45	0.6	1.9	254	31	<3	119	0.013
KM135	19.21	41.35	5.20	23.37	5.58	1.855	6.30	1.11	6.42	1.25	3.97	0.601	3.59	0.541	4.6	0.89	<0.5	0.25	<0.1	2.59	0.51	0.6	1.2	270	58	6	117	0.011
KM136	20.01	42.60	5.27	23.75	5.70	1.903	6.40	1.11	6.68	1.28	4.09	0.605	3.70	0.555	4.6	0.89	<0.5	0.08	<0.1	2.65	0.50	0.8	1.2	282	40	8	117	0.011
KM137	16.51	34.80	4.45	19.90	4.83	1.604	5.32	0.93	5.53	1.07	3.34	0.490	3.00	0.449	3.9	0.79	<0.5	0.09	<0.1	2.20	0.43	0.6	0.5	225	43	9	103	0.024
KM138	26.69	57.00	7.08	30.71	6.94	2.326	7.08	1.20	6.77	1.28	3.95	0.575	3.52	0.504	5.4	1.24	<0.5	0.06	<0.1	3.46	0.72	0.5	0.4	243	27	6	124	0.031
KM139	16.94	32.87	4.39	19.42	4.62	1.608	5.16	0.85	5.03	0.99	3.03	0.439	2.64	0.399	3.6	0.67	<0.5	<0.05	<0.1	2.08	0.39	0.5	<0.3	203	65	12	90	0.012
KM140	27.82	59.63	7.53	33.32	7.59	2.466	7.88	1.26	7.14	1.34	4.13	0.592	3.59	0.524	5.3	1.19	<0.5	0.10	<0.1	3.56	0.72	0.8	0.4	238	23	11	118	0.012
KM141	17.01	36.93	4.87	22.39	5.49	1.954	5.62	0.91	5.11	0.92	2.76	0.385	2.31	0.324	4.1	0.80	<0.5	0.06	<0.1	1.98	0.42	0.5	0.8	163	58	<3	91	0.013
KM142	33.52	73.27	9.45	43.03	9.51	3.173	9.21	1.42	7.59	1.34	3.95	0.530	3.14	0.437	7.4	1.72	<0.5	0.08	<0.1	3.48	0.76	1.0	0.9	37	<1	10	129	0.037
KM143	23.95	51.84	6.73	30.84	7.26	2.433	7.33	1.14	6.23	1.13	3.37	0.465	2.78	0.393	5.5	1.16	<0.5	0.17	<0.1	2.56	0.56	0.7	<0.3	264	46	<3	115	0.013
KM144	20.39	45.39	5.43	24.78	6.27	1.967	6.75	1.23	7.02	1.35	4.18	0.624	3.81	0.542	4.6	0.82	<0.5	0.06	<0.1	1.86	0.37	0.8	0.7	256	14	21	121	0.049
KM145	20.12	42.45	5.12	22.55	5.46	1.801	5.91	1.07	6.24	1.22	3.88	0.555	3.51	0.491	4.1	0.74	<0.5	0.05	<0.1	1.87	0.40	0.7	0.6	248	37	12	101	0.011
KM146	20.36	44.43	5.31	22.92	5.39	1.833	5.79	1.04	5.93	1.14	3.62	0.542	3.33	0.486	4.0	0.80	<0.5	0.08	<0.1	1.87	0.46	0.6	1.6	213	26	7	107	0.012
KM147	36.35	80.47	9.76	42.97	9.66	3.197	9.48	1.59	8.49	1.57	4.70	0.633	3.71	0.524	6.5	1.53	<0.5	0.09	<0.1	2.96	0.66	0.8	0.5	89	<1	5	128	0.008
KM148	40.10	89.53	10.72	45.50	9.84	3.076	9.48	1.58	8.68	1.60	4.88	0.658	3.97	0.536	6.8	1.77	<0.5	0.11	<0.1	3.57	0.77	0.7	1.0	139	<1	8	122	0.037
KM150	39.90	87.64	10.40	44.61	9.75	3.131	9.55	1.57	8.55	1.57	4.82	0.680	4.16	0.593	7.0	1.77	<0.5	0.10	<0.1	3.47	0.75	0.7	1.1	150	7	<3	127	0.009
KM151	41.39	92.68	11.10	48.89	10.74	3.432	10.08	1.64	8.49	1.50	4.46	0.572	3.53	0.481	7.7	1.92	<0.5	0.13	<0.1	3.37	0.73	1.2	13.1	126	<1	21	110	0.009
KM152	32.24	73.42	8.92	39.12	8.88	2.930	8.36	1.36	7.17	1.31	3.89	0.525	3.20	0.442	6.7	1.52	<0.5	0.10	<0.1	2.82	0.59	0.9	15.0	85	2	7	101	0.015
KM153	30.13	68.11	8.37	37.09	8.61	2.908	8.44	1.38	7.25	1.29	3.89	0.518	3.17	0.448	5.9	1.40	<0.5	0.11	<0.1	2.63	0.59	0.8	13.4	146	17	10	97	0.009
KM154	33.50	74.62	9.02	39.28	8.57	2.821	8.36	1.39	7.38	1.32	4.02	0.546	3.43	0.480	6.4	1.56	<0.5	0.08	<0.1	3.04	0.65	0.9	13.5	144	15	12	102	0.009
KM155	33.04	73.90	8.94	39.54	8.57	2.804	8.39	1.39	7.51	1.34	4.12	0.558	3.38	0.468	6.5	1.58	<0.5	0.08	<0.1	2.99	0.64	0.8	14.6	142	14	15	101	0.007
KM156	14.11	31.73	3.80	16.64	3.86	1.403	4.20	0.74	4.22	0.78	2.45	0.348	2.15	0.308	3.1	0.60	<0.5	0.06	<0.1	0.87	8.82	0.4	12.8	146	52	5	75	0.008
KM157	17.92	39.68	4.75	20.98	4.97	1.641	5.31	0.93	5.36	1.03	3.20	0.467	2.86	0.418	3.8	0.74	<0.5	0.11	<0.1	1.88	0.46	0.6	11.1	180	42	10	79	0.011
KM158	19.13	42.66	5.09	22.28	5.43	1.775	5.95	1.08	6.41	1.25	3.96	0.576	3.52	0.521	4.2	0.82	<0.5	0.08	<0.1	1.94	0.42	0.6	12.7	150	22	18	88	0.010
KM159	30.53	44.85	6.00	26.42	5.95	2.141	8.22	1.38	8.08	1.71	5.40	0.762	4.38	0.670	3.8	0.71	<0.5	0.12	<0.1	1.73	0.43	0.5	12.8	217	55	8	139	0.009
KM160	15.90	35.67	4.27	18.81	4.50	1.537	4.71	0.86	4.95	0.96	2.95	0.437	2.62	0.382	3.3	0.77	<0.5	0.06	<0.1	1.59	0.40	0.6	12.1	197	43	4	77	0.010
KM161	18.79	41.14	4.88	21.25	4.83	1.667	5.18	0.92	5.41	1.03	3.23	0.473	2.95	0.418	3.9	0.79	<0.5	0.05	<0.1	1.88	0.96	0.8	13.3	192	21	17	84	0.011
KM162	23.27	49.33	6.04	26.51	6.38	2.071	6.48	1.14	6.82	1.37	4.11	0.603	3.65	0.539	4.8	0.90	<0.5	0.08	<0.1	2.83	0.45	0.8	13.8	257	38	20	92	0.023
KM163	18.64	39.40	4.91	21.03	5.12	1.702	5.20	0.93	5.46	1.08	3.18	0.475	2.82	0.412	3.8	0.71	<0.5	0.09	0.1	2.20	0.39	0.7	13.2	197	44	27	79	0.020
KN001	13.92	33.72	4.03	18.19	4.51	1.500	4.60	0.80	4.55	0.88	2.55	0.359	2.09	0.292	3.4	0.65	<0.5	0.18	<0.1	1.98	0.38	<0.3	<0.3	130	246	<3	75	0.010
KN002	4.96	11.72	1.40	6.65	1.69	0.634	1.86	0.32	1.93	0.41	1.12	0.161	0.97	0.143	1.1	0.14	<0.5	<0.05	<0.1	0.48	0.07	<0.3	0.8	49	356	<3	59	0.002
KN003	10.42	25.90	3.28	15.56	3.80	1.446	4.06	0.68	3.93	0.79	2.25	0.321	1.84	0.261	2.6	0.30	<0.5	0.07	<0.1	0.47	0.10	<0.3	<0.3	123	211	11	67	0.019
KN005	21.06	47.49	5.40	23.25	5.77	1.752	6.27	1.09	6.75	1.34	3.98	0.573	3.42	0.478	4.5	0.75	<0.5	0.55	0.1	4.39	0.88	<0.3	<0.3	205	29	<3	108	<0.001
KN006	12.37	28.40	3.35	15.12	4.03	1.361	4.71	0.84	5.53	1.13	3.43	0.476	2.98	0.427	3.1	0.44	<0.5	0.15	<0.1	2.20	0.41	<0.3	<0.3	204	49	<3	100	<0.001
KN009	12.93	30.00	3.56	16.26	4.12	1.409	4.50	0.78	4.76	0.97	2.84	0.403	2.35	0.336	3.9	0.60	<0.5	0.34	0.1	2.32	0.65	<0.3	<0.3	167	61	<3	83	<0.001
KN010	14.80	33.70	3.95	17.59	4.33	1.326	4.77	0.85	5.20	1.05	3.17	0.441	2.59	0.386	3.4	0.53	<0.5	0.14	<0.1	3.21	0.70	<0.3	0.7	167	51	10	96	<0.001
KN011	14.95	33.83	3.96	17.36	4.38	1.401	4.88	0.88	5.35	1.08	3.20	0.465	2.69	0.389	3.6	0.54	<0.5	0.36	<0.1	3.32	0.72	<0.3	0.5	151	51	<3	93	<0.001
KN012	12.95	29.15	3.46	15.34	4.04	1.364	4.61	0.85	5.28	1.13	3.30	0.466	2.88	0.414	3.0	0.44	<0.5	0.12	<0.1	2.14	0.44	<0.3	0.6	132	44	<3	88	<0.001
KN014	31.02	70.31	8.13	35.17	7.68	2.524	7.49	1.17	6.54	1.30	3.68	0.478	2.74	0.401	5.8	1.50	<0.5	0.14	<0.1	3.08	0.64	<0.3	0.5	186	34	7	119	<0.001
KN016	23.15	52.83	6.02	27.23	6.34	1.989	6.86	1.17	7.09	1.44	4.29	0.597	3.52	0.507	5.3	1.04	<0.5	0.17	<0.1	2.55	0.47	<0.3	<0.3	210	37	<3	127	<0.001
KN017	20.21	45.11	5.17	22.91	5.16	1.748	5.25	0.90	5.37	1.04	3.08	0.430	2.54	0.357	3.9	0.88	<0.5	0.12	<0.1	2.23	0.48	<0.3	0.6	198	67	<3	98	<0.001
KN018	37.11	84.43	9.76	41.84	9.02	2.909	8.38	1.35	7.28	1.47	4.21	0.572	3.27	0.468	6.7	1.84	<0.5	0.17	<0.1	3.69	0.75	<0.3	<0.3	179	27	21	121	<0.001
KN019	19.26	43.19	4.87	21.66	4.87	1.715	4.92	0.82	4.79	0.94	2.72	0.405	2.24	0.321	3.6	0.83	<0.5	0.06	<0.1	2.02	0.38	<0.3	<0.3	233	60	<3	91	<0.001
KN020	22.37	50.46	5.77	25.14	5.56	1.829	5.60	0.91	5.43	1.05	3.08	0.440	2.50	0.381	4.3	0.99	<0.5	0.11	<0.1	2.39	0.42	<0.3	<0.3	238	51	<3	99	<0.001

Geochemical grade assay for rocks, drill cores and drill cuttings samples

Sample No.	Pd	Pt	Ir	Rh	Re	Au
	ppb	ppb	ppb	ppb	ppb	ppb
Detection Limit	0.2	0.2	0.1	0.2	0.1	2
KM122	15.2	16.0				4
KM124	12.2	4.4				3
KM125	8.8	8.1				4
KM126	18.6	8.7				5
KM128	0.3	0.7				<2
KM129	3.9	3.3				<2
KM130A	5.6	2.9				<2
KM130B	15.4	8.8				4
KM131	14.3	7.0				4
KM133	17.3	6.7				6
KM134	12.4	6.0				5
KM135	15.3	6.0				5
KM136	20.0	5.9				7
KM137	15.2	8.5				4
KM138	1.9	1.7				<2
KM139	14.9	7.3				4
KM140	4.4	4.5				2
KM141	10.0	14.9				3
KM142	0.7	0.4				<2
KM143	9.7	7.4				4
KM144	16.4	4.4				4
KM145	11.9	8.1				4
KM146	15.1	5.0				4
KM147	0.4	<0.2				<2
KM148	0.5	0.4				<2
KM150	0.4	<0.2				<2
KM151	0.4	<0.2				<2
KM152	0.5	<0.2				<2
KM153	0.8	0.7				<2
KM154	3.2	4.3				<2
KM155	3.7	4.1				3
KM156	4.3	2.7				<2
KM157	18.4	10.7				5
KM158	10.7	3.3				5
KM159	11.2	7.3				15
KM160	17.9	12.8				4
KM161	16.8	7.3				4
KM162	18.1	5.9				5
KM163	16.0	7.5				4
KN001	0.8	0.7	<0.1	0.3	<0.1	2
KN002	0.3	1.2	<0.1	0.3	0.2	<1
KN003	8.4	8.5				3
KN005	10.1	4.6				3
KN006	7.4	3.0				3
KN009	13.5	12.0				4
KN010	9.6	3.0				3
KN011	6.3	2.7				1
KN012	11.4	4.5				3
KN014	0.2	0.2				<1
KN016	16.1	6.3				2
KN017	12.2	18.1				5
KN018	0.6	0.6				<1
KN019	18.5	14.6				6
KN020	17.5	12.1				6

Geochemical grade assay for rocks, drill cores and drill cuttings samples

Sample No.	SiO_2	Al_2O_3	Fe_2O_3	MnO	MgO	CaO	Na_2O	K_2O	TiO_2	P_2O_5	LOI	Total	Be	V	Cr	Co	Ga	Ge	As	Rb	Sr	Y	Zr	Nb	Mo	In	Sn	Sb	Cs	Ba	Sc
	%	%	%	%	%	%	%	%	%	%	%	%	ppm	ppm	ppm	ppm	ppm	ppm	ppm	ppm	ppm	ppm	ppm	ppm	ppm	ppm	ppm	ppm	ppm	ppm	ppm	ppm
Detection Limit	0.01	0.01	0.01	0.001	0.01	0.01	0.01	0.01	0.001	0.01	0.01		1	5	20	1	1	0.5	5	1	2	0.5	1	0.2	2	0.1	1	0.2	0.1	3	1
KN021	50.05	13.29	14.20	0.200	5.84	10.01	2.45	0.98	2.144	0.24	1.05	100.45	<1	423	100	44	21	1.5	<5	24	368	27.5	153	14.1	<2	<0.1	<1	<0.2	0.4	326	39
KN022A	49.95	13.33	13.87	0.206	5.62	10.04	2.49	1.04	2.107	0.24	1.31	100.21	<1	433	92	40	20	1.7	<5	21	354	26.0	143	13.3	<2	<0.1	<1	0.2	0.1	305	38
KN022B	52.26	11.21	17.01	0.209	3.28	5.59	2.66	2.41	3.025	0.43	2.04	100.12	1	298	<20	35	24	1.7	<5	83	326	41.6	287	25.2	<2	<0.1	2	<0.2	0.3	556	32
KN023A	50.28	13.32	14.10	0.201	5.67	9.95	2.52	1.02	2.145	0.24	1.06	100.50	<1	416	96	43	22	1.8	<5	24	383	28.5	160	14.8	<2	<0.1	<1	<0.2	0.1	339	38
KN023B	50.01	11.39	17.67	0.220	3.78	7.31	2.63	1.60	3.509	0.40	1.81	100.34	1	497	<20	40	25	1.7	<5	49	347	39.2	247	23.2	<2	<0.1	1	<0.2	0.4	453	37
KN024A	50.23	13.37	14.19	0.203	5.91	10.06	2.49	0.98	2.130	0.23	0.64	100.45	<1	441	101	45	22	1.9	<5	23	389	27.7	153	14.5	<2	<0.1	<1	<0.2	0.1	326	38
KN024B	51.30	11.99	15.92	0.172	3.38	5.78	2.77	3.24	2.843	0.42	1.69	99.50	1	397	<20	35	25	1.7	<5	161	367	42.9	259	23.3	<2	<0.1	1	<0.2	0.8	483	33
KN025A	49.73	13.32	13.95	0.190	5.98	10.18	2.34	0.80	1.810	0.21	1.63	100.12	<1	420	147	44	21	1.6	<5	15	321	28.1	127	10.8	<2	<0.1	<1	<0.2	0.1	265	39
KN025B	54.24	10.36	15.40	0.344	3.61	6.99	2.73	1.99	3.045	0.37	1.20	100.28	<1	556	<20	35	22	1.7	<5	57	328	32.9	224	22.7	<2	<0.1	2	<0.2	0.5	447	33
KN026	49.93	13.21	14.14	0.205	5.81	10.19	2.45	0.98	2.132	0.24	0.82	100.10	<1	434	100	44	22	1.9	<5	21	398	28.0	155	14.6	<2	<0.1	<1	<0.2	0.1	324	39
KN027	50.73	12.64	15.01	0.212	4.82	8.78	2.56	1.33	2.304	0.27	0.50	99.15	<1	420	52	41	22	1.5	<5	32	265	36.7	175	14.9	<2	0.1	1	0.3	0.2	311	41
KN028	51.43	12.49	15.33	0.220	4.88	8.75	2.61	1.30	2.236	0.27	0.71	100.24	<1	428	53	41	21	1.8	<5	29	266	39.4	189	15.2	<2	0.1	3	<0.2	0.4	335	42
KN029	51.22	12.68	16.16	0.229	4.09	8.38	2.87	1.42	2.604	0.33	0.25	100.24	<1	489	41	38	22	2.1	<5	35	242	44.3	210	19.0	<2	0.1	2	<0.2	0.6	381	41
KN030	52.07	12.22	14.67	0.224	4.67	8.65	2.71	1.28	2.174	0.25	0.68	99.60	<1	438	50	37	20	1.5	<5	31	235	35.6	171	14.1	<2	<0.1	1	0.3	0.3	341	41
KN031	51.31	12.56	15.85	0.227	4.57	8.73	2.65	1.24	2.367	0.28	0.22	100.01	<1	450	27	40	21	1.7	<5	29	290	38.8	186	16.2	<2	<0.1	2	<0.2	0.2	368	42
KN032	50.66	13.56	13.20	0.204	6.31	10.29	2.43	0.87	1.660	0.18	0.86	100.22	<1	376	84	40	18	1.6	<5	19	275	27.1	127	10.3	<2	<0.1	1	<0.2	0.2	243	43
KN033	52.09	12.56	15.37	0.209	4.42	8.40	2.68	1.45	2.391	0.30	0.34	100.21	<1	443	26	38	22	1.7	<5	36	280	38.1	198	16.5	<2	<0.1	2	<0.2	0.3	375	41
KN034A	50.61	13.39	12.89	0.155	5.19	8.59	2.82	1.58	4.453	0.39	0.12	100.19	1	366	72	22	18	0.6	<5	38	751	28.7	229	20.5	<2	<0.1	1	<0.2	0.8	501	27
KN034B	54.47	12.92	13.34	0.159	2.68	6.38	3.11	2.76	2.925	0.74	0.62	100.11	3	271	<20	29	29	1.7	<5	72	727	48.8	443	37.4	2	0.1	4	<0.2	1.5	910	19
KN035A	51.21	13.10	14.95	0.213	4.96	9.10	2.47	1.09	2.246	0.26	0.68	100.28	<1	423	54	39	21	1.6	<5	28	274	37.8	186	14.7	<2	<0.1	1	<0.2	1.0	331	42
KN036A	50.98	12.44	15.78	0.220	4.28	8.06	2.69	1.64	3.451	0.50	0.13	100.18	1	458	21	38	25	1.7	<5	48	381	40.4	267	25.1	<2	<0.1	3	<0.2	1.0	515	33
KN036B	50.23	12.93	15.25	0.218	4.29	8.14	2.70	1.47	3.708	0.44	0.88	100.26	1	509	20	39	25	1.2	<5	38	400	37.3	247	23.6	<2	<0.1	2	<0.2	0.5	450	34
KN037	49.99	14.83	14.86	0.196	3.69	8.90	2.83	1.30	2.775	0.36	0.58	100.31	<1	514	<20	36	23	1.7	<5	36	378	34.2	176	16.5	<2	<0.1	2	<0.2	1.9	398	32
KN038	53.12	12.59	14.65	0.221	3.13	7.02	3.10	1.74	3.171	0.46	1.27	100.49	2	306	<20	27	23	1.4	<5	40	366	47.2	289	24.7	<2	<0.1	3	<0.2	0.6	528	29
KN039A	49.79	13.50	14.13	0.201	6.27	9.99	2.53	0.94	2.133	0.28	0.41	100.17	<1	396	135	42	20	1.7	<5	26	339	29.7	139	13.4	<2	<0.1	1	<0.2	0.7	305	39
KN039B	49.70	11.98	17.56	0.238	4.22	8.43	2.49	1.25	3.598	0.40	0.63	100.48	<1	592	<20	43	23	1.2	<5	35	340	40.4	212	19.9	<2	<0.1	2	<0.2	0.9	409	40
KN040A	50.37	12.99	14.77	0.208	5.70	9.64	2.41	1.04	2.358	0.39	0.51	100.40	<1	446	100	43	21	1.5	<5	32	340	32.7	165	15.6	<2	<0.1	1	<0.2	0.8	355	39
KN040B	50.02	13.17	14.64	0.204	5.64	9.67	2.48	0.96	2.372	0.32	0.75	100.22	<1	441	97	42	21	1.7	<5	29	338	32.4	165	15.6	<2	<0.1	2	<0.2	1.0	303	38
KN040C	46.94	11.66	19.22	0.238	5.22	9.09	2.32	1.02	3.871	0.29	0.40	100.26	<1	916	<20	54	23	1.7	<5	27	314	31.6	156	15.0	<2	<0.1	3	<0.2	0.8	354	45
KN042	52.81	13.95	12.56	0.183	5.62	9.14	2.27	1.27	1.111	0.13	0.93	99.98	<1	357	32	46	20	1.9	<5	45	201	22.9	105	10.4	<2	<0.1	4	<0.2	1.4	239	44
KN043	68.13	12.39	5.56	0.073	0.67	2.74	2.72	4.47	0.708	0.21	2.07	99.73	3	27	<20	6	19	1.7	<5	195	98	53.8	295	25.0	<2	<0.1	9	0.3	10.3	650	18
KN044	52.38	13.98	11.39	0.165	5.85	9.60	2.20	0.82	1.118	0.14	1.72	99.36	<1	305	75	36	19	1.6	<5	18	192	25.8	132	8.4	<2	0.2	55	<0.2	1.6	294	39
KN045	54.60	13.78	12.35	0.175	4.59	8.02	2.65	1.76	1.322	0.20	0.96	100.41	1	322	<20	37	21	1.8	<5	62	211	31.9	141	12.1	<2	<0.1	<1	<0.2	2.2	345	38
KN046A	53.20	13.74	11.83	0.193	5.80	9.50	2.46	1.12	1.137	0.13	0.70	99.81	<1	311	31	38	19	1.8	<5	37	192	25.1	97	7.0	<2	<0.1	12	<0.2	1.0	211	42
KN047	49.56	12.57	15.74	0.214	4.31	8.37	2.68	1.45	3.472	0.55	0.81	99.71	1	441	<20	37	23	1.8	<5	33	390	41.7	235	23.8	<2	<0.1	3	<0.2	0.4	511	34
KN048A	53.60	13.18	13.72	0.190	4.02	7.66	2.84	1.73	1.725	0.26	1.02	99.96	1	393	<20	36	22	1.7	<5	59	232	39.5	187	17.3	<2	<0.1	<1	<0.2	1.6	457	37
KN048B	57.20	11.94	13.74	0.155	2.22	5.01	3.01	2.61	1.800	0.40	1.30	99.39	2	230	<20	27	23	2.0	<5	92	195	55.8	289	25.5	2	<0.1	1	<0.2	2.3	673	29
KN049	49.86	13.47	13.87	0.208	5.78	9.84	2.43	0.90	1.926	0.22	0.94	99.44	<1	399	103	41	20	1.6	<5	19	317	28.8	137	12.7	<2	<0.1	<1	<0.2	0.2	300	41
KN050	49.76	13.65	14.25	0.224	5.78	10.10	2.43	0.85	2.153	0.27	0.97	100.43	<1	415	116	41	20	1.6	<5	12	331	31.0	144	13.4	<2	<0.1	<1	<0.2	0.3	329	40
KN051	50.81	12.73	15.76	0.209	4.89	8.72	2.45	1.35	2.313	0.28	0.52	100.04	<1	429	43	38	20	1.7	<5	38	272	37.3	164	14.2	<2	<0.1	<1	<0.2	0.4	332	43
KN052	49.51	13.60	13.85	0.187	6.21	10.24	2.38	0.86	1.877	0.19	0.64	99.56	<1	408	118	43	20	1.8	<5	17	320	26.8	129	12.2	<2	<0.1	<1	<0.2	0.1	283	42
KN104	50.25	13.16	14.23	0.161	4.52	8.75	2.55	1.27	2.997	0.39	1.51	99.80	2	458	43	43	23	1.5	<5	27	445	34.9	216	19.6	2	<0.1	2	<0.2	0.5	524	32
KN105	51.62	12.24	16.00	0.225	4.63	8.46	2.48	1.15	2.419	0.30	0.67	100.19	1	451	60	44	22	1.7	<5	26	285	42.3	205	16.1	<2	<0.1	2	<0.2	0.6	398	41
KN108	51.39	12.57	15.75	0.227	4.45	8.44	2.43	1.17	2.447	0.30	0.77	99.94	1	440	50	42	21	1.6	<5	24	257	43.8	191	15.4	<2	<0.1	1	<0.2	0.1	329	41
KN110A	49.47	12.68	14.89	0.204	5.66	9.23	2.41	0.97	2.630	0.28	1.59	100.02	1	475	108	45	22	1.7	<5	20	404	31.0	180	14.8	<2	<0.1	1	<0.2	0.2	313	35
KN112	51.20	13.04	14.58	0.211	5.27	9.13	2.61	0.96	2.092	0.26	0.71	100.07	1	423	77	42	20	1.9	<5	22	315	35.7	164	13.9	<2	<0.1	1	<0.2	0.3	335	41
KN115	50.62	12.22	15.76	0.212	4.28	8.06	2.71	1.48	3.023	0.34	1.68	100.39	1	485	<20	38	23	1.5	<5	33	372	38.7	227	19.9	<2	<0.1	2	0.2	1.3	455	32
KN117	50.33	13.40	15.19	0.203	3.61	8.41	2.64	1.26	3.016	0.40	1.12	99.57	1	467	<20	35	23	1.2	<5	33	375	50.7	205	18.1	<2	<0.1	1	<0.2	0.9	434	35
KN118	50.01	12.65	15.50	0.211	4.70	8.80	2.41	1.13	2.720	0.39	1.41	99.93	1	459	53	40	21	1.6	<5	28	506	38.8	195	17.1	<2	<0.1	1	<0.2	0.5	391	37
KN119	50.24	12.61	16.82	0.220	4.18	8.31	2.55	1.22	3.104	0.40	0.69	100.35	1	563	<20	42	23	1.7	<5	29	342	39.7	193	17.9	<2	<0.1	2	<0.2	1.1	447	37
KN121	50.48	12.76	15.82	0.215	4.65	8.65	2.53	1.27	3.005	0.36	0.51	100.24	1	444	43	41	22	1.4	<5	26	394	35.9	207	19.6	<2	<0.1	1	<0.2	0.5	447	34
KN123	50.03	11.98	17.08	0.231	4.88	8.83	2.34	0.97	2.912	0.28	0.62	100.17	1	565	40	46	21	1.5	<5	22	264	43.5	190	15.5	<2	<0.1	1	<0.2	0.3	350	44
KN124	52.54	13.69	14.83	0.185	3.07	7.73	2.70	1.51	2.577	0.39	1.21	100.41	2	300	21	37	24	1.6	<5	36	298	47.2	247	20.3	<2	<0.1	2	0.4	0.4	492	32
KN125	49.95	13.22	14.53	0.200	5.28	9.55	2.36	1.06	2.361	0.32	1.07	99.90	1	417	108	40	21	1.7	<5	28	366	33.8	166	15.7	<2	<0.1	1	<0.2	1.4	429	36
KN126A	51.56	12.43	15.57	0.216	4.22	8.43	2.44	1.26	2.694	0.34	1.06	100.22	1	406	48	39	22	1.3	<5	27	254	47.9	232	19.0	<2	<0.1	2	<0.2	0.2	383	39
KN128	49.89	12.56	15.02	0.204	4.17	7.70	2.74	1.76	4.038	0.73	1.25	100.06	2	369	<20	35	26	1.5	<5	37	636	46.4	313	28.2	<2	<0.1	2	0.2	0.8	615	26

Geochemical grade assay for rocks, drill cores and drill cuttings samples

Sample No.	La	Ce	Pr	Nd	Sm	Eu	Gd	Tb	Dy	Ho	Er	Tm	Yb	Lu	Hf	Ta	W	Tl	Bi	Th	U	Ag	Cd	Cu	Ni	Pb	Zn	S
	ppm	ppm	ppm	ppm	ppm	ppm	ppm	ppm	ppm	ppm	ppm	ppm	ppm	ppm	ppm	ppm	ppm	ppm	ppm	ppm	ppm	ppm	ppm	ppm	ppm	ppm	ppm	%
Detection Limit	0.05	0.05	0.01	0.05	0.01	0.005	0.01	0.01	0.01	0.01	0.01	0.005	0.01	0.002	0.1	0.01	0.5	0.05	0.1	0.05	0.01	0.3	0.3	1	1	3	30	0.001
KN021	22.56	51.31	5.83	25.12	5.56	1.873	5.74	0.90	5.45	1.07	3.14	0.440	2.62	0.381	4.3	1.00	<0.5	0.19	<0.1	2.36	0.45	<0.3	0.5	246	57	7	104	<0.001
KN022A	21.83	48.38	5.49	24.04	5.30	1.779	5.40	0.87	5.15	1.01	3.06	0.431	2.37	0.332	4.1	0.95	<0.5	0.14	<0.1	2.29	0.42	<0.3	0.9	234	55	<3	100	<0.001
KN022B	42.58	94.55	10.43	44.24	9.26	2.891	8.56	1.42	8.58	1.68	4.83	0.744	4.28	0.600	7.8	1.80	<0.5	0.21	<0.1	4.46	0.87	<0.3	0.5	273	10	<3	134	<0.001
KN023A	23.05	51.57	5.96	25.55	5.56	1.904	5.88	0.92	5.44	1.09	3.27	0.459	2.61	0.373	4.5	1.00	<0.5	0.14	<0.1	2.47	0.45	<0.3	0.6	239	49	8	95	<0.001
KN023B	35.69	81.17	9.13	38.92	8.24	2.696	8.33	1.33	7.68	1.56	4.36	0.626	3.63	0.517	6.7	1.59	<0.5	0.41	<0.1	3.69	0.73	<0.3	0.7	372	14	<3	137	<0.001
KN024A	22.30	50.15	5.63	24.68	5.34	1.888	5.55	0.90	5.37	1.04	2.95	0.430	2.59	0.344	4.4	0.99	<0.5	0.11	<0.1	2.32	0.45	<0.3	0.6	226	55	<3	96	<0.001
KN024B	37.91	85.26	9.50	40.88	8.84	2.835	8.63	1.42	8.28	1.63	4.62	0.671	3.71	0.555	6.9	1.63	<0.5	0.34	<0.1	3.90	0.80	<0.3	<0.3	232	14	<3	145	0.004
KN025A	18.12	40.33	4.64	20.77	4.81	1.700	5.06	0.87	5.27	1.05	3.13	0.459	2.45	0.372	3.6	0.73	<0.5	0.12	<0.1	2.19	0.50	<0.3	<0.3	227	64	8	96	<0.001
KN025B	32.95	74.66	8.47	35.85	7.48	2.382	7.31	1.15	6.62	1.25	3.61	0.514	2.79	0.433	6.5	1.61	<0.5	0.33	<0.1	3.33	0.54	<0.3	0.6	1315	16	<3	120	0.012
KN026	22.26	49.87	5.63	24.74	5.46	1.868	5.56	0.91	5.44	1.06	3.06	0.424	2.39	0.357	4.3	0.95	<0.5	0.12	<0.1	2.32	0.42	<0.3	0.8	241	53	<3	99	<0.001
KN027	23.08	53.12	6.12	26.11	6.20	2.011	6.52	1.13	6.88	1.41	4.08	0.603	3.25	0.484	4.8	1.01	<0.5	0.23	<0.1	2.55	0.50	<0.3	0.6	273	41	<3	117	<0.001
KN028	21.86	46.08	5.98	25.85	6.32	1.974	7.49	1.19	7.18	1.52	4.43	0.653	4.02	0.596	5.4	1.08	<0.5	0.15	<0.1	2.62	0.50	<0.3	0.5	269	40	<3	113	<0.001
KN029	27.72	59.09	7.47	31.91	7.26	2.246	8.72	1.35	8.29	1.72	4.93	0.715	4.38	0.610	6.4	1.29	<0.5	0.28	<0.1	3.35	0.55	<0.3	0.3	289	33	7	122	<0.001
KN030	21.06	44.63	5.60	24.07	5.86	1.854	6.81	1.10	6.75	1.41	4.08	0.602	3.81	0.523	5.1	1.01	<0.5	0.14	<0.1	2.31	0.57	<0.3	<0.3	240	36	15	114	<0.001
KN031	24.51	50.91	6.51	27.62	6.38	2.000	7.31	1.19	7.16	1.47	4.20	0.614	3.71	0.541	5.6	1.12	<0.5	0.16	<0.1	2.92	0.51	<0.3	1.4	268	32	18	125	<0.001
KN032	15.74	33.21	4.26	17.80	4.31	1.416	4.75	0.80	4.79	1.03	2.87	0.441	2.59	0.375	3.5	0.69	<0.5	0.09	<0.1	1.86	0.35	<0.3	0.3	172	54	<3	93	<0.001
KN033	24.74	51.06	6.50	27.62	6.39	2.058	6.91	1.17	6.98	1.45	4.16	0.627	3.77	0.518	5.4	1.16	<0.5	0.19	<0.1	2.86	0.50	<0.3	<0.3	185	27	13	120	<0.001
KN034A	31.15	64.92	8.45	36.43	8.03	2.729	7.71	1.14	6.00	1.07	2.85	0.366	2.28	0.302	6.4	1.71	<0.5	0.10	<0.1	3.36	0.73	<0.3	<0.3	111	66	<3	93	<0.001
KN034B	62.62	131.47	16.97	69.70	15.00	4.521	13.85	2.04	10.66	1.98	5.20	0.629	3.88	0.535	11.8	2.58	0.6	0.45	<0.1	7.23	1.56	<0.3	0.4	251	15	8	140	0.011
KN035A	22.24	46.71	5.94	26.16	6.20	1.950	6.76	1.14	7.05	1.45	4.22	0.608	3.71	0.529	5.2	1.01	<0.5	0.24	<0.1	2.71	0.49	0.4	0.9	256	43	<3	115	0.031
KN036A	35.71	75.77	9.82	41.33	9.04	2.908	9.39	1.40	7.99	1.60	4.36	0.584	3.64	0.523	7.5	1.71	<0.5	0.24	<0.1	4.45	0.84	<0.3	0.7	235	33	<3	133	0.037
KN036B	31.98	66.95	8.70	37.58	8.18	2.641	8.40	1.27	7.32	1.44	3.92	0.547	3.39	0.474	6.9	1.61	<0.5	0.18	<0.1	3.91	0.73	<0.3	0.7	243	33	5	131	0.696
KN037	26.38	55.18	6.98	29.17	6.49	2.275	6.74	1.11	6.64	1.34	3.89	0.572	3.38	0.500	5.3	1.20	<0.5	0.22	<0.1	3.23	0.63	<0.3	0.7	238	26	4	116	0.055
KN038	37.19	78.46	10.04	43.06	9.47	3.059	9.92	1.52	8.90	1.82	4.90	0.687	4.29	0.590	8.0	1.79	<0.5	0.23	<0.1	4.03	0.81	<0.3	0.6	124	4	<3	133	0.137
KN039A	20.62	43.07	5.46	23.51	5.28	1.778	5.63	0.91	5.48	1.10	3.21	0.465	2.92	0.408	4.1	0.92	<0.5	0.17	<0.1	2.43	0.51	<0.3	0.9	190	64	<3	96	0.051
KN039B	29.74	62.43	7.92	33.46	7.52	2.481	8.40	1.31	7.65	1.55	4.49	0.646	4.06	0.569	6.0	1.39	<0.5	0.15	<0.1	3.52	0.70	<0.3	0.3	348	21	<3	136	0.127
KN040A	24.40	50.50	6.39	28.02	6.07	2.006	6.90	1.04	6.30	1.28	3.68	0.529	3.23	0.452	4.7	1.11	<0.5	0.22	<0.1	2.89	0.58	<0.3	0.5	211	56	11	107	0.068
KN040B	24.43	50.24	6.36	26.94	6.13	2.004	6.70	1.03	6.32	1.27	3.63	0.524	3.24	0.451	4.8	1.03	<0.5	0.27	<0.1	2.87	0.57	<0.3	<0.3	210	54	8	107	0.104
KN040C	21.91	45.49	5.87	24.92	5.67	1.946	6.49	0.99	5.83	1.24	3.49	0.496	3.08	0.441	4.5	0.97	<0.5	0.12	<0.1	2.48	0.49	<0.3	0.5	416	43	<3	133	0.087
KN042	15.87	34.71	3.94	16.99	3.84	1.238	4.36	0.74	4.28	0.86	2.44	0.366	2.20	0.342	3.2	0.78	<0.5	0.28	0.1	4.77	0.98	<0.3	0.6	122	57	10	87	0.010
KN043	53.32	109.06	12.06	48.88	10.17	1.945	10.58	1.73	10.00	2.01	5.74	0.887	5.37	0.785	8.9	2.37	1.8	1.02	0.2	18.97	3.67	0.4	0.3	27	1	26	94	0.003
KN044	16.63	35.00	4.16	18.07	4.20	1.300	4.59	0.80	4.93	0.96	2.75	0.415	2.57	0.376	4.0	1.74	<0.5	0.08	0.2	4.94	1.13	<0.3	0.5	91	46	10	88	0.011
KN045	21.49	47.06	5.31	22.52	5.13	1.538	5.57	0.98	5.77	1.15	3.31	0.491	2.96	0.458	4.2	1.02	0.6	0.39	0.1	6.26	1.57	<0.3	0.5	65	31	8	95	0.009
KN046A	13.43	29.91	3.45	15.47	3.79	1.292	4.34	0.79	4.74	0.95	2.68	0.405	2.48	0.365	3.1	0.72	<0.5	0.15	<0.1	3.65	0.90	<0.3	0.6	127	32	9	87	0.011
KN047	36.52	81.58	9.45	41.45	8.87	2.977	8.84	1.41	8.21	1.54	4.14	0.597	3.66	0.552	6.9	1.89	<0.5	0.11	<0.1	4.43	0.87	0.4	0.8	146	27	4	125	0.032
KN048A	29.90	63.30	6.96	29.61	6.62	1.996	6.86	1.23	7.19	1.46	4.12	0.624	3.79	0.557	5.6	1.29	0.6	0.27	<0.1	7.17	1.55	<0.3	0.8	141	26	7	112	0.009
KN048B	45.31	96.46	10.81	45.13	9.67	2.615	10.51	1.74	10.43	2.08	5.85	0.867	5.33	0.804	8.5	1.81	1.3	0.54	<0.1	11.05	2.42	0.3	0.8	193	7	13	118	0.008
KN049	19.46	43.09	4.95	21.78	5.00	1.759	5.39	0.93	5.48	1.05	2.98	0.437	2.79	0.402	4.1	0.93	<0.5	0.06	<0.1	2.45	0.44	<0.3	0.7	210	65	<3	102	0.010
KN050	21.59	48.56	5.57	24.03	5.50	1.944	5.85	1.03	5.97	1.17	3.34	0.476	3.03	0.444	4.4	1.00	<0.5	0.06	<0.1	2.82	0.57	<0.3	0.9	206	70	3	108	0.012
KN051	23.29	51.75	5.88	25.63	6.03	2.011	6.58	1.19	7.09	1.43	4.00	0.609	3.68	0.546	5.0	1.07	<0.5	0.09	<0.1	2.91	0.55	0.3	1.0	280	43	<3	118	0.011
KN052	17.86	39.98	4.61	20.11	4.61	1.666	5.04	0.86	5.02	1.01	2.85	0.413	2.62	0.388	3.7	0.84	<0.5	0.06	<0.1	2.18	0.41	<0.3	<0.3	200	53	<3	103	<0.001
KN104	31.99	67.88	8.39	36.55	7.80	2.668	8.14	1.24	6.85	1.29	3.51	0.475	2.86	0.400	5.6	1.56	<0.5	0.12	<0.1	3.29	0.69	0.6	1.1	234	30	16	126	0.066
KN105	25.67	54.04	6.56	28.93	6.77	2.182	7.75	1.22	6.98	1.42	4.05	0.600	3.68	0.536	5.0	1.06	<0.5	0.05	<0.1	2.90	0.55	0.7	1.7	228	24	17	113	0.031
KN108	24.57	51.92	6.36	28.57	6.70	2.178	7.73	1.28	7.49	1.49	4.45	0.648	3.99	0.578	5.0	1.16	<0.5	0.07	<0.1	2.80	0.55	0.7	1.7	249	26	13	115	0.071
KN110A	21.73	47.80	6.00	26.98	6.16	2.229	6.88	1.10	5.97	1.13	3.19	0.432	2.63	0.360	4.7	1.01	<0.5	0.15	<0.1	2.30	0.48	0.5	0.8	212	60	16	101	0.075
KN112	21.52	45.68	5.66	24.86	5.65	1.941	6.59	1.08	6.15	1.24	3.60	0.526	3.26	0.468	4.2	0.92	<0.5	0.05	<0.1	2.55	0.51	0.5	0.4	195	33	12	98	0.016
KN115	28.97	61.44	7.83	34.25	7.88	2.630	7.60	1.34	7.53	1.45	4.33	0.586	3.51	0.486	6.2	1.34	0.5	0.16	<0.1	2.93	0.62	0.7	1.0	243	30	14	127	0.107
KN117	29.48	59.49	7.45	32.73	7.46	2.580	8.46	1.38	7.91	1.57	4.53	0.660	4.02	0.556	5.1	1.20	<0.5	0.06	0.1	3.49	0.74	0.6	1.3	245	<1	15	115	0.035
KN118	27.08	57.32	7.03	31.23	6.89	2.340	7.76	1.26	7.04	1.38	3.98	0.589	3.58	0.512	5.1	1.15	0.5	0.11	0.1	3.32	0.74	0.6	1.4	203	23	8	112	0.050
KN119	28.07	59.18	7.27	32.55	7.22	2.421	7.92	1.25	7.06	1.41	4.09	0.587	3.68	0.522	5.1	1.25	<0.5	0.12	<0.1	3.49	0.73	0.6	1.5	232	9	9	119	0.080
KN121	29.20	61.07	7.52	32.94	7.20	2.441	7.63	1.18	6.59	1.29	3.65	0.511	3.13	0.424	5.4	1.32	<0.5	0.08	<0.1	3.00	0.72	0.7	0.5	181	19	11	114	0.040
KN123	22.28	47.14	5.79	25.65	6.02	2.035	6.93	1.13	6.58	1.32	3.75	0.580	3.38	0.482	4.7	1.01	<0.5	0.05	<0.1	2.71	0.56	0.5	1.6	259	21	7	120	0.027
KN124	35.04	71.72	8.59	37.46	8.25	2.618	9.11	1.49	8.32	1.62	4.69	0.707	4.24	0.606	6.4	1.39	<0.5	0.11	<0.1	4.34	0.81	0.9	0.5	298	5	14	120	0.023
KN125	22.55	48.57	6.09	26.83	5.98	2.050	6.53	1.06	6.06	1.19	3.39	0.490	2.98	0.422	4.3	1.03	<0.5	0.12	<0.1	2.85	0.58	0.5	0.9	219	43	15	100	0.074
KN126A	28.44	60.05	7.29	31.93	7.41	2.285	8.44	1.41	8.16	1.68	4.79	0.732	4.38	0.644	6.2	1.25	<0.5	0.08	<0.1	3.42	0.66	0.8	1.6	268	21	12	120	0.102
KN128	43.17	95.23	12.04	54.34	11.77	3.983	11.65	1.64	8.53	1.56	4.11	0.522	3.14	0.417	7.4	2.05	<0.5	0.19	<0.1	3.88	0.87	0.8	1.7	95	14	15	123	0.023

Geochemical grade assay for rocks, drill cores and drill cuttings samples

Sample No.	Pd	Pt	Ir	Rh	Re	Au
	ppb	ppb	ppb	ppb	ppb	ppb
Detection Limit	0.2	0.2	0.1	0.2	0.1	2
KN021	16.1	12.6				6
KN022A	17.8	12.9				5
KN022B	27.4	2.5				12
KN023A	12.9	11.8				5
KN023B	27.4	2.4				11
KN024A	21.9	13.4				6
KN024B	28.4	2.3				9
KN025A	18.4	16.8				6
KN025B	22.0	2.6				8
KN026	13.0	11.9				5
KN027	20.3	4.6				6
KN028	7.0	5.0				4
KN029	6.2	10.7				1
KN030	7.8	8.7				1
KN031	16.5	4.9				6
KN032	13.4	7.8				4
KN033	18.3	4.6				7
KN034A	5.3	7.9				3
KN034B	9.0	1.0				6
KN035A	15.1	6.7				6
KN036A	3.2	4.3				4
KN036B	3.8	4.4				1
KN037	7.3	6.8				6
KN038	<0.2	<0.2				<2
KN039A	5.6	5.7				3
KN039B	10.1	14.1				7
KN040A	6.5	6.4				3
KN040B	6.3	6.0				3
KN040C	14.1	14.7				9
KN042	1.0	3.6				<2
KN043	<0.2	0.2				<2
KN044	6.0	7.6				4
KN045	0.2	0.9				<2
KN046A	7.4	5.6				3
KN047	<0.2	0.2				<2
KN048A	3.4	5.2				2
KN048B	8.9	2.6				2
KN049	14.4	6.6				4
KN050	10.4	14.5				4
KN051	20.6	4.0				6
KN052	13.2	8.2				9
KN104	133.8	18.7	0.1	<0.2	1.4	41
KN105	35.7	6.0				6
KN108	31.6	10.5				3
KN110A	43.4	16.5	0.2	0.8	1.3	8
KN112	47.0	5.6	<0.1	0.7	0.7	6
KN115	2.3	3.5				<2
KN117	13.2	7.9				3
KN118	41.7	14.7				17
KN119	14.9	9.5				4
KN121	9.0	2.4				<2
KN123	24.2	3.9				6
KN124	24.8	8.0				6
KN125	15.3	11.1				4
KN126A	17.3	6.6				3
KN128	<0.2	<0.2				<2

Geochemical grade assay for rocks, drill cores and drill cuttings samples

Sample No.	SiO_2	Al_2O_3	Fe_2O_3	MnO	MgO	CaO	Na_2O	K_2O	TiO_2	P_2O_5	LOI	Total	Be	V	Cr	Co	Ga	Ge	As	Rb	Sr	Y	Zr	Nb	Mo	In	Sn	Sb	Cs	Ba	Sc
	%	%	%	%	%	%	%	%	%	%	%	%	ppm	ppm	ppm	ppm	ppm	ppm	ppm	ppm	ppm	ppm	ppm	ppm	ppm	ppm	ppm	ppm	ppm	ppm	ppm	ppm
Detection Limit	0.01	0.01	0.01	0.001	0.01	0.01	0.01	0.01	0.001	0.01	0.01		1	5	20	1	1	0.5	5	1	2	0.5	1	0.2	2	0.1	1	0.2	0.1	3	1
KN134	53.73	13.65	12.15	0.170	3.34	6.69	3.15	2.40	3.019	0.74	0.98	100.02	3	226	<20	27	26	1.6	<5	62	878	42.6	325	32.8	<2	<0.1	2	<0.2	1.1	838	20
KN141	50.02	13.00	15.05	0.209	5.19	9.44	2.36	1.07	2.570	0.34	1.13	100.37	1	481	95	49	24	1.5	<5	23	371	34.6	176	18.9	<2	<0.1	1	<0.2	0.2	377	37
KN142	51.58	11.89	16.46	0.229	3.37	7.39	2.67	1.63	3.163	0.51	1.14	100.03	2	414	<20	47	26	1.6	<5	40	335	51.5	258	24.1	<2	<0.1	2	<0.2	0.5	520	33
KN143	50.52	12.98	15.86	0.217	3.50	8.29	2.65	1.44	3.137	0.42	0.74	99.75	2	465	<20	42	26	1.7	<5	34	380	42.0	225	21.5	<2	<0.1	2	<0.2	0.4	452	34
KN144	50.59	12.14	15.37	0.226	4.04	7.75	2.63	1.59	3.836	0.64	1.05	99.85	2	430	26	48	27	2.0	<5	26	479	45.1	311	27.7	<2	<0.1	2	<0.2	0.4	561	29
KN145	50.58	12.43	15.10	0.219	4.18	7.65	2.72	1.74	3.404	0.45	1.36	99.83	2	437	21	44	28	1.9	<5	38	490	40.9	290	25.4	<2	<0.1	2	<0.2	0.3	540	27
KN146	53.79	13.36	11.53	0.161	3.45	7.21	3.73	1.94	3.051	0.46	1.45	100.14	2	312	31	30	26	1.4	<5	46	521	37.6	300	25.6	<2	<0.1	2	<0.2	0.7	544	22
KN148	51.13	13.42	14.68	0.201	4.53	9.14	2.57	1.01	2.153	0.27	1.26	100.36	1	428	76	48	24	1.5	<5	23	324	37.5	170	16.0	<2	<0.1	1	<0.2	0.4	326	38
KN150	54.63	12.90	12.91	0.177	3.26	6.78	3.14	2.15	3.106	0.60	0.66	100.31	2	326	23	32	29	2.0	<5	51	497	48.3	375	30.3	<2	<0.1	3	<0.2	0.6	661	23
KN151	58.77	13.11	10.44	0.134	2.76	5.03	3.56	3.21	1.873	0.59	0.93	100.40	3	247	53	29	30	1.5	5	129	371	27.7	355	23.9	<2	<0.1	2	<0.2	1.2	713	19
KN152	66.65	12.92	6.54	0.097	0.73	1.96	3.45	4.23	1.201	0.32	2.28	100.37	4	20	<20	5	27	1.6	<5	139	341	60.1	574	46.1	2	<0.1	5	<0.2	3.1	1230	13
KN153	50.96	12.57	14.57	0.203	4.11	8.01	2.71	1.54	3.583	0.51	1.26	100.02	2	413	<20	42	28	1.8	<5	33	495	42.3	292	25.3	<2	<0.1	3	<0.2	0.3	467	29
KN154	53.06	12.86	12.43	0.185	3.90	7.54	2.98	1.33	3.370	0.53	1.50	99.68	2	345	43	35	26	1.8	<5	44	499	42.7	328	28.7	<2	<0.1	2	<0.2	0.7	548	25
KN156	53.44	12.48	13.03	0.188	4.12	7.32	2.69	2.11	2.643	0.36	1.12	99.51	2	388	92	37	25	1.6	<5	55	387	41.4	278	25.4	<2	<0.1	2	0.2	0.3	520	28
KN157	50.74	12.90	14.60	0.211	5.06	9.00	2.49	1.29	2.392	0.31	1.12	100.11	1	417	94	48	22	1.7	<5	34	267	40.3	199	18.7	<2	<0.1	2	<0.2	0.4	350	39
KN158	50.47	12.52	15.19	0.217	4.78	9.26	2.50	0.74	2.120	0.24	1.48	99.52	1	427	57	48	22	1.5	<5	20	330	37.2	159	14.3	<2	<0.1	1	<0.2	0.2	345	42
KN159	49.94	12.88	14.51	0.182	5.24	9.00	2.26	1.61	2.341	0.30	1.39	99.63	1	403	101	45	22	1.9	<5	44	263	40.7	195	16.9	<2	<0.1	1	<0.2	0.5	352	39
KN160	52.14	12.75	13.10	0.161	4.04	7.94	2.61	1.63	2.415	0.35	1.53	98.66	2	359	79	33	23	0.9	<5	61	385	34.5	283	20.4	<2	<0.1	1	<0.2	0.7	544	30
KN161	51.96	13.09	14.81	0.211	4.62	8.81	2.54	0.99	2.153	0.28	0.59	100.04	1	377	51	48	24	1.8	<5	25	302	36.8	174	15.5	<2	<0.1	1	<0.2	0.2	356	39
KN162	55.01	11.84	15.56	0.226	1.85	5.79	2.99	2.46	2.298	0.88	1.25	100.14	3	49	<20	26	30	1.9	<5	61	442	63.9	452	35.5	2	<0.1	3	<0.2	0.9	807	21
KN163	52.02	12.84	14.13	0.196	4.33	7.98	2.71	1.52	3.369	0.44	0.79	100.32	2	402	39	32	24	1.3	<5	32	470	38.1	262	20.1	<2	<0.1	2	<0.2	0.3	502	28
KN164	51.35	13.16	13.35	0.200	6.27	10.12	2.23	0.83	1.726	0.20	0.51	99.95	1	378	131	40	18	1.0	<5	17	245	30.5	137	11.2	<2	<0.1	1	<0.2	0.3	265	42
KN165	51.54	12.73	13.66	0.139	3.57	6.41	3.34	2.00	3.372	0.55	2.34	99.65	2	362	32	32	25	1.5	<5	50	534	39.3	294	22.0	<2	<0.1	2	<0.2	2.4	532	25
KN166	53.78	12.41	14.28	0.230	2.91	6.58	2.84	1.76	2.947	0.48	1.88	100.10	2	231	<20	30	24	1.7	<5	40	390	60.3	310	25.3	<2	<0.1	2	<0.2	0.5	588	27
KN167B	52.04	11.52	16.46	0.233	2.97	6.98	2.71	1.73	3.306	0.57	1.10	99.61	2	257	<20	35	23	1.4	<5	44	300	54.2	282	24.2	<2	<0.1	2	<0.2	0.7	536	34
KN168	64.91	13.24	7.49	0.142	1.05	2.86	3.73	3.90	1.367	0.42	1.08	100.19	4	18	<20	5	26	1.3	<5	111	410	123.7	558	44.2	3	<0.1	4	<0.2	2.0	1110	14
KN169	52.06	12.81	15.22	0.218	4.62	8.71	2.47	0.99	2.155	0.26	0.26	99.78	1	409	51	43	22	1.4	<5	24	234	40.0	187	17.0	<2	<0.1	1	<0.2	0.5	306	41
KN170	51.69	12.33	15.82	0.222	4.53	8.70	2.40	0.98	2.611	0.32	0.37	99.97	1	432	37	42	22	1.8	<5	21	221	46.5	210	17.1	<2	<0.1	2	<0.2	0.5	282	42
KN171	51.67	12.85	15.14	0.210	4.60	8.88	2.43	0.95	2.593	0.31	0.56	100.20	1	420	47	42	22	1.5	<5	21	230	45.0	206	16.6	<2	<0.1	1	<0.2	0.2	272	41
KN172	51.48	12.55	14.79	0.216	3.92	7.74	2.91	1.52	3.511	0.64	0.67	99.95	2	346	<20	37	25	1.7	<5	34	462	44.3	263	23.8	<2	<0.1	2	<0.2	0.5	520	30
KN173	51.85	12.83	15.29	0.221	4.94	8.95	2.46	1.02	2.203	0.28	0.22	100.26	1	419	68	44	22	1.6	<5	23	256	39.7	183	15.9	<2	<0.1	1	<0.2	0.3	338	42
KN174A	51.73	12.78	14.98	0.205	4.93	8.97	2.39	0.91	2.173	0.26	0.61	99.93	1	408	57	44	21	1.9	<5	23	249	39.7	183	15.1	<2	<0.1	1	<0.2	0.5	302	41
KN175	52.17	12.87	12.87	0.151	4.41	7.57	2.76	1.85	3.830	0.51	0.96	99.95	2	317	60	40	26	1.7	<5	43	696	39.6	306	26.8	<2	<0.1	2	<0.2	1.1	593	24
KN176	51.84	12.75	15.20	0.219	4.77	8.79	2.40	1.03	2.218	0.28	0.47	99.97	1	407	140	45	22	1.7	<5	23	240	41.5	192	16.3	<2	<0.1	1	<0.2	0.4	329	42
TM101	45.95	9.42	11.76	0.172	9.30	12.82	1.33	2.77	3.450	0.56	1.58	99.11	2	293	303	50	18	1.6	<5	61	799	28.3	277	74.0	3	<0.1	3	<0.2	1.8	1020	40
TM102	48.86	14.02	14.32	0.183	5.36	9.82	2.48	0.86	2.962	0.30	0.62	99.80	1	581	106	48	25	1.4	<5	17	480	25.8	151	23.0	<2	<0.1	1	<0.2	0.2	329	33
TM103	47.15	13.09	16.47	0.203	4.45	8.65	2.61	1.28	4.878	0.33	0.48	99.58	1	640	<20	38	24	0.9	<5	26	472	30.5	184	23.6	<2	0.1	1	<0.2	0.3	409	33
TM104	49.97	13.10	14.36	0.208	4.53	8.67	2.72	1.14	3.396	0.41	1.79	100.30	1	488	76	44	26	1.5	<5	24	464	33.8	215	22.9	<2	<0.1	2	<0.2	0.2	378	32
TM105	50.18	12.01	16.28	0.216	3.81	7.80	2.66	1.42	3.960	0.48	1.31	100.12	2	445	<20	41	26	1.8	<5	29	460	41.4	260	26.8	<2	<0.1	3	0.2	0.3	464	32
TM106	48.44	14.07	14.61	0.183	5.34	9.81	2.58	0.90	3.019	0.27	0.48	99.73	1	663	72	51	26	1.5	<5	19	500	25.1	149	16.8	<2	<0.1	1	<0.2	0.2	309	33
TM107	48.63	11.73	18.83	0.242	4.50	8.61	2.32	0.92	3.152	0.26	0.80	99.99	<1	910	<20	56	24	1.4	<5	23	257	38.3	160	15.5	<2	<0.1	1	<0.2	0.5	332	46
TM109	51.12	12.56	14.95	0.196	4.05	8.04	2.58	1.46	3.327	0.45	1.48	100.20	2	399	40	41	27	1.7	<5	35	612	41.9	257	23.2	<2	<0.1	2	<0.2	0.6	503	30
TM110	47.82	14.41	11.09	0.102	5.70	4.54	3.00	1.82	3.934	0.52	7.46	100.39	2	462	47	49	27	1.1	<5	42	1220	41.7	301	26.8	<2	<0.1	3	<0.2	1.0	750	35
TM111	51.27	12.60	14.47	0.184	4.23	7.72	2.57	1.52	3.381	0.45	1.72	100.12	2	402	42	40	26	1.3	<5	34	520	43.0	262	24.5	<2	<0.1	2	<0.2	0.4	515	30
TM112	51.01	12.41	14.84	0.191	4.03	7.87	2.55	1.52	3.385	0.44	1.73	99.99	2	414	43	40	27	1.3	<5	36	553	43.3	267	24.8	<2	<0.1	2	<0.2	0.5	491	31
TM113	53.53	12.64	13.88	0.228	3.38	6.75	3.03	2.11	2.933	0.62	0.66	99.75	2	244	42	32	26	2.0	<5	44	462	47.4	311	28.3	<2	<0.1	2	<0.2	0.3	719	24
TM114	51.98	12.34	13.35	0.214	3.46	6.87	2.53	2.26	2.938	0.62	2.12	98.68	2	235	40	31	25	1.9	<5	48	584	48.7	305	27.8	<2	<0.1	3	<0.2	0.2	680	25
TM115	50.52	12.65	14.96	0.189	4.63	8.83	2.55	1.14	2.871	0.30	0.94	99.59	1	469	65	42	24	1.9	<5	25	377	37.4	202	18.9	<2	<0.1	2	<0.2	0.2	370	34
TM116	49.08	12.44	14.48	0.194	5.04	8.83	2.49	0.86	3.768	0.40	2.49	100.07	1	437	79	40	24	1.6	<5	20	474	32.8	197	19.9	<2	<0.1	2	<0.2	0.3	424	33
TM117	44.74	10.63	11.51	0.191	7.27	12.80	1.73	2.27	3.545	0.71	4.51	99.91	2	417	142	41	14	1.7	<5	105	901	34.0	296	91.9	<2	<0.1	2	<0.2	4.8	3590	31
TM118	49.86	12.36	14.98	0.200	4.47	8.51	2.63	0.95	3.582	0.49	1.75	99.77	2	422	43	42	25	1.7	<5	23	496	36.6	242	30.8	<2	<0.1	2	<0.2	0.3	479	31
TM119	49.35	12.56	15.32	0.202	4.22	8.23	2.65	0.81	4.050	0.54	2.14	100.06	2	435	<20	50	27	1.9	<5	24	513	43.3	246	26.0	<2	<0.1	2	<0.2	0.5	505	31
TM120	52.06	12.70	12.15	0.189	4.58	7.71	2.95	1.96	3.519	0.50	1.34	99.66	2	383	39	34	26	1.6	<5	42	485	37.1	294	24.9	<2	<0.1	2	0.3	0.3	527	27

Geochemical grade assay for rocks, drill cores and drill cuttings samples

Sample No.	La	Ce	Pr	Nd	Sm	Eu	Gd	Tb	Dy	Ho	Er	Tm	Yb	Lu	Hf	Ta	W	Tl	Bi	Th	U	Ag	Cd	Cu	Ni	Pb	Zn	S
	ppm	ppm	ppm	ppm	ppm	ppm	ppm	ppm	ppm	ppm	ppm	ppm	ppm	ppm	ppm	ppm	ppm	ppm	ppm	ppm	ppm	ppm	ppm	ppm	ppm	ppm	ppm	%
Detection Limit	0.05	0.05	0.01	0.05	0.01	0.005	0.01	0.01	0.01	0.01	0.01	0.005	0.01	0.002	0.1	0.01	0.5	0.05	0.1	0.05	0.01	0.3	0.3	1	1	3	30	0.001
KN134	54.96	116.90	14.25	60.30	11.90	3.913	11.28	1.59	8.20	1.47	3.87	0.501	3.11	0.419	8.0	2.32	0.6	0.23	<0.1	6.72	1.59	0.8	0.6	56	<1	8	93	0.048
KN141	23.98	52.77	6.30	27.50	6.05	2.072	6.37	1.02	5.85	1.17	3.44	0.487	3.05	0.429	4.6	1.08	<0.5	0.18	<0.1	2.68	0.56	0.5	1.0	202	34	<3	99	0.049
KN142	35.22	76.00	9.08	39.96	8.95	2.899	9.52	1.59	9.04	1.77	5.34	0.746	4.65	0.671	6.6	1.57	<0.5	0.20	<0.1	4.40	0.93	0.7	1.5	222	<1	8	125	0.060
KN143	30.77	66.73	8.03	34.83	7.68	2.600	8.10	1.29	7.25	1.43	4.37	0.618	3.80	0.552	5.8	1.41	<0.5	0.16	<0.1	3.62	0.77	0.6	1.1	285	<1	7	121	0.052
KN144	38.70	86.75	10.67	46.49	10.12	3.295	10.05	1.51	8.13	1.49	4.32	0.565	3.45	0.472	7.6	1.87	<0.5	0.31	<0.1	3.92	0.79	0.8	<0.3	205	11	8	118	0.010
KN145	35.22	78.40	9.59	41.52	9.10	3.019	9.06	1.39	7.46	1.36	3.88	0.503	3.10	0.422	7.1	1.60	<0.5	0.13	<0.1	3.35	0.71	1.0	0.4	97	3	17	112	0.013
KN146	36.07	79.74	9.67	41.81	8.92	3.166	8.55	1.33	7.02	1.28	3.69	0.471	2.96	0.402	7.4	1.71	<0.5	<0.05	<0.1	3.77	0.81	0.6	0.7	42	7	9	98	0.021
KN148	20.97	45.85	5.49	24.01	5.71	1.904	6.19	1.09	6.15	1.20	3.74	0.530	3.27	0.466	4.3	0.88	<0.5	0.10	<0.1	2.48	0.47	0.7	0.9	231	25	3	104	0.035
KN150	47.12	104.77	12.77	55.95	11.88	3.675	11.26	1.74	9.07	1.63	4.75	0.634	3.77	0.508	9.5	2.13	<0.5	0.18	<0.1	4.92	1.04	1.1	1.0	49	<1	18	124	0.054
KN151	56.84	108.02	11.42	43.26	7.87	2.362	6.41	0.92	4.86	0.90	2.68	0.350	2.19	0.308	9.0	1.89	0.7	0.31	<0.1	14.15	2.61	1.2	1.0	96	14	21	103	0.029
KN152	76.14	158.45	18.89	76.44	15.53	3.925	13.82	2.07	11.14	2.05	6.01	0.815	4.97	0.681	13.7	3.26	0.9	0.39	<0.1	12.63	2.74	1.9	1.1	11	<1	26	99	0.002
KN153	33.49	75.81	9.43	42.26	9.57	3.246	9.45	1.44	7.76	1.42	4.11	0.545	3.33	0.438	7.4	1.59	<0.5	0.14	<0.1	3.28	0.69	0.7	1.2	44	2	12	114	0.010
KN154	41.06	91.38	10.87	47.12	10.42	3.301	10.04	1.54	8.32	1.51	4.33	0.565	3.49	0.479	8.5	2.03	<0.5	0.21	0.1	4.20	0.89	0.9	<0.3	44	13	18	109	0.060
KN156	34.96	76.46	9.19	39.93	8.77	2.782	8.49	1.38	7.61	1.45	4.25	0.577	3.56	0.495	7.2	1.62	0.5	0.22	<0.1	4.03	0.87	0.9	0.8	87	31	13	106	0.007
KN157	25.09	53.87	6.52	28.09	6.43	2.040	7.13	1.19	6.91	1.36	4.22	0.617	3.77	0.539	5.2	1.10	<0.5	0.14	<0.1	2.92	0.56	0.6	1.2	223	34	4	107	0.007
KN158	19.58	43.22	5.20	22.46	5.43	1.828	6.29	1.10	6.38	1.27	3.91	0.562	3.53	0.512	4.2	0.80	<0.5	0.07	<0.1	2.20	0.42	0.5	0.9	222	22	<3	104	0.015
KN159	24.67	53.62	6.52	28.68	6.52	2.087	6.91	1.17	6.76	1.33	3.99	0.578	3.50	0.504	4.9	1.04	<0.5	0.11	<0.1	2.78	0.50	0.7	0.5	172	38	12	104	0.014
KN160	39.04	78.89	8.88	35.96	7.46	2.435	7.45	1.17	6.32	1.15	3.46	0.458	2.83	0.392	6.6	1.28	<0.5	0.13	<0.1	8.12	1.53	0.8	0.8	247	20	6	109	0.009
KN161	22.13	48.40	5.84	25.24	5.73	1.942	6.04	1.02	5.91	1.15	3.58	0.515	3.21	0.468	4.4	0.91	<0.5	0.11	<0.1	2.44	0.47	0.7	0.5	208	20	13	102	0.018
KN162	60.93	133.07	16.05	69.53	14.73	4.523	14.26	2.20	11.59	2.14	6.29	0.818	4.92	0.661	10.8	2.40	0.5	0.22	<0.1	6.53	1.32	1.5	1.7	241	<1	14	146	0.069
KN163	33.57	74.85	9.23	41.50	9.24	3.029	9.19	1.42	7.66	1.39	4.09	0.531	3.23	0.443	7.1	1.63	<0.5	0.12	<0.1	3.40	0.73	0.8	0.9	63	29	9	105	0.049
KN164	16.85	36.46	4.43	19.39	4.66	1.618	5.23	0.91	5.47	1.06	3.29	0.473	2.86	0.415	3.7	0.71	<0.5	<0.05	<0.1	1.89	0.36	0.6	0.4	167	49	11	91	0.031
KN165	39.84	87.18	10.70	47.81	10.23	3.389	9.92	1.42	7.49	1.33	3.78	0.480	2.91	0.391	7.5	1.60	<0.5	0.14	<0.1	3.88	0.77	0.7	0.7	76	13	10	122	0.071
KN166	40.71	88.64	10.75	47.50	10.77	3.509	11.71	1.87	10.47	2.04	6.19	0.866	5.26	0.751	8.2	1.76	<0.5	0.21	<0.1	4.23	0.87	1.0	1.4	65	<1	15	134	0.025
KN167B	41.00	88.40	10.58	45.56	10.16	3.239	10.92	1.76	9.93	1.93	5.91	0.844	5.09	0.728	7.5	1.68	<0.5	0.14	<0.1	4.79	0.98	0.9	1.4	260	<1	10	121	0.038
KN168	86.00	167.85	20.82	89.69	19.25	5.638	22.21	3.42	19.45	4.08	12.84	1.801	10.38	1.536	14.2	3.13	1.1	0.23	<0.1	9.30	2.11	2.0	0.4	4	<1	19	119	0.004
KN169	23.92	51.23	6.17	26.69	6.42	2.083	7.36	1.25	7.19	1.44	4.41	0.640	3.96	0.555	5.2	1.00	<0.5	0.10	<0.1	2.58	0.49	0.7	1.3	197	18	5	102	0.028
KN170	24.13	53.94	6.64	29.95	7.40	2.418	8.70	1.46	8.33	1.62	5.02	0.743	4.42	0.632	5.6	1.04	<0.5	0.08	<0.1	2.29	0.46	0.7	1.1	245	20	8	111	0.038
KN171	23.88	52.87	6.59	29.59	7.29	2.390	8.28	1.44	8.22	1.62	4.94	0.698	4.30	0.620	5.5	1.02	<0.5	0.14	<0.1	2.27	0.46	0.6	0.9	229	16	15	105	0.044
KN172	38.58	85.10	10.38	46.08	10.08	3.420	10.28	1.57	8.36	1.51	4.41	0.592	3.63	0.491	6.6	1.63	<0.5	0.12	0.1	3.32	0.67	0.7	1.0	62	<1	16	120	0.080
KN173	24.35	52.68	6.31	27.28	6.63	2.158	7.16	1.20	7.02	1.41	4.30	0.620	3.81	0.544	4.8	0.93	<0.5	0.13	<0.1	2.40	0.45	0.6	1.3	219	34	9	106	0.029
KN174A	22.61	49.08	5.92	25.52	6.11	2.004	6.87	1.17	6.87	1.35	4.16	0.592	3.66	0.517	4.8	0.91	<0.5	0.09	<0.1	2.28	0.42	0.6	1.5	210	27	10	110	0.032
KN175	44.48	96.72	11.61	50.06	10.97	3.532	10.85	1.58	8.00	1.40	3.98	0.512	2.99	0.399	7.9	1.89	<0.5	0.13	<0.1	4.24	0.91	0.9	<0.3	149	45	10	98	0.023
KN176	24.12	52.25	6.21	27.01	6.51	2.128	7.46	1.25	7.16	1.41	4.37	0.634	3.84	0.551	5.1	0.95	<0.5	0.08	<0.1	2.40	0.46	0.6	1.1	222	28	12	106	0.035
TM101	76.52	157.57	17.20	66.58	11.49	3.100	9.10	1.20	5.88	1.00	2.87	0.349	2.24	0.301	7.3	5.81	<0.5	0.22	<0.1	10.37	2.53	0.6	0.8	81	144	23	64	0.026
TM102	24.98	53.49	6.64	28.99	6.43	2.261	6.11	0.95	5.16	0.94	2.78	0.361	2.22	0.304	4.3	1.04	<0.5	0.06	<0.1	1.97	0.41	0.4	0.7	102	55	9	93	0.052
TM103	26.30	56.34	7.04	30.48	6.88	2.485	6.73	1.08	5.86	1.08	3.22	0.428	2.63	0.362	5.0	1.41	<0.5	<0.05	<0.1	2.20	0.46	0.5	1.4	235	13	8	111	0.083
TM104	30.85	65.79	8.28	36.16	8.04	2.602	7.63	1.17	6.45	1.18	3.48	0.460	2.82	0.397	5.7	1.39	<0.5	0.10	<0.1	2.76	0.57	0.4	1.5	135	37	26	106	0.096
TM105	38.34	81.02	10.07	43.52	9.54	3.192	9.18	1.44	7.83	1.45	4.29	0.585	3.49	0.473	6.9	1.76	<0.5	0.10	0.1	3.39	0.71	0.7	1.1	262	<1	13	125	0.036
TM106	21.39	45.57	5.66	24.70	5.59	1.994	5.43	0.85	4.72	0.85	2.53	0.338	2.07	0.286	4.0	0.95	<0.5	0.09	<0.1	1.90	0.39	0.3	0.8	100	62	9	96	0.052
TM107	20.98	44.55	5.58	24.98	5.97	1.951	6.40	1.13	6.65	1.31	4.00	0.601	3.60	0.521	4.5	0.91	<0.5	0.06	<0.1	2.25	0.44	<0.3	1.1	232	36	9	119	0.028
TM109	34.58	75.91	9.67	42.61	9.85	3.212	9.39	1.48	8.02	1.48	4.29	0.565	3.35	0.466	7.0	1.56	<0.5	0.13	<0.1	3.39	0.77	0.8	0.4	207	18	12	110	0.111
TM110	38.50	84.76	10.87	48.19	10.99	3.451	10.07	1.60	8.54	1.54	4.51	0.607	3.64	0.497	8.1	1.82	0.6	0.25	0.1	3.88	0.87	0.8	1.2	232	35	10	131	0.109
TM111	36.74	80.86	10.28	45.36	10.48	3.325	9.98	1.58	8.50	1.56	4.56	0.596	3.55	0.495	7.5	1.69	<0.5	0.10	<0.1	3.53	0.81	0.8	1.0	202	23	12	105	0.215
TM112	35.65	77.07	9.80	43.64	10.05	3.167	9.69	1.52	8.31	1.51	4.32	0.576	3.40	0.486	7.3	1.65	<0.5	0.09	<0.1	3.49	0.79	0.9	0.6	213	13	23	114	0.822
TM113	44.63	96.52	12.01	51.48	11.28	3.582	10.82	1.66	9.14	1.68	4.87	0.658	3.91	0.544	8.4	1.91	<0.5	0.19	<0.1	4.30	0.83	1.1	0.7	57	5	15	121	0.021
TM114	44.80	96.30	12.20	52.55	11.48	3.630	10.97	1.72	9.46	1.72	5.04	0.668	4.03	0.568	8.2	1.90	<0.5	0.17	0.1	4.30	0.90	1.0	0.5	60	<1	5	122	0.010
TM115	25.17	53.94	6.87	29.95	7.16	2.310	7.22	1.17	6.69	1.28	3.81	0.540	3.21	0.463	5.5	1.12	<0.5	0.09	<0.1	2.71	0.57	0.6	0.7	237	36	10	105	0.010
TM116	27.04	58.76	7.45	32.62	7.52	2.554	7.25	1.15	6.37	1.16	3.38	0.446	2.76	0.377	5.5	1.32	<0.5	0.08	<0.1	2.57	0.52	0.6	1.0	123	29	24	105	0.035
TM117	98.93	168.08	20.04	76.62	11.93	3.301	9.58	1.19	5.86	1.01	2.85	0.367	2.08	0.281	7.9	7.03	<0.5	0.10	0.1	11.61	2.36	0.8	0.5	93	55	24	65	0.017
TM118	32.32	70.71	9.16	40.57	9.26	3.007	8.77	1.34	7.33	1.34	3.83	0.506	3.03	0.405	6.7	1.52	<0.5	0.13	<0.1	2.91	0.63	0.7	1.4	127	20	<3	113	0.038
TM119	34.33	74.10	9.62	43.34	10.12	3.379	9.88	1.53	8.23	1.50	4.30	0.555	3.34	0.451	6.8	1.52	<0.5	0.26	<0.1	2.91	0.61	0.8	0.9	61	4	<3	124	0.043
TM120	36.07	83.78	9.96	44.44	9.69	3.300	9.51	1.44	7.72	1.45	3.80	0.528	3.16	0.433	7.6	1.84	<0.5	0.14	<0.1	3.78	0.81	0.9	0.6	49	19	9	105	0.015

Geochemical grade assay for rocks, drill cores and drill cuttings samples

Sample No.	Pd	Pt	Ir	Rh	Re	Au
	ppb	ppb	ppb	ppb	ppb	ppb
Detection Limit	0.2	0.2	0.1	0.2	0.1	2
KN134	0.3	<0.2				<2
KN141	7.7	6.9				2
KN142	<0.2	6.3				2
KN143	11.8	9.4				3
KN144	0.9	4.1				3
KN145	<0.2	<0.2				<2
KN146	<0.2	<0.2				<2
KN148	16.6	8.8				4
KN150	76.1	11.2	<0.1	<0.2	2.0	24
KN151	4.6	1.9				<2
KN152	1.3	<0.2				<2
KN153	0.7	<0.2				<2
KN154	1.0	<0.2				<2
KN156	2.4	3.1				<2
KN157	17.0	8.7				5
KN158	17.3	3.8				4
KN159	14.4	9.1				5
KN160	11.6	9.2				4
KN161	16.3	5.5				4
KN162	3.7	0.4				<2
KN163	<0.2	0.2				<2
KN164	13.9	11.1				3
KN165	0.4	0.4				<2
KN166	<0.2	<0.2				<2
KN167B	<0.2	0.7				<2
KN168	1.8	<0.2				3
KN169	12.9	5.3				4
KN170	14.9	6.3				5
KN171	14.5	6.0				4
KN172	<0.2	<0.2				<2
KN173	59.3	13.6	<0.1	0.6	0.7	17
KN174A	16.7	6.0				4
KN175	6.6	4.3				3
KN176	16.0	6.2				4
TM101	3.6	2.9				<2
TM102	6.7	4.6				<2
TM103	13.0	17.0				6
TM104	5.6	5.8				<2
TM105	3.0	1.6				<2
TM106	3.7	3.9				<2
TM107	19.4	5.0				6
TM109	7.7	10.0				7
TM110	8.6	11.0				4
TM111	6.5	9.5				4
TM112	6.7	9.8				7
TM113	1.0	0.6				<2
TM114	0.3	0.7				<2
TM115	3.1	3.9				<2
TM116	1.3	1.7				<2
TM117	2.8	3.4				<2
TM118	3.4	3.8				<2
TM119	0.2	<0.2				<2
TM120	9.1	2.3				3

Geochemical grade assay for rocks, drill cores and drill cuttings samples

Sample No.	SiO_2	Al_2O_3	Fe_2O_3	MnO	MgO	CaO	Na_2O	K_2O	TiO_2	P_2O_5	LOI	Total	Be	V	Cr	Co	Ga	Ge	As	Rb	Sr	Y	Zr	Nb	Mo	In	Sn	Sb	Cs	Ba	Sc
	%	%	%	%	%	%	%	%	%	%	%	%	ppm	ppm	ppm	ppm	ppm	ppm	ppm	ppm	ppm	ppm	ppm	ppm	ppm	ppm	ppm	ppm	ppm	ppm	ppm	ppm
Detection Limit	0.01	0.01	0.01	0.001	0.01	0.01	0.01	0.01	0.001	0.01	0.01		1	5	20	1	1	0.5	5	1	2	0.5	1	0.2	2	0.1	1	0.2	0.1	3	1
TM121	49.26	12.40	14.66	0.206	4.62	8.78	2.79	0.72	3.664	0.45	1.65	99.21	1	438	61	40	25	2.0	<5	21	511	36.0	216	23.1	<2	<0.1	2	<0.2	0.3	436	32
TM122	51.12	12.67	14.04	0.182	3.68	7.50	2.66	1.93	3.471	0.53	2.27	100.06	2	379	27	37	25	1.5	<5	51	506	39.7	274	24.0	<2	<0.1	3	<0.2	0.8	614	27
TM123	50.73	12.58	14.69	0.199	4.01	8.09	2.88	0.87	3.585	0.52	2.22	100.37	2	387	<20	36	25	1.7	<5	26	547	39.7	254	21.4	<2	<0.1	2	<0.2	0.4	514	29
TM124	49.37	12.97	14.32	0.200	5.12	9.06	2.63	0.71	3.387	0.41	1.98	100.17	1	422	117	42	24	1.8	<5	23	565	33.3	205	19.0	<2	<0.1	2	<0.2	0.3	439	30
TM125	52.99	12.51	13.52	0.167	3.79	6.08	3.03	2.13	2.884	0.63	2.33	100.04	2	242	42	27	25	1.8	<5	46	427	47.7	320	27.7	<2	<0.1	2	0.2	0.3	690	24
TM126	50.58	12.16	15.18	0.210	3.76	7.73	2.87	1.16	3.721	0.61	1.68	99.65	2	386	<20	39	25	1.7	<5	33	572	42.8	294	28.4	<2	<0.1	2	<0.2	0.5	582	28
TM127	52.11	12.60	13.76	0.189	3.77	7.64	2.69	1.66	3.379	0.51	1.70	100.01	2	364	<20	34	25	1.8	<5	37	480	41.7	284	24.7	<2	<0.1	2	<0.2	0.3	535	27
TM128	49.46	12.69	14.28	0.192	4.67	8.72	2.46	1.03	3.444	0.42	1.95	99.31	1	431	57	41	24	1.7	<5	16	469	35.0	223	21.3	<2	<0.1	2	<0.2	0.2	461	32
TM129	50.13	12.78	14.38	0.200	4.72	8.99	2.55	1.11	3.448	0.43	1.49	100.23	1	428	52	39	24	1.8	<5	23	620	35.4	226	21.1	<2	<0.1	2	<0.2	0.3	442	32
TM130	50.28	12.82	14.42	0.194	4.68	8.93	2.64	1.03	3.477	0.42	1.32	100.21	1	412	52	39	24	1.2	<5	23	497	34.4	215	20.4	<2	<0.1	2	<0.2	0.3	501	32
TM131	50.01	12.38	14.41	0.195	4.02	7.91	2.43	1.19	3.441	0.48	3.82	100.29	2	367	<20	35	25	1.7	<5	31	522	38.2	257	22.2	<2	<0.1	2	<0.2	0.4	425	28
TM132	50.77	12.42	14.32	0.196	3.95	7.92	2.70	1.05	3.466	0.49	2.78	100.04	2	361	<20	35	24	1.5	<5	37	497	38.3	256	22.7	<2	<0.1	2	<0.2	0.7	485	28
TM133	51.03	12.20	15.45	0.214	3.81	7.76	2.46	1.70	3.793	0.64	1.17	100.23	2	359	<20	37	26	1.9	<5	39	505	42.4	289	27.7	<2	<0.1	2	<0.2	0.5	574	29
TM134	50.93	12.47	14.80	0.173	4.23	7.89	2.56	1.44	3.962	0.43	1.39	100.27	2	461	24	43	25	1.5	<5	30	434	39.3	249	23.6	<2	<0.1	2	<0.2	0.3	481	33
TM135	51.60	12.07	15.10	0.206	3.71	6.84	2.78	1.98	3.900	0.54	1.07	99.80	2	428	<20	41	28	1.7	<5	45	495	45.5	295	29.0	<2	<0.1	2	<0.2	0.3	574	29
TM136	50.06	13.00	13.95	0.181	4.04	7.99	2.86	1.44	3.923	0.62	1.41	99.48	2	399	<20	42	28	1.7	<5	38	676	40.2	271	28.6	<2	<0.1	2	<0.2	1.1	596	25
TM137	53.25	12.15	14.74	0.194	3.00	6.43	2.97	1.95	3.262	0.60	1.58	100.13	2	314	<20	35	29	1.7	<5	47	409	50.3	338	31.3	<2	<0.1	3	<0.2	0.4	618	26
TM138	49.36	12.76	14.58	0.195	4.48	8.17	3.01	1.54	3.564	0.44	1.31	99.42	2	422	40	42	26	1.6	<5	35	448	38.4	259	25.2	<2	<0.1	2	<0.2	0.3	467	32
TM139	54.28	12.31	13.47	0.180	2.63	6.57	2.83	2.06	2.716	0.66	2.26	99.96	2	228	<20	31	28	1.8	<5	42	485	53.4	360	31.3	<2	<0.1	3	<0.2	0.5	668	23
TM140	51.45	12.38	15.09	0.223	3.76	7.85	2.66	1.58	3.339	0.57	1.16	100.06	2	332	<20	41	26	2.0	<5	36	472	45.6	255	26.5	<2	<0.1	2	<0.2	0.2	543	31
TM141	50.79	13.39	13.46	0.181	5.43	9.06	2.56	1.19	2.963	0.36	1.00	100.38	1	416	104	61	26	1.6	<5	27	471	37.7	210	21.3	<2	<0.1	2	<0.2	0.9	415	32
TM142	50.99	13.04	13.64	0.186	5.32	9.04	2.53	1.26	3.063	0.37	0.76	100.21	1	330	74	38	23	1.6	<5	27	458	32.6	208	18.4	<2	<0.1	2	<0.2	0.7	422	32
TM143	37.93	10.76	13.77	0.255	5.27	14.44	2.65	2.19	6.079	1.76	3.72	98.82	4	439	<20	44	21	1.6	<5	119	2310	73.2	572	197.4	2	<0.1	4	<0.2	1.1	2130	14
TM144	50.72	12.50	15.41	0.228	4.24	7.84	2.58	1.48	3.521	0.52	1.12	100.15	2	337	<20	45	25	1.9	<5	33	401	40.7	238	41.9	<2	<0.1	2	<0.2	0.5	498	31
TM145	52.76	12.52	15.02	0.215	3.11	7.13	2.77	1.80	3.082	0.71	1.32	100.42	2	262	<20	35	27	1.5	<5	41	400	51.5	289	35.5	<2	<0.1	2	<0.2	0.5	587	27
TM146	49.88	12.90	15.15	0.209	4.94	8.80	2.56	1.32	3.420	0.48	0.76	100.40	1	426	54	44	24	1.7	<5	28	441	34.3	203	27.0	<2	<0.1	2	<0.2	0.4	432	32
TM147	49.68	12.98	16.22	0.220	4.11	8.51	2.49	1.28	3.726	0.43	0.74	100.37	1	473	<20	46	25	1.5	<5	22	460	35.6	211	25.4	<2	<0.1	2	<0.2	0.3	425	32
TM148	51.16	13.37	13.37	0.205	3.06	7.22	3.28	1.80	3.036	0.65	1.37	98.52	2	238	<20	31	26	2.0	14	38	462	43.6	268	29.9	<2	<0.1	2	0.4	0.4	570	24
TM149	51.02	12.15	15.89	0.220	3.57	7.83	2.77	1.66	3.655	0.67	0.95	100.39	2	368	<20	38	26	1.6	<5	36	432	45.5	274	30.3	<2	<0.1	2	<0.2	0.3	571	30
TM150	51.68	12.67	14.66	0.192	4.05	7.74	2.72	1.74	3.291	0.43	1.13	100.30	2	365	<20	39	25	1.7	<5	35	449	37.8	264	26.1	<2	<0.1	2	<0.2	0.4	479	27
TM151	50.68	12.15	15.44	0.210	3.81	7.78	2.67	1.49	3.813	0.62	1.41	100.07	2	364	<20	40	26	1.6	<5	35	488	44.1	300	30.5	<2	<0.1	2	<0.2	0.3	552	28
TM152	48.76	12.19	15.75	0.208	3.28	7.44	2.54	1.80	3.693	0.70	3.30	99.65	2	360	<20	33	25	1.7	<5	39	415	48.9	285	26.4	<2	<0.1	2	0.2	0.6	583	30
TM153	50.65	13.22	13.58	0.174	4.89	9.01	2.53	1.09	3.045	0.35	1.52	100.06	1	395	89	39	22	1.5	<5	23	442	32.3	182	16.8	<2	<0.1	2	<0.2	0.4	382	33
TM154	39.99	16.05	20.99	0.267	1.47	0.48	0.18	0.91	3.547	0.23	15.18	99.29	2	499	74	53	26	2.1	<5	34	34	31.0	227	20.2	<2	<0.1	2	<0.2	0.5	592	53
TM155	49.71	13.16	14.06	0.196	5.39	8.68	2.08	0.88	1.791	0.22	2.59	98.75	2	365	74	40	18	1.8	<5	25	231	30.5	136	12.6	<2	<0.1	2	<0.2	4.5	307	42
TM156	50.59	13.52	13.25	0.213	5.61	9.49	2.33	0.71	1.868	0.22	2.18	99.99	<1	392	91	43	20	1.4	<5	11	279	31.3	135	12.5	<2	<0.1	1	<0.2	0.1	302	42
TM157	50.69	12.86	14.72	0.200	4.91	8.74	2.53	1.04	2.034	0.25	2.26	100.21	1	385	50	42	19	1.6	<5	23	264	39.3	152	13.8	<2	<0.1	1	<0.2	0.2	351	41
TM158	51.20	11.35	15.67	0.205	4.15	7.45	2.60	1.49	3.494	0.55	1.84	100.01	2	346	<20	33	21	1.5	<5	37	317	45.8	235	23.1	<2	<0.1	2	<0.2	0.6	509	35
TM159	48.75	12.09	14.98	0.188	5.14	9.02	2.44	1.14	3.068	0.38	1.93	99.11	1	407	131	39	21	1.8	<5	24	414	31.9	187	19.0	<2	<0.1	2	<0.2	0.2	411	33
TM160	48.45	12.14	14.52	0.169	4.78	7.23	2.37	1.70	3.359	0.41	3.76	98.88	1	416	74	37	22	1.6	<5	45	354	32.4	202	20.7	<2	<0.1	3	<0.2	0.3	457	31
TM161	51.61	12.46	15.04	0.180	4.69	8.80	2.41	1.03	2.110	0.27	1.32	99.92	1	377	56	41	20	1.5	<5	27	233	41.1	176	15.6	<2	<0.1	1	<0.2	0.5	327	42
TM162	51.48	12.89	14.32	0.216	5.24	9.49	2.42	0.94	1.943	0.23	1.29	100.45	<1	379	51	44	19	1.6	<5	19	267	37.6	138	13.4	<2	<0.1	1	<0.2	0.2	314	42
TM163	49.98	13.53	13.47	0.174	5.92	9.63	2.41	0.98	2.570	0.28	1.09	100.06	1	347	120	43	21	1.6	<5	18	443	26.5	147	13.9	<2	<0.1	1	<0.2	0.2	326	33
TM164	49.84	12.26	15.16	0.207	3.83	8.06	2.57	1.45	3.630	0.58	1.46	99.03	2	373	<20	35	21	1.5	<5	31	394	41.0	228	23.8	<2	<0.1	2	<0.2	0.3	523	33
TM165	50.08	12.41	14.55	0.183	3.68	7.28	2.73	1.55	3.761	0.49	2.04	98.75	2	337	<20	31	23	1.5	<5	33	528	37.7	255	23.1	<2	<0.1	2	<0.2	1.1	555	28
TM166	51.63	12.61	14.69	0.250	5.14	9.14	2.38	0.86	2.008	0.24	1.00	99.95	1	373	80	44	19	1.7	<5	20	229	38.5	158	14.7	<2	<0.1	1	<0.2	0.2	298	43
TM167	51.46	12.52	15.13	0.180	4.57	8.53	2.54	0.96	2.212	0.27	1.80	100.19	<1	383	56	41	20	1.5	<5	21	224	41.9	174	15.1	<2	<0.1	1	<0.2	0.2	312	41
TM168	50.54	13.04	14.41	0.190	5.32	9.46	2.41	0.92	2.083	0.24	1.35	99.96	1	377	62	41	19	1.5	<5	15	332	30.0	145	14.0	<2	<0.1	1	<0.2	0.1	337	39
TM169	49.68	12.05	15.35	0.218	3.81	7.26	2.64	1.75	3.808	0.56	2.48	99.60	2	417	<20	44	22	1.7	<5	37	400	51.5	263	23.6	<2	<0.1	2	<0.2	0.4	631	30
TM170	50.05	12.06	15.26	0.191	4.16	7.80	2.70	1.68	3.899	0.56	1.31	99.67	2	404	<20	35	24	1.8	<5	38	428	40.7	277	26.2	<2	<0.1	2	<0.2	0.5	536	31
TM171	50.15	12.25	15.30	0.206	5.04	8.41	2.54	1.22	2.573	0.31	1.32	99.31	1	447	98	41	19	1.3	<5	25	228	40.9	189	18.0	<2	<0.1	2	<0.2	0.2	375	41
TM172	51.43	12.48	14.51	0.194	5.10	9.17	2.62	0.95	2.443	0.29	0.77	99.96	<1	396	72	40	20	1.4	<5	22	255	43.0	180	16.2	<2	<0.1	1	<0.2	0.3	272	41
TM173	51.20	12.50	14.65	0.215	4.83	8.88	2.75	1.13	2.490	0.31	1.02	99.96	1	403	70	38	20	1.5	<5	24	236	48.9	184	16.3	<2	<0.1	1	<0.2	0.4	277	41

Geochemical grade assay for rocks, drill cores and drill cuttings samples

(5continuded/8)

Sample No.	La	Ce	Pr	Nd	Sm	Eu	Gd	Tb	Dy	Ho	Er	Tm	Yb	Lu	Hf	Ta	W	Tl	Bi	Th	U	Ag	Cd	Cu	Ni	Pb	Zn	S
	ppm	ppm	ppm	ppm	ppm	ppm	ppm	ppm	ppm	ppm	ppm	ppm	ppm	ppm	ppm	ppm	ppm	ppm	ppm	ppm	ppm	ppm	ppm	ppm	ppm	ppm	ppm	%
Detection Limit	0.05	0.05	0.01	0.05	0.01	0.005	0.01	0.01	0.01	0.01	0.01	0.005	0.01	0.002	0.1	0.01	0.5	0.05	0.1	0.05	0.01	0.3	0.3	1	1	3	30	0.001
TM121	29.37	63.32	8.21	35.83	8.16	2.776	7.96	1.28	6.83	1.25	3.60	0.484	2.90	0.408	5.9	1.43	<0.5	0.12	0.1	2.79	0.59	0.6	0.3	102	16	15	105	0.041
TM122	40.97	88.78	11.13	47.43	10.36	3.247	9.83	1.47	7.87	1.44	4.28	0.545	3.39	0.463	7.5	1.88	0.6	0.19	<0.1	5.07	1.25	0.8	1.0	153	29	13	107	0.007
TM123	33.99	74.54	9.62	42.76	9.72	3.246	9.59	1.46	7.94	1.44	4.16	0.552	3.31	0.456	7.1	1.57	<0.5	0.14	<0.1	3.22	0.69	0.8	0.7	50	<1	7	112	0.041
TM124	28.22	61.48	8.03	35.35	8.02	2.760	8.09	1.22	6.59	1.19	3.45	0.452	2.68	0.369	5.8	1.32	<0.5	0.15	<0.1	2.55	0.54	1.0	11.9	145	48	<3	92	0.036
TM125	44.58	99.01	11.70	51.54	10.98	3.680	11.01	1.71	9.47	1.82	4.92	0.694	4.15	0.575	8.4	1.96	<0.5	0.17	<0.1	4.44	1.03	1.3	11.9	66	<1	4	104	0.008
TM126	41.64	91.14	11.47	50.20	11.06	3.570	10.88	1.63	8.64	1.54	4.45	0.578	3.57	0.489	7.8	2.01	<0.5	0.13	<0.1	3.86	0.82	0.9	13.9	116	8	8	94	0.048
TM127	37.77	81.63	10.33	45.93	10.35	3.366	10.31	1.57	8.39	1.52	4.39	0.571	3.48	0.482	7.8	1.66	<0.5	0.14	<0.1	3.81	0.87	1.2	13.1	45	<1	<3	92	0.012
TM128	30.21	66.34	8.44	36.87	8.33	2.709	8.01	1.25	6.80	1.25	3.71	0.490	2.95	0.407	6.2	1.40	<0.5	0.09	<0.1	2.82	0.60	0.7	11.7	135	29	12	84	0.015
TM129	30.92	68.06	8.61	38.18	8.56	2.823	8.29	1.28	6.92	1.29	3.73	0.483	3.00	0.412	6.1	1.42	<0.5	0.11	<0.1	2.81	0.63	0.9	11.6	143	25	11	82	0.026
TM130	29.16	63.83	8.15	35.56	8.08	2.688	8.12	1.25	6.77	1.24	3.61	0.472	2.94	0.401	6.0	1.37	<0.5	0.07	<0.1	2.72	0.56	0.7	11.2	142	33	11	82	0.024
TM131	32.78	73.13	9.45	42.78	9.61	3.153	9.19	1.44	7.75	1.41	4.08	0.544	3.23	0.440	7.2	1.55	<0.5	0.11	<0.1	3.25	0.69	0.7	12.4	43	<1	13	89	0.031
TM132	35.78	77.87	9.99	44.10	10.17	3.258	9.44	1.48	7.88	1.43	4.23	0.539	3.21	0.445	7.2	1.61	<0.5	0.16	<0.1	3.23	0.68	0.9	13.3	40	<1	4	90	0.053
TM133	40.96	89.73	11.40	49.85	11.09	3.574	10.41	1.56	8.30	1.49	4.33	0.557	3.39	0.468	7.7	1.86	<0.5	0.12	<0.1	3.60	0.77	1.3	14.2	130	<1	16	100	0.055
TM134	33.42	71.85	9.06	40.02	9.05	2.872	8.76	1.38	7.50	1.40	4.15	0.566	3.40	0.471	6.7	1.58	<0.5	0.09	<0.1	3.10	0.65	0.5	13.3	136	39	23	89	0.024
TM135	44.30	94.11	11.98	51.14	11.06	3.493	10.96	1.69	8.75	1.65	4.73	0.633	3.75	0.507	8.1	1.91	<0.5	0.13	<0.1	3.73	0.67	0.6	12.1	188	<1	22	100	0.026
TM136	45.65	96.37	12.29	51.59	10.77	3.465	10.16	1.50	7.69	1.41	4.07	0.510	3.13	0.420	7.2	1.82	<0.5	0.21	0.1	4.17	0.93	0.9	12.2	72	18	21	87	0.021
TM137	50.64	107.23	13.64	57.20	12.21	3.886	11.91	1.84	9.70	1.74	5.02	0.683	4.21	0.573	8.9	1.99	<0.5	0.16	<0.1	4.21	0.85	1.2	12.4	168	<1	6	102	0.028
TM138	38.01	81.07	10.38	43.52	9.34	3.073	9.46	1.44	7.71	1.38	4.08	0.531	3.24	0.447	6.9	1.54	<0.5	0.11	<0.1	3.09	0.63	0.4	13.9	154	19	16	89	0.022
TM139	52.54	110.90	14.03	60.48	12.80	3.955	12.44	1.90	10.09	1.85	5.29	0.718	4.44	0.585	9.4	2.00	<0.5	0.16	<0.1	4.57	0.93	1.7	11.4	157	<1	19	109	0.084
TM140	40.76	85.12	10.81	45.79	9.91	3.210	9.89	1.58	8.41	1.59	4.62	0.632	3.82	0.529	6.7	1.61	<0.5	0.12	<0.1	3.44	0.69	0.9	13.2	87	<1	18	100	0.096
TM141	31.01	64.68	8.23	35.64	7.90	2.657	8.08	1.30	6.77	1.27	3.63	0.486	2.96	0.425	5.5	1.25	<0.5	0.12	<0.1	2.52	0.52	0.8	11.2	125	107	19	84	0.049
TM142	28.33	60.48	7.69	33.96	7.47	2.477	6.83	1.18	6.39	1.17	3.19	0.449	2.74	0.376	5.5	1.32	<0.5	0.10	<0.1	2.78	0.58	0.9	11.7	137	39	18	84	0.053
TM143	224.70	445.11	49.26	187.37	31.02	9.298	25.58	2.96	12.65	1.98	5.14	0.649	2.98	0.367	13.9	15.19	1.1	0.16	<0.1	21.92	4.88	1.1	11.8	70	2	16	55	0.017
TM144	40.03	82.06	10.29	43.39	9.19	3.041	9.16	1.43	7.66	1.46	4.21	0.568	3.45	0.480	6.3	1.63	<0.5	0.14	<0.1	3.16	0.62	0.8	13.8	63	<1	15	100	0.067
TM145	45.95	95.64	11.99	50.97	11.07	3.484	11.04	1.73	9.33	1.72	5.13	0.709	4.28	0.580	7.3	1.81	<0.5	0.22	<0.1	3.88	0.79	1.1	14.4	76	<1	19	108	0.095
TM146	33.51	69.83	8.83	37.43	7.98	2.663	8.17	1.28	6.64	1.24	3.52	0.481	2.91	0.401	5.5	1.45	<0.5	0.11	<0.1	2.71	0.56	0.6	13.2	58	11	21	93	0.069
TM147	33.27	68.83	8.74	37.07	8.07	2.693	7.94	1.28	6.88	1.29	3.77	0.514	3.18	0.442	5.8	1.48	<0.5	0.09	<0.1	2.82	0.56	0.7	14.5	154	11	7	96	0.093
TM148	43.47	90.09	11.34	46.94	9.86	3.263	9.89	1.53	8.20	1.52	4.40	0.611	3.64	0.509	7.1	1.86	<0.5	0.10	0.1	3.66	0.74	0.7	11.0	16	<1	<3	99	0.053
TM149	44.86	93.13	11.76	49.40	10.54	3.347	10.55	1.65	8.74	1.65	4.70	0.630	3.80	0.520	7.4	1.89	<0.5	0.09	<0.1	3.76	0.75	0.8	13.4	65	<1	13	106	0.041
TM150	37.03	79.24	10.24	43.16	9.27	2.975	8.94	1.37	7.33	1.34	3.82	0.488	3.04	0.419	7.1	1.56	<0.5	0.13	<0.1	3.17	0.67	0.9	12.7	85	<1	4	97	0.008
TM151	44.02	93.14	12.03	51.06	10.84	3.525	10.55	1.64	8.65	1.58	4.43	0.588	3.59	0.487	7.9	1.94	<0.5	0.11	<0.1	3.60	0.75	0.9	14.4	133	<1	12	106	0.053
TM152	42.38	90.37	11.44	50.02	10.93	3.502	10.96	1.68	9.11	1.70	4.84	0.657	4.03	0.551	7.6	1.97	<0.5	0.13	<0.1	3.72	0.69	1.0	13.3	130	<1	20	112	0.009
TM153	25.63	53.68	7.15	32.12	7.44	2.594	7.48	1.14	6.28	1.16	3.27	0.427	2.66	0.361	5.2	1.08	<0.5	0.11	<0.1	2.08	0.45	0.6	10.2	228	53	14	97	0.010
TM154	16.90	46.50	4.42	19.18	4.69	1.492	4.90	0.93	5.70	1.17	3.61	0.548	3.53	0.494	6.4	1.32	<0.5	0.21	<0.1	2.67	0.64	1.1	18.7	313	44	23	159	0.001
TM155	18.38	36.98	4.76	20.77	4.99	1.637	5.46	0.93	5.54	1.07	3.24	0.477	2.97	0.416	3.8	0.73	<0.5	0.14	<0.1	1.79	0.37	0.5	12.9	186	57	4	207	0.010
TM156	17.99	37.40	4.78	20.93	4.94	1.708	5.45	0.95	5.54	1.10	3.29	0.482	2.98	0.430	3.8	0.73	<0.5	<0.05	<0.1	1.83	0.37	0.6	11.0	184	44	11	79	0.009
TM157	22.93	43.68	5.95	25.73	6.19	2.059	6.71	1.14	6.79	1.33	4.03	0.583	3.58	0.513	4.2	0.83	<0.5	0.09	<0.1	1.98	0.37	0.6	11.4	177	23	21	90	0.005
TM158	37.31	78.39	9.70	41.11	9.19	2.877	9.26	1.53	8.56	1.66	4.89	0.704	4.27	0.609	6.6	1.60	<0.5	0.14	<0.1	3.68	0.80	0.9	12.6	110	<1	12	103	0.008
TM159	27.03	57.50	7.18	31.39	6.96	2.360	6.85	1.10	6.08	1.13	3.25	0.428	2.70	0.381	5.0	1.23	<0.5	0.09	<0.1	2.30	0.48	0.7	0.8	99	43	12	96	0.014
TM160	31.38	63.17	8.24	35.83	7.86	2.603	7.65	1.17	6.60	1.20	3.48	0.467	2.90	0.391	5.4	1.40	<0.5	0.13	<0.1	2.54	0.49	0.5	0.5	110	19	8	102	0.011
TM161	21.71	46.59	5.89	25.44	6.21	1.978	6.82	1.21	7.22	1.45	4.24	0.617	3.82	0.549	4.7	0.89	<0.5	0.06	<0.1	2.17	0.43	0.6	0.4	217	24	6	110	0.016
TM162	21.91	43.52	5.56	24.04	5.74	1.885	6.35	1.06	6.35	1.27	3.85	0.565	3.49	0.504	3.8	0.75	<0.5	0.08	<0.1	1.82	0.37	0.5	0.5	197	38	8	99	0.014
TM163	20.65	45.30	5.88	26.15	6.07	2.136	6.16	0.95	5.24	0.95	2.75	0.364	2.25	0.318	4.2	0.88	<0.5	0.08	<0.1	1.67	0.36	0.5	0.4	177	67	<3	92	0.012
TM164	37.73	77.32	9.65	41.76	8.97	2.936	8.88	1.41	7.92	1.48	4.30	0.586	3.66	0.520	6.2	1.60	<0.5	0.10	<0.1	3.31	0.70	0.7	0.9	157	1	10	119	0.017
TM165	34.63	75.70	9.70	43.03	9.77	3.244	9.37	1.48	7.83	1.41	3.97	0.503	3.12	0.430	7.1	1.58	<0.5	0.10	<0.1	2.70	0.64	0.8	0.6	26	<1	10	110	0.014
TM166	20.22	42.67	5.38	23.54	5.63	1.848	6.48	1.12	6.68	1.33	4.04	0.583	3.60	0.526	4.3	0.81	<0.5	0.08	<0.1	1.93	0.39	0.5	<0.3	207	33	4	101	0.013
TM167	23.42	46.81	6.13	26.59	6.57	2.094	7.13	1.25	7.42	1.47	4.45	0.657	4.01	0.571	4.7	0.91	<0.5	0.05	<0.1	2.20	0.49	0.7	1.2	126	14	11	108	0.016
TM168	21.33	44.97	5.51	24.04	5.35	1.819	5.66	0.95	5.38	1.06	3.20	0.466	2.82	0.403	4.0	0.81	<0.5	0.05	<0.1	2.01	0.40	0.7	0.8	212	26	8	93	0.013
TM169	41.41	81.14	10.79	47.34	10.63	3.416	10.73	1.73	9.60	1.81	5.22	0.705	4.41	0.628	7.2	1.81	<0.5	0.12	0.1	3.60	0.87	1.0	1.5	289	7	22	138	0.009
TM170	37.92	83.97	9.86	43.54	9.50	3.196	9.53	1.46	8.00	1.54	4.05	0.594	3.60	0.503	7.3	1.94	0.5	0.12	<0.1	3.98	0.86	0.7	0.8	220	12	14	132	0.014
TM171	24.07	51.03	6.32	27.74	6.37	2.029	7.03	1.23	7.14	1.43	4.34	0.627	3.87	0.568	5.4	1.14	<0.5	0.06	<0.1	2.52	0.37	0.7	1.3	250	32	16	114	0.012
TM172	21.06	45.37	5.87	26.73	6.67	2.114	7.35	1.30	7.77	1.49	4.48	0.660	3.97	0.577	5.2	1.00	<0.5	<0.05	<0.1	2.09	0.36	1.0	0.5	111	30	13	112	0.016
TM173	22.64	46.49	6.11	28.35	6.89	2.194	7.90	1.37	7.86	1.57	4.67	0.657	4.01	0.560	5.2	1.06	<0.5	0.06	<0.1	2.06	0.38	0.7	0.5	230	28	9	119	0.017

Geochemical grade assay for rocks, drill cores and drill cuttings samples

Sample No.	Pd	Pt	Ir	Rh	Re	Au
	ppb	ppb	ppb	ppb	ppb	ppb
Detection Limit	0.2	0.2	0.1	0.2	0.1	2
TM121	2.8	2.6				<2
TM122	5.7	6.9				2
TM123	1.6	0.9				<2
TM124	5.0	6.3				<2
TM125	3.3	2.3				<2
TM126	22.8	4.1	0.2	<0.2	0.6	8
TM127	0.4	0.8				<2
TM128	5.9	9.2				2
TM129	17.7	10.1	0.3	0.7	0.7	2
TM130	8.1	9.5	1.8	0.7	0.6	4
TM131	0.3	0.8				<2
TM132	0.7	0.5				<2
TM133	0.5	0.7				<2
TM134	9.0	9.2				3
TM135	8.0	11.2				3
TM136	0.7	1.1				<2
TM137	0.4	4.7				<2
TM138	7.5	9.9				3
TM139	<0.2	2.5				<2
TM140	2.0	2.4				<2
TM141	6.1	7.9				<2
TM142	11.6	9.3				27
TM143	2.8	2.5				<2
TM144	1.7	1.7				<2
TM145	4.0	1.4				<2
TM146	1.8	1.3				<2
TM147	1.6	2.9				<2
TM148	1.5	1.2				<2
TM149	0.8	1.7				<2
TM150	0.3	0.9				<2
TM151	0.4	0.9				<2
TM152	0.5	1.9				<2
TM153	10.3	12.1	0.1	0.3	0.6	3
TM154	27.4	8.7				6
TM155	21.7	6.2				3
TM156	15.1	10.6				3
TM157	10.8	4.6				<2
TM158	<0.2	0.6				<2
TM159	1.6	2.6				<2
TM160	1.4	2.8				<2
TM161	9.3	5.7				3
TM162	6.5	3.5				6
TM163	9.0	13.8				4
TM164	9.4	1.7	<0.1	0.5	1.3	2
TM165	0.3	<0.2				<2
TM166	15.5	5.4				3
TM167	18.8	5.8				5
TM168	7.8	6.2				3
TM169	1.2	2.8				<2
TM170	4.1	3.9				3
TM171	18.5	6.5				<2
TM172	10.3	7.8				3
TM173	4.8	7.3				<2

Geochemical grade assay for rocks, drill cores and drill cuttings samples

Sample No.	SiO_2	Al_2O_3	Fe_2O_3	MnO	MgO	CaO	Na_2O	K_2O	TiO_2	P_2O_5	LOI	Total	Be	V	Cr	Co	Ga	Ge	As	Rb	Sr	Y	Zr	Nb	Mo	In	Sn	Sb	Cs	Ba	Sc
	%	%	%	%	%	%	%	%	%	%	%	%	ppm	ppm	ppm	ppm	ppm	ppm	ppm	ppm	ppm	ppm	ppm	ppm	ppm	ppm	ppm	ppm	ppm	ppm	ppm	ppm
Detection Limit	0.01	0.01	0.01	0.001	0.01	0.01	0.01	0.01	0.001	0.01	0.01		1	5	20	1	1	0.5	5	1	2	0.5	1	0.2	2	0.1	1	0.2	0.1	3	1
TM174	50.57	11.85	15.92	0.224	5.47	8.30	2.32	1.11	2.203	0.23	1.62	99.83	<1	405	102	45	18	1.7	<5	20	235	61.9	137	12.9	<2	<0.1	1	<0.2	0.2	351	42
TM175	49.30	12.78	14.38	0.199	5.54	9.00	2.45	0.58	2.093	0.25	3.39	99.96	<1	419	62	40	19	1.5	<5	16	284	33.4	145	13.8	<2	<0.1	1	<0.2	0.3	290	41
TM176	52.16	12.49	15.37	0.214	4.42	8.47	2.57	1.05	2.284	0.28	0.47	99.78	1	433	33	40	20	1.5	<5	22	283	38.7	172	15.5	<2	<0.1	1	0.3	0.2	390	41
TM177	52.04	11.83	15.15	0.213	5.52	8.94	2.55	1.08	2.081	0.24	0.60	100.23	<1	401	90	42	18	1.7	<5	23	218	35.3	148	13.1	<2	<0.1	1	<0.2	0.2	289	45
TM178	49.79	12.83	15.24	0.232	4.99	8.82	2.84	1.30	2.339	0.27	1.26	99.91	1	357	53	40	19	1.6	<5	26	272	36.3	153	14.2	<2	<0.1	1	<0.2	0.2	356	42
TM179	51.37	13.08	14.32	0.219	5.34	9.31	2.46	0.94	2.009	0.24	0.99	100.27	<1	392	73	42	18	1.5	<5	18	259	32.0	132	12.6	<2	<0.1	1	<0.2	0.1	298	42
WW017	66.40	13.24	6.38	0.108	1.16	2.30	2.68	4.19	0.968	0.28	2.79	100.50	3	95	<20	13	22	2.0	<5	247	113	49.6	273	21.6	<2	<0.1	5	0.3	10.1	893	19
WW024	52.52	13.73	13.17	0.185	4.92	8.46	2.53	1.39	1.397	0.19	1.44	99.93	1	341	26	40	22	1.7	<5	43	225	31.9	158	12.7	<2	<0.1	2	0.3	1.3	331	37
WW026	67.34	12.53	6.45	0.099	1.04	2.72	3.21	4.26	1.014	0.31	1.48	100.44	3	78	<20	10	18	1.7	<5	182	129	43.8	255	20.5	<2	<0.1	4	0.3	5.9	628	17
WW031	52.75	12.98	14.34	0.219	4.20	8.11	2.72	1.41	1.695	0.21	1.06	99.70	<1	413	<20	38	21	1.8	<5	64	172	37.0	164	9.8	<2	<0.1	1	<0.2	2.9	295	40
WW056	49.66	13.05	14.30	0.206	5.54	9.80	2.28	0.94	2.180	0.27	2.11	100.34	<1	428	96	40	20	1.6	<5	40	323	28.6	147	13.4	<2	<0.1	<1	<0.2	4.1	324	39
WW068	69.33	13.94	3.74	0.069	1.17	2.40	3.64	2.84	0.456	0.14	2.62	100.32	2	52	62	9	16	1.2	<5	74	476	18.8	155	9.1	<2	<0.1	<1	0.3	0.9	1210	8
WW069	65.83	12.75	6.81	0.136	1.43	3.48	3.15	3.95	1.037	0.29	1.57	100.43	3	101	<20	13	19	1.5	<5	180	142	37.5	243	19.9	<2	<0.1	4	<0.2	7.0	573	19
WW073	54.69	12.25	15.44	0.200	3.09	6.82	2.75	2.38	1.872	0.27	0.60	100.37	1	479	<20	38	21	1.9	<5	145	153	41.6	172	12.2	<2	<0.1	2	0.3	9.3	329	39
WW076	50.90	15.44	10.67	0.150	5.58	9.89	2.21	1.23	1.181	0.17	1.46	98.86	<1	257	148	38	20	1.4	<5	42	215	25.1	135	9.7	<2	<0.1	<1	<0.2	0.7	285	35
WW077	52.88	14.71	10.64	0.155	6.19	9.16	2.38	1.48	1.044	0.16	1.57	100.37	<1	232	209	38	17	1.7	<5	48	195	21.7	122	8.2	<2	<0.1	<1	<0.2	0.9	309	35
WW083	53.03	12.99	14.48	0.199	4.40	8.41	2.79	1.35	1.686	0.22	0.69	100.24	<1	415	<20	38	21	1.6	<5	48	191	102.0	158	10.9	<2	<0.1	1	0.7	1.0	331	39
WW092	51.04	13.55	13.12	0.213	6.30	10.45	2.41	0.50	1.195	0.13	1.47	100.37	<1	351	30	42	18	1.7	<5	18	161	27.1	95	5.8	<2	<0.1	<1	<0.2	0.7	140	42
WW095	49.51	13.20	14.35	0.196	5.85	9.61	2.20	0.20	1.427	0.14	3.85	100.53	<1	406	49	45	20	1.6	<5	6	161	30.6	105	5.5	<2	<0.1	<1	0.2	0.4	80	42
WW099	53.57	14.64	10.03	0.163	6.49	8.76	2.22	1.61	1.059	0.17	1.72	100.43	<1	244	181	37	19	1.5	<5	60	202	22.9	130	8.7	<2	<0.1	1	<0.2	1.5	343	34
WW117A	53.12	13.78	12.23	0.180	5.00	8.91	2.43	1.32	1.289	0.18	1.49	99.92	1	351	40	42	21	1.8	<5	84	234	35.2	130	9.8	<2	<0.1	2	<0.2	4.2	716	37
WW122	50.48	13.02	13.13	0.165	4.06	7.89	2.50	1.85	4.126	0.60	2.22	100.04	2	337	26	32	26	1.6	<5	25	778	36.1	340	30.8	<2	<0.1	3	<0.2	0.7	673	22
WW129	54.35	14.04	11.80	0.206	4.44	8.41	2.71	1.17	1.429	0.19	1.62	100.38	1	368	20	42	22	1.7	<5	62	234	37.1	155	13.1	<2	<0.1	1	<0.2	2.3	387	37
WW130	51.71	14.08	11.64	0.206	6.10	10.60	2.53	0.50	1.320	0.12	0.07	98.86	<1	361	71	34	18	1.2	<5	18	158	27.3	89	5.0	<2	<0.1	<1	<0.2	0.4	118	42
WW134	55.47	13.76	11.47	0.178	4.84	7.64	2.96	1.68	1.092	0.15	0.85	100.09	<1	288	<20	38	19	1.9	<5	71	216	29.2	132	9.4	<2	<0.1	1	<0.2	2.0	368	39
WW161	51.70	15.23	11.19	0.150	5.81	9.82	2.22	1.24	1.061	0.17	1.35	99.93	1	252	71	43	18	1.7	<5	38	236	23.8	126	8.7	<2	<0.1	1	<0.2	0.8	330	36
WW162	56.55	12.43	12.97	0.200	2.25	5.84	2.66	2.55	1.784	0.24	1.71	99.18	2	375	<20	40	21	1.7	<5	99	190	40.5	235	16.5	<2	<0.1	2	<0.2	2.9	497	34
WW163	57.08	12.70	13.64	0.181	2.24	6.00	2.75	2.59	1.776	0.25	0.80	100.00	2	365	<20	38	22	1.9	<5	99	190	42.7	245	17.9	<2	<0.1	2	<0.2	2.8	508	35
WW164	51.69	14.09	10.89	0.168	6.36	9.99	2.26	1.08	1.061	0.15	1.33	99.07	1	278	112	40	17	1.6	<5	24	197	22.5	107	8.8	<2	<0.1	1	<0.2	0.5	243	37
WW165	56.85	12.31	12.85	0.163	2.26	5.57	2.71	2.58	1.744	0.26	1.48	98.79	2	398	<20	34	21	1.9	7	102	178	39.9	219	16.4	<2	<0.1	3	<0.2	4.5	500	33
WW166	57.81	12.32	13.15	0.166	2.36	5.60	2.59	2.69	1.726	0.24	1.25	99.90	2	326	<20	35	20	1.6	<5	96	175	39.9	229	16.6	<2	<0.1	2	<0.2	2.5	465	33
WW167	52.66	13.56	12.21	0.222	5.20	8.83	2.52	0.95	1.318	0.19	2.12	99.77	1	320	30	39	19	1.4	<5	36	212	28.7	140	11.4	<2	<0.1	1	<0.2	1.9	332	36
WW174	53.01	13.21	13.18	0.184	5.00	8.85	2.07	0.81	1.285	0.16	2.30	100.05	1	378	22	48	19	1.7	<5	41	207	29.2	129	9.8	<2	<0.1	1	<0.2	1.1	325	42
WW175	52.39	14.29	10.94	0.171	6.78	10.22	2.01	0.88	0.882	0.10	1.20	99.86	<1	283	72	46	17	1.6	<5	32	185	18.3	83	6.5	<2	<0.1	<1	<0.2	0.9	178	43
WW177	56.96	12.39	13.30	0.194	2.33	5.84	2.60	2.80	1.704	0.24	0.92	99.27	2	350	<20	37	22	1.8	<5	102	186	43.1	235	16.5	<2	<0.1	2	<0.2	2.3	499	34
WW181	52.45	14.53	10.84	0.173	6.59	10.20	2.31	1.02	0.962	0.11	1.05	100.22	<1	280	96	42	18	1.7	<5	30	191	21.7	95	7.1	<2	<0.1	<1	<0.2	0.7	252	40
WW183A	52.62	13.60	12.52	0.197	5.07	8.81	2.66	0.94	1.358	0.18	1.42	99.38	1	322	32	40	20	1.7	<5	52	222	29.9	127	10.5	<2	<0.1	1	<0.2	2.8	311	36
WW184	52.97	13.77	11.37	0.204	6.19	9.92	2.38	1.05	1.091	0.13	1.06	100.13	<1	306	56	41	18	1.7	<5	35	187	22.5	98	6.9	<2	<0.1	<1	<0.2	0.8	197	40
WW191	55.62	14.56	10.19	0.150	3.87	7.77	2.38	2.23	1.275	0.20	1.93	100.19	2	228	61	31	19	1.6	<5	70	204	29.4	193	13.6	<2	<0.1	2	<0.2	0.6	455	32
WW196	56.92	12.51	13.43	0.180	2.43	6.01	2.65	2.52	1.698	0.24	1.36	99.95	2	339	<20	37	22	1.7	<5	93	193	41.1	234	16.8	<2	<0.1	2	<0.2	2.3	505	34
WW197	52.52	14.11	11.18	0.199	6.40	10.34	2.24	1.08	1.069	0.13	0.90	100.17	1	298	87	40	18	1.8	<5	33	198	22.5	108	7.8	<2	<0.1	1	<0.2	0.9	232	39
WW203	56.85	12.33	13.61	0.154	2.31	4.78	2.72	2.74	1.778	0.24	2.29	99.81	2	386	<20	36	22	2.0	<5	104	200	40.9	227	15.6	<2	<0.1	3	<0.2	4.1	541	33
WW204	57.79	12.52	13.45	0.181	2.27	5.95	2.79	2.61	1.769	0.25	0.47	100.04	2	405	22	37	22	2.0	<5	101	201	42.4	236	15.8	<2	<0.1	3	<0.2	2.5	511	34
WW205	53.55	13.82	11.44	0.171	5.73	9.65	2.44	1.15	1.121	0.14	0.72	99.93	1	315	76	42	19	2.1	<5	42	192	24.5	120	8.5	<2	<0.1	1	<0.2	1.1	267	38
WW209	53.05	13.69	12.55	0.187	4.81	8.87	2.69	1.05	1.346	0.18	1.31	99.73	1	365	38	41	21	1.9	<5	57	233	30.8	131	9.8	<2	<0.1	2	<0.2	4.5	430	37
WW210	52.22	14.18	10.93	0.179	6.65	10.67	2.18	0.68	1.012	0.12	1.18	100.01	<1	313	97	42	19	1.5	<5	13	212	21.6	86	6.1	<2	<0.1	<1	<0.2	0.8	209	39
WW219	71.10	12.06	5.11	0.115	0.58	1.68	2.67	5.18	0.665	0.20	1.05	100.41	4	24	<20	5	18	1.2	<5	206	88	49.3	271	21.1	<2	<0.1	6	<0.2	9.5	678	16
WW221	69.04	12.25	5.22	0.049	0.49	1.29	2.46	5.13	0.688	0.20	2.48	99.29	4	22	<20	4	18	1.7	<5	234	77	54.4	281	21.7	<2	<0.1	6	0.3	10.6	701	16
WW222	54.08	13.63	11.62	0.170	5.08	8.68	2.43	1.47	1.295	0.18	1.36	100.00	1	338	84	39	20	1.6	<5	50	201	29.2	135	10.6	<2	<0.1	2	<0.2	1.8	343	35
WW223	53.06	13.22	13.33	0.165	4.59	8.25	2.48	1.55	1.499	0.17	1.49	99.79	1	449	144	45	20	1.7	<5	56	202	28.8	137	10.3	<2	<0.1	2	<0.2	1.8	361	40
YM105	55.09	12.58	14.31	0.198	3.42	6.92	2.83	1.81	1.850	0.26	0.84	100.11	2	418	<20	41	23	1.4	<5	66	208	40.7	190	12.9	<2	<0.1	2	<0.2	2.0	396	34
YM108	53.27	13.77	12.71	0.210	4.87	8.35	2.72	1.46	1.532	0.22	1.23	100.35	2	357	23	42	22	1.5	<5	46	247	33.1	176	14.8	<2	<0.1	1	<0.2	0.9	409	36
YM109	51.25	13.82	12.72	0.203	6.06	10.06	2.48	0.94	1.642	0.22	0.83	100.23	1	381	63	46	22	1.7	<5	29	268	30.3	136	10.3	<2	<0.1	1	<0.2	0.6	260	39
YM114	49.45	13.88	13.18	0.223	6.32	10.85	2.35	0.51	1.317	0.14	1.78	100.02	<1	356	142	46	18	1.6	<5	9	183	27.4	101	6.6	<2	<0.1	<1	<0.2	0.1	152	43

Geochemical grade assay for rocks, drill cores and drill cuttings samples

(6continued/8)

Sample No.	La	Ce	Pr	Nd	Sm	Eu	Gd	Tb	Dy	Ho	Er	Tm	Yb	Lu	Hf	Ta	W	Tl	Bi	Th	U	Ag	Cd	Cu	Ni	Pb	Zn	S
	ppm	ppm	ppm	ppm	ppm	ppm	ppm	ppm	ppm	ppm	ppm	ppm	ppm	ppm	ppm	ppm	ppm	ppm	ppm	ppm	ppm	ppm	ppm	ppm	ppm	ppm	ppm	%
Detection Limit	0.05	0.05	0.01	0.05	0.01	0.005	0.01	0.01	0.01	0.01	0.01	0.005	0.01	0.002	0.1	0.01	0.5	0.05	0.1	0.05	0.01	0.3	0.3	1	1	3	30	0.001
TM174	31.03	39.36	7.53	34.32	7.83	2.730	9.91	1.61	9.58	1.96	5.86	0.838	4.95	0.735	4.1	0.78	1.8	0.08	<0.1	1.88	0.41	0.5	1.5	227	59	4	128	0.014
TM175	20.74	42.95	5.30	23.08	5.38	1.779	5.85	1.03	6.07	1.17	3.47	0.494	3.07	0.443	4.3	0.84	<0.5	<0.05	<0.1	2.01	0.18	0.6	<0.3	166	29	16	105	0.017
TM176	22.94	47.94	6.06	26.47	6.12	2.010	6.67	1.16	6.82	1.35	4.05	0.587	3.64	0.537	4.7	0.96	<0.5	<0.05	0.2	2.37	0.68	0.6	1.4	156	14	16	114	0.015
TM177	19.03	40.19	5.04	22.42	5.53	1.754	6.28	1.07	6.38	1.27	3.85	0.574	3.45	0.500	4.3	0.82	<0.5	0.09	<0.1	2.00	0.39	0.5	1.1	229	46	12	108	0.014
TM178	21.14	44.44	5.66	24.67	5.83	1.902	6.30	1.10	6.72	1.32	3.99	0.578	3.58	0.526	4.4	0.90	<0.5	0.15	<0.1	2.26	0.55	0.8	0.5	711	23	8	114	0.015
TM179	18.32	38.71	4.86	21.64	5.07	1.726	5.68	0.97	5.72	1.14	3.47	0.515	3.19	0.462	3.9	0.76	<0.5	0.06	<0.1	1.92	0.39	0.6	1.2	256	33	8	102	0.011
WW017	47.93	104.87	11.58	45.69	9.58	2.085	9.22	1.54	9.33	1.79	5.33	0.788	4.84	0.719	7.3	1.97	1.3	1.46	0.7	12.98	4.40	<0.3	<0.3	61	2	19	89	<0.001
WW024	24.82	51.96	5.93	24.16	5.43	1.665	5.71	0.99	5.93	1.22	3.58	0.532	3.24	0.487	4.2	0.87	<0.5	0.15	0.2	5.36	1.16	<0.3	0.5	176	33	<3	100	<0.001
WW026	41.87	88.14	9.56	39.14	8.28	1.782	8.21	1.37	7.83	1.58	4.65	0.683	3.70	0.552	7.4	1.83	1.1	1.34	1.0	12.26	3.76	<0.3	0.4	126	1	18	85	<0.001
WW031	19.50	42.41	5.03	22.83	5.85	1.703	6.38	1.14	6.77	1.39	4.10	0.607	3.37	0.500	4.6	0.66	<0.5	0.53	0.2	4.31	0.99	<0.3	0.4	179	28	6	107	<0.001
WW056	20.35	45.76	5.34	23.37	5.22	1.755	5.47	0.91	5.37	1.10	3.14	0.468	2.54	0.383	4.2	0.90	<0.5	0.46	<0.1	2.42	0.50	<0.3	<0.3	265	54	<3	105	<0.001
WW068	43.97	81.25	8.21	29.90	5.01	1.457	3.98	0.57	3.28	0.63	1.96	0.280	1.60	0.233	4.0	0.70	<0.5	0.71	0.1	6.46	0.71	<0.3	<0.3	12	25	23	49	0.004
WW069	39.81	85.18	9.31	37.34	7.99	1.680	7.40	1.24	7.22	1.38	4.19	0.599	3.36	0.489	6.9	1.77	1.2	1.44	0.3	12.30	4.27	<0.3	<0.3	55	5	26	87	0.003
WW073	23.85	51.34	6.00	25.58	6.30	1.884	6.98	1.25	7.76	1.58	4.70	0.707	3.92	0.595	5.1	0.98	0.7	0.91	0.2	6.18	1.75	<0.3	<0.3	250	23	10	126	<0.001
WW076	18.13	40.69	4.57	19.32	4.47	1.307	4.61	0.77	4.61	0.94	2.80	0.403	2.24	0.351	3.8	0.63	<0.5	0.31	<0.1	3.90	0.63	<0.3	0.3	80	86	6	84	<0.001
WW077	16.62	36.61	4.11	17.53	3.95	1.162	4.08	0.69	4.04	0.81	2.41	0.344	1.98	0.284	3.4	0.58	<0.5	0.42	0.1	3.46	0.85	<0.3	<0.3	151	103	<3	82	<0.001
WW083	31.52	45.89	7.68	34.16	9.21	3.174	12.77	2.42	15.81	3.41	10.09	1.391	6.83	0.943	4.5	0.70	<0.5	0.36	<0.1	4.30	0.90	<0.3	<0.3	167	30	<3	113	<0.001
WW092	10.66	24.37	2.94	13.26	3.62	1.231	4.31	0.78	4.94	1.04	2.95	0.441	2.60	0.363	2.9	0.42	<0.5	0.50	<0.1	2.44	0.69	<0.3	<0.3	166	48	<3	88	<0.001
WW095	10.79	26.22	3.15	14.81	4.10	1.423	5.00	0.92	5.92	1.17	3.45	0.523	2.92	0.420	3.2	0.41	<0.5	0.20	<0.1	2.39	0.60	<0.3	0.6	217	43	<3	101	<0.001
WW099	19.71	44.13	4.85	20.43	4.58	1.266	4.52	0.76	4.37	0.90	2.62	0.390	2.24	0.301	3.9	0.66	<0.5	0.54	<0.1	4.49	0.99	<0.3	0.4	63	117	9	78	0.002
WW117A	20.72	44.41	5.16	22.45	5.30	1.644	6.07	1.05	6.21	1.26	3.72	0.539	3.12	0.428	3.7	0.72	<0.5	2.38	0.1	4.37	1.23	<0.3	<0.3	239	41	8	100	<0.001
WW122	47.79	108.98	12.48	54.97	11.73	3.722	10.24	1.54	8.13	1.41	3.78	0.473	2.79	0.349	9.2	2.31	<0.5	0.22	<0.1	4.56	1.03	<0.3	0.5	226	40	7	115	<0.001
WW129	25.76	55.77	6.17	26.00	5.98	1.693	6.26	1.10	6.77	1.36	4.05	0.587	3.38	0.503	4.3	0.85	<0.5	0.95	<0.1	5.64	1.25	<0.3	<0.3	183	31	8	102	<0.001
WW130	8.53	20.97	2.60	12.38	3.67	1.281	4.39	0.84	5.25	1.09	3.19	0.453	2.63	0.366	2.7	0.37	<0.5	0.14	<0.1	1.64	0.48	<0.3	<0.3	186	57	<3	94	0.012
WW134	20.62	45.05	4.96	21.00	4.69	1.332	4.90	0.81	4.94	0.97	2.94	0.428	2.34	0.341	3.9	0.70	<0.5	0.77	0.1	5.17	1.19	<0.3	<0.3	88	40	8	93	<0.001
WW161	23.85	47.62	5.72	23.66	5.05	1.504	5.12	0.85	4.93	0.96	2.92	0.422	2.58	0.364	3.3	0.51	<0.5	0.23	<0.1	2.97	0.59	<0.3	<0.3	106	270	7	87	<0.001
WW162	45.84	89.46	10.54	42.51	9.03	2.176	8.59	1.44	8.16	1.58	4.79	0.699	4.21	0.593	6.0	1.11	0.7	0.49	<0.1	7.71	1.66	0.4	<0.3	92	8	15	131	<0.001
WW163	45.59	89.52	10.59	43.27	9.19	2.232	8.64	1.44	8.42	1.62	5.02	0.709	4.34	0.604	6.3	1.11	0.9	0.51	<0.1	7.83	1.69	0.4	<0.3	94	<1	13	136	<0.001
WW164	19.73	38.58	4.67	19.82	4.47	1.361	4.63	0.79	4.73	0.91	2.88	0.403	2.43	0.352	2.9	0.46	<0.5	0.13	<0.1	2.68	0.60	<0.3	<0.3	110	155	<3	88	<0.001
WW165	43.11	80.97	9.84	39.72	8.69	2.162	8.70	1.45	8.19	1.56	4.84	0.706	4.23	0.593	5.8	1.20	1.2	0.58	0.3	7.21	1.91	<0.3	<0.3	109	32	13	124	<0.001
WW166	43.64	85.97	10.22	41.21	8.77	2.159	8.44	1.43	8.18	1.58	4.87	0.708	4.22	0.614	6.1	1.09	0.7	0.49	0.2	7.51	1.50	<0.3	<0.3	77	6	10	126	<0.001
WW167	27.05	53.17	6.38	26.47	5.90	1.748	6.10	1.03	6.00	1.16	3.52	0.514	3.10	0.434	3.8	0.68	<0.5	0.30	<0.1	3.98	0.86	<0.3	<0.3	153	123	10	99	<0.001
WW174	26.18	49.58	6.41	26.97	6.06	1.819	6.53	1.06	6.10	1.19	3.54	0.497	3.08	0.424	3.5	0.61	<0.5	0.47	<0.1	3.72	0.86	<0.3	<0.3	156	150	11	108	<0.001
WW175	14.38	29.58	3.63	15.23	3.61	1.143	3.64	0.65	3.79	0.74	2.25	0.328	1.93	0.280	2.3	0.39	<0.5	0.18	<0.1	2.36	0.58	<0.3	<0.3	172	261	<3	82	<0.001
WW177	42.03	82.93	9.96	39.73	8.56	2.073	8.12	1.39	8.26	1.58	4.83	0.724	4.24	0.602	6.0	1.10	0.8	0.45	<0.1	8.03	1.68	0.4	<0.3	76	7	13	139	<0.001
WW181	18.49	30.04	4.50	18.96	4.28	1.361	4.51	0.79	4.47	0.84	2.60	0.361	2.14	0.296	2.5	0.40	<0.5	0.14	<0.1	2.35	0.49	<0.3	<0.3	71	179	4	85	<0.001
WW183A	19.75	41.03	5.17	20.51	4.72	1.509	5.03	0.92	5.34	1.16	3.00	0.472	2.79	0.410	3.5	0.67	<0.5	0.53	0.2	4.94	1.18	<0.3	<0.3	157	130	5	104	<0.001
WW184	14.57	30.05	3.78	16.09	4.00	1.283	4.26	0.78	4.54	0.87	2.63	0.386	2.32	0.323	2.7	0.43	<0.5	0.22	<0.1	2.51	0.61	<0.3	<0.3	142	118	<3	86	<0.001
WW191	35.65	71.08	8.48	33.71	7.03	1.745	6.52	1.07	6.06	1.16	3.61	0.513	3.17	0.445	5.1	0.87	<0.5	0.35	<0.1	7.24	0.86	0.3	<0.3	79	189	12	97	<0.001
WW196	39.06	78.09	9.34	38.03	8.19	1.939	7.81	1.33	7.78	1.52	4.63	0.678	4.06	0.589	6.1	4.62	0.8	0.49	0.1	8.44	1.80	0.4	<0.3	85	12	10	119	<0.001
WW197	15.89	32.60	3.98	16.76	4.08	1.227	4.28	0.75	4.38	0.85	2.61	0.372	2.27	0.332	2.9	0.47	<0.5	0.15	<0.1	3.21	0.88	0.4	1.2	92	51	12	82	0.018
WW203	38.25	73.68	9.18	37.53	7.90	1.987	7.75	1.33	7.50	1.44	4.44	0.638	3.91	0.544	5.8	1.16	1.0	0.59	0.2	8.54	2.82	0.6	1.0	71	5	25	117	0.006
WW204	36.94	74.09	8.88	35.51	7.61	1.908	7.38	1.27	7.41	1.39	4.31	0.617	3.77	0.530	5.8	1.12	0.8	0.56	0.1	8.58	2.29	0.5	0.7	82	5	18	117	0.008
WW205	17.32	34.73	4.29	18.32	4.31	1.299	4.39	0.79	4.53	0.88	2.72	0.407	2.39	0.346	3.1	0.52	<0.5	0.22	<0.1	3.65	0.79	0.3	1.0	31	48	11	81	0.009
WW209	20.22	40.39	5.02	21.18	4.89	1.458	5.22	0.94	5.38	1.08	3.34	0.471	2.86	0.418	3.7	0.73	<0.5	0.45	<0.1	4.79	1.12	0.3	0.8	141	38	14	93	0.016
WW210	11.99	24.89	3.15	13.69	3.37	1.058	3.77	0.65	3.92	0.77	2.32	0.335	2.13	0.303	2.5	0.42	<0.5	0.12	<0.1	2.91	0.73	0.3	0.9	114	49	12	73	0.015
WW219	44.88	90.23	10.87	42.87	9.08	1.724	8.85	1.54	8.73	1.69	5.31	0.789	4.89	0.713	7.7	2.03	1.5	0.50	0.7	16.16	5.28	0.5	0.5	19	<1	32	81	0.002
WW221	43.74	83.71	10.53	41.42	8.81	1.725	8.80	1.54	9.34	1.84	5.88	0.888	5.33	0.775	8.1	2.19	1.3	1.27	0.3	17.07	4.72	0.6	<0.3	16	<1	27	82	<0.001
WW222	20.68	40.94	5.09	21.54	4.89	1.368	5.08	0.91	5.34	1.03	3.20	0.471	2.79	0.407	3.9	0.76	0.5	0.26	<0.1	5.11	1.29	0.4	0.6	104	37	12	92	0.008
WW223	21.83	44.68	5.54	23.35	5.29	1.421	5.34	0.95	5.44	1.05	3.24	0.474	2.96	0.412	4.1	0.77	<0.5	0.31	<0.1	5.65	1.40	0.4	1.0	140	36	15	97	0.007
YM105	26.88	55.12	6.83	28.70	7.08	1.995	7.05	1.24	7.33	1.45	4.37	0.649	3.79	0.572	5.2	0.96	0.7	0.34	0.2	6.45	1.80	0.9	13.7	148	<1	17	95	0.010
YM108	25.77	52.10	6.03	24.55	5.84	1.709	5.69	1.01	5.92	1.15	3.46	0.513	3.10	0.449	4.4	0.92	<0.5	0.18	<0.1	5.49	1.07	0.5	10.8	100	25	15	82	0.008
YM109	16.71	36.35	4.60	19.73	5.03	1.647	5.20	0.89	5.33	1.03	3.16	0.472	2.76	0.398	3.4	0.63	<0.5	0.15	<0.1	2.93	0.71	0.6	11.0	156	47	13	73	0.011
YM114	10.21	22.41	2.91	13.40	3.81	1.349	4.32	0.82	5.03	1.02	3.00	0.455	2.67	0.409	2.8	0.35	<0.5	0.06	<0.1	1.71	0.47	0.4	12.1	144	49	19	67	0.009

Geochemical grade assay for rocks, drill cores and drill cuttings samples

Sample No.	Pd	Pt	Ir	Rh	Re	Au
	ppb	ppb	ppb	ppb	ppb	ppb
Detection Limit	0.2	0.2	0.1	0.2	0.1	2
TM174	4.7	7.3				3
TM175	23.3	6.8				2
TM176	14.1	4.4				3
TM177	10.1	5.2				5
TM178	18.2	3.2				5
TM179	14.6	4.8				4
WW017	1.4	1.3				1
WW024	11.7	9.9				3
WW026	1.7	1.2				3
WW031	8.8	6.9				3
WW056	14.3	11.3				5
WW068	0.2	0.1				<1
WW069	0.4	1.5				1
WW073	4.8	8.8				1
WW076	6.9	4.9				16
WW077	5.6	5.7				2
WW083	9.2	3.8				4
WW092	8.7	2.3				2
WW095	8.8	4.8				3
WW099	1.1	2.5				2
WW117A	12.8	10.6				3
WW122	6.9	3.7				5
WW129	11.5	9.7				3
WW130	12.1	5.5				3
WW134	13.7	12.6	0.2	1.0	0.8	3
WW161	8.3	5.5				3
WW162	0.5	1.3				<2
WW163	0.8	1.9				<2
WW164	6.3	5.7				<2
WW165	0.3	0.4				<2
WW166	0.4	1.2				<2
WW167	9.4	8.9				3
WW174	1.7	2.5				5
WW175	33.4	11.8	<0.1	<0.2	0.6	<2
WW177	0.8	1.6				<2
WW181	2.8	5.2				2
WW183A	10.7	8.4				3
WW184	20.6	6.1	0.3	0.8	1.2	7
WW191	2.7	3.2				5
WW196	0.7	1.3				3
WW197	3.2	6.0				6
WW203	0.3	0.7				<2
WW204	0.4	0.6				<2
WW205	3.4	4.5				3
WW209	10.3	9.1				3
WW210	10.3	10.1				3
WW219	0.5	0.2				<2
WW221	0.5	<0.2				<2
WW222	5.4	4.7				<2
WW223	5.4	8.6				3
YM105	12.1	14.7				3
YM108	16.2	7.8	0.1	0.2	0.4	5
YM109	11.9	10.7				3
YM114	8.8	3.8	<0.1	0.6	0.9	<2

Geochemical grade assay for rocks, drill cores and drill cuttings samples

Sample No.	SiO_2	Al_2O_3	Fe_2O_3	MnO	MgO	CaO	Na_2O	K_2O	TiO_2	P_2O_5	LOI	Total	Be	V	Cr	Co	Ga	Ge	As	Rb	Sr	Y	Zr	Nb	Mo	In	Sn	Sb	Cs	Ba	Sc
	%	%	%	%	%	%	%	%	%	%	%	%	ppm	ppm	ppm	ppm	ppm	ppm	ppm	ppm	ppm	ppm	ppm	ppm	ppm	ppm	ppm	ppm	ppm	ppm	ppm	ppm
Detection Limit	0.01	0.01	0.01	0.001	0.01	0.01	0.01	0.01	0.001	0.01	0.01		1	5	20	1	1	0.5	5	1	2	0.5	1	0.2	2	0.1	1	0.2	0.1	3	1
YM115	52.51	12.55	16.01	0.225	4.12	8.20	2.65	1.20	1.890	0.22	0.73	100.29	1	493	<20	46	22	1.5	<5	45	176	42.9	163	10.2	<2	<0.1	2	<0.2	1.5	269	41
YM117	50.16	12.54	15.65	0.222	4.81	8.68	2.67	1.20	2.319	0.28	1.49	100.01	1	443	52	44	21	1.6	<5	28	263	39.6	181	13.1	<2	<0.1	1	<0.2	0.3	334	42
YM118	49.36	13.03	14.52	0.263	5.35	9.91	2.39	0.90	2.385	0.31	1.75	100.17	1	414	106	41	20	1.5	<5	13	339	30.7	157	13.3	<2	<0.1	<1	<0.2	0.2	321	37
YM119	50.17	13.37	13.09	0.215	6.17	10.10	2.34	0.85	1.756	0.20	1.88	100.13	<1	384	87	43	19	1.7	<5	16	283	27.9	130	11.3	<2	<0.1	<1	<0.2	0.1	252	44
YM120	50.61	12.79	13.64	0.179	5.81	9.87	2.33	1.50	1.721	0.19	1.58	100.22	1	388	102	44	19	1.6	<5	48	266	28.6	131	10.4	<2	<0.1	<1	<0.2	0.5	262	44
YM121	51.20	12.54	15.16	0.225	4.74	8.64	2.55	1.48	2.330	0.28	0.89	100.03	1	446	50	42	20	1.6	<5	39	263	38.0	179	14.3	<2	<0.1	1	<0.2	0.4	322	42
YM122	51.35	12.65	15.27	0.202	4.88	8.78	2.49	1.27	2.329	0.28	0.74	100.23	1	414	46	40	20	1.6	<5	26	248	35.8	170	13.6	<2	<0.1	<1	<0.2	0.2	305	42
YM124	49.40	12.11	15.58	0.214	4.91	8.51	2.63	1.42	3.374	0.47	1.45	100.06	1	447	<20	42	23	2.0	<5	29	415	35.2	231	19.2	<2	0.1	2	<0.2	0.4	410	34
YM125	51.06	12.61	15.19	0.221	4.64	8.73	2.56	1.28	2.444	0.27	1.05	100.04	1	445	70	43	21	1.6	<5	26	248	39.5	192	15.4	<2	<0.1	2	<0.2	0.2	343	41
YM126	51.04	12.78	14.95	0.219	4.93	8.79	2.40	1.32	2.315	0.27	1.36	100.36	1	430	61	42	20	1.2	<5	31	245	38.3	184	14.3	<2	<0.1	<1	<0.2	1.0	332	41
YM127	51.83	12.42	15.28	0.230	4.65	8.66	2.43	1.38	2.277	0.26	0.97	100.39	1	447	53	43	21	1.6	<5	31	247	38.1	182	14.1	<2	<0.1	1	<0.2	0.5	321	41
YM128	51.31	12.46	15.20	0.202	4.75	8.61	2.52	1.25	2.260	0.27	0.87	99.70	1	430	55	39	20	1.5	<5	29	242	38.3	173	14.0	<2	<0.1	2	<0.2	0.4	315	41
YM129	49.44	11.94	15.97	0.207	5.53	8.77	2.57	1.08	2.267	0.25	1.81	99.84	1	454	72	46	18	1.6	<5	15	218	35.1	159	13.0	<2	<0.1	2	<0.2	<0.1	277	44
YM130	50.43	13.37	13.61	0.202	6.00	9.99	2.38	0.89	1.843	0.22	1.34	100.27	<1	437	150	44	19	1.6	<5	19	304	29.3	129	11.0	<2	<0.1	1	<0.2	0.2	282	40
YM131	50.90	12.38	15.65	0.216	4.64	8.67	2.67	1.26	2.364	0.27	0.98	99.99	<1	467	60	42	20	1.9	<5	28	248	39.5	176	14.2	<2	<0.1	2	<0.2	0.3	327	42
YM132	50.77	13.28	14.08	0.207	5.71	9.80	2.51	0.96	1.960	0.24	0.78	100.31	<1	408	97	42	19	1.5	<5	19	306	28.0	138	12.0	<2	<0.1	1	<0.2	0.1	297	40
YM133	50.35	12.98	13.20	0.192	6.13	9.85	2.35	1.07	1.633	0.19	1.68	99.63	<1	377	93	42	17	1.6	<5	19	242	26.2	117	10.0	<2	<0.1	1	<0.2	0.2	233	43
YM134	51.19	12.69	15.22	0.206	5.05	9.00	2.58	1.17	2.225	0.27	0.75	100.35	1	440	54	40	20	1.7	<5	24	262	36.6	164	13.5	<2	<0.1	2	<0.2	0.2	312	42
YM135	50.82	12.52	15.56	0.231	4.72	8.84	2.60	1.20	2.336	0.34	0.96	100.14	1	456	69	42	21	1.5	<5	30	257	41.0	184	12.6	<2	<0.1	1	0.9	0.4	363	41
YM136	49.81	12.51	15.22	0.235	5.03	9.06	2.36	0.81	2.261	0.27	1.71	99.28	<1	433	55	40	19	1.6	<5	14	240	36.1	164	12.9	<2	<0.1	2	<0.2	0.8	302	41
YM137	49.18	13.40	13.22	0.200	6.44	10.31	2.32	0.92	1.887	0.21	1.21	99.30	<1	402	153	47	19	1.4	<5	18	367	25.1	133	12.6	<2	<0.1	1	<0.2	0.2	290	37
YM138	48.97	12.84	14.73	0.185	4.62	8.84	2.63	1.26	3.139	0.43	1.73	99.36	1	460	26	40	22	1.5	<5	24	425	31.3	199	17.7	<2	<0.1	2	<0.2	0.2	378	32
YM139	53.92	11.92	14.48	0.157	2.80	5.82	2.91	2.40	2.670	0.79	2.25	100.11	3	222	<20	26	27	1.7	<5	51	438	54.1	378	27.8	<2	<0.1	3	<0.2	0.5	657	23
YM140	50.17	12.53	14.90	0.250	5.34	8.92	2.37	1.06	2.148	0.26	1.46	99.40	<1	416	76	41	19	1.6	<5	20	240	36.8	173	14.6	<2	<0.1	2	<0.2	0.2	315	41
YM141	49.91	12.17	15.77	0.226	4.38	8.46	2.64	1.38	3.555	0.53	1.27	100.27	2	461	21	39	22	1.3	<5	26	413	35.8	229	20.9	<2	<0.1	2	<0.2	0.5	430	32
YM142	51.18	12.43	15.16	0.215	4.69	8.51	2.55	1.37	2.195	0.27	1.35	99.91	1	457	56	41	20	1.7	<5	23	236	37.5	170	14.7	<2	<0.1	2	<0.2	0.1	304	40
YM143	50.56	12.42	15.42	0.214	4.88	8.75	2.39	1.17	2.219	0.27	1.98	100.27	1	429	56	42	21	1.5	<5	32	250	38.2	170	12.0	<2	<0.1	1	<0.2	0.4	320	40
YM144	50.91	12.53	15.17	0.207	4.09	8.19	2.73	1.65	3.133	0.50	1.07	100.17	2	388	38	36	22	1.6	<5	33	401	39.8	256	21.9	<2	<0.1	2	<0.2	0.3	507	31
YM145	51.10	12.51	15.27	0.223	4.19	8.10	2.73	1.66	3.121	0.49	0.96	100.35	2	414	39	37	24	1.7	<5	34	414	41.9	267	23.5	<2	<0.1	2	<0.2	0.3	522	30
YM146	49.60	13.39	14.06	0.209	5.66	10.39	2.48	0.33	1.434	0.14	1.55	99.23	<1	357	43	43	18	1.7	<5	4	148	29.0	86	6.3	<2	<0.1	1	<0.2	0.2	118	41
YM147	53.22	12.70	15.36	0.218	4.20	8.04	2.68	1.24	1.730	0.21	0.65	100.25	1	439	32	44	21	1.5	<5	37	182	39.0	146	8.9	<2	<0.1	2	<0.2	0.8	273	38
YM148	51.35	12.73	15.31	0.232	4.84	8.89	2.50	1.17	2.182	0.28	0.86	100.33	1	421	67	43	21	1.5	<5	36	258	40.3	183	13.9	<2	<0.1	2	<0.2	0.8	327	41
YM150	50.89	13.32	13.38	0.259	5.07	8.24	2.37	1.65	1.498	0.21	2.81	99.70	2	330	24	39	21	1.5	<5	81	241	36.7	165	11.1	<2	<0.1	1	<0.2	1.8	340	37
YM151	63.30	13.65	6.85	0.100	2.20	3.62	2.53	3.76	1.074	0.23	2.69	100.00	2	140	32	16	20	1.5	<5	132	157	34.6	200	16.2	<2	<0.1	<1	<0.2	1.6	711	19
YM152	62.63	13.83	7.33	0.111	2.19	5.19	2.24	2.45	1.055	0.24	3.14	100.41	2	147	33	18	20	1.5	<5	62	365	34.6	240	16.3	<2	<0.1	2	<0.2	3.7	674	20
YM153	52.73	15.33	10.56	0.164	5.08	7.78	2.81	2.34	1.170	0.20	2.01	100.17	2	229	119	39	20	1.6	<5	62	286	29.3	167	13.2	<2	<0.1	1	<0.2	0.4	413	33
YM154	54.73	12.79	13.71	0.177	3.28	7.49	2.09	2.09	1.615	0.21	1.68	99.87	1	420	<20	42	20	1.7	<5	44	197	34.0	183	12.5	<2	<0.1	2	<0.2	1.2	434	36
YM155	52.90	14.07	11.79	0.181	5.26	9.10	2.58	0.85	1.195	0.17	1.86	99.95	1	261	36	42	20	1.7	<5	35	244	30.5	150	11.0	<2	<0.1	1	<0.2	1.2	388	37
YM156	50.61	14.73	11.96	0.158	5.41	9.41	2.57	1.22	1.776	0.22	1.35	99.40	1	304	150	42	23	1.5	<5	35	327	29.0	169	12.0	<2	<0.1	1	<0.2	1.0	333	26
YM157	66.18	12.61	5.93	0.101	1.01	2.94	2.78	4.00	0.871	0.28	2.68	99.38	4	47	<20	10	19	1.6	<5	172	145	42.6	253	18.5	<2	<0.1	5	<0.2	8.6	641	16
YM158	54.54	13.67	12.45	0.184	4.40	7.86	2.80	1.76	1.401	0.20	0.83	100.09	2	318	<20	36	21	1.4	<5	60	198	32.7	153	12.0	<2	<0.1	2	<0.2	1.3	340	34
YM159	67.97	12.41	5.65	0.103	1.32	2.74	3.07	3.99	0.892	0.28	1.35	99.77	4	63	<20	10	18	1.3	<5	164	120	39.4	231	19.9	<2	<0.1	5	<0.2	5.1	600	17
YM160	66.13	12.61	5.71	0.103	1.23	3.54	3.20	2.91	0.884	0.28	3.09	99.69	4	66	<20	10	20	1.7	<5	194	155	41.3	251	19.8	<2	<0.1	5	<0.2	11.3	616	18
YM161	53.40	12.44	15.45	0.189	3.83	7.16	3.01	1.49	1.795	0.24	1.30	100.30	1	424	20	43	21	1.9	<5	55	171	42.4	167	11.9	<2	<0.1	2	<0.2	2.7	313	38
YM162	66.27	12.52	6.13	0.104	1.32	3.42	3.29	3.35	0.934	0.27	2.42	100.03	3	94	<20	13	19	1.8	6	155	148	39.7	246	19.5	<2	<0.1	5	<0.2	8.6	569	18
YM163	51.97	13.87	11.98	0.182	5.86	9.55	2.48	1.00	1.220	0.17	1.66	99.94	1	357	81	43	20	1.5	<5	28	200	28.1	117	9.9	<2	<0.1	2	<0.2	1.3	245	36
YM164	56.75	13.12	12.47	0.158	3.30	5.90	2.90	2.52	1.590	0.29	1.02	100.02	2	332	23	38	22	1.5	<5	98	177	52.8	220	17.0	<2	<0.1	3	<0.2	2.5	496	31
YM165	53.15	13.40	13.64	0.199	4.50	8.16	2.77	1.58	1.566	0.24	0.99	100.20	1	381	<20	40	21	1.6	<5	40	235	35.1	167	15.6	<2	<0.1	2	<0.2	0.7	441	35
YM166	56.60	12.83	12.82	0.173	3.29	6.80	2.79	2.18	1.665	0.26	0.63	100.03	2	423	<20	36	22	1.8	<5	83	195	36.0	175	15.4	<2	<0.1	3	<0.2	2.8	447	33
YM167	52.35	14.25	11.59	0.184	6.03	9.48	2.24	0.87	1.083	0.17	1.93	100.17	1	288	100	46	20	1.4	<5	15	261	30.7	141	11.4	<2	<0.1	<1	<0.2	0.1	377	36
YM168	55.37	13.14	12.50	0.186	4.42	8.09	2.64	1.57	1.261	0.17	0.64	99.97	1	373	<20	46	21	1.7	<5	57	197	29.7	144	10.7	<2	<0.1	2	<0.2	1.2	331	39
YM169	52.48	12.76	14.14	0.202	4.77	8.35	2.80	1.25	1.431	0.22	0.61	99.00	1	437	<20	47	20	1.6	<5	47	186	38.2	154	12.2	<2	<0.1	2	<0.2	1.2	302	39
YM170	54.16	12.26	15.47	0.209	3.37	7.40	2.95	1.51	1.871	0.27	0.71	100.19	1	501	<20	44	20	1.8	<5	52	153	42.0	162	11.6	<2	<0.1	2	<0.2	2.4	280	38

Geochemical grade assay for rocks, drill cores and drill cuttings samples

(7continuded/8)

Sample No.	La	Ce	Pr	Nd	Sm	Eu	Gd	Tb	Dy	Ho	Er	Tm	Yb	Lu	Hf	Ta	W	Tl	Bi	Th	U	Ag	Cd	Cu	Ni	Pb	Zn	S
	ppm	ppm	ppm	ppm	ppm	ppm	ppm	ppm	ppm	ppm	ppm	ppm	ppm	ppm	ppm	ppm	ppm	ppm	ppm	ppm	ppm	ppm	ppm	ppm	ppm	ppm	ppm	%
Detection Limit	0.05	0.05	0.01	0.05	0.01	0.005	0.01	0.01	0.01	0.01	0.01	0.005	0.01	0.002	0.1	0.01	0.5	0.05	0.1	0.05	0.01	0.3	0.3	1	1	3	30	0.001
YM115	19.09	40.83	5.07	22.00	6.07	1.871	6.66	1.25	7.46	1.51	4.56	0.684	4.18	0.603	4.4	0.70	0.5	0.21	<0.1	4.56	1.14	0.8	13.8	200	9	16	104	0.010
YM117	24.30	50.82	6.27	26.96	6.50	2.080	6.76	1.19	7.08	1.42	4.24	0.620	3.73	0.536	4.7	0.86	<0.5	0.11	<0.1	2.48	0.50	0.7	14.6	302	27	10	101	0.011
YM118	22.93	48.27	5.92	25.18	5.91	1.995	5.92	1.00	5.71	1.13	3.35	0.482	2.87	0.415	4.0	0.86	<0.5	0.10	<0.1	2.56	0.51	0.7	12.2	227	48	18	85	0.011
YM119	17.79	37.96	4.63	20.06	4.89	1.667	4.81	0.86	5.09	1.02	3.01	0.443	2.63	0.386	3.3	1.25	<0.5	<0.05	<0.1	1.91	0.31	0.6	10.7	182	42	20	77	0.010
YM120	17.22	36.15	4.37	19.05	4.75	1.605	4.74	0.84	5.04	1.01	3.00	0.447	2.73	0.391	3.4	0.60	<0.5	0.09	<0.1	1.75	0.37	0.5	11.2	78	43	11	79	0.011
YM121	24.07	50.47	6.19	26.65	6.48	2.041	6.60	1.13	6.73	1.34	4.00	0.601	3.65	0.525	4.7	0.89	3.2	0.06	<0.1	3.46	0.42	0.8	13.1	252	25	13	90	0.007
YM122	23.53	49.25	6.07	26.25	6.26	2.036	6.27	1.11	6.66	1.33	4.06	0.595	3.49	0.535	4.6	0.86	<0.5	0.07	<0.1	2.51	0.40	0.8	15.1	231	24	9	97	0.006
YM124	30.50	65.84	8.31	35.03	8.23	2.741	7.54	1.23	6.73	1.26	3.56	0.494	2.88	0.419	5.5	1.30	<0.5	0.09	<0.1	2.66	0.44	0.9	13.8	85	13	9	101	0.010
YM125	25.49	53.74	6.69	28.53	6.88	2.155	6.79	1.18	7.12	1.44	4.25	0.640	3.73	0.562	4.9	0.94	<0.5	0.07	<0.1	2.66	0.50	0.7	13.0	192	22	21	94	0.010
YM126	24.68	51.81	6.46	27.57	6.87	2.095	6.85	1.18	6.93	1.39	4.07	0.630	3.76	0.547	4.8	0.91	<0.5	<0.05	<0.1	2.55	0.39	1.3	10.7	254	31	18	92	0.008
YM127	23.56	49.70	6.18	26.45	6.69	2.112	6.61	1.19	7.08	1.41	4.26	0.621	3.74	0.561	4.8	0.94	<0.5	0.06	<0.1	2.44	0.44	0.7	13.5	238	22	14	100	0.011
YM128	20.65	44.78	5.43	24.35	5.93	1.979	6.73	1.09	6.78	1.34	4.02	0.629	3.72	0.542	4.8	0.86	<0.5	0.09	<0.1	2.47	0.49	0.8	14.2	255	20	16	98	0.011
YM129	19.36	41.97	5.00	22.05	5.40	1.808	6.44	1.06	6.42	1.29	3.83	0.571	3.56	0.507	4.4	0.79	<0.5	<0.05	<0.1	2.38	0.89	0.7	13.5	214	44	5	100	0.008
YM130	16.82	36.46	4.37	19.53	4.61	1.651	5.24	0.83	5.16	1.01	3.03	0.445	2.72	0.396	3.4	0.64	<0.5	0.08	<0.1	2.27	0.45	0.6	11.2	209	61	13	84	0.010
YM131	21.50	46.14	5.52	25.11	6.09	1.978	6.88	1.11	6.77	1.35	4.01	0.616	3.58	0.529	4.6	0.87	<0.5	0.09	<0.1	2.46	0.55	0.7	15.4	104	23	15	101	0.009
YM132	18.82	40.33	4.82	21.31	4.97	1.718	5.35	0.86	5.17	1.04	3.04	0.453	2.65	0.385	3.8	0.75	<0.5	0.07	<0.1	2.14	0.42	0.6	12.3	208	49	26	89	0.009
YM133	15.74	33.99	4.07	18.22	4.37	1.542	4.85	0.82	4.91	0.96	2.82	0.426	2.61	0.383	3.3	0.61	<0.5	0.05	<0.1	1.86	0.36	0.4	12.6	153	51	3	77	0.009
YM134	21.43	47.06	5.66	24.72	5.98	2.000	6.66	1.10	6.54	1.30	3.91	0.581	3.62	0.517	4.5	0.86	<0.5	0.09	<0.1	2.58	0.50	0.8	14.0	231	21	8	97	0.009
YM135	23.64	50.13	6.48	27.07	6.26	2.082	6.82	1.22	7.05	1.57	4.05	0.632	3.82	0.559	4.9	1.01	<0.5	0.07	<0.1	2.70	0.58	0.8	13.8	109	22	16	99	0.009
YM136	21.09	46.26	5.54	24.18	5.96	1.967	6.66	1.08	6.65	1.32	3.90	0.591	3.54	0.508	4.6	0.81	<0.5	<0.05	<0.1	2.45	0.45	0.7	11.6	252	23	19	102	0.008
YM137	19.41	41.59	4.87	21.18	4.82	1.686	4.96	0.78	4.59	0.87	2.60	0.379	2.22	0.326	3.5	0.76	<0.5	0.09	<0.1	2.07	0.41	0.5	11.9	166	81	6	83	0.010
YM138	28.79	62.76	7.69	34.15	7.40	2.579	7.51	1.15	6.52	1.19	3.39	0.475	2.79	0.389	5.2	1.23	0.5	0.09	<0.1	2.76	0.56	0.9	12.1	119	23	11	105	0.011
YM139	49.08	111.28	14.61	60.94	13.20	4.175	12.43	1.99	10.35	2.10	5.08	0.705	4.26	0.602	9.7	2.02	<0.5	0.20	<0.1	4.74	1.05	1.6	13.2	76	<1	5	127	0.010
YM140	21.81	47.57	5.71	24.98	6.00	1.965	6.59	1.09	6.53	1.28	3.83	0.578	3.56	0.521	4.5	0.82	<0.5	0.06	<0.1	2.44	0.47	0.7	13.3	213	34	16	100	0.007
YM141	32.51	70.01	8.58	37.78	8.46	2.861	8.37	1.30	7.41	1.33	3.77	0.524	3.15	0.432	6.0	1.40	<0.5	0.06	<0.1	2.99	0.62	0.8	14.7	82	11	9	112	0.019
YM142	21.72	46.93	5.68	24.85	5.94	2.007	6.66	1.12	6.71	1.32	3.90	0.593	3.56	0.528	4.5	0.84	<0.5	0.08	<0.1	2.44	0.50	0.7	13.7	213	19	14	101	0.008
YM143	21.19	45.64	5.54	24.24	5.79	1.979	6.61	1.13	6.81	1.37	4.04	0.595	3.67	0.522	4.6	0.87	<0.5	0.09	<0.1	2.53	0.50	0.7	12.8	273	18	10	100	0.007
YM144	35.72	75.20	9.07	39.60	8.64	2.871	8.74	1.30	7.29	1.36	3.95	0.559	3.43	0.461	6.7	1.56	<0.5	0.10	<0.1	3.75	0.80	1.1	14.1	206	9	12	112	0.006
YM145	36.13	78.01	9.34	40.73	8.86	2.914	8.94	1.37	7.63	1.43	4.16	0.590	3.41	0.497	7.0	1.61	<0.5	0.11	<0.1	3.91	0.79	1.0	13.8	204	16	8	116	0.005
YM146	6.93	16.32	2.21	10.91	3.41	1.244	4.50	0.80	5.02	1.01	3.00	0.459	2.62	0.389	2.5	0.31	<0.5	<0.05	<0.1	1.26	0.39	0.5	11.5	170	34	29	85	0.011
YM147	17.51	38.20	4.65	20.40	5.46	1.775	6.39	1.10	6.77	1.38	4.07	0.620	3.73	0.547	4.1	0.58	<0.5	0.21	<0.1	4.33	1.03	0.5	12.0	166	12	16	102	0.004
YM148	22.10	47.66	5.80	25.43	6.05	2.035	6.96	1.13	6.94	1.37	4.06	0.615	3.81	0.563	5.0	0.90	<0.5	0.07	<0.1	2.66	0.52	0.7	14.3	236	29	15	106	0.009
YM150	24.32	50.47	6.10	25.50	5.95	1.741	6.44	1.05	6.31	1.27	3.74	0.570	3.48	0.488	4.6	0.64	<0.5	0.31	<0.1	5.53	0.93	0.8	12.6	129	5	5	93	0.014
YM151	42.29	87.26	10.27	38.12	7.58	1.680	6.84	1.10	6.12	1.30	3.39	0.515	3.09	0.448	5.3	1.09	0.9	0.12	<0.1	11.52	2.08	1.0	7.2	20	<1	32	82	0.004
YM152	40.09	82.83	9.24	36.91	7.63	1.674	7.17	1.08	6.21	1.16	3.53	0.527	3.15	0.442	6.4	1.02	0.6	0.34	0.1	12.34	2.04	1.0	6.0	23	6	32	80	0.025
YM153	24.48	50.38	5.80	24.42	5.31	1.524	5.33	0.87	5.10	0.97	2.92	0.441	2.70	0.380	4.4	0.78	<0.5	0.35	<0.1	5.85	1.00	0.8	8.4	90	53	15	79	0.014
YM154	26.52	56.03	6.58	27.02	6.17	1.669	6.29	1.03	6.00	1.17	3.46	0.521	3.20	0.455	5.0	0.84	<0.5	0.17	0.2	7.33	1.84	0.8	12.3	295	13	33	98	0.017
YM155	22.19	45.98	5.32	22.59	5.04	1.528	5.39	0.89	5.32	1.03	3.08	0.463	2.82	0.413	4.0	0.56	<0.5	0.24	<0.1	4.89	0.80	0.6	10.8	82	26	18	86	0.016
YM156	21.14	45.70	5.67	24.58	5.70	1.840	5.96	0.91	5.23	0.97	2.85	0.399	2.40	0.337	4.5	0.75	<0.5	0.17	<0.1	4.24	0.72	0.7	11.0	108	78	4	85	0.010
YM157	43.10	89.12	9.96	39.89	8.56	1.752	8.18	1.30	7.47	1.42	4.32	0.649	3.92	0.545	7.0	1.65	1.6	0.89	0.8	15.71	5.50	1.2	5.1	20	<1	31	83	0.009
YM158	21.92	45.65	5.29	22.56	5.40	1.563	5.77	0.93	5.62	1.10	3.34	0.503	3.05	0.434	4.2	0.76	0.7	0.32	<0.1	6.13	1.65	<0.3	<0.3	148	91	8	106	<0.001
YM159	41.51	85.03	10.18	37.41	7.45	1.564	7.03	1.22	7.05	1.47	3.76	0.581	3.56	0.521	6.2	1.71	1.4	0.66	0.1	13.88	4.62	0.6	<0.3	45	1	21	84	<0.001
YM160	38.78	80.71	9.22	36.90	7.74	1.643	7.82	1.22	7.03	1.32	4.00	0.593	3.59	0.508	6.7	1.64	1.6	1.25	0.7	14.45	5.12	0.5	<0.3	51	1	18	84	<0.001
YM161	21.36	44.24	5.53	23.92	6.22	1.853	7.24	1.21	7.48	1.51	4.40	0.680	4.05	0.581	4.6	0.69	0.9	0.36	0.2	5.23	1.38	0.4	<0.3	213	86	10	131	<0.001
YM162	40.66	81.58	9.48	38.19	7.95	1.668	7.88	1.23	6.96	1.35	3.93	0.599	3.77	0.509	6.6	1.54	1.5	1.00	1.1	13.43	4.69	0.6	<0.3	74	<1	19	86	<0.001
YM163	16.60	33.85	4.10	18.19	4.35	1.367	5.05	0.84	4.99	0.99	2.84	0.430	2.61	0.369	3.3	0.57	<0.5	0.13	<0.1	3.98	1.13	<0.3	<0.3	138	174	<3	93	<0.001
YM164	36.15	70.05	8.33	34.67	7.80	2.015	8.76	1.39	8.17	1.71	4.95	0.724	4.28	0.616	5.8	1.11	0.8	0.59	0.1	9.73	2.31	0.5	<0.3	118	57	12	126	<0.001
YM165	25.99	51.45	6.16	25.96	5.91	1.739	6.34	1.04	6.21	1.26	3.59	0.541	3.26	0.482	4.6	0.91	0.6	0.24	0.1	5.65	1.24	0.4	<0.3	164	88	<3	119	<0.001
YM166	27.72	57.22	7.08	28.11	6.20	1.673	6.18	1.11	6.45	1.39	3.64	0.546	3.28	0.483	4.8	1.15	0.9	0.50	0.4	7.58	2.26	0.3	<0.3	113	47	12	115	<0.001
YM167	21.95	44.24	5.25	22.00	4.95	1.466	5.42	0.89	5.24	1.08	3.13	0.470	2.94	0.424	3.9	0.51	<0.5	0.10	<0.1	4.44	0.72	<0.3	<0.3	85	226	<3	98	<0.001
YM168	21.63	44.76	5.40	22.47	5.24	1.453	5.53	0.92	5.37	1.06	3.02	0.456	2.80	0.400	4.0	0.64	<0.5	0.32	0.1	5.75	1.33	<0.3	<0.3	163	118	3	105	<0.001
YM169	20.62	42.55	5.14	21.79	5.46	1.690	6.24	1.08	6.52	1.33	3.83	0.586	3.62	0.531	4.3	0.74	<0.5	0.30	0.2	5.11	1.21	0.4	<0.3	197	121	<3	116	0.026
YM170	21.46	44.58	5.55	24.37	6.07	1.805	7.20	1.22	7.45	1.51	4.47	0.677	4.18	0.578	4.6	0.76	0.7	0.36	0.2	5.92	1.63	0.4	<0.3	209	54	6	132	0.051

Geochemical grade assay for rocks, drill cores and drill cuttings samples

(7continuded/8)

Sample No.	Pd	Pt	Ir	Rh	Re	Au
	ppb	ppb	ppb	ppb	ppb	ppb
Detection Limit	0.2	0.2	0.1	0.2	0.1	2
YM115	12.9	12.4	0.1	0.7	0.8	3
YM117	18.9	6.5				5
YM118	10.3	10.3				5
YM119	41.1	5.8	0.5	0.8	0.4	4
YM120	8.7	5.3				<2
YM121	18.1	3.8				5
YM122	17.3	3.6				4
YM124	<0.2	0.2				<2
YM125	23.3	4.8	<0.1	0.5	0.6	4
YM126	10.6	6.6				<2
YM127	14.2	7.6				7
YM128	17.1	7.3				4
YM129	16.7	5.4				4
YM130	24.2	16.1	0.2	0.4	0.6	7
YM131	9.0	5.3				9
YM132	13.6	6.8				2
YM133	20.0	6.0				5
YM134	18.1	4.4				5
YM135	13.6	6.1				5
YM136	15.0	7.2				5
YM137	14.0	22.8				4
YM138	0.3	0.4				<2
YM139	<0.2	<0.2				<2
YM140	13.3	7.0				6
YM141	<0.2	<0.2				<2
YM142	7.3	7.1				<2
YM143	17.3	8.2				5
YM144	0.8	0.9				<2
YM145	0.6	0.9				<2
YM146	13.0	5.5	0.1	0.3	1.4	6
YM147	11.9	14.9				4
YM148	10.8	6.1				2
YM150	8.1	4.5				2
YM151	0.2	0.3				<2
YM152	0.4	0.7				<2
YM153	2.5	2.0				<2
YM154	1.1	4.2				3
YM155	0.9	1.2				<2
YM156	5.4	6.6				2
YM157	0.5	<0.2				<2
YM158	6.7	8.2				<2
YM159	9.8	2.7				4
YM160	1.1	0.9				<2
YM161	9.1	12.2				2
YM162	1.4	1.3				<2
YM163	11.9	10.9				2
YM164	2.7	2.6				<2
YM165	7.0	8.2				3
YM166	4.5	3.0				<2
YM167	1.3	1.7				2
YM168	16.2	12.3	0.6	0.8	1.0	4
YM169	8.2	2.3				3
YM170	9.6	9.9				3

Geochemical grade assay for rocks, drill cores and drill cuttings samples

Sample No.	SiO_2	Al_2O_3	Fe_2O_3	MnO	MgO	CaO	Na_2O	K_2O	TiO_2	P_2O_5	LOI	Total	Be	V	Cr	Co	Ga	Ge	As	Rb	Sr	Y	Zr	Nb	Mo	In	Sn	Sb	Cs	Ba	Sc
	%	%	%	%	%	%	%	%	%	%	%	%	ppm	ppm	ppm	ppm	ppm	ppm	ppm	ppm	ppm	ppm	ppm	ppm	ppm	ppm	ppm	ppm	ppm	ppm	ppm	ppm
Detection Limit	0.01	0.01	0.01	0.001	0.01	0.01	0.01	0.01	0.001	0.01	0.01		1	5	20	1	1	0.5	5	1	2	0.5	1	0.2	2	0.1	1	0.2	0.1	3	1
YM171	53.45	12.09	15.76	0.216	3.48	7.55	2.88	1.48	1.892	0.26	0.82	99.87	1	549	<20	46	22	1.6	<5	55	168	43.0	169	12.1	<2	<0.1	2	<0.2	2.5	295	39
YM172	53.65	12.23	15.60	0.211	3.57	7.70	2.84	1.42	1.849	0.25	0.58	99.92	1	539	<20	44	22	1.4	<5	54	176	41.6	166	12.0	<2	<0.1	2	<0.2	2.6	295	39
YM173	57.08	11.90	15.04	0.206	1.91	6.13	3.17	1.98	1.831	0.37	0.79	100.41	2	210	<20	34	24	1.7	<5	84	182	58.9	248	16.8	<2	<0.1	3	<0.2	5.8	435	31
YM174	54.15	12.13	15.50	0.209	3.28	7.40	2.90	1.61	1.791	0.29	0.64	99.89	1	502	<20	44	23	1.8	<5	62	182	46.0	182	12.8	<2	<0.1	2	<0.2	3.3	322	38
YM175	53.88	12.22	15.60	0.209	3.34	7.74	2.80	1.61	1.861	0.27	0.90	100.43	1	533	<20	44	23	1.6	<5	58	186	43.7	173	12.5	<2	<0.1	2	<0.2	2.3	311	38
YM176	55.62	11.41	15.95	0.215	2.37	6.49	2.81	1.84	1.871	0.35	1.18	100.12	2	287	<20	37	22	1.5	<5	70	158	62.2	242	15.7	<2	<0.1	3	0.4	3.7	359	35
YM177	53.92	12.66	15.53	0.216	3.75	7.81	2.83	1.40	1.754	0.23	-0.01	100.10	1	484	27	40	21	1.5	<5	53	166	44.0	165	11.2	<2	<0.1	2	<0.2	2.8	279	38
YM178	52.82	14.36	12.46	0.195	4.48	8.58	2.60	1.31	1.343	0.20	1.32	99.67	1	261	29	42	22	1.5	<5	39	258	32.2	178	13.7	<2	<0.1	<1	<0.2	0.6	462	36
YM179	52.72	12.96	11.82	0.147	4.32	7.71	2.61	1.93	3.386	0.49	1.86	99.95	2	291	65	32	25	1.5	<5	29	571	34.2	281	23.8	<2	<0.1	2	<0.2	0.2	688	22
YM180	50.75	14.98	9.57	0.152	8.13	10.89	2.04	0.60	0.778	0.09	2.07	100.04	<1	233	278	42	18	1.5	<5	14	189	17.1	70	7.1	<2	<0.1	<1	<0.2	<0.1	146	37
YM181	49.34	12.75	12.78	0.156	4.93	8.84	2.49	0.69	3.629	0.49	3.24	99.33	2	315	93	36	25	1.5	<5	9	781	34.8	268	24.1	<2	<0.1	2	<0.2	0.5	465	24
YM182	50.63	12.84	13.49	0.183	4.36	8.02	2.58	1.61	3.404	0.49	2.11	99.72	2	339	37	39	27	1.5	<5	33	613	39.1	289	26.6	<2	<0.1	2	<0.2	0.9	636	27
YM183	50.80	13.61	13.68	0.205	6.01	10.27	2.59	0.57	1.374	0.15	0.33	99.58	<1	352	67	45	21	1.7	<5	20	165	30.5	97	8.0	<2	<0.1	<1	3.2	0.5	129	40
YM184	49.67	12.98	12.53	0.178	5.28	7.45	3.55	1.63	3.253	0.45	2.16	99.13	2	295	89	37	25	1.7	<5	36	616	32.6	257	22.1	<2	<0.1	2	<0.2	0.5	561	24
YM185	51.10	13.81	13.56	0.206	6.01	10.51	2.51	0.59	1.392	0.15	0.38	100.21	<1	334	66	42	20	1.7	<5	16	172	29.4	90	7.1	<2	<0.1	<1	<0.2	0.8	122	40
YM186	51.67	14.02	11.98	0.184	6.86	9.77	2.54	1.08	1.039	0.11	0.69	99.95	<1	293	74	43	19	1.5	<5	45	204	24.8	82	6.0	<2	<0.1	<1	<0.2	1.1	248	42
YM187	77.42	12.02	1.38	0.022	0.08	0.59	3.27	4.70	0.086	0.02	0.55	100.14	3	<5	<20	<1	20	0.9	<5	276	17	66.6	128	18.7	<2	<0.1	3	<0.2	3.3	25	4
YM188	51.78	13.10	12.75	0.159	4.33	7.85	2.87	1.69	3.575	0.50	0.94	99.56	2	307	43	35	27	1.8	<5	39	697	38.1	293	24.2	<2	<0.1	2	<0.2	0.8	645	24
YM189	52.84	12.94	12.16	0.161	3.95	7.48	3.03	2.05	3.415	0.51	0.57	99.12	2	274	59	32	27	1.9	<5	67	682	39.1	326	29.3	<2	<0.1	2	<0.2	3.3	741	22
YM190	51.64	13.06	12.52	0.156	4.63	8.26	2.77	1.70	3.588	0.48	0.58	99.37	2	311	73	36	27	1.5	<5	44	752	36.9	304	28.0	<2	<0.1	2	<0.2	2.2	618	24
YM191	52.33	12.87	12.92	0.159	3.96	7.58	2.88	1.92	3.586	0.55	0.80	99.56	2	308	54	32	26	1.6	<5	40	693	39.3	313	27.2	<2	<0.1	2	<0.2	0.7	687	23
YM192	53.09	14.17	11.61	0.189	5.29	9.00	2.51	1.40	1.148	0.17	1.11	99.68	1	255	27	40	21	1.6	<5	40	232	28.5	146	13.0	<2	<0.1	<1	<0.2	0.6	415	37
YM193	53.67	13.04	13.01	0.180	3.81	7.72	2.67	1.47	1.656	0.25	2.07	99.54	2	375	<20	39	20	1.5	<5	41	252	32.4	171	14.7	<2	<0.1	2	<0.2	1.6	383	34
YM194	54.09	13.39	12.24	0.174	3.32	6.64	2.56	2.16	1.666	0.29	3.08	99.62	2	307	22	35	21	1.6	<5	61	195	39.0	224	17.3	<2	<0.1	2	<0.2	2.3	463	31
YM195	52.27	13.36	13.23	0.198	4.67	8.60	2.60	1.14	1.570	0.23	1.77	99.63	1	364	37	43	21	1.6	<5	39	244	32.0	177	15.3	<2	<0.1	1	<0.2	1.4	372	34
YM197	52.26	13.36	12.49	0.198	4.89	8.34	2.64	1.41	1.344	0.18	1.58	98.69	1	357	<20	43	19	1.9	<5	62	197	29.8	140	11.2	<2	<0.1	1	<0.2	1.7	301	35
YM198	51.03	13.70	13.86	0.207	6.00	10.52	2.53	0.54	1.397	0.15	0.21	100.13	<1	378	65	48	19	1.4	<5	16	156	29.3	98	6.6	<2	<0.1	<1	<0.2	0.5	114	42
YM199	50.44	14.22	10.91	0.162	6.99	11.13	2.24	0.40	1.010	0.12	1.50	99.12	<1	299	219	45	17	1.6	<5	20	178	20.7	86	6.4	<2	<0.1	1	<0.2	2.8	138	38
YM200	52.94	14.15	12.15	0.170	5.15	9.07	2.36	1.01	1.257	0.19	1.98	100.42	1	275	28	44	20	1.6	<5	27	241	29.7	164	11.4	<2	<0.1	1	<0.2	0.6	390	38
YM201	50.78	13.02	12.41	0.159	4.71	8.42	2.88	1.71	3.501	0.48	1.02	99.09	2	324	65	37	23	1.7	<5	33	672	34.0	290	22.6	<2	<0.1	2	<0.2	0.3	596	24
YM205	51.78	13.89	11.81	0.183	6.82	10.15	2.42	1.10	0.992	0.11	0.34	99.60	<1	296	94	44	17	1.5	<5	46	292	23.5	91	7.8	<2	<0.1	<1	<0.2	1.3	201	42
YM206	50.45	13.80	13.65	0.207	5.96	10.87	2.48	0.41	1.365	0.15	0.71	100.06	<1	372	66	46	19	1.5	<5	13	176	29.0	93	6.2	<2	<0.1	1	<0.2	0.5	154	41
YM207	53.04	12.52	15.99	0.228	4.07	8.09	2.74	1.31	1.766	0.22	0.20	100.17	<1	476	<20	45	20	1.8	<5	48	180	41.5	162	10.1	<2	<0.1	2	<0.2	2.0	256	41
YM208	51.81	12.77	12.38	0.162	4.91	8.56	2.63	1.74	3.443	0.45	0.11	98.96	2	313	99	36	23	1.8	<5	31	671	33.0	256	20.1	<2	<0.1	2	<0.2	0.2	495	24
YM210	52.13	13.00	12.55	0.155	4.82	8.18	2.82	1.87	3.647	0.46	0.45	100.07	2	317	79	36	23	1.6	<5	37	642	33.6	268	23.8	<2	<0.1	2	<0.2	0.4	567	25
YM211	51.93	12.92	12.92	0.160	4.57	8.18	2.57	1.76	3.724	0.51	0.95	100.21	2	314	69	37	24	1.5	<5	31	981	37.0	300	27.0	<2	<0.1	2	<0.2	1.1	630	24
YM212	50.70	13.06	12.56	0.131	4.62	8.02	2.66	1.92	3.818	0.51	2.01	100.03	2	328	66	38	25	1.4	<5	42	754	38.7	306	28.2	<2	<0.1	2	<0.2	0.9	682	24
YM215	68.39	12.00	5.09	0.061	0.92	1.68	2.61	4.96	0.729	0.22	1.94	98.60	4	19	<20	6	17	1.8	8	215	86	55.2	291	23.8	<2	<0.1	6	0.4	9.3	651	17
YM218	49.34	12.75	14.97	0.219	4.89	8.71	2.60	1.27	3.572	0.48	1.23	100.03	1	421	31	42	21	1.6	<5	30	410	35.6	214	22.9	<2	<0.1	1	<0.2	0.4	461	33
YM219	51.59	13.48	13.73	0.232	5.70	9.97	2.56	0.99	1.371	0.17	0.55	100.35	<1	364	39	45	19	1.6	<5	30	183	30.1	118	10.5	<2	<0.1	<1	<0.2	0.4	248	43
YM222	50.63	12.57	13.05	0.165	4.05	7.28	2.69	2.53	4.014	0.60	1.02	98.61	2	319	41	35	24	1.8	<5	58	735	37.6	329	30.4	<2	<0.1	3	<0.2	0.4	720	22
YM223	50.58	13.01	13.82	0.159	4.43	8.00	2.71	1.98	4.055	0.51	1.11	100.35	2	352	39	41	24	1.5	<5	45	804	34.5	293	28.6	<2	<0.1	2	<0.2	0.6	628	24
YM225	49.47	12.97	13.95	0.161	4.21	8.01	2.76	1.84	4.077	0.51	1.93	99.88	2	401	<20	40	24	1.6	<5	36	836	33.0	271	27.2	<2	<0.1	2	<0.2	0.5	615	23
YM227	49.74	14.22	12.19	0.191	7.13	11.72	2.26	0.54	1.096	0.12	1.10	100.30	<1	323	167	46	17	1.6	<5	7	181	23.6	80	8.7	<2	<0.1	<1	<0.2	0.1	143	43
YM228	52.42	12.42	15.53	0.220	4.18	8.22	2.69	0.86	1.817	0.23	1.18	99.78	1	448	21	44	21	1.2	<5	39	162	42.5	148	11.0	<2	<0.1	2	<0.2	1.5	265	40
YM229	50.09	13.59	13.03	0.168	5.97	10.36	2.41	1.07	1.902	0.22	0.95	99.77	<1	388	152	42	19	1.5	<5	21	353	25.4	133	12.8	<2	<0.1	<1	<0.2	0.5	302	39
YM230	52.06	12.44	15.58	0.226	4.17	7.99	2.66	1.41	1.767	0.23	0.56	99.09	<1	447	20	42	19	1.4	<5	52	154	40.7	144	11.0	<2	<0.1	1	<0.2	1.4	250	41
YM231	53.40	12.86	14.49	0.220	4.40	8.23	2.66	1.41	1.664	0.21	0.55	100.08	<1	424	41	42	20	1.7	<5	53	181	38.7	158	10.0	<2	<0.1	1	<0.2	1.3	303	39

Geochemical grade assay for rocks, drill cores and drill cuttings samples

(8continued/8)

Sample No.	La	Ce	Pr	Nd	Sm	Eu	Gd	Tb	Dy	Ho	Er	Tm	Yb	Lu	Hf	Ta	W	Tl	Bi	Th	U	Ag	Cd	Cu	Ni	Pb	Zn	S
	ppm	ppm	ppm	ppm	ppm	ppm	ppm	ppm	ppm	ppm	ppm	ppm	ppm	ppm	ppm	ppm	ppm	ppm	ppm	ppm	ppm	ppm	ppm	ppm	ppm	ppm	ppm	%
Detection Limit	0.05	0.05	0.01	0.05	0.01	0.005	0.01	0.01	0.01	0.01	0.01	0.005	0.01	0.002	0.1	0.01	0.5	0.05	0.1	0.05	0.01	0.3	0.3	1	1	3	30	0.001
YM171	21.09	44.49	5.52	24.15	6.06	1.795	7.13	1.20	7.55	1.51	4.41	0.673	4.21	0.594	4.7	0.79	0.6	0.32	0.1	5.99	1.65	0.4	<0.3	213	59	6	137	0.059
YM172	20.83	43.21	5.36	23.29	5.92	1.778	7.05	1.21	7.20	1.47	4.27	0.657	4.14	0.572	4.5	0.76	0.6	0.28	0.1	5.91	1.61	0.3	<0.3	206	62	8	132	0.043
YM173	30.41	62.89	7.79	33.33	8.45	2.306	9.43	1.60	9.69	1.95	5.79	0.882	5.52	0.790	6.6	1.13	1.0	0.47	0.3	8.84	2.40	0.6	<0.3	305	3	15	146	0.058
YM174	22.80	46.91	5.85	25.43	6.48	1.854	7.41	1.27	7.79	1.56	4.58	0.696	4.34	0.603	4.9	0.83	0.7	0.38	0.3	6.47	1.76	0.4	<0.3	217	45	11	133	0.027
YM175	22.26	46.15	5.72	24.94	6.22	1.844	7.36	1.22	7.49	1.54	4.52	0.691	4.09	0.612	4.8	0.82	0.7	0.26	0.2	6.26	1.73	0.3	<0.3	213	56	4	135	0.005
YM176	28.69	60.94	7.66	34.34	8.77	2.483	10.45	1.79	11.03	2.20	6.52	0.981	6.06	0.861	6.7	1.05	0.8	0.41	0.2	8.04	2.11	0.5	<0.3	312	9	6	151	0.036
YM177	18.96	40.17	5.04	22.59	5.88	1.786	6.96	1.24	7.49	1.54	4.47	0.691	4.24	0.608	4.5	0.71	<0.5	0.26	<0.1	5.25	1.40	0.3	<0.3	226	78	5	128	0.003
YM178	25.25	53.29	6.08	25.64	5.56	1.742	5.95	0.99	5.95	1.14	3.58	0.542	3.26	0.475	4.9	0.68	<0.5	0.19	<0.1	4.83	0.84	0.4	<0.3	80	120	5	110	0.006
YM179	38.48	84.87	10.20	45.11	9.71	3.338	9.08	1.35	7.04	1.22	3.43	0.453	2.71	0.356	7.4	1.60	<0.5	0.13	<0.1	3.95	0.88	0.6	<0.3	155	166	6	113	<0.001
YM180	8.70	19.14	2.26	10.34	2.57	0.951	2.94	0.50	3.09	0.60	1.86	0.282	1.67	0.244	2.0	0.26	<0.5	<0.05	<0.1	1.85	0.38	<0.3	<0.3	137	400	<3	70	<0.001
YM181	35.66	79.80	9.64	42.79	9.37	3.313	9.26	1.34	7.14	1.20	3.34	0.441	2.65	0.350	6.9	1.66	<0.5	<0.05	<0.1	3.63	0.85	0.4	<0.3	173	259	3	121	<0.001
YM182	42.29	92.44	10.88	47.67	10.14	3.408	9.93	1.47	7.98	1.41	3.99	0.533	3.20	0.433	7.6	1.82	<0.5	0.18	<0.1	5.18	1.19	0.5	<0.3	172	130	6	127	<0.001
YM183	8.71	20.61	2.65	12.85	3.74	1.414	4.94	0.94	5.52	1.08	3.32	0.485	2.91	0.415	2.8	0.34	<0.5	0.09	0.1	1.68	0.53	<0.3	<0.3	180	184	7	103	<0.001
YM184	34.05	75.83	9.11	41.07	9.04	3.216	8.82	1.33	6.95	1.21	3.36	0.435	2.55	0.345	6.8	1.49	<0.5	0.18	<0.1	3.46	0.78	0.5	<0.3	152	225	5	113	<0.001
YM185	8.57	20.22	2.58	12.72	3.76	1.398	4.83	0.88	5.38	1.05	3.23	0.497	2.94	0.420	2.6	0.33	<0.5	0.08	<0.1	1.63	0.47	<0.3	<0.3	187	204	3	105	<0.001
YM186	9.10	20.42	2.50	11.39	3.09	1.086	3.91	0.70	4.32	0.86	2.63	0.405	2.37	0.352	2.4	0.44	<0.5	0.33	<0.1	2.22	0.81	<0.3	<0.3	131	205	<3	84	<0.001
YM187	15.12	41.29	5.48	25.16	8.17	0.251	9.78	1.87	11.35	2.19	6.85	1.111	6.40	0.895	5.7	1.69	<0.5	1.45	0.5	21.27	5.17	0.4	<0.3	3	<1	25	57	0.006
YM188	37.90	83.82	10.28	46.54	10.19	3.618	10.09	1.51	7.94	1.35	3.90	0.502	2.96	0.397	7.7	1.67	<0.5	0.18	<0.1	3.69	0.82	0.5	<0.3	169	148	9	125	0.011
YM189	45.72	99.56	11.76	50.81	10.78	3.634	10.41	1.53	8.13	1.39	3.89	0.508	3.03	0.407	8.6	2.05	0.7	0.39	0.1	5.94	1.66	0.5	<0.3	132	162	9	119	0.031
YM190	40.33	89.72	10.67	47.38	10.16	3.580	9.93	1.44	7.70	1.29	3.67	0.479	2.87	0.370	8.1	1.84	<0.5	0.17	<0.1	4.38	0.95	0.4	<0.3	159	211	5	123	0.012
YM191	44.01	98.10	11.70	52.00	11.25	3.846	10.78	1.62	8.46	1.46	4.13	0.546	3.20	0.433	8.7	1.87	<0.5	0.15	0.1	4.76	1.02	0.5	<0.3	175	146	4	131	0.019
YM192	21.65	45.55	5.32	22.53	5.04	1.566	5.24	0.87	5.31	1.01	3.16	0.485	2.94	0.410	4.1	0.59	<0.5	0.21	<0.1	4.61	0.78	<0.3	<0.3	75	151	<3	103	<0.001
YM193	30.20	59.54	6.87	28.02	5.99	1.757	6.51	1.05	6.01	1.20	3.44	0.507	3.03	0.441	4.2	0.98	<0.5	0.22	0.2	5.99	1.70	<0.3	<0.3	144	55	4	114	<0.001
YM194	41.02	79.35	9.13	35.37	7.30	1.900	7.76	1.21	7.04	1.39	4.07	0.620	3.63	0.511	5.3	1.10	<0.5	0.42	0.2	8.75	2.08	0.4	<0.3	105	54	11	123	<0.001
YM195	29.71	57.75	6.74	27.68	5.86	1.818	6.44	1.01	5.94	1.19	3.43	0.509	3.06	0.435	4.1	0.86	<0.5	0.24	<0.1	4.65	0.97	0.4	<0.3	154	100	10	110	0.009
YM197	22.74	44.55	5.26	21.46	4.88	1.531	5.58	0.90	5.38	1.09	3.12	0.457	2.74	0.393	3.3	0.60	<0.5	0.27	0.1	4.28	1.12	0.4	<0.3	169	99	7	103	<0.001
YM198	10.08	21.72	2.85	13.61	3.79	1.415	5.03	0.88	5.36	1.09	3.13	0.473	2.79	0.398	2.5	0.31	<0.5	0.25	<0.1	1.43	0.40	<0.3	<0.3	180	179	<3	100	0.006
YM199	12.01	24.70	3.05	13.19	3.27	1.137	3.81	0.65	3.91	0.78	2.24	0.332	1.96	0.285	2.1	0.36	<0.5	0.29	0.1	2.05	0.58	<0.3	<0.3	132	361	<3	81	<0.001
YM200	26.75	52.93	6.23	25.55	5.34	1.656	5.76	0.90	5.30	1.08	3.13	0.474	2.90	0.406	3.8	0.58	<0.5	0.22	<0.1	4.38	0.78	<0.3	<0.3	82	132	6	110	<0.001
YM201	43.52	88.37	10.95	47.50	10.07	3.503	10.08	1.41	7.45	1.34	3.53	0.449	2.69	0.357	6.8	1.59	<0.5	0.12	<0.1	3.32	0.68	0.5	<0.3	154	184	<3	117	<0.001
YM205	11.24	23.09	2.85	12.45	3.16	1.108	3.94	0.70	4.20	0.86	2.54	0.385	2.29	0.325	2.3	0.32	<0.5	0.17	<0.1	2.12	0.58	<0.3	<0.3	132	210	<3	86	<0.001
YM206	9.05	20.19	2.73	12.90	3.74	1.396	4.98	0.86	5.38	1.09	3.22	0.481	2.81	0.395	2.4	0.30	<0.5	0.10	<0.1	1.23	0.38	<0.3	<0.3	181	178	<3	101	0.009
YM207	20.50	42.39	5.29	22.99	5.87	1.885	7.12	1.23	7.56	1.56	4.50	0.696	4.18	0.595	4.1	0.65	<0.5	0.28	0.2	3.92	1.01	<0.3	<0.3	238	82	4	132	0.004
YM208	38.77	81.07	10.33	45.33	9.66	3.325	9.31	1.36	7.16	1.27	3.37	0.438	2.54	0.346	7.0	1.54	<0.5	0.11	0.1	3.06	0.82	0.4	<0.3	138	225	<3	110	<0.001
YM210	44.87	92.97	11.59	48.35	10.25	3.501	9.91	1.44	7.71	1.35	3.58	0.455	2.66	0.357	7.4	1.75	<0.5	0.12	<0.1	3.83	0.86	0.5	<0.3	130	214	<3	109	<0.001
YM211	49.28	101.48	12.52	53.48	11.12	3.792	10.67	1.58	8.14	1.47	3.82	0.495	2.91	0.392	8.1	1.93	<0.5	0.14	<0.1	4.12	0.87	0.5	<0.3	172	202	3	120	0.002
YM212	51.33	104.65	12.93	54.73	11.47	3.908	10.90	1.59	8.43	1.50	4.00	0.511	3.06	0.401	8.1	1.93	<0.5	1.24	<0.1	3.99	0.93	0.4	<0.3	168	211	<3	123	0.245
YM215	57.47	114.05	13.16	50.35	10.32	2.065	10.51	1.73	10.29	2.07	6.24	0.932	5.55	0.802	8.1	2.04	1.6	1.31	0.7	14.94	4.17	0.8	<0.3	24	<1	24	108	<0.001
YM218	37.45	76.22	9.44	39.81	8.37	2.863	8.27	1.27	7.20	1.40	3.88	0.546	3.25	0.451	5.8	1.54	<0.5	0.11	<0.1	2.93	0.59	<0.3	<0.3	169	102	6	129	<0.001
YM219	17.73	36.70	4.57	19.86	4.75	1.588	5.53	0.96	5.86	1.18	3.47	0.528	3.18	0.465	3.5	0.55	<0.5	0.16	<0.1	2.56	0.50	<0.3	<0.3	170	131	<3	106	<0.001
YM222	57.28	117.59	14.63	62.05	12.54	4.052	11.47	1.61	8.56	1.51	3.92	0.499	2.96	0.382	8.8	2.18	<0.5	0.15	<0.1	3.92	0.86	0.4	<0.3	147	141	<3	122	<0.001
YM223	51.99	107.70	13.45	57.09	11.75	3.946	10.75	1.51	8.15	1.43	3.68	0.461	2.76	0.374	8.1	1.99	<0.5	0.13	<0.1	3.91	0.91	0.4	<0.3	128	175	7	123	<0.001
YM225	48.08	99.95	12.63	53.77	10.84	3.745	9.99	1.41	7.64	1.35	3.55	0.444	2.57	0.357	7.4	1.83	<0.5	0.11	<0.1	3.56	0.82	0.3	<0.3	146	119	<3	122	<0.001
YM227	11.28	23.37	3.03	13.79	3.56	1.324	4.32	0.75	4.71	0.96	2.76	0.395	2.45	0.359	2.5	0.35	<0.5	<0.05	<0.1	1.42	0.27	<0.3	<0.3	144	260	<3	85	<0.001
YM228	18.67	40.42	5.23	21.96	5.66	1.793	6.36	1.23	7.41	1.64	4.26	0.680	4.05	0.609	4.3	0.75	<0.5	0.28	<0.1	4.50	1.20	0.3	<0.3	251	80	<3	133	<0.001
YM229	23.88	48.17	5.85	25.00	5.36	1.890	5.58	0.90	5.20	1.02	2.97	0.404	2.54	0.356	3.6	0.80	<0.5	0.06	<0.1	1.80	0.33	0.4	<0.3	221	270	<3	107	<0.001
YM230	21.83	44.71	5.63	24.27	6.03	1.958	7.26	1.26	7.86	1.62	4.78	0.715	4.32	0.610	4.2	0.72	<0.5	0.16	<0.1	3.60	0.93	<0.3	<0.3	222	79	5	135	<0.001
YM231	24.38	48.40	6.19	27.23	6.54	1.978	7.23	1.26	7.54	1.49	4.55	0.656	3.95	0.574	4.3	0.59	<0.5	0.24	<0.1	3.19	0.78	<0.3	<0.3	213	103	6	126	<0.001

Geochemical grade assay for rocks, drill cores and drill cuttings samples

Sample No.	Pd	Pt	Ir	Rh	Re	Au
	ppb	ppb	ppb	ppb	ppb	ppb
Detection Limit	0.2	0.2	0.1	0.2	0.1	2
YM171	9.2	10.7				4
YM172	9.4	12.2				4
YM173	14.9	0.9				6
YM174	10.2	8.2				4
YM175	14.5	10.3				5
YM176	13.2	1.1				4
YM177	10.5	11.8				3
YM178	4.5	5.2				2
YM179	5.6	3.6				2
YM180	7.5	6.8				3
YM181	8.2	5.6				3
YM182	8.6	6.8	0.2	0.6	0.2	4
YM183	10.3	5.7				3
YM184	7.3	5.8	0.3	1.0	0.9	3
YM185	10.2	5.6				3
YM186	6.0	5.9				<2
YM187	<0.2	<0.2				<2
YM188	8.0	5.3				3
YM189	4.8	4.6				2
YM190	7.1	6.3				3
YM191	6.9	5.5				4
YM192	0.4	1.1				<2
YM193	9.0	4.8				5
YM194	3.6	2.9				<2
YM195	8.1	8.6				3
YM197	11.3	12.0				3
YM198	11.6	5.9				3
YM199	9.6	11.4				2
YM200	1.4	2.0				<2
YM201	4.1	3.8				3
YM205	6.0	6.0				<2
YM206	10.1	6.5				3
YM207	11.5	11.8				3
YM208	10.3	4.3	0.3	0.7	0.3	2
YM210	7.4	6.3	0.2	0.5	0.8	<2
YM211	6.5	3.7				3
YM212	6.8	4.0				3
YM215	0.4	0.2				<2
YM218	1.2	0.4				<2
YM219	9.7	2.8				<2
YM222	4.8	4.4				2
YM223	7.1	7.3	0.2	0.7	1.0	3
YM225	<0.2	<0.2				<2
YM227	6.2	6.4				<2
YM228	10.1	9.7				4
YM229	14.0	11.8				4
YM230	12.2	10.3				4
YM231	7.6	7.6				<2

APPENDIX 7

Geochemical grade assay for pan concentrated samples collected in the Lajes districts

Sample No.	Ag	Cd	Cu	Mn	Mo	Ni	Pb	Zn	S	Pd	Pt
	ppm	ppm	ppm	ppm	ppm	ppm	ppm	ppm	%	ppb	ppb
AS027P	< 0.2	< 0.5	68	318	< 2	45	7	68	0.006	1.0	1.0
AS022P-1	< 0.2	< 0.5	79	1236	6	51	6	75	3.966	<1.0	4.0
AS022P-2	< 0.2	< 0.5	75	758	< 2	109	6	66	9.976	3.0	3.0
AS022P-3	< 0.2	< 0.5	130	922	< 2	105	5	50	10.026	3.0	3.0
AS022P-4	< 0.2	< 0.5	53	5397	< 2	1161	14	86	3.192	5.0	6.0

APPENDIX 8

Geochemical grade assay for stream sediments collected in the Lomba Grande district

Sample No.	UTM_E	UTM_N	Latitude	Longitude	Location	Ag	Cd	Cu	Mn	Mo	Ni	Pb	Zn	Al	As	Ba	Be	Bi	Ca	Co	Cr	Fe	K	Mg	Na	P	Sb	Sc	Sn
						ppm	ppm	ppm	ppm	ppm	ppm	ppm	ppm	%	ppm	ppm	ppm	ppm	%	ppm	ppm	%	%	%	%	%	ppm	ppm	ppm
CK-S-001	495450	6698500	-51.0471	-29.8439	Lomba Grande	<0.2	<0.5	8	133	<2	7	6	8	0.53	<10	67	<1	<10	0.02	6	11	1.06	0.04	0.04	0.02	0.006	<10	3	<10
CK-S-002	494900	6699000	-51.0528	-29.8394	Lomba Grande	<0.2	<0.5	7	82	<2	4	6	7	0.38	<10	43	<1	<10	0.04	2	7	0.58	0.03	0.05	0.02	0.004	<10	1	<10
CK-S-003	492450	6698150	-51.0782	-29.8470	Lomba Grande	<0.2	<0.5	5	58	<2	3	6	8	0.37	<10	40	<1	<10	0.03	2	8	0.62	0.03	0.03	0.02	0.004	<10	1	<10
CK-S-004	493000	6699100	-51.0725	-29.8385	Lomba Grande	<0.2	<0.5	5	79	<2	3	6	9	0.24	<10	37	<1	<10	0.02	2	7	0.58	0.03	0.03	0.02	0.004	<10	<1	<10
CK-S-005	494800	6699550	-51.0538	-29.8344	Lomba Grande	<0.2	<0.5	7	141	<2	4	7	10	0.26	<10	40	<1	<10	0.02	4	21	1.36	0.03	0.03	0.01	0.006	<10	1	<10
CK-S-006	495000	6699650	-51.0518	-29.8335	Lomba Grande	<0.2	<0.5	10	362	<2	24	6	13	0.44	<10	57	<1	<10	0.15	9	27	1.86	0.02	0.32	0.03	0.011	<10	2	<10
CK-S-007	495700	6700200	-51.0445	-29.8286	Lomba Grande	<0.2	<0.5	8	159	<2	11	7	12	0.25	<10	37	<1	<10	0.07	5	16	1.81	0.01	0.14	0.02	0.009	<10	1	<10
CK-S-008	495850	6700400	-51.0430	-29.8267	Lomba Grande	<0.2	<0.5	26	799	<2	227	4	34	1.50	<10	62	<1	<10	1.09	46	95	4.87	0.02	3.88	0.16	0.011	<10	7	<10
CK-S-009	494250	6700350	-51.0595	-29.8272	Lomba Grande	<0.2	<0.5	5	95	<2	4	7	8	0.33	<10	42	<1	<10	0.03	2	9	1.17	0.03	0.06	0.02	0.005	<10	1	<10
CK-S-010	494150	6701550	-51.0605	-29.8164	Lomba Grande	<0.2	<0.5	9	204	<2	7	12	19	0.71	<10	96	<1	<10	0.05	7	21	2.08	0.03	0.06	0.02	0.023	<10	2	<10
CK-S-011	493200	6700600	-51.0704	-29.8249	Lomba Grande	<0.2	<0.5	7	586	<2	3	11	13	0.75	<10	114	<1	<10	0.04	5	10	1.34	0.05	0.04	0.02	0.007	<10	5	<10
CK-S-012	493100	6701400	-51.0714	-29.8177	Lomba Grande	<0.2	<0.5	9	94	<2	4	11	15	1.42	<10	130	<1	<10	0.04	2	9	1.28	0.04	0.05	0.02	0.010	<10	3	<10
CK-S-013	492200	6702000	-51.0807	-29.8123	Lomba Grande	<0.2	<0.5	5	147	<2	3	7	10	0.69	<10	79	<1	<10	0.03	2	7	0.91	0.03	0.03	0.02	0.006	<10	1	<10
CK-S-014	498150	6698500	-51.0192	-29.8439	Lomba Grande	<0.2	<0.5	5	260	<2	6	4	7	0.29	<10	42	<1	<10	0.04	5	12	0.60	0.02	0.04	0.02	0.006	<10	1	<10
CK-S-015	497700	6698500	-51.0238	-29.8439	Lomba Grande	<0.2	<0.5	4	76	<2	4	5	6	0.18	<10	39	<1	<10	0.02	3	8	0.71	0.02	0.04	0.02	0.005	<10	<1	<10
CK-S-016	499300	6699550	-51.0072	-29.8344	Lomba Grande	<0.2	<0.5	30	475	<2	36	13	26	2.23	<10	121	1	<10	0.15	19	146	5.77	0.04	0.14	0.03	0.014	<10	18	<10
CK-S-017	498800	6699350	-51.0124	-29.8362	Lomba Grande	<0.2	<0.5	9	254	<2	9	6	10	0.31	<10	44	<1	<10	0.07	5	17	1.03	0.02	0.10	0.02	0.008	<10	2	<10
CK-S-018	499100	6699650	-51.0093	-29.8335	Lomba Grande	<0.2	<0.5	4	78	<2	3	4	6	0.16	<10	25	<1	<10	0.03	2	7	0.41	0.01	0.02	0.02	0.003	<10	<1	<10
CK-S-019	499550	6701100	-51.0047	-29.8204	Lomba Grande	<0.2	<0.5	4	58	<2	2	5	5	0.23	<10	27	<1	<10	0.02	2	7	0.58	0.02	0.03	0.02	0.003	<10	<1	<10
CK-S-020	498200	6703000	-51.0186	-29.8033	Lomba Grande	<0.2	<0.5	6	145	<2	5	6	13	0.33	<10	101	<1	<10	0.06	4	14	1.08	0.08	0.07	0.02	0.008	<10	1	<10
CK-S-021	499050	6703100	-51.0098	-29.8024	Lomba Grande	<0.2	<0.5	6	86	<2	5	7	12	0.43	<10	48	<1	<10	0.06	3	15	1.08	0.06	0.07	0.03	0.008	<10	1	<10
CK-S-022	498500	6704000	-51.0155	-29.7943	Lomba Grande	<0.2	<0.5	6	83	<2	4	5	9	0.23	<10	58	<1	<10	0.02	3	15	1.24	0.04	0.04	0.02	0.008	<10	<1	<10
CK-S-023	498700	6704000	-51.0135	-29.7943	Lomba Grande	<0.2	<0.5	5	181	<2	3	6	7	0.27	<10	46	<1	<10	0.03	3	6	0.52	0.03	0.03	0.02	0.006	<10	<1	<10
CK-S-024	498650	6704650	-51.0140	-29.7884	Lomba Grande	<0.2	<0.5	5	178	<2	4	6	9	0.39	<10	59	<1	<10	0.08	3	8	0.89	0.04	0.05	0.03	0.012	<10	1	<10
CK-S-025	498650	6705000	-51.0140	-29.7852	Lomba Grande	<0.2	<0.5	4	58	<2	2	4	7	0.20	<10	31	<1	<10	0.02	2	7	0.71	0.03	0.03	0.02	0.005	<10	<1	<10
CK-S-026	498300	6705200	-51.0176	-29.7834	Lomba Grande	<0.2	<0.5	5	78	<2	3	5	5	0.27	<10	33	<1	<10	0.03	2	6	0.46	0.02	0.03	0.02	0.003	<10	<1	<10
CK-S-027	499150	6705850	-51.0088	-29.7780	Lomba Grande	<0.2	<0.5	5	85	<2	2	6	10	0.31	<10	53	<1	<10	0.04	2	5	0.62	0.03	0.04	0.02	0.009	<10	<1	<10
CK-S-028	496450	6706100	-51.0367	-29.7753	Lomba Grande	<0.2	<0.5	4	45	<2	3	4	5	0.19	<10	23	<1	<10	0.04	1	10	0.86	<0.01	0.03	0.02	0.003	<10	<1	<10
CK-S-029	494200	6705600	-51.0600	-29.7798	Lomba Grande	<0.2	<0.5	8	201	<2	4	4	10	0.20	<10	41	<1	<10	0.06	4	6	0.52	0.01	0.04	0.03	0.006	<10	<1	<10
CK-S-030	496900	6703400	-51.0321	-29.7997	Lomba Grande	<0.2	<0.5	11	266	<2	15	5	13	0.69	<10	62	<1	<10	0.31	6	25	1.21	0.03	0.17	0.07	0.009	<10	3	<10
CK-S-032	496100	6704400	-51.0404	-29.7907	Lomba Grande	<0.2	<0.5	5	36	<2	3	5	6	0.28	<10	30	<1	<10	0.02	<1	7	0.45	0.03	0.02	0.03	0.004	<10	<1	<10
CK-S-033	495250	6704300	-51.0491	-29.7915	Lomba Grande	<0.2	<0.5	8	102	<2	7	5	11	0.87	<10	42	<1	<10	0.31	4	15	1.76	0.02	0.14	0.09	0.011	<10	3	<10
CK-S-034	494100	6702900	-51.0611	-29.8042	Lomba Grande	<0.2	<0.5	13	199	<2	9	10	23	0.97	<10	80	<1	<10	0.05	6	20	1.85	0.04	0.05	0.03	0.010	<10	3	<10
CK-S-035	493800	6704000	-51.0642	-29.7943	Lomba Grande	<0.2	<0.5	3	27	<2	<1	3	1	0.17	<10	13	<1	<10	0.01	<1	1	0.10	0.01	<0.01	0.03	0.001	<10	<1	<10
CK-S-036	494750	6703700	-51.0543	-29.7970	Lomba Grande	<0.2	<0.5	5	108	<2	4	4	7	0.31	<10	39	<1	<10	0.04	3	6	0.54	0.02	0.05	0.03	0.005	<10	1	<10
CK-S-037	494900	6703700	-51.0528	-29.7970	Lomba Grande	<0.2	<0.5	4	137	<2	4	4	6	0.38	<10	41	<1	<10	0.08	2	7	0.55	0.02	0.06	0.04	0.006	<10	1	<10
CK-S-038	495300	6702750	-51.0486	-29.8055	Lomba Grande	<0.2	<0.5	7	324	<2	10	5	10	0.57	<10	64	<1	<10	0.17	5	13	1.03	0.03	0.17	0.05	0.010	<10	2	<10
CK-S-039	493350	6704900	-51.0688	-29.7861	Lomba Grande	<0.2	<0.5	6	64	<2	2	6	6	0.46	<10	30	<1	<10	0.04	1	4	0.65	0.02	0.02	0.03	0.004	<10	1	<10
CK-S-040	493200	6704900	-51.0704	-29.7861	Lomba Grande	<0.2	<0.5	3	18	<2	2	4	12	0.20	<10	20	<1	<10	0.01	<1	2	0.23	0.01	0.01	0.03	0.004	<10	<1	<10
CK-S-041	492300	6703450	-51.0797	-29.7992	Lomba Grande	<0.2	<0.5	4	175	<2	5	12	10	0.14	<10	87	<1	<10	0.01	4	19	2.52	0.01	0.01	0.03	0.007	<10	1	<10
CK-S-042	503750	6705700	-50.9612	-29.7789	Lomba Grande	<0.2	<0.5	4	195	<2	6	7	16	0.66	<10	62	<1	<10	0.06	5	11	1.19	0.04	0.06	0.03	0.012	<10	2	<10
CK-S-043	502850	6705300	-50.9705	-29.7825	Lomba Grande	<0.2	<0.5	5	176	<2	5	9	19	0.83	<10	49	<1	<10	0.05	5	13	1.29	0.04	0.04	0.03	0.012	<10	2	<10
CK-S-044	502900	6705450	-50.9700	-29.7812	Lomba Grande	<0.2	<0.5	2	104	<2	3	3	8	0.26	<10	36	<1	<10	0.03	2	5	0.68	0.02	0.02	0.02	0.009	<10	<1	<10
CK-S-045	502400	6705350	-50.9752	-29.7821	Lomba Grande	<0.2	<0.5	6	989	<2	5	7	18	0.51	<10	86	<1	<10	0.07	10	8	1.15	0.03	0.04	0.02	0.018	<10	1	<10
CK-S-046	502700	6703000	-50.9721	-29.8033	Lomba Grande	<0.2	<0.5	6	303	<2	11	9	16	0.40	<10	72	<1	<10	0.09	6	14	0.95	0.03	0.07	0.02	0.010	<10	1	<10
CK-S-047	502900	6703050	-50.9700	-29.8028	Lomba Grande	<0.2	<0.5	5	140	<2	5	7	12	0.43	<10	45	<1	<10	0.11	3	10	1.02	0.03	0.06	0.03	0.006	<10	2	<10
CK-S-048	501750	6703600	-50.9819	-29.7979	Lomba Grande	<0.2	<0.5	5	271	<2	5	10	12	0.29	<10	53	<1	<10	0.10	5	10	1.00	0.02	0.05	0.03	0.007	<10	1	<10
CK-S-049	507400	6706700	-50.9235	-29.7699	Lomba Grande	<0.2	<0.5	9	792	<2	11	11	29	0.72	<10	99	<1	<10	0.20	17	25	2.46	0.02	0.10	0.04	0.021	<10	4	<10
CK-S-050	509500	6705950	-50.9017	-29.7766	Lomba Grande	<0.2	<0.5	9	608	<2	8	7	25	0.89	<10	83	<1	<10	0.20	10	18	2.17	0.02	0.10	0.04	0.017	<10	4	<10
CK-S-051	509400	6703850	-50.9027	-29.7956	Lomba Grande	<0.2	<0.5	4	265	<2	4	8	15	0.52	<10	48	<1	<10	0.05	5	14	1.73	0.02	0.03	0.02	0.009	<10	2	<10
CK-S-052	510000	6703900	-50.8965	-29.7951	Lomba Grande	<0.2	<0.5	8	147	<2	5	9	18	0.68	<10	58	<1	<10	0.15	4	11	1.28	0.02	0.09	0.04	0.011	<10	2	<10
CK-S-053	509000	6703500	-50.9069	-29.7987	Lomba Grande	<0.2	<0.5	6	157	<2	5	9	19	0.85	<10	61	<1	<10	0.07	4	12	1.40	0.02	0.05	0.02	0.012	<10	2	<10
CK-S-054	507950	6703000	-50.9177	-29.8033	Lomba Grande	<0.2	<0.5	4	148	<2	4	7	15	0.66	<10	46	<1	<10	0.05	4	11	1.52	0.02	0.04	0.02	0.012	<10	2	<10

Geochemical grade assay for stream sediments collected in the Lomba Grande district

(1continuerd/4)

Sample No.	Sr	Ti	V	W	Y	Zr	S
	ppm	%	ppm	ppm	ppm	ppm	%
CK-S-001	15	0.01	20	<10	5	5	0.036
CK-S-002	7	0.03	15	<10	3	4	0.011
CK-S-003	5	0.02	15	<10	3	5	0.007
CK-S-004	6	0.02	12	<10	3	2	0.007
CK-S-005	7	0.03	28	<10	4	4	0.007
CK-S-006	9	0.03	33	<10	3	4	0.007
CK-S-007	5	0.03	41	<10	2	4	0.009
CK-S-008	50	0.06	53	<10	4	12	0.006
CK-S-009	7	0.02	25	<10	2	3	0.004
CK-S-010	13	0.05	57	<10	4	4	0.009
CK-S-011	10	0.03	33	<10	6	4	0.006
CK-S-012	11	0.03	28	<10	3	11	0.007
CK-S-013	7	0.02	20	<10	2	4	0.005
CK-S-014	7	0.02	12	<10	2	2	0.003
CK-S-015	7	0.02	13	<10	2	2	0.004
CK-S-016	11	0.07	113	<10	8	29	0.008
CK-S-017	5	0.02	22	<10	3	4	0.006
CK-S-018	3	0.01	9	<10	1	1	0.003
CK-S-019	5	0.02	14	<10	2	2	0.003
CK-S-020	15	0.03	23	<10	3	4	0.004
CK-S-021	15	0.03	24	<10	4	4	0.004
CK-S-022	11	0.06	28	<10	2	4	0.004
CK-S-023	12	0.01	8	<10	2	2	0.005
CK-S-024	18	0.02	11	<10	2	2	0.004
CK-S-025	8	0.02	14	<10	1	2	0.003
CK-S-026	9	<0.01	9	<10	2	2	0.003
CK-S-027	9	0.01	11	<10	2	1	0.005
CK-S-028	4	0.02	27	<10	1	4	0.003
CK-S-029	4	0.01	10	<10	2	2	0.005
CK-S-030	17	0.05	30	<10	4	5	0.004
CK-S-032	7	0.02	13	<10	3	2	0.004
CK-S-033	18	0.04	29	<10	3	9	0.004
CK-S-034	18	0.05	46	<10	4	6	0.007
CK-S-035	3	<0.01	4	<10	<1	2	0.002
CK-S-036	8	0.02	13	<10	2	2	0.004
CK-S-037	8	0.02	12	<10	2	2	0.003
CK-S-038	12	0.02	18	<10	3	3	0.004
CK-S-039	5	<0.01	16	<10	1	6	0.005
CK-S-040	4	<0.01	7	<10	2	2	0.004
CK-S-041	19	0.04	49	<10	1	8	0.003
CK-S-042	11	0.03	28	<10	2	3	0.005
CK-S-043	8	0.03	29	<10	2	6	0.009
CK-S-044	6	0.02	13	<10	1	2	0.004
CK-S-045	10	0.02	15	<10	3	5	0.009
CK-S-046	12	0.01	20	<10	3	2	0.007
CK-S-047	10	0.02	25	<10	2	4	0.003
CK-S-048	8	0.02	21	<10	2	3	0.004
CK-S-049	11	0.05	51	<10	4	7	0.011
CK-S-050	12	0.05	43	<10	4	8	0.007
CK-S-051	6	0.04	42	<10	2	5	0.004
CK-S-052	13	0.02	22	<10	2	4	0.008
CK-S-053	9	0.04	30	<10	3	5	0.006
CK-S-054	6	0.04	29	<10	2	4	0.006

Geochemical grade assay for stream sediments collected in the Lomba Grande district

Sample No.	UTM_E	UTM_N	Latitude	Longitude	Location	Ag	Cd	Cu	Mn	Mo	Ni	Pb	Zn	Al	As	Ba	Be	Bi	Ca	Co	Cr	Fe	K	Mg	Na	P	Sb	Sc	Sn
						ppm	ppm	ppm	ppm	ppm	ppm	ppm	ppm	%	ppm	ppm	ppm	ppm	%	ppm	ppm	%	%	%	%	%	ppm	ppm	ppm
CK-S-055	504750	6703850	-50.9509	-29.7956	Lomba Grande	<0.2	<0.5	2	97	<2	3	6	9	0.24	<10	26	<1	<10	0.02	3	7	0.65	<0.01	0.01	0.01	0.005	<10	1	<10
CK-S-056	506300	6704050	-50.9348	-29.7938	Lomba Grande	<0.2	<0.5	3	159	<2	1	6	10	0.34	<10	29	<1	<10	0.04	2	4	0.58	<0.01	0.02	0.02	0.007	<10	<1	<10
CK-S-057	505700	6703800	-50.9410	-29.7961	Lomba Grande	<0.2	<0.5	9	192	<2	3	8	18	0.54	<10	44	<1	<10	0.12	4	8	1.00	0.02	0.06	0.02	0.011	<10	2	<10
CK-S-058	506700	6703200	-50.9307	-29.8015	Lomba Grande	<0.2	<0.5	4	44	<2	2	5	12	0.30	<10	27	<1	<10	0.05	1	4	0.45	<0.01	0.03	0.02	0.007	<10	<1	<10
CK-S-059	506450	6703150	-50.9333	-29.8019	Lomba Grande	<0.2	<0.5	5	134	<2	5	6	17	0.66	<10	45	<1	<10	0.08	3	8	0.98	0.02	0.08	0.02	0.016	<10	2	<10
CK-S-061	507150	6702000	-50.9260	-29.8123	Lomba Grande	<0.2	<0.5	3	72	<2	2	4	10	0.28	<10	27	<1	<10	0.03	2	4	0.53	<0.01	0.02	0.02	0.008	<10	<1	<10
CK-S-062	506650	6701700	-50.9312	-29.8150	Lomba Grande	<0.2	<0.5	7	62	<2	1	4	9	0.24	<10	24	<1	<10	0.03	1	4	0.42	0.01	0.02	0.01	0.004	<10	<1	<10
CK-S-063	506700	6701450	-50.9307	-29.8173	Lomba Grande	<0.2	<0.5	6	46	<2	2	6	14	0.21	<10	21	<1	<10	0.02	1	3	0.29	0.01	0.01	0.01	0.004	<10	<1	<10
CK-S-064	505800	6702150	-50.9400	-29.8109	Lomba Grande	<0.2	<0.5	5	163	<2	2	6	15	0.43	<10	33	<1	<10	0.04	2	8	0.96	0.01	0.03	0.02	0.006	<10	1	<10
CK-S-065	504850	6702500	-50.9498	-29.8078	Lomba Grande	<0.2	<0.5	9	346	<2	8	9	22	0.98	<10	75	<1	<10	0.38	6	17	1.22	0.02	0.13	0.07	0.013	<10	2	<10
CK-S-066	503900	6702950	-50.9596	-29.8037	Lomba Grande	<0.2	<0.5	4	129	<2	2	5	12	0.31	<10	33	<1	<10	0.03	2	5	0.52	0.01	0.02	0.01	0.006	<10	<1	<10
CK-S-067	503900	6702100	-50.9596	-29.8114	Lomba Grande	<0.2	<0.5	4	100	<2	1	6	10	0.28	<10	25	<1	<10	0.02	2	7	0.93	0.01	0.02	<0.01	0.004	<10	<1	<10
CK-S-068	503900	6701100	-50.9596	-29.8204	Lomba Grande	<0.2	<0.5	6	101	<2	3	7	13	0.21	<10	25	<1	<10	0.03	2	9	0.99	0.01	0.02	0.01	0.004	<10	<1	<10
CK-S-069	505500	6701250	-50.9431	-29.8191	Lomba Grande	<0.2	<0.5	10	168	<2	7	9	17	0.53	<10	60	<1	<10	0.23	4	16	1.38	0.02	0.10	0.04	0.008	<10	2	<10
CK-S-070	505100	6700550	-50.9472	-29.8254	Lomba Grande	<0.2	<0.5	4	104	<2	4	7	12	0.23	<10	30	<1	<10	0.08	2	12	1.27	0.01	0.04	0.02	0.006	<10	<1	<10
CK-S-071	504900	6699650	-50.9493	-29.8335	Lomba Grande	<0.2	<0.5	4	161	<2	3	7	13	0.31	<10	40	<1	<10	0.08	2	10	0.82	0.03	0.05	0.02	0.008	<10	1	<10
CK-S-072	504900	6699550	-50.9493	-29.8344	Lomba Grande	<0.2	<0.5	5	351	<2	3	7	16	0.23	<10	69	<1	<10	0.05	5	9	1.02	0.03	0.04	0.01	0.016	<10	<1	<10
CK-S-073	504800	6698950	-50.9503	-29.8398	Lomba Grande	<0.2	<0.5	6	350	<2	2	8	17	0.23	<10	48	<1	<10	0.07	4	6	0.59	0.02	0.04	0.01	0.007	<10	<1	<10
CK-S-074	504850	6699250	-50.9498	-29.8371	Lomba Grande	<0.2	<0.5	7	610	<2	3	6	18	0.25	<10	73	<1	<10	0.07	5	6	0.68	0.02	0.05	0.01	0.010	<10	<1	<10
CK-S-075	502050	6700200	-50.9788	-29.8286	Lomba Grande	<0.2	<0.5	5	118	<2	4	8	14	0.19	<10	35	<1	<10	0.03	3	15	1.34	0.02	0.03	0.01	0.006	<10	<1	<10
CK-S-076	502550	6699550	-50.9736	-29.8344	Lomba Grande	<0.2	<0.5	5	289	<2	4	7	18	0.30	<10	75	<1	<10	0.08	4	11	0.81	0.07	0.08	0.01	0.010	<10	1	<10
CK-S-077	502600	6701150	-50.9731	-29.8200	Lomba Grande	<0.2	<0.5	3	183	<2	3	6	12	0.15	<10	41	<1	<10	0.04	3	7	0.59	0.02	0.03	0.01	0.007	<10	<1	<10
CK-S-078	503100	6700350	-50.9679	-29.8272	Lomba Grande	<0.2	<0.5	2	238	<2	2	5	10	0.13	<10	38	<1	<10	0.04	2	9	0.64	0.02	0.03	0.01	0.006	<10	<1	<10
CK-S-079	503000	6700200	-50.9689	-29.8286	Lomba Grande	<0.2	<0.5	14	126	<2	4	7	19	0.13	<10	34	<1	<10	0.04	2	8	0.69	0.02	0.03	0.01	0.008	<10	<1	<10
CK-S-080	503400	6700100	-50.9648	-29.8295	Lomba Grande	<0.2	<0.5	5	239	<2	3	6	15	0.13	<10	36	<1	<10	0.05	3	5	0.43	0.02	0.03	0.01	0.006	<10	<1	<10
CK-S-081	503400	6698900	-50.9648	-29.8403	Lomba Grande	<0.2	<0.5	4	171	<2	3	6	16	0.14	<10	50	<1	<10	0.05	3	9	0.71	0.03	0.05	0.01	0.009	<10	<1	<10
CK-S-082	503900	6700150	-50.9596	-29.8290	Lomba Grande	<0.2	<0.5	3	61	<2	2	4	10	0.17	<10	20	<1	<10	0.02	1	5	0.65	<0.01	0.01	<0.01	0.004	<10	<1	<10
CK-S-083	503850	6700050	-50.9601	-29.8299	Lomba Grande	<0.2	<0.5	4	217	<2	2	4	12	0.10	<10	30	<1	<10	0.04	2	5	0.40	0.02	0.02	<0.01	0.005	<10	<1	<10
CK-S-084	503950	6699800	-50.9591	-29.8322	Lomba Grande	<0.2	<0.5	6	186	<2	4	10	28	0.17	<10	44	<1	<10	0.08	3	6	0.62	0.02	0.05	0.02	0.009	<10	<1	<10
CK-S-085	502700	6698100	-50.9720	-29.8475	Lomba Grande	<0.2	<0.5	4	72	<2	4	10	21	0.31	<10	44	<1	<10	0.07	2	6	0.53	0.02	0.03	0.02	0.010	<10	<1	<10
CK-S-086	501750	6698900	-50.9819	-29.8403	Lomba Grande	<0.2	<0.5	4	292	<2	5	9	23	0.37	<10	82	<1	<10	0.12	4	11	1.02	0.08	0.10	0.02	0.013	<10	1	<10
CK-S-087	500700	6698400	-50.9928	-29.8448	Lomba Grande	<0.2	<0.5	13	485	<2	20	9	27	0.95	<10	93	<1	<10	0.22	10	49	1.95	0.03	0.14	0.04	0.012	<10	5	<10
CK-S-088	501000	6697550	-50.9886	-29.8525	Lomba Grande	<0.2	<0.5	1	35	<2	1	6	8	0.17	<10	28	<1	<10	0.01	1	4	0.41	0.01	0.02	0.02	0.005	<10	<1	<10
CK-S-089	501050	6700200	-50.9891	-29.8286	Lomba Grande	<0.2	<0.5	1	46	<2	2	4	9	0.18	<10	27	<1	<10	0.02	1	7	0.46	0.02	0.02	0.02	0.004	<10	<1	<10
CK-S-090	501450	6701400	-50.9850	-29.8177	Lomba Grande	<0.2	<0.5	3	121	<2	2	8	12	0.20	<10	34	<1	<10	0.03	3	8	0.62	0.02	0.02	0.02	0.006	<10	<1	<10
CK-S-091	501200	6701600	-50.9876	-29.8159	Lomba Grande	<0.2	<0.5	3	182	<2	3	9	15	0.32	<10	55	<1	<10	0.04	4	8	0.88	0.02	0.03	0.02	0.009	<10	<1	<10
CK-S-092	501100	6701100	-50.9886	-29.8204	Lomba Grande	<0.2	<0.5	3	99	<2	3	6	11	0.22	<10	38	<1	<10	0.05	2	8	0.80	0.03	0.04	0.02	0.008	<10	<1	<10
CK-S-093	500050	6700950	-50.9995	-29.8218	Lomba Grande	<0.2	<0.5	3	113	<2	2	6	11	0.15	<10	33	<1	<10	0.02	3	6	0.59	0.01	0.02	0.02	0.004	<10	<1	<10
CK-S-094	502250	6694300	-50.9767	-29.8818	Lomba Grande	<0.2	<0.5	1	80	<2	1	5	10	0.16	<10	29	<1	<10	0.04	2	3	0.48	<0.01	0.01	0.01	0.012	<10	<1	<10
CK-S-095	500200	6693250	-50.9979	-29.8913	Lomba Grande	<0.2	<0.5	6	62	<2	3	7	16	0.17	<10	23	<1	<10	0.05	2	4	0.32	0.02	0.03	0.02	0.008	<10	<1	<10
CK-S-096	501700	6691650	-50.9824	-29.9057	Lomba Grande	<0.2	<0.5	6	220	<2	4	13	56	0.71	<10	66	<1	<10	0.10	6	10	1.52	0.08	0.10	0.02	0.012	<10	2	<10
CK-S-097	513500	6704750	-50.8603	-29.7874	Lomba Grande	<0.2	<0.5	2	178	<2	3	5	11	0.29	<10	32	<1	<10	0.04	3	7	0.66	0.02	0.03	0.02	0.005	<10	<1	<10
CK-S-098	513400	6704200	-50.8614	-29.7924	Lomba Grande	<0.2	<0.5	6	203	<2	7	8	21	0.57	<10	67	<1	<10	0.12	7	17	1.59	0.02	0.09	0.03	0.012	<10	3	<10
CK-S-100	511500	6702450	-50.8810	-29.8082	Lomba Grande	<0.2	<0.5	<1	405	<2	2	4	11	0.24	<10	48	<1	<10	0.02	4	5	0.71	0.03	0.02	0.02	0.008	<10	<1	<10
CK-S-102	513950	6705950	-50.8557	-29.7766	Lomba Grande	<0.2	<0.5	12	454	<2	16	10	36	0.92	<10	79	<1	<10	0.34	15	35	3.16	0.02	0.19	0.05	0.020	<10	5	<10
CK-S-103	515100	6705200	-50.8438	-29.7833	Lomba Grande	<0.2	<0.5	22	412	<2	34	12	57	1.61	<10	154	1	<10	0.54	26	50	4.21	0.03	0.47	0.08	0.030	<10	10	<10
CK-S-104	515700	6706700	-50.8376	-29.7698	Lomba Grande	<0.2	<0.5	66	1283	<2	36	20	80	2.79	<10	183	1	<10	0.31	40	65	6.43	0.06	0.27	0.05	0.025	<10	19	<10
CK-S-105	515750	6703400	-50.8370	-29.7996	Lomba Grande	<0.2	<0.5	11	413	<2	7	15	35	2.20	<10	98	<1	<10	0.15	6	19	2.23	0.04	0.10	0.04	0.014	<10	5	<10
CK-S-106	509600	6697650	-50.9006	-29.8515	Lomba Grande	<0.2	<0.5	1	134	<2	2	5	10	0.24	<10	41	<1	<10	0.03	3	7	0.45	0.04	0.03	0.02	0.005	<10	<1	<10
CK-S-107	510200	6698000	-50.8944	-29.8484	Lomba Grande	<0.2	<0.5	3	92	<2	5	5	12	0.56	<10	47	<1	<10	0.13	3	11	0.72	0.03	0.07	0.04	0.011	<10	2	<10
CK-S-108	511100	6698200	-50.8851	-29.8466	Lomba Grande	<0.2	<0.5	2	219	<2	5	7	16	0.31	<10	64	<1	<10	0.06	5	12	0.92	0.06	0.06	0.02	0.010	<10	1	<10
CK-S-109	511600	6698700	-50.8799	-29.8420	Lomba Grande	<0.2	<0.5	3	187	<2	4	5	14	0.31	<10	68	<1	<10	0.12	4	11	0.73	0.06	0.08	0.03	0.006	<10	1	<10
CK-S-110	512300	6698250	-50.8727	-29.8461	Lomba Grande	<0.2	<0.5	2	56	<2	3	5	10	0.16	<10	33	<1	<10	0.02	2	12	0.60	0.03	0.03	0.02	0.003	<10	<1	<10

Geochemical grade assay for stream sediments collected in the Lomba Grande district

Sample No.	Sr	Ti	V	W	Y	Zr	S
	ppm	%	ppm	ppm	ppm	ppm	%
CK-S-055	2	0.09	27	<10	2	3	0.006
CK-S-056	5	0.01	12	<10	2	2	0.006
CK-S-057	8	0.02	22	<10	2	3	0.008
CK-S-058	4	0.01	11	<10	1	2	0.004
CK-S-059	6	0.02	23	<10	2	3	0.007
CK-S-061	3	0.01	13	<10	1	2	0.004
CK-S-062	3	0.01	10	<10	1	1	0.003
CK-S-063	3	<0.01	7	<10	<1	1	0.004
CK-S-064	5	0.02	23	<10	2	3	0.004
CK-S-065	21	0.03	29	<10	8	4	0.008
CK-S-066	4	0.01	12	<10	2	2	0.005
CK-S-067	3	0.01	25	<10	1	2	0.003
CK-S-068	3	0.02	26	<10	1	2	0.004
CK-S-069	14	0.03	37	<10	4	7	0.004
CK-S-070	5	0.02	34	<10	2	4	0.002
CK-S-071	6	0.01	17	<10	2	4	0.005
CK-S-072	5	0.01	13	<10	2	3	0.005
CK-S-073	5	<0.01	11	<10	2	2	0.004
CK-S-074	6	0.01	10	<10	2	2	0.005
CK-S-075	6	0.02	32	<10	2	3	0.003
CK-S-076	8	0.01	12	<10	3	2	0.005
CK-S-077	6	0.01	13	<10	2	1	0.003
CK-S-078	5	<0.01	13	<10	1	1	0.002
CK-S-079	3	0.01	12	<10	1	2	0.005
CK-S-080	3	<0.01	7	<10	1	2	0.004
CK-S-081	4	<0.01	12	<10	2	2	0.003
CK-S-082	2	0.01	16	<10	<1	2	0.002
CK-S-083	3	<0.01	6	<10	<1	1	0.002
CK-S-084	5	0.01	10	<10	2	2	0.005
CK-S-085	5	0.01	12	<10	3	1	0.010
CK-S-086	11	0.01	16	<10	4	3	0.004
CK-S-087	15	0.05	54	<10	5	10	0.005
CK-S-088	3	0.01	8	<10	1	1	0.004
CK-S-089	3	0.01	10	<10	2	3	0.002
CK-S-090	4	0.01	14	<10	2	2	0.004
CK-S-091	6	0.02	18	<10	2	2	0.006
CK-S-092	5	<0.01	14	<10	2	3	0.004
CK-S-093	3	0.01	12	<10	1	2	0.002
CK-S-094	3	<0.01	11	<10	1	2	0.004
CK-S-095	4	<0.01	9	<10	2	2	0.004
CK-S-096	11	0.01	26	<10	4	6	0.005
CK-S-097	5	0.02	15	<10	1	2	0.003
CK-S-098	11	0.04	45	<10	3	5	0.006
CK-S-100	6	<0.01	8	<10	2	2	0.005
CK-S-102	17	0.08	96	<10	5	11	0.005
CK-S-103	25	0.10	112	<10	10	20	0.008
CK-S-104	22	0.03	115	<10	12	13	0.012
CK-S-105	22	0.02	48	<10	4	10	0.011
CK-S-106	9	<0.01	8	<10	2	2	0.003
CK-S-107	11	0.01	17	<10	3	4	0.005
CK-S-108	12	0.01	16	<10	3	3	0.004
CK-S-109	13	0.01	14	<10	3	3	0.003
CK-S-110	5	0.01	13	<10	3	3	0.002

Geochemical grade assay for stream sediments collected in the Lomba Grande district

Sample No.	UTM_E	UTM_N	Latitude	Longitude	Location	Ag	Cd	Cu	Mn	Mo	Ni	Pb	Zn	Al	As	Ba	Be	Bi	Ca	Co	Cr	Fe	K	Mg	Na	P	Sb	Sc	Sn
						ppm	ppm	ppm	ppm	ppm	ppm	ppm	ppm	%	ppm	ppm	ppm	ppm	%	ppm	ppm	%	%	%	%	%	ppm	ppm	ppm
CK-S-111	512250	6696900	-50.8732	-29.8583	Lomba Grande	<0.2	<0.5	6	207	<2	5	9	18	0.17	<10	53	<1	<10	0.05	5	18	1.35	0.04	0.04	0.02	0.006	<10	<1	<10
CK-S-112	511850	6697650	-50.8773	-29.8515	Lomba Grande	<0.2	<0.5	13	158	<2	3	8	16	0.13	<10	44	<1	<10	0.04	4	11	0.74	0.03	0.03	0.01	0.007	<10	<1	<10
CK-S-113	511050	6697450	-50.8856	-29.8533	Lomba Grande	<0.2	<0.5	2	30	<2	1	5	8	0.14	<10	22	<1	<10	0.02	1	5	0.39	0.01	0.01	0.01	0.002	<10	<1	<10
CK-S-114	510850	6696700	-50.8877	-29.8601	Lomba Grande	<0.2	<0.5	3	122	<2	5	8	13	0.15	<10	47	<1	<10	0.02	4	23	2.97	0.03	0.02	0.02	0.004	<10	<1	<10
CK-S-115	510750	6696450	-50.8887	-29.8624	Lomba Grande	<0.2	<0.5	3	90	<2	3	4	11	0.21	<10	43	<1	<10	0.03	2	5	0.53	0.04	0.03	0.02	0.005	<10	<1	<10
CK-S-116	510150	6697000	-50.8949	-29.8574	Lomba Grande	<0.2	<0.5	3	162	<2	5	7	12	0.29	<10	52	<1	<10	0.04	3	9	0.61	0.04	0.04	0.02	0.007	<10	<1	<10
CK-S-117	509600	6696150	-50.9006	-29.8651	Lomba Grande	<0.2	<0.5	3	84	<2	<1	4	8	0.15	<10	21	<1	<10	0.06	<1	3	0.63	0.09	0.01	0.03	0.003	<10	<1	<10
CK-S-118	508850	6696350	-50.9084	-29.8615	Lomba Grande	<0.2	<0.5	2	73	<2	3	6	15	0.29	<10	54	<1	<10	0.07	3	4	0.59	0.04	0.06	0.01	0.006	<10	1	<10
CK-S-119	511400	6695950	-50.8820	-29.8669	Lomba Grande	<0.2	<0.5	3	52	<2	2	7	12	0.12	<10	39	<1	<10	0.02	2	7	0.43	0.03	0.02	0.01	0.005	<10	<1	<10
CK-S-120	510950	6694250	-50.8866	-29.8822	Lomba Grande	<0.2	<0.5	2	87	<2	1	7	11	0.15	<10	43	<1	<10	0.04	2	3	0.47	0.02	0.02	0.01	0.003	<10	<1	<10
CK-S-121	510100	6695550	-50.8954	-29.8705	Lomba Grande	<0.2	<0.5	2	77	<2	2	5	12	0.13	<10	33	<1	<10	0.03	3	10	0.52	0.02	0.02	0.01	0.004	<10	<1	<10
CK-S-122	509550	6695000	-50.9011	-29.8755	Lomba Grande	<0.2	<0.5	4	22	<2	<1	6	14	0.09	<10	23	<1	<10	0.01	1	4	0.29	0.01	<0.01	0.01	0.004	<10	<1	<10
CK-S-123	514950	6699950	-50.8453	-29.8307	Lomba Grande	<0.2	<0.5	5	53	<2	1	7	14	0.19	<10	36	<1	<10	0.03	<1	6	0.41	0.01	0.02	0.01	0.003	<10	1	<10
CK-S-124	514250	6699600	-50.8525	-29.8339	Lomba Grande	<0.2	<0.5	4	72	<2	1	7	13	0.09	<10	31	<1	<10	0.02	2	7	0.44	0.01	0.01	<0.01	0.003	<10	<1	<10
CK-S-125	514900	6699050	-50.8458	-29.8388	Lomba Grande	<0.2	<0.5	4	77	<2	2	7	14	0.37	<10	54	<1	<10	0.04	2	9	0.86	0.03	0.04	0.02	0.005	<10	1	<10
CK-S-126	513350	6699000	-50.8618	-29.8393	Lomba Grande	<0.2	<0.5	3	141	<2	4	7	15	0.36	<10	45	<1	<10	0.09	3	14	1.09	0.03	0.05	0.02	0.007	<10	1	<10
CK-S-127	515700	6699400	-50.8375	-29.8357	Lomba Grande	<0.2	<0.5	2	48	<2	1	5	12	0.16	<10	35	<1	<10	0.02	1	5	0.32	0.02	0.02	0.01	0.004	<10	<1	<10
CK-S-128	515600	6699200	-50.8385	-29.8375	Lomba Grande	<0.2	<0.5	7	66	<2	2	7	17	0.24	<10	46	<1	<10	0.05	2	6	0.51	0.02	0.03	0.01	0.006	<10	1	<10
CK-S-129	516300	6698250	-50.8313	-29.8461	Lomba Grande	<0.2	<0.5	3	168	<2	3	5	17	0.21	<10	51	<1	<10	0.05	4	6	0.57	0.03	0.05	0.01	0.006	<10	<1	<10
CK-S-130	507350	6701050	-50.9239	-29.8209	Lomba Grande	<0.2	<0.5	2	71	<2	2	5	12	0.23	<10	22	<1	<10	0.05	2	8	0.84	<0.01	0.02	0.01	0.004	<10	<1	<10
CK-S-131	507450	6601100	-50.9229	-29.8204	Lomba Grande	<0.2	<0.5	2	48	<2	1	5	11	0.15	<10	17	<1	<10	0.02	1	3	0.37	<0.01	0.02	<0.01	0.005	<10	<1	<10
CK-S-132	507700	6700300	-50.9203	-29.8276	Lomba Grande	<0.2	<0.5	3	130	<2	2	4	13	0.18	<10	29	<1	<10	0.04	2	5	0.65	<0.01	0.02	<0.01	0.007	<10	<1	<10
CK-S-133	508450	6701250	-50.9125	-29.8191	Lomba Grande	<0.2	<0.5	5	142	<2	1	5	14	0.12	<10	26	<1	<10	0.02	2	4	0.46	<0.01	0.01	<0.01	0.004	<10	<1	<10
CK-S-134	517550	6700450	-50.8184	-29.8262	Lomba Grande	<0.2	<0.5	3	51	<2	<1	5	13	0.06	<10	19	<1	<10	0.03	1	1	0.22	<0.01	0.01	<0.01	0.003	<10	<1	<10
CK-S-135	516550	6700350	-50.8287	-29.8271	Lomba Grande	<0.2	<0.5	4	130	<2	4	4	15	0.31	<10	38	<1	<10	0.10	3	5	0.46	0.02	0.06	0.02	0.006	<10	<1	<10
CK-S-136	516750	6699250	-50.8266	-29.8370	Lomba Grande	<0.2	<0.5	6	88	<2	8	11	21	0.77	<10	84	<1	<10	0.20	5	10	1.47	0.02	0.17	0.03	0.011	<10	3	<10
CK-S-137	516650	6698900	-50.8276	-29.8402	Lomba Grande	<0.2	<0.5	2	56	<2	2	4	11	0.13	<10	31	<1	<10	0.02	1	4	0.27	0.01	0.02	<0.01	0.004	<10	<1	<10
CK-S-138	517500	6698250	-50.8188	-29.8460	Lomba Grande	<0.2	<0.5	6	38	<2	1	8	15	0.11	<10	26	<1	<10	0.02	<1	3	0.24	0.01	0.02	<0.01	0.004	<10	<1	<10
CK-S-139	517400	6698050	-50.8199	-29.8478	Lomba Grande	<0.2	<0.5	6	50	<2	2	8	17	0.10	<10	26	<1	<10	0.03	1	3	0.29	0.01	0.02	<0.01	0.004	<10	<1	<10
CK-S-140	517900	6699500	-50.8147	-29.8347	Lomba Grande	<0.2	<0.5	5	132	<2	1	6	16	0.16	<10	34	<1	<10	0.03	2	3	0.46	0.02	0.03	<0.01	0.008	<10	<1	<10
CK-S-141	518900	6697800	-50.8043	-29.8501	Lomba Grande	<0.2	<0.5	4	130	<2	<1	6	16	0.13	<10	32	<1	<10	0.03	2	2	0.37	0.01	0.02	<0.01	0.008	<10	<1	<10
CK-S-142	517350	6696050	-50.8204	-29.8659	Lomba Grande	<0.2	<0.5	3	51	<2	<1	6	14	0.14	<10	20	<1	<10	0.02	1	2	0.52	<0.01	0.01	<0.01	0.013	<10	<1	<10
CK-S-143	515500	6698400	-50.8395	-29.8447	Lomba Grande	<0.2	<0.5	2	77	<2	1	5	12	0.07	<10	28	<1	<10	0.02	1	3	0.27	<0.01	0.02	<0.01	0.003	<10	<1	<10
CK-S-144	515600	6698450	-50.8385	-29.8443	Lomba Grande	<0.2	<0.5	4	41	<2	<1	7	15	0.07	<10	26	<1	<10	0.03	1	2	0.28	<0.01	0.02	<0.01	0.002	<10	<1	<10
CK-S-145	516550	6696650	-50.8286	-29.8605	Lomba Grande	<0.2	<0.5	4	20	<2	3	5	14	0.09	<10	11	<1	<10	0.03	<1	4	0.25	<0.01	0.03	0.01	0.003	<10	<1	<10
CK-S-146	513800	6695850	-50.8571	-29.8677	Lomba Grande	<0.2	<0.5	2	41	<2	2	7	15	0.15	<10	29	<1	<10	0.02	1	4	0.40	0.02	0.02	0.01	0.004	<10	<1	<10
CK-S-147	514050	6695850	-50.8545	-29.8677	Lomba Grande	<0.2	<0.5	4	27	<2	<1	5	12	0.10	<10	21	<1	<10	<0.01	1	3	0.33	<0.01	<0.01	0.01	0.003	<10	<1	<10
CK-S-148	512700	6695450	-50.8685	-29.8894	Lomba Grande	<0.2	<0.5	3	37	<2	2	4	12	0.09	<10	28	<1	<10	0.02	1	3	0.26	0.01	0.01	0.01	0.003	<10	<1	<10
CK-S-149	515550	6694200	-50.8392	-29.8826	Lomba Grande	<0.2	<0.5	25	36	<2	7	6	18	0.07	<10	26	<1	<10	0.01	2	4	0.43	0.01	0.01	<0.01	0.009	<10	<1	<10
CK-S-150	515550	6694200	-50.8390	-29.8826	Lomba Grande	<0.2	<0.5	10	25	<2	4	6	<1	0.06	<10	11	<1	<10	37.17	<1	1	0.33	<0.01	<0.01	<0.01	0.005	<10	<1	<10
CK-S-151	515400	6694000	-50.8405	-29.8844	Lomba Grande	<0.2	<0.5	8	15	<2	3	6	12	0.06	<10	20	<1	<10	<0.01	<1	1	0.22	<0.01	<0.01	0.01	0.005	<10	<1	<10
CK-S-152	514450	6692450	-50.8503	-29.8984	Lomba Grande	<0.2	<0.5	5	29	<2	2	4	11	0.06	<10	12	<1	<10	0.02	<1	1	0.19	<0.01	<0.01	0.01	0.003	<10	<1	<10
CK-S-153	514050	6692150	-50.8545	-29.9011	Lomba Grande	<0.2	<0.5	5	29	<2	<1	4	11	0.06	<10	9	<1	<10	0.01	<1	2	0.31	<0.01	<0.01	<0.01	0.007	<10	<1	<10
CK-S-154	512850	6690900	-50.8669	-29.9124	Lomba Grande	<0.2	<0.5	3	67	<2	1	4	11	0.04	<10	15	<1	<10	0.02	2	1	0.41	<0.01	<0.01	0.01	0.004	<10	<1	<10
CK-S-157	515500	6693000	-50.8395	-29.8934	Lomba Grande	<0.2	<0.5	4	167	<2	2	8	12	0.10	<10	37	<1	<10	0.03	3	4	0.79	<0.01	0.01	0.01	0.007	<10	2	<10
CK-S-158	514700	6691250	-50.8477	-29.9092	Lomba Grande	<0.2	<0.5	<1	18	<2	<1	4	9	0.15	<10	34	<1	<10	<0.01	1	2	0.14	<0.01	<0.01	0.02	0.003	<10	<1	<10
CK-S-159	511800	6690900	-50.8778	-29.9124	Lomba Grande	<0.2	<0.5	1	55	<2	<1	4	12	0.09	<10	12	<1	<10	0.01	1	2	0.27	<0.01	<0.01	0.02	0.003	<10	<1	<10
CK-S-161	513050	6689200	-50.8648	-29.9278	Lomba Grande	<0.2	<0.5	20	112	<2	5	14	25	1.24	<10	38	<1	<10	0.09	3	22	2.93	0.03	0.09	0.02	0.010	<10	7	<10
CK-S-162	513350	6688800	-50.8617	-29.9314	Lomba Grande	<0.2	<0.5	10	103	<2	3	10	19	0.72	<10	32	<1	<10	0.07	3	14	1.94	0.02	0.06	0.01	0.009	<10	4	<10
CK-S-163	514350	6690150	-50.8513	-29.9192	Lomba Grande	<0.2	<0.5	3	128	<2	<1	6	13	0.17	<10	23	<1	<10	0.03	3	3	0.69	<0.01	0.01	0.01	0.008	<10	<1	<10
CK-S-164	515000	6689600	-50.8446	-29.9241	Lomba Grande	<0.2	<0.5	5	156	<2	4	7	13	0.30	<10	29	<1	<10	0.03	3	5	0.73	<0.01	0.02	0.01	0.006	<10	2	<10
CK-S-165	512450	6689550	-50.8710	-29.9246	Lomba Grande	<0.2	<0.5	11	152	<2	4	8	18	0.34	<10	22	<1	<10	0.05	3	6	1.74	<0.01	0.02	0.02	0.017	<10	2	<10
CK-S-166	509700	6692700	-50.8995	-29.8962	Lomba Grande	<0.2	<0.5	3	50	<2	3	5	11	0.31	<10	24	<1	<10	0.04	2	4	0.47	0.02	0.04	0.03	0.006	<10	<1	<10

Geochemical grade assay for stream sediments collected in the Lomba Grande district

Sample No.	Sr	Ti	V	W	Y	Zr	S
	ppm	%	ppm	ppm	ppm	ppm	%
CK-S-111	6	0.01	32	<10	3	3	0.004
CK-S-112	4	0.01	17	<10	2	2	0.006
CK-S-113	3	<0.01	12	<10	2	2	0.003
CK-S-114	7	0.04	74	<10	2	7	0.002
CK-S-115	7	<0.01	8	<10	2	2	0.004
CK-S-116	9	0.01	11	<10	3	2	0.003
CK-S-117	6	<0.01	9	<10	2	2	0.003
CK-S-118	8	<0.01	14	<10	6	4	0.002
CK-S-119	4	<0.01	11	<10	5	2	0.003
CK-S-120	3	<0.01	9	<10	3	3	0.003
CK-S-121	3	<0.01	11	<10	2	2	0.003
CK-S-122	1	<0.01	7	<10	2	1	0.004
CK-S-123	3	<0.01	14	<10	2	3	0.002
CK-S-124	2	<0.01	11	<10	1	1	0.004
CK-S-125	8	<0.01	22	<10	4	5	0.003
CK-S-126	9	0.02	24	<10	2	3	0.004
CK-S-127	5	<0.01	7	<10	1	1	0.003
CK-S-128	6	<0.01	12	<10	4	3	0.006
CK-S-129	5	<0.01	11	<10	3	2	0.003
CK-S-130	3	0.02	24	<10	1	2	0.002
CK-S-131	2	<0.01	9	<10	<1	1	0.003
CK-S-132	3	<0.01	14	<10	1	2	0.004
CK-S-133	2	<0.01	11	<10	1	1	0.004
CK-S-134	2	<0.01	4	<10	<1	<1	0.003
CK-S-135	7	0.01	10	<10	2	2	0.008
CK-S-136	16	0.02	27	<10	5	11	0.006
CK-S-137	3	<0.01	6	<10	2	<1	0.003
CK-S-138	3	<0.01	5	<10	1	<1	0.004
CK-S-139	3	<0.01	6	<10	2	1	0.003
CK-S-140	3	<0.01	7	<10	2	1	0.004
CK-S-141	3	<0.01	4	<10	1	<1	0.004
CK-S-142	2	<0.01	15	<10	1	1	0.004
CK-S-143	2	<0.01	6	<10	1	<1	0.002
CK-S-144	2	<0.01	7	<10	2	1	0.002
CK-S-145	2	<0.01	8	<10	<1	1	0.003
CK-S-146	3	<0.01	13	<10	2	2	0.003
CK-S-147	2	<0.01	7	<10	2	2	0.003
CK-S-148	3	<0.01	7	<10	2	1	0.003
CK-S-149	2	<0.01	6	<10	1	1	0.006
CK-S-150	1	<0.01	8	<10	<1	1	<0.001
CK-S-151	1	<0.01	4	<10	1	<1	0.003
CK-S-152	1	<0.01	5	<10	<1	<1	0.003
CK-S-153	1	<0.01	13	<10	<1	1	0.004
CK-S-154	1	<0.01	10	<10	<1	1	0.003
CK-S-157	3	<0.01	25	<10	3	3	0.005
CK-S-158	2	<0.01	6	<10	1	2	0.003
CK-S-159	1	<0.01	8	<10	<1	2	0.002
CK-S-161	10	0.03	94	<10	3	27	0.004
CK-S-162	6	0.02	62	<10	2	16	0.004
CK-S-163	2	<0.01	18	<10	1	3	0.004
CK-S-164	3	<0.01	21	<10	2	5	0.004
CK-S-165	3	0.02	32	<10	1	6	0.008
CK-S-166	3	0.01	11	<10	2	3	0.004

Geochemical grade assay for stream sediments collected in the Lomba Grande district

Sample No.	UTM_E	UTM_N	Latitude	Longitude	Location	Ag	Cd	Cu	Mn	Mo	Ni	Pb	Zn	Al	As	Ba	Be	Bi	Ca	Co	Cr	Fe	K	Mg	Na	P	Sb	Sc	Sn
						ppm	ppm	ppm	ppm	ppm	ppm	ppm	ppm	%	ppm	ppm	ppm	ppm	%	ppm	ppm	%	%	%	%	%	ppm	ppm	ppm
CK-S-167	509600	6692850	-50.9006	-29.8949	Lomba Grande	<0.2	<0.5	2	57	<2	3	6	8	0.18	<10	27	<1	<10	0.02	2	3	0.27	0.02	0.02	0.02	0.005	<10	<1	<10
CK-S-168	508300	6689550	-50.9140	-29.9246	Lomba Grande	<0.2	<0.5	10	347	<2	7	12	43	0.86	<10	56	<1	<10	0.09	10	15	2.45	0.03	0.09	0.02	0.010	<10	5	<10
CK-S-169	508250	6689800	-50.9145	-29.9224	Lomba Grande	<0.2	<0.5	20	100	<2	8	7	21	0.50	12	29	<1	<10	0.26	4	9	0.82	0.02	0.10	0.05	0.016	<10	1	<10
CK-S-170	506550	6690350	-50.9321	-29.9174	Lomba Grande	<0.2	<0.5	2	81	<2	3	5	12	0.24	<10	19	<1	<10	0.05	2	6	0.74	0.01	0.02	0.03	0.005	<10	1	<10
CK-S-172	503150	6690450	-50.9674	-29.9165	Lomba Grande	<0.2	<0.5	2	48	<2	<1	7	15	0.22	<10	30	<1	<10	0.04	2	3	0.33	0.04	0.04	0.02	0.004	<10	<1	<10
CK-S-173	502950	6690250	-50.9694	-29.9184	Lomba Grande	<0.2	<0.5	4	156	<2	2	9	19	0.34	<10	66	<1	<10	0.06	4	6	0.73	0.03	0.05	0.02	0.006	<10	1	<10
CK-S-174	503200	6691950	-50.9669	-29.9030	Lomba Grande	<0.2	<0.5	2	39	<2	<1	5	14	0.13	<10	23	<1	<10	0.04	1	2	0.27	0.02	0.03	0.01	0.003	<10	<1	<10
CK-S-175	505400	6692600	-50.9441	-29.8971	Lomba Grande	<0.2	<0.5	6	139	<2	6	9	21	0.67	<10	58	<1	<10	0.28	4	12	0.89	0.07	0.14	0.04	0.008	<10	2	<10
CK-S-176	505950	6690700	-50.9384	-29.9143	Lomba Grande	<0.2	<0.5	7	80	<2	9	8	20	0.46	<10	39	<1	<10	0.11	3	14	0.63	0.04	0.10	0.02	0.006	<10	1	<10
CK-S-177	508150	6692950	-50.9156	-29.8940	Lomba Grande	<0.2	<0.5	3	137	<2	2	6	18	0.38	<10	39	<1	<10	0.06	3	6	0.58	0.04	0.05	0.02	0.010	<10	1	<10
CK-S-178	504650	6695800	-50.9519	-29.8683	Lomba Grande	<0.2	<0.5	<1	80	<2	2	5	10	0.32	<10	31	<1	<10	0.04	2	4	0.38	0.04	0.04	0.02	0.006	<10	<1	<10
CK-S-179	507900	6694450	-50.9182	-29.8804	Lomba Grande	<0.2	<0.5	2	178	<2	3	6	14	0.42	<10	41	<1	<10	0.04	3	6	0.44	0.06	0.06	0.02	0.009	<10	1	<10
CK-S-180	506100	6695350	-50.9368	-29.8723	Lomba Grande	<0.2	<0.5	<1	402	<2	3	8	17	0.53	<10	61	<1	<10	0.07	5	7	0.65	0.07	0.07	0.02	0.013	<10	1	<10
CK-S-181	504550	6696400	-50.9529	-29.8628	Lomba Grande	<0.2	<0.5	<1	163	<2	4	7	15	0.45	<10	43	<1	<10	0.06	3	6	0.56	0.10	0.09	0.02	0.010	<10	1	<10
CK-S-182	491600	6698850	-51.0870	-29.8407	Lomba Grande	<0.2	<0.5	10	55	<2	3	14	32	0.28	<10	27	<1	<10	0.05	1	4	0.35	0.03	0.03	0.02	0.005	<10	<1	<10

Geochemical grade assay for stream sediments collected in the Lomba Grande district

(4continuerd/4)

Sample No.	Sr	Ti	V	W	Y	Zr	S
	ppm	%	ppm	ppm	ppm	ppm	%
CK-S-167	3	<0.01	6	<10	2	2	0.003
CK-S-168	8	0.05	66	<10	3	15	0.003
CK-S-169	10	0.03	24	<10	2	6	0.011
CK-S-170	3	0.04	31	<10	1	6	0.002
CK-S-172	3	<0.01	8	<10	2	2	0.003
CK-S-173	6	<0.01	16	<10	3	4	0.005
CK-S-174	3	<0.01	6	<10	1	2	0.002
CK-S-175	12	0.02	23	<10	4	7	0.003
CK-S-176	7	0.02	18	<10	3	4	0.003
CK-S-177	7	0.01	11	<10	3	2	0.005
CK-S-178	6	<0.01	8	<10	3	3	0.003
CK-S-179	7	0.01	9	<10	4	2	0.006
CK-S-180	10	<0.01	10	<10	3	2	0.006
CK-S-181	10	<0.01	7	<10	3	3	0.004
CK-S-182	6	<0.01	8	<10	1	2	0.003

Geochemical grade assay for stream sediments collected in the São Gabriel district

Sample No.	UTM_E	UTM_N	Latitude	Longitude	Location	Ag	Cd	Cu	Mn	Mo	Ni	Pb	Zn	Al	As	Ba	Be	Bi	Ca	Co	Cr	Fe	K	Mg	Na	P	Sb	Sc	Sn
						ppm	ppm	ppm	ppm	ppm	ppm	ppm	ppm	%	ppm	ppm	ppm	ppm	%	ppm	ppm	%	%	%	%	%	ppm	ppm	ppm
SJ-001			-29.80532	-55.78368	São Gabriel	<0.2	<0.5	21	320	<2	11	8	26	0.61	<10	62	<1	<10	0.18	8	10	1.48	0.02	0.08	0.04	0.007	<10	5	<10
SJ-002			-29.57620	-55.98628	São Gabriel	<0.2	<0.5	45	1731	4	22	15	53	2.04	<10	225	1	<10	0.70	44	27	4.19	0.05	0.27	0.08	0.016	<10	15	<10
SJ-003			-29.72000	-55.85834	São Gabriel	<0.2	<0.5	72	1553	3	36	8	65	2.95	<10	262	1	<10	1.11	40	54	4.17	0.05	0.44	0.11	0.006	<10	24	<10
SJ-004			-29.72481	-56.05511	São Gabriel	<0.2	<0.5	69	1823	3	32	12	81	3.22	<10	270	2	<10	1.00	37	45	4.06	0.05	0.42	0.08	0.008	<10	25	<10
SJ-005			-29.81949	-55.77008	São Gabriel	<0.2	<0.5	18	307	<2	11	7	28	0.89	<10	79	<1	<10	0.17	9	11	1.40	0.02	0.09	0.04	0.016	<10	6	<10
SJ-006			-29.97298	-55.74703	São Gabriel	<0.2	<0.5	38	563	3	16	<2	47	1.59	<10	105	<1	<10	0.53	16	19	2.92	0.03	0.23	0.06	0.008	<10	14	<10
SJ-007			-29.95093	-55.59867	São Gabriel	<0.2	<0.5	16	99	3	9	7	26	0.80	<10	56	<1	<10	0.12	5	12	1.18	0.02	0.07	0.03	0.010	<10	5	<10
SJ-008			-30.15953	-55.57694	São Gabriel	<0.2	<0.5	40	569	<2	16	9	56	2.22	<10	216	1	<10	0.50	18	15	3.54	0.04	0.17	0.03	0.026	<10	17	<10
SJ-009			-30.07010	-55.77653	São Gabriel	<0.2	<0.5	61	1433	<2	25	7	68	2.26	<10	221	1	17	0.60	38	25	5.28	0.05	0.32	0.06	0.012	<10	21	<10
SJ-010			-30.02345	-55.86850	São Gabriel	<0.2	<0.5	44	1289	<2	19	6	55	1.85	<10	193	1	<10	0.67	31	23	3.80	0.05	0.27	0.07	0.016	<10	16	<10
SJ-011			-29.92994	-55.86998	São Gabriel	<0.2	<0.5	53	830	5	20	8	58	2.04	<10	169	1	<10	0.80	20	28	4.13	0.03	0.31	0.05	0.011	<10	19	<10
SJ-012			-29.73854	-56.25440	São Gabriel	<0.2	<0.5	53	861	5	25	11	52	2.00	<10	162	<1	<10	1.22	33	32	4.53	0.06	0.46	0.18	0.020	<10	21	<10
SJ-013			-29.78532	-56.36606	São Gabriel	<0.2	<0.5	64	1600	2	25	12	71	2.56	<10	248	1	12	1.00	32	29	4.32	0.06	0.37	0.09	0.022	<10	20	<10
SJ-014			-29.71876	-56.67583	São Gabriel	<0.2	<0.5	85	1631	3	30	11	71	3.09	<10	336	2	<10	1.24	33	35	4.86	0.06	0.48	0.13	0.024	11	23	<10
SJ-015			-29.74362	-56.69124	São Gabriel	<0.2	<0.5	71	1903	4	28	15	77	3.03	<10	369	2	21	0.98	39	26	5.85	0.07	0.44	0.07	0.024	<10	24	<10
SJ-016			-29.91547	-56.04875	São Gabriel	<0.2	<0.5	87	2779	<2	44	3	54	3.34	<10	342	1	16	1.14	55	46	5.15	0.04	0.47	0.17	0.022	<10	22	<10
SJ-017			-30.16495	-55.91664	São Gabriel	<0.2	<0.5	82	1620	<2	34	7	81	3.25	<10	282	2	29	0.89	42	47	6.53	0.07	0.41	0.08	0.016	<10	28	<10
SJ-018			-30.24133	-55.89169	São Gabriel	<0.2	<0.5	73	2431	6	25	16	86	2.56	10	354	2	10	0.94	52	20	6.92	0.08	0.34	0.09	0.031	11	22	<10
SJ-019			-30.61477	-55.93910	São Gabriel	<0.2	<0.5	84	3307	5	33	8	78	2.87	<10	569	2	16	1.03	70	32	6.51	0.06	0.40	0.10	0.021	<10	23	<10
SJ-020			-30.55491	-56.10691	São Gabriel	<0.2	<0.5	58	1056	4	19	8	60	2.16	<10	232	1	<10	0.78	27	19	4.39	0.06	0.38	0.08	0.021	<10	17	<10
SJ-021			-30.49425	-56.20588	São Gabriel	<0.2	<0.5	56	1332	<2	22	4	72	2.31	<10	232	2	11	0.72	26	22	4.66	0.05	0.32	0.04	0.022	<10	22	<10
SJ-022			-30.45125	-56.30272	São Gabriel	<0.2	<0.5	24	717	2	10	9	34	0.93	<10	139	<1	<10	0.20	16	9	2.40	0.02	0.09	0.02	0.014	<10	9	<10
SJ-023			-30.38882	-56.43548	São Gabriel	<0.2	<0.5	63	1461	5	23	11	134	2.23	<10	328	1	20	1.30	34	22	4.01	0.04	0.39	0.11	0.021	<10	14	<10
SJ-024			-30.24397	-56.30597	São Gabriel	<0.2	<0.5	74	1800	6	30	13	94	2.56	<10	257	1	12	1.43	34	38	4.41	0.05	0.40	0.09	0.041	<10	19	<10
SJ-025			-30.62659	-55.68289	São Gabriel	<0.2	<0.5	59	1463	<2	24	7	77	2.83	<10	302	2	21	0.71	35	26	5.84	0.07	0.36	0.04	0.020	<10	26	<10
SJ-026			-30.45639	-55.71204	São Gabriel	<0.2	<0.5	64	1558	4	26	3	72	2.17	<10	257	2	<10	0.68	49	32	5.60	0.04	0.30	0.07	0.018	<10	20	<10
SJ-027			-30.44213	-55.74472	São Gabriel	<0.2	<0.5	84	2615	3	46	<2	77	3.43	<10	361	2	16	1.22	65	65	6.79	0.05	0.44	0.11	0.018	<10	30	<10
SJ-028			-30.87885	-55.85689	São Gabriel	<0.2	<0.5	50	1159	<2	12	14	88	2.55	<10	304	3	24	0.63	32	11	6.69	0.07	0.22	0.03	0.044	<10	24	<10
SJ-029			-30.91931	-55.95766	São Gabriel	<0.2	<0.5	63	1214	<2	17	12	94	2.52	<10	281	3	<10	0.52	33	26	7.80	0.08	0.32	0.04	0.036	<10	25	<10
SJ-030			-30.82867	-55.84183	São Gabriel	<0.2	<0.5	56	1566	2	15	20	112	2.54	<10	452	3	<10	0.62	29	10	5.47	0.08	0.15	0.02	0.063	<10	23	<10
SJ-031			-30.25256	-56.50440	São Gabriel	<0.2	<0.5	51	1116	5	19	13	57	1.98	<10	231	1	<10	0.73	25	27	3.90	0.05	0.33	0.06	0.016	<10	17	<10
SJ-032			-30.19128	-56.53511	São Gabriel	<0.2	<0.5	4	63	<2	3	3	7	0.09	<10	36	<1	<10	0.03	2	1	0.36	<0.01	0.01	0.01	0.003	<10	<1	<10
SJ-033			-30.14058	-56.55071	São Gabriel	<0.2	<0.5	67	1926	3	24	10	72	2.13	<10	273	2	14	0.89	33	30	3.88	0.04	0.33	0.04	0.031	<10	18	<10
SJ-034			-30.12144	-56.42154	São Gabriel	<0.2	<0.5	68	2087	3	30	11	83	2.83	<10	316	2	<10	1.05	35	35	4.68	0.06	0.38	0.06	0.031	<10	22	<10
SJ-035			-30.01502	-56.82671	São Gabriel	<0.2	<0.5	48	1655	2	17	12	59	1.77	<10	320	1	10	0.68	32	16	3.27	0.05	0.26	0.04	0.035	<10	12	<10
SJ-036			-30.08952	-56.76924	São Gabriel	<0.2	<0.5	60	2712	2	30	14	68	2.82	<10	479	2	13	0.87	40	33	4.26	0.06	0.39	0.06	0.018	<10	20	<10
SJ-037			-29.88367	-57.11540	São Gabriel	<0.2	<0.5	59	3329	3	26	20	62	2.48	<10	608	2	<10	0.99	45	21	4.06	0.05	0.34	0.06	0.018	<10	16	<10
SJ-038			-29.75201	-56.99299	São Gabriel	<0.2	<0.5	39	1070	<2	19	11	50	1.75	<10	214	1	<10	0.76	22	22	2.66	0.03	0.25	0.04	0.023	<10	11	<10
SJ-039			-29.65353	-56.89146	São Gabriel	<0.2	<0.5	70	1748	6	30	4	75	3.15	<10	426	2	13	0.94	38	26	4.85	0.06	0.39	0.05	0.019	<10	21	<10
SJ-040			-29.49741	-56.59528	São Gabriel	<0.2	<0.5	37	836	4	22	17	64	2.59	<10	166	1	12	0.73	19	28	3.30	0.06	0.37	0.03	0.009	<10	15	<10
SJ-041			-29.46838	-56.47515	São Gabriel	<0.2	<0.5	67	1461	6	26	11	84	3.11	<10	231	2	11	0.63	21	34	4.88	0.06	0.42	0.05	0.028	<10	25	<10
SJ-042			-29.46535	-56.29649	São Gabriel	<0.2	<0.5	22	920	2	9	6	26	0.62	<10	125	<1	<10	0.24	15	9	1.34	0.02	0.10	0.01	0.011	<10	5	<10
LA-S-001	690295	6836812	-28.58159	-55.05425	São Gabriel	<0.2	<0.5	97	1798	3	21	16	62	1.61	<10	245	2	<10	0.29	46	13	8.67	0.03	0.08	0.02	0.026	<10	26	<10
LA-S-002	698984	6837330	-28.57562	-54.96554	São Gabriel	<0.2	<0.5	130	1553	4	20	12	80	1.93	<10	203	3	<10	0.30	51	8	10.03	0.04	0.10	0.02	0.026	<10	28	<10
LA-S-003	701552	6832278	-28.62079	-54.93841	São Gabriel	<0.2	<0.5	120	1233	<2	24	16	73	2.74	<10	204	2	<10	0.35	42	14	9.81	0.06	0.16	0.03	0.028	<10	30	<10
LA-S-004	646828	6844846	-28.51474	-55.49958	São Gabriel	<0.2	<0.5	94	3764	2	31	18	62	2.16	<10	599	2	17	1.47	82	35	6.85	0.02	0.31	0.05	0.016	<10	21	<10
LA-S-005	683088	6847434	-28.48680	-55.12960	São Gabriel	<0.2	<0.5	34	756	3	10	23	38	0.62	<10	96	<1	<10	0.06	20	17	3.84	<0.01	0.04	0.02	0.004	<10	11	<10
LA-S-006	684412	6849632	-28.46678	-55.11643	São Gabriel	<0.2	<0.5	83	1752	2	25	12	60	2.03	<10	194	2	14	0.28	45	28	7.62	0.02	0.11	0.03	0.022	<10	23	<10
LA-S-007	646303	6857350	-28.40197	-55.50653	São Gabriel	<0.2	<0.5	97	1255	<2	21	21	54	1.19	<10	184	1	14	0.28	32	46	5.75	0.01	0.14	0.03	0.006	<10	16	<10
LA-S-008	644599	6863989	-28.34225	-55.52475	São Gabriel	<0.2	<0.5	111	2729	<2	19	14	54	1.98	<10	235	2	<10	0.24	45	37	7.61	0.02	0.08	0.02	0.026	<10	22	<10
LA-S-009	667090	6865557	-28.32543	-55.29559	São Gabriel	<0.2	<0.5	103	1250	3	25	17	97	0.69	<10	95	1	<10	0.07	35	19	7.48	<0.01	<0.01	0.02	0.008	<10	11	<10
LA-S-010	660981	6880219	-28.19390	-55.35991	São Gabriel	<0.2	<0.5	103	1682	4	39	14	70	2.43	<10	242	2	<10	0.23	50	36	9.11	0.02	0.06	0.03	0.030	<10	29	<10
LA-S-011	666390	6885614	-28.14455	-55.30559	São Gabriel	<0.2	<0.5	64	913	<2	19	8	72	0.74	<10	85	1	<10	0.11	26	14	5.69	0.01	0.05	0.02	0.010	<10	9	<10
LA-S-012	678269	6994800	-28.06012	-55.18607	São Gabriel	<0.2	<0.5	100	1673	4	24	9	71	1.21	<10	241	2	18	0.38	44	24	7.19	0.03	0.16	0.03	0.012	<10	16	<10

Geochemical grade assay for stream sediments collected in the São Gabriel district

Sample No.	Sr	Ti	V	W	Y	Zr	S
	ppm	%	ppm	ppm	ppm	ppm	%
SJ-001	25	0.10	75	<10	6	24	0.009
SJ-002	52	0.08	130	<10	20	36	0.010
SJ-003	94	0.01	34	<10	31	24	0.009
SJ-004	81	<0.01	25	<10	35	24	0.011
SJ-005	16	0.04	57	<10	6	13	0.013
SJ-006	55	0.09	117	<10	16	31	0.009
SJ-007	12	0.04	45	<10	4	13	0.012
SJ-008	33	0.02	106	<10	23	30	0.017
SJ-009	48	0.12	214	<10	26	52	0.012
SJ-010	65	0.13	159	<10	20	66	0.010
SJ-011	51	0.07	168	<10	24	70	0.014
SJ-012	73	0.18	155	<10	16	86	0.005
SJ-013	71	0.14	157	<10	26	53	0.024
SJ-014	81	0.11	179	<10	28	55	0.026
SJ-015	64	0.11	219	<10	30	66	0.023
SJ-016	59	0.11	196	<10	19	60	0.029
SJ-017	87	0.16	273	<10	35	75	0.017
SJ-018	76	0.20	353	<10	30	81	0.029
SJ-019	106	0.18	307	<10	31	78	0.027
SJ-020	70	0.13	181	<10	23	73	0.017
SJ-021	47	0.09	182	<10	31	56	0.021
SJ-022	16	0.04	102	<10	15	29	0.019
SJ-023	42	0.09	158	<10	19	58	0.022
SJ-024	72	0.10	169	<10	28	46	0.072
SJ-025	129	0.17	258	<10	38	76	0.022
SJ-026	102	0.24	316	<10	23	87	0.011
SJ-027	98	0.18	302	<10	24	88	0.017
SJ-028	84	0.24	300	<10	49	77	0.043
SJ-029	58	0.34	380	<10	39	97	0.015
SJ-030	60	0.19	258	<10	67	49	0.066
SJ-031	46	0.11	171	<10	24	47	0.021
SJ-032	2	<0.01	14	<10	2	4	0.003
SJ-033	50	0.05	154	<10	27	42	0.033
SJ-034	59	0.09	179	<10	30	46	0.037
SJ-035	50	0.09	125	<10	22	42	0.023
SJ-036	60	0.11	170	<10	30	49	0.025
SJ-037	60	0.12	170	<10	24	70	0.027
SJ-038	34	0.07	107	<10	15	31	0.032
SJ-039	56	0.13	190	<10	26	74	0.021
SJ-040	36	0.07	106	<10	16	59	0.015
SJ-041	42	0.05	159	<10	36	46	0.024
SJ-042	14	<0.01	57	<10	10	15	0.014
LA-S-001	25	0.19	406	<10	45	86	0.012
LA-S-002	23	0.37	547	<10	38	112	0.014
LA-S-003	30	0.31	469	<10	34	121	0.010
LA-S-004	71	0.29	340	<10	40	82	0.007
LA-S-005	6	0.49	201	<10	10	75	0.006
LA-S-006	23	0.30	333	<10	25	90	0.010
LA-S-007	23	0.42	300	<10	20	80	0.005
LA-S-008	19	0.17	330	<10	22	74	0.014
LA-S-009	7	0.54	638	<10	8	91	0.004
LA-S-010	25	0.33	420	<10	32	91	0.012
LA-S-011	8	0.39	485	<10	8	73	0.005
LA-S-012	28	0.35	499	<10	21	96	0.005

Geochemical grade assay for stream sediments collected in the São Gabriel district

Sample No.	UTM_E	UTM_N	Latitude	Longitude	Location	Ag	Cd	Cu	Mn	Mo	Ni	Pb	Zn	Al	As	Ba	Be	Bi	Ca	Co	Cr	Fe	K	Mg	Na	P	Sb	Sc	Sn
						ppm	ppm	ppm	ppm	ppm	ppm	ppm	ppm	%	ppm	ppm	ppm	ppm	%	ppm	ppm	%	%	%	%	%	ppm	ppm	ppm
LA-S-013	678715	6865756	-28.32210	-55.17709	São Gabriel	<0.2	<0.5	105	1926	4	26	14	61	2.61	<10	231	2	12	0.38	44	26	7.95	0.02	0.11	0.03	0.025	<10	32	<10
LA-S-014	670601	6875187	-28.23809	-55.26120	São Gabriel	<0.2	<0.5	61	1075	3	21	9	49	1.90	<10	141	1	19	0.26	32	19	5.62	0.03	0.12	0.03	0.015	<10	17	<10
LA-S-015	692292	6888533	-28.11470	-55.04242	São Gabriel	<0.2	<0.5	105	1142	<2	23	12	60	1.46	<10	182	1	10	0.21	30	34	6.48	0.02	0.10	0.03	0.010	<10	15	<10
LA-S-016	704910	6897978	-28.02760	-54.91568	São Gabriel	<0.2	<0.5	168	1434	2	37	5	94	2.70	<10	267	2	<10	0.47	41	52	9.23	0.05	0.25	0.05	0.028	<10	24	<10
LA-S-017	707321	6898486	-28.02264	-54.89125	São Gabriel	<0.2	<0.5	145	1739	3	34	15	84	2.76	<10	245	2	15	0.31	50	45	9.41	0.04	0.14	0.03	0.028	<10	28	<10
LA-S-018	710181	6886946	-28.12629	-54.86012	São Gabriel	<0.2	<0.5	183	1489	4	42	6	105	2.69	12	249	2	<10	0.28	43	57	11.26	0.04	0.12	0.03	0.025	<10	30	<10
LA-S-019	698640	6893994	-28.06449	-54.97875	São Gabriel	<0.2	<0.5	110	2050	<2	25	10	65	2.93	<10	252	2	<10	0.27	38	21	7.84	0.03	0.13	0.03	0.013	<10	36	<10
LA-S-020	717359	6893424	-28.06670	-54.78828	São Gabriel	<0.2	<0.5	125	1542	5	30	9	92	2.22	<10	221	2	<10	0.26	41	43	8.92	0.03	0.09	0.03	0.025	<10	23	<10
LA-S-021	720613	6893845	-28.06236	-54.75527	São Gabriel	<0.2	<0.5	186	1557	<2	46	9	90	2.61	<10	227	2	<10	0.47	46	63	9.90	0.03	0.25	0.05	0.020	<10	29	<10
LA-S-022	732160	6895270	-28.04754	-54.63814	São Gabriel	<0.2	<0.5	249	1626	4	45	7	105	1.91	11	202	2	<10	0.35	49	56	12.01	0.03	0.18	0.04	0.016	<10	26	<10
LA-S-023	738718	6895599	-28.04341	-54.57154	São Gabriel	<0.2	<0.5	203	1814	<2	43	13	83	2.91	11	219	2	29	0.31	53	57	12.35	0.04	0.09	0.03	0.024	15	41	<10
LA-S-024	741162	6889130	-28.10131	-54.54537	São Gabriel	<0.2	<0.5	227	1939	<2	44	12	100	2.54	<10	231	2	<10	0.24	57	74	13.78	0.03	0.07	0.03	0.025	16	35	<10
LA-S-025	726450	6872786	-28.25133	-54.69184	São Gabriel	<0.2	<0.5	97	1503	<2	32	6	60	2.44	<10	129	2	<10	0.08	36	32	8.67	0.02	0.06	0.03	0.024	<10	23	<10
LA-S-026	713768	6871981	-28.26071	-54.82088	São Gabriel	<0.2	<0.5	82	1096	<2	25	20	71	2.25	<10	223	2	<10	0.19	37	20	8.91	0.02	0.04	0.03	0.029	<10	25	<10
LA-S-027	727067	6855844	-28.40403	-54.68224	São Gabriel	<0.2	<0.5	122	1709	<2	35	11	75	2.53	<10	226	2	<10	0.31	52	27	9.63	0.02	0.09	0.03	0.032	<10	35	<10
LA-S-028	734611	6830270	-28.63334	-54.60007	São Gabriel	<0.2	<0.5	137	1613	<2	41	12	89	2.46	<10	271	2	<10	0.45	45	54	8.90	0.03	0.18	0.03	0.033	20	31	<10
LA-S-029	724366	6836447	-28.57944	-54.70601	São Gabriel	<0.2	<0.5	95	1244	<2	27	11	61	1.04	<10	196	1	<10	0.20	36	27	6.27	0.02	0.08	0.03	0.010	<10	15	<10
LA-S-030	714120	6838077	-28.56647	-54.81101	São Gabriel	<0.2	<0.5	99	1116	<2	32	12	70	1.61	<10	182	2	<10	0.25	37	33	8.80	0.02	0.10	0.03	0.014	<10	23	<10
LA-S-031	729830	6881020	-28.17647	-54.65904	São Gabriel	<0.2	<0.5	102	701	<2	23	15	74	0.75	<10	109	1	<10	0.16	31	21	7.56	0.01	0.05	0.03	0.014	15	11	<10
LA-S-032	742237	6821786	-28.70844	-54.52032	São Gabriel	<0.2	<0.5	226	1219	<2	46	21	121	1.38	<10	161	2	<10	0.17	42	74	10.28	0.01	0.05	0.02	0.025	<10	23	<10
LA-S-033	741963	6803978	-28.86908	-54.51932	São Gabriel	<0.2	<0.5	151	1101	<2	27	16	116	0.62	<10	98	2	29	0.12	40	17	10.64	<0.01	0.02	0.02	0.010	<10	15	<10
LA-S-034	752853	6818595	-28.73518	-54.41103	São Gabriel	<0.2	<0.5	145	1864	<2	35	12	85	1.59	<10	269	2	25	0.37	55	57	9.09	0.03	0.11	0.03	0.027	<10	22	<10
LA-S-035	759587	6812089	-28.79250	-54.34065	São Gabriel	<0.2	<0.5	121	1627	<2	34	10	80	2.20	<10	286	2	<10	0.53	48	40	8.95	0.04	0.22	0.03	0.022	<10	28	<10
LA-S-036	756246	6823024	-28.69458	-54.37732	São Gabriel	<0.2	<0.5	140	1452	<2	36	12	73	2.35	<10	230	2	16	0.31	38	52	8.94	0.03	0.12	0.03	0.025	<10	28	<10
LA-S-037	758759	6825844	-28.66865	-54.35226	São Gabriel	<0.2	<0.5	104	1002	<2	25	7	60	1.29	<10	135	1	<10	0.19	27	36	6.31	0.02	0.08	0.02	0.014	<10	16	<10
LA-S-038	766999	6844085	-28.50251	-54.27227	São Gabriel	<0.2	<0.5	135	1878	<2	34	16	82	2.08	<10	251	2	<10	0.35	50	53	9.72	0.03	0.11	0.02	0.036	<10	29	<10
LA-S-039	751743	6831213	-28.62162	-54.42517	São Gabriel	<0.2	<0.5	182	1796	<2	40	18	89	2.39	<10	287	2	<10	0.39	55	66	10.29	0.03	0.16	0.03	0.025	16	32	<10
LA-S-040	740823	6861566	-28.34996	-54.54312	São Gabriel	<0.2	<0.5	239	1772	<2	52	20	137	1.25	<10	207	2	19	0.25	51	71	11.41	0.02	0.11	0.03	0.014	19	19	<10
LA-S-041	741185	6855620	-28.40352	-54.53820	São Gabriel	<0.2	<0.5	262	1756	<2	50	15	129	1.83	<10	234	2	<10	0.32	56	76	12.14	0.02	0.14	0.03	0.021	31	27	<10
LA-S-042	749813	6856306	-28.39571	-54.45035	São Gabriel	<0.2	<0.5	152	1649	<2	35	20	82	2.09	<10	244	2	12	0.28	48	59	10.31	0.03	0.09	0.02	0.031	<10	31	<10
LA-S-043	756998	6856119	-28.39601	-54.37704	São Gabriel	<0.2	<0.5	168	1637	<2	41	13	85	2.10	<10	249	2	<10	0.31	50	69	11.20	0.03	0.10	0.02	0.030	14	32	<10
LA-S-044	764067	6854714	-28.40727	-54.30463	São Gabriel	<0.2	<0.5	116	1253	<2	29	11	73	1.52	<10	233	2	<10	0.32	39	42	7.74	0.03	0.11	0.02	0.037	<10	24	<10
LA-S-045	780758	6827138	-28.65240	-54.12770	São Gabriel	<0.2	0.6	274	1369	<2	41	24	132	1.57	<10	264	2	33	0.26	45	74	11.49	0.02	0.15	0.02	0.037	<10	27	<10
LA-S-046	779947	6825929	-28.66347	-54.13569	São Gabriel	<0.2	0.5	151	2025	<2	37	39	105	1.94	<10	323	2	<10	0.34	55	53	8.59	0.03	0.17	0.02	0.038	<10	25	<10
LA-S-047	784150	6834740	-28.58312	-54.09492	São Gabriel	<0.2	<0.5	193	1077	2	37	23	122	1.37	<10	182	2	22	0.20	37	57	8.79	0.02	0.09	0.02	0.026	<10	19	<10
LA-S-048	775631	6858111	-28.37426	-54.18752	São Gabriel	<0.2	<0.5	238	1828	<2	50	20	130	2.61	<10	236	2	24	0.24	51	94	11.81	0.03	0.07	0.02	0.039	11	34	<10
LA-S-049	783240	6858348	-28.37050	-54.11002	São Gabriel	<0.2	<0.5	243	2799	<2	57	30	130	2.63	<10	288	2	<10	0.28	71	90	11.91	0.04	0.11	0.02	0.037	13	30	<10
LA-S-050	790826	6856768	-28.38308	-54.03230	São Gabriel	<0.2	<0.5	267	1473	<2	48	17	153	2.00	<10	214	2	14	0.26	50	68	11.72	0.03	0.11	0.02	0.029	<10	27	<10
LA-S-051	774040	6870330	-28.26442	-54.20662	São Gabriel	<0.2	<0.5	240	1576	<2	41	27	120	2.84	<10	245	2	18	0.26	40	52	11.05	0.03	0.11	0.02	0.042	<10	35	<10
LA-S-052	782936	6872300	-28.24478	-54.11651	São Gabriel	<0.2	<0.5	175	2206	<2	40	24	121	2.67	<10	382	2	<10	0.43	62	70	10.93	0.04	0.15	0.02	0.041	<10	33	<10
LA-S-053	769730	6868957	-28.27769	-54.25019	São Gabriel	<0.2	<0.5	221	3032	2	33	28	127	1.58	<10	571	2	27	0.29	65	68	12.02	0.02	0.06	0.02	0.045	11	23	<10
LA-S-054	772445	6897766	-28.01738	-54.22924	São Gabriel	<0.2	<0.5	112	1244	<2	34	20	87	2.01	<10	204	2	14	0.26	35	63	10.69	0.01	0.02	0.01	0.046	<10	36	<10
LA-S-055	778410	6900530	-27.99122	-54.16929	São Gabriel	<0.2	<0.5	264	1626	<2	42	12	130	1.54	<10	196	2	25	0.18	52	55	12.37	0.01	0.03	0.01	0.025	<10	28	<10
LA-S-056	762574	6882315	-28.15869	-54.32609	São Gabriel	<0.2	<0.5	211	1653	<2	40	26	133	1.87	<10	231	2	13	0.30	50	60	11.66	0.02	0.10	0.02	0.030	<10	31	<10
LA-S-057	751767	6868237	-28.28775	-54.43301	São Gabriel	<0.2	<0.5	328	2286	<2	51	21	155	1.64	<10	251	2	<10	0.33	62	67	12.90	0.03	0.14	0.02	0.020	<10	24	<10
LA-S-058	743601	6871091	-28.26355	-54.51680	São Gabriel	<0.2	<0.5	236	1896	<2	53	12	125	2.49	<10	361	2	<10	0.49	52	69	10.67	0.04	0.25	0.03	0.028	<10	27	<10
LA-S-059	711520	6925944	-27.77428	-54.85346	São Gabriel	<0.2	<0.5	243	1371	<2	61	7	125	2.31	<10	306	2	15	0.50	41	67	9.83	0.06	0.33	0.05	0.042	<10	20	<10
LA-S-060	689954	6910597	-27.91597	-55.06976	São Gabriel	<0.2	<0.5	242	1737	<2	58	26	129	2.04	<10	311	2	<10	0.53	50	60	10.74	0.05	0.30	0.05	0.027	<10	20	<10
LA-S-061	713891	6902733	-27.98329	-54.82524	São Gabriel	<0.2	<0.5	184	1782	<2	45	20	113	2.86	<10	385	2	<10	0.58	52	66	9.73	0.05	0.30	0.04	0.036	<10	27	<10
LA-S-062	731607	6910134	-27.91357	-54.64667	São Gabriel	<0.2	<0.5	240	1796	<2	44	23	122	2.75	<10	281	2	13	0.32	55	59	11.91	0.05	0.15	0.02	0.032	<10	35	<10
LA-S-063	741277	6910411	-27.90936	-54.54855	São Gabriel	<0.2	<0.5	300	1582	<2	42	33	143	1.67	<10	208	2	29	0.23	51	65	12.96	0.02	0.07	0.02	0.021	<10	28	<10
LA-S-064	734222	6926491	-27.76558	-54.62334	São Gabriel	<0.2	<0.5	169	1858	4	44	21	107	2.39	<10	318	2	<10	0.39	63	62	10.25	0.04	0.17	0.03	0.045	<10	32	<10
LA-S-065	743344	6941004	-27.63306	-54.53379	São Gabriel	<0.2	<0.5	166	1855	<2	53	12	96	2.42	<10	312	2	<10	0.55	47	73	8.24	0.03	0.36	0.02	0.038	<10	29	<10
LA-S-066	710112	6934811	-27.69451	-54.86930	São Gabriel	<0.2	<0.5	174	1342	<2	50	13	101	1.62	<10	226	2	11	0.41	40	43	9.88	0.03	0.21	0.03	0.030	<10	21	<10

Geochemical grade assay for stream sediments collected in the São Gabriel district

(2continued/7)

Sample No.	Sr	Ti	V	W	Y	Zr	S
	ppm	%	ppm	ppm	ppm	ppm	%
LA-S-013	29	0.15	296	<10	37	70	0.025
LA-S-014	18	0.16	256	<10	16	62	0.008
LA-S-015	19	0.36	366	<10	13	72	0.006
LA-S-016	39	0.29	400	<10	25	82	0.014
LA-S-017	26	0.28	416	<10	25	84	0.012
LA-S-018	22	0.39	623	<10	24	101	0.011
LA-S-019	24	0.22	305	<10	55	85	0.011
LA-S-020	23	0.37	476	<10	24	82	0.013
LA-S-021	40	0.41	487	<10	27	103	0.011
LA-S-022	29	0.69	830	<10	19	138	0.009
LA-S-023	24	0.45	603	<10	27	114	0.012
LA-S-024	18	0.50	730	<10	24	118	0.010
LA-S-025	11	0.28	343	<10	20	79	0.005
LA-S-026	18	0.21	335	<10	23	75	0.012
LA-S-027	22	0.22	431	<10	36	80	0.024
LA-S-028	42	0.28	374	<10	36	73	0.013
LA-S-029	20	0.38	350	<10	16	68	0.004
LA-S-030	19	0.38	478	<10	23	84	0.008
LA-S-031	12	0.44	590	<10	12	80	0.006
LA-S-032	15	0.81	696	<10	17	101	0.010
LA-S-033	11	0.66	952	<10	12	114	0.005
LA-S-034	48	0.44	499	<10	24	97	0.009
LA-S-035	72	0.37	465	<10	33	104	0.011
LA-S-036	43	0.37	426	<10	27	100	0.010
LA-S-037	16	0.35	365	<10	15	73	0.008
LA-S-038	29	0.28	418	<10	29	88	0.014
LA-S-039	44	0.38	513	<10	43	106	0.012
LA-S-040	29	1.08	859	<10	17	130	0.007
LA-S-041	30	0.88	791	<10	24	138	0.009
LA-S-042	25	0.36	492	<10	27	99	0.014
LA-S-043	32	0.44	532	<10	28	109	0.012
LA-S-044	26	0.30	350	<10	24	99	0.015
LA-S-045	17	0.48	765	<10	29	149	0.006
LA-S-046	30	0.39	486	<10	30	112	0.012
LA-S-047	16	0.66	626	<10	15	128	0.009
LA-S-048	19	0.68	703	<10	21	143	0.015
LA-S-049	25	0.60	754	<10	21	135	0.014
LA-S-050	19	0.91	805	<10	20	155	0.011
LA-S-051	15	0.66	639	<10	22	126	0.013
LA-S-052	31	0.40	571	<10	35	124	0.013
LA-S-053	20	0.49	680	15	23	118	0.009
LA-S-054	17	0.24	547	<10	30	132	0.013
LA-S-055	13	0.57	855	<10	19	146	0.013
LA-S-056	21	0.57	728	<10	25	139	0.014
LA-S-057	25	0.81	947	<10	17	158	0.009
LA-S-058	38	0.61	672	<10	24	141	0.011
LA-S-059	31	0.51	669	<10	15	111	0.012
LA-S-060	40	0.48	755	<10	19	132	0.012
LA-S-061	48	0.46	530	<10	28	124	0.013
LA-S-062	24	0.53	657	<10	27	145	0.012
LA-S-063	17	0.93	934	<10	21	155	0.010
LA-S-064	26	0.34	510	<10	32	106	0.013
LA-S-065	36	0.29	398	<10	25	102	0.029
LA-S-066	24	0.35	678	<10	20	105	0.014

Geochemical grade assay for stream sediments collected in the São Gabriel district

Sample No.	UTM_E	UTM_N	Latitude	Longitude	Location	Ag	Cd	Cu	Mn	Mo	Ni	Pb	Zn	Al	As	Ba	Be	Bi	Ca	Co	Cr	Fe	K	Mg	Na	P	Sb	Sc	Sn
						ppm	ppm	ppm	ppm	ppm	ppm	ppm	ppm	%	ppm	ppm	ppm	ppm	%	ppm	ppm	%	%	%	%	%	ppm	ppm	ppm
LA-S-067	711278	6933431	-27.70678	-54.85724	São Gabriel	<0.2	<0.5	203	1666	<2	42	19	108	2.32	<10	279	2	17	0.49	53	56	10.39	0.04	0.25	0.04	0.040	<10	27	<10
LA-S-068	705163	6921590	-27.81455	-54.91719	São Gabriel	<0.2	<0.5	219	2737	<2	51	18	120	2.36	<10	416	2	<10	0.53	77	67	10.25	0.05	0.29	0.04	0.037	<10	25	<10
LA-S-069	698840	6911486	-27.90666	-54.97966	São Gabriel	<0.2	<0.5	237	4116	<2	78	20	97	4.15	17	745	3	24	0.51	127	117	12.64	0.07	0.21	0.03	0.055	12	38	<10
LA-S-070	760476	6924632	-27.77751	-54.35675	São Gabriel	<0.2	<0.5	247	1460	<2	57	29	120	3.45	<10	226	2	<10	0.25	49	85	12.95	0.04	0.09	0.02	0.032	<10	38	<10
LA-S-071	759730	6924498	-27.77886	-54.36429	São Gabriel	<0.2	<0.5	255	1705	<2	61	22	147	3.16	<10	296	2	<10	0.32	62	87	14.07	0.04	0.15	0.03	0.032	<10	36	<10
LA-S-072	760607	6913856	-27.87466	-54.35307	São Gabriel	<0.2	<0.5	300	1664	<2	54	23	139	3.01	<10	272	2	<10	0.28	57	75	13.96	0.05	0.13	0.03	0.029	<10	34	<10
LA-S-073	766473	6912307	-27.88747	-54.29319	São Gabriel	<0.2	<0.5	367	1726	<2	75	21	210	1.55	<10	160	3	33	0.16	63	83	18.49	0.02	0.03	0.02	0.014	<10	24	<10
LA-S-074	781780	6918283	-27.83045	-54.13928	São Gabriel	<0.2	<0.5	215	1594	<2	57	14	139	2.88	<10	307	2	11	0.40	50	81	10.93	0.04	0.23	0.04	0.029	<10	33	<10
LA-S-075	781549	6929161	-27.73242	-54.14419	São Gabriel	<0.2	<0.5	254	1751	<2	65	11	140	3.14	<10	332	2	<10	0.48	57	77	12.78	0.05	0.28	0.04	0.040	<10	34	<10
LA-S-076	781636	6939138	-27.64244	-54.14565	São Gabriel	<0.2	<0.5	221	1848	<2	56	19	133	2.70	<10	340	2	11	0.41	56	83	11.45	0.05	0.22	0.03	0.039	<10	31	<10
LA-S-077	776860	6943227	-27.60656	-54.19494	São Gabriel	<0.2	<0.5	323	1883	<2	76	24	211	1.97	<10	286	2	21	0.35	61	101	14.42	0.03	0.19	0.03	0.030	<10	24	<10
LA-S-078	786963	6944986	-27.58860	-54.09311	São Gabriel	<0.2	<0.5	346	1767	<2	66	14	181	2.21	<10	234	2	30	0.28	55	68	15.94	0.04	0.12	0.03	0.028	<10	29	<10
LA-S-079	773423	6952723	-27.52163	-54.23188	São Gabriel	<0.2	<0.5	430	2248	<2	87	18	270	1.85	<10	273	3	21	0.29	70	125	19.20	0.03	0.12	0.05	0.022	<10	21	<10
LA-S-080	757496	6943709	-27.60604	-54.39106	São Gabriel	<0.2	<0.5	306	1963	<2	56	29	142	3.13	<10	247	2	10	0.31	61	79	14.75	0.04	0.12	0.03	0.035	12	36	<10
LA-S-081	729619	6940494	-27.64006	-54.67270	São Gabriel	<0.2	<0.5	231	2130	<2	53	22	131	3.29	<10	342	2	13	0.45	64	69	12.18	0.05	0.20	0.05	0.044	<10	36	<10
LA-S-082	786279	6976058	-27.30858	-54.10735	São Gabriel	<0.2	<0.5	305	2192	<2	65	24	163	3.03	<10	367	2	21	0.49	67	67	14.00	0.07	0.29	0.05	0.042	<10	29	<10
LA-S-083	780134	6966659	-27.39461	-54.16722	São Gabriel	<0.2	<0.5	289	1852	<2	60	10	147	3.65	<10	331	2	27	0.47	57	80	13.48	0.06	0.26	0.05	0.045	<10	36	<10
LA-S-084	779126	6963307	-27.42504	-54.17664	São Gabriel	<0.2	<0.5	267	2170	4	67	11	134	2.84	14	304	2	18	0.43	68	93	14.28	0.05	0.25	0.04	0.044	<10	30	<10
LA-S-085	764980	6956491	-27.48933	-54.31811	São Gabriel	<0.2	<0.5	293	1656	5	67	16	145	1.71	16	174	3	20	0.21	59	88	16.40	0.03	0.12	0.03	0.019	<10	21	<10
LA-S-086	752217	6957031	-27.48689	-54.44729	São Gabriel	<0.2	<0.5	331	2115	4	70	11	129	2.78	11	277	3	22	0.19	67	119	16.30	0.03	0.09	0.03	0.026	<10	31	<10
LA-S-087	749799	6954311	-27.51187	-54.47118	São Gabriel	<0.2	<0.5	342	1559	6	78	12	137	2.60	<10	206	2	17	0.49	57	93	14.02	0.04	0.33	0.06	0.033	<10	24	<10
LA-S-088	216075	6764591	-29.21552	-53.92045	São Gabriel	<0.2	<0.5	8	808	<2	4	20	32	0.74	11	223	2	<10	0.10	7	4	2.48	0.02	0.04	0.03	0.026	<10	5	<10
LA-S-089	213641	6776632	-29.10644	-53.94236	São Gabriel	<0.2	<0.5	10	145	<2	5	12	12	0.39	<10	53	<1	<10	0.05	3	5	0.78	0.01	0.02	0.03	0.006	<10	2	<10
LA-S-090	231349	6782842	-29.05432	-53.75909	São Gabriel	<0.2	<0.5	7	321	<2	4	10	17	0.63	<10	97	<1	<10	0.06	5	6	0.92	0.02	0.04	0.03	0.011	<10	3	<10
LA-S-091	255640	6785915	-29.03151	-53.50916	São Gabriel	<0.2	<0.5	28	372	<2	9	12	38	0.98	<10	86	<1	<10	0.06	10	10	2.77	0.02	0.05	0.03	0.012	<10	6	<10
LA-S-092	275942	6788421	-29.01264	-53.30033	São Gabriel	<0.2	<0.5	25	310	<2	7	10	32	0.86	<10	65	<1	<10	0.04	8	8	2.34	0.01	0.03	0.02	0.010	<10	5	<10
LA-S-093	242100	6776568	-29.11311	-53.65023	São Gabriel	<0.2	<0.5	17	437	<2	6	13	32	0.76	<10	135	2	<10	0.12	9	5	1.94	0.02	0.07	0.03	0.021	<10	5	<10
LA-S-094	215895	6755411	-29.29823	-53.92465	São Gabriel	<0.2	<0.5	9	817	<2	4	24	36	0.72	<10	241	2	<10	0.17	6	4	2.37	0.03	0.06	0.02	0.024	<10	5	<10
LA-S-095	221698	6746389	-29.38085	-53.86725	São Gabriel	<0.2	<0.5	13	544	<2	6	25	34	0.81	<10	213	2	<10	0.18	5	5	2.22	0.03	0.06	0.02	0.025	<10	6	<10
LA-S-096	244353	6753835	-29.31853	-53.63233	São Gabriel	<0.2	<0.5	8	229	<2	4	7	17	0.36	<10	72	<1	<10	0.06	5	3	0.96	0.01	0.03	0.02	0.011	<10	3	<10
LA-S-097	260324	6762303	-29.24532	-53.46618	São Gabriel	<0.2	<0.5	5	91	<2	3	5	8	0.25	<10	42	<1	<10	0.04	2	2	0.42	<0.01	0.02	0.02	0.006	<10	1	<10
LA-S-098	277190	6758656	-29.28129	-53.29349	São Gabriel	<0.2	<0.5	25	471	<2	6	11	42	0.50	<10	96	1	<10	0.08	10	4	3.70	0.02	0.05	0.02	0.010	<10	5	<10
LA-S-099	275095	6739850	-29.45051	-53.31888	São Gabriel	<0.2	<0.5	43	984	<2	9	22	88	1.54	<10	265	2	<10	0.32	17	7	5.81	0.07	0.18	0.03	0.029	<10	11	<10
LA-S-100	251473	6735511	-29.48517	-53.56322	São Gabriel	<0.2	<0.5	49	702	<2	13	19	64	1.08	<10	213	2	<10	0.35	16	9	4.09	0.05	0.18	0.04	0.024	<10	8	<10
LA-S-101	222594	6725312	-29.57104	-53.86337	São Gabriel	<0.2	<0.5	43	935	<2	13	14	56	1.49	<10	273	2	<10	0.46	17	11	4.37	0.05	0.22	0.06	0.032	<10	12	<10
LA-S-102	242605	6710415	-29.70963	-53.66054	São Gabriel	<0.2	<0.5	18	637	3	8	13	39	0.83	<10	155	1	<10	0.23	10	4	2.13	0.05	0.10	0.02	0.026	<10	6	<10
LA-S-103	267330	6709300	-29.72457	-53.40541	São Gabriel	<0.2	<0.5	7	176	<2	5	9	16	0.43	<10	71	<1	<10	0.11	3	3	0.95	0.04	0.06	0.02	0.010	<10	2	<10
LA-S-104	232103	6698853	-29.81163	-53.77186	São Gabriel	<0.2	<0.5	4	66	<2	4	4	9	0.29	<10	50	<1	<10	0.07	2	3	0.31	0.02	0.03	0.02	0.006	<10	<1	<10
LA-S-105	233879	6684973	-29.93713	-53.75694	São Gabriel	<0.2	<0.5	4	151	<2	3	5	8	0.16	<10	51	<1	<10	0.05	2	3	0.26	0.01	0.02	0.02	0.006	<10	<1	<10
LA-S-106	217670	6678987	-29.98746	-53.92627	São Gabriel	<0.2	<0.5	8	58	<2	5	12	13	0.19	<10	49	<1	<10	0.07	<1	4	0.21	0.02	0.02	0.01	0.007	<10	<1	<10
LA-S-107	259186	6725412	-29.57774	-53.48596	São Gabriel	<0.2	<0.5	16	225	<2	6	9	26	0.41	<10	80	<1	<10	0.13	5	3	1.60	0.04	0.07	0.02	0.011	<10	3	<10
LA-S-108	278621	6727272	-29.56457	-53.28509	São Gabriel	<0.2	<0.5	75	738	2	19	12	90	0.90	<10	137	1	<10	0.29	22	14	5.66	0.05	0.17	0.03	0.020	<10	8	<10
LA-S-109	290746	6708611	-29.73496	-53.16361	São Gabriel	<0.2	<0.5	15	229	<2	6	6	23	0.37	<10	54	<1	<10	0.07	6	4	1.48	0.04	0.06	0.02	0.007	<10	3	<10
LA-S-110	301036	6707126	-29.75005	-53.05755	São Gabriel	<0.2	<0.5	14	224	<2	7	6	21	0.50	<10	63	<1	<10	0.13	6	5	1.24	0.05	0.09	0.02	0.008	<10	3	<10
LA-S-111	311020	6713832	-29.69113	-52.95318	São Gabriel	<0.2	<0.5	26	295	<2	12	15	30	0.59	<10	68	<1	<10	0.19	7	7	1.63	0.06	0.11	0.03	0.010	<10	4	<10
LA-S-112	313087	6716353	-29.66870	-52.93139	São Gabriel	<0.2	<0.5	37	455	<2	15	9	50	0.72	<10	108	<1	<10	0.32	13	11	3.36	0.05	0.17	0.04	0.015	<10	5	<10
LA-S-113	313482	6715898	-29.67287	-52.92739	São Gabriel	<0.2	<0.5	34	757	2	16	9	39	0.99	<10	138	<1	<10	0.30	20	13	2.74	0.06	0.19	0.03	0.016	<10	7	<10
LA-S-114	344940	6713105	-29.70239	-52.60284	São Gabriel	<0.2	<0.5	33	537	<2	20	6	44	0.68	<10	122	<1	<10	0.25	18	20	3.32	0.04	0.15	0.03	0.011	<10	5	<10
LA-S-115	325014	6722680	-29.61337	-52.80718	São Gabriel	<0.2	<0.5	54	602	<2	22	7	61	0.61	<10	98	<1	<10	0.29	20	19	4.00	0.04	0.17	0.03	0.013	<10	6	<10
LA-S-116	325582	6728406	-29.56180	-52.80040	São Gabriel	<0.2	<0.5	65	939	3	24	19	81	1.66	<10	394	3	<10	0.59	25	21	5.25	0.08	0.31	0.04	0.046	<10	13	<10
LA-S-117	326706	6727414	-29.57090	-52.78896	São Gabriel	<0.2	<0.5	90	1309	2	32	13	97	2.01	12	286	3	<10	0.57	37	28	7.42	0.07	0.34	0.04	0.040	<10	18	<10
LA-S-118	348397	6739148	-29.46787	-52.56349	São Gabriel	<0.2	<0.5	69	1147	4	37	14	91	1.99	<10	280	2	<10	0.63	34	33	7.86	0.09	0.35	0.06	0.031	<10	15	<10
LA-S-119	348821	6745112	-29.41411	-52.55829	São Gabriel	<0.2	<0.5	57	971	3	20	14	83	1.38	<10	209	2	11	0.27	28	14	7.16	0.05	0.17	0.03	0.025	<10	11	<10
LA-S-120	348897	6745095	-29.41427	-52.55751	São Gabriel	<0.2	<0.5	59	994	3	21	16	100	1.14	<10	189	2	<10	0.26	26	24	8.65	0.05	0.18	0.03	0.017	<10	11	<10

Geochemical grade assay for stream sediments collected in the São Gabriel district

Sample No.	Sr	Ti	V	W	Y	Zr	S
	ppm	%	ppm	ppm	ppm	ppm	%
LA-S-067	31	0.40	604	<10	25	122	0.014
LA-S-068	42	0.51	611	<10	26	132	0.012
LA-S-069	42	0.37	596	<10	32	136	0.023
LA-S-070	17	0.58	756	<10	23	147	0.011
LA-S-071	23	0.65	871	<10	25	156	0.013
LA-S-072	19	0.69	908	<10	21	160	0.009
LA-S-073	12	1.03	1624	<10	15	187	0.009
LA-S-074	30	0.53	643	<10	30	126	0.013
LA-S-075	34	0.59	775	<10	25	146	0.015
LA-S-076	30	0.54	704	<10	26	124	0.014
LA-S-077	25	0.89	1208	<10	18	160	0.009
LA-S-078	20	0.82	1194	<10	19	169	0.011
LA-S-079	21	1.15	1660	<10	15	184	0.010
LA-S-080	22	0.61	869	<10	26	149	0.012
LA-S-081	28	0.44	636	<10	30	117	0.016
LA-S-082	38	0.58	823	<10	19	133	0.017
LA-S-083	33	0.54	701	<10	25	137	0.015
LA-S-084	28	0.51	860	<10	18	97	0.019
LA-S-085	16	0.73	1216	<10	12	100	0.005
LA-S-086	17	0.64	968	<10	14	95	0.010
LA-S-087	34	0.59	968	<10	16	92	0.006
LA-S-088	17	0.07	34	<10	16	46	0.010
LA-S-089	5	0.06	27	<10	4	18	0.008
LA-S-090	9	0.05	24	<10	7	22	0.006
LA-S-091	9	0.21	114	<10	10	52	0.007
LA-S-092	6	0.17	94	<10	7	43	0.006
LA-S-093	18	0.08	59	<10	10	40	0.007
LA-S-094	27	0.06	35	<10	25	74	0.014
LA-S-095	25	0.06	30	<10	20	72	0.020
LA-S-096	9	0.05	28	<10	7	22	0.005
LA-S-097	5	0.03	13	<10	3	10	0.004
LA-S-098	13	0.24	142	<10	8	77	0.003
LA-S-099	49	0.40	184	<10	20	149	0.011
LA-S-100	62	0.30	200	<10	15	91	0.014
LA-S-101	54	0.17	162	<10	23	78	0.015
LA-S-102	26	0.09	81	<10	17	45	0.013
LA-S-103	11	0.04	31	<10	6	24	0.005
LA-S-104	5	0.01	10	<10	3	4	0.005
LA-S-105	5	<0.01	7	<10	3	4	0.009
LA-S-106	6	<0.01	6	<10	3	2	0.009
LA-S-107	19	0.09	68	<10	8	52	0.006
LA-S-108	32	0.50	434	<10	10	125	0.004
LA-S-109	9	0.13	84	<10	6	41	0.003
LA-S-110	14	0.08	63	<10	6	29	0.004
LA-S-111	17	0.10	79	<10	6	36	0.010
LA-S-112	33	0.24	206	<10	9	85	0.003
LA-S-113	36	0.12	133	<10	10	46	0.008
LA-S-114	31	0.22	238	<10	6	70	0.002
LA-S-115	29	0.31	309	<10	7	83	0.008
LA-S-116	73	0.22	196	<10	26	195	0.021
LA-S-117	62	0.38	389	<10	23	144	0.012
LA-S-118	63	0.37	429	<10	19	138	0.012
LA-S-119	28	0.36	370	<10	16	145	0.011
LA-S-120	28	0.46	481	<10	15	173	0.004

Geochemical grade assay for stream sediments collected in the São Gabriel district

Sample No.	UTM_E	UTM_N	Latitude	Longitude	Location	Ag	Cd	Cu	Mn	Mo	Ni	Pb	Zn	Al	As	Ba	Be	Bi	Ca	Co	Cr	Fe	K	Mg	Na	P	Sb	Sc	Sn
						ppm	ppm	ppm	ppm	ppm	ppm	ppm	ppm	%	ppm	ppm	ppm	ppm	%	ppm	ppm	%	%	%	%	%	ppm	ppm	ppm
LA-S-121	340280	6765127	-29.23248	-52.64340	São Gabriel	<0.2	<0.5	32	1122	3	8	33	85	2.14	<10	384	3	<10	0.32	18	8	5.35	0.10	0.25	0.02	0.041	<10	12	<10
LA-S-122	341012	6762249	-29.25854	-52.63629	São Gabriel	<0.2	<0.5	32	993	<2	10	33	77	1.83	<10	316	3	<10	0.36	12	9	4.02	0.08	0.25	0.02	0.034	<10	11	<10
LA-S-123	338737	6773400	-29.15765	-52.65807	São Gabriel	<0.2	<0.5	27	947	3	7	32	92	1.80	<10	533	3	<10	0.31	12	8	4.98	0.08	0.19	0.02	0.032	<10	13	<10
LA-S-124	338291	6773566	-29.15609	-52.66263	São Gabriel	<0.2	<0.5	20	965	3	6	35	81	1.87	<10	380	3	<10	0.27	10	9	4.51	0.06	0.16	0.02	0.028	<10	11	<10
LA-S-125	339716	6785653	-29.04723	-52.64625	São Gabriel	<0.2	<0.5	16	927	<2	6	31	59	1.57	<10	280	3	<10	0.23	7	5	3.15	0.04	0.10	0.02	0.031	<10	9	<10
LA-S-126	297150	6749211	-29.36985	-53.08988	São Gabriel	<0.2	<0.5	38	952	2	6	21	76	1.21	<10	220	2	<10	0.25	17	3	5.12	0.04	0.14	0.02	0.034	<10	10	<10
LA-S-127	298020	6760697	-29.26639	-53.07882	São Gabriel	<0.2	<0.5	51	1144	3	8	34	83	1.49	11	270	3	10	0.30	20	4	5.79	0.05	0.16	0.02	0.036	<10	12	<10
LA-S-128	299625	6764784	-29.22978	-53.06157	São Gabriel	<0.2	<0.5	59	1393	3	9	29	97	1.74	<10	407	3	<10	0.41	26	7	6.25	0.08	0.21	0.02	0.036	<10	15	<10
LA-S-129	310790	6774069	-29.14775	-52.94518	São Gabriel	<0.2	<0.5	32	1115	<2	8	27	91	1.58	<10	322	2	<10	0.20	19	11	5.69	0.06	0.12	0.02	0.022	<10	12	<10
LA-S-130	308072	6779075	-29.10219	-52.97224	São Gabriel	<0.2	<0.5	46	934	<2	9	23	77	1.74	<10	279	3	<10	0.19	15	13	5.52	0.05	0.10	0.02	0.026	<10	13	<10
LA-S-131	302174	6786242	-29.03663	-53.03155	São Gabriel	<0.2	<0.5	26	695	2	6	29	58	1.68	<10	344	3	<10	0.22	11	8	3.89	0.06	0.12	0.02	0.024	<10	11	<10
LA-S-132	311509	6815761	-28.77176	-52.93080	São Gabriel	<0.2	<0.5	63	860	2	16	27	72	2.25	<10	241	2	<10	0.16	21	23	6.36	0.04	0.08	0.02	0.028	<10	17	<10
LA-S-133	312680	6816568	-28.76465	-52.91867	São Gabriel	<0.2	<0.5	89	865	3	21	27	86	1.67	<10	143	2	<10	0.14	23	25	6.51	0.03	0.06	0.02	0.023	<10	14	<10
LA-S-134	319769	6820299	-28.73200	-52.84550	São Gabriel	<0.2	<0.5	143	896	2	28	14	93	1.16	<10	86	1	<10	0.09	30	35	7.97	0.02	0.05	0.02	0.015	<10	14	<10
LA-S-135	324731	6821593	-28.72101	-52.79451	São Gabriel	<0.2	<0.5	104	899	2	27	18	79	2.08	12	163	2	<10	0.15	26	43	7.32	0.03	0.09	0.02	0.027	<10	20	<10
LA-S-136	335275	6825509	-28.68707	-52.68603	São Gabriel	<0.2	<0.5	67	870	2	14	21	78	1.69	<10	220	2	<10	0.19	18	19	5.84	0.04	0.10	0.02	0.025	<10	15	<10
LA-S-137	342208	6831244	-28.63619	-52.61430	São Gabriel	<0.2	<0.5	22	769	2	7	37	65	2.41	<10	294	3	<10	0.21	10	8	4.93	0.05	0.09	0.02	0.027	<10	14	<10
LA-S-138	340868	6843431	-28.52607	-52.62631	São Gabriel	<0.2	<0.5	121	1869	4	35	25	63	2.62	11	207	1	11	0.20	42	64	8.27	0.05	0.09	0.03	0.039	<10	28	<10
LA-S-139	337288	6851779	-28.45030	-52.66171	São Gabriel	<0.2	<0.5	185	1952	5	56	18	89	3.65	<10	306	2	15	0.26	66	109	12.07	0.04	0.12	0.03	0.043	<10	41	<10
LA-S-140	333102	6853877	-28.43084	-52.70414	São Gabriel	<0.2	<0.5	176	1022	3	45	12	91	2.07	<10	123	2	15	0.13	36	126	10.62	0.02	0.08	0.03	0.030	<10	26	<10
LA-S-141	315312	6845861	-28.50077	-52.88699	São Gabriel	<0.2	<0.5	182	1117	4	45	18	82	3.46	<10	133	2	15	0.19	38	66	11.66	0.03	0.10	0.04	0.028	<10	37	<10
LA-S-142	312190	6845399	-28.50449	-52.91895	São Gabriel	<0.2	<0.5	157	1720	3	46	19	86	3.55	<10	190	2	14	0.30	55	59	11.36	0.04	0.15	0.04	0.032	<10	37	<10
LA-S-143	309529	6846914	-28.49043	-52.94588	São Gabriel	<0.2	<0.5	187	1369	3	43	14	96	2.88	10	160	2	15	0.23	47	58	12.00	0.03	0.12	0.04	0.028	<10	33	<10
LA-S-144	298777	6843430	-28.52024	-53.05627	São Gabriel	<0.2	<0.5	164	1339	4	35	23	95	2.78	12	161	2	16	0.19	34	47	11.70	0.03	0.10	0.04	0.038	<10	32	<10
LA-S-145	295689	6832322	-28.61996	-53.08979	São Gabriel	<0.2	<0.5	145	1170	5	29	17	110	1.79	<10	127	2	13	0.11	30	34	10.85	0.02	0.06	0.03	0.026	<10	21	<10
LA-S-146	680292	6820933	-28.72628	-55.15397	São Gabriel	<0.2	<0.5	98	2279	3	20	21	60	2.12	<10	402	2	<10	0.49	59	11	7.86	0.06	0.22	0.07	0.017	<10	24	<10
LA-S-147	681893	6821386	-28.72196	-55.13766	São Gabriel	<0.2	<0.5	97	1333	4	21	21	53	2.17	<10	332	2	<10	0.49	46	20	7.74	0.06	0.27	0.04	0.016	<10	23	<10
LA-S-148	684440	6821704	-28.71873	-55.11165	São Gabriel	<0.2	<0.5	81	1542	4	22	22	61	1.43	<10	294	1	<10	0.46	32	13	5.32	0.04	0.19	0.06	0.016	<10	14	<10
LA-S-149	684561	6821666	-28.71906	-55.11040	São Gabriel	<0.2	<0.5	90	1476	3	20	17	67	1.81	<10	319	2	<10	0.54	41	14	6.54	0.04	0.24	0.05	0.015	<10	20	<10
LA-S-150	691568	6820436	-28.72913	-55.03849	São Gabriel	<0.2	<0.5	111	2271	3	23	20	75	2.69	<10	506	3	10	0.60	53	14	8.58	0.07	0.26	0.05	0.023	<10	26	<10
LA-S-151	692468	6820412	-28.72922	-55.02927	São Gabriel	<0.2	<0.5	97	2499	4	23	21	65	2.71	<10	483	3	11	0.48	53	16	9.04	0.05	0.18	0.05	0.031	<10	27	<10
LA-S-152	696261	6817332	-28.75643	-54.98992	São Gabriel	<0.2	<0.5	110	1749	3	28	16	73	2.85	11	347	3	11	0.46	50	16	8.77	0.06	0.21	0.04	0.029	<10	32	<10
LA-S-153	699864	6815697	-28.77062	-54.95275	São Gabriel	<0.2	<0.5	110	1347	4	19	23	69	2.64	<10	267	3	11	0.33	40	15	9.92	0.04	0.12	0.03	0.032	<10	28	<10
LA-S-154	702134	6815047	-28.77613	-54.92940	São Gabriel	<0.2	<0.5	125	1428	3	21	32	82	2.19	10	227	3	10	0.31	38	17	9.64	0.04	0.11	0.03	0.030	<10	25	<10
LA-S-155	707166	6815930	-28.76737	-54.87804	São Gabriel	<0.2	<0.5	121	1722	3	22	22	73	2.37	<10	255	2	12	0.32	45	26	10.10	0.03	0.12	0.03	0.031	<10	27	<10
LA-S-156	707904	6811035	-28.81140	-54.86959	São Gabriel	<0.2	<0.5	150	1403	4	21	19	83	2.07	<10	233	3	12	0.24	43	19	10.11	0.03	0.10	0.03	0.023	<10	28	<10
LA-S-157	685577	6813177	-28.79550	-55.09862	São Gabriel	<0.2	<0.5	83	2948	3	16	20	62	2.12	<10	371	3	<10	0.43	47	15	5.96	0.03	0.15	0.03	0.023	<10	25	<10
LA-S-158	692002	6808479	-28.83693	-55.03202	São Gabriel	<0.2	<0.5	75	1219	<2	14	12	59	1.46	<10	295	2	<10	0.54	30	8	5.97	0.05	0.23	0.03	0.025	<10	18	<10
LA-S-159	698749	6801997	-28.89438	-54.96176	São Gabriel	<0.2	<0.5	81	1132	3	14	17	62	1.77	<10	342	3	<10	0.48	23	9	5.41	0.05	0.18	0.03	0.015	<10	20	<10
LA-S-160	701745	6797919	-28.93069	-54.93032	São Gabriel	<0.2	<0.5	27	1191	2	10	42	58	1.48	<10	607	4	<10	0.31	13	10	3.96	0.09	0.10	0.03	0.028	<10	11	<10
LA-S-161	703028	6796237	-28.94566	-54.91686	São Gabriel	<0.2	<0.5	15	656	<2	5	25	46	1.26	<10	391	3	<10	0.19	7	5	3.13	0.07	0.09	0.03	0.021	<10	8	<10
LA-S-162	707300	6801928	-28.89364	-54.87410	São Gabriel	<0.2	<0.5	118	1507	3	17	12	73	1.70	<10	330	2	11	0.54	41	12	7.26	0.06	0.25	0.06	0.023	<10	21	<10
LA-S-163	705800	6798750	-28.92255	-54.88890	São Gabriel	<0.2	<0.5	83	1764	4	18	20	60	2.02	<10	378	2	<10	0.38	45	16	5.94	0.05	0.17	0.04	0.021	<10	22	<10
LA-S-164	717182	6795126	-28.95336	-54.77151	São Gabriel	<0.2	<0.5	66	803	<2	11	16	45	1.09	<10	279	2	<10	0.24	16	13	3.55	0.03	0.10	0.03	0.019	<10	10	<10
LA-S-165	717935	6795342	-28.95128	-54.76383	São Gabriel	<0.2	<0.5	108	884	<2	23	29	60	1.54	<10	283	2	<10	0.42	21	28	4.97	0.05	0.18	0.06	0.023	<10	15	<10
LA-S-166	769257	6730061	-29.53001	-54.22183	São Gabriel	<0.2	<0.5	30	382	<2	11	7	26	0.51	<10	54	<1	<10	0.11	12	6	2.44	0.02	0.07	0.03	0.004	<10	5	<10
LA-S-167	764454	6733471	-29.50030	-54.27217	São Gabriel	<0.2	<0.5	57	2016	3	19	15	68	1.95	<10	273	2	<10	0.42	52	13	6.59	0.05	0.18	0.03	0.045	<10	20	<10
LA-S-168	765918	6736746	-29.47046	-54.25788	São Gabriel	<0.2	<0.5	82	885	2	16	11	88	1.00	<10	140	2	<10	0.22	31	6	6.57	0.04	0.14	0.03	0.024	<10	11	<10
LA-S-169	761708	6738635	-29.45432	-54.30170	São Gabriel	<0.2	<0.5	98	1078	4	24	13	98	1.15	<10	167	2	<10	0.27	38	7	7.69	0.03	0.14	0.03	0.024	<10	14	<10
LA-S-170	760824	6739746	-29.44449	-54.31107	São Gabriel	<0.2	<0.5	120	1307	4	20	19	125	1.53	<10	302	3	<10	0.41	35	7	8.90	0.07	0.18	0.03	0.032	<10	17	<10
LA-S-171	759886	6738728	-29.45386	-54.32049	São Gabriel	<0.2	<0.5	133	1373	5	27	25	131	1.70	<10	234	3	11	0.38	42	9	9.25	0.06	0.19	0.05	0.033	<10	18	<10
LA-S-172	769759	6742952	-29.41370	-54.21983	São Gabriel	<0.2	<0.5	111	1699	3	16	28	129	1.86	11	388	3	10	0.49	41	5	9.45	0.09	0.24	0.03	0.041	<10	17	<10
LA-S-173	770330	6739791	-29.44207	-54.21318	São Gabriel	<0.2	<0.5	169	1592	5	28	19	171	1.85	<10	261	3	10	0.38	52	8	12.30	0.06	0.20	0.04	0.032	<10	19	<10
LA-S-174	779144	6737334	-29.46228	-54.12178	São Gabriel	<0.2	<0.5	92	1015	3	16	14	103	1.52	<10	286	3	<10	0.32	26	5	7.46	0.05	0.18	0.05	0.027	<10	14	<10

Geochemical grade assay for stream sediments collected in the São Gabriel district

(4continued/7)

Sample No.	Sr	Ti	V	W	Y	Zr	S
	ppm	%	ppm	ppm	ppm	ppm	%
LA-S-121	51	0.30	107	<10	26	198	0.010
LA-S-122	41	0.25	78	<10	28	157	0.022
LA-S-123	48	0.37	105	<10	32	222	0.015
LA-S-124	35	0.28	67	<10	26	248	0.016
LA-S-125	32	0.12	43	<10	27	137	0.023
LA-S-126	24	0.25	139	<10	22	159	0.008
LA-S-127	32	0.28	150	<10	25	176	0.018
LA-S-128	53	0.41	229	<10	27	224	0.017
LA-S-129	34	0.45	155	<10	24	236	0.014
LA-S-130	29	0.35	181	<10	23	175	0.011
LA-S-131	39	0.24	81	<10	33	197	0.013
LA-S-132	25	0.36	241	<10	26	168	0.013
LA-S-133	14	0.51	308	<10	13	124	0.013
LA-S-134	7	0.87	554	<10	8	114	0.006
LA-S-135	16	0.48	353	<10	19	153	0.009
LA-S-136	25	0.42	212	<10	24	201	0.013
LA-S-137	32	0.24	57	<10	34	319	0.014
LA-S-138	18	0.31	333	<10	19	96	0.021
LA-S-139	23	0.47	535	<10	21	120	0.016
LA-S-140	13	0.56	657	<10	11	100	0.010
LA-S-141	17	0.52	575	<10	18	123	0.008
LA-S-142	33	0.46	510	<10	21	105	0.012
LA-S-143	24	0.70	616	<10	17	120	0.009
LA-S-144	22	0.49	543	<10	19	122	0.013
LA-S-145	13	0.58	622	<10	12	106	0.007
LA-S-146	61	0.29	378	<10	44	100	0.011
LA-S-147	64	0.22	407	<10	40	114	0.005
LA-S-148	68	0.29	297	<10	24	97	0.013
LA-S-149	77	0.34	343	<10	30	109	0.007
LA-S-150	104	0.24	365	<10	50	101	0.009
LA-S-151	70	0.19	370	<10	49	88	0.016
LA-S-152	59	0.24	404	<10	48	96	0.019
LA-S-153	36	0.27	500	<10	37	103	0.016
LA-S-154	34	0.33	510	<10	33	101	0.018
LA-S-155	32	0.31	493	<10	32	104	0.010
LA-S-156	23	0.46	603	<10	34	127	0.009
LA-S-157	47	0.11	266	<10	59	46	0.017
LA-S-158	86	0.21	318	<10	36	97	0.012
LA-S-159	72	0.22	251	<10	61	155	0.008
LA-S-160	123	0.24	70	<10	46	188	0.030
LA-S-161	69	0.20	54	<10	28	148	0.018
LA-S-162	58	0.30	400	<10	32	115	0.007
LA-S-163	66	0.26	260	<10	47	119	0.013
LA-S-164	46	0.26	166	<10	22	85	0.009
LA-S-165	67	0.28	238	<10	28	124	0.017
LA-S-166	9	0.21	201	<10	5	47	0.002
LA-S-167	48	0.20	269	<10	30	94	0.018
LA-S-168	26	0.43	532	<10	12	109	0.009
LA-S-169	30	0.43	681	<10	14	114	0.009
LA-S-170	66	0.73	664	<10	25	177	0.015
LA-S-171	49	0.75	742	<10	23	145	0.017
LA-S-172	100	0.63	587	<10	23	184	0.021
LA-S-173	43	1.02	1020	<10	17	171	0.016
LA-S-174	52	0.52	555	<10	26	147	0.008

Geochemical grade assay for stream sediments collected in the São Gabriel district

Sample No.	UTM_E	UTM_N	Latitude	Longitude	Location	Ag	Cd	Cu	Mn	Mo	Ni	Pb	Zn	Al	As	Ba	Be	Bi	Ca	Co	Cr	Fe	K	Mg	Na	P	Sb	Sc	Sn
						ppm	ppm	ppm	ppm	ppm	ppm	ppm	ppm	%	ppm	ppm	ppm	ppm	%	ppm	ppm	%	%	%	%	%	ppm	ppm	ppm
LA-S-175	778615	6737862	-29.45764	-54.12736	São Gabriel	<0.2	<0.5	68	1013	<2	12	18	84	1.36	<10	266	3	<10	0.33	22	4	6.14	0.05	0.14	0.04	0.030	<10	12	<10
LA-S-176	775010	6738416	-29.45345	-54.16463	São Gabriel	<0.2	<0.5	100	1217	2	21	22	104	1.65	<10	219	2	11	0.39	33	5	7.71	0.06	0.21	0.04	0.030	<10	16	<10
OC-S-001	749452	6677037	-30.01220	-54.41370	São Gabriel	<0.2	<0.5	3	113	<2	2	6	6	0.23	<10	32	<1	<10	0.05	2	5	0.43	0.02	0.04	0.02	0.004	<10	<1	<10
OC-S-002	743334	6719986	-29.62620	-54.48680	São Gabriel	<0.2	<0.5	5	157	<2	2	5	6	0.28	<10	38	<1	<10	0.05	4	3	0.78	0.03	0.04	0.02	0.010	<10	1	<10
OC-S-003	746934	6727577	-29.55700	-54.45140	São Gabriel	<0.2	<0.5	52	611	<2	13	9	64	0.98	<10	88	1	<10	0.20	20	7	4.71	0.04	0.16	0.04	0.016	<10	8	<10
OC-S-004	757402	6728272	-29.54860	-54.34360	São Gabriel	<0.2	0.6	84	1032	<2	19	16	95	2.12	<10	184	2	<10	0.41	34	9	7.60	0.07	0.27	0.05	0.044	<10	17	<10
OC-S-005	713417	6725964	-29.57780	-54.79680	São Gabriel	<0.2	<0.5	6	164	<2	1	5	5	0.22	<10	33	<1	<10	0.03	3	4	0.57	0.01	0.02	0.02	0.005	<10	1	<10
OC-S-006	709896	6734156	-29.50450	-54.83470	São Gabriel	<0.2	<0.5	33	536	<2	10	11	58	0.73	<10	86	1	<10	0.11	16	10	4.36	0.03	0.09	0.03	0.014	<10	6	<10
OC-S-007	714938	6736604	-29.48150	-54.78320	São Gabriel	<0.2	<0.5	33	944	<2	9	10	45	0.72	<10	139	1	<10	0.20	18	8	3.36	0.04	0.12	0.03	0.022	<10	5	<10
OC-S-008	718243	6733629	-29.50780	-54.74850	São Gabriel	<0.2	<0.5	8	149	<2	2	6	13	0.28	<10	51	<1	<10	0.05	4	2	0.99	0.02	0.04	0.02	0.009	<10	2	<10
OC-S-009	725561	6734940	-29.49470	-54.67340	São Gabriel	<0.2	<0.5	17	343	<2	3	8	24	0.30	<10	74	<1	<10	0.09	8	4	2.00	0.02	0.05	0.02	0.012	<10	3	<10
OC-S-010	717935	6747374	-29.38390	-54.75440	São Gabriel	<0.2	<0.5	25	401	<2	5	8	26	0.46	<10	56	<1	<10	0.09	14	5	2.57	0.01	0.05	0.02	0.011	<10	5	<10
OC-S-011	722586	6756366	-29.30200	-54.70840	São Gabriel	<0.2	<0.5	46	406	<2	6	14	51	0.86	<10	193	1	<10	0.20	11	4	3.83	0.05	0.15	0.03	0.020	<10	7	<10
OC-S-012	693459	6718308	-29.65010	-55.00130	São Gabriel	<0.2	<0.5	16	295	<2	3	10	17	0.57	<10	83	<1	<10	0.15	6	5	1.31	0.03	0.06	0.02	0.022	<10	2	<10
OC-S-013	689626	6729172	-29.55270	-55.04280	São Gabriel	<0.2	<0.5	35	529	<2	11	9	43	1.14	<10	122	1	<10	0.19	15	12	3.18	0.04	0.14	0.02	0.017	<10	8	<10
OC-S-014	681295	6730710	-29.54000	-55.12900	São Gabriel	<0.2	<0.5	13	233	<2	4	6	18	0.46	<10	55	<1	<10	0.06	5	5	1.39	0.02	0.05	0.02	0.008	<10	3	<10
OC-S-015	735210	6745722	-29.39570	-54.57620	São Gabriel	<0.2	0.7	109	2457	<2	20	23	97	2.80	<10	453	3	<10	0.51	67	7	10.12	0.12	0.38	0.04	0.039	<10	22	<10
OC-S-016	740679	6754916	-29.31170	-54.52190	São Gabriel	<0.2	<0.5	20	812	<2	2	30	67	2.00	<10	790	4	<10	0.39	10	6	4.31	0.13	0.21	0.03	0.034	<10	12	<10
OC-S-017	745378	6750329	-29.35220	-54.47250	São Gabriel	<0.2	<0.5	106	1628	<2	8	24	108	2.08	<10	384	4	<10	0.39	31	4	8.04	0.11	0.29	0.03	0.036	<10	18	<10
OC-S-018	750549	6756538	-29.29520	-54.42070	São Gabriel	<0.2	<0.5	19	768	<2	1	28	56	1.58	<10	439	3	<10	0.34	9	5	4.52	0.09	0.21	0.02	0.033	<10	11	<10
OC-S-019	748576	6758731	-29.27580	-54.44150	São Gabriel	<0.2	<0.5	15	847	<2	<1	25	49	1.41	<10	406	3	<10	0.30	8	4	3.59	0.07	0.15	0.02	0.036	<10	10	<10
OC-S-020	741667	6746175	-29.39040	-54.50980	São Gabriel	<0.2	<0.5	52	778	<2	11	18	57	1.20	<10	273	3	<10	0.40	19	5	6.09	0.06	0.23	0.04	0.035	<10	12	<10
OC-S-021	719653	6765616	-29.21910	-54.74040	São Gabriel	<0.2	<0.5	23	521	<2	2	18	44	0.64	<10	360	2	<10	0.26	7	5	2.96	0.06	0.12	0.02	0.026	<10	7	<10
OC-S-022	724096	6758623	-29.28140	-54.69330	São Gabriel	<0.2	<0.5	12	200	<2	2	10	15	0.30	<10	87	<1	<10	0.08	3	3	1.25	0.02	0.05	0.02	0.008	<10	2	<10
OC-S-023	729996	6774916	-29.13340	-54.63600	São Gabriel	<0.2	<0.5	6	212	<2	1	10	8	0.18	<10	50	<1	<10	0.04	3	4	0.88	<0.01	0.02	0.01	0.005	<10	2	<10
OC-S-024	736256	6772521	-29.15380	-54.57120	São Gabriel	<0.2	<0.5	9	223	<2	2	18	10	0.20	<10	42	<1	<10	0.04	3	7	1.22	<0.01	0.03	0.01	0.004	<10	2	<10
OC-S-025	754262	6769994	-29.17310	-54.38560	São Gabriel	<0.2	<0.5	9	290	<2	2	15	13	0.37	<10	108	<1	<10	0.08	5	6	1.72	0.02	0.04	0.01	0.009	<10	3	<10
OC-S-026	764506	6732177	-29.51200	-54.27130	São Gabriel	<0.2	<0.5	38	301	<2	8	8	52	0.44	<10	68	<1	<10	0.05	12	4	3.64	0.02	0.08	0.02	0.011	<10	4	<10
OC-S-027	760121	6737189	-29.46770	-54.31770	São Gabriel	<0.2	0.7	99	976	<2	16	17	104	1.77	<10	222	3	<10	0.40	31	6	8.26	0.07	0.27	0.05	0.035	<10	14	<10
OC-S-028	768829	6734566	-29.48950	-54.22740	São Gabriel	<0.2	<0.5	44	623	<2	8	12	60	1.12	<10	165	2	<10	0.22	15	5	4.18	0.04	0.17	0.03	0.023	<10	9	<10
OC-S-029	773601	6735397	-29.48100	-54.17840	São Gabriel	<0.2	0.6	107	969	<2	15	18	137	1.40	<10	251	3	<10	0.30	30	6	9.09	0.06	0.21	0.03	0.031	<10	13	<10
OC-S-030	757320	6761953	-29.24500	-54.35230	São Gabriel	<0.2	<0.5	17	2012	<2	<1	29	50	1.54	<10	313	4	<10	0.25	17	4	3.70	0.06	0.14	0.02	0.035	<10	10	<10
OC-S-031	683848	6771203	-29.17440	-55.10940	São Gabriel	<0.2	<0.5	59	988	<2	10	16	73	1.22	<10	271	3	<10	0.38	28	7	6.50	0.06	0.23	0.02	0.035	<10	14	<10
OC-S-032	682503	6768304	-29.20070	-55.12280	São Gabriel	<0.2	<0.5	37	901	<2	7	11	46	1.15	<10	176	2	<10	0.22	20	7	3.75	0.05	0.13	0.02	0.019	<10	9	<10
OC-S-033	668340	6764920	-29.23320	-55.26790	São Gabriel	<0.2	<0.5	7	120	<2	1	6	7	0.34	<10	30	<1	<10	0.02	4	4	0.62	0.01	0.01	0.01	0.005	<10	2	<10
OC-S-034	657860	6760208	-29.27710	-55.37500	São Gabriel	<0.2	<0.5	40	951	<2	14	6	39	1.28	<10	135	1	<10	0.27	27	20	3.92	0.04	0.21	0.03	0.011	<10	10	<10
OC-S-035	667107	6737859	-29.47750	-55.27650	São Gabriel	<0.2	<0.5	4	115	<2	<1	3	2	0.08	<10	9	<1	<10	<0.01	2	2	0.18	<0.01	<0.01	0.01	0.001	<10	<1	<10
OC-S-036	679830	6746596	-29.39690	-55.14670	São Gabriel	<0.2	<0.5	20	432	<2	5	6	21	0.51	<10	78	<1	<10	0.07	9	8	1.60	0.02	0.06	0.02	0.009	<10	4	<10
OC-S-037	695403	6744187	-29.41630	-54.98590	São Gabriel	<0.2	<0.5	48	1084	<2	10	26	70	2.57	<10	852	4	<10	0.54	21	9	5.99	0.14	0.37	0.03	0.041	<10	15	<10
OC-S-038	744773	6788167	-29.01110	-54.48710	São Gabriel	<0.2	<0.5	8	112	<2	2	9	5	0.35	<10	31	<1	<10	0.03	2	5	0.87	0.01	0.02	0.01	0.004	<10	2	<10
OC-S-039	734126	6801663	-28.89140	-54.59910	São Gabriel	<0.2	<0.5	50	388	<2	6	9	38	0.32	<10	51	<1	<10	0.05	11	11	2.85	0.01	0.03	0.02	0.007	<10	3	<10
OC-S-040	734974	6795105	-28.95040	-54.58910	São Gabriel	<0.2	<0.5	12	159	<2	2	12	12	0.56	<10	65	<1	<10	0.06	3	6	1.30	0.02	0.04	0.01	0.007	<10	3	<10
OC-S-041	717193	6795287	-28.95190	-54.77140	São Gabriel	<0.2	1.3	204	1745	<2	23	18	96	0.98	<10	335	5	<10	0.34	59	64	14.87	0.03	0.15	0.04	0.071	<10	10	<10
OC-S-042	710396	6807158	-28.84600	-54.84330	São Gabriel	<0.2	<0.5	63	812	<2	7	16	46	0.79	<10	241	2	<10	0.31	26	7	4.53	0.03	0.15	0.02	0.020	<10	11	<10
OC-S-043	706529	6806355	-28.85380	-54.88280	São Gabriel	<0.2	1.1	198	3478	<2	23	21	99	2.04	<10	557	4	<10	0.54	91	39	16.01	0.07	0.30	0.05	0.048	<10	20	<10
OC-S-044	699751	6809395	-28.82750	-54.95280	São Gabriel	<0.2	0.5	112	1924	<2	11	25	84	1.51	<10	347	3	<10	0.32	42	10	7.66	0.07	0.20	0.03	0.029	<10	14	<10
OC-S-045	697921	6813713	-28.78880	-54.97230	São Gabriel	<0.2	1.4	142	2250	<2	24	30	91	3.21	<10	356	4	<10	0.50	76	60	17.67	0.06	0.28	0.06	0.060	<10	28	<10
OC-S-046	702390	6800399	-28.90820	-54.92420	São Gabriel	<0.2	<0.5	61	1270	<2	10	26	64	2.14	<10	385	3	<10	0.41	22	15	5.38	0.08	0.26	0.04	0.028	<10	15	<10
OC-S-047	763510	6779063	-29.08950	-54.29280	São Gabriel	<0.2	<0.5	34	742	<2	3	24	58	1.47	<10	217	2	<10	0.15	11	14	4.87	0.04	0.08	0.02	0.038	<10	9	<10
OC-S-048	758499	6777794	-29.10190	-54.34390	São Gabriel	<0.2	<0.5	9	211	<2	1	4	8	0.22	<10	41	<1	<10	0.04	5	2	0.91	0.01	0.02	0.02	0.008	<10	1	<10
OC-S-049	673842	6809030	-28.83450	-55.21820	São Gabriel	<0.2	1.0	117	1735	<2	22	19	92	2.20	<10	362	3	<10	0.36	63	29	9.80	0.05	0.24	0.04	0.036	<10	19	<10
OC-S-050	689942	6814835	-28.77990	-55.05420	São Gabriel	<0.2	1.1	161	4818	<2	26	21	79	2.42	<10	1325	4	<10	0.66	126	14	14.03	0.10	0.41	0.07	0.051	<10	19	<10
OC-S-051	684363	6820599	-28.72870	-55.11230	São Gabriel	<0.2	0.9	118	3152	<2	22	19	71	2.40	<10	511	3	<10	0.70	83	13	9.55	0.07	0.42	0.05	0.034	<10	21	<10
OC-S-052	683149	6774434	-29.14530	-55.11720	São Gabriel	<0.2	0.9	94	1463	<2	12	20	81	1.94	<10	291	3	<10	0.37	38	11	8.68	0.08	0.23	0.03	0.030	<10	18	<10

Geochemical grade assay for stream sediments collected in the São Gabriel district

(5continued/7)

Sample No.	Sr	Ti	V	W	Y	Zr	S
	ppm	%	ppm	ppm	ppm	ppm	%
LA-S-175	51	0.41	352	<10	28	131	0.017
LA-S-176	57	0.51	499	<10	20	147	0.015
OC-S-001	4	0.04	10	<10	3	5	0.004
OC-S-002	3	0.03	23	<10	4	6	0.003
OC-S-003	19	0.32	355	<10	10	32	0.006
OC-S-004	44	0.39	450	<10	25	49	0.010
OC-S-005	3	0.06	19	<10	3	9	0.002
OC-S-006	12	0.32	342	<10	10	34	0.005
OC-S-007	26	0.20	201	<10	10	34	0.005
OC-S-008	6	0.07	44	<10	5	18	0.003
OC-S-009	12	0.13	116	<10	7	25	0.003
OC-S-010	8	0.12	175	<10	7	20	0.004
OC-S-011	38	0.25	203	<10	15	60	0.005
OC-S-012	10	0.02	33	<10	8	6	0.006
OC-S-013	25	0.19	169	<10	14	42	0.006
OC-S-014	11	0.10	72	<10	6	23	0.003
OC-S-015	123	0.49	489	<10	33	105	0.011
OC-S-016	114	0.26	56	<10	37	133	0.016
OC-S-017	69	0.64	447	<10	37	116	0.014
OC-S-018	99	0.18	53	<10	32	119	0.011
OC-S-019	52	0.10	40	<10	37	58	0.013
OC-S-020	68	0.21	293	<10	25	70	0.012
OC-S-021	63	0.16	81	<10	20	67	0.007
OC-S-022	15	0.09	41	<10	5	29	0.003
OC-S-023	7	0.08	22	<10	3	18	0.003
OC-S-024	7	0.20	54	<10	4	21	0.003
OC-S-025	23	0.11	55	<10	6	32	0.003
OC-S-026	9	0.32	303	<10	7	49	0.003
OC-S-027	43	0.55	532	<10	23	99	0.009
OC-S-028	30	0.26	232	<10	19	63	0.006
OC-S-029	40	0.61	739	<10	27	88	0.009
OC-S-030	44	0.10	41	<10	38	62	0.013
OC-S-031	57	0.24	318	<10	27	76	0.009
OC-S-032	41	0.20	184	<10	18	57	0.007
OC-S-033	2	0.04	19	<10	4	4	0.005
OC-S-034	31	0.15	186	<10	12	40	0.004
OC-S-035	<1	0.03	9	<10	1	2	0.002
OC-S-036	10	0.11	97	<10	6	22	0.003
OC-S-037	140	0.25	122	<10	32	105	0.020
OC-S-038	3	0.08	47	<10	4	11	0.003
OC-S-039	7	0.25	241	<10	4	29	0.003
OC-S-040	16	0.08	53	<10	7	20	0.004
OC-S-041	33	0.26	779	<10	26	71	0.006
OC-S-042	34	0.12	234	<10	28	41	0.009
OC-S-043	58	0.37	897	<10	42	91	0.004
OC-S-044	58	0.40	424	<10	34	70	0.008
OC-S-045	42	0.23	670	<10	38	78	0.009
OC-S-046	82	0.23	174	<10	47	83	0.012
OC-S-047	24	0.22	89	<10	20	81	0.012
OC-S-048	4	0.03	24	<10	3	13	0.003
OC-S-049	48	0.42	483	<10	29	68	0.005
OC-S-050	101	0.25	649	<10	39	51	0.005
OC-S-051	86	0.27	438	<10	38	85	0.006
OC-S-052	50	0.36	433	<10	34	110	0.008

Geochemical grade assay for stream sediments collected in the São Gabriel district

Sample No.	UTM_E	UTM_N	Latitude	Longitude	Location	Ag	Cd	Cu	Mn	Mo	Ni	Pb	Zn	Al	As	Ba	Be	Bi	Ca	Co	Cr	Fe	K	Mg	Na	P	Sb	Sc	Sn
						ppm	ppm	ppm	ppm	ppm	ppm	ppm	ppm	%	ppm	ppm	ppm	ppm	%	ppm	ppm	%	%	%	%	%	ppm	ppm	ppm
OC-S-053	667712	6772539	-29.16460	-55.27550	São Gabriel	<0.2	<0.5	6	694	<2	<1	3	5	0.12	<10	51	<1	<10	0.02	11	2	0.54	<0.01	<0.01	0.01	0.004	<10	<1	<10
OC-S-054	653950	6771219	-29.17820	-55.41680	São Gabriel	<0.2	<0.5	5	40	<2	<1	2	3	0.03	<10	10	<1	<10	<0.01	1	1	0.36	<0.01	<0.01	0.01	0.002	<10	<1	<10
OC-S-055	651211	6766038	-29.22530	-55.44420	São Gabriel	<0.2	<0.5	14	250	<2	4	5	15	0.45	<10	40	<1	<10	0.07	8	9	1.46	0.02	0.06	0.03	0.009	<10	3	<10
OC-S-056	646632	6776400	-29.13240	-55.49270	São Gabriel	<0.2	<0.5	4	98	<2	<1	4	2	0.18	<10	16	<1	<10	0.01	1	3	0.23	<0.01	0.01	0.02	0.002	<10	<1	<10
OC-S-057	650688	6809979	-28.82890	-55.45550	São Gabriel	<0.2	<0.5	83	1344	<2	21	14	63	2.43	<10	240	1	<10	0.90	30	37	5.78	0.04	0.44	0.06	0.016	<10	20	<10
OC-S-058	652061	6810714	-28.82210	-55.44160	São Gabriel	<0.2	<0.5	27	829	<2	6	10	25	0.66	<10	99	<1	<10	0.17	17	7	2.30	0.02	0.11	0.04	0.011	<10	6	<10
OC-S-059	691728	6797049	-28.94010	-55.03290	São Gabriel	<0.2	<0.5	81	1044	<2	3	30	76	2.07	<10	799	3	<10	0.35	13	8	4.97	0.13	0.24	0.04	0.028	<10	13	<10
OC-S-060	680011	6804166	-28.87760	-55.15420	São Gabriel	<0.2	<0.5	91	1821	<2	16	22	77	2.00	<10	439	3	<10	0.59	41	12	7.26	0.09	0.36	0.07	0.050	<10	15	<10
OC-S-061	679613	6804012	-28.87900	-55.15820	São Gabriel	<0.2	0.5	82	1547	<2	15	17	66	2.62	<10	336	2	<10	0.60	38	13	6.49	0.07	0.36	0.05	0.028	<10	20	<10
OC-S-062	688088	6819383	-28.73910	-55.07390	São Gabriel	<0.2	1.4	174	4485	<2	29	25	83	2.61	<10	1133	5	<10	0.63	120	22	17.60	0.08	0.39	0.06	0.052	<10	21	<10
OC-S-063	676238	6821283	-28.72370	-55.19550	São Gabriel	<0.2	0.5	88	1845	<2	11	21	66	2.49	<10	343	2	<10	0.43	42	12	6.37	0.06	0.26	0.04	0.032	<10	22	<10
OC-S-064	645986	6818924	-28.74870	-55.50490	São Gabriel	<0.2	<0.5	38	1079	<2	9	15	30	0.69	<10	153	<1	<10	0.28	25	13	2.99	0.02	0.13	0.02	0.023	<10	9	<10
OC-S-065	652937	6821710	-28.72280	-55.43410	São Gabriel	<0.2	0.7	100	1638	<2	14	28	87	1.63	<10	288	4	<10	0.37	60	27	10.99	0.05	0.22	0.04	0.075	<10	16	<10
OC-S-066	660655	6828961	-28.65640	-55.35610	São Gabriel	<0.2	<0.5	56	1390	<2	12	18	54	1.38	<10	242	2	<10	0.37	36	15	5.17	0.03	0.21	0.04	0.032	<10	14	<10
OC-S-067	661702	6830855	-28.63920	-55.34570	São Gabriel	<0.2	<0.5	79	1831	<2	22	15	63	1.84	<10	376	2	<10	0.68	59	20	7.41	0.03	0.36	0.06	0.035	<10	17	<10
OC-S-068	670807	6831543	-28.63180	-55.25260	São Gabriel	<0.2	<0.5	77	1467	<2	16	13	58	1.48	<10	280	1	<10	0.50	36	16	5.86	0.03	0.24	0.05	0.037	<10	13	<10
OC-S-069	614562	6831469	-28.63870	-55.82790	São Gabriel	<0.2	1.0	187	4556	<2	44	40	65	2.91	<10	1209	3	<10	0.51	91	66	13.59	0.05	0.29	0.03	0.054	<10	26	<10
OC-S-070	648250	6730780	-29.54380	-55.46990	São Gabriel	<0.2	<0.5	19	641	<2	5	6	26	0.56	<10	75	<1	<10	0.05	18	23	2.69	0.01	0.03	0.02	0.015	<10	4	<10
OC-S-071	673348	6713331	-29.69790	-55.20820	São Gabriel	<0.2	<0.5	5	54	<2	<1	6	2	0.20	<10	14	<1	<10	<0.01	<1	3	0.18	<0.01	<0.01	0.02	0.003	<10	<1	<10
OC-S-072	663042	6716303	-29.67250	-55.31520	São Gabriel	<0.2	<0.5	2	62	<2	1	4	1	0.23	<10	19	<1	<10	0.01	2	4	0.31	<0.01	<0.01	0.02	0.003	<10	<1	<10
OC-S-073	653766	6717666	-29.66140	-55.41120	São Gabriel	<0.2	<0.5	1	52	<2	1	5	1	0.17	<10	17	<1	<10	<0.01	1	3	0.21	<0.01	<0.01	0.02	0.003	<10	<1	<10
OC-S-074	641336	6711507	-29.71850	-55.53880	São Gabriel	<0.2	<0.5	3	44	<2	<1	4	2	0.12	<10	14	<1	<10	0.01	1	3	0.21	<0.01	<0.01	0.02	0.002	<10	<1	<10
OC-S-075	636711	6723270	-29.61280	-55.58810	São Gabriel	<0.2	<0.5	24	295	<2	5	9	36	0.48	<10	58	<1	<10	0.08	13	7	3.02	0.01	0.08	0.01	0.009	<10	6	<10
OC-S-076	641759	6720638	-29.63600	-55.53560	São Gabriel	<0.2	<0.5	9	419	<2	2	3	10	0.12	<10	39	<1	<10	0.02	12	6	1.02	<0.01	0.01	0.02	0.007	<10	1	<10
OC-S-077	651729	6725389	-29.59200	-55.43330	São Gabriel	<0.2	<0.5	5	183	<2	<1	3	3	0.07	<10	22	<1	<10	0.01	2	2	0.20	<0.01	<0.01	0.01	0.002	<10	<1	<10
OC-S-078	625607	6757150	-29.30830	-55.70660	São Gabriel	<0.2	<0.5	7	174	<2	<1	5	6	0.16	<10	23	<1	<10	0.03	3	3	0.49	<0.01	0.01	0.01	0.004	<10	1	<10
OC-S-079	625780	6741563	-29.44890	-55.70300	São Gabriel	<0.2	<0.5	5	97	<2	2	6	6	0.24	<10	28	<1	<10	0.01	4	6	0.56	<0.01	0.01	0.01	0.004	<10	2	<10
OC-S-080	621048	6744863	-29.41960	-55.75220	São Gabriel	<0.2	0.6	88	1697	<2	16	18	52	1.79	<10	305	2	<10	0.61	41	14	6.58	0.04	0.39	0.03	0.025	<10	19	<10
OC-S-081	615071	6748132	-29.39070	-55.81410	São Gabriel	<0.2	<0.5	9	136	<2	1	5	8	0.25	<10	29	<1	<10	0.04	3	4	0.86	<0.01	0.03	0.01	0.005	<10	2	<10
OC-S-082	628005	6790056	-29.01120	-55.68570	São Gabriel	<0.2	<0.5	11	489	<2	2	16	13	0.21	<10	61	<1	<10	0.03	10	8	1.29	<0.01	0.03	0.01	0.004	<10	4	<10
OC-S-083	697509	6757846	-29.29280	-54.96670	São Gabriel	<0.2	<0.5	35	894	<2	7	26	25	0.73	<10	133	<1	<10	0.27	25	15	3.34	0.02	0.14	0.02	0.022	<10	7	<10
OC-S-084	671231	6725320	-29.59010	-55.23200	São Gabriel	<0.2	<0.5	5	84	<2	<1	2	2	0.08	<10	14	<1	<10	0.01	1	1	0.14	<0.01	<0.01	0.01	0.002	<10	<1	<10
OC-S-085	676452	6733361	-29.51680	-55.17940	São Gabriel	<0.2	<0.5	4	576	<2	<1	<2	1	0.07	<10	40	<1	<10	0.01	4	1	0.22	<0.01	<0.01	0.02	0.002	<10	<1	<10
OC-S-086	706016	6722050	-29.61430	-54.87240	São Gabriel	<0.2	<0.5	6	265	<2	<1	3	4	0.10	<10	39	<1	<10	0.05	4	2	0.43	<0.01	0.02	0.01	0.006	<10	<1	<10
OC-S-087	748111	6706649	-29.74550	-54.43450	São Gabriel	<0.2	<0.5	5	24	<2	<1	3	2	0.05	<10	19	<1	<10	0.02	<1	<1	0.12	<0.01	<0.01	0.01	0.002	<10	<1	<10
OC-S-088	746927	6710745	-29.70880	-54.44760	São Gabriel	<0.2	<0.5	3	77	<2	1	4	4	0.12	<10	28	<1	<10	0.04	2	2	0.35	0.01	0.02	0.01	0.005	<10	<1	<10
OC-S-089	727661	6703170	-29.78080	-54.64500	São Gabriel	<0.2	<0.5	6	32	<2	<1	2	2	0.08	<10	23	<1	<10	0.02	<1	1	0.11	<0.01	<0.01	0.01	0.003	<10	<1	<10
OC-S-090	614851	6841533	-28.54790	-55.82600	São Gabriel	<0.2	<0.5	138	855	<2	30	7	55	1.33	<10	180	<1	<10	0.79	25	18	4.85	0.06	0.55	0.13	0.042	<10	9	10
OC-S-091	622000	6833087	-28.62340	-55.75200	São Gabriel	<0.2	1.0	106	4709	<2	23	31	55	1.76	<10	530	2	<10	0.61	72	32	9.58	0.03	0.28	0.03	0.045	<10	18	<10
OC-S-092	623391	6833752	-28.61730	-55.73780	São Gabriel	<0.2	<0.5	40	960	<2	7	19	32	0.45	<10	129	<1	<10	0.16	18	13	2.77	0.01	0.09	0.02	0.014	<10	7	<10
OC-S-093	645793	6845261	-28.51110	-55.51020	São Gabriel	<0.2	<0.5	23	229	<2	6	13	22	0.10	<10	87	<1	<10	0.08	6	13	2.21	<0.01	0.05	0.02	0.003	<10	5	<10
OC-S-094	646282	6857338	-28.40210	-55.50670	São Gabriel	<0.2	0.7	84	1157	<2	18	24	49	0.79	<10	203	1	<10	0.24	35	40	5.81	0.01	0.15	0.01	0.012	<10	13	<10
OC-S-095	599394	6836458	-28.59490	-55.98350	São Gabriel	<0.2	0.8	138	3902	<2	26	19	93	2.69	<10	404	3	<10	0.49	75	47	11.39	0.05	0.29	0.02	0.094	<10	34	<10
OC-S-097	635415	6851770	-28.45350	-55.61700	São Gabriel	<0.2	0.8	122	2923	<2	33	36	54	1.42	<10	435	3	<10	0.63	84	60	10.64	0.02	0.30	0.02	0.047	<10	20	<10
OC-S-098	638820	6826393	-28.68210	-55.57920	São Gabriel	<0.2	<0.5	31	1180	<2	6	16	37	0.42	<10	142	<1	<10	0.21	25	9	2.46	0.01	0.09	0.02	0.021	<10	7	<10
OC-S-099	637910	6810143	-28.82890	-55.58650	São Gabriel	<0.2	1.0	109	4925	<2	22	36	56	1.03	<10	949	4	<10	0.37	73	46	12.90	0.03	0.13	0.02	0.059	<10	15	<10
OC-S-101	626278	6827152	-28.67660	-55.70760	São Gabriel	<0.2	0.6	74	2489	<2	23	21	58	1.26	<10	360	2	<10	0.65	54	33	5.83	0.03	0.32	0.03	0.030	<10	14	<10
OC-S-102	613835	6806050	-28.86820	-55.83280	São Gabriel	<0.2	<0.5	50	886	<2	16	29	55	0.85	<10	225	<1	<10	0.48	17	41	3.28	0.02	0.19	0.04	0.011	<10	11	<10
OC-S-103	614126	6804405	-28.88300	-55.82960	São Gabriel	<0.2	<0.5	52	919	<2	12	17	64	1.99	<10	217	1	<10	0.59	20	16	4.88	0.04	0.34	0.03	0.030	<10	16	<10
OC-S-104	612119	6851998	-28.45370	-55.85490	São Gabriel	<0.2	0.8	143	2231	<2	25	31	46	2.49	<10	360	3	<10	0.35	65	59	11.02	0.04	0.21	0.02	0.034	<10	27	<10
OC-S-105	596765	6822993	-28.71670	-56.00920	São Gabriel	<0.2	1.0	96	2513	<2	16	48	35	1.94	<10	401	3	<10	0.40	52	46	11.00	0.03	0.20	0.02	0.036	<10	15	<10
OC-S-106	585675	6818400	-28.75890	-56.12240	São Gabriel	<0.2	1.1	127	3736	<2	28	50	80	2.61	20	565	6	<10	0.63	96	51	16.79	0.05	0.30	0.02	0.180	<10	27	<10
OC-S-107	610055	6795223	-28.96620	-55.87050	São Gabriel	<0.2	<0.5	29	563	<2	6	11	27	0.91	<10	99	<1	<10	0.23	15	10	2.97	0.02	0.13	0.02	0.018	<10	8	<10
OC-S-109	581510	6747284	-29.40100	-56.15990	São Gabriel	<0.2	0.7	84	11209	<2	65	60	36	1.40	10	2495	2	<10	1.28	299	19	6.17	0.04	0.29	0.04	0.037	<10	10	<10

Geochemical grade assay for stream sediments collected in the São Gabriel district

(6continued/7)

Sample No.	Sr	Ti	V	W	Y	Zr	S
	ppm	%	ppm	ppm	ppm	ppm	%
OC-S-053	2	0.01	22	<10	2	3	0.002
OC-S-054	<1	0.01	24	<10	<1	3	0.002
OC-S-055	9	0.06	72	<10	4	13	0.003
OC-S-056	2	0.04	10	<10	2	3	0.002
OC-S-057	54	0.27	206	<10	29	46	0.005
OC-S-058	14	0.29	107	<10	9	29	0.004
OC-S-059	108	0.27	113	<10	39	66	0.014
OC-S-060	88	0.25	314	<10	39	37	0.007
OC-S-061	58	0.21	239	<10	41	56	0.010
OC-S-062	89	0.22	870	<10	53	81	0.005
OC-S-063	56	0.22	229	<10	46	58	0.009
OC-S-064	21	0.08	140	<10	17	20	0.008
OC-S-065	37	0.24	505	<10	37	54	0.009
OC-S-066	39	0.31	251	<10	26	45	0.006
OC-S-067	57	0.28	387	<10	27	47	0.005
OC-S-068	39	0.30	281	<10	22	40	0.006
OC-S-069	51	0.15	527	<10	40	53	0.005
OC-S-070	5	0.05	109	<10	5	16	0.004
OC-S-071	<1	0.04	9	<10	4	3	0.003
OC-S-072	1	0.03	12	<10	2	2	0.003
OC-S-073	<1	0.02	7	<10	2	2	0.003
OC-S-074	1	0.02	11	<10	1	2	0.002
OC-S-075	6	0.12	183	<10	9	30	0.005
OC-S-076	3	0.01	35	<10	2	4	0.002
OC-S-077	1	0.01	9	<10	1	3	0.002
OC-S-078	3	0.03	23	<10	2	7	0.002
OC-S-079	2	0.03	24	<10	3	4	0.003
OC-S-080	39	0.13	228	<10	32	82	0.005
OC-S-081	4	0.07	43	<10	3	13	0.002
OC-S-082	3	0.19	58	<10	4	25	0.002
OC-S-083	16	0.13	185	<10	17	37	0.004
OC-S-084	1	<0.01	6	<10	1	2	0.002
OC-S-085	2	<0.01	11	<10	<1	2	0.001
OC-S-086	4	<0.01	15	<10	3	4	0.002
OC-S-087	2	<0.01	4	<10	1	1	0.002
OC-S-088	3	<0.01	11	<10	2	3	0.003
OC-S-089	2	<0.01	3	<10	1	1	0.003
OC-S-090	49	0.16	222	<10	21	51	0.003
OC-S-091	47	0.14	337	<10	32	60	0.005
OC-S-092	15	0.33	164	<10	12	48	0.003
OC-S-093	7	0.68	157	<10	4	44	0.004
OC-S-094	20	0.32	306	<10	21	61	0.003
OC-S-095	43	0.25	407	<10	44	54	0.013
OC-S-097	53	0.03	475	<10	44	35	0.008
OC-S-098	19	0.10	137	<10	15	25	0.005
OC-S-099	36	0.07	638	<10	40	43	0.008
OC-S-101	51	0.12	232	<10	28	48	0.006
OC-S-102	30	0.26	195	<10	18	48	0.003
OC-S-103	42	0.20	172	<10	22	52	0.008
OC-S-104	31	0.11	409	<10	36	57	0.004
OC-S-105	36	0.08	502	<10	23	60	0.004
OC-S-106	58	0.11	699	<10	59	61	0.007
OC-S-107	17	0.11	110	<10	11	30	0.003
OC-S-109	46	0.14	441	<10	47	44	0.003

Geochemical grade assay for stream sediments collected in the São Gabriel district

Sample No.	UTM_E	UTM_N	Latitude	Longitude	Location	Ag	Cd	Cu	Mn	Mo	Ni	Pb	Zn	Al	As	Ba	Be	Bi	Ca	Co	Cr	Fe	K	Mg	Na	P	Sb	Sc	Sn
						ppm	ppm	ppm	ppm	ppm	ppm	ppm	ppm	%	ppm	ppm	ppm	ppm	%	ppm	ppm	%	%	%	%	%	ppm	ppm	ppm
OC-S-110	601429	6750601	-29.36960	-55.95490	São Gabriel	<0.2	<0.5	10	232	<2	2	5	10	0.24	<10	51	<1	<10	0.15	6	5	0.93	0.01	0.07	0.02	0.007	<10	3	<10
OC-S-111	583293	6759756	-29.28830	-56.14250	São Gabriel	<0.2	<0.5	26	383	<2	9	22	38	0.51	<10	122	<1	<10	0.34	18	12	2.42	0.02	0.16	0.02	0.026	<10	4	<10
OC-S-112	589562	6807613	-28.85600	-56.08180	São Gabriel	<0.2	<0.5	42	3375	<2	14	33	23	0.57	<10	329	1	<10	0.30	68	14	3.24	0.02	0.14	0.02	0.041	<10	7	<10
OC-S-113	595938	6800499	-28.91970	-56.01580	São Gabriel	<0.2	<0.5	26	1230	<2	6	15	20	0.65	<10	152	<1	<10	0.19	22	11	3.41	0.02	0.09	0.02	0.028	<10	6	<10
OC-S-114	567077	6799146	-28.93380	-56.31180	São Gabriel	<0.2	1.6	162	4090	<2	30	33	101	2.68	<10	616	6	<10	0.51	114	68	19.89	0.04	0.25	0.03	0.154	<10	28	<10
OC-S-115	558464	6781967	-29.08920	-56.39920	São Gabriel	<0.2	0.9	177	2125	<2	29	16	98	3.05	<10	517	3	<10	0.87	71	24	10.40	0.08	0.72	0.06	0.039	<10	39	11
OC-S-116	679090	6697570	-29.83930	-55.14630	São Gabriel	<0.2	<0.5	4	305	<2	1	4	5	0.21	<10	38	<1	<10	0.04	4	7	0.58	0.01	0.02	0.02	0.008	<10	<1	<10
OC-S 117	698335	6696393	-29.84700	-54.94700	São Gabriel	<0.2	<0.5	2	66	<2	1	3	2	0.21	<10	26	<1	<10	0.04	1	3	0.23	0.01	0.03	0.02	0.004	<10	<1	<10
OC-S-118	720018	6694685	-29.85870	-54.72230	São Gabriel	<0.2	<0.5	6	38	<2	<1	3	1	0.06	<10	17	<1	<10	0.01	1	2	0.23	<0.01	<0.01	0.02	0.003	<10	<1	<10
OC-S-119	732056	6696733	-29.83800	-54.59820	São Gabriel	<0.2	<0.5	4	24	<2	<1	3	<1	0.04	<10	16	<1	<10	<0.01	<1	2	0.20	<0.01	<0.01	0.02	0.002	<10	<1	<10
OC-S-120	730391	6667313	-30.10360	-54.60910	São Gabriel	<0.2	<0.5	2	26	<2	<1	4	2	0.19	<10	28	<1	<10	0.03	<1	3	0.21	0.02	0.02	0.02	0.003	<10	<1	<10
OC-S-121	716817	6681180	-29.98100	-54.75270	São Gabriel	<0.2	<0.5	3	30	<2	<1	4	<1	0.07	<10	16	<1	<10	0.01	<1	4	0.18	<0.01	<0.01	0.02	0.001	<10	<1	<10
OC-S-122	723068	6674922	-30.03630	-54.68660	São Gabriel	<0.2	<0.5	7	26	<2	<1	3	1	0.04	<10	16	<1	<10	<0.01	<1	1	0.12	<0.01	<0.01	0.02	0.001	<10	<1	<10
OC-S-123	734021	6706247	-29.75180	-54.58000	São Gabriel	<0.2	<0.5	3	22	<2	<1	5	1	0.13	<10	30	<1	<10	0.03	<1	3	0.12	<0.01	0.01	0.02	0.004	<10	<1	<10
OC-S-124	770280	6712366	-29.68930	-54.20690	São Gabriel	<0.2	<0.5	8	174	<2	2	7	10	0.42	<10	52	<1	<10	0.08	4	3	0.88	0.02	0.04	0.02	0.010	<10	3	<10
OC-S-125	760917	6706194	-29.74690	-54.30210	São Gabriel	<0.2	<0.5	7	31	<2	<1	3	2	0.10	<10	23	<1	<10	0.02	<1	2	0.15	0.01	0.01	0.02	0.003	<10	<1	<10
OC-S 126	766001	6715174	-29.66490	-54.25180	São Gabriel	<0.2	<0.5	12	324	<2	1	4	4	0.14	<10	46	<1	<10	0.03	6	2	0.60	0.01	0.01	0.03	0.006	<10	<1	<10
OC-S-127	717867	6700412	-29.80740	-54.74570	São Gabriel	<0.2	<0.5	6	45	<2	<1	2	<1	0.07	<10	19	<1	<10	0.01	<1	2	0.11	0.01	<0.01	0.03	0.003	<10	<1	<10
OC-S-128	778046	6689295	-29.89550	-54.12080	São Gabriel	<0.2	<0.5	6	264	<2	2	9	7	0.51	<10	152	<1	<10	0.11	4	5	0.86	0.03	0.05	0.03	0.011	<10	1	<10
OC-S-129	770896	6686082	-29.92610	-54.19390	São Gabriel	<0.2	<0.5	13	1831	<2	7	25	23	1.27	18	243	3	<10	0.29	20	16	4.69	0.08	0.17	0.03	0.059	<10	3	<10
OC-S-130	779023	6671786	-30.05310	-54.10610	São Gabriel	<0.2	<0.5	4	88	<2	2	5	5	0.36	<10	72	<1	<10	0.09	2	3	0.41	0.05	0.08	0.03	0.006	<10	<1	<10
OC-S-131	771336	6658828	-30.17160	-54.18240	São Gabriel	<0.2	<0.5	11	169	<2	5	6	14	0.56	<10	187	<1	<10	0.22	4	7	0.89	0.06	0.13	0.04	0.014	<10	2	<10
OC-S-132	739211	6663886	-30.13280	-54.51690	São Gabriel	<0.2	<0.5	2	108	<2	1	5	2	0.22	<10	37	<1	<10	0.05	1	3	0.25	0.02	0.03	0.02	0.004	<10	<1	<10
OC-S-133	734452	6662894	-30.14270	-54.56600	São Gabriel	<0.2	<0.5	9	230	<2	3	14	14	0.67	<10	114	<1	<10	0.16	5	5	1.11	0.05	0.09	0.03	0.013	<10	2	<10
OC-S-133A	735648	6663170	-30.13990	-54.55370	São Gabriel	<0.2	<0.5	2	149	<2	1	4	<1	0.24	<10	47	<1	<10	25.80	1	3	0.29	0.03	0.04	0.02	0.005	<10	<1	<10
OC-S-134	755461	6706181	-29.74820	-54.35840	São Gabriel	<0.2	<0.5	7	55	<2	<1	3	3	0.12	<10	25	<1	<10	0.02	2	2	0.50	0.01	0.01	0.02	0.007	<10	<1	<10
OC-S-135	772034	6740928	-29.43150	-54.19590	São Gabriel	<0.2	0.8	103	1341	<2	13	17	86	2.43	<10	429	3	<10	0.52	32	6	8.76	0.11	0.38	0.05	0.051	<10	21	<10

Geochemical grade assay for stream sediments collected in the São Gabriel district

Sample No.	Sr	Ti	V	W	Y	Zr	S
	ppm	%	ppm	ppm	ppm	ppm	%
OC-S-110	22	0.04	49	<10	5	13	0.003
OC-S-111	26	0.14	216	<10	13	30	0.010
OC-S-112	26	0.06	169	<10	16	26	0.002
OC-S-113	14	0.06	134	<10	11	24	0.003
OC-S-114	49	0.20	889	<10	56	72	0.009
OC-S-115	90	0.22	352	<10	85	114	0.008
OC-S-116	4	<0.01	13	<10	3	3	0.003
OC-S 117	3	0.02	7	<10	2	2	0.003
OC-S-118	2	<0.01	5	<10	1	2	0.003
OC-S-119	1	<0.01	6	<10	1	2	0.002
OC-S-120	3	0.01	5	<10	2	2	0.003
OC-S-121	2	0.02	5	<10	1	3	0.002
OC-S-122	1	<0.01	3	<10	<1	2	0.002
OC-S-123	2	0.02	5	<10	6	1	0.003
OC-S-124	14	0.04	28	<10	7	17	0.003
OC-S-125	2	0.01	4	<10	2	2	0.003
OC-S 126	2	<0.01	17	<10	2	4	0.002
OC-S-127	2	<0.01	3	<10	1	2	0.002
OC-S-128	10	0.03	19	<10	7	5	0.004
OC-S-129	26	<0.01	66	<10	14	13	0.006
OC-S-130	13	0.01	7	<10	4	7	0.004
OC-S-131	25	<0.01	14	<10	5	7	0.022
OC-S-132	5	0.02	5	<10	3	3	0.003
OC-S-133	20	<0.01	22	<10	6	8	0.006
OC-S-133A	6	<0.01	7	<10	3	4	<0.001
OC-S-134	3	<0.01	11	<10	2	3	0.002
OC-S-135	66	0.33	313	<10	32	76	0.007

Geochemical grade assay for stream sediments collected in the Ponta Grossa district

Sample No.	UTM_E	UTM_N	Latitude	Longitude	Location	Ag	Cd	Cu	Mn	Mo	Ni	Pb	Zn	Al	As	Ba	Be	Bi	Ca	Co	Cr	Fe	K	Mg	Na	P	Sb	Sc	Sn
						ppm	ppm	ppm	ppm	ppm	ppm	ppm	ppm	%	ppm	ppm	ppm	ppm	%	ppm	ppm	%	%	%	%	%	ppm	ppm	ppm
ES-S-49	518065	7289248	-24.51035	-50.82168	Ponta Grossa	<0.2	<0.5	71	269	<2	14	19	54	1.85	<10	86	2	15	0.07	10	44	7.51	<0.01	<0.01	0.01	0.076	<10	24	<10
ES-S-50	517121	7286093	-24.53885	-50.83096	Ponta Grossa	<0.2	<0.5	103	1211	4	35	3	76	1.91	<10	174	1	17	0.65	36	21	7.40	0.02	0.35	0.03	0.108	<10	25	<10
ES-S-51	519727	7282463	-24.57161	-50.80518	Ponta Grossa	<0.2	<0.5	22	389	<2	13	18	54	1.43	<10	150	1	<10	0.16	13	12	3.26	0.08	0.13	0.02	0.030	<10	7	<10
ES-S-52	519951	7282870	-24.56793	-50.80297	Ponta Grossa	<0.2	<0.5	24	632	3	17	14	84	1.07	<10	134	1	<10	0.22	20	13	4.48	0.04	0.16	0.02	0.038	<10	7	<10
ES-S-53	515871	7287894	-24.52260	-50.84332	Ponta Grossa	<0.2	<0.5	29	331	3	8	12	41	1.81	<10	84	<1	<10	0.10	7	11	4.37	0.03	0.06	0.02	0.036	<10	12	<10
ES-S-54	518900	7276105	-24.62904	-50.81326	Ponta Grossa	<0.2	<0.5	133	759	<2	19	6	74	2.88	<10	213	2	17	0.28	27	13	8.43	0.04	0.15	0.03	0.089	<10	27	<10
ES-S-55	519211	7276841	-24.62239	-50.81020	Ponta Grossa	<0.2	<0.5	46	803	<2	14	9	70	1.56	<10	144	1	<10	0.18	20	15	5.08	0.04	0.09	0.02	0.041	<10	11	<10
ES-S-56	515438	7275863	-24.63126	-50.84746	Ponta Grossa	<0.2	<0.5	62	643	<2	10	14	54	2.43	<10	146	1	13	0.11	13	9	6.43	0.03	0.05	0.02	0.058	<10	20	<10
ES-S-57	519160	7274059	-24.64752	-50.81066	Ponta Grossa	<0.2	<0.5	75	772	<2	32	19	93	1.74	<10	111	1	<10	0.16	30	66	6.92	0.03	0.07	0.02	0.046	<10	19	<10
ES-S-58	519062	7271757	-24.66831	-50.81160	Ponta Grossa	<0.2	<0.5	135	1310	2	48	5	111	1.78	<10	176	2	21	0.44	35	59	7.78	0.04	0.29	0.03	0.048	<10	23	<10
ES-S-59	516496	7268915	-24.69400	-50.83693	Ponta Grossa	<0.2	<0.5	55	783	<2	19	7	78	0.91	<10	110	1	<10	0.10	20	24	5.88	0.02	0.03	0.02	0.024	<10	13	<10
ES-S-60	516637	7267877	-24.70338	-50.83552	Ponta Grossa	<0.2	<0.5	11	438	<2	11	10	31	0.81	<10	124	<1	<10	0.10	9	10	1.81	0.03	0.07	0.01	0.020	<10	4	<10
ES-S-61	516769	7264933	-24.72996	-50.83418	Ponta Grossa	<0.2	<0.5	22	454	<2	12	15	57	1.38	<10	174	1	<10	0.27	15	12	3.57	0.05	0.15	0.02	0.046	<10	7	<10
ES-S-62	519637	7271135	-24.67392	-50.80591	Ponta Grossa	<0.2	<0.5	21	342	2	13	18	43	0.58	<10	85	<1	<10	0.09	10	18	2.12	0.02	0.04	0.02	0.014	<10	4	<10
ES-S-63	518218	7261590	-24.76014	-50.81981	Ponta Grossa	<0.2	<0.5	11	181	2	8	9	30	0.79	<10	87	<1	<10	0.11	6	10	1.75	0.07	0.09	0.02	0.015	<10	3	<10
ES-S-64	522086	7256979	-24.80173	-50.78148	Ponta Grossa	<0.2	<0.5	5	75	<2	4	5	15	0.24	<10	37	<1	<10	0.03	2	3	0.57	0.01	0.02	0.02	0.006	<10	1	<10
ES-S-65	518149	7257901	-24.79346	-50.82045	Ponta Grossa	<0.2	<0.5	19	492	<2	10	12	73	1.08	<10	100	<1	<10	0.16	12	12	3.60	0.03	0.10	0.02	0.027	<10	7	<10
ES-S-66	519708	7251349	-24.85261	-50.80493	Ponta Grossa	<0.2	<0.5	13	287	<2	9	8	35	1.07	<10	112	<1	<10	0.12	7	8	1.65	0.07	0.11	0.02	0.011	<10	3	<10
ES-S-67	526520	7252182	-24.84498	-50.73752	Ponta Grossa	<0.2	<0.5	11	98	<2	3	<2	18	0.25	<10	42	<1	<10	0.03	3	4	0.53	0.01	0.02	0.02	0.006	<10	1	<10
ES-S-68	505014	7248283	-24.88042	-50.95036	Ponta Grossa	<0.2	<0.5	39	852	2	21	21	113	1.09	<10	184	2	<10	0.37	24	19	5.59	0.06	0.23	0.03	0.040	<10	8	<10
ES-S-69	503925	7244764	-24.91220	-50.96113	Ponta Grossa	<0.2	<0.5	34	656	<2	16	19	102	0.96	<10	164	1	<10	0.21	20	19	5.08	0.04	0.16	0.02	0.039	<10	7	<10
ES-S-70	500941	7238934	-24.96486	-50.99068	Ponta Grossa	<0.2	<0.5	15	445	<2	12	14	55	0.52	10	137	<1	<10	0.17	10	10	2.11	0.04	0.13	0.02	0.019	<10	3	<10
ES-S-71	513098	7236573	-24.98612	-50.87022	Ponta Grossa	<0.2	<0.5	78	1409	4	27	21	78	3.02	21	247	2	<10	0.21	25	34	6.78	0.09	0.14	0.03	0.039	<10	16	<10
ES-S-72	509655	7244348	-24.91593	-50.90439	Ponta Grossa	<0.2	<0.5	25	673	<2	15	15	61	0.98	<10	207	1	<10	0.24	13	14	2.37	0.11	0.20	0.03	0.019	<10	4	<10
ES-S-73	512655	7242867	-24.92929	-50.87466	Ponta Grossa	<0.2	<0.5	22	364	<2	13	11	44	1.20	<10	166	1	<10	0.22	9	11	2.02	0.11	0.16	0.03	0.014	<10	4	<10
ES-S-74	512681	7242699	-24.93080	-50.87440	Ponta Grossa	<0.2	<0.5	23	624	5	15	15	56	1.32	<10	199	1	<10	0.22	11	16	2.66	0.13	0.21	0.03	0.017	<10	5	<10
ES-S-75	510963	7246620	-24.89541	-50.89145	Ponta Grossa	<0.2	<0.5	21	492	<2	12	10	51	0.96	<10	173	<1	<10	0.20	10	11	2.07	0.10	0.19	0.03	0.015	<10	4	<10
ES-S-76	507787	7245836	-24.90251	-50.92289	Ponta Grossa	<0.2	<0.5	23	654	5	15	19	78	0.93	<10	144	1	<10	0.27	17	17	3.50	0.06	0.20	0.03	0.039	<10	5	<10
ES-S-77	511163	7242725	-24.93058	-50.88944	Ponta Grossa	<0.2	<0.5	16	723	2	11	13	31	0.87	<10	169	<1	<10	0.12	10	10	1.80	0.07	0.11	0.03	0.013	<10	3	<10
ES-S-78	522315	7240572	-24.94990	-50.77895	Ponta Grossa	<0.2	<0.5	12	90	3	8	10	21	0.50	<10	58	<1	<10	0.05	3	5	0.62	0.03	0.03	0.02	0.008	<10	1	<10
ES-S-79	520233	7242329	-24.93406	-50.79960	Ponta Grossa	<0.2	<0.5	50	499	3	15	19	43	2.82	<10	235	1	<10	0.18	12	20	4.47	0.12	0.15	0.02	0.023	<10	11	<10
ES-S-80	519952	7243194	-24.92626	-50.80240	Ponta Grossa	<0.2	<0.5	16	367	<2	15	20	48	1.62	<10	183	1	<10	0.13	12	11	2.94	0.07	0.10	0.02	0.025	<10	4	<10
ES-S-81	530733	7243008	-24.92776	-50.69562	Ponta Grossa	<0.2	<0.5	14	122	<2	5	4	17	0.40	<10	49	<1	<10	0.02	3	6	0.87	0.01	0.02	0.02	0.010	<10	1	<10
ES-S-82	530742	7242859	-24.92910	-50.69553	Ponta Grossa	<0.2	<0.5	6	35	<2	3	2	8	0.19	<10	22	<1	<10	0.01	1	2	0.34	<0.01	<0.01	0.02	0.003	<10	<1	<10
ES-S-83	532808	7242176	-24.93523	-50.67505	Ponta Grossa	<0.2	<0.5	17	209	<2	12	8	27	1.52	<10	96	<1	<10	0.04	9	14	2.19	0.03	0.03	0.02	0.023	<10	4	<10
ES-S-84	534277	7241304	-24.94307	-50.66048	Ponta Grossa	<0.2	<0.5	16	353	<2	15	3	29	1.82	<10	106	<1	<10	0.06	11	18	2.25	0.06	0.05	0.02	0.033	<10	4	<10
ES-S-85	465141	7284184	-24.55580	-51.34422	Ponta Grossa	<0.2	<0.5	13	391	<2	9	11	27	1.38	<10	100	<1	<10	0.11	7	12	1.89	0.05	0.10	0.02	0.017	<10	3	<10
ES-S-86	459837	7281766	-24.57751	-51.39666	Ponta Grossa	<0.2	<0.5	135	2178	2	25	7	108	1.88	<10	217	2	<10	0.28	52	11	10.28	0.04	0.12	0.03	0.035	<10	23	<10
ES-S-87	459099	7286107	-24.53828	-51.40382	Ponta Grossa	<0.2	<0.5	46	632	<2	10	7	61	0.75	<10	81	<1	<10	0.11	15	12	3.97	0.03	0.05	0.02	0.016	<10	6	<10
ES-S-88	466908	7280306	-24.59086	-51.32686	Ponta Grossa	<0.2	<0.5	30	410	<2	10	3	45	0.71	<10	59	<1	<10	0.09	10	7	3.09	0.01	0.04	0.02	0.016	<10	6	<10
ES-S-89	473241	7276588	-24.62456	-51.26438	Ponta Grossa	<0.2	<0.5	28	250	<2	10	10	36	0.40	<10	53	<1	<10	0.09	7	7	1.88	0.03	0.05	0.02	0.009	<10	3	<10
ES-S-90	476688	7274711	-24.64157	-51.23035	Ponta Grossa	<0.2	<0.5	29	363	<2	10	4	36	0.44	<10	65	<1	<10	0.10	9	6	2.15	0.02	0.06	0.01	0.010	<10	4	<10
ES-S-91	478377	7264601	-24.73290	-51.21382	Ponta Grossa	<0.2	<0.5	18	271	<2	7	<2	27	0.29	<10	62	<1	<10	0.11	7	4	1.24	0.03	0.06	0.01	0.011	<10	2	<10
ES-S-92	479068	7266894	-24.71220	-51.20695	Ponta Grossa	<0.2	<0.5	38	441	3	10	4	36	0.59	<10	104	<1	<10	0.28	12	8	2.22	0.05	0.14	0.02	0.023	<10	7	<10
ES-S-93	483807	7260747	-24.76778	-51.16017	Ponta Grossa	<0.2	<0.5	11	258	<2	6	7	28	0.48	<10	86	<1	<10	0.14	4	6	0.72	0.04	0.12	0.02	0.012	<10	2	<10
ES-S-94	485061	7258348	-24.78945	-51.14779	Ponta Grossa	<0.2	<0.5	14	218	<2	8	7	32	0.92	<10	113	<1	<10	0.15	4	8	0.92	0.08	0.16	0.02	0.010	<10	2	<10
ES-S-95	486301	7264397	-24.73483	-51.13547	Ponta Grossa	<0.2	<0.5	16	312	<2	9	11	43	0.71	<10	104	<1	<10	0.18	6	10	1.47	0.06	0.16	0.02	0.016	<10	3	<10
ES-S-96	486683	7264052	-24.73795	-51.13169	Ponta Grossa	<0.2	<0.5	14	219	2	8	8	35	0.88	<10	122	<1	<10	0.22	4	9	1.04	0.12	0.26	0.03	0.013	<10	2	<10
ES-S-97	493663	7255074	-24.81908	-51.06271	Ponta Grossa	<0.2	<0.5	20	447	<2	11	13	64	0.83	<10	147	<1	<10	0.26	10	12	2.57	0.07	0.19	0.03	0.021	<10	4	<10
ES-S-98	491299	7254691	-24.82253	-51.08610	Ponta Grossa	<0.2	<0.5	14	437	<2	7	9	39	0.57	<10	101	<1	<10	0.19	8	8	1.59	0.04	0.12	0.02	0.023	<10	3	<10
ES-S-99	491270	7253761	-24.83093	-51.08639	Ponta Grossa	<0.2	<0.5	22	497	2	12	17	72	1.09	<10	185	<1	<10	0.33	11	15	2.55	0.11	0.28	0.03	0.021	<10	4	<10
ES-S-100	488942	7253532	-24.83298	-51.10944	Ponta Grossa	<0.2	<0.5	19	553	<2	10	20	73	0.73	<10	138	<1	15	0.27	11	13	2.45	0.05	0.18	0.02	0.031	<10	3	<10
ES-S-101	486738	7253098	-24.83688	-51.13125	Ponta Grossa	<0.2	<0.5	34	824	3	13	18	72	1.03	<10	201	1	<10	0.38	15	14	2.75	0.08	0.29	0.02	0.042	<10	4	<10
ES-S-102	487657	7250778	-24.85784	-51.12218	Ponta Grossa	<0.2	<0.5	25	623	3	12	17	68	1.07	13	191	1	<10	0.40	14	13	3.12	0.06	0.23	0.02	0.036	<10	4	<10

Geochemical grade assay for stream sediments collected in the Ponta Grossa district

(1continued/2)

Sample No.	Sr	Ti	V	W	Y	Zr	S
	ppm	%	ppm	ppm	ppm	ppm	%
ES-S-49	7	0.19	327	<10	6	77	0.022
ES-S-50	34	0.25	343	<10	31	60	0.008
ES-S-51	16	0.14	152	<10	8	32	0.011
ES-S-52	17	0.35	369	<10	7	42	0.007
ES-S-53	11	0.28	146	<10	7	51	0.010
ES-S-54	23	0.24	291	<10	24	74	0.013
ES-S-55	19	0.30	251	11	10	51	0.010
ES-S-56	17	0.24	239	<10	12	61	0.017
ES-S-57	12	0.41	469	<10	11	61	0.019
ES-S-58	25	0.45	572	<10	21	68	0.008
ES-S-59	10	0.37	508	<10	8	55	0.011
ES-S-60	10	0.04	57	<10	7	15	0.008
ES-S-61	20	0.05	135	<10	11	28	0.007
ES-S-62	8	0.20	142	<10	6	22	0.011
ES-S-63	10	0.10	81	<10	7	19	0.004
ES-S-64	2	0.12	30	<10	4	13	0.003
ES-S-65	13	0.30	266	<10	6	38	0.007
ES-S-66	11	0.07	36	<10	6	22	0.004
ES-S-67	3	0.05	25	<10	4	6	0.002
ES-S-68	25	0.32	526	<10	11	45	0.011
ES-S-69	16	0.31	404	<10	8	44	0.009
ES-S-70	14	0.13	113	<10	6	21	0.008
ES-S-71	23	0.22	232	<10	19	61	0.051
ES-S-72	23	0.11	95	<10	7	24	0.016
ES-S-73	17	0.06	46	<10	6	23	0.007
ES-S-74	21	0.08	68	<10	8	27	0.013
ES-S-75	19	0.08	72	<10	6	22	0.013
ES-S-76	22	0.24	231	<10	8	33	0.013
ES-S-77	14	0.03	44	<10	6	14	0.011
ES-S-78	4	0.01	12	<10	5	7	0.009
ES-S-79	25	0.06	106	<10	13	54	0.010
ES-S-80	20	<0.01	43	<10	10	27	0.010
ES-S-81	2	<0.01	12	<10	3	6	0.005
ES-S-82	1	<0.01	8	<10	2	3	0.002
ES-S-83	4	0.02	44	<10	6	15	0.009
ES-S-84	7	<0.01	41	<10	5	16	0.010
ES-S-85	12	0.04	47	<10	5	15	0.010
ES-S-86	21	0.41	617	<10	18	106	0.011
ES-S-87	10	0.31	316	<10	6	45	0.009
ES-S-88	7	0.23	218	<10	5	37	0.006
ES-S-89	8	0.16	142	<10	3	24	0.009
ES-S-90	9	0.15	151	<10	4	25	0.006
ES-S-91	10	0.09	85	<10	4	15	0.003
ES-S-92	15	0.07	101	<10	8	29	0.003
ES-S-93	13	0.05	26	<10	4	7	0.006
ES-S-94	16	0.03	19	<10	4	11	0.006
ES-S-95	17	0.17	88	<10	5	17	0.009
ES-S-96	19	0.04	26	<10	5	14	0.006
ES-S-97	19	0.27	194	<10	7	29	0.006
ES-S-98	12	0.15	100	<10	5	17	0.005
ES-S-99	24	0.27	134	<10	7	32	0.007
ES-S-100	18	0.26	203	<10	7	27	0.010
ES-S-101	26	0.15	131	<10	10	29	0.008
ES-S-102	27	0.16	128	<10	8	37	0.013

Geochemical grade assay for stream sediments collected in the Ponta Grossa district

Sample No.	UTM_E	UTM_N	Latitude	Longitude	Location	Ag	Cd	Cu	Mn	Mo	Ni	Pb	Zn	Al	As	Ba	Be	Bi	Ca	Co	Cr	Fe	K	Mg	Na	P	Sb	Sc	Sn
						ppm	ppm	ppm	ppm	ppm	ppm	ppm	ppm	%	ppm	ppm	ppm	ppm	%	ppm	ppm	%	%	%	%	%	ppm	ppm	ppm
ES-S-103	495310	7245126	-24.90893	-51.04644	Ponta Grossa	<0.2	<0.5	19	385	3	13	16	66	0.95	<10	172	<1	<10	0.29	7	13	1.88	0.08	0.25	0.02	0.022	<10	3	<10
ES-S-104	632899	7337603	-24.06813	-49.69276	Ponta Grossa	<0.2	<0.5	13	77	<2	9	10	29	1.21	<10	48	<1	<10	0.05	3	16	1.68	0.02	0.02	0.02	0.016	<10	4	<10
ES-S-105	631097	7333799	-24.10263	-49.71014	Ponta Grossa	<0.2	<0.5	27	582	<2	12	15	34	1.20	<10	110	<1	<10	0.09	9	15	2.95	0.03	0.02	0.02	0.018	<10	6	<10
ES-S-106	633006	7335930	-24.08323	-49.69155	Ponta Grossa	<0.2	<0.5	30	691	<2	11	5	36	0.76	<10	83	<1	<10	0.06	10	16	3.65	0.01	<0.01	0.02	0.014	<10	8	<10
ES-S-107	635733	7336561	-24.07730	-49.66479	Ponta Grossa	<0.2	<0.5	67	556	3	13	5	70	0.84	<10	89	1	11	0.29	16	8	5.43	0.04	0.07	0.02	0.055	<10	10	<10
ES-S-108	635568	7337025	-24.07312	-49.66646	Ponta Grossa	<0.2	<0.5	67	567	<2	11	9	72	1.07	<10	116	1	<10	0.27	17	8	4.59	0.04	0.07	0.02	0.061	<10	9	<10
ES-S-109	636146	7333699	-24.10311	-49.66046	Ponta Grossa	<0.2	<0.5	12	114	<2	2	2	12	0.27	<10	30	<1	<10	0.03	2	3	0.96	<0.01	<0.01	0.02	0.011	<10	2	<10
ES-S-110	637923	7336405	-24.07852	-49.64324	Ponta Grossa	<0.2	<0.5	73	560	3	15	5	89	0.77	<10	81	1	13	0.32	18	8	6.03	0.04	0.08	0.03	0.053	<10	9	<10
ES-S-111	636675	7337458	-24.06912	-49.65561	Ponta Grossa	<0.2	<0.5	42	615	2	13	5	65	0.56	<10	69	<1	<10	0.11	15	22	4.87	0.02	0.05	0.02	0.023	<10	7	<10
ES-S-112	633900	7333800	-24.10239	-49.68256	Ponta Grossa	<0.2	<0.5	59	369	<2	8	6	53	0.74	<10	87	1	12	0.13	13	5	5.20	0.02	0.02	0.01	0.043	<10	11	<10

Geochemical grade assay for stream sediments collected in the Ponta Grossa district

(2continued/2)

Sample No.	Sr	Ti	V	W	Y	Zr	S
	ppm	%	ppm	ppm	ppm	ppm	%
ES-S-103	23	0.12	70	<10	6	20	0.009
ES-S-104	6	0.04	55	<10	5	16	0.018
ES-S-105	10	0.11	92	<10	6	30	0.010
ES-S-106	7	0.23	233	<10	6	34	0.008
ES-S-107	16	0.22	408	<10	14	44	0.005
ES-S-108	16	0.16	246	<10	18	32	0.016
ES-S-109	4	0.12	42	<10	2	10	0.006
ES-S-110	17	0.26	493	<10	12	44	0.006
ES-S-111	8	0.19	473	<10	8	40	0.005
ES-S-112	9	0.12	306	<10	15	48	0.008

List of stream water collected in the Lomba Grande district

Sample No.	E-W		N-S	
CK-A- 1	22J	495450	UTM	6698500
CK-A- 2	22J	494900	UTM	6699000
CK-A- 3	22J	492450	UTM	6698150
CK-A- 4	22J	493000	UTM	6699100
CK-A- 5	22J	494800	UTM	6699550
CK-A- 6	22J	495000	UTM	6699650
CK-A- 7	22J	495700	UTM	6700200
CK-A- 8	22J	495850	UTM	6700400
CK-A- 9	22J	494250	UTM	6700350
CK-A- 10	22J	494150	UTM	6701550
CK-A- 11	22J	493200	UTM	6700600
CK-A- 12	22J	493100	UTM	6701400
CK-A- 13	22J	492200	UTM	6702000
CK-A- 14	22J	498150	UTM	6698500
CK-A- 15	22J	497700	UTM	6698500
CK-A- 16	22J	499300	UTM	6699550
CK-A- 17	22J	498800	UTM	6699350
CK-A- 18	22J	499100	UTM	6699650
CK-A- 19	22J	499550	UTM	6701100
CK-A- 20	22J	498200	UTM	6703000
CK-A- 21	22J	499050	UTM	6703100
CK-A- 22	22J	498500	UTM	6704000
CK-A- 23	22J	498700	UTM	6704000
CK-A- 24	22J	498650	UTM	6704650
CK-A- 25	22J	498650	UTM	6705000
CK-A- 26	22J	498300	UTM	6705200
CK-A- 27	22J	499150	UTM	6705800
CK-A- 28	22J	496450	UTM	6706100
CK-A- 29	22J	494200	UTM	6705600
CK-A- 30	22J	496900	UTM	6703400
CK-A- 31	22J	496050	UTM	6704250
CK-A- 32	22J	496100	UTM	6704400
CK-A- 33	22J	495250	UTM	6704300
CK-A- 34	22J	494100	UTM	6702900
CK-A- 35	22J	493800	UTM	6704000
CK-A- 36	22J	494750	UTM	6703700
CK-A- 37	22J	494900	UTM	6703700
CK-A- 38	22J	495300	UTM	6702750
CK-A- 39	22J	493350	UTM	6704900
CK-A- 40	22J	493200	UTM	6704900
CK-A- 41	22J	492300	UTM	6703450
CK-A- 42	22J	503750	UTM	6705700
CK-A- 43	22J	502850	UTM	6705300
CK-A- 44	22J	502900	UTM	6705450
CK-A- 45	22J	502400	UTM	6705350
CK-A- 46	22J	502700	UTM	6703000
CK-A- 47	22J	502900	UTM	6703050
CK-A- 48	22J	501750	UTM	6703600
CK-A- 49	22J	507400	UTM	6706700
CK-A- 50	22J	509500	UTM	6705950
CK-A- 51	22J	509400	UTM	6703850
CK-A- 52	22J	510000	UTM	6703900
CK-A- 53	22J	509000	UTM	6703500
CK-A- 54	22J	507950	UTM	6703000
CK-A- 55	22J	504750	UTM	6703850
CK-A- 56	22J	506300	UTM	6704050
CK-A- 57	22J	505700	UTM	6703800
CK-A- 58	22J	506700	UTM	6703200
CK-A- 59	22J	506450	UTM	6703150
CK-A- 60	22J	506600	UTM	6702900
CK-A- 61	22J	507150	UTM	6702000
CK-A- 62	22J	506650	UTM	6701700
CK-A- 63	22J	506700	UTM	6701450
CK-A- 64	22J	505800	UTM	6702150
CK-A- 65	22J	504850	UTM	6702500
CK-A- 66	22J	503900	UTM	6702950
CK-A- 67	22J	503900	UTM	6702100
CK-A- 68	22J	503900	UTM	6701100

Sample No.	E-W		N-S	
CK-A- 69	22J	505500	UTM	6701250
CK-A- 70	22J	505100	UTM	6700550
CK-A- 71	22J	504900	UTM	6699650
CK-A- 72	22J	504900	UTM	6699550
CK-A- 73	22J	504800	UTM	6698950
CK-A- 74	22J	504850	UTM	6699250
CK-A- 75	22J	502050	UTM	6700200
CK-A- 76	22J	502550	UTM	6699550
CK-A- 77	22J	502600	UTM	6701150
CK-A- 78	22J	503100	UTM	6700350
CK-A- 79	22J	503000	UTM	6700200
CK-A- 80	22J	503400	UTM	6700100
CK-A- 81	22J	503400	UTM	6698900
CK-A- 82	22J	503900	UTM	6700150
CK-A- 83	22J	503850	UTM	6700050
CK-A- 84	22J	503950	UTM	6699800
CK-A- 85	22J	502700	UTM	6698100
CK-A- 86	22J	501750	UTM	6698900
CK-A- 87	22J	500700	UTM	6698400
CK-A- 88	22J	501100	UTM	6697550
CK-A- 89	22J	501050	UTM	6700200
CK-A- 90	22J	501450	UTM	6701400
CK-A- 91	22J	501200	UTM	6701600
CK-A- 92	22J	501100	UTM	6701100
CK-A- 93	22J	500050	UTM	6700950
CK-A- 94	22J	502250	UTM	6694300
CK-A- 95	22J	500200	UTM	6693250
CK-A- 96	22J	501700	UTM	6691650
CK-A- 97	22J	513500	UTM	6704750
CK-A- 98	22J	513400	UTM	6704200
CK-A- 99	22J	511950	UTM	6703750
CK-A- 100	22J	511500	UTM	6702450
CK-A- 101	22J	512850	UTM	6701750
CK-A- 102	22J	513950	UTM	6705950
CK-A- 103	22J	515100	UTM	6705200
CK-A- 104	22J	515700	UTM	6706700
CK-A- 105	22J	515750	UTM	6703400
CK-A- 106	22J	509600	UTM	6697650
CK-A- 107	22J	510200	UTM	6698000
CK-A- 108	22J	511100	UTM	6698200
CK-A- 109	22J	511600	UTM	6698700
CK-A- 110	22J	512300	UTM	6698250
CK-A- 111	22J	512250	UTM	6696900
CK-A- 112	22J	511850	UTM	6697650
CK-A- 113	22J	511050	UTM	6697450
CK-A- 114	22J	510850	UTM	6696700
CK-A- 115	22J	510750	UTM	6696450
CK-A- 116	22J	510150	UTM	6697000
CK-A- 117	22J	509600	UTM	6696150
CK-A- 118	22J	508850	UTM	6696550
CK-A- 119	22J	511400	UTM	6695950
CK-A- 120	22J	510950	UTM	6694250
CK-A- 121	22J	510100	UTM	6695550
CK-A- 122	22J	509550	UTM	6695000
CK-A- 123	22J	514950	UTM	6699950
CK-A- 124	22J	514250	UTM	6699600
CK-A- 125	22J	514900	UTM	6699050
CK-A- 126	22J	513350	UTM	6699000
CK-A- 127	22J	515700	UTM	6699400
CK-A- 128	22J	515600	UTM	6699200
CK-A- 129	22J	516300	UTM	6698250
CK-A- 130	22J	507350	UTM	6701050
CK-A- 131	22J	507450	UTM	6601100
CK-A- 132	22J	507700	UTM	6700300
CK-A- 133	22J	508450	UTM	6701250
CK-A- 134	22J	517550	UTM	6700450
CK-A- 135	22J	516550	UTM	6700350
CK-A- 136	22J	516750	UTM	6699250

List of stream water collected in the Lomba Grande district

Sample No.	E-W		N-S	
CK-A- 137	22J	516650	UTM	6698900
CK-A- 138	22J	517500	UTM	6698250
CK-A- 139	22J	517400	UTM	6698050
CK-A- 140	22J	517900	UTM	6699500
CK-A- 141	22J	518900	UTM	6697800
CK-A- 142	22J	517350	UTM	6696050
CK-A- 143	22J	515500	UTM	6698400
CK-A- 144	22J	515600	UTM	6698450
CK-A- 145	22J	516550	UTM	6696650
CK-A- 146	22J	513800	UTM	6695850
CK-A- 147	22J	514050	UTM	6695850
CK-A- 148	22J	512700	UTM	6693450
CK-A- 149	22J	515530	UTM	6694200
CK-A- 150	22J	515550	UTM	6694200
CK-A- 151	22J	515400	UTM	6694000
CK-A- 152	22J	514450	UTM	6692450
CK-A- 153	22J	514050	UTM	6692150
CK-A- 154	22J	512850	UTM	6690900
CK-A- 155	22J	512950	UTM	6691100
CK-A- 156	22J	513650	UTM	6690400
CK-A- 157	22J	515500	UTM	6693000
CK-A- 158	22J	514700	UTM	6691250
CK-A- 159	22J	511800	UTM	6690900
CK-A- 160	22J	512950	UTM	6687850
CK-A- 161	22J	513050	UTM	6689200
CK-A- 162	22J	513350	UTM	6688800
CK-A- 163	22J	514350	UTM	6690150
CK-A- 164	22J	515000	UTM	6689600
CK-A- 165	22J	512450	UTM	6689550
CK-A- 166	22J	509700	UTM	6692700
CK-A- 167	22J	509600	UTM	6692850
CK-A- 168	22J	508300	UTM	6689550
CK-A- 169	22J	508250	UTM	6689800
CK-A- 170	22J	506550	UTM	6690350
CK-A- 171	22J	505800	UTM	6689800
CK-A- 172	22J	503150	UTM	6690450
CK-A- 173	22J	502950	UTM	6690250
CK-A- 174	22J	503200	UTM	6691950
CK-A- 175	22J	505400	UTM	6692600
CK-A- 176	22J	505950	UTM	6690700
CK-A- 177	22J	508150	UTM	6692950
CK-A- 178	22J	504650	UTM	6695800
CK-A- 179	22J	507900	UTM	6694450
CK-A- 180	22J	506100	UTM	6695350
CK-A- 181	22J	504550	UTM	6696400
CK-A- 182	22J	491600	UTM	6698850

Geochemical grade assay of stream water collected in the Lomba Grande district

Sample No.	Li	Be	Na	Mg	Al	Si	K	Ca	Sc	Ti	V	Cr	Mn	Fe	Co	Ni	Cu	Zn	Ga	Ge	As	Se	Br	Rb	Sr	Y	Zr	Nb	Mo	Ru	Pd	Ag	Cd	In
CK-A-01	<1	<0.1	2470	813	170	4440	1040	982	4	4.3	0.42	1.4	82.2	704	0.533	0.6	10.4	23.4	0.05	<0.01	0.43	<0.2	54	3.093	11.64	0.900	0.16	0.013	<0.1	<0.01	<0.01	<0.2	0.07	<0.001
CK-A-02	<1	<0.1	3370	1910	103	4220	599	2490	4	2.9	0.44	0.8	224.9	1310	1.099	0.6	1.4	5.1	0.04	<0.01	0.59	<0.2	107	2.356	23.63	0.251	0.08	<0.005	<0.1	<0.01	<0.01	<0.2	0.09	<0.001
CK-A-03	2	<0.1	3140	1150	85	6070	1380	1540	5	3.6	0.64	0.7	78.9	706	0.650	0.6	12.5	8.6	0.03	<0.01	0.76	<0.2	38	4.457	13.92	0.362	0.10	<0.005	<0.1	<0.01	<0.01	<0.2	0.05	<0.001
CK-A-04	2	<0.1	3080	975	54	6590	1700	1450	5	3.4	0.49	0.9	24.7	337	0.211	0.4	0.8	5.0	0.02	<0.01	0.29	<0.2	40	5.252	11.93	0.208	0.08	<0.005	<0.1	<0.01	<0.01	<0.2	0.03	<0.001
CK-A-05	<1	<0.1	3380	1290	84	4550	1860	2730	4	3.1	0.43	1.1	426.2	1160	1.334	0.9	1.7	6.6	0.05	<0.01	0.59	<0.2	48	6.141	19.07	0.271	0.07	<0.005	<0.1	<0.01	<0.01	<0.2	0.02	<0.001
CK-A-06	<1	<0.1	7300	7050	161	10400	1840	6230	8	5.1	0.83	1.7	323.8	991	1.678	2.0	5.4	10.1	0.05	<0.01	0.23	<0.2	59	5.247	32.96	0.473	0.04	<0.005	<0.1	<0.01	<0.01	<0.2	0.08	<0.001
CK-A-07	<1	<0.1	4590	1610	38	6820	2790	1810	5	3.9	0.48	0.8	88.4	611	0.653	1.1	5.9	5.0	0.03	<0.01	0.41	<0.2	48	7.862	17.87	0.211	0.06	<0.005	<0.1	<0.01	<0.01	<0.2	0.02	<0.001
CK-A-08	<1	<0.1	16500	9210	136	12100	1370	11800	9	6.7	1.63	1.5	184.5	470	0.716	1.3	1.4	1.8	0.06	0.02	0.16	0.4	55	3.222	47.51	0.174	0.05	<0.005	<0.1	<0.01	<0.01	<0.2	0.01	<0.001
CK-A-09	<1	<0.1	3850	752	82	6290	1850	959	4	3.3	0.61	0.7	30.2	184	0.181	0.5	1.1	4.3	0.03	0.01	1.22	<0.2	41	6.069	11.15	0.183	0.06	<0.005	<0.1	<0.01	<0.01	<0.2	0.03	<0.001
CK-A-10	<1	<0.1	4410	1530	81	6230	4960	1400	4	7.8	1.32	0.9	90.0	474	0.905	0.7	1.7	11.1	0.03	0.02	0.59	<0.2	48	11.456	17.36	0.946	0.36	<0.005	<0.1	<0.01	<0.01	<0.2	0.02	<0.001
CK-A-11	<1	<0.1	2950	538	61	4690	2090	<50	4	2.7	0.52	1.0	22.3	190	0.099	<0.3	0.6	3.3	0.03	0.01	0.17	<0.2	35	7.338	8.63	0.413	0.05	<0.005	<0.1	<0.01	<0.01	<0.2	0.01	<0.001
CK-A-12	<1	<0.1	2420	804	61	4240	954	203	3	2.7	0.40	0.9	31.8	266	0.247	<0.3	3.6	6.9	0.03	<0.01	0.35	<0.2	37	3.103	8.94	0.169	0.08	<0.005	<0.1	<0.01	<0.01	<0.2	0.02	<0.001
CK-A-13	<1	<0.1	2590	727	41	3860	968	134	3	2.6	0.34	0.8	35.3	195	0.228	<0.3	0.5	6.0	0.02	0.01	0.34	<0.2	34	3.238	8.32	0.141	0.10	<0.005	<0.1	<0.01	<0.01	<0.2	<0.01	<0.001
CK-A-14	<1	<0.1	5040	2590	65	9840	1570	2900	7	4.9	0.56	1.4	199.3	888	0.995	1.0	0.9	3.4	0.05	<0.01	0.31	<0.2	46	4.459	23.05	0.213	0.07	<0.005	<0.1	<0.01	<0.01	<0.2	0.02	<0.001
CK-A-15	1	<0.1	3540	1100	56	6540	2410	1690	5	3.6	0.36	1.6	265.5	721	1.191	0.5	0.7	3.6	0.05	<0.01	0.33	<0.2	42	6.465	15.80	0.162	0.04	<0.005	<0.1	<0.01	<0.01	<0.2	0.02	<0.001
CK-A-16	<1	<0.1	6890	5650	36	11000	884	5540	9	5.6	0.60	1.5	208.3	960	0.954	1.0	0.7	2.3	0.05	<0.01	0.30	<0.2	46	2.304	29.15	0.108	0.05	<0.005	<0.1	<0.01	<0.01	<0.2	0.01	<0.001
CK-A-17	<1	<0.1	5040	2450	52	9540	2900	2450	7	5.0	0.58	1.1	218.1	903	0.753	0.7	0.8	1.4	0.06	<0.01	0.30	<0.2	40	7.958	20.52	0.158	0.03	<0.005	<0.1	<0.01	<0.01	<0.2	0.01	<0.001
CK-A-18	<1	<0.1	4980	1850	71	9420	1580	2310	7	5.0	0.59	1.3	103.3	602	0.644	0.7	2.4	2.8	0.05	<0.01	0.31	<0.2	42	4.706	19.83	0.243	0.16	<0.005	<0.1	<0.01	<0.01	<0.2	0.01	<0.001
CK-A-19	<1	<0.1	4280	916	68	9300	1730	1080	7	4.5	0.57	1.0	65.8	334	0.611	0.4	0.4	1.4	0.04	<0.01	0.26	<0.2	42	4.885	13.51	0.272	0.06	<0.005	<0.1	<0.01	<0.01	<0.2	0.02	<0.001
CK-A-20	2	<0.1	8230	3250	35	13600	2700	5690	10	6.4	1.20	1.1	50.2	369	0.404	0.4	0.7	0.9	0.03	<0.01	0.33	<0.2	48	6.584	30.11	0.161	0.05	<0.005	<0.1	<0.01	<0.01	<0.2	0.01	<0.001
CK-A-21	1	<0.1	5820	1080	61	11500	1650	1710	8	5.3	0.77	1.0	37.9	266	0.441	0.8	2.2	2.8	0.03	<0.01	0.28	<0.2	33	4.240	16.13	0.190	0.12	<0.005	<0.1	<0.01	<0.01	<0.2	0.01	<0.001
CK-A-22	1	<0.1	6240	2310	108	9850	2650	3750	7	5.1	1.30	1.1	104.3	563	0.980	0.8	1.8	3.7	0.05	<0.01	0.30	<0.2	40	6.305	22.82	0.375	0.11	<0.005	<0.1	<0.01	<0.01	<0.2	0.03	<0.001
CK-A-23	1	0.1	4260	1170	207	7370	1860	1780	5	4.0	1.17	1.2	139.9	993	0.968	0.9	2.9	6.2	0.08	0.01	0.50	<0.2	41	4.990	17.24	0.551	0.22	<0.005	<0.1	<0.01	<0.01	<0.2	0.04	<0.001
CK-A-24	<1	<0.1	4760	1260	87	7520	2430	2010	5	3.7	0.71	0.9	164.2	693	0.853	0.5	0.9	3.0	0.06	<0.01	0.44	<0.2	39	6.136	17.71	0.255	0.12	<0.005	<0.1	<0.01	<0.01	<0.2	0.02	<0.001
CK-A-25	<1	0.1	4470	675	146	7320	1150	717	5	4.1	0.57	0.9	54.4	253	0.569	0.5	0.6	2.9	0.05	<0.01	0.31	<0.2	32	3.315	11.33	0.261	0.15	<0.005	<0.1	<0.01	<0.01	<0.2	0.03	<0.001
CK-A-26	<1	<0.1	3290	1360	169	6240	2010	1030	5	3.3	1.11	1.6	102.4	1010	1.017	0.7	4.0	3.3	0.07	<0.01	0.53	<0.2	38	6.292	17.31	0.601	0.15	<0.005	<0.1	<0.01	<0.01	<0.2	0.02	<0.001
CK-A-27	<1	<0.1	4390	836	127	7330	2250	928	5	4.1	0.89	0.9	17.2	143	0.211	0.3	1.2	2.7	0.04	<0.01	0.26	<0.2	33	6.106	13.03	0.445	0.14	<0.005	<0.1	<0.01	<0.01	<0.2	0.02	<0.001
CK-A-28	<1	0.1	3710	1810	288	6320	3380	2120	4	3.5	3.59	1.4	32.3	480	0.402	0.7	1.2	2.7	0.08	0.01	0.52	<0.2	49	9.206	21.10	0.672	0.20	<0.005	<0.1	<0.01	<0.01	<0.2	0.02	0.001
CK-A-29	<1	<0.1	3480	1330	214	6420	2060	1380	4	3.3	1.69	1.3	58.1	912	0.602	0.7	4.5	4.7	0.07	<0.01	0.51	<0.2	42	6.355	15.11	0.594	0.17	<0.005	<0.1	<0.01	<0.01	<0.2	0.01	<0.001
CK-A-30	<1	<0.1	4350	2780	279	8250	2680	2940	6	7.9	1.15	1.9	22.4	373	0.299	0.9	1.3	2.0	0.08	<0.01	0.21	<0.2	45	7.580	20.67	0.358	0.17	0.014	<0.1	<0.01	<0.01	<0.2	0.03	<0.001
CK-A-31	<1	<0.1	3790	1890	112	7530	2420	2110	5	4.1	0.87	1.4	97.7	576	0.838	0.9	1.4	3.0	0.05	0.01	0.34	<0.2	41	7.299	19.35	0.288	0.09	<0.005	<0.1	<0.01	<0.01	<0.2	0.02	<0.001
CK-A-32	1	0.1	3070	918	59	7450	2430	573	5	3.5	0.89	1.3	37.4	236	0.384	0.4	0.5	2.3	0.03	0.01	0.26	<0.2	34	7.661	13.97	0.253	0.06	<0.005	<0.1	<0.01	<0.01	<0.2	0.02	<0.001
CK-A-33	<1	<0.1	2840	1660	130	4730	1090	1890	4	2.4	0.97	1.1	54.8	1230	0.522	0.6	2.8	4.3	0.05	<0.01	0.80	<0.2	39	4.015	21.00	0.341	0.13	<0.005	<0.1	<0.01	<0.01	<0.2	0.01	<0.001
CK-A-34	<1	<0.1	5200	1500	75	7630	2380	1490	5	3.7	0.76	1.3	26.7	230	0.261	0.4	0.8	2.3	0.03	<0.01	0.24	<0.2	45	6.081	16.58	0.211	0.11	<0.005	<0.1	<0.01	<0.01	<0.2	0.01	<0.001
CK-A-35	<1	<0.1	3410	1410	101	2960	1810	988	2	1.8	1.12	1.1	44.5	688	0.251	<0.3	0.7	1.9	0.04	<0.01	0.60	<0.2	44	5.591	17.80	0.324	0.14	<0.005	<0.1	<0.01	<0.01	<0.2	<0.01	<0.001
CK-A-36	2	<0.1	5230	1810	109	10100	2440	2540	7	4.6	1.03	1.7	67.7	720	0.643	0.6	1.1	3.1	0.05	<0.01	0.49	<0.2	55	6.463	21.23	0.314	0.13	<0.005	<0.1	<0.01	<0.01	<0.2	0.01	<0.001
CK-A-37	<1	<0.1	3280	1130	54	5840	1580	1280	4	2.7	0.54	1.1	62.7	474	0.326	0.4	0.4	1.8	0.03	0.01	0.36	<0.2	42	4.736	14.16	0.170	0.08	<0.005	<0.1	<0.01	<0.01	<0.2	0.01	<0.001
CK-A-38	<1	<0.1	3510	1110	59	5180	2000	1240	4	2.8	0.56	1.2	91.7	571	0.402	0.3	1.3	2.8	0.04	<0.01	0.41	<0.2	44	6.155	12.96	0.180	0.09	<0.005	<0.1	<0.01	<0.01	<0.2	0.01	<0.001
CK-A-39	1	<0.1	4040	1570	66	7590	1850	1670	5	3.3	0.89	1.1	48.0	631	0.532	0.5	0.6	3.5	0.04	<0.01	0.52	<0.2	46	6.229	19.82	0.303	0.09	<0.005	<0.1	<0.01	<0.01	<0.2	0.01	<0.001
CK-A-40	2	0.1	5710	3590	126	9270	2960	2230	6	4.4	1.35	1.3	61.5	708	0.950	0.7	1.3	2.9	0.05	0.01	0.65	<0.2	42	9.477	23.26	0.481	0.21	<0.005	0.4	<0.01	<0.01	<0.2	0.02	<0.001
CK-A-41	<1	<0.1	5040	1300	48	6830	1980	1570	4	3.2	0.56	1.3	132.6	452	0.721	0.7	0.7	4.7	0.05	0.01	0.33	<0.2	57	5.769	16.50	0.237	0.07	<0.005	0.1	<0.01	<0.01	<0.2	0.02	<0.001
CK-A-42	<1	<0.1	4710	1770	127	7920	2590	2620	5	3.9	1.10	1.3	26.3	149	0.215	0.4	0.7	9.3	0.04	<0.01	0.26	0.2	45	6.597	18.29	0.209	0.06	<0.005	<0.1	<0.01	<0.01	<0.2	0.02	<0.001
CK-A-43	<1	<0.1	6630	2740	48	7630	2580	5050	5	3.9	1.22	1.5	203.2	758	1.008	0.4	1.5	6.0	0.06	<0.01	0.55	<0.2	50	7.062	26.04	0.128	0.06	<0.005	<0.1	<0.01	<0.01	<0.2	<0.01	<0.001
CK-A-44	<1	<0.1	4690	1790	65	7780	2370	2960	5	3.9	0.70	1.5	98.8	443	0.619	0.3	0.7	1.9	0.05	<0.01	0.35	<0.2	43	5.986	19.53	0.159	0.09	<0.005	<0.1	<0.01	<0.01	<0.2	0.01	<0.001
CK-A-45	<1	<0.1	4440	1270	40	7170	1630	1850	5	3.2	0.51	1.1	115.8	920	0.478	<0.3	0.3	1.1	0.05	<0.01	0.45	<0.2	40	4.977	17.65	0.134	0.06	<0.005	<0.1	<0.01	<0.01	<0.2	0.01	<0.001
CK-A-46	<1	<0.1	3510	915	36	6570	1830	918	4	2.9	0.51	1.4	12.7	138	0.130	<0.3	0.4	1.3	0.02	<0.01	0.21	<0.2	35	4.997	10.77	0.097	0.03	<0.005	<0.1	<0.01	<0.01	<0.2	0.01	<0.001
CK-A-47	<1	<0.1	2430	755	40	5130	1690	841	4	2.8	0.38	0.8	6.7	140	0.075	<0.3	0.3	0.9	0.01	<0.01	0.18	<0.2	38	5.599	11.93	0.140	0.04	<0.005	<0.1	<0.01	<0.01	<0.2	<0.01	<0.001
CK-A-48	<1	<0.1	3490	1200	20	6840	1370	1860	6	3.4	0.31	0.8	50.6	225	0.358	<0.3	0.4	0.7	0.01	<0.01	0.18	<0.2	31	4.344	15.22	0.102	0.03	<0.005	<0.1	<0.01	<0.01	<0.2	<0.01	<0.001
CK-A-49	<1	<0.1	4160	2350	100	10100	1570	3540	8	4.8	0.46	1.2	70.5	463	0.688	0.5	1.9	2.4	0.03	<0.01	0.21	<0.2	34	5.129	22.67	0.090	0.02	<0.005	<0.1	<0.01	<0.01	<0.2	0.01	<0.001
CK-A-50	<1	<0.1	3970	1770	49	8260	1330	2980	6	4.2	0.58	1.1	68.5	437	0.429	0.4	0.4	1.4	0.03	<0.01	0.23	<0.2	39	4.440	20.79	0.122	0.05	<0.005	<0.1	<0.01	<0.01	<0.2	0.01	<0.001
CK-A-51	<1	<0.1	3570	1530	43	7440	1320	2550	6	3.7	0.47	1.1	33.7	430	0.224	0.6	0.5	1.3	0.02	<0.01	0.26	<0.2	39	4.474	18.93	0.121	0.05	<0.005	<0.1	<0.01	<0.01	<0.2	0.01	<0.001
CK-A-52	<1	<0.1	2620	751	32	4890	848	894	3	2.2	0.17	0.9	23.8	392	0.116	<0.3	0.3	1.6	0.02	<0.01	0.31	<0.2	38	3.293	11.86	0.068	0.06	<0.005	<0.1	<0.01	<0.01	<0.2	0.01	<0.001
CK-A-53	<1	<0.1	2690	1200	68	5990	1150	1490	4	3.2	0.55	1.0	53.1	662	0.279	0.3	3.5	2.2	0.03	0.01	0.35	<0.2	42	3.978	15.04	0.132	0.08	<0.005	<0.1	<0.01	<0.01	<0.2	0.01	<0.001
CK-A-54	<1	<0.1	3040	1430	69	6740	1280	1900	5	4.4	0.63	1.0	60.8	651	0.375	0.3	3.1	1.4	0.03	<0.01	0.31	<0.2	47	4.390	17.01	0.128	0.09	<0.005	<0.1	<0.01	<0.01	<0.2	<0.01	<0.001
CK-A-55	<1	<0.1	3030	1150	55	5190	1070	1250	4	3.0	0.50	0.9	30.5	183	0.399	<0.3	0.3	1.5	0.03	<0.01	0.18	<0.2	35	3.079	14.02	0.165	0.05	<0.005	<0.1	<0.01	<0.01	<0.2	<0.01	<0.001
CK-A-56	<1	<0.1	2230	748	79	3520	1400	645	3	3.0	0.45	1.0	30.5	486	0.217	<0.3	0.3	1.1	0.03	<0.01	0.45	<0.2	42	4.081	10.79	0.179	0.12	<0.005	<0.1	<0.01	<0.01	<0.2	<0.01	<0.001
CK-A-57	<1	<0.1	2660	1050	97	3540	2330	1270	3	3.2	0.66	1.1	70.9	744	0.421	<0.3	0.5	1.3	0.05	<0.01	0.49	<0.2	41	5.705	14.34	0.184	0.12	0.006	<0.1	<0.01	<0.01	<0.2	<0.01	<0.001
CK-A-58	<1	<0.1	2060	704	87	3530	1280	599	3	2.8	0.49	0.9	18.3	511	0.127	<0.3	0.5	2.6	0.03	<0.01	0.34	<0.2	38	3.669	9.89	0.149	0.09	<0.005	<0.1	<0.01	<0.01	<0.2	<0.01	<0.001
CK-A-59	<1	<0.1	2260	1010	66	3170	1400	1140	3	2.3	0.47	0.9	31.9	696	0.177	<0.3	1.4	2.7	0.03	<0.01	0.37	<0.2	39	3.957	14.19	0.141	0.08	<0.005	<0.1	<0.01	<0.01	<0.2	0.01	<0.001
CK-A-60	<1	<0.1	2190	918	73	3420	1370	969	3	2.5	0.52	1.1	31.8	650	0.198	<0.3	0.4	1.8	0.03	<0.01	0.38	<0.2	39	3.959	12.67	0.152	0.09	<0.005	<0.1	<0.01	<0.01	<0.2	0.01	<0.001
CK-A-61	<1	<0.1	2290	847	85	3370	1370	927	3	2.5	0.60	1.0	23.8	623	0.178	<0.3	0.5	1.6	0.03	<0.01	0.38	<0.2	38	4.169	12.78	0.156	0.09	<0.005	<0.1	<0.01	<0.01	<0.2	<0.01	<0.001

Geochemical grade assay of stream water collected in the Lomba Grande district

(1continued/3)

Sample No.	Sn	Sb	Te	I	Cs	Ba	La	Ce	Pr	Nd	Sm	Eu	Gd	Tb	Dy	Ho	Er	Tm	Yb	Lu	Hf	Ta	W	Re	Os	Pt	Au	Hg	Tl	Pb	Bi	Th
CK-A-01	33.9	0.39	<0.01	8	0.028	57.4	0.935	1.113	0.248	0.937	0.359	0.033	0.283	0.039	0.142	0.026	0.068	0.007	0.045	0.007	0.008	<0.001	0.08	<0.001	<0.002	<0.01	<0.002	<0.2	0.029	44.5	0.01	0.057
CK-A-02	<0.1	0.07	<0.01	13	0.038	43.0	0.278	0.718	0.083	0.333	0.092	0.024	0.084	0.009	0.043	0.008	0.021	0.003	0.022	0.005	0.003	<0.001	<0.02	<0.001	<0.002	<0.01	<0.002	<0.2	0.015	0.8	0.01	0.046
CK-A-03	<0.1	0.10	<0.01	7	0.032	44.9	0.279	0.660	0.078	0.330	0.105	0.032	0.099	0.012	0.052	0.011	0.030	0.004	0.032	0.005	0.004	<0.001	<0.02	<0.001	<0.002	<0.01	<0.002	<0.2	0.020	1.0	0.01	0.039
CK-A-04	<0.1	0.12	0.01	10	0.035	47.8	0.133	0.314	0.039	0.173	0.052	0.023	0.050	0.007	0.033	0.007	0.019	0.002	0.017	0.003	0.005	<0.001	<0.02	<0.001	<0.002	<0.01	<0.002	<0.2	0.023	0.3	0.01	0.024
CK-A-05	<0.1	0.03	0.02	12	0.034	55.8	0.162	0.422	0.050	0.219	0.068	0.026	0.074	0.008	0.039	0.007	0.022	0.003	0.023	0.003	<0.002	<0.001	<0.02	<0.001	<0.002	<0.01	<0.002	<0.2	0.032	0.6	<0.01	0.033
CK-A-06	<0.1	0.04	<0.01	12	0.121	43.6	0.539	1.256	0.149	0.549	0.169	0.040	0.147	0.019	0.077	0.016	0.046	0.006	0.040	0.006	<0.002	<0.001	<0.02	<0.001	<0.002	<0.01	<0.002	<0.2	0.042	3.9	<0.01	0.029
CK-A-07	<0.1	0.04	0.02	11	0.048	53.8	0.073	0.192	0.023	0.109	0.038	0.014	0.039	0.005	0.031	0.006	0.021	0.003	0.022	0.003	0.002	<0.001	<0.02	<0.001	<0.002	<0.01	<0.002	<0.2	0.036	0.7	0.01	0.016
CK-A-08	<0.1	0.07	<0.01	19	0.026	26.9	0.131	0.285	0.039	0.153	0.047	0.016	0.042	0.007	0.029	0.005	0.016	0.003	0.017	0.003	0.002	<0.001	<0.02	<0.001	<0.002	<0.01	<0.002	<0.2	0.014	0.3	<0.01	0.018
CK-A-09	<0.1	0.05	<0.01	7	0.055	40.3	0.108	0.264	0.030	0.121	0.041	0.016	0.042	0.007	0.026	0.006	0.017	0.002	0.017	0.003	<0.002	<0.001	<0.02	<0.001	<0.002	<0.01	<0.002	<0.2	0.019	0.5	<0.01	0.017
CK-A-10	<0.1	0.05	<0.01	7	0.131	51.9	0.203	0.484	0.060	0.263	0.075	0.028	0.088	0.015	0.103	0.027	0.075	0.009	0.078	0.010	0.014	<0.001	<0.02	<0.001	<0.002	<0.01	<0.002	<0.2	0.061	0.4	0.02	0.014
CK-A-11	<0.1	0.04	<0.01	5	0.114	36.6	0.080	0.178	0.025	0.106	0.044	0.017	0.055	0.010	0.052	0.010	0.030	0.004	0.032	0.005	0.004	<0.001	<0.02	<0.001	<0.002	<0.01	<0.002	<0.2	0.032	0.2	<0.01	0.009
CK-A-12	<0.1	0.05	<0.01	3	0.050	25.5	0.131	0.351	0.045	0.182	0.050	0.015	0.047	0.006	0.026	0.005	0.016	0.003	0.018	0.003	0.003	<0.001	<0.02	<0.001	<0.002	<0.01	<0.002	<0.2	0.021	0.3	<0.01	0.015
CK-A-13	<0.1	0.05	<0.01	3	0.041	28.2	0.084	0.212	0.026	0.104	0.031	0.011	0.032	0.005	0.017	0.004	0.013	0.002	0.013	0.002	0.003	<0.001	<0.02	<0.001	<0.002	<0.01	<0.002	<0.2	0.019	0.2	<0.01	0.011
CK-A-14	<0.1	0.07	0.02	8	0.043	41.7	0.164	0.398	0.048	0.186	0.056	0.023	0.050	0.007	0.036	0.007	0.021	0.002	0.016	0.003	0.004	<0.001	<0.02	<0.001	<0.002	<0.01	<0.002	<0.2	0.017	0.3	<0.01	0.026
CK-A-15	<0.1	0.08	<0.01	7	0.032	76.6	0.075	0.202	0.022	0.094	0.033	0.022	0.041	0.005	0.025	0.005	0.017	0.002	0.012	0.002	<0.002	<0.001	<0.02	<0.001	<0.002	<0.01	<0.002	<0.2	0.028	0.3	<0.01	0.021
CK-A-16	<0.1	0.07	<0.01	10	0.027	39.1	0.106	0.275	0.029	0.112	0.032	0.014	0.034	0.004	0.018	0.004	0.011	0.002	0.010	0.002	<0.002	<0.001	<0.02	<0.001	<0.002	<0.01	<0.002	<0.2	0.008	0.2	<0.01	0.017
CK-A-17	<0.1	0.07	<0.01	7	0.028	50.3	0.120	0.299	0.032	0.137	0.043	0.017	0.038	0.006	0.025	0.005	0.012	0.002	0.016	0.002	<0.002	<0.001	<0.02	<0.001	<0.002	<0.01	<0.002	<0.2	0.016	0.2	<0.01	0.020
CK-A-18	0.1	0.09	<0.01	8	0.025	41.0	0.171	0.385	0.047	0.200	0.064	0.021	0.062	0.009	0.035	0.008	0.024	0.003	0.020	0.003	0.003	<0.001	<0.02	<0.001	<0.002	<0.01	<0.002	<0.2	0.017	0.4	<0.01	0.027
CK-A-19	<0.1	0.08	<0.01	6	0.034	42.1	0.136	0.352	0.039	0.172	0.060	0.023	0.063	0.009	0.040	0.009	0.022	0.003	0.025	0.003	0.004	<0.001	<0.02	<0.001	<0.002	<0.01	<0.002	<0.2	0.028	0.3	<0.01	0.022
CK-A-20	<0.1	0.09	<0.01	5	0.019	59.6	0.084	0.220	0.029	0.108	0.038	0.021	0.038	0.004	0.024	0.005	0.015	0.002	0.015	0.003	<0.002	<0.001	<0.02	<0.001	<0.002	<0.01	<0.002	<0.2	0.016	0.2	<0.01	0.020
CK-A-21	<0.1	0.07	<0.01	3	0.020	43.0	0.121	0.294	0.037	0.170	0.062	0.019	0.053	0.006	0.031	0.006	0.017	0.002	0.019	0.003	0.005	<0.001	<0.02	<0.001	<0.002	<0.01	<0.002	<0.2	0.016	0.4	<0.01	0.019
CK-A-22	<0.1	0.07	0.01	5	0.042	61.2	0.215	0.561	0.067	0.289	0.100	0.037	0.098	0.012	0.059	0.012	0.031	0.004	0.032	0.005	0.005	<0.001	<0.02	<0.001	<0.002	<0.01	<0.002	<0.2	0.026	0.4	<0.01	0.039
CK-A-23	<0.1	0.09	0.03	8	0.043	49.7	0.454	1.140	0.134	0.548	0.178	0.052	0.177	0.019	0.092	0.018	0.053	0.006	0.047	0.006	0.012	<0.001	<0.02	<0.001	<0.002	<0.01	<0.002	<0.2	0.023	1.1	<0.01	0.072
CK-A-24	<0.1	0.07	<0.01	6	0.048	52.1	0.141	0.373	0.043	0.171	0.058	0.022	0.057	0.008	0.038	0.008	0.021	0.003	0.023	0.003	0.005	<0.001	<0.02	<0.001	<0.002	<0.01	<0.002	<0.2	0.029	0.4	<0.01	0.038
CK-A-25	<0.1	0.06	<0.01	4	0.032	30.6	0.099	0.260	0.029	0.121	0.047	0.021	0.049	0.008	0.043	0.008	0.024	0.003	0.022	0.004	0.009	<0.001	<0.02	<0.001	<0.002	<0.01	<0.002	<0.2	0.017	0.3	<0.01	0.027
CK-A-26	<0.1	0.07	<0.01	4	0.054	47.1	0.410	1.005	0.120	0.512	0.166	0.048	0.157	0.021	0.108	0.019	0.054	0.007	0.051	0.007	0.007	<0.001	<0.02	<0.001	<0.002	<0.01	<0.002	<0.2	0.030	0.8	<0.01	0.047
CK-A-27	<0.1	0.10	<0.01	4	0.062	35.3	0.121	0.305	0.042	0.175	0.068	0.028	0.077	0.012	0.065	0.012	0.040	0.005	0.037	0.006	0.007	<0.001	<0.02	<0.001	<0.002	<0.01	<0.002	<0.2	0.027	0.3	0.01	0.012
CK-A-28	<0.1	0.06	0.02	4	0.116	47.4	0.974	2.241	0.261	0.956	0.267	0.068	0.237	0.029	0.129	0.023	0.063	0.007	0.055	0.008	0.011	<0.001	<0.02	<0.001	<0.002	<0.01	<0.002	<0.2	0.039	1.0	<0.01	0.041
CK-A-29	<0.1	0.06	<0.01	6	0.063	43.2	0.533	1.348	0.151	0.585	0.189	0.050	0.181	0.022	0.101	0.020	0.052	0.006	0.044	0.008	0.007	<0.001	<0.02	<0.001	<0.002	<0.01	<0.002	<0.2	0.033	1.0	<0.01	0.058
CK-A-30	<0.1	0.07	<0.01	6	0.072	51.4	0.199	0.508	0.059	0.265	0.094	0.034	0.090	0.012	0.061	0.012	0.031	0.004	0.036	0.005	0.008	<0.001	<0.02	<0.001	<0.002	<0.01	<0.002	<0.2	0.028	0.4	<0.01	0.033
CK-A-31	<0.1	0.06	<0.01	5	0.078	51.7	0.221	0.558	0.062	0.250	0.079	0.030	0.083	0.010	0.045	0.010	0.027	0.003	0.027	0.004	0.004	<0.001	<0.02	<0.001	<0.002	<0.01	<0.002	<0.2	0.036	0.5	<0.01	0.026
CK-A-32	<0.1	0.05	<0.01	3	0.070	58.7	0.120	0.350	0.039	0.162	0.056	0.026	0.062	0.008	0.042	0.007	0.023	0.003	0.020	0.003	0.003	<0.001	<0.02	<0.001	<0.002	<0.01	<0.002	<0.2	0.044	0.3	<0.01	0.014
CK-A-33	<0.1	0.05	<0.01	7	0.060	31.2	0.455	1.048	0.130	0.517	0.143	0.037	0.130	0.015	0.059	0.012	0.030	0.003	0.031	0.005	0.007	<0.001	<0.02	<0.001	<0.002	<0.01	<0.002	<0.2	0.017	0.6	<0.01	0.059
CK-A-34	<0.1	0.06	0.01	4	0.038	41.2	0.130	0.371	0.040	0.160	0.060	0.020	0.056	0.007	0.033	0.006	0.022	0.002	0.023	0.004	0.005	<0.001	<0.02	<0.001	<0.002	<0.01	<0.002	<0.2	0.024	0.3	<0.01	0.024
CK-A-35	<0.1	0.09	<0.01	4	0.069	31.4	0.472	1.008	0.127	0.503	0.146	0.039	0.126	0.015	0.063	0.011	0.034	0.004	0.028	0.004	0.007	<0.001	<0.02	<0.001	<0.002	<0.01	<0.002	<0.2	0.017	0.6	0.01	0.044
CK-A-36	<0.1	0.07	<0.01	5	0.063	56.2	0.254	0.701	0.080	0.330	0.096	0.034	0.094	0.011	0.053	0.010	0.033	0.004	0.034	0.005	0.005	<0.001	<0.02	<0.001	<0.002	<0.01	<0.002	<0.2	0.028	0.4	<0.01	0.042
CK-A-37	<0.1	0.04	<0.01	7	0.030	37.4	0.124	0.313	0.037	0.156	0.040	0.019	0.049	0.007	0.028	0.005	0.017	0.002	0.017	0.003	0.003	<0.001	<0.02	<0.001	<0.002	<0.01	<0.002	<0.2	0.016	0.2	<0.01	0.024
CK-A-38	<0.1	0.04	<0.01	9	0.038	39.3	0.112	0.286	0.033	0.130	0.042	0.018	0.051	0.006	0.028	0.006	0.019	0.002	0.017	0.002	0.005	<0.001	<0.02	<0.001	<0.002	<0.01	<0.002	<0.2	0.021	0.3	<0.01	0.023
CK-A-39	<0.1	0.04	0.02	8	0.045	50.2	0.285	0.696	0.085	0.344	0.104	0.033	0.096	0.012	0.054	0.009	0.029	0.003	0.029	0.004	0.005	<0.001	<0.02	<0.001	<0.002	<0.01	<0.002	<0.2	0.023	0.5	<0.01	0.037
CK-A-40	<0.1	10.56	<0.01	6	0.113	82.2	0.397	1.066	0.120	0.507	0.157	0.048	0.147	0.016	0.075	0.015	0.042	0.006	0.040	0.006	0.008	<0.001	<0.02	<0.001	<0.002	<0.01	<0.002	<0.2	0.039	0.5	0.01	0.050
CK-A-41	<0.1	0.07	<0.01	6	0.045	50.7	0.098	0.239	0.034	0.142	0.041	0.022	0.046	0.006	0.029	0.007	0.020	0.002	0.022	0.003	0.004	<0.001	<0.02	<0.001	<0.002	<0.01	<0.002	<0.2	0.028	0.3	0.01	0.019
CK-A-42	<0.1	0.04	0.01	5	0.041	42.3	0.088	0.206	0.024	0.094	0.034	0.017	0.040	0.007	0.029	0.006	0.016	0.002	0.020	0.003	0.003	<0.001	<0.02	<0.001	<0.002	<0.01	<0.002	<0.2	0.020	0.3	<0.01	0.012
CK-A-43	<0.1	0.04	0.01	11	0.038	47.9	0.122	0.315	0.033	0.125	0.035	0.020	0.038	0.005	0.021	0.004	0.014	0.002	0.013	0.002	0.002	<0.001	<0.02	<0.001	<0.002	<0.01	<0.002	<0.2	0.021	0.4	<0.01	0.018
CK-A-44	<0.1	0.04	<0.01	6	0.052	44.4	0.080	0.216	0.022	0.101	0.030	0.014	0.034	0.005	0.020	0.005	0.015	0.002	0.015	0.003	<0.002	<0.001	<0.02	<0.001	<0.002	<0.01	<0.002	<0.2	0.022	0.2	<0.01	0.017
CK-A-45	<0.1	0.03	<0.01	7	0.025	33.9	0.085	0.242	0.026	0.105	0.031	0.014	0.035	0.004	0.023	0.004	0.015	0.001	0.011	0.002	0.003	<0.001	<0.02	<0.001	<0.002	<0.01	<0.002	<0.2	0.011	0.2	<0.01	0.023
CK-A-46	<0.1	0.06	0.02	4	0.040	23.5	0.051	0.119	0.016	0.059	0.023	0.010	0.023	0.003	0.014	0.003	0.010	0.001	0.010	0.002	<0.002	<0.001	<0.02	<0.001	<0.002	<0.01	<0.002	<0.2	0.009	0.3	<0.01	0.010
CK-A-47	<0.1	0.02	<0.01	4	0.045	30.1	0.073	0.176	0.023	0.100	0.032	0.013	0.036	0.005	0.022	0.004	0.013	0.002	0.012	0.002	0.002	<0.001	<0.02	<0.001	<0.002	<0.01	<0.002	<0.2	0.014	0.3	<0.01	0.014
CK-A-48	<0.1	0.02	<0.01	7	0.017	36.8	0.050	0.143	0.015	0.061	0.022	0.013	0.023	0.004	0.017	0.003	0.008	<0.001	0.010	0.002	0.003	<0.001	<0.02	<0.001	<0.002	<0.01	<0.002	<0.2	0.013	0.2	<0.01	0.013
CK-A-49	<0.1	0.05	<0.01	7	0.049	43.2	0.060	0.180	0.017	0.063	0.020	0.013	0.025	0.004	0.016	0.003	0.008	0.001	0.012	0.002	<0.002	<0.001	<0.02	<0.001	<0.002	<0.01	<0.002	<0.2	0.020	0.2	<0.01	0.011
CK-A-50	<0.1	0.02	<0.01	7	0.050	31.9	0.119	0.307	0.032	0.126	0.039	0.013	0.033	0.004	0.022	0.004	0.012	0.001	0.011	0.002	<0.002	<0.001	<0.02	<0.001	<0.002	<0.01	<0.002	<0.2	0.014	0.2	<0.01	0.019
CK-A-51	<0.1	0.02	<0.01	7	0.037	29.3	0.100	0.254	0.029	0.114	0.025	0.011	0.037	0.004	0.016	0.004	0.013	0.001	0.011	0.002	0.004	<0.001	<0.02	<0.001	<0.002	<0.01	<0.002	<0.2	0.014	0.2	<0.01	0.017
CK-A-52	<0.1	0.03	<0.01	4	0.047	22.5	0.049	0.124	0.016	0.065	0.015	0.008	0.017	0.002	0.010	0.002	0.005	<0.001	0.008	0.002	0.003	<0.001	<0.02	<0.001	<0.002	<0.01	<0.002	<0.2	0.009	0.2	<0.01	0.014
CK-A-53	<0.1	0.02	<0.01	7	0.060	26.7	0.141	0.379	0.038	0.174	0.049	0.014	0.042	0.005	0.022	0.005	0.015	0.001	0.016	0.002	0.002	<0.001	<0.02	<0.001	<0.002	<0.01	<0.002	<0.2	0.020	0.3	<0.01	0.024
CK-A-54	<0.1	0.02	<0.01	7	0.061	31.1	0.120	0.342	0.034	0.139	0.039	0.015	0.039	0.004	0.024	0.004	0.012	0.002	0.013	0.002	0.004	<0.001	<0.02	<0.001	<0.002	<0.01	<0.002	<0.2	0.021	0.3	<0.01	0.023
CK-A-55	<0.1	0.02	<0.01	3	0.050	31.4	0.091	0.260	0.026	0.099	0.031	0.014	0.044	0.005	0.027	0.006	0.015	0.002	0.016	0.002	0.004	<0.001	<0.02	<0.001	<0.002	<0.01	<0.002	<0.2	0.019	0.3	<0.01	0.013
CK-A-56	<0.1	0.02	<0.01	5	0.077	23.0	0.150	0.413	0.044	0.189	0.055	0.015	0.048	0.007	0.030	0.006	0.019	0.002	0.016	0.002	0.003	<0.001	<0.02	<0.001	<0.002	<0.01	<0.002	<0.2	0.021	0.2	<0.01	0.021
CK-A-57	<0.1	0.02	<0.01	5	0.088	31.1	0.165	0.437	0.046	0.182	0.057	0.017	0.055	0.006	0.033	0.006	0.017	0.002	0.020	0.002	0.005	<0.001	<0.02	<0.001	<0.002	<0.01	<0.002	<0.2	0.026	0.3	<0.01	0.026
CK-A-58	<0.1	0.02	0.02	4	0.063	21.0	0.137	0.375	0.040	0.164	0.045	0.014	0.044	0.005	0.027	0.004	0.016	0.002	0.015	0.002	0.004	<0.001	<0.02	<0.001	<0.002	<0.01	<0.002	<0.2	0.016	0.2	<0.01	0.018
CK-A-59	<0.1	0.02	<0.01	5	0.050	26.6	0.120	0.318	0.034	0.132	0.037	0.014	0.044	0.005	0.023	0.004	0.014	0.002	0.014	0.003	0.003	<0.001	<0.02	<0.001	<0.002	<0.01	<0.002	<0.2	0.015	0.6	<0.01	0.020
CK-A-60	<0.1	0.04	<0.01	5	0.065	24.4	0.132	0.361	0.040	0.142	0.047	0.013	0.045	0.005	0.027	0.005	0.015	0.002	0.017	0.003	0.006	<0.001	<0.02	<0.001	<0.002	<0.01	<0.002	<0.2	0.016	0.2	<0.01	0.022
CK-A-61	<0.1	0.01	<0.01	5	0.055	24.1	0.141	0.414	0.042	0.151	0.044	0.013	0.045	0.005	0.031	0.005	0.014	0.002	0.013	0.003	0.005	<0.001	<0.02	<0.001	<0.002	<0.01	<0.002	<0.2	0.016	0.3	<0.01	0.024

Geochemical grade assay of stream water collected in the Lomba Grande district

(1continued/3)

Sample No.	U	SO_4
CK-A-01	0.040	14
CK-A-02	0.023	9
CK-A-03	0.024	16
CK-A-04	0.014	15
CK-A-05	0.013	15
CK-A-06	0.025	26
CK-A-07	0.012	18
CK-A-08	0.022	52
CK-A-09	0.013	18
CK-A-10	0.020	11
CK-A-11	0.010	12
CK-A-12	0.013	14
CK-A-13	0.010	15
CK-A-14	0.016	15
CK-A-15	0.010	17
CK-A-16	0.011	11
CK-A-17	0.012	18
CK-A-18	0.015	16
CK-A-19	0.014	18
CK-A-20	0.018	18
CK-A-21	0.014	16
CK-A-22	0.027	15
CK-A-23	0.043	14
CK-A-24	0.017	16
CK-A-25	0.021	19
CK-A-26	0.034	12
CK-A-27	0.020	14
CK-A-28	0.081	12
CK-A-29	0.046	13
CK-A-30	0.020	17
CK-A-31	0.018	13
CK-A-32	0.017	14
CK-A-33	0.039	9
CK-A-34	0.014	20
CK-A-35	0.039	9
CK-A-36	0.024	19
CK-A-37	0.013	16
CK-A-38	0.015	17
CK-A-39	0.026	14
CK-A-40	0.041	15
CK-A-41	0.009	15
CK-A-42	0.010	16
CK-A-43	0.017	17
CK-A-44	0.010	17
CK-A-45	0.010	14
CK-A-46	0.006	15
CK-A-47	0.011	14
CK-A-48	0.005	17
CK-A-49	0.008	10
CK-A-50	0.007	12
CK-A-51	0.007	11
CK-A-52	0.005	11
CK-A-53	0.012	10
CK-A-54	0.012	9
CK-A-55	0.010	14
CK-A-56	0.020	11
CK-A-57	0.020	13
CK-A-58	0.015	10
CK-A-59	0.013	11
CK-A-60	0.015	9
CK-A-61	0.017	10

Geochemical grade assay of stream water collected in the Lomba Grande district

Sample No.	Li	Be	Na	Mg	Al	Si	K	Ca	Sc	Ti	V	Cr	Mn	Fe	Co	Ni	Cu	Zn	Ga	Ge	As	Se	Br	Rb	Sr	Y	Zr	Nb	Mo	Ru	Pd	Ag	Cd	In
CK-A-62	<1	<0.1	2050	669	79	3570	1200	563	3	2.8	0.39	0.8	27.4	294	0.184	<0.3	0.4	1.6	0.03	0.01	0.27	<0.2	32	4.428	11.49	0.163	0.08	<0.005	<0.1	<0.01	<0.01	<0.2	<0.01	<0.001
CK-A-63	<1	<0.1	2030	769	98	4470	1080	352	3	3.6	0.58	0.9	10.4	170	0.101	0.5	0.5	1.1	0.03	<0.01	0.20	<0.2	32	4.382	12.20	0.203	0.10	0.005	<0.1	<0.01	<0.01	<0.2	0.01	<0.001
CK-A-64	<1	<0.1	1970	648	66	3660	1220	401	3	2.4	0.40	0.9	30.6	253	0.169	<0.3	0.3	0.5	0.02	<0.01	0.20	<0.2	31	4.542	10.97	0.220	0.07	<0.005	<0.1	<0.01	<0.01	<0.2	<0.01	<0.001
CK-A-65	<1	<0.1	2020	630	50	3190	1030	226	3	2.3	0.23	0.8	9.1	53	0.072	0.6	0.9	3.3	0.02	<0.01	0.08	<0.2	29	3.047	9.88	0.363	0.04	<0.005	<0.1	<0.01	<0.01	<0.2	0.01	<0.001
CK-A-66	<1	<0.1	1850	537	43	3710	1090	106	3	2.2	0.23	0.8	10.5	95	0.079	<0.3	1.0	4.4	0.01	<0.01	0.12	<0.2	29	3.972	8.61	0.236	0.09	<0.005	<0.1	<0.01	<0.01	<0.2	0.01	<0.001
CK-A-67	<1	<0.1	2280	661	57	3760	1330	464	3	2.4	0.40	0.9	37.1	269	0.210	<0.3	0.6	0.8	0.02	0.01	0.26	<0.2	37	4.539	10.35	0.171	0.08	<0.005	<0.1	<0.01	<0.01	<0.2	<0.01	<0.001
CK-A-68	<1	<0.1	2300	658	62	4830	1560	486	3	2.5	0.41	0.8	23.1	261	0.160	<0.3	0.5	1.6	0.02	<0.01	0.28	<0.2	37	5.379	10.76	0.211	0.07	<0.005	<0.1	<0.01	<0.01	<0.2	<0.01	<0.001
CK-A-69	<1	<0.1	2300	565	87	6110	1980	164	4	3.3	0.58	1.1	7.8	67	0.095	<0.3	0.5	1.7	0.03	<0.01	0.09	<0.2	26	6.707	9.65	0.319	0.04	<0.005	<0.1	<0.01	<0.01	<0.2	0.01	<0.001
CK-A-70	<1	<0.1	3460	765	81	6840	1580	1170	5	3.5	0.61	0.8	8.3	112	0.090	<0.3	0.4	1.1	0.02	<0.01	0.18	<0.2	32	5.045	12.09	0.178	0.06	<0.005	<0.1	<0.01	<0.01	<0.2	0.01	<0.001
CK-A-71	<1	<0.1	3980	1160	28	6790	1280	1920	4	3.3	0.17	0.8	122.0	394	0.352	<0.3	1.2	2.6	0.04	<0.01	0.31	<0.2	37	3.778	18.23	0.092	0.05	<0.005	<0.1	<0.01	<0.01	<0.2	0.03	<0.001
CK-A-72	1	<0.1	4830	1090	66	10300	2380	2300	7	5.0	0.58	1.3	101.9	404	0.437	0.4	0.3	2.4	0.05	0.02	0.35	<0.2	34	6.153	16.03	0.122	0.05	<0.005	<0.1	<0.01	<0.01	<0.2	0.04	<0.001
CK-A-73	1	<0.1	5120	2020	63	7230	1700	3360	5	3.4	0.44	1.0	87.1	878	0.469	0.5	0.5	1.7	0.05	<0.01	0.52	<0.2	59	3.855	30.59	0.195	0.09	<0.005	<0.1	<0.01	<0.01	<0.2	0.02	<0.001
CK-A-74	1	<0.1	4960	1570	89	9060	1870	3910	6	4.4	0.58	1.3	177.6	812	0.385	0.4	0.5	1.6	0.07	0.01	0.45	<0.2	51	5.543	25.29	0.201	0.09	<0.005	<0.1	<0.01	<0.01	<0.2	0.02	<0.001
CK-A-75	1	0.1	5390	1050	65	10200	2270	1200	6	4.5	0.89	0.9	23.7	237	0.290	0.5	0.8	2.4	0.03	<0.01	0.21	<0.2	39	5.896	15.07	0.164	0.04	<0.005	<0.1	<0.01	<0.01	<0.2	0.02	<0.001
CK-A-76	1	<0.1	6290	2020	69	9260	2680	6230	6	4.9	0.64	0.9	127.2	539	0.454	0.3	1.3	1.3	0.05	<0.01	0.38	<0.2	44	5.293	29.99	0.191	0.06	<0.005	<0.1	<0.01	<0.01	<0.2	0.02	<0.001
CK-A-77	<1	0.1	5290	1070	28	9170	1330	1750	6	3.9	1.21	1.0	11.9	63	0.098	0.3	0.5	1.3	0.01	0.01	0.22	<0.2	43	3.440	14.91	0.161	0.06	<0.005	<0.1	<0.01	<0.01	<0.2	0.02	<0.001
CK-A-78	<1	<0.1	5420	1430	39	9030	1560	3770	6	3.8	0.56	0.9	191.8	316	0.478	0.4	0.4	1.2	0.06	<0.01	0.38	<0.2	45	4.079	23.55	0.134	0.06	0.020	<0.1	<0.01	<0.01	<0.2	0.01	<0.001
CK-A-79	1	<0.1	5810	1380	80	10200	2220	3340	7	4.9	0.63	1.1	116.3	696	0.444	0.4	1.6	1.7	0.06	0.02	0.40	<0.2	45	5.530	22.06	0.197	0.36	0.006	<0.1	<0.01	<0.01	<0.2	0.03	<0.001
CK-A-80	1	<0.1	6270	2080	47	9180	1810	5640	6	4.8	0.62	1.3	110.0	619	0.318	0.4	0.4	1.1	0.05	0.01	0.43	<0.2	46	3.815	29.61	0.158	0.07	<0.005	<0.1	<0.01	<0.01	<0.2	0.01	<0.001
CK-A-81	1	<0.1	5670	1700	32	8660	2060	3080	6	4.0	0.67	0.9	60.1	188	0.238	0.4	1.7	2.2	0.03	<0.01	0.25	<0.2	39	5.778	24.09	0.112	0.03	<0.005	<0.1	<0.01	<0.01	<0.2	0.01	<0.001
CK-A-82	<1	<0.1	2470	718	106	5150	1590	733	3	2.8	0.63	1.0	92.3	564	0.431	0.4	1.3	2.7	0.05	<0.01	0.32	<0.2	39	5.331	12.17	0.277	0.09	<0.005	<0.1	<0.01	<0.01	<0.2	0.01	<0.001
CK-A-83	1	<0.1	5110	1480	58	9240	1870	4480	7	5.3	0.56	1.2	99.0	603	0.320	0.4	1.1	2.0	0.04	0.01	0.42	<0.2	42	4.805	24.65	0.165	0.07	0.006	<0.1	<0.01	<0.01	<0.2	0.02	<0.001
CK-A-84	1	<0.1	5740	1930	46	9220	1840	4160	7	4.5	0.60	1.0	131.9	572	0.415	0.4	0.6	1.5	0.04	<0.01	0.42	<0.2	44	5.039	27.15	0.155	0.05	<0.005	<0.1	<0.01	<0.01	<0.2	<0.01	<0.001
CK-A-85	<1	<0.1	3680	1020	48	7240	2440	1670	5	3.4	0.68	1.0	12.6	41	0.100	0.4	1.0	4.0	0.01	<0.01	0.15	<0.2	36	8.614	16.23	0.176	0.03	<0.005	<0.1	<0.01	<0.01	<0.2	0.03	<0.001
CK-A-86	<1	<0.1	3600	1260	55	6250	1510	3730	5	3.4	0.75	1.0	15.8	119	0.107	<0.3	0.3	1.0	0.02	<0.01	0.25	<0.2	43	4.006	17.97	0.165	0.07	<0.005	<0.1	<0.01	<0.01	<0.2	<0.01	<0.001
CK-A-87	<1	<0.1	4270	1730	78	9760	1740	2280	7	5.3	0.75	2.2	26.2	294	0.213	0.8	0.4	1.1	0.03	<0.01	0.20	<0.2	39	5.047	16.36	0.217	0.08	<0.005	<0.1	<0.01	<0.01	<0.2	0.01	<0.001
CK-A-88	<1	<0.1	3040	726	51	6950	2270	579	5	3.8	0.57	0.9	20.5	180	0.261	0.4	0.4	1.8	0.02	<0.01	0.20	<0.2	36	6.998	10.71	0.221	0.06	0.006	<0.1	<0.01	<0.01	<0.2	<0.01	<0.001
CK-A-89	1	<0.1	4650	1050	153	10100	2430	1600	7	6.2	1.00	1.0	38.5	529	0.453	0.5	1.0	2.3	0.05	0.01	0.44	<0.2	42	7.517	17.89	0.451	0.15	0.007	<0.1	<0.01	<0.01	<0.2	0.01	<0.001
CK-A-90	1	<0.1	30200	1080	126	9160	12400	1850	6	125	0.75	1.3	44.8	414	0.404	<0.3	2.6	6.7	0.17	<0.01	0.40	<0.2	45	5.276	18.53	0.227	0.12	0.018	0.1	<0.01	<0.01	<0.2	0.02	<0.001
CK-A-92	<1	<0.1	5180	1580	89	8470	2010	3350	6	7.5	0.66	0.9	93.4	910	0.602	0.5	0.6	1.6	0.05	<0.01	0.65	<0.2	52	6.330	23.40	0.283	0.16	0.007	<0.1	<0.01	<0.01	<0.2	<0.01	<0.001
CK-A-93	<1	<0.1	3740	1030	68	7430	1350	1420	5	4.8	0.54	0.9	62.8	493	0.446	0.4	0.5	2.4	0.04	<0.01	0.38	<0.2	39	4.320	15.76	0.234	0.10	<0.005	<0.1	<0.01	<0.01	<0.2	0.01	<0.001
CK-A-94	<1	<0.1	6950	2230	142	2800	2370	4050	3	5.0	1.33	0.9	69.5	1250	0.491	0.6	1.2	2.7	0.06	0.01	1.07	<0.2	56	5.672	32.51	0.392	0.31	0.008	<0.1	<0.01	<0.01	<0.2	0.02	<0.001
CK-A-95	<1	<0.1	5120	2150	186	4700	2140	3900	4	8.0	1.50	1.1	38.3	1040	0.424	0.7	1.3	2.3	0.07	<0.01	0.90	<0.2	52	4.241	30.78	0.453	0.40	0.014	<0.1	<0.01	<0.01	<0.2	0.01	<0.001
CK-A-96	<1	<0.1	4140	1540	88	2870	696	2040	3	3.3	0.64	0.9	104.9	1370	0.463	<0.3	0.5	11.9	0.05	<0.01	0.59	<0.2	71	1.946	24.07	0.272	0.19	0.005	<0.1	<0.01	<0.01	<0.2	0.01	<0.001
CK-A-100	<1	<0.1	2160	493	134	2940	883	468	3	3.7	0.51	0.9	41.3	359	0.212	0.4	0.7	2.3	0.04	<0.01	0.28	<0.2	23	2.905	7.83	0.237	0.22	0.009	<0.1	<0.01	<0.01	<0.2	<0.01	<0.001
CK-A-101	<1	<0.1	1930	384	111	2550	476	<50	2	2.7	0.51	0.7	32.3	201	0.227	0.4	0.7	2.8	0.03	<0.01	0.21	<0.2	25	1.985	5.99	0.273	0.23	<0.005	<0.1	<0.01	<0.01	<0.2	0.01	<0.001
CK-A-102	<1	<0.1	3290	1770	339	7460	960	2870	6	12.2	2.24	1.3	34.0	579	0.412	0.6	1.1	4.3	0.10	0.01	0.16	<0.2	28	3.453	17.98	0.507	0.34	0.018	<0.1	<0.01	<0.01	<0.2	0.01	<0.001
CK-A-103	<1	<0.1	3400	1620	345	7660	833	2480	6	11.1	2.23	1.5	23.4	453	0.381	0.5	1.5	6.2	0.09	0.01	0.14	<0.2	27	2.821	16.74	0.527	0.32	0.018	<0.1	<0.01	<0.01	<0.2	0.01	<0.001
CK-A-104	<1	<0.1	3480	1860	352	8040	743	2730	6	11.5	2.18	1.6	24.1	451	0.361	0.6	1.0	8.6	0.09	0.01	0.11	<0.2	26	2.508	19.35	0.566	0.37	0.018	<0.1	<0.01	<0.01	<0.2	<0.01	<0.001
CK-A-105	<1	<0.1	2600	868	68	1870	256	309	2	1.7	0.25	0.9	34.9	153	0.179	<0.3	0.3	2.3	0.02	<0.01	0.22	<0.2	43	0.896	11.98	0.179	0.14	<0.005	<0.1	<0.01	<0.01	<0.2	<0.01	<0.001
CK-A-106	1	<0.1	3510	1300	244	6320	1330	3150	5	6.8	1.09	1.1	162.3	738	0.664	1.0	0.7	7.0	0.09	<0.01	0.49	<0.2	39	3.562	18.98	0.445	0.27	0.013	<0.1	<0.01	<0.01	<0.2	0.01	<0.001
CK-A-107	<1	<0.1	2660	1270	147	4510	1030	1360	3	3.9	1.03	0.9	33.8	620	0.286	0.6	14.4	31.3	0.05	<0.01	0.39	<0.2	41	3.054	16.13	0.530	0.22	0.006	<0.1	<0.01	<0.01	<0.2	0.03	<0.001
CK-A-108	1	<0.1	3810	1050	145	7380	1370	2420	6	5.4	1.02	1.2	82.7	495	0.481	0.7	9.3	6.1	0.06	<0.01	0.33	<0.2	31	3.811	15.95	0.335	0.15	0.009	<0.1	<0.01	<0.01	<0.2	0.02	<0.001
CK-A-109	2	0.1	4340	1080	302	7830	1900	2290	6	8.9	1.13	1.3	72.0	506	0.502	0.8	5.2	3.9	0.10	<0.01	0.30	<0.2	33	4.581	16.53	0.544	0.31	0.019	<0.1	<0.01	<0.01	<0.2	0.01	<0.001
CK-A-110	2	0.1	5680	1010	294	9710	1990	1450	7	9.9	1.54	1.4	47.7	333	0.638	0.8	1.0	3.2	0.10	0.01	0.27	<0.2	37	4.713	13.17	0.661	0.31	0.021	<0.1	<0.01	<0.01	<0.2	0.02	<0.001
CK-A-111	2	0.1	4560	1220	185	9010	1670	2510	7	7.9	1.27	1.4	55.7	235	0.511	0.8	1.4	3.7	0.07	<0.01	0.22	<0.2	28	4.276	15.48	0.325	0.21	0.022	<0.1	<0.01	<0.01	<0.2	0.01	<0.001
CK-A-112	2	<0.1	3810	971	169	7650	1420	1940	5	7.0	0.99	1.1	30.9	180	0.273	0.5	1.0	4.3	0.06	<0.01	0.21	<0.2	28	3.787	13.94	0.317	0.38	0.013	<0.1	<0.01	<0.01	<0.2	0.01	<0.001
CK-A-113	<1	<0.1	2410	1030	253	3380	1000	769	3	6.8	1.03	1.1	60.3	709	0.454	1.2	3.0	5.6	0.08	<0.01	0.38	<0.2	45	3.563	15.85	0.772	0.26	0.016	<0.1	<0.01	<0.01	<0.2	<0.01	<0.001
CK-A-114	1	<0.1	3610	1030	178	6810	1650	2750	5	7.4	0.73	0.9	164.4	451	0.606	0.5	0.9	4.7	0.07	0.01	0.25	<0.2	35	4.136	16.54	0.352	0.23	0.014	<0.1	<0.01	<0.01	<0.2	0.01	<0.001
CK-A-115	2	0.1	3840	950	219	6850	1170	1950	5	7.6	0.79	1.0	124.3	512	0.801	0.5	0.7	5.9	0.09	<0.01	0.34	<0.2	35	2.925	13.92	0.461	0.30	0.015	<0.1	<0.01	<0.01	<0.2	0.01	<0.001
CK-A-116	1	<0.1	3690	1430	196	6890	1430	3760	5	7.5	0.93	1.1	207.6	668	0.772	0.7	0.6	10.5	0.10	<0.01	0.49	<0.2	39	3.543	20.16	0.380	0.34	0.017	<0.1	<0.01	<0.01	<0.2	0.01	<0.001
CK-A-117	<1	<0.1	2990	1260	376	3110	1230	1510	3	11.0	1.00	1.0	28.6	902	0.361	0.5	0.7	8.0	0.12	0.01	0.52	<0.2	46	3.438	18.23	0.692	0.46	0.035	<0.1	<0.01	<0.01	<0.2	<0.01	<0.001
CK-A-118	<1	<0.1	3700	1530	179	3160	1300	2010	3	4.5	0.70	0.9	47.3	712	0.439	0.4	1.0	1.7	0.07	<0.01	0.61	<0.2	48	3.137	22.81	0.485	0.23	0.011	<0.1	<0.01	<0.01	<0.2	<0.01	<0.001
CK-A-119	3	0.2	5910	1130	189	9790	1890	1080	7	7.8	1.64	1.5	21.1	199	0.404	1.0	1.4	2.4	0.07	0.01	0.20	<0.2	45	4.747	12.70	0.671	0.18	0.019	<0.1	<0.01	<0.01	<0.2	<0.01	<0.001
CK-A-120	2	<0.1	3730	1010	175	6970	851	1090	5	5.8	0.97	0.8	37.3	515	0.356	0.6	0.8	1.9	0.06	<0.01	0.47	<0.2	38	2.677	14.51	0.516	0.19	0.011	<0.1	<0.01	<0.01	<0.2	0.01	<0.001
CK-A-121	2	0.1	5060	1210	390	7560	1190	1540	5	7.2	0.94	1.7	33.3	248	0.434	1.0	0.6	3.2	0.11	0.01	0.20	<0.2	50	2.993	14.13	0.637	0.21	0.021	<0.1	<0.01	<0.01	<0.2	0.01	<0.001
CK-A-122	3	0.1	3780	917	207	7940	915	912	6	6.8	0.84	1.1	41.7	319	0.529	0.8	0.6	5.1	0.07	<0.01	0.34	<0.2	41	2.534	12.78	0.708	0.20	0.015	<0.1	<0.01	<0.01	<0.2	<0.01	<0.001
CK-A-123	1	<0.1	3250	767	55	5960	1080	385	4	3.1	0.71	1.0	13.7	67	0.119	0.3	0.7	8.2	0.02	<0.01	0.12	<0.2	28	3.322	8.54	0.225	0.09	<0.005	<0.1	<0.01	<0.01	<0.2	<0.01	<0.001
CK-A-124	1	<0.1	3090	786	124	6460	1300	108	5	3.4	0.70	1.0	41.2	200	0.487	0.5	0.7	26.2	0.04	<0.01	0.19	<0.2	31	4.334	9.07	0.282	0.10	<0.005	<0.1	<0.01	<0.01	<0.2	<0.01	<0.001
CK-A-125	1	<0.1	3150	935	175	4920	984	1100	4	2.6	1.31	1.0	49.9	607	0.322	0.5	1.6	49.2	0.06	<0.01	0.45	<0.2	38	3.772	13.18	0.557	0.17	<0.005	<0.1	<0.01	<0.01	<0.2	0.01	<0.001
CK-A-126	<1	<0.1	3250	678	155	5790	1770	1160	5	3.7	0.91	1.0	26.6	184	0.202	0.5	0.7	49.3	0.03	<0.01	0.22	<0.2	40	5.316	10.76	0.428	0.20	<0.005	<0.1	<0.01	<0.01	<0.2	0.01	<0.001

Geochemical grade assay of stream water collected in the Lomba Grande district

(2continued/3)

Sample No.	Sn	Sb	Te	I	Cs	Ba	La	Ce	Pr	Nd	Sm	Eu	Gd	Tb	Dy	Ho	Er	Tm	Yb	Lu	Hf	Ta	W	Re	Os	Pt	Au	Hg	Tl	Pb	Bi	Th
CK-A-62	<0.1	0.01	<0.01	3	0.062	28.5	0.104	0.263	0.029	0.129	0.033	0.014	0.041	0.005	0.030	0.006	0.017	0.002	0.021	0.003	0.004	<0.001	<0.02	<0.001	<0.002	<0.01	<0.002	<0.2	0.019	0.3	<0.01	0.018
CK-A-63	<0.1	0.01	<0.01	2	0.082	30.5	0.146	0.376	0.045	0.189	0.057	0.022	0.061	0.008	0.033	0.007	0.021	0.003	0.018	0.003	0.004	<0.001	<0.02	<0.001	<0.002	<0.01	<0.002	<0.2	0.023	0.3	<0.01	0.013
CK-A-64	<0.1	<0.01	<0.01	3	0.065	29.1	0.092	0.253	0.030	0.122	0.045	0.015	0.049	0.006	0.034	0.006	0.021	0.003	0.024	0.003	0.004	<0.001	<0.02	<0.001	<0.002	<0.01	<0.002	<0.2	0.022	0.2	<0.01	0.013
CK-A-65	<0.1	<0.01	<0.01	3	0.061	26.1	0.094	0.206	0.032	0.141	0.054	0.021	0.073	0.010	0.055	0.013	0.038	0.004	0.042	0.006	0.003	<0.001	<0.02	<0.001	<0.002	<0.01	<0.002	<0.2	0.024	0.3	<0.01	0.006
CK-A-66	<0.1	0.02	<0.01	7	0.057	28.9	0.066	0.173	0.022	0.094	0.029	0.014	0.045	0.007	0.031	0.007	0.022	0.003	0.021	0.003	0.004	<0.001	<0.02	<0.001	<0.002	<0.01	<0.002	<0.2	0.019	0.3	<0.01	0.007
CK-A-67	<0.1	0.02	<0.01	4	0.058	24.5	0.098	0.276	0.030	0.121	0.035	0.015	0.040	0.006	0.029	0.005	0.017	0.002	0.019	0.003	0.003	<0.001	<0.02	<0.001	<0.002	<0.01	<0.002	<0.2	0.023	0.2	<0.01	0.016
CK-A-68	<0.1	0.01	<0.01	4	0.046	26.7	0.106	0.284	0.030	0.138	0.038	0.016	0.041	0.006	0.034	0.006	0.021	0.002	0.019	0.003	0.002	<0.001	<0.02	<0.001	<0.002	<0.01	<0.002	<0.2	0.019	0.3	<0.01	0.016
CK-A-69	<0.1	<0.01	<0.01	3	0.088	32.8	0.131	0.293	0.038	0.185	0.054	0.020	0.066	0.011	0.053	0.011	0.032	0.004	0.036	0.006	0.002	<0.001	<0.02	<0.001	<0.002	<0.01	<0.002	<0.2	0.028	0.3	<0.01	0.007
CK-A-70	<0.1	0.05	<0.01	3	0.034	26.6	0.096	0.216	0.028	0.112	0.035	0.014	0.042	0.006	0.032	0.006	0.018	0.002	0.020	0.003	<0.002	<0.001	<0.02	<0.001	<0.002	<0.01	<0.002	<0.2	0.014	0.2	<0.01	0.010
CK-A-71	<0.1	0.01	<0.01	5	0.014	34.6	0.049	0.116	0.015	0.062	0.019	0.010	0.023	0.003	0.012	0.003	0.009	<0.001	0.008	0.002	0.003	<0.001	<0.02	<0.001	<0.002	<0.01	<0.002	<0.2	0.009	0.2	<0.01	0.012
CK-A-72	<0.1	0.02	<0.01	7	0.035	43.0	0.095	0.252	0.026	0.112	0.032	0.014	0.035	0.004	0.022	0.004	0.012	0.001	0.012	0.003	0.003	<0.001	<0.02	<0.001	<0.002	<0.01	<0.002	<0.2	0.016	0.2	<0.01	0.019
CK-A-73	0.4	0.02	<0.01	10	0.020	66.3	0.161	0.397	0.049	0.203	0.054	0.023	0.057	0.007	0.035	0.006	0.016	0.002	0.019	0.003	0.005	<0.001	<0.02	<0.001	<0.002	<0.01	<0.002	<0.2	0.013	0.8	<0.01	0.035
CK-A-74	<0.1	0.02	<0.01	12	0.042	42.5	0.136	0.358	0.040	0.185	0.046	0.019	0.049	0.007	0.030	0.007	0.017	0.003	0.021	0.003	0.004	<0.001	<0.02	<0.001	<0.002	<0.01	<0.002	<0.2	0.016	0.3	<0.01	0.036
CK-A-75	<0.1	0.01	<0.01	11	0.025	45.0	0.107	0.286	0.033	0.144	0.049	0.019	0.046	0.006	0.028	0.005	0.014	0.003	0.016	0.002	0.002	<0.001	<0.02	<0.001	<0.002	<0.01	<0.002	<0.2	0.023	0.4	<0.01	0.018
CK-A-76	<0.1	0.02	<0.01	9	0.021	66.1	0.106	0.285	0.034	0.135	0.043	0.022	0.043	0.006	0.032	0.006	0.015	0.002	0.013	0.002	<0.002	<0.001	<0.02	<0.001	<0.002	<0.01	<0.002	<0.2	0.012	0.3	<0.01	0.027
CK-A-77	<0.1	<0.01	<0.01	5	0.022	33.2	0.041	0.096	0.014	0.077	0.027	0.012	0.027	0.004	0.027	0.005	0.016	0.003	0.019	0.003	0.004	<0.001	<0.02	<0.001	<0.002	<0.01	<0.002	<0.2	0.011	0.1	<0.01	0.009
CK-A-78	<0.1	<0.01	<0.01	10	0.013	47.0	0.054	0.131	0.017	0.076	0.023	0.012	0.029	0.004	0.018	0.004	0.010	0.001	0.014	0.002	0.003	<0.001	<0.02	<0.001	<0.002	<0.01	<0.002	<0.2	0.013	0.2	<0.01	0.019
CK-A-79	<0.1	0.04	<0.01	9	0.032	51.8	0.149	0.375	0.044	0.169	0.055	0.020	0.052	0.007	0.029	0.005	0.018	0.002	0.017	0.003	0.010	<0.001	<0.02	<0.001	<0.002	<0.01	<0.002	<0.2	0.015	0.3	<0.01	0.031
CK-A-80	<0.1	0.01	<0.01	9	0.022	56.9	0.096	0.242	0.028	0.129	0.045	0.019	0.045	0.005	0.027	0.005	0.012	0.002	0.015	0.002	0.005	<0.001	<0.02	<0.001	<0.002	<0.01	<0.002	<0.2	0.008	0.2	<0.01	0.025
CK-A-81	<0.1	<0.01	<0.01	5	0.020	49.5	0.060	0.144	0.018	0.076	0.023	0.013	0.027	0.003	0.017	0.004	0.010	<0.001	0.009	0.001	<0.002	<0.001	<0.02	<0.001	<0.002	<0.01	<0.002	<0.2	0.016	0.2	<0.01	0.012
CK-A-82	<0.1	<0.01	<0.01	5	0.055	28.9	0.171	0.483	0.047	0.196	0.059	0.020	0.070	0.009	0.047	0.010	0.027	0.003	0.026	0.004	0.006	<0.001	<0.02	<0.001	<0.002	<0.01	<0.002	<0.2	0.022	0.4	<0.01	0.027
CK-A-83	<0.1	0.03	<0.01	9	0.033	43.4	0.119	0.296	0.034	0.155	0.048	0.016	0.046	0.007	0.030	0.006	0.016	0.002	0.014	0.003	0.004	<0.001	0.09	<0.001	<0.002	<0.01	<0.002	<0.2	0.016	0.3	<0.01	0.034
CK-A-84	<0.1	0.03	<0.01	6	0.018	51.6	0.102	0.254	0.029	0.119	0.037	0.018	0.039	0.005	0.029	0.004	0.012	0.002	0.016	0.002	0.002	<0.001	<0.02	<0.001	<0.002	<0.01	<0.002	<0.2	0.012	0.2	0.04	0.022
CK-A-85	<0.1	0.02	<0.01	2	0.102	43.6	0.097	0.224	0.025	0.097	0.029	0.015	0.033	0.005	0.027	0.005	0.017	0.002	0.016	0.003	<0.002	<0.001	<0.02	<0.001	<0.002	<0.01	<0.002	<0.2	0.023	0.5	<0.01	0.008
CK-A-86	<0.1	0.07	<0.01	5	0.024	37.9	0.083	0.182	0.027	0.126	0.038	0.015	0.039	0.005	0.032	0.006	0.018	0.002	0.015	0.003	0.006	<0.001	<0.02	<0.001	<0.002	<0.01	<0.002	<0.2	0.012	0.2	<0.01	0.015
CK-A-87	<0.1	0.02	<0.01	6	0.031	40.1	0.137	0.301	0.039	0.163	0.050	0.020	0.051	0.007	0.034	0.007	0.020	0.002	0.020	0.003	0.003	<0.001	<0.02	<0.001	<0.002	<0.01	<0.002	<0.2	0.018	0.2	0.01	0.018
CK-A-88	<0.1	0.02	<0.01	3	0.041	42.7	0.102	0.258	0.031	0.121	0.042	0.017	0.052	0.006	0.034	0.006	0.019	0.003	0.018	0.003	0.004	<0.001	<0.02	<0.001	<0.002	<0.01	<0.002	<0.2	0.031	0.3	<0.01	0.012
CK-A-89	<0.1	0.03	<0.01	5	0.046	50.6	0.308	0.826	0.092	0.399	0.117	0.042	0.116	0.017	0.075	0.014	0.043	0.006	0.040	0.005	0.011	<0.001	<0.02	<0.001	<0.002	<0.01	<0.002	<0.2	0.033	0.4	<0.01	0.043
CK-A-90	<0.1	0.06	<0.01	7	0.036	37.0	0.151	0.439	0.050	0.211	0.064	0.021	0.061	0.008	0.039	0.007	0.023	0.002	0.022	0.004	0.005	<0.001	<0.02	<0.001	<0.002	<0.01	<0.002	<0.2	0.022	1.2	<0.01	0.028
CK-A-92	<0.1	0.03	<0.01	10	0.027	37.5	0.195	0.487	0.064	0.258	0.074	0.024	0.083	0.010	0.044	0.010	0.029	0.003	0.021	0.004	0.008	<0.001	<0.02	<0.001	<0.002	<0.01	<0.002	<0.2	0.014	0.3	<0.01	0.043
CK-A-93	<0.1	0.03	<0.01	7	0.028	30.7	0.132	0.342	0.039	0.176	0.056	0.018	0.058	0.007	0.033	0.007	0.021	0.003	0.021	0.003	0.004	<0.001	<0.02	<0.001	<0.002	<0.01	<0.002	<0.2	0.016	0.2	<0.01	0.026
CK-A-94	<0.1	0.05	<0.01	14	0.076	50.4	0.544	1.181	0.143	0.597	0.154	0.043	0.139	0.016	0.073	0.014	0.042	0.005	0.033	0.005	0.012	<0.001	<0.02	<0.001	<0.002	<0.01	<0.002	<0.2	0.022	0.6	<0.01	0.073
CK-A-95	<0.1	0.06	<0.01	11	0.048	49.1	0.571	1.361	0.162	0.629	0.170	0.046	0.159	0.019	0.086	0.016	0.043	0.006	0.041	0.006	0.013	0.001	<0.02	<0.001	<0.002	<0.01	<0.002	<0.2	0.018	0.6	<0.01	0.073
CK-A-96	<0.1	0.03	<0.01	21	0.023	27.4	0.258	0.731	0.088	0.369	0.109	0.028	0.100	0.011	0.049	0.009	0.028	0.004	0.025	0.005	0.008	<0.001	<0.02	<0.001	<0.002	<0.01	<0.002	<0.2	0.009	0.3	<0.01	0.051
CK-A-100	<0.1	0.03	<0.01	6	0.031	18.7	0.146	0.419	0.044	0.201	0.055	0.017	0.055	0.008	0.041	0.008	0.027	0.003	0.024	0.004	0.011	<0.001	<0.02	<0.001	<0.002	<0.01	<0.002	<0.2	0.014	0.4	<0.01	0.029
CK-A-101	<0.1	0.02	<0.01	6	0.038	13.2	0.135	0.402	0.047	0.213	0.064	0.016	0.060	0.009	0.046	0.009	0.026	0.004	0.031	0.004	0.008	<0.001	<0.02	<0.001	<0.002	<0.01	<0.002	<0.2	0.017	0.3	<0.01	0.020
CK-A-102	<0.1	0.01	<0.01	5	0.049	25.1	0.425	0.989	0.125	0.500	0.137	0.041	0.140	0.019	0.100	0.019	0.053	0.007	0.053	0.008	0.012	0.001	<0.02	<0.001	<0.002	<0.01	<0.002	<0.2	0.019	0.3	<0.01	0.040
CK-A-103	<0.1	0.01	<0.01	4	0.048	23.2	0.472	1.070	0.137	0.566	0.155	0.041	0.154	0.020	0.100	0.019	0.052	0.007	0.057	0.009	0.013	0.001	<0.02	<0.001	<0.002	<0.01	<0.002	<0.2	0.014	0.4	<0.01	0.033
CK-A-104	<0.1	0.03	<0.01	4	0.049	23.6	0.522	1.215	0.155	0.640	0.178	0.044	0.171	0.021	0.104	0.020	0.061	0.008	0.060	0.009	0.012	0.001	<0.02	<0.001	<0.002	<0.01	<0.002	<0.2	0.014	0.3	<0.01	0.030
CK-A-105	<0.1	0.01	<0.01	3	0.028	18.6	0.219	0.561	0.067	0.281	0.065	0.019	0.066	0.007	0.037	0.006	0.019	0.002	0.017	0.003	0.008	<0.001	<0.02	<0.001	<0.002	<0.01	<0.002	<0.2	0.010	0.3	<0.01	0.016
CK-A-106	3.7	0.03	<0.01	9	0.046	56.2	0.309	0.875	0.096	0.431	0.132	0.035	0.130	0.017	0.073	0.015	0.040	0.005	0.035	0.005	0.010	0.001	<0.02	<0.001	<0.002	<0.01	<0.002	<0.2	0.025	0.5	<0.01	0.066
CK-A-107	0.1	0.02	<0.01	7	0.038	38.4	0.433	1.107	0.138	0.589	0.177	0.047	0.168	0.022	0.105	0.020	0.055	0.006	0.051	0.008	0.012	<0.001	<0.02	<0.001	<0.002	<0.01	<0.002	<0.2	0.016	0.4	<0.01	0.050
CK-A-108	<0.1	0.02	<0.01	14	0.034	47.1	0.176	0.527	0.061	0.265	0.081	0.026	0.087	0.013	0.062	0.011	0.033	0.004	0.033	0.005	0.008	<0.001	<0.02	<0.001	<0.002	<0.01	<0.002	<0.2	0.025	0.4	<0.01	0.039
CK-A-109	<0.1	0.02	<0.01	8	0.060	54.0	0.290	0.796	0.091	0.413	0.132	0.039	0.135	0.021	0.100	0.018	0.052	0.007	0.049	0.007	0.012	0.002	<0.02	<0.001	<0.002	<0.01	<0.002	<0.2	0.022	0.4	<0.01	0.065
CK-A-110	<0.1	0.02	<0.01	5	0.063	40.3	0.264	0.709	0.087	0.386	0.142	0.041	0.144	0.021	0.109	0.022	0.067	0.008	0.057	0.009	0.014	0.002	<0.02	<0.001	<0.002	<0.01	<0.002	<0.2	0.032	0.4	<0.01	0.062
CK-A-111	<0.1	0.02	<0.01	4	0.047	53.7	0.146	0.528	0.050	0.241	0.079	0.032	0.088	0.014	0.060	0.014	0.034	0.004	0.028	0.004	0.006	0.001	<0.02	<0.001	<0.002	<0.01	<0.002	<0.2	0.025	0.3	<0.01	0.043
CK-A-112	<0.1	0.03	<0.01	4	0.044	47.4	0.142	0.396	0.046	0.225	0.069	0.023	0.076	0.010	0.059	0.011	0.032	0.004	0.031	0.004	0.011	<0.001	<0.02	<0.001	<0.002	<0.01	<0.002	<0.2	0.021	0.3	<0.01	0.029
CK-A-113	<0.1	0.02	<0.01	8	0.055	33.7	0.617	1.648	0.201	0.826	0.247	0.067	0.240	0.032	0.153	0.027	0.073	0.009	0.069	0.011	0.013	0.002	<0.02	<0.001	<0.002	<0.01	<0.002	<0.2	0.026	0.7	<0.01	0.068
CK-A-114	<0.1	0.02	<0.01	7	0.042	58.8	0.207	0.607	0.063	0.292	0.092	0.033	0.090	0.013	0.066	0.012	0.034	0.004	0.030	0.005	0.007	0.002	<0.02	<0.001	<0.002	<0.01	<0.002	<0.2	0.030	0.4	<0.01	0.057
CK-A-115	<0.1	0.02	<0.01	6	0.039	52.8	0.249	0.728	0.081	0.373	0.122	0.037	0.120	0.018	0.087	0.016	0.044	0.005	0.040	0.006	0.010	0.001	<0.02	<0.001	<0.002	<0.01	<0.002	<0.2	0.021	0.4	<0.01	0.074
CK-A-116	0.7	0.02	<0.01	9	0.042	65.8	0.243	0.690	0.080	0.334	0.109	0.034	0.101	0.014	0.069	0.013	0.034	0.004	0.029	0.005	0.012	0.001	<0.02	<0.001	<0.002	<0.01	<0.002	<0.2	0.024	0.4	<0.01	0.068
CK-A-117	<0.1	0.02	<0.01	10	0.061	33.5	0.592	1.421	0.176	0.745	0.211	0.052	0.195	0.026	0.113	0.021	0.060	0.007	0.055	0.007	0.017	0.002	<0.02	<0.001	<0.002	<0.01	<0.002	<0.2	0.018	0.5	<0.01	0.092
CK-A-118	<0.1	0.02	<0.01	15	0.040	55.7	0.426	1.080	0.137	0.566	0.169	0.043	0.165	0.018	0.089	0.017	0.045	0.006	0.050	0.007	0.012	<0.001	<0.02	<0.001	<0.002	<0.01	<0.002	<0.2	0.016	0.4	<0.01	0.063
CK-A-119	<0.1	0.01	<0.01	4	0.043	62.3	0.276	0.663	0.089	0.416	0.144	0.051	0.148	0.023	0.122	0.025	0.063	0.008	0.067	0.010	0.011	0.001	<0.02	<0.001	<0.002	<0.01	<0.002	<0.2	0.046	0.4	<0.01	0.048
CK-A-120	<0.1	0.02	<0.01	4	0.033	41.9	0.457	1.162	0.141	0.566	0.160	0.044	0.161	0.021	0.093	0.017	0.049	0.005	0.042	0.006	0.011	<0.001	<0.02	<0.001	<0.002	<0.01	<0.002	<0.2	0.016	0.5	<0.01	0.061
CK-A-121	<0.1	0.02	<0.01	4	0.052	42.9	0.328	0.933	0.120	0.561	0.179	0.047	0.177	0.024	0.116	0.022	0.060	0.008	0.051	0.009	0.009	0.001	<0.02	<0.001	<0.002	<0.01	<0.002	<0.2	0.018	0.6	<0.01	0.051
CK-A-122	<0.1	0.02	<0.01	3	0.039	43.7	0.556	1.371	0.182	0.754	0.237	0.056	0.224	0.028	0.130	0.025	0.066	0.008	0.056	0.009	0.010	0.001	<0.02	<0.001	<0.002	<0.01	<0.002	<0.2	0.016	0.5	<0.01	0.054
CK-A-123	<0.1	0.02	<0.01	4	0.037	22.6	0.081	0.235	0.029	0.132	0.038	0.014	0.044	0.006	0.035	0.008	0.022	0.003	0.024	0.003	0.004	<0.001	<0.02	<0.001	<0.002	<0.01	<0.002	<0.2	0.016	0.1	<0.01	0.011
CK-A-124	<0.1	0.01	<0.01	3	0.033	32.1	0.121	0.370	0.040	0.170	0.057	0.019	0.061	0.009	0.046	0.010	0.027	0.004	0.029	0.005	0.005	<0.001	<0.02	<0.001	<0.002	<0.01	<0.002	<0.2	0.029	0.2	<0.01	0.015
CK-A-125	<0.1	0.02	<0.01	6	0.041	33.0	0.430	1.115	0.134	0.536	0.153	0.041	0.152	0.021	0.097	0.020	0.052	0.007	0.045	0.007	0.010	<0.001	<0.02	<0.001	<0.002	<0.01	<0.002	<0.2	0.020	0.6	<0.01	0.038
CK-A-126	<0.1	0.02	<0.01	6	0.045	24.4	0.217	0.534	0.064	0.259	0.081	0.025	0.093	0.014	0.067	0.013	0.036	0.005	0.041	0.006	0.009	<0.001	0.03	<0.001	<0.002	<0.01	<0.002	<0.2	0.024	0.3	<0.01	0.022

Geochemical grade assay of stream water collected in the Lomba Grande district

Sample No.	U	SO_4
CK-A-62	0.011	12
CK-A-63	0.017	10
CK-A-64	0.011	12
CK-A-65	0.020	13
CK-A-66	0.007	15
CK-A-67	0.010	11
CK-A-68	0.013	15
CK-A-69	0.013	16
CK-A-70	0.010	16
CK-A-71	0.005	9
CK-A-72	0.010	16
CK-A-73	0.014	14
CK-A-74	0.013	14
CK-A-75	0.016	18
CK-A-76	0.016	16
CK-A-77	0.014	18
CK-A-78	0.008	17
CK-A-79	0.015	17
CK-A-80	0.014	17
CK-A-81	0.010	12
CK-A-82	0.020	13
CK-A-83	0.016	15
CK-A-84	0.013	15
CK-A-85	0.008	16
CK-A-86	0.013	16
CK-A-87	0.016	17
CK-A-88	0.010	18
CK-A-89	0.027	14
CK-A-90	0.021	3
CK-A-92	0.017	9
CK-A-93	0.011	13
CK-A-94	0.050	14
CK-A-95	0.055	13
CK-A-96	0.024	15
CK-A-100	0.017	12
CK-A-101	0.018	9
CK-A-102	0.023	11
CK-A-103	0.027	10
CK-A-104	0.028	12
CK-A-105	0.013	10
CK-A-106	0.033	15
CK-A-107	0.041	11
CK-A-108	0.024	15
CK-A-109	0.030	16
CK-A-110	0.035	19
CK-A-111	0.022	16
CK-A-112	0.020	17
CK-A-113	0.052	11
CK-A-114	0.022	17
CK-A-115	0.029	17
CK-A-116	0.028	17
CK-A-117	0.041	13
CK-A-118	0.033	13
CK-A-119	0.028	21
CK-A-120	0.042	14
CK-A-121	0.037	18
CK-A-122	0.044	17
CK-A-123	0.012	16
CK-A-124	0.017	18
CK-A-125	0.041	15
CK-A-126	0.025	15

Geochemical grade assay of stream water collected in the Lomba Grande district

Sample No.	Li	Be	Na	Mg	Al	Si	K	Ca	Sc	Ti	V	Cr	Mn	Fe	Co	Ni	Cu	Zn	Ga	Ge	As	Se	Br	Rb	Sr	Y	Zr	Nb	Mo	Ru	Pd	Ag	Cd	In
CK-A-127	2	0.1	2790	621	97	6780	845	418	6	3.6	0.86	1.1	21.1	217	0.231	0.4	0.5	9.0	0.03	<0.01	0.23	<0.2	29	2.881	7.82	0.326	0.56	<0.005	<0.1	<0.01	<0.01	<0.2	0.01	<0.001
CK-A-128	1	<0.1	3020	983	121	6210	892	945	5	3.3	1.18	0.9	19.5	563	0.293	0.6	1.0	5.7	0.03	<0.01	0.46	<0.2	36	3.481	12.76	0.461	0.19	<0.005	<0.1	<0.01	<0.01	<0.2	0.01	<0.001
CK-A-129	1	<0.1	2840	776	182	5250	978	1120	4	3.3	1.18	1.0	26.9	563	0.325	0.5	1.1	8.0	0.05	<0.01	0.37	<0.2	33	3.275	11.20	0.601	0.22	<0.005	<0.1	<0.01	<0.01	<0.2	0.01	<0.001
CK-A-130	<1	<0.1	2010	772	119	3200	1130	787	3	2.7	0.77	0.9	20.6	402	0.179	<0.3	1.6	7.0	0.03	<0.01	0.32	<0.2	30	4.237	12.46	0.313	0.17	<0.005	<0.1	<0.01	<0.01	<0.2	0.01	<0.001
CK-A-131	<1	<0.1	2080	868	119	2560	1200	878	3	3.8	0.87	0.9	22.1	691	0.199	0.3	1.6	15.7	0.04	<0.01	0.44	<0.2	35	3.615	12.05	0.232	0.19	0.006	<0.1	<0.01	<0.01	<0.2	<0.01	<0.001
CK-A-132	<1	<0.1	2330	997	119	4410	1140	1330	4	2.9	0.93	0.9	46.6	704	0.307	0.3	0.8	17.4	0.04	<0.01	0.39	<0.2	36	3.761	14.15	0.280	0.16	<0.005	<0.1	<0.01	<0.01	<0.2	0.01	<0.001
CK-A-133	<1	<0.1	1590	463	111	3010	659	129	3	2.4	0.50	1.0	8.3	314	0.090	<0.3	0.6	21.7	0.03	<0.01	0.16	<0.2	27	2.775	7.42	0.279	0.19	<0.005	<0.1	<0.01	<0.01	<0.2	<0.01	<0.001
CK-A-134	1	<0.1	3080	741	48	5660	654	1000	4	3.1	0.37	1.0	58.7	377	0.263	0.6	2.3	4.8	0.02	<0.01	0.31	<0.2	31	2.184	10.37	0.142	0.14	<0.005	<0.1	<0.01	<0.01	<0.2	0.01	<0.001
CK-A-135	2	<0.1	3020	766	37	5840	687	632	5	2.9	0.35	0.8	40.1	452	0.232	0.6	1.2	4.0	0.02	<0.01	0.33	<0.2	36	2.871	10.69	0.111	0.10	<0.005	<0.1	<0.01	<0.01	<0.2	0.01	<0.001
CK-A-136	<1	<0.1	2260	966	141	2360	326	800	3	3.2	0.51	0.8	12.7	688	0.150	<0.3	0.6	3.5	0.04	<0.01	0.45	<0.2	48	1.512	14.31	0.311	0.21	0.007	<0.1	<0.01	<0.01	<0.2	0.01	<0.001
CK-A-137	2	<0.1	2970	742	77	6560	707	583	5	3.3	0.79	0.8	17.9	355	0.197	0.3	0.7	3.3	0.02	<0.01	0.34	<0.2	35	2.590	10.00	0.291	0.13	<0.005	<0.1	<0.01	<0.01	<0.2	<0.01	<0.001
CK-A-138	1	<0.1	2980	1020	104	5610	937	1410	4	3.2	0.80	0.9	31.3	511	0.280	0.4	0.8	2.6	0.03	0.01	0.62	<0.2	38	3.367	15.90	0.387	0.18	<0.005	<0.1	<0.01	<0.01	<0.2	<0.01	<0.001
CK-A-139	1	<0.1	3190	967	108	5980	889	1240	5	3.5	0.84	0.9	32.9	540	0.297	0.4	1.1	1.7	0.03	<0.01	0.35	<0.2	36	2.883	13.89	0.383	0.16	<0.005	<0.1	<0.01	<0.01	<0.2	<0.01	<0.001
CK-A-140	1	<0.1	3210	799	54	5740	656	1090	4	3.0	0.53	0.9	61.0	621	0.273	<0.3	0.7	2.7	0.03	<0.01	0.47	<0.2	35	2.417	12.82	0.184	0.14	<0.005	<0.1	<0.01	<0.01	<0.2	0.01	<0.001
CK-A-141	<1	<0.1	3180	862	63	5310	633	1120	4	3.0	0.57	0.9	58.8	736	0.292	<0.3	0.5	2.8	0.03	<0.01	0.48	<0.2	36	2.447	13.72	0.215	0.18	<0.005	<0.1	<0.01	<0.01	<0.2	<0.01	<0.001
CK-A-142	<1	<0.1	3630	1230	179	1370	789	1350	2	5.3	1.41	1.0	29.5	790	0.374	0.5	4.1	7.9	0.05	<0.01	1.04	<0.2	52	2.656	14.57	0.417	0.55	0.009	<0.1	<0.01	<0.01	<0.2	<0.01	<0.001
CK-A-143	1	<0.1	3480	1010	101	7140	1170	1610	6	3.8	0.83	1.0	31.1	454	0.273	0.6	1.5	16.1	0.03	<0.01	0.32	<0.2	35	3.689	13.39	0.324	0.14	<0.005	<0.1	<0.01	<0.01	<0.2	0.03	<0.001
CK-A-144	1	<0.1	3360	1120	145	6840	731	1870	5	4.0	1.07	1.0	24.5	645	0.273	0.7	0.9	19.9	0.05	<0.01	0.50	<0.2	41	2.694	16.43	0.483	0.17	<0.005	<0.1	<0.01	<0.01	<0.2	0.02	<0.001
CK-A-145	<1	<0.1	4250	1290	142	849	944	1320	1	5.0	0.86	1.0	39.6	905	0.412	1.1	2.3	33.3	0.04	<0.01	0.86	<0.2	62	2.780	15.89	0.370	0.51	0.014	<0.1	<0.01	<0.01	<0.2	0.02	<0.001
CK-A-146	4	0.2	4480	1200	196	9720	1270	1900	8	6.2	1.31	1.2	62.0	562	0.678	1.1	1.7	34.3	0.06	0.01	0.36	<0.2	41	3.405	16.02	0.774	0.19	0.006	<0.1	<0.01	<0.01	<0.2	0.02	<0.001
CK-A-147	1	<0.1	2630	705	87	6210	955	582	5	3.3	0.85	0.9	30.3	646	0.356	0.4	0.7	2.9	0.03	<0.01	0.39	<0.2	30	3.741	10.57	0.457	0.14	<0.005	<0.1	<0.01	<0.01	<0.2	<0.01	<0.001
CK-A-148	4	0.1	3700	1030	107	8380	1090	1370	6	3.9	1.01	0.9	32.1	555	0.369	0.5	0.6	5.6	0.03	<0.01	0.43	<0.2	35	3.155	14.40	0.479	0.21	<0.005	<0.1	<0.01	<0.01	<0.2	0.01	<0.001
CK-A-149	3	0.1	3460	830	73	8940	1450	520	7	4.2	1.00	1.1	27.8	253	0.560	0.9	0.8	5.5	0.03	<0.01	0.25	<0.2	33	4.778	10.49	0.465	0.08	<0.005	<0.1	<0.01	<0.01	<0.2	0.01	<0.001
CK-A-150	<1	<0.1	3300	1800	67	2830	399	2150	3	2.1	0.88	0.9	84.2	1490	0.507	0.6	4.9	11.6	0.03	<0.01	0.85	<0.2	53	1.784	23.98	0.261	0.21	<0.005	<0.1	<0.01	<0.01	<0.2	0.02	<0.001
CK-A-151	3	<0.1	3440	1120	60	7870	1010	1340	6	3.9	0.79	0.9	31.7	831	0.353	0.6	0.8	13.3	0.03	<0.01	0.52	<0.2	35	3.498	16.44	0.377	0.13	<0.005	<0.1	<0.01	<0.01	<0.2	0.03	<0.001
CK-A-152	<1	<0.1	3000	1550	128	2890	536	1630	3	2.2	1.68	0.9	69.8	1490	0.580	0.6	1.7	19.4	0.05	<0.01	1.35	<0.2	63	2.170	19.27	0.421	0.25	<0.005	<0.1	<0.01	<0.01	<0.2	<0.01	<0.001
CK-A-153	<1	<0.1	7030	2060	176	1610	2160	2720	2	9.8	2.87	1.0	71.4	2010	0.714	0.7	1.5	11.0	0.07	<0.01	1.66	<0.2	82	5.796	24.75	0.374	0.47	0.018	<0.1	<0.01	<0.01	<0.2	0.01	<0.001
CK-A-154	<1	<0.1	3370	1780	162	3020	1130	2670	3	5.3	1.64	1.1	58.3	914	0.607	0.7	3.5	7.3	0.06	<0.01	0.73	<0.2	60	3.986	19.14	0.441	0.72	0.012	<0.1	<0.01	<0.01	<0.2	0.02	<0.001
CK-A-155	<1	<0.1	4970	2690	215	2450	7430	4580	3	6.7	4.79	1.1	75.3	1170	0.661	0.5	2.6	4.4	0.08	0.01	1.23	<0.2	66	12.786	24.76	0.542	0.83	0.011	<0.1	<0.01	<0.01	<0.2	0.02	<0.001
CK-A-156	<1	<0.1	2910	1230	124	1320	1040	1660	2	2.4	2.91	1.1	34.0	1010	0.300	0.4	1.1	3.7	0.06	<0.01	1.01	<0.2	48	2.816	13.57	0.289	0.51	<0.005	<0.1	<0.01	<0.01	<0.2	<0.01	<0.001
CK-A-157	2	<0.1	3110	1220	115	5360	1000	1560	4	3.2	1.15	1.0	60.6	1200	0.556	0.5	0.8	2.7	0.04	<0.01	0.65	<0.2	42	3.515	16.69	0.496	0.23	<0.005	<0.1	<0.01	<0.01	<0.2	0.01	<0.001
CK-A-158	<1	<0.1	3800	1530	103	3700	1320	1950	4	3.0	1.64	1.0	62.6	1690	0.506	0.5	0.9	3.2	0.04	<0.01	0.97	<0.2	57	4.433	20.30	0.487	0.39	0.006	<0.1	<0.01	<0.01	<0.2	0.02	<0.001
CK-A-159	<1	<0.1	4520	1630	115	4310	798	2020	4	3.7	1.20	1.2	90.1	847	0.739	0.5	1.2	17.8	0.06	<0.01	0.56	<0.2	73	2.778	19.37	0.247	0.37	0.007	<0.1	<0.01	<0.01	<0.2	0.02	<0.001
CK-A-160	<1	<0.1	2820	1260	137	4160	540	1420	4	3.4	1.21	1.5	51.1	1380	0.546	0.9	1.7	48.8	0.05	<0.01	0.55	<0.2	70	1.838	13.88	0.530	0.24	0.006	<0.1	<0.01	<0.01	<0.2	0.02	<0.001
CK-A-161	<1	<0.1	2810	1230	116	2150	445	1450	2	3.8	1.40	1.2	34.0	1270	0.334	33.4	2.4	55.6	0.04	<0.01	0.67	<0.2	53	1.698	15.37	0.324	1.00	0.008	<0.1	<0.01	<0.01	<0.2	0.01	<0.001
CK-A-162	<1	<0.1	2760	1350	89	2420	560	1780	3	2.3	1.41	1.1	44.5	1220	0.441	0.4	1.2	13.7	0.03	<0.01	0.66	<0.2	54	1.987	17.38	0.403	0.33	<0.005	<0.1	<0.01	<0.01	<0.2	0.01	<0.001
CK-A-163	<1	<0.1	2830	1220	99	1500	826	1590	2	2.2	2.35	1.0	23.0	1110	0.228	1.1	77.4	8.6	0.03	<0.01	0.94	<0.2	50	2.505	14.40	0.288	0.32	0.005	<0.1	<0.01	<0.01	<0.2	0.08	0.001
CK-A-164	<1	<0.1	2620	1130	105	2370	697	1350	3	2.2	1.41	0.9	42.1	1170	0.407	0.5	3.2	8.3	0.03	<0.01	0.74	<0.2	46	2.562	15.25	0.528	0.30	<0.005	<0.1	<0.01	<0.01	<0.2	<0.01	0.001
CK-A-165	<1	<0.1	2610	1310	57	1640	247	1420	2	1.6	1.08	1.0	77.8	1190	0.454	<0.3	1.7	29.9	0.03	<0.01	0.62	<0.2	51	1.071	16.43	0.191	0.17	<0.005	<0.1	<0.01	<0.01	<0.2	<0.01	<0.001
CK-A-166	<1	<0.1	2780	1160	123	2870	470	1430	3	2.8	1.08	1.1	44.4	1140	0.339	<0.3	1.4	30.2	0.04	<0.01	0.73	<0.2	53	1.646	17.51	0.421	0.23	0.006	<0.1	<0.01	<0.01	<0.2	<0.01	<0.001
CK-A-167	1	<0.1	3810	1240	87	6040	857	1820	5	4.1	0.84	1.0	62.0	1020	0.453	0.4	0.7	42.9	0.03	<0.01	0.75	<0.2	44	2.796	20.14	0.515	0.20	<0.005	<0.1	<0.01	<0.01	<0.2	0.01	<0.001
CK-A-168	<1	<0.1	4220	1790	46	2680	801	3190	3	2.3	0.71	0.9	33.2	662	0.292	0.3	1.0	13.3	0.02	<0.01	0.46	<0.2	70	2.236	26.83	0.212	0.13	<0.005	<0.1	<0.01	<0.01	<0.2	<0.01	<0.001
CK-A-169	<1	<0.1	8790	2570	108	2840	1510	4380	3	4.1	1.14	1.5	91.3	1310	0.565	0.5	1.5	19.4	0.04	0.01	1.10	<0.2	77	4.137	32.06	0.285	0.24	0.006	0.2	<0.01	<0.01	<0.2	0.01	<0.001
CK-A-170	<1	<0.1	5780	2670	45	3120	974	4830	3	2.7	0.70	0.8	249.4	1210	0.719	0.5	1.2	12.1	0.04	0.01	0.67	<0.2	86	2.804	36.36	0.201	0.17	<0.005	<0.1	<0.01	<0.01	<0.2	<0.01	<0.001
CK-A-171	1	<0.1	8420	3430	82	4430	2020	6940	4	6.6	1.18	1.0	184.9	3030	0.605	0.6	3.7	2.7	0.05	0.01	1.94	<0.2	80	5.400	46.22	0.197	0.22	0.012	<0.1	<0.01	<0.01	<0.2	0.01	<0.001
CK-A-172	1	<0.1	6020	1700	169	7960	1380	3320	8	5.1	1.16	0.8	27.9	620	0.306	0.4	1.0	2.0	0.06	<0.01	0.61	<0.2	43	2.868	32.94	0.635	0.23	0.006	<0.1	<0.01	<0.01	<0.2	<0.01	<0.001
CK-A-173	1	<0.1	4410	2170	143	5700	1090	3120	5	3.7	1.23	0.9	24.7	966	0.301	0.4	0.9	2.5	0.04	<0.01	0.71	<0.2	49	2.910	32.35	0.420	0.19	<0.005	<0.1	<0.01	<0.01	<0.2	<0.01	<0.001
CK-A-174	2	<0.1	6350	1650	318	9420	1140	3510	9	12.8	1.09	1.0	14.0	409	0.203	0.4	0.6	1.9	0.08	<0.01	0.51	<0.2	47	2.328	29.03	0.470	0.41	0.023	<0.1	<0.01	<0.01	<0.2	<0.01	<0.001
CK-A-175	2	<0.1	8250	3020	122	8210	1520	8700	7	5.6	1.25	0.9	32.7	600	0.247	0.9	0.8	20.9	0.04	<0.01	0.79	<0.2	65	2.756	51.16	0.494	0.21	0.006	<0.1	<0.01	<0.01	<0.2	<0.01	<0.001
CK-A-176	2	<0.1	6850	3400	221	8240	1680	6820	7	5.9	1.79	1.2	43.8	879	0.451	0.9	1.3	18.8	0.06	<0.01	0.91	<0.2	55	3.154	46.15	0.748	0.27	0.008	<0.1	<0.01	<0.01	<0.2	<0.01	<0.001
CK-A-177	<1	<0.1	3500	1470	94	4640	673	1730	4	3.1	1.06	1.0	74.8	1490	0.468	0.4	0.7	30.6	0.04	<0.01	0.97	<0.2	51	2.227	22.09	0.417	0.22	<0.005	<0.1	<0.01	<0.01	<0.2	<0.01	<0.001
CK-A-178	<1	<0.1	4680	1590	89	6030	972	3330	6	4.0	0.78	1.3	54.0	1030	0.381	0.4	0.9	37.1	0.03	<0.01	0.75	<0.2	45	2.562	30.38	0.506	0.22	<0.005	<0.1	<0.01	<0.01	<0.2	<0.01	<0.001
CK-A-179	<1	<0.1	5700	1990	65	6210	1120	4760	6	4.0	0.75	1.2	59.4	1190	0.246	0.5	0.7	34.2	0.03	<0.01	0.75	<0.2	52	2.722	36.54	0.352	0.16	<0.005	<0.1	<0.01	<0.01	<0.2	0.01	<0.001
CK-A-180	1	<0.1	5880	1930	61	6750	1230	4590	6	4.2	0.68	1.2	90.6	1080	0.337	0.5	1.4	61.4	0.03	<0.01	0.73	<0.2	50	3.033	36.64	0.333	0.15	<0.005	<0.1	<0.01	<0.01	<0.2	<0.01	<0.001
CK-A-181	1	<0.1	6760	2190	44	7210	1490	5550	7	4.6	0.57	1.1	189.8	1090	0.542	0.4	0.5	32.3	0.04	<0.01	0.82	<0.2	53	3.548	38.96	0.230	0.10	<0.005	<0.1	<0.01	<0.01	<0.2	<0.01	<0.001
CK-A-182	1	<0.1	2550	996	81	5020	1130	1070	5	4.2	0.56	1.1	27.9	315	0.238	0.3	0.5	41.9	0.03	<0.01	0.36	<0.2	39	4.045	14.33	0.235	0.16	0.006	<0.1	<0.01	<0.01	<0.2	<0.01	<0.001

Geochemical grade assay of stream water collected in the Lomba Grande district

(3continued/3)

Sample No.	Sn	Sb	Te	I	Cs	Ba	La	Ce	Pr	Nd	Sm	Eu	Gd	Tb	Dy	Ho	Er	Tm	Yb	Lu	Hf	Ta	W	Re	Os	Pt	Au	Hg	Tl	Pb	Bi	Th
CK-A-127	<0.1	0.02	<0.01	3	0.033	29.5	0.200	0.482	0.061	0.255	0.079	0.026	0.075	0.011	0.054	0.012	0.034	0.005	0.035	0.005	0.020	<0.001	<0.02	<0.001	<0.002	<0.01	<0.002	<0.2	0.021	0.2	<0.01	0.021
CK-A-128	<0.1	0.03	<0.01	7	0.037	32.8	0.378	0.930	0.117	0.454	0.129	0.036	0.131	0.017	0.075	0.015	0.044	0.006	0.042	0.006	0.008	<0.001	<0.02	<0.001	<0.002	<0.01	<0.002	<0.2	0.019	0.5	<0.01	0.044
CK-A-129	<0.1	0.03	<0.01	6	0.038	36.2	0.444	1.093	0.134	0.566	0.156	0.047	0.163	0.023	0.102	0.020	0.058	0.008	0.057	0.008	0.011	<0.001	<0.02	<0.001	<0.002	<0.01	<0.002	<0.2	0.020	0.5	<0.01	0.047
CK-A-130	<0.1	0.03	<0.01	4	0.055	25.3	0.211	0.582	0.063	0.275	0.073	0.022	0.081	0.012	0.059	0.011	0.031	0.004	0.031	0.005	0.008	<0.001	<0.02	<0.001	<0.002	<0.01	<0.002	<0.2	0.030	0.4	<0.01	0.033
CK-A-131	<0.1	0.04	<0.01	6	0.051	18.1	0.223	0.614	0.066	0.262	0.069	0.019	0.075	0.009	0.041	0.008	0.025	0.003	0.026	0.004	0.006	<0.001	<0.02	<0.001	<0.002	<0.01	<0.002	<0.2	0.022	0.4	<0.01	0.040
CK-A-132	<0.1	0.02	<0.01	8	0.054	23.1	0.260	0.706	0.075	0.297	0.081	0.022	0.090	0.011	0.048	0.010	0.028	0.003	0.027	0.005	0.007	<0.001	<0.02	<0.001	<0.002	<0.01	<0.002	<0.2	0.022	0.4	<0.01	0.037
CK-A-133	<0.1	0.02	<0.01	5	0.055	17.3	0.211	0.571	0.068	0.274	0.080	0.021	0.084	0.011	0.047	0.009	0.029	0.003	0.028	0.005	0.007	<0.001	<0.02	<0.001	<0.002	<0.01	<0.002	<0.2	0.015	0.3	<0.01	0.024
CK-A-134	<0.1	0.02	0.01	5	0.015	21.4	0.082	0.196	0.027	0.115	0.033	0.011	0.037	0.004	0.023	0.004	0.013	0.002	0.017	0.003	0.005	<0.001	<0.02	<0.001	<0.002	<0.01	<0.002	<0.2	0.009	0.2	<0.01	0.023
CK-A-135	<0.1	0.02	<0.01	7	0.021	27.6	0.083	0.189	0.028	0.116	0.034	0.011	0.032	0.004	0.020	0.004	0.011	0.001	0.013	0.002	0.003	<0.001	<0.02	<0.001	<0.002	<0.01	<0.002	<0.2	0.012	0.1	<0.01	0.022
CK-A-136	<0.1	0.02	<0.01	12	0.041	23.3	0.419	0.929	0.125	0.515	0.136	0.033	0.120	0.014	0.064	0.012	0.037	0.004	0.032	0.005	0.007	<0.001	<0.02	<0.001	<0.002	<0.01	<0.002	<0.2	0.012	0.3	<0.01	0.050
CK-A-137	<0.1	0.02	<0.01	5	0.026	28.6	0.195	0.478	0.064	0.266	0.073	0.022	0.072	0.010	0.049	0.010	0.028	0.004	0.028	0.004	0.004	<0.001	<0.02	<0.001	<0.002	<0.01	<0.002	<0.2	0.013	0.2	<0.01	0.030
CK-A-138	<0.1	0.03	<0.01	8	0.044	33.8	0.314	0.734	0.094	0.397	0.112	0.033	0.108	0.014	0.064	0.013	0.037	0.005	0.032	0.005	0.009	<0.001	<0.02	<0.001	<0.002	<0.01	<0.002	<0.2	0.017	0.3	<0.01	0.037
CK-A-139	<0.1	0.02	<0.01	6	0.025	36.3	0.274	0.635	0.087	0.362	0.106	0.030	0.109	0.012	0.065	0.012	0.033	0.004	0.036	0.005	0.009	<0.001	<0.02	<0.001	<0.002	<0.01	<0.002	<0.2	0.014	0.4	<0.01	0.041
CK-A-140	<0.1	0.02	<0.01	6	0.017	23.3	0.135	0.324	0.043	0.179	0.054	0.015	0.052	0.007	0.032	0.005	0.015	0.002	0.021	0.003	0.005	<0.001	<0.02	<0.001	<0.002	<0.01	<0.002	<0.2	0.010	0.3	<0.01	0.034
CK-A-141	<0.1	0.02	<0.01	10	0.019	23.8	0.182	0.409	0.054	0.235	0.072	0.019	0.067	0.008	0.036	0.008	0.019	0.003	0.020	0.003	0.009	<0.001	<0.02	<0.001	<0.002	<0.01	<0.002	<0.2	0.010	0.2	<0.01	0.037
CK-A-142	<0.1	0.03	<0.01	22	0.074	23.7	0.572	1.404	0.169	0.671	0.182	0.041	0.173	0.022	0.101	0.015	0.048	0.006	0.042	0.006	0.017	<0.001	<0.02	<0.001	<0.002	<0.01	<0.002	<0.2	0.016	0.5	<0.01	0.055
CK-A-143	<0.1	0.02	<0.01	7	0.027	41.5	0.192	0.455	0.057	0.239	0.072	0.025	0.081	0.010	0.056	0.011	0.032	0.004	0.030	0.004	0.005	<0.001	<0.02	<0.001	<0.002	<0.01	<0.002	<0.2	0.019	0.6	<0.01	0.034
CK-A-144	<0.1	0.02	<0.01	8	0.035	48.1	0.411	0.974	0.131	0.554	0.151	0.043	0.145	0.019	0.085	0.016	0.048	0.006	0.044	0.007	0.008	<0.001	<0.02	<0.001	<0.002	<0.01	<0.002	<0.2	0.012	0.5	<0.01	0.047
CK-A-145	<0.1	0.04	0.01	12	0.061	22.4	0.431	1.022	0.133	0.516	0.147	0.035	0.128	0.017	0.075	0.013	0.041	0.005	0.038	0.006	0.018	<0.001	<0.02	<0.001	<0.002	<0.01	<0.002	<0.2	0.019	0.4	<0.01	0.064
CK-A-146	<0.1	0.02	<0.01	6	0.038	78.7	0.455	1.332	0.152	0.613	0.191	0.060	0.195	0.027	0.124	0.026	0.071	0.010	0.067	0.011	0.010	<0.001	<0.02	<0.001	<0.002	<0.01	<0.002	<0.2	0.020	0.6	<0.01	0.066
CK-A-147	<0.1	0.03	<0.01	3	0.039	39.0	0.273	0.663	0.083	0.364	0.109	0.034	0.127	0.017	0.082	0.015	0.043	0.005	0.042	0.006	0.006	<0.001	<0.02	<0.001	<0.002	<0.01	<0.002	<0.2	0.019	0.4	<0.01	0.049
CK-A-148	<0.1	0.02	<0.01	4	0.030	63.9	0.287	0.809	0.095	0.410	0.119	0.041	0.129	0.017	0.079	0.016	0.044	0.006	0.041	0.006	0.008	<0.001	<0.02	<0.001	<0.002	<0.01	<0.002	<0.2	0.022	0.4	<0.01	0.050
CK-A-149	<0.1	0.01	<0.01	2	0.034	66.4	0.239	0.617	0.077	0.339	0.104	0.041	0.116	0.016	0.083	0.016	0.044	0.006	0.043	0.006	0.007	<0.001	<0.02	<0.001	<0.002	<0.01	<0.002	<0.2	0.039	0.4	<0.01	0.029
CK-A-150	<0.1	0.02	<0.01	11	0.043	32.7	0.354	0.826	0.104	0.421	0.108	0.028	0.098	0.013	0.056	0.010	0.028	0.004	0.026	0.004	0.009	<0.001	<0.02	<0.001	<0.002	<0.01	<0.002	<0.2	0.012	0.5	<0.01	0.057
CK-A-151	<0.1	0.02	<0.01	5	0.026	59.7	0.268	0.604	0.085	0.353	0.101	0.035	0.105	0.014	0.070	0.013	0.039	0.004	0.035	0.006	0.006	<0.001	<0.02	<0.001	<0.002	<0.01	<0.002	<0.2	0.018	0.5	<0.01	0.047
CK-A-152	<0.1	0.03	0.01	17	0.055	28.6	0.573	1.506	0.169	0.686	0.181	0.044	0.174	0.019	0.092	0.015	0.042	0.005	0.041	0.005	0.009	<0.001	<0.02	<0.001	<0.002	<0.01	<0.002	<0.2	0.012	0.8	<0.01	0.083
CK-A-153	<0.1	0.02	0.01	26	0.269	21.6	0.598	1.563	0.173	0.659	0.169	0.040	0.164	0.019	0.084	0.015	0.044	0.005	0.039	0.005	0.019	0.001	<0.02	<0.001	<0.002	<0.01	<0.002	<0.2	0.021	0.7	<0.01	0.099
CK-A-154	<0.1	0.02	<0.01	11	0.140	28.3	0.596	1.516	0.158	0.624	0.168	0.041	0.163	0.020	0.089	0.016	0.048	0.006	0.041	0.006	0.020	<0.001	<0.02	<0.001	<0.002	<0.01	<0.002	<0.2	0.021	0.8	<0.01	0.074
CK-A-155	<0.1	0.06	0.01	12	0.146	25.1	0.795	2.098	0.214	0.816	0.225	0.053	0.210	0.024	0.108	0.019	0.056	0.007	0.051	0.006	0.030	<0.001	<0.02	<0.001	<0.002	<0.01	<0.002	<0.2	0.032	0.9	<0.01	0.073
CK-A-156	<0.1	0.03	<0.01	8	0.077	15.6	0.395	1.136	0.107	0.415	0.122	0.029	0.102	0.014	0.065	0.010	0.030	0.004	0.028	0.004	0.017	<0.001	<0.02	<0.001	<0.002	<0.01	<0.002	<0.2	0.012	0.6	<0.01	0.052
CK-A-157	<0.1	0.03	<0.01	7	0.038	46.2	0.486	1.187	0.143	0.571	0.167	0.044	0.169	0.020	0.096	0.017	0.053	0.007	0.046	0.006	0.012	<0.001	<0.02	<0.001	<0.002	<0.01	<0.002	<0.2	0.016	0.4	<0.01	0.067
CK-A-158	<0.1	0.03	<0.01	12	0.098	42.2	0.589	1.428	0.172	0.655	0.195	0.049	0.189	0.022	0.099	0.019	0.053	0.006	0.048	0.007	0.016	<0.001	<0.02	<0.001	<0.002	<0.01	<0.002	<0.2	0.023	0.6	<0.01	0.076
CK-A-159	<0.1	0.03	<0.01	13	0.072	28.2	0.284	0.884	0.085	0.344	0.096	0.026	0.090	0.010	0.047	0.009	0.028	0.003	0.027	0.004	0.011	<0.001	<0.02	<0.001	<0.002	<0.01	<0.002	<0.2	0.022	0.4	<0.01	0.056
CK-A-160	<0.1	0.02	<0.01	20	0.077	23.1	0.681	1.857	0.203	0.799	0.205	0.047	0.203	0.024	0.099	0.019	0.058	0.008	0.060	0.009	0.014	<0.001	<0.02	<0.001	<0.002	<0.01	<0.002	<0.2	0.017	0.6	<0.01	0.065
CK-A-161	<0.1	0.02	<0.01	14	0.077	18.8	0.467	1.183	0.130	0.501	0.125	0.030	0.127	0.014	0.060	0.012	0.035	0.004	0.030	0.005	0.014	<0.001	<0.02	<0.001	<0.002	<0.01	<0.002	<0.2	0.013	0.5	0.02	0.065
CK-A-162	<0.1	0.03	0.02	13	0.071	21.7	0.543	1.429	0.154	0.589	0.165	0.037	0.147	0.018	0.074	0.015	0.044	0.006	0.044	0.006	0.013	<0.001	<0.02	<0.001	<0.002	<0.01	<0.002	<0.2	0.015	0.4	<0.01	0.063
CK-A-163	<0.1	0.04	<0.01	8	0.071	16.2	0.402	1.098	0.117	0.450	0.118	0.028	0.116	0.013	0.057	0.010	0.030	0.004	0.029	0.005	0.016	<0.001	0.03	<0.001	<0.002	<0.01	<0.002	<0.2	0.013	0.8	<0.01	0.051
CK-A-164	<0.1	0.03	<0.01	9	0.056	26.7	0.608	1.532	0.177	0.727	0.187	0.046	0.183	0.024	0.096	0.020	0.051	0.007	0.054	0.008	0.014	<0.001	<0.02	<0.001	<0.002	<0.01	<0.002	<0.2	0.015	0.5	<0.01	0.069
CK-A-165	<0.1	0.02	<0.01	10	0.061	19.6	0.260	0.753	0.077	0.293	0.080	0.019	0.071	0.009	0.037	0.006	0.018	0.003	0.014	0.003	0.006	<0.001	<0.02	<0.001	<0.002	<0.01	<0.002	<0.2	0.010	0.3	<0.01	0.051
CK-A-166	<0.1	0.04	<0.01	10	0.044	29.7	0.562	1.417	0.169	0.688	0.182	0.040	0.167	0.020	0.081	0.015	0.041	0.006	0.038	0.007	0.011	<0.001	<0.02	<0.001	<0.002	<0.01	<0.002	<0.2	0.012	0.5	<0.01	0.064
CK-A-167	<0.1	0.03	<0.01	8	0.026	45.3	0.526	1.289	0.166	0.670	0.183	0.045	0.178	0.021	0.097	0.017	0.046	0.006	0.045	0.007	0.010	<0.001	<0.02	<0.001	<0.002	<0.01	<0.002	<0.2	0.013	0.5	<0.01	0.070
CK-A-168	0.7	0.03	<0.01	31	0.052	33.6	0.254	0.626	0.072	0.268	0.077	0.021	0.072	0.008	0.041	0.008	0.022	0.002	0.023	0.003	0.006	<0.001	<0.02	<0.001	<0.002	<0.01	<0.002	<0.2	0.018	0.3	<0.01	0.031
CK-A-169	<0.1	0.07	<0.01	32	0.069	39.7	0.392	1.041	0.112	0.431	0.124	0.030	0.115	0.013	0.052	0.008	0.031	0.004	0.027	0.004	0.012	<0.001	<0.02	0.001	<0.002	<0.01	<0.002	<0.2	0.015	0.5	<0.01	0.052
CK-A-170	<0.1	0.03	<0.01	37	0.035	41.9	0.242	0.646	0.069	0.280	0.070	0.019	0.071	0.008	0.037	0.006	0.019	0.002	0.019	0.003	0.006	<0.001	<0.02	<0.001	<0.002	<0.01	<0.002	<0.2	0.017	0.3	<0.01	0.037
CK-A-171	<0.1	0.06	<0.01	26	0.043	43.3	0.256	0.689	0.077	0.280	0.069	0.022	0.076	0.009	0.037	0.007	0.019	0.003	0.019	0.003	0.007	<0.001	<0.02	<0.001	<0.002	<0.01	<0.002	<0.2	0.009	1.3	<0.01	0.045
CK-A-172	<0.1	0.03	<0.01	8	0.033	45.1	0.502	1.232	0.165	0.736	0.214	0.052	0.211	0.026	0.117	0.020	0.057	0.007	0.054	0.009	0.010	<0.001	<0.02	<0.001	<0.002	<0.01	<0.002	<0.2	0.011	0.7	<0.01	0.061
CK-A-173	<0.1	0.03	<0.01	10	0.030	40.4	0.467	1.104	0.133	0.506	0.160	0.037	0.145	0.018	0.080	0.014	0.040	0.005	0.036	0.006	0.011	<0.001	<0.02	<0.001	<0.002	<0.01	<0.002	<0.2	0.012	0.8	<0.01	0.078
CK-A-174	<0.1	0.04	<0.01	7	0.040	43.4	0.341	0.831	0.118	0.496	0.150	0.040	0.148	0.020	0.091	0.017	0.047	0.006	0.047	0.007	0.014	0.002	<0.02	<0.001	<0.002	<0.01	<0.002	<0.2	0.010	0.6	<0.01	0.069
CK-A-175	<0.1	0.03	<0.01	15	0.028	68.3	0.397	0.888	0.128	0.537	0.155	0.042	0.154	0.019	0.082	0.016	0.046	0.006	0.041	0.007	0.010	<0.001	<0.02	<0.001	<0.002	<0.01	<0.002	<0.2	0.013	0.6	<0.01	0.059
CK-A-176	<0.1	0.03	<0.01	13	0.035	58.5	0.695	1.591	0.220	0.883	0.253	0.058	0.248	0.031	0.143	0.024	0.064	0.009	0.063	0.009	0.014	<0.001	<0.02	<0.001	<0.002	<0.01	<0.002	<0.2	0.015	0.7	<0.01	0.083
CK-A-177	<0.1	0.03	<0.01	11	0.030	37.2	0.519	1.402	0.155	0.640	0.170	0.039	0.160	0.019	0.081	0.014	0.040	0.005	0.037	0.006	0.010	<0.001	<0.02	<0.001	<0.002	<0.01	<0.002	<0.2	0.012	0.6	<0.01	0.076
CK-A-178	<0.1	0.03	<0.01	14	0.017	44.4	0.468	1.077	0.150	0.603	0.172	0.045	0.168	0.020	0.088	0.018	0.052	0.007	0.046	0.007	0.009	<0.001	<0.02	<0.001	<0.002	<0.01	<0.002	<0.2	0.009	0.7	<0.01	0.069
CK-A-179	<0.1	0.04	<0.01	17	0.019	42.9	0.323	0.759	0.102	0.416	0.106	0.032	0.111	0.013	0.057	0.011	0.030	0.003	0.027	0.004	0.008	<0.001	<0.02	<0.001	<0.002	<0.01	<0.002	<0.2	0.009	0.3	<0.01	0.053
CK-A-180	<0.1	0.04	<0.01	16	0.014	46.1	0.295	0.719	0.091	0.389	0.109	0.030	0.110	0.013	0.055	0.011	0.030	0.003	0.028	0.004	0.007	<0.001	<0.02	<0.001	<0.002	<0.01	<0.002	<0.2	0.010	0.4	<0.01	0.052
CK-A-181	<0.1	0.04	<0.01	18	0.016	52.8	0.160	0.374	0.049	0.208	0.053	0.022	0.060	0.007	0.033	0.007	0.018	0.003	0.015	0.003	0.004	<0.001	<0.02	<0.001	<0.002	<0.01	<0.002	<0.2	0.010	0.2	<0.01	0.035
CK-A-182	<0.1	0.02	<0.01	5	0.035	41.4	0.173	0.348	0.045	0.207	0.061	0.022	0.058	0.007	0.034	0.007	0.019	0.002	0.020	0.004	0.005	<0.001	<0.02	<0.001	<0.002	<0.01	<0.002	<0.2	0.021	0.3	<0.01	0.025

Geochemical grade assay of stream water collected in the Lomba Grande district

Sample No.	U	SO_4
CK-A-127	0.025	14
CK-A-128	0.039	14
CK-A-129	0.040	13
CK-A-130	0.022	11
CK-A-131	0.024	8
CK-A-132	0.022	10
CK-A-133	0.025	11
CK-A-134	0.010	13
CK-A-135	0.010	13
CK-A-136	0.034	8
CK-A-137	0.021	14
CK-A-138	0.030	13
CK-A-139	0.028	13
CK-A-140	0.015	13
CK-A-141	0.017	9
CK-A-142	0.052	6
CK-A-143	0.021	14
CK-A-144	0.035	13
CK-A-145	0.032	5
CK-A-146	0.039	18
CK-A-147	0.032	13
CK-A-148	0.028	16
CK-A-149	0.025	19
CK-A-150	0.034	9
CK-A-151	0.024	13
CK-A-152	0.056	8
CK-A-153	0.052	4
CK-A-154	0.059	6
CK-A-155	0.090	10
CK-A-156	0.050	6
CK-A-157	0.036	9
CK-A-158	0.047	8
CK-A-159	0.027	9
CK-A-160	0.053	12
CK-A-161	0.040	8
CK-A-162	0.041	7
CK-A-163	0.046	8
CK-A-164	0.050	7
CK-A-165	0.026	8
CK-A-166	0.050	9
CK-A-167	0.038	12
CK-A-168	0.022	13
CK-A-169	0.057	14
CK-A-170	0.022	9
CK-A-171	0.025	9
CK-A-172	0.091	11
CK-A-173	0.111	10
CK-A-174	0.073	14
CK-A-175	0.111	14
CK-A-176	0.118	13
CK-A-177	0.045	10
CK-A-178	0.034	11
CK-A-179	0.026	11
CK-A-180	0.021	12
CK-A-181	0.012	11
CK-A-182	0.014	13

APPENDIX 9

Electron microprove analysis for olivine in the Paraná basaltic lava and intrusion

Sample No.	Ni	Mn	Mg	Fe	O	Total
	(wt%)					
AS004A Point9-1-core	0.015	0.389	12.131	18.169	29.334	60.038
AS004A Point9-2-core	0.064	0.431	10.451	19.875	30.979	61.800
AS004A Point10-1-core	0.043	0.379	13.097	16.436	29.911	59.866
AS004A Point10-2-core	—	0.435	12.176	17.497	31.521	61.629
AS004A Point10-3-core	0.035	0.212	10.668	7.993	23.800	42.708
AS021 Point7-1-core	0.020	0.303	13.317	14.772	33.057	61.469
AS021 Point7-2-core	0.035	0.297	14.300	14.185	31.566	60.383
AS021 Point8-1-core	—	0.231	9.953	10.547	22.245	42.976
KN003 Point5-1-core	0.195	0.155	29.989	9.177	38.155	77.671
KN003 Point5-2-core	0.120	0.204	28.709	12.287	36.573	77.893
KN003 Point5-3-core	0.183	0.168	28.117	11.979	38.350	78.797
KN003 Point6-1-core	0.214	0.118	28.472	10.027	41.271	80.102
KN003 Point6-2-core	0.243	0.127	29.746	9.340	39.757	79.213
TG62-226.3 Point1-1-core	0.184	0.211	27.577	13.517	37.950	79.439
TG62-226.3 Point1-1-rim	0.202	0.212	27.988	13.188	38.762	80.352
TG62-226.3 Point1-2-core	0.180	0.217	28.130	14.359	36.683	79.569
TG62-226.3 Point1-2-rim	0.166	0.209	27.015	13.913	39.886	81.189
TG62-226.3 Point2-1-core	0.136	0.172	28.494	11.824	36.054	76.680
TG62-226.3 Point2-1-rim	0.209	0.215	26.668	13.105	35.975	76.172
TG62-226.3 Point2-2-core	0.176	0.224	28.236	13.091	37.747	79.474
TG62-226.3 Point2-2-rim	0.204	0.179	28.291	11.310	35.888	75.872
TG114-289.9 Point3-1-core	0.160	0.231	26.470	14.638	36.858	78.357
TG114-289.9 Point3-1-rim	0.121	0.327	24.348	17.660	38.077	80.533
TG114-289.9 Point3-2-core	0.090	0.346	24.728	19.051	35.981	80.196
TG114-289.9 Point3-2-rim	0.193	0.307	23.273	18.155	39.814	81.742
TG114-289.9 Point4-1-core	0.176	0.224	26.244	14.149	37.686	78.479
TG114-289.9 Point4-1-rim	0.201	0.237	26.816	13.963	37.628	78.845
TG114-289.9 Point4-2-core	0.129	0.290	23.769	17.815	37.130	79.133
TG114-289.9 Point4-2-rim	0.114	0.328	24.446	18.794	36.823	80.505

Measuring Points of EPMA

AS004 Point 9 (Lava: Ribeira)

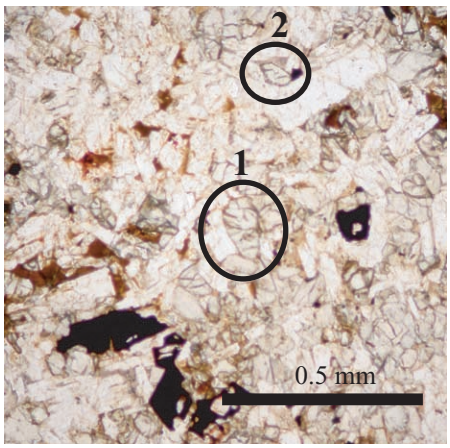

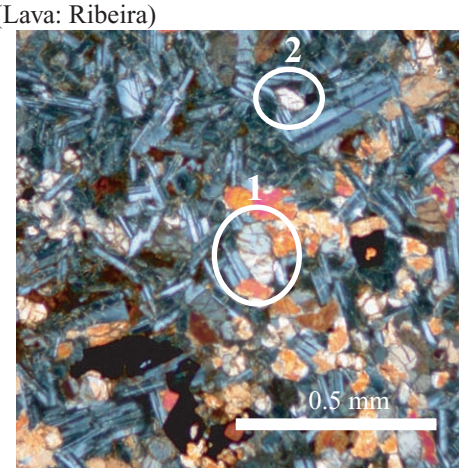

AS004A Point 10 (Lava: Ribeira)

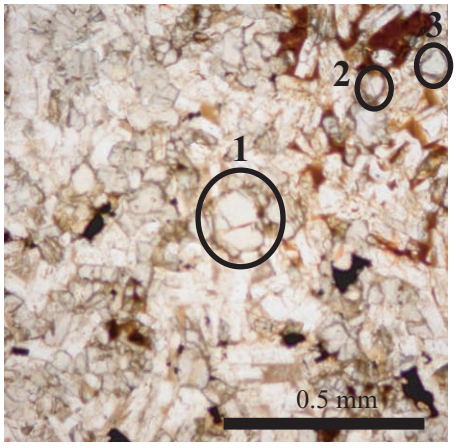

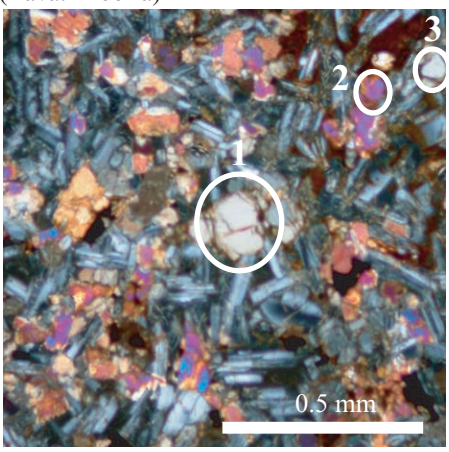

AS021 Point 7 (Lava: Gramado)

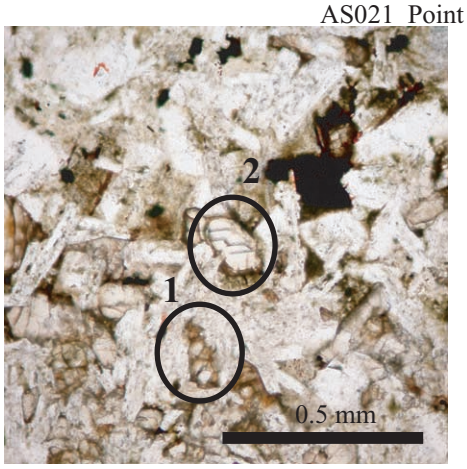

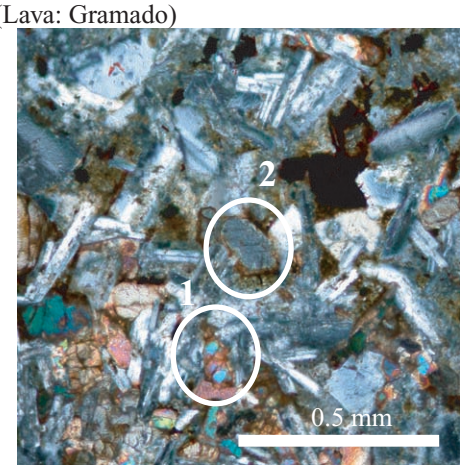

AS021 Point 8 (Lava: Gramado)

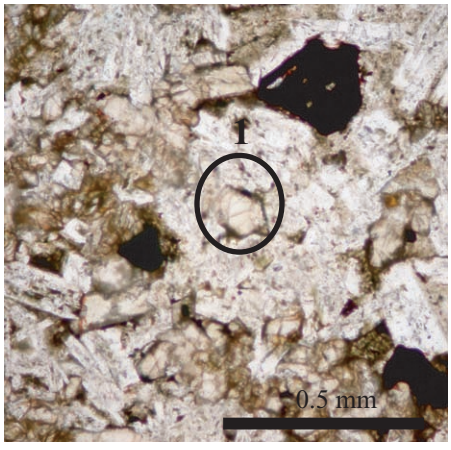

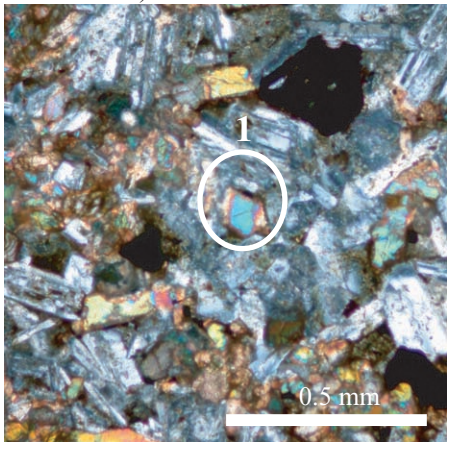

Measuring Points of EPMA

KN003 Point 5 (Feeder Dyke)

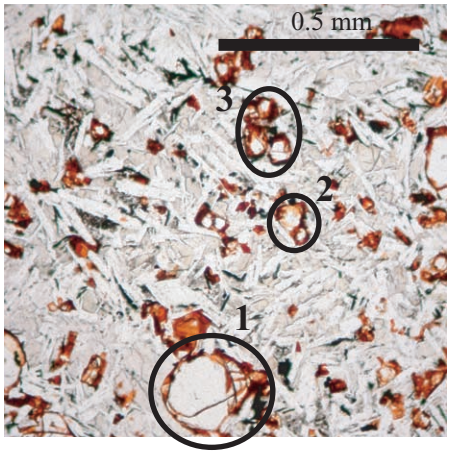

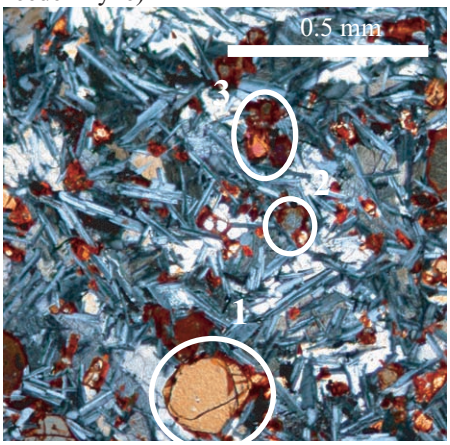

KN003 Point 6 (Feeder Dyke)

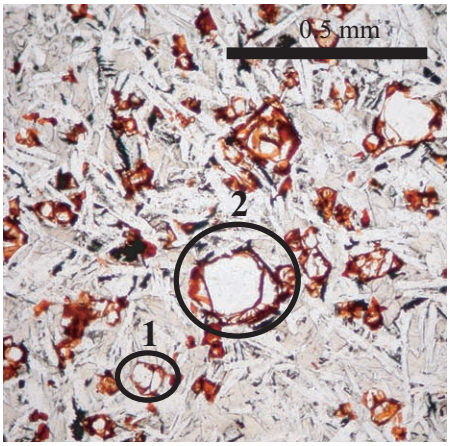

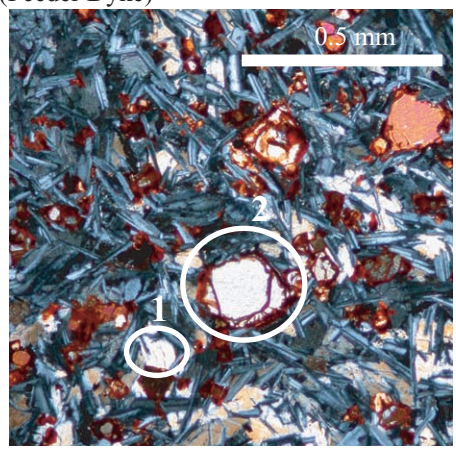

TG62-226.3 Point 1 (Intrusion: Drill Core)

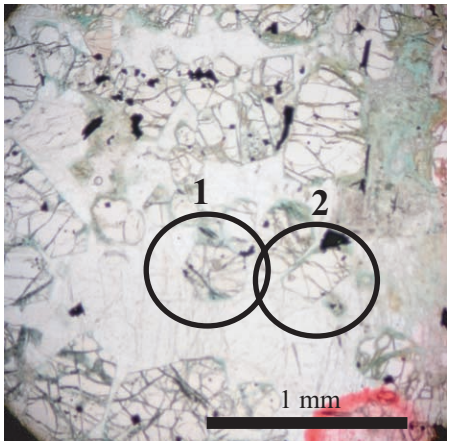

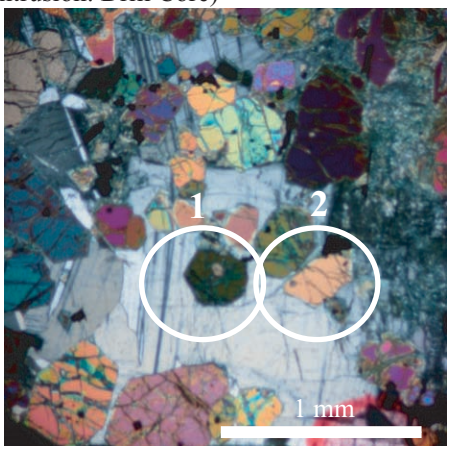

TG62-226.3 Point 2 (Intrusion: Drill Core)

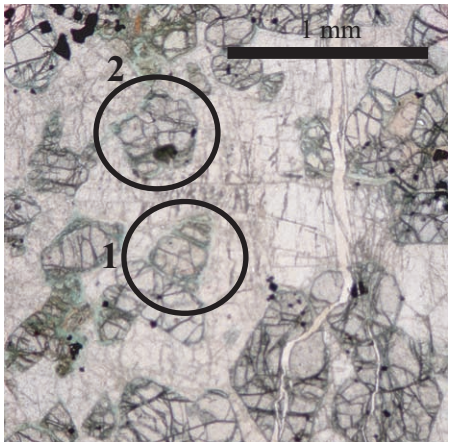

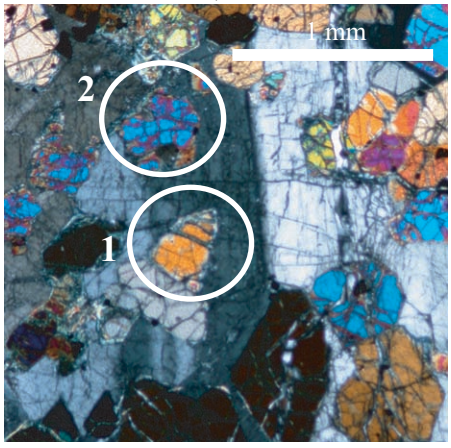

Measuring Points of EPMA

TG114-289.9 Point 3 (Intrusion: Drill Core)

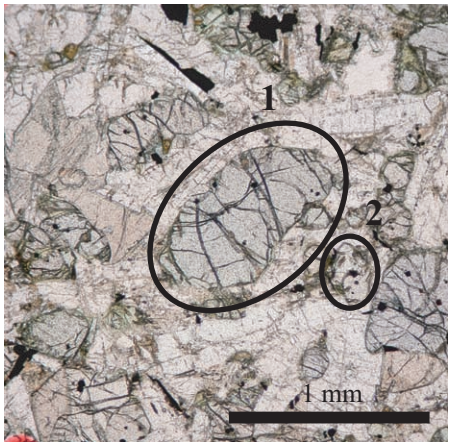

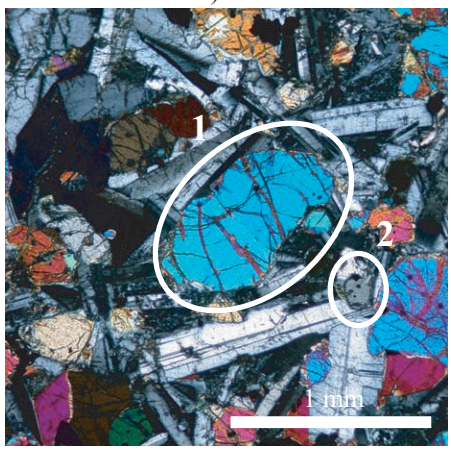

TG114-289.9 Point 4 (Intrusion: Drill Core)

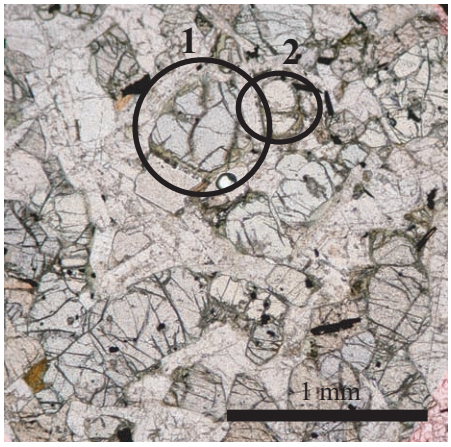

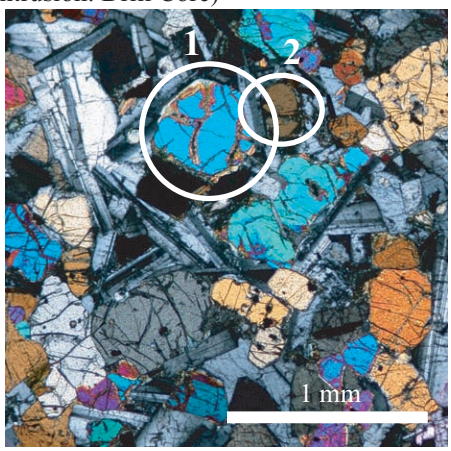

APPENDIX 10

$^{143}Nd/^{144}Nd$ and $^{87}Sr/^{86}Sr$ isotopic ratios for the Paraná basaltic lava and intrusion

Sample	$(^{143}Nd/^{144}Nd)$ p	Err	$(^{87}Sr/^{86}Sr)$ p	Err	Sm (ppm)	Nd (ppm)	Rb (ppm)	Sr (ppm)	^{147}Sm	^{144}Nd	^{87}Rb	^{86}Sr	$(^{147}Sm/^{144}Nd)$ p	$(^{87}Rb/^{86}Sr)$ p	λ (Sm)	λ (Rb)	$(^{143}Nd/^{144}Nd)$ initial	$(^{87}Sr/^{86}Sr)$ initial	ε Nd	ε Sr
AS001	0.512373	6	0.711215	15	3.8	17.0	40.9	210.0	0.5624785	4.0578098	11.3709620	20.7060000	0.1386163	0.5491627	6.53912E-12	1.42038E-11	0.512255	0.710200	-7.47	80.91
AS003	0.512368	7	0.706376	13	3.9	17.6	21.6	316.0	0.5877084	4.1976001	6.0230663	31.1576000	0.1400106	0.1933097	6.53912E-12	1.42038E-11	0.512249	0.706019	-7.59	21.56
AS006	0.512407	6	0.706153	15	6.2	26.9	28.6	353.0	0.9339879	6.4019680	7.9690529	34.8058000	0.1458908	0.2289576	6.53912E-12	1.42038E-11	0.512283	0.705730	-6.93	17.46
AS011	0.512394	4	0.706363	14	6.5	29.4	31.8	345.0	0.9804617	6.9916089	8.8410105	34.0170000	0.1402341	0.2598998	6.53912E-12	1.42038E-11	0.512275	0.705883	-7.09	19.63
AS014	0.512379	5	0.706311	17	13.2	62.3	53.3	471.0	1.9779968	14.8291710	14.8217148	46.4406000	0.1333855	0.3191542	6.53912E-12	1.42038E-11	0.512266	0.705721	-7.27	17.33
AS023	0.512336	5	0.710155	16	6.3	26.2	46.4	216.0	0.9388733	6.2432498	12.9085414	21.2976000	0.1503821	0.6061031	6.53912E-12	1.42038E-11	0.512208	0.709035	-8.39	64.37
AS024A	0.512570	5	0.706881	16	3.7	12.5	16.8	162.0	0.5480981	2.9836813	4.6683581	15.9732000	0.1836986	0.2922619	6.53912E-12	1.42038E-11	0.512414	0.706341	-4.37	26.13
KM106	0.512397	8	0.705923	17	9.5	43.1	25.2	462.5	1.4190925	10.2587142	7.0256880	45.6013375	0.1383304	0.1540676	6.53912E-12	1.42038E-11	0.512279	0.705638	-7.00	16.16
KM120	0.512413	4	0.70618	14	6.4	26.7	22.8	218.3	0.9660897	6.3479746	6.3463187	21.5204135	0.1521887	0.2948976	6.53912E-12	1.42038E-11	0.512284	0.705635	-6.91	16.11
KM142	0.512418	5	0.706235	15	9.5	43.0	29.5	564.7	1.4259549	10.2416203	8.2107531	55.6836932	0.1392314	0.1474535	6.53912E-12	1.42038E-11	0.512300	0.705962	-6.60	20.76
KM153	0.512399	4	0.706208	14	8.6	37.1	27.0	512.4	1.2912470	8.8277634	7.5108976	50.5188503	0.1462711	0.1486751	6.53912E-12	1.42038E-11	0.512275	0.705933	-7.09	20.34
KN002	0.512502	6	0.706743	13	1.7	6.6	5.9	174.0	0.2534079	1.5825298	1.6463975	17.1564000	0.1601284	0.0959640	6.53912E-12	1.42038E-11	0.512366	0.706566	-5.31	29.32
KN003	0.512567	5	0.705988	16	3.8	15.6	8.5	318.0	0.5695040	3.7033471	2.3753072	31.3548000	0.1537809	0.0757558	6.53912E-12	1.42038E-11	0.512436	0.705848	-3.94	19.13
KN005	0.512334	5	0.709502	18	5.8	23.3	48.8	188.0	0.8649026	5.5336090	13.5696982	18.5368000	0.1562999	0.7320410	6.53912E-12	1.42038E-11	0.512201	0.708149	-8.52	51.80
KN006	0.512421	6	0.706829	18	4.0	15.1	14.7	170.0	0.6047099	3.5974490	4.0937012	16.7620000	0.1680941	0.2442251	6.53912E-12	1.42038E-11	0.512278	0.706378	-7.02	26.65
KN009	0.512510	7	0.707613	16	4.1	16.3	58.3	213.0	0.6181273	3.8704729	16.2196563	21.0018000	0.1597033	0.7722984	6.53912E-12	1.42038E-11	0.512374	0.706186	-5.15	23.93
KN012	0.512400	5	0.706922	19	4.0	15.3	17.4	185.0	0.6053614	3.6502805	4.8375080	18.2410000	0.1658397	0.2651997	6.53912E-12	1.42038E-11	0.512259	0.706432	-7.39	27.42
KN014	0.512384	6	0.705917	16	7.7	35.2	33.4	399.0	1.1509931	8.3706240	9.2931987	39.3414000	0.1375039	0.2362193	6.53912E-12	1.42038E-11	0.512267	0.705480	-7.24	13.92
KN016	0.512456	5	0.706240	19	6.3	27.2	28.1	229.0	0.9498608	6.4816711	7.8119840	22.5794000	0.1465457	0.3459784	6.53912E-12	1.42038E-11	0.512331	0.705601	-5.98	15.62
KN019	0.512391	4	0.705804	17	4.9	21.7	10.3	355.0	0.7292740	5.1555955	2.8579493	35.0030000	0.1414529	0.0816487	6.53912E-12	1.42038E-11	0.512271	0.705653	-7.16	16.37
KN020	0.512370	6	0.706225	14	5.6	25.1	23.0	360.0	0.8331737	5.9840361	6.4119399	35.4960000	0.1392327	0.1806384	6.53912E-12	1.42038E-11	0.512252	0.705891	-7.54	19.75
KN022A	0.512387	5	0.706141	17	5.3	24.0	21.3	370.0	0.7946826	5.7210771	5.9292316	36.4820000	0.1389044	0.1625249	6.53912E-12	1.42038E-11	0.512269	0.705841	-7.20	19.03
KN024A	0.512376	7	0.706238	15	5.3	24.7	23.3	375.0	0.7999073	5.8743148	6.4853952	36.9750000	0.1361703	0.1753995	6.53912E-12	1.42038E-11	0.512260	0.705914	-7.37	20.07
KN027	0.512399	6	0.706497	18	6.2	26.1	31.9	264.0	0.9299938	6.2144668	8.8805558	26.0304000	0.1496498	0.3411609	6.53912E-12	1.42038E-11	0.512272	0.705866	-7.14	19.40
KN031	0.512376	4	0.706416	15	6.4	27.6	29.3	289.0	0.9564408	6.5738732	8.1561515	28.4954000	0.1454912	0.2862270	6.53912E-12	1.42038E-11	0.512252	0.705887	-7.52	19.69
KN032	0.512413	8	0.706190	20	4.3	17.8	19.3	285.0	0.6464084	4.2362829	5.3577339	28.1010000	0.1525886	0.1906599	6.53912E-12	1.42038E-11	0.512283	0.705838	-6.92	18.99
KN040A	0.512373	5	0.706457	17	6.1	28.0	32.2	336.0	0.9096085	6.6689402	8.9655759	33.1296000	0.1363948	0.2706213	6.53912E-12	1.42038E-11	0.512257	0.705957	-7.43	20.68
KN050	0.512384	6	0.705936	17	5.5	24.0	12.0	355.0	0.8237702	5.7196655	3.3351901	35.0030000	0.1440242	0.0952830	6.53912E-12	1.42038E-11	0.512262	0.705760	-7.34	17.88
KN052	0.512382	4	0.706136	19	4.6	20.1	17.3	335.0	0.6905617	4.7850638	4.8133479	33.0310000	0.1443161	0.1457221	6.53912E-12	1.42038E-11	0.512259	0.705867	-7.39	19.40
KN104	0.512397	5	0.705907	13	7.8	36.5	27.1	444.8	1.1695365	8.6985927	7.5455805	43.8586560	0.1344512	0.1720431	6.53912E-12	1.42038E-11	0.512283	0.705589	-6.93	15.46
KN110A	0.512439	4	0.705882	15	6.2	27.0	20.4	404.2	0.9230642	6.4203630	5.6839369	39.8552619	0.1437713	0.1426145	6.53912E-12	1.42038E-11	0.512317	0.705618	-6.27	15.88
KN112	0.512393	5	0.70715	12	5.6	24.9	21.8	314.6	0.8462054	5.9173233	6.0741563	31.0181589	0.1430048	0.1958258	6.53912E-12	1.42038E-11	0.512271	0.706788	-7.15	32.48
KN128	0.512425	7	0.705976	17	11.8	54.3	37.4	635.9	1.7637871	12.9330554	10.4093462	62.7002360	0.1363782	0.1660177	6.53912E-12	1.42038E-11	0.512309	0.705669	-6.42	16.60
KN150	0.51242	5	0.706188	18	11.9	56.0	51.0	497.3	1.7810230	13.3169042	14.2054548	49.0350653	0.1337415	0.2896999	6.53912E-12	1.42038E-11	0.512306	0.705653	-6.47	16.36
KN163	0.512453	4	0.706134	14	9.2	41.5	31.7	470.2	1.3848660	9.8778985	8.8132834	46.3604733	0.1401984	0.1901034	6.53912E-12	1.42038E-11	0.512334	0.705783	-5.93	18.21
KN172	0.512384	6	0.706064	11	10.1	46.1	34.4	462.0	1.5114620	10.9664400	9.5715577	45.5484128	0.1378261	0.2101403	6.53912E-12	1.42038E-11	0.512267	0.705676	-7.24	16.69
KN173	0.512419	6	0.70612	13	6.6	27.3	23.1	256.4	0.9935032	6.4934437	6.4248046	25.2761400	0.1530010	0.2541846	6.53912E-12	1.42038E-11	0.512289	0.705650	-6.81	16.33
TM107	0.512425	9	0.706454	17	6.0	25.0	22.8	257.3	0.8948684	5.9460892	6.3316590	25.3663490	0.1504970	0.2496086	6.53912E-12	1.42038E-11	0.512297	0.705993	-6.65	21.19
TM121	0.512386	8	0.705887	14	8.2	35.8	21.0	511.0	1.2231840	8.5204000	5.8443000	50.3846000	0.1435595	0.1159938	6.53912E-12	1.42038E-11	0.512264	0.705673	-7.30	16.64

$^{143}Nd/^{144}Nd$ and $^{87}Sr/^{86}Sr$ isotopic ratios for the Paraná basaltic lava and intrusion

Sample	$(^{143}Nd/^{144}Nd)$ p	Err	$(^{87}Sr/^{86}Sr)$ p	Err	Sm (ppm)	Nd (ppm)	Rb (ppm)	Sr (ppm)	^{147}Sm	^{144}Nd	^{87}Rb	^{86}Sr	$(^{147}Sm/^{144}Nd)$ p	$(^{87}Rb/^{86}Sr)$ p	λ (Sm)	λ (Rb)	$(^{143}Nd/^{144}Nd)$ initial	$(^{87}Sr/^{86}Sr)$ initial	ε Nd	ε Sr
TM126	0.512415	6	0.706844	14	11.1	50.2	33.0	572.0	1.6638900	11.9476000	9.1839000	56.3992000	0.1392656	0.1628374	6.53912E-12	1.42038E-11	0.512297	0.706543	-6.66	29.00
TM130	0.512393	6	0.705894	11	8.1	35.6	22.7	497.0	1.2107679	8.4628697	6.3099897	49.0010217	0.1430682	0.1287726	6.53912E-12	1.42038E-11	0.512271	0.705656	-7.15	16.41
TM153	0.512395	5	0.705907	18	7.4	32.1	23.0	442.0	1.1152560	7.6398000	6.4009000	43.5812000	0.1459797	0.1468730	6.53912E-12	1.42038E-11	0.512271	0.705636	-7.16	16.12
TM164	0.512404	4	0.705974	13	9.0	41.8	31.2	394.3	1.3447529	9.9389488	8.6948632	38.8730595	0.1353013	0.2236732	6.53912E-12	1.42038E-11	0.512289	0.705561	-6.81	15.05
WW024	0.512254	5	0.709798	17	5.4	24.2	43.5	232.0	0.8134024	5.7501593	12.0994777	22.8752000	0.1414574	0.5289343	6.53912E-12	1.42038E-11	0.512134	0.708820	-9.84	61.33
WW099	0.512289	4	0.711683	20	4.6	20.4	60.0	214.0	0.6860673	4.8621924	16.6955276	21.1004000	0.1411025	0.7912422	6.53912E-12	1.42038E-11	0.512169	0.710221	-9.15	81.20
WW122	0.512399	5	0.705282	22	11.7	55.0	25.4	801.0	1.7584785	13.0833829	7.0652077	78.9786000	0.1344055	0.0894572	6.53912E-12	1.42038E-11	0.512285	0.705117	-6.89	8.75
WW184	0.512348	8	0.71049	11	4.0	16.1	34.9	186.9	0.5992366	3.8285242	9.7060723	18.4319831	0.1565190	0.5265886	6.53912E-12	1.42038E-11	0.512215	0.709517	-8.25	71.21
YM141	0.512366	5	0.706006	12	8.5	37.8	25.9	412.7	1.2683321	8.9922736	7.2217116	40.6887299	0.1410469	0.1774868	6.53912E-12	1.42038E-11	0.512246	0.705678	-7.65	16.72
YM187	0.51237	7	1.066095	22	8.2	25.2	276.5	16.9	1.2249614	5.9872910	76.9457196	1.6637323	0.2045936	46.2488577	6.53912E-12	1.42038E-11	0.512196	0.980618	-8.62	3919.34
YM198	0.512592	7	0.706465	17	3.8	13.6	15.7	155.8	0.5683626	3.2389701	4.3590071	15.3652065	0.1754763	0.2836934	6.53912E-12	1.42038E-11	0.512443	0.705941	-3.81	20.45
YM223	0.512431	6	0.705551	16	11.7	57.1	44.6	803.8	1.7607918	13.5869352	12.4230192	79.2504875	0.1295945	0.1567564	6.53912E-12	1.42038E-11	0.512321	0.705261	-6.19	10.81
AT03-519.2	0.512331	4	0.711547	17	6.1	27.5	61.0	241.0	0.9128910	6.5450000	16.9763000	23.7626000	0.1394791	0.7144126	6.53912E-12	1.42038E-11	0.512212	0.710227	-8.30	81.29
AT08-845.1	0.512334	4	0.712020	16	6.5	29.4	64.0	210.0	0.9698530	6.9972000	17.8112000	20.7060000	0.1386059	0.8601951	6.53912E-12	1.42038E-11	0.512216	0.710430	-8.23	84.18
CA-86RS 496.25-496.75	0.512252	5	0.717142	13	7.8	35.5	100.2	180.3	1.1744862	8.4422560	27.8981657	17.7821379	0.1391200	1.5688870	6.53912E-12	1.42038E-11	0.512134	0.714242	-9.84	138.29
5AT09 657.70-657.90	0.512405	7	0.710139	13	3.2	13.5	25.0	244.7	0.4730667	3.2051217	6.9706853	24.1274814	0.1475971	0.2889106	6.53912E-12	1.42038E-11	0.512279	0.709605	-6.99	72.46
PP-02-SP 1120-1130	0.51239	6	0.70596	12	8.4	37.6	28.5	429.6	1.2537206	8.9520861	7.9248533	42.3585684	0.1400479	0.1870897	6.53912E-12	1.42038E-11	0.512271	0.705614	-7.16	15.82
PP-02-SP 1280-1290	0.512403	4	0.706128	16	10.3	46.2	24.7	545.5	1.5504314	10.9958625	6.8845459	53.7819187	0.1410013	0.1280086	6.53912E-12	1.42038E-11	0.512283	0.705891	-6.92	19.75
PP-02-SP 1380-1390	0.512479	5	0.706405	13	9.2	38.4	34.6	337.5	1.3834765	9.1442556	9.6157492	33.2810382	0.1512946	0.2889258	6.53912E-12	1.42038E-11	0.512350	0.705871	-5.61	19.46
PP-02-SP 1460-1470	0.512925	6	0.706703	12	10.4	49.4	41.7	526.8	1.5594034	11.7660993	11.5959659	51.9424312	0.1325336	0.2232465	6.53912E-12	1.42038E-11	0.512812	0.706290	3.40	25.41
PP-02-SP 1540-1550	0.512411	5	0.706803	11	10.0	46.2	45.2	512.9	1.5033242	11.0066218	12.5897354	50.5710526	0.1365836	0.2489514	6.53912E-12	1.42038E-11	0.512295	0.706343	-6.69	26.16
PP-02-SP 1590-1600	0.512316	5	0.709391	11	6.0	25.7	54.6	348.6	0.8973651	6.1280904	15.1861419	34.3673049	0.1464347	0.4418776	6.53912E-12	1.42038E-11	0.512191	0.708574	-8.71	57.83
PP-02-SP 280-290	0.512412	4	0.706481	14	6.0	24.6	23.3	270.3	0.8934496	5.8567380	6.4856218	26.6509778	0.1525507	0.2433540	6.53912E-12	1.42038E-11	0.512282	0.706031	-6.94	21.74
PP-02-SP 440-450	0.51241	7	0.706261	13	5.0	20.6	21.9	255.6	0.7453952	4.8925446	6.0884737	25.2057334	0.1523533	0.2415511	6.53912E-12	1.42038E-11	0.512280	0.705815	-6.98	18.66
PP-02-SP 600-610	0.512362	6	0.706151	11	7.3	32.6	28.5	369.5	1.0897918	7.7584766	7.9358408	36.4333075	0.1404647	0.2178183	6.53912E-12	1.42038E-11	0.512243	0.705748	-7.71	17.72
PP-02-SP 760-770	0.512397	5	0.706355	14	9.2	41.2	35.7	358.2	1.3775181	9.8154215	9.9364482	35.3206227	0.1403422	0.2813214	6.53912E-12	1.42038E-11	0.512278	0.705835	-7.03	18.95
PP-02-SP 800-810	0.51238	6	0.706062	13	8.4	37.8	24.9	435.4	1.2621617	8.9849258	6.9372239	42.9316296	0.1404755	0.1615877	6.53912E-12	1.42038E-11	0.512261	0.705763	-7.36	17.93
PP-02-SP 960-970	0.512371	6	0.70624	12	8.2	36.4	29.2	436.6	1.2223740	8.6734076	8.1316249	43.0508834	0.1409335	0.1888840	6.53912E-12	1.42038E-11	0.512251	0.705891	-7.55	19.74
SW01 556.55-556.70	0.512383	4	0.717506	12	6.6	26.3	72.0	210.3	0.9939850	6.2523059	20.0299762	20.7378074	0.1589790	0.9658676	6.53912E-12	1.42038E-11	0.512248	0.715721	-7.61	159.27
TG114-289.9	0.512864	5	0.705162	15	2.5	9.7	9.8	188.0	0.3719789	2.3108101	2.7338333	18.5368000	0.1609734	0.1474814	6.53912E-12	1.42038E-11	0.512727	0.704889	1.74	5.53
TG228-817	0.512219	4	0.710876	17	5.2	23.6	37.0	243.0	0.7764820	5.6168000	10.2971000	23.9598000	0.1382428	0.4297657	6.53912E-12	1.42038E-11	0.512101	0.710082	-10.47	79.23
TG62-237.6	0.512851	7	0.705398	19	2.3	9.2	12.1	189.0	0.3472032	2.1880149	3.3702364	18.6354000	0.1586841	0.1808513	6.53912E-12	1.42038E-11	0.512716	0.705064	1.52	8.00
TG95-756.3	0.512210	5	0.710140	16	4.6	21.3	32.0	236.0	0.6925380	5.0694000	8.9056000	23.2696000	0.1366114	0.3827139	6.53912E-12	1.42038E-11	0.512094	0.709433	-10.62	70.02

$^{143}Nd/^{144}Nd$ CHUR: 0.512638 (Faure, 1986)
$^{87}Sr/^{86}Nd$ UR: 0.7045 (White and Hofmann, 1982)

APPENDIX 11

^{40}Ar-^{39}Ar dating for the Paraná basaltic lava and intrusion

AS001

Inc.	39/40	(39/40)err	36/40	(36/40)err
351	1.07E-02	3.10E-04	1.91E-03	3.00E-05
519	8.12E-03	1.70E-05	6.39E-04	3.20E-06
595	9.84E-03	9.00E-06	3.45E-04	2.10E-06
689	1.08E-02	9.90E-06	3.88E-04	3.00E-06
769	1.05E-02	1.00E-05	4.90E-04	5.30E-06
845	9.33E-03	1.30E-05	8.83E-04	7.90E-06
1102	1.14E-02	1.20E-05	7.86E-04	4.00E-06
1422	9.08E-03	5.20E-05	1.18E-03	1.00E-05

Inc.	% 39Ar	Age (Ma)	Age Err	%40Arrad
351	2.68	68.8	2.3	44
519	17.87	163.7	0.4	81
595	23.54	150.3	0.2	90
689	17.62	135.9	0.2	89
769	11.51	134.4	0.3	86
845	5.37	131.1	0.4	74
1102	17.53	111.6	0.2	77
1422	3.87	119.2	0.9	65

AS003

Inc.	39/40	(39/40)err	36/40	(36/40)err
421	1.79E-04	3.00E-06	3.29E-03	1.20E-05
512	4.54E-03	7.80E-06	1.68E-03	9.40E-06
590	9.41E-03	9.70E-06	5.87E-04	4.60E-06
688	1.01E-02	9.40E-06	5.28E-04	4.60E-06
769	1.05E-02	1.20E-05	4.61E-04	5.30E-06
841	9.57E-03	1.00E-05	8.12E-04	9.00E-06
1097	9.34E-03	1.00E-05	1.25E-03	8.00E-06
1422	6.02E-03	1.50E-05	1.84E-03	1.90E-05

Inc.	% 39Ar	Age (Ma)	Age Err	%40Arrad
421	2.08	239.4	29	2.6
512	6.32	181.1	1	50
590	21.05	145	0.3	82
688	25.17	137.7	0.3	84
769	16	135.9	0.3	86
841	10.4	131.5	0.5	76
1097	16.44	112.5	0.4	63
1422	2.55	125.6	1.6	46

AS006

Inc.	39/40	(39/40)err	36/40	(36/40)err
444	8.41E-03	8.10E-06	6.29E-04	9.20E-06
530	9.42E-03	1.10E-05	3.60E-04	8.00E-06
590	9.90E-03	1.10E-05	4.39E-04	6.10E-06
690	1.10E-02	1.10E-05	3.11E-04	3.90E-06
770	1.06E-02	1.10E-05	5.05E-04	4.70E-06
910	8.67E-03	2.50E-05	1.15E-03	2.80E-05
1100	8.34E-03	1.70E-05	1.55E-03	1.20E-05
1420	5.56E-03	7.10E-05	1.99E-03	3.00E-05

Inc.	% 39Ar	Age (Ma)	Age Err	%40Arrad
444	7.72	159.3	0.5	83
530	11.6	156.3	0.4	89
590	15.82	145.3	0.3	87
690	31	136.9	0.2	91
770	23.07	133.4	0.3	85
910	3.15	126.5	1.6	66
1100	6.18	108.6	0.7	54
1420	1.46	123.2	3	41

AS023

Inc.	39/40	(39/40)err	36/40	(36/40)err
432	1.08E-02	3.30E-05	1.39E-03	1.60E-05
514	1.03E-02	1.10E-05	9.64E-04	1.10E-05
588	9.22E-03	1.10E-05	9.40E-04	9.00E-06
771	8.84E-03	9.30E-06	1.02E-03	1.20E-05
845	7.69E-03	2.00E-05	1.75E-03	2.20E-05
909	6.39E-03	2.20E-05	2.20E-03	3.90E-05
1106	5.80E-03	8.20E-06	2.12E-03	1.60E-05
1420	2.79E-03	1.50E-05	2.28E-03	1.70E-05

Inc.	% 39Ar	Age (Ma)	Age Err	%40Arrad
432	27.89	91.2	0.8	59
514	24.19	116.2	0.5	71
588	22.98	130.3	0.5	72
771	12.18	131.5	0.7	70
845	4.6	105.3	1.4	48
909	1.98	92.1	3	35
1106	4.1	107.8	1.4	37
1420	2.09	191.2	2.9	33

AS024A

Inc.	39/40	(39/40)err	36/40	(36/40)err
438	3.62E-03	3.50E-05	2.29E-03	1.30E-05
523	5.23E-03	2.20E-05	1.72E-03	1.00E-05
590	7.01E-03	7.20E-06	1.30E-03	7.20E-06
690	7.15E-03	6.60E-06	1.37E-03	5.50E-06
767	6.20E-03	7.00E-06	1.55E-03	9.10E-06
843	5.74E-03	1.50E-05	1.79E-03	1.40E-05
908	5.54E-03	6.40E-06	1.94E-03	1.50E-05
1105	5.68E-03	8.50E-06	2.04E-03	9.00E-06
1424	3.25E-03	7.90E-06	2.39E-03	1.30E-05

Inc.	% 39Ar	Age (Ma)	Age Err	%40Arrad
438	5.18	148.3	2	32
523	12.68	155.7	1.1	49
590	16.97	145.5	0.5	61
690	30.18	138.5	0.4	59
767	10.64	144.9	0.7	54
843	5.05	136.6	1.2	47
908	4.77	128.8	1.3	43
1105	11.18	116.7	0.8	40
1424	3.35	150.2	2	29

KN002

Inc.	39/40	(39/40)err	36/40	(36/40)err
432	7.20E-03	1.90E-04	2.55E-03	4.50E-05
515	5.78E-03	1.80E-04	2.11E-03	5.80E-05
600	5.20E-03	1.70E-05	1.83E-03	1.70E-05
688	5.38E-03	7.10E-06	1.85E-03	8.10E-06
769	6.11E-03	9.70E-06	1.54E-03	1.00E-05
917	5.32E-03	1.50E-05	1.84E-03	2.00E-05
1110	5.06E-03	5.70E-06	2.06E-03	9.00E-06
1420	2.31E-03	7.60E-06	2.70E-03	1.70E-05

Inc.	% 39Ar	Age (Ma)	Age Err	%40Arrad
432	7.21	57.1	3.1	25
515	11.24	106.3	5.5	37
600	6.84	143	1.5	46
688	30.73	136.8	0.7	45
769	14.34	144.1	0.8	54
917	5.92	139.3	1.8	46
1110	19.15	125.4	0.8	39
1420	4.57	141.8	3.4	20

KN003

Inc.	39/40	(39/40)err	36/40	(36/40)err
450	3.23E-03	5.20E-06	2.11E-03	9.90E-06
550	4.52E-03	1.30E-05	1.84E-03	1.00E-05
600	4.51E-03	2.30E-05	1.92E-03	1.40E-05
690	4.12E-03	7.20E-06	2.09E-03	9.40E-06
770	5.82E-03	2.30E-05	1.47E-03	2.10E-05
910	5.34E-03	1.40E-05	1.70E-03	1.60E-05
1110	5.81E-03	8.10E-06	1.81E-03	1.20E-05
1410	3.40E-03	3.00E-05	2.26E-03	3.10E-05

Inc.	% 39Ar	Age (Ma)	Age Err	%40Arrad
450	15.15	185.8	1.4	37
550	14.24	163.2	1.1	46
600	12.48	155.4	1.5	43
690	19.54	150	1.1	38
770	7.12	156.9	1.8	56
910	8.61	151.1	1.4	50
1110	19.61	130.4	1	46
1410	3.26	157.1	4.4	33

KN005

Inc.	39/40	(39/40)err	36/40	(36/40)err
444	8.19E-03	4.90E-05	6.59E-04	1.70E-05
522	9.67E-03	1.10E-05	2.57E-04	4.90E-06
600	1.07E-02	1.10E-05	2.08E-04	3.30E-06
693	1.11E-02	1.10E-05	2.25E-04	4.00E-06
770	1.07E-02	1.70E-05	4.04E-04	1.40E-05
910	1.01E-02	2.60E-05	7.23E-04	1.40E-05
1110	1.04E-02	1.80E-05	1.13E-03	1.70E-05
1420	7.75E-03	2.30E-05	1.34E-03	2.90E-05

Inc.	% 39Ar	Age (Ma)	Age Err	%40Arrad
444	4.29	159	1.3	81
522	19.92	154.7	0.3	92
600	29.81	142.6	0.2	94
693	23.97	137	0.2	93
770	7.01	134.3	0.6	88
910	5.67	126.8	0.7	79
1110	6.98	105.2	0.8	67
1420	2.35	127.3	1.8	60

KN012

Inc.	39/40	(39/40)err	36/40	(36/40)err
370	7.35E-03	7.80E-06	1.07E-03	9.60E-06
530	8.51E-03	1.10E-05	4.70E-04	9.00E-06
595	9.60E-03	8.90E-06	3.88E-04	4.20E-06
688	9.86E-03	1.10E-05	4.86E-04	7.40E-06
769	9.38E-03	1.30E-05	6.44E-04	9.70E-06
910	7.75E-03	1.20E-05	1.21E-03	1.40E-05
1100	5.81E-03	2.20E-05	2.33E-03	1.80E-05
1420	3.23E-03	1.90E-05	2.57E-03	3.10E-05

Inc.	% 39Ar	Age (Ma)	Age Err	%40Arrad
370	10.97	151.3	0.6	68
530	16.01	163.6	0.5	86
595	29.49	149.8	0.2	88
688	20.41	141.4	0.4	86
769	11.85	140.5	0.5	81
910	5.65	135.4	0.9	64
1100	4.16	88.7	1.5	31
1420	1.45	122.1	4.5	24

KN016

Inc.	39/40	(39/40)err	36/40	(36/40)err
435	1.10E-04	1.80E-06	3.31E-03	1.20E-05
522	6.05E-03	5.50E-05	1.56E-03	1.50E-05
597	9.08E-03	1.10E-05	6.54E-04	6.40E-06
681	1.00E-02	9.40E-06	5.53E-04	2.60E-06
761	1.01E-02	1.00E-05	5.88E-04	4.70E-06
921	9.44E-03	1.10E-05	9.18E-04	6.00E-06
1110	9.26E-03	1.10E-05	1.28E-03	9.30E-06
1434	5.91E-03	1.10E-05	1.85E-03	1.20E-05

Inc.	% 39Ar	Age (Ma)	Age Err	%40Arrad
435	0.64	307.1	45	2
522	4.79	145	1.7	54
597	11.07	144.7	0.4	81
681	35.91	136	0.2	84
761	18.1	133.3	0.3	83
921	13.83	126.4	0.3	73
1110	12.01	110.6	0.5	62
1434	3.66	125.4	1	45

KN020

Inc.	39/40	(39/40)err	36/40	(36/40)err
438	7.51E-03	1.70E-05	6.52E-04	1.50E-05
525	9.29E-03	1.70E-05	3.50E-04	7.30E-06
593	9.91E-03	1.10E-05	3.26E-04	1.10E-05
686	1.07E-02	1.10E-05	3.33E-04	4.80E-06
776	1.08E-02	1.40E-05	3.64E-04	8.50E-06
840	9.62E-03	2.20E-05	7.18E-04	1.30E-05
1098	7.68E-03	1.60E-05	1.38E-03	2.10E-05
1420	5.26E-03	3.10E-05	2.03E-03	3.80E-05

Inc.	% 39Ar	Age (Ma)	Age Err	%40Arrad
438	5.24	173.8	1	55
525	28.52	156.8	0.5	69
593	12.84	148.5	0.5	77
686	22.33	137.9	0.3	80
776	17.41	135.1	0.4	85
840	7.25	134	0.7	87
1098	5.14	126.5	1.3	73
1420	1.25	124.4	3.5	55

KN024A

Inc.	39/40	(39/40)err	36/40	(36/40)err
433	6.70E-03	6.80E-05	6.31E-04	4.90E-05
533	9.44E-03	1.00E-05	3.35E-04	7.40E-06
602	1.04E-02	1.10E-05	2.36E-04	7.30E-06
693	1.11E-02	1.00E-05	2.91E-04	4.60E-06
771	9.48E-03	1.00E-05	7.62E-04	1.40E-05
912	8.03E-03	2.40E-05	1.25E-03	2.10E-05
1102	7.47E-03	2.90E-05	2.00E-03	2.60E-05
1418	4.77E-03	9.00E-05	1.99E-03	6.90E-05

Inc.	% 39Ar	Age (Ma)	Age Err	%40Arrad
433	1.44	195.7	3.8	81
533	34	155.5	0.4	90
602	17.75	145.8	0.4	93
693	31.38	135.3	0.2	91
771	7.86	133.9	0.7	77
912	3.86	128.9	1.3	63
1102	2.95	91	1.7	41
1418	0.77	141.6	7.2	41

^{40}Ar-^{39}Ar dating for the Paraná basaltic lava and intrusion

KN027

Inc.	39/40	(39/40)err	36/40	(36/40)err
458	4.87E-03	2.20E-05	1.53E-03	1.50E-05
535	5.50E-03	2.40E-05	1.05E-03	1.50E-05
606	7.16E-03	1.10E-05	7.72E-04	8.90E-06
693	8.59E-03	1.30E-05	6.58E-04	6.20E-06
771	9.82E-03	1.20E-05	5.07E-04	7.80E-06
845	1.07E-02	9.90E-06	4.48E-04	2.20E-06
1100	1.11E-02	1.50E-05	8.97E-04	1.30E-05
1420	8.42E-03	2.60E-05	1.53E-03	2.90E-05

Inc.	% 39Ar	Age (Ma)	Age Err	%40Arrad
458	4.3	181.8	1.6	55
535	3.29	202.2	1.5	69
606	7.48	174.8	0.6	77
693	9.17	153.1	0.4	80
771	10.13	141.8	0.4	85
845	51.8	132.8	0.2	87
1100	11.33	109.5	0.6	73
1420	2.5	107.5	1.7	55

KN031

Inc.	39/40	(39/40)err	36/40	(36/40)err
437	6.65E-03	1.00E-05	1.09E-03	1.50E-05
520	8.37E-03	1.30E-05	6.10E-04	1.20E-05
601	9.58E-03	1.00E-05	4.93E-04	7.30E-06
693	1.05E-02	1.00E-05	3.60E-04	3.60E-06
772	1.05E-02	1.00E-05	5.26E-04	4.00E-06
916	1.00E-02	1.10E-05	7.08E-04	6.60E-06
1108	9.21E-03	1.30E-05	1.24E-03	6.40E-06
1430	7.74E-03	1.60E-05	1.50E-03	1.40E-05

Inc.	% 39Ar	Age (Ma)	Age Err	%40Arrad
437	3.9	166.3	1.1	68
520	4.54	159.8	0.7	81
601	23.91	146.2	0.4	85
693	21.61	139.7	0.2	89
772	20.18	131.8	0.2	84
916	11.73	129.9	0.3	79
1108	10.27	114	0.4	63
1430	3.85	119.1	0.9	56

KN050

Inc.	39/40	(39/40)err	36/40	(36/40)err
429	5.83E-03	1.90E-05	1.35E-03	1.90E-05
530	7.61E-03	8.80E-06	8.12E-04	5.40E-06
594	8.64E-03	9.00E-06	7.04E-04	5.20E-06
688	9.53E-03	8.80E-06	6.56E-04	4.70E-06
770	9.41E-03	1.20E-05	8.07E-04	8.20E-06
912	8.18E-03	1.30E-05	1.24E-03	1.00E-05
1151	6.02E-03	1.40E-05	2.01E-03	1.20E-05
1424	2.86E-03	2.60E-05	2.67E-03	2.30E-05

Inc.	% 39Ar	Age (Ma)	Age Err	%40Arrad
429	4.19	168.4	1.6	60
530	18.19	163.2	0.4	76
594	17.55	150.3	0.3	79
688	29.71	139.2	0.3	81
770	13.61	133.4	0.4	58
912	9.01	127.8	0.6	63
1151	6.47	112.1	1	41
1424	1.28	122.8	4	21

KN052

Inc.	39/40	(39/40)err	36/40	(36/40)err
264	4.99E-03	3.00E-04	3.05E-03	1.40E-05
419	4.32E-03	6.30E-06	2.01E-03	9.60E-06
517	7.28E-03	7.10E-06	1.02E-03	4.40E-06
589	7.68E-03	7.00E-06	1.12E-03	6.50E-06
687	8.52E-03	8.00E-06	9.78E-04	4.40E-06
770	9.42E-03	9.60E-06	8.25E-04	5.60E-06
841	8.11E-03	9.90E-06	1.20E-03	9.20E-06
1103	5.54E-03	9.40E-06	2.08E-03	9.70E-06
1418	2.85E-03	2.20E-05	2.50E-03	1.80E-05

Inc.	% 39Ar	Age (Ma)	Age Err	%40Arrad
264	8.5	33.6	2.4	9.8
419	5.76	154.1	1	40.6
517	25.27	157.7	0.3	70
589	13.96	143.3	0.4	67
687	19.85	137.7	0.3	71
770	12.38	132.6	0.3	76
841	6.39	131.4	0.6	65
1103	6.48	115.3	0.9	38
1418	1.41	151	3.3	26